

• REVIEW •

The prognostic molecular markers in hepatocellular carcinoma

Lun-Xiu Qin, Zhao-You Tang

Lun-Xiu Qin, Zhao-You Tang, Liver Cancer Institute and Zhongshan Hospital, Fudan University, Shanghai, China

Correspondence to: Zhao-You Tang, M.D., Professor of Surgery & Chairman, Liver Cancer Institute & Zhongshan Hospital, Fudan University, 136 Yi Xue Yuan Road, Shanghai 200032, China. zytang@srcap.stc.sh.cn
Telephone: +86-21-64037181 Fax: +86-21-64037181

Received 2002-03-19 Accepted 2002-05-08

Abstract

The prognosis of hepatocellular carcinoma (HCC) still remains dismal, although many advances in its clinical study have been made. It is important for tumor control to identify the factors that predispose patients to death. With new discoveries in cancer biology, the pathological and biological prognostic factors of HCC have been studied quite extensively. Analyzing molecular markers (biomarkers) with prognostic significance is a complementary method. A large number of molecular factors have been shown to associate with the invasiveness of HCC, and have potential prognostic significance. One important aspect is the analysis of molecular markers for the cellular malignancy phenotype. These include alterations in DNA ploidy, cellular proliferation markers (PCNA, Ki-67, MCM2, MIB1, MIA, and CSE1L/CAS protein), nuclear morphology, the p53 gene and its related molecule MDM2, other cell cycle regulators (cyclin A, cyclin D, cyclin E, cdc2, p27, p73), oncogenes and their receptors (such as ras, c-myc, c-fms, HGF, c-met, and erb-B receptor family members), apoptosis related factors (Fas and FasL), as well as telomerase activity. Another important aspect is the analysis of molecular markers involved in the process of cancer invasion and metastasis. Adhesion molecules (E-cadherin, catenins, serum intercellular adhesion molecule-1, CD44 variants), proteinases involved in the degradation of extracellular matrix (MMP-2, MMP-9, uPA, uPAR, PAI), as well as other molecules have been regarded as biomarkers for the malignant phenotype of HCC, and are related to prognosis and therapeutic outcomes. Tumor angiogenesis is critical to both the growth and metastasis of cancers including HCC, and has drawn much attention in recent years. Many angiogenesis-related markers, such as vascular endothelial growth factor (VEGF), basic fibroblast growth factor (bFGF), platelet-derived endothelial cell growth factor (PD-ECGF), thrombospondin (TSP), angiogenin, pleiotrophin, and endostatin (ES) levels, as well as intratumor microvessel density (MVD) have been evaluated and found to be of prognostic significance. Body fluid (particularly blood and urinary) testing for biomarkers is easily accessible and useful in clinical patients. The prognostic significance of circulating DNA in plasma or serum, and its genetic alterations in HCC are other important trends. More attention should be paid to these two areas in future. As the progress of the human genome project advances, so does a clearer understanding of tumor biology, and more and more new prognostic markers with high sensitivity and specificity will be found and used in

clinical assays. However, the combination of some items, i.e., the pathological features and some biomarkers mentioned above, seems to be more practical for now.

Qin LX, Tang ZY. The prognostic molecular markers in hepatocellular carcinoma. *World J Gastroenterol* 2002;8(3):385-392

INTRODUCTION

Liver cancer is one of the common malignancies worldwide, and has been ranked the 2nd cancer killer in China since the 1990s. Although many advances in the clinical study of hepatocellular carcinoma (HCC) have been made, and long-term survival of patients has been obtained in some clinical centers, only a definitive subset of cases is cured by surgery, and the overall dismal outcome of patients with HCC has not been completely changed. Lack of control of metastatic foci and recurrence are the most prevalent causes of death in patients with HCC, and it is important for tumor control to identify the factors that predispose patients to death. Much effort has been made to predict HCC behavior, but specific prognostic indicators are still lacking^[1].

Prognostic factors in HCC conventionally consist of staging with the tumor node metastasis system (TNM) and grading by tumor cellular differentiation. There are also other factors useful in prognostic predication but most of them are clinical. With new discoveries in cancer biology, pathological and biological factors of HCC in relation to prognosis have been studied quite extensively. Morphological features of the tumor, both gross and histological, have been found to significantly associate with tumor recurrence and patient survival^[2-4]. A complementary way is to analyze molecular markers for their prognostic significance with reference to tumor recurrence and survival term in HCC. A large number of molecular biological factors have been shown to associate with the invasiveness of HCC, and have potential prognostic significance. However, routine biomarkers for the prediction of HCC prognosis are not yet available. In this review, we will focus on the recent advances in this aspect.

Cellular malignancy is a very important aspect for patient prognosis. In recent years, with the development of cellular and molecular biological techniques, many molecular markers related to invasion, metastasis, recurrence and survival have been explored. In HCC, DNA ploidy, the proliferating activity of tumor cells, tumor suppressor and promoter genes, cell cycle controllers, proteinases that degrade extracellular matrix, adhesion molecules, angiogenic factors, and metabolic genes, have been regarded as biomarkers for the malignant phenotype of HCC, and are related to prognosis and therapeutic outcomes^[5].

CELLULAR MALIGNANCY-RELATED MARKERS

DNA-ploidy

Controversy still exists regarding the prognostic significance of DNA ploidy in HCC patients. Many reports indicate that DNA ploidy could be a predictive marker for HCC prognosis^[6,7]. The overall survival rate of patients with aneuploid cells is much lower than that of patients with diploid ones, and those with multiple G0/G1 peaks have the

worst prognosis. Patients with higher cell proportions in proliferating stages have a higher early recurrence rate^[7]. However, other studies could not find a relationship between DNA ploidy and prognosis.

Proliferating activity of HCC cells

Many antigens, such as proliferating cell nuclear antigen (PCNA), Ki-67, MCM2, MIB1, MIA, and CSE1L/CAS protein (CAS), have been used as proliferation markers for cancer cells. The detection of PCNA with immunohistochemical methods is a common way to study the proliferating activity of cancer cells^[8]. Combined with histopathological characteristics, the PCNA labeling index (PCNA-LI) is one useful marker for evaluating malignant grade, and for predicting recurrence time and the patients' prognosis of HCC^[9].

The expression of the human Ki-67 protein is strictly associated with cell proliferation. The fact that the Ki-67 protein is present during all active phases of the cell cycle, but is absent from resting cells, makes it an excellent marker for determining the so-called growth fraction of a given cell population. Ki-67 protein expression is an absolute requirement for progression through the cell-division cycle. The fraction of Ki-67-positive tumor cells (the Ki-67 labeling index) is often correlated with the clinical course of the disease^[10,11]. Higher Ki-67 labeling index (Ki-67-LI) has a very similar clinical significance to PCNA-LI, reflecting the existence of biologically aggressive phenotypes and poor overall and disease-free survival rates in HCC. This could be a useful factor for predicting the long-term survival of patients with HCC following hepatic resection^[12,13].

The CSE1L/CAS protein (CAS) is a Ran-binding protein with a function as a nuclear transport (export) factor. This protein plays a role in the mitotic spindle checkpoint, which assures genomic stability during cell division. This checkpoint is frequently disturbed in neoplasias of various origins, including hepatic tumors. The degree of CAS expression correlates with the grade of tumor dedifferentiation, and could be a prognostic marker for HCC^[14].

Nuclear morphology

Nuclear profiles have been reported as useful prognostic predictors in various cancers, including HCC. The nuclear area of HCC correlates with cell differentiation and cell proliferating activity, and HCC with a large nuclear area has high potential for blood vessel invasion and intrahepatic metastasis. Computerized nuclear morphometry is more objective and quicker than conventional microscopic analysis^[15]. Recently, quantitative nuclear morphometry of cancer cells followed by computer-assisted image analysis (termed Quantitative nuclear grade, QNG) has proven to have potential use in cancer detection and predicting outcomes such as tumor stage, recurrence, and progression^[16].

p53 gene and its related molecule MDM2

P53 protein plays a central role in cellular responses, including cell-cycle arrest and cell death in response to DNA damage. p53 dysfunction can induce abnormal cell growth, increased cell survival, genetic instability, and drug resistance. Mutations in the p53 gene are the most frequently reported somatic gene alteration in human cancer. Associations of p53 mutation or positive immunohistochemistry staining with higher grade and more advanced stage has been noted for cancers of various origins. In addition, p53 mutation is considered as a strong marker predicting an increased risk of local relapse, treatment failure, and overall and disease-free survival in many kinds of human carcinomas, such as breast^[17-19], colorectal^[20], esophageal^[21], head and neck^[22], lung^[23,24], and ovarian^[25], as well as sarcoma^[26]. An increased intracellular concentration of the P53 protein, although not identical to, is sometimes seen in tumors with p53 mutation, and has been correlated with poor prognosis in some tumor types. Several studies have shown a relationship between the nuclear accumulation of p53 protein and poor disease-free and overall survival of cancer

patients^[27,28]. The presence of serum anti-p53 antibody has also been shown to associate with survival of patients with breast, ovarian, and colorectal cancer^[29,30]. p53 mutations in plasma DNA could also be detected in cancer patients, and may be used as a prognostic factor and an early marker to indicate recurrence or distant metastasis^[31]. However, there is still a great controversy as to whether alteration of the p53 gene adversely affects survival of cancer patients. Many reports failed to show the independent prognostic value of p53 in the carcinomas of tongue^[32], breast^[33,34], stomach^[35], lung^[36], ovarian^[37], bladder^[38], colorectal^[39], and non-Hodgkin's lymphoma^[40].

In a similar situation, there are many very controversial results with the prognostic value of p53 overexpression or p53 gene mutation in HCC patients. Many studies showed that p53 mutation was involved in determining the dedifferentiation, the proliferating activity, and tumor progression^[41], was strongly related to the invasiveness of HCC, and may also influence the postoperative course (particularly the recurrence within 1 year)^[42,43]. Mutations in the p53 gene or positive immunostaining for mutant P53 protein expression could be used as a significant indicator of poor prognosis. HCCs with p53 mutations have a high malignant potential, and p53 mutation in the primary lesion is useful as an indicator for the biological behavior of recurrent HCCs. It is also a useful independent prognostic factor affecting survival after recurrence^[9,44,45].

In a recent prospective study, we found the 3-year and 5-year overall survival rates of HCC patients with positive P53 nuclear accumulation were much lower than those of the HCC patients with negative P53 expression. In univariate and multivariate Cox analysis, p53 overexpression was the most significant factor that associated with the overall survival rates of HCC patients after resection. Its significance was even greater than that of factors such as tumor size, vascular invasion, and tumor capsule, though they were also related to the overall survival. p53 mutation or nuclear accumulation of p53 expression could be a valuable marker for predicting the prognosis of HCC patients after resection^[46].

Serum anti-p53 antibody also could be a useful prognostic factor for HCC patients^[47]. However, many different results showed that neither the immunohistochemical detection of p53 expression, nor the serum anti-p53 antibodies had a significant prognostic value for outcome of patients with HCC^[48,49].

The transcription of the mdm2 gene is activated by p53 and this limits the growth-suppressing activity of p53 by direct binding. It has been reported that MDM2 protein is overexpressed in several types of cancers. Endo found MDM2 overexpression correlated positively with p53 mutation, and is a useful predictor of poor prognosis in patients with HCC following hepatic resection^[50].

Cell cycle regulators

Disruption of the G1/S and G2/M checkpoints leads to uncontrolled cell growth, resulting in the development and progression of cancers. Overexpression of cyclin A, cyclin D, and cyclin E have been found to correlate with the tumor relapse of human HCC, and are independent predictive markers for their recurrence and prognosis^[51,52]. The enhanced expression of cyclin E correlates with hyperphosphorylation of pRb and a high frequency of Ki-67-positive cells. HCCs with enhanced cyclin E expression probably contain a relatively large number of proliferating cancer cells^[52]. cdc2 overexpression seems to play the most crucial role of the modulators in cell cycle progression and cell proliferation of HCC, and significantly predicts recurrence^[53].

The p27 protein binds and inhibits cyclin/cyclin-dependent kinase complexes, is a negative regulator of cell-cycle progression. The central role of p27 makes it important in a variety of disease processes, particularly in neoplasia, that involve aberrations in cellular proliferation and other cell fates. Loss of p27 cooperates with mutations in several oncogenes and tumor suppressor genes to facilitate

tumor growth, indicating that p27 may be a “nodal point” for tumor suppression. In most tumor types, reduced p27 expression correlates with poor prognosis, making p27 a novel and powerful prognostic marker^[54]. High p27 expression, correlated with prolonged survival, is a favorable independent prognostic parameter for HCC^[55,56].

The protein p73, the first identified homologue of p53 gene, has been shown to induce apoptosis. P73 expression status is significantly related to prognosis of HCC patients, and could serve as a useful indicator of prognosis in HCC patients^[57]. There is still controversy with the prognostic value of the p16INK4a and p15INK4B genes^[58].

Tumor promoter genes and their receptors

Aberrations of many tumor promoter genes, such as ras, c-myc, c-fms have been indicated as indicators of malignant potential and poor prognosis in HCC^[9,59-61]. c-myc amplification and p53 alteration may be participating events in the progression of HCC. Disease-free survival in patients showing c-myc amplification is significantly shorter than in those without amplification. Hepatocyte growth factor/scatter factor (HGF/SF) is one of the most important humoral mediators of liver regeneration. It is potentially related to molecular mechanisms of hepatocarcinogenesis via a paracrine system involving its cellular receptor, c-met. Up-regulation of c-met plays an important role in the development and progression of HCC, and may be a prognostic marker. Its expression level is inversely correlated with survival coordinated with uPA expression^[62,63]. However, there is no significant correlation between the HGF level in tumor and the survival rate of HCC patients^[5].

Among of the erb-B receptor family members, c-erbB-2 (Her-2/neu) represents a well-established prognostic marker and therapeutic target in several human tumor types, especially breast cancer. However, c-erbB-2 is neither a prognostic marker nor a relevant therapeutic target in human HCCs^[9,64]. EGF-R and c-erbB-3 play important roles in the progression of HCC, affecting disease-free survival of HCC patients^[5,65].

ets-1 has also been shown to link to cancer invasion and metastasis. ets-1 expression was observed with high incidence. However, the average labeling index (LI) in HCC is lower than in noncancerous lesions. Even lower expression levels were found in HCCs of high TNM stage, poor differentiation, portal invasion, intrahepatic metastasis, large tumor size, and high Ki-67-LI. HCC patients with high ets-1 expression showed better outcomes for disease-free survival than those with low ets-1 expression^[66].

Apoptosis related

The expression of Fas and Fas ligand (Fas L) play a role in apoptosis of cancer cells including HCCs, and associates with the prognosis of cancer patients. Fas expression level is significantly decreased in poorly differentiated HCC and of large size, while Fas L expression in carcinoma cells is observed exclusively in moderately or poorly differentiated cases. Each of them has prognostic significance for disease-free survival (DFS)^[5,67,68].

Telomerase activity

The ribonucleoprotein telomerase extends telomeres in cancer cells and has been proposed as a prognostic marker for cancer. Telomerase activity can be identified as an independent predictor for recurrence after resection of HCC^[69]. The peripheral blood telomerase activity can also be used as a molecular marker for the detection of circulating hepatoma cells in blood of HCC patients, which reflect haematogenous micrometastasis. This is potentially a practical diagnostic/predictive marker of HCC^[70]. Quantitative analysis of telomerase activity shows that the patients with positive telomerase activity in noncancerous liver tissue have a higher recurrence rate after HCC resection. The relative telomerase activity (RTA) of early recurrent patients is significantly higher than those without recurrence.

So, RTA could be a predictive marker for early recurrence after HCC resection^[71].

CELL ADHESION AND EXTRACELLULAR MATRIX RELATED

Adhesion molecules

The expression level of E-cadherin inversely correlates with HCC histological grade and prognosis. E-cadherin underexpression might have some contribution to the early recurrence of HCC^[72,73]. In contrast, alpha-, beta-, and gamma-catenin expression significantly correlated positively with HCC grade, being the highest in poorly differentiated HCC. Significant positive associations were found between gamma-catenin high expression and capsular invasion or presence of satellite nodules, and between beta-catenin high expression and vascular invasion. HCC patients with underexpression of E-cadherin, alpha-catenin, and gamma-catenin, and patients with overexpression of beta-catenin, had poorer survival rates^[73]. HCCs with a nonnuclear type of beta-catenin overexpression were frequently larger than 5cm in diameter and had poorer cellular differentiation, more invasiveness, and the patients had significantly shorter disease-free survival lengths^[74,75]. beta-catenin mutation associates with nuclear expression of the protein, and is a favorable prognostic factor related to low stage^[76].

Serum concentration of intercellular adhesion molecule-1 (sICAM-1) in patients with HCC is a marker for disease progression and prognosis. Higher sICAM-1 levels are more frequently observed in those patients with multiple lesions and intrahepatic metastasis, and their prognosis is also very poor. Detecting sICAM-1 is of important value in predicting tumor recurrence after surgery^[77-79]. The CD44 proteins form a ubiquitously expressed family of cell surface adhesion molecules involved in cell-cell and cell-matrix interactions. The major physiological role of CD44 is to maintain organ and tissue structure via cell-cell and cell-matrix adhesion, but certain variant isoforms can also mediate lymphocyte activation and homing, and the presentation of chemical factors and hormones. The expression of multiple CD44 isoforms is greatly upregulated in neoplasia. CD44, particularly its variants, may be useful as a diagnostic or prognostic marker of malignancy in at least some human cancers^[80]. Up-regulation of CD44 isoforms such as CD44s, CD44v5, CD44v6, CD44v7-8, and CD44v10, correlates with high histological grade, being the highest in poorly differentiated HCC. CD44 positivity was an independent factor. Positivity for one or more CD44 isoforms was the most useful independent factor for overall survival^[81].

Degradation of extracellular matrix

The matrix metalloproteinases (MMP) and the plasminogen activation system (PA) play crucial roles in the process of cancer invasion and metastasis. Their expression levels were found correlated to recurrence and survival after HCC resection^[82,83].

MMP-2, MMP-9, and tissue inhibitors of metalloproteinases -1, -2 (TIMP-1, TIMP-2) have been found to be of prognostic significance in HCC. The content of MMP-2, MMP-9 in HCC being higher than that in surrounding liver parenchyma could be used as an important index to judge the invasion and metastasis of HCC^[84,85]. Plasma MMP-9 levels can also be a candidate for a novel marker for HCC. The levels appear to reflect the potential and ongoing activity of vascular invasion^[5].

In several tumor types, elevated levels of urokinase plasminogen activator (uPA), its receptor (uPAR) or its inhibitor plasminogen activator inhibitor-1 (PAI-1) is associated with a poorer prognosis^[85]. uPA activity may be the most sensitive factor affecting HCC invasion in the plasminogen activation system and is a strong predictor for the recurrence and prognosis of HCC^[86,87]. The PAI-1 protein is a multifaceted proteolytic factor. It not only functions as an inhibitor of the protease uPA, but also plays an important role in signal

transduction, cell adherence, and cell migration. Thus, an apparent paradox considering its name—although it inhibits uPA during blood coagulation, it actually promotes invasion and metastasis. In many malignancies including HCC, elevated PAI-1 is associated with tumor aggressiveness and poor patient outcome^[86].

ANGIOGENESIS RELATED

Tumor angiogenesis is critical to both the growth and metastasis of cancer, and is regulated by angiogenic factors. Circulating angiogenesis regulators have been evaluated not only as diagnostic and/or prognostic factors but also as predictive factors in cancer patients. They could be used to determine the risk of developing cancer, to screen for early detection, to distinguish benign from malignant disease, and to distinguish between different types of malignancies. In established malignancies, they can be used to determine prognosis, to predict the response to therapy, and to monitor the clinical course^[5,83,88]. HCC is typically a hypervascular tumor with a rich blood supply. In recent years, many angiogenesis-related markers, such as vascular endothelial growth factor (VEGF), basic fibroblast growth factor (bFGF), platelet-derived endothelial cell growth factor (PD-ECGF), thrombospondin (TSP), angiogenin, pleiotrophin and endostatin (ES) levels, as well as intratumor microvessel density (MVD) have been evaluated and found to relate to HCC prognosis.

Intratumor microvessel density (MVD)

The intratumor MVD is a direct reflection of tumor angiogenesis. It can be visualized by immunohistochemical staining with antibodies to anti-CD34, Factor VIII, and alpha smooth muscle actin^[89]. MVD levels have a close relationship with the tumor capsule status, tumor size (HCC with 2-5cm in diameter has the highest MVD level), intrahepatic recurrence and disease-free survival, and can be a predictive marker for disease-free survival^[90]. In the authors' institute, three types of intratumor microvessels, including capillary-like, sinusoid-like, and mixed-type, were found in HCC. The MVD level was not related to tumor size, capsule status, Edmondson's grade, or alpha-fetoprotein level; was an independent factor of disease-free survival in small HCC patients; and was a predictive marker for early recurrence^[91].

Vascular endothelial growth factor (VEGF)

A substantial number of studies have demonstrated a strong association between elevated tumor expression of VEGF and advanced disease or poor prognosis in various cancers. Circulating VEGF seems to be a reliable surrogate marker of angiogenic activity and tumor progression in cancer patients. It may be predictive of tumor status and prognosis in patients with different types of cancer, and may be useful in predicting and monitoring tumor response to anticancer therapies and in follow-up surveillance for tumor relapse. It may provide new prognostic information that is not afforded by conventional clinicopathologic prognostic indicators^[92]. In HCC, a high serum VEGF level significantly correlates with absence of tumor capsule, presence of intrahepatic metastasis, presence of microscopic venous invasion, and advanced stage, and it may be useful as a biologic marker of tumor invasiveness and a prognostic factor in HCC^[93]. The data of the authors' institute also shows serum VEGF is a predictor of invasion and metastasis of HCC and a potential biomarker of metastatic recurrence after curative resection^[94,95].

Platelet-derived endothelial cell growth factor (PD-ECGF)

PD-ECGF may not be a major regulator of angiogenesis of HCC, but may play an important role in hepatocarcinogenesis, cooperating with hepatitis C virus. PD-ECGF expression associates with the venous invasion of HCC^[96].

GENOMICS AND PROTEOMICS RELATED

Molecular genetic analyses have clarified that accumulation of genomic changes provides important steps in carcinogenesis and have identified a number of valuable genetic markers for certain cancers. The association of these genomic aberrations with the progression and prognosis of cancer has drawn more and more attention. To date, allelic loss of 1p, 1q21-23, 2p21-16.3, 3p24-p25, 8p22, 8p23, 9p21, 9q, 10, 13q12, 17p13.3, and 22q13 have been proposed to be related to the survival and prognosis of cancer patients^[97-101].

Many chromosomal aberrations, including gain of 1q, 8q, and 20q, and loss of 16q, 4q, 17p, 1p, and 8p have been identified in HCC^[102]. However, the relationship between these recurrent alterations and the clinical phenotypes and prognosis is still unknown. Towards the end of 1999, we compared the differences of chromosomal aberrations between the primary HCC tumors and their matched metastatic lesions using a comparative genomic hybridization (CGH) technique, and found chromosome 8p deletions might contribute to HCC metastasis^[103]. This result was further confirmed by comparison between nude mice models of HCC with different metastatic potentials^[104]. In addition, a more accurate location was identified on 8p23.3, 8p11.2^[105]. These findings provide new targets for exploring new predictive markers for the recurrence and prognosis of HCC. Recently, Itano *et al.* used restriction landmark genomic scanning (RLGS), a new high-speed screening method for multiple genomic changes, to detect unknown genetic alterations in HCC. They found the disease-free survival rate for patients with ≥ 16 changed RLGS spots was significantly lower than that for patients with fewer changed RLGS spots (≤ 15 spots). In multivariate analysis, the number of changed spots was proven to retain an independent prognostic value. These results suggest that the number of changed RLGS spots may be a useful biological marker for recurrence of HCC^[106].

One important trend in this area that should be paid attention to is the prognostic value of circulating DNA in plasma or serum, and its genetic alterations in cancer patients. Small amounts of DNA circulate in both healthy and diseased human plasma/serum, and increased concentrations of DNA are present in the plasma of cancer patients. Characteristics of tumor DNA have been found in genetic material extracted from the plasma of cancer patients. These features include decreased strand stability, the presence of specific oncogene or tumor suppressor gene mutations, microsatellite alterations, Ig rearrangements and hypermethylation of several genes. The results obtained in many different cancers have opened a new research area indicating that plasma DNA might eventually be a suitable target for the development of noninvasive diagnostic, prognostic and follow-up tests for cancer^[107]. Blood testing for circulating tumor genetic markers may provide valuable prognostic information and guide future therapy^[108].

However, there is still controversy over the prognostic significance^[109]. We found loss of heterozygosity (LOH) on chromosome 14q (D14S62 and D14S51) could be detected in plasma DNA, and could be of prognostic significance in HCC patients^[11].

Proteomics, regarded as a sister technology to genomics, is one of the technologies rapidly changing our approach to understanding tumor biology. By comparing the proteins present in diseased samples with those present in normal samples, it is possible to identify changes in expression of proteins that potentially may be related to tumor progression, invasion and metastasis, and prognosis. This technique has now made it possible to analyze proteins using high throughput, automated techniques. Proteomic profiling can be applied to tissue samples as well as body fluids (e.g. serum, urine, etc.), and it can provide surrogate markers of disease processes, potential response to treatment, possibility of recurrence and metastasis for cancers including HCC^[110].

OTHERS

In addition, higher levels of urinary TGF-beta 1^[111], heat shock protein-27 (HSP-27)^[112] and Glutamine synthetase (GS) expression

in the tumor^[113], increased levels of cyclooxygenase-2 (COX-2) in nontumor liver tissue^[114], preoperative serum IL-10^[115], and HFE mutation s^[116] or down-regulation of DRH1^[117] are also powerful prognostic indicators for shorter disease-free survival and poor prognosis, related to tumor progression of HCC.

The RECK (reversion-inducing-cysteine-rich protein with Kazal motifs) gene suppresses the invasive and metastatic activities of cancers, has negative effects on the invasiveness of HCC, and can be regarded as a promising prognostic molecular marker for HCC^[118].

EXPERIENCES OF THE AUTHORS' INSTITUTE

At the authors' institute, many molecular factors have been investigated and found to be related to HCC invasiveness in recent years. They could be divided into two groups: one is positive invasiveness-related factors, including p16 and p53 mutations, H-ras, c-erbB2, mdm2, TGF- α , epidermal growth factor receptor (EGFR), MMP-2, uPA, uPA-R and PAI-1, ICAM-1, VEGF, PD-ECGF, bFGF, and osteopontin (OPN), etc. The other group is negative invasiveness-related factors, including nm23-H1, Kai-1, TIMP-2, integrin $\alpha 5$, E-cadherin, etc. These factors could be potential predictive markers for the prognosis of HCC. Serum ICAM-1 and PAI-1 levels were higher in patients with metastasis than those without metastasis, while serum Thrombomodulin concentration negatively associated with the intrahepatic spreading and portal vein thrombosis of HCC. Deletions of chromosome 8p and 17p, overexpression of MMP-2, TGF- α , and EGFR in HCC tissues, and LOH on chromosome 14q (D14S62 and D14S51) in plasma DNA were also related to metastatic recurrence and prognosis of HCC patients. p53 mutation or nuclear accumulation of p53 expression could be a valuable marker for predicting the prognosis of HCC patients after resection. E-cadherin, nm23, TIMP-2 are promising prognostic markers^[1, 43, 46, 77, 84, 86, 91, 94-96, 104-106].

To search for metastasis-associated genes on a global genomic scale, we recently used cDNA microarrays containing approximately 9984 human transcripts to investigate the gene expression profiles of primary tumors and their corresponding metastatic lesions (intrahepatic metastasis or tumor thrombosis of portal vein). A total of 79 significantly upregulated and 69 downregulated genes were identified. Some of them have proven to promote HCC metastasis^[119]. These will provide new prognostic markers for predicting the possibility of metastatic recurrence and survival after operation.

QUESTIONS AND PROSPECTS

In summary, pathologic factors indicative of tumor invasiveness such as tumor size, number, capsule state, venous invasion, presence of satellite nodules, and advanced pTNM stage, are the best-established risk factors for recurrence and important aspects affecting the prognosis of patients with HCC. Recent molecular research has identified many tumor biological factors as potential prognostic markers (biomarkers). However, to date, none of them has been proved to be specific enough, and most of the studies for specific molecular parameters were correlative and retrospective. Methodologies, sample sizes, and definitions differ. Consideration should be given to the design of prospective clinical trials in evaluating the prognostic significance of these markers.

These biomarkers could be detected both in tissue and body fluids (serum, urine, bile, etc.). Body fluid (particularly blood and urinary) testing is easily accessible and useful in clinical patients, and is more important in "predicting" the possibility or "early diagnosis" of recurrence and metastasis. So, future work should be focused on serum or urinary markers.

The prognostic significance of circulating DNA in plasma or serum, and its genetic alterations in HCC, are important trends that deserve attention. Proteomics and cDNA array provide other ways to explore new prognostic markers. So, we can believe, with the

continuing progress of human genome project, the development of new molecular and cytogenetic techniques, and a more complete understanding of tumor biology, more and more new prognostic markers with high sensitivity and specificity will soon be found and used in clinical assays. However, the combination of some items, i.e., pathological features and some biomarkers mentioned above, seems to be more practical now.

REFERENCES

- 1 Tang ZY. Hepatocellular carcinoma-Cause, treatment and metastasis. *World J Gastroenterol* 2001;7:445-454
- 2 Qin LX, Tang ZY. The prognostic significance of clinical and pathological features in hepatocellular carcinoma. *World J Gastroenterol* 2002;8:193-199
- 3 Zhao WH, Ma ZM, Zhou XR, Feng YZ, Fang BS. Prediction of recurrence and prognosis in patients with hepatocellular carcinoma after resection by use of CLIP score. *World J Gastroenterol* 2002;8:237-242
- 4 Zheng N, Ye SL, Sun RX, Zhao Y, Tang ZY. Effects of cryopreservation and phenylacetate on biological characters of adherent LAK cells from patients with hepatocellular carcinoma. *World J Gastroenterol* 2002;8:233-236
- 5 Korn WM. Moving toward an understanding of the metastatic process in hepatocellular carcinoma. *World J Gastroenterol* 2001;7:777-778
- 6 Mise K, Tashiro S, Yogita S, Wada D, Harada M, Fukuda Y, Miyake H, Isikawa M, Izumi K, Sano N. Assessment of the biological malignancy of hepatocellular carcinoma: relationship to clinicopathological factors and prognosis. *Clin Cancer Res* 1998;4:1475-1482
- 7 Nolte M, Werner M, Nasarek A, Bektas H, von Wasielewski R, Klempnauer J, Georgii A. Expression of proliferation associated antigens and detection of numerical chromosome aberrations in primary human liver tumours: relevance to tumor characteristics and prognosis. *J Clin Pathol* 1998;51:47-51
- 8 Weber JC, Nakano H, Bachellier P, Oussoultzoglou E, Inoue K, Shimura H, Wolf P, Chenard-Neu MP, Jaeck D. Is a proliferation index of cancer cells a reliable prognostic factor after hepatectomy in patients with colorectal liver metastases? *Am J Surg* 2001;182:81-88
- 9 Lin GY, Chen ZL, Lu CM, Li Y, Ping XJ, Huang R. Immunohistochemical study on p53, H-rasp21, c-erbB-2 protein and PCNA expression in HCC tissues of Han and minority ethnic patients. *World J Gastroenterol* 2000;6:234-238
- 10 Scholzen T, Gerdes J. The Ki-67 protein: from the known and the unknown. *J Cell Physiol* 2000;182:311-322
- 11 Hernandez-Rodriguez NA, Correa E, Sotelo R, Contreras-Paredes A, Gomez-Ruiz C, Green L, Mohar A. Ki-67: a proliferative marker that may predict pulmonary metastases and mortality of primary osteosarcoma. *Cancer Detect Prev* 2001;25:210-215
- 12 Ito Y, Matsuura N, Sakon M, Takeda T, Umeshita K, Nagano H, Nakamori S, Dono K, Tsujimoto M, Nakahara M, Nakao K, Monden M. Both cell proliferation and apoptosis significantly predict shortened disease-free survival in hepatocellular carcinoma. *Br J Cancer* 1999;81:747-751
- 13 Ouchi K, Sugawara T, Ono H, Fujiya T, Kamiyama Y, Kakugawa Y, Mikuni J, Yamanami H, Komatsu S, Horikoshi A. Mitotic index is the best predictive factor for survival of patients with resected hepatocellular carcinoma. *Dig Surg* 2000;17:42-48
- 14 Wellmann A, Flemming P, Behrens P, Wuppermann K, Lang H, Oldhafer K, Pastan I, Brinkmann U. High expression of the proliferation and apoptosis associated CSE1L/CAS gene in hepatitis and liver neoplasms: correlation with tumor progression. *Int J Mol Med* 2001;7:489-494
- 15 Ikeguchi M, Sato N, Hirooka Y, Kaibara N. Computerized nuclear morphology of hepatocellular carcinoma and its relation to proliferative activity. *J Surg Oncol* 1998;68:225-230
- 16 Veltri RW, Partin AW, Miller MC. Quantitative nuclear grade

- (QNG): a new image analysis-based biomarker of clinically relevant nuclear structure alterations. *J Cell Biochem* 2000;Suppl 35:151-157
- 17 Overgaard J, Yilmaz M, Guldberg P, Hansen LL, Alsner J. TP53 mutation is an independent prognostic marker for poor outcome in both node-negative and node-positive breast cancer. *Acta Oncol* 2000;39:327-333
 - 18 Takahashi M, Tonoki H, Tada M, Kashiwazaki H, Furuuchi K, Hamada J, Fujioaka Y, Sato Y, Takahashi H, Todo S, Sakuragi N, Moriuchi T. Distinct prognostic values of p53 mutations and loss of estrogen receptor and their cumulative effect in primary breast cancers. *Int J Cancer* 2000;89:92-99
 - 19 Blaszyk H, Hartmann A, Cunningham JM, Schaid D, Wold LE, Kovach JS, Sommer SS. A prospective trial of midwest breast cancer patients: a p53 gene mutation is the most important predictor of adverse outcome. *Int J Cancer* 2000;89:32-38
 - 20 Kahlenberg MS, Stoler DL, Rodriguez-Bigas MA, Weber TK, Driscoll DL, Anderson GR, Petrelli NJ. p53 tumor suppressor gene mutations predict decreased survival of patients with sporadic colorectal carcinoma. *Cancer* 2000;88:1814-1819
 - 21 Ireland AP, Shibata DK, Chandrasoma P, Lord RV, Peters JH, DeMeester TR. Clinical significance of p53 mutations in adenocarcinoma of the esophagus and cardia. *Ann Surg* 2000;231:179-187
 - 22 Tamas L, Kraxner H, Mechtler L, Repassy G, Ribari O, Hirschberg A, Szentkuti G, Jaray B, Szentirmay Z. Prognostic significance of P53 histochemistry and DNA histogram parameters in head and neck malignancies. *Anticancer Res* 2000;20:4031-4037
 - 23 Murakami I, Hiyama K, Ishioka S, Yamakido M, Kasagi F, Yokosaki Y. p53 gene mutations are associated with shortened survival in patients with advanced non-small cell lung cancer: an analysis of medically managed patients. *Clin Cancer Res* 2000;6:526-530
 - 24 Mitsudomi T, Hamajima N, Ogawa M, Takahashi T. Prognostic significance of p53 alterations in patients with non-small cell lung cancer: a meta-analysis. *Clin Cancer Res* 2000;6:4055-4063
 - 25 Shahin MS, Hughes JH, Sood AK, Buller RE. The prognostic significance of p53 tumor suppressor gene alterations in ovarian carcinoma. *Cancer* 2000;89:2006-2017
 - 26 de Alava E, Antonescu CR, Panizo A, Leung D, Meyers PA, Huvos AG, Pardo-Mindan FJ, Healey JH, Ladanyi M. Prognostic impact of P53 status in Ewing sarcoma. *Cancer* 2000;89:783-792
 - 27 Leibovich BC, Cheng L, Weaver AL, Myers RP, Bostwick DG. Outcome prediction with p53 immunostaining after radical prostatectomy in patients with locally advanced prostate cancer. *J Urol* 2000;163:1756-1760
 - 28 Osaki T, Kimura T, Tatamoto Y, Dapeng L, Yoneda K, Yamamoto T. Diffuse mode of tumor cell invasion and expression of mutant p53 protein but not of p21 protein are correlated with treatment failure in oral carcinomas and their metastatic foci. *Oncology* 2000;59:36-43
 - 29 Suzuki M, Ohwada M, Saga Y, Kohno T, Takei Y, Sato I. Micrometastatic p53-positive cells in the lymph nodes of early stage epithelial ovarian cancer: prognostic significance. *Oncology* 2001;60:170-175
 - 30 Shiota G, Ishida M, Noguchi N, Oyama K, Takano Y, Okubo M, Katayama S, Tomie Y, Harada K, Hori K, Ashida K, Kishimoto Y, Hosoda A, Suou T, Kanbe T, Tanaka K, Nosaka K, Tanida O, Kojo H, Miura K, Ito H, Kaibara N, Kawasaki H. Circulating p53 antibody in patients with colorectal cancer: relation to clinicopathologic features and survival. *Dig Dis Sci* 2000;45:122-128
 - 31 Shao ZM, Wu J, Shen ZZ, Nguyen M. p53 mutation in plasma DNA and its prognostic value in breast cancer patients. *Clin Cancer Res* 2001;7:2222-2227
 - 32 Kantola S, Parikka M, Jokinen K, Hyrynkangas K, Soini Y, Alho OP, Salo T. Prognostic factors in tongue cancer - relative importance of demographic, clinical and histopathological factors. *Br J Cancer* 2000;83:614-619
 - 33 Ferrero JM, Ramaoli A, Formento JL, Francoual M, Etienne MC, Peyrotte S, Ettore F, Leblanc-Talent P, Namer M, Milano G. P53 determination alongside classical prognostic factors in node-negative breast cancer: an evaluation at more than 10-year follow-up. *Ann Oncol* 2000;11:393-397
 - 34 Reed W, Hannisdal E, Boehler PJ, Gundersen S, Host H, Marthin J. The prognostic value of p53 and c-erb B-2 immunostaining is overrated for patients with lymph node negative breast carcinoma: a multivariate analysis of prognostic factors in 613 patients with a follow-up of 14-30 years. *Cancer* 2000;88:804-813
 - 35 Kaye PV, Radebold K, Isaacs S, Dent DM. Expression of p53 and p21waf1/cip1 in gastric carcinoma: lack of inter-relationship or correlation with prognosis. *Eur J Surg Oncol* 2000;26:39-43
 - 36 Schiller JH, Adak S, Feins RH, Keller SM, Fry WA, Livingston RB, Hammond ME, Wolf B, Sabatini L, Jett J, Kohman L, Johnson DH. Lack of prognostic significance of p53 and K-ras mutations in primary resected non-small-cell lung cancer on E4592: a Laboratory Ancillary Study on an Eastern Cooperative Oncology Group Prospective Randomized Trial of Postoperative Adjuvant Therapy. *J Clin Oncol* 2001;19:448-457
 - 37 Gadducci A, Cianci C, Cosio S, Carnino F, Fanucchi A, Buttitta F, Conte PF, Genazzani AR. p53 status is neither a predictive nor a prognostic variable in patients with advanced ovarian cancer treated with a paclitaxel-based regimen. *Anticancer Res* 2000;20:4793-4799
 - 38 Fleshner N, Kapusta L, Ezer D, Herschorn S, Klotz L. p53 nuclear accumulation is not associated with decreased disease-free survival in patients with node positive transitional cell carcinoma of the bladder. *J Urol* 2000;164:1177-1182
 - 39 Gallego MG, Acenero MJ, Ortega S, Delgado AA, Cantero JL. Prognostic influence of p53 nuclear overexpression in colorectal carcinoma. *Colon Rectum* 2000;43:971-975
 - 40 Nieder C, Petersen S, Petersen C, Thames HD. The challenge of p53 as a prognostic and predictive factor in Hodgkin's or non-Hodgkin's lymphoma. *Ann Hematol* 2001;80:2-8
 - 41 Itoh T, Shiro T, Seki T, Nakagawa T, Wakabayashi M, Inoue K, Okamura A. Relationship between p53 overexpression and the proliferative activity in hepatocellular carcinoma. *Int J Mol Med* 2000;6:137-142
 - 42 Jeng KS, Sheen IS, Chen BF, Wu JY. Is the p53 gene mutation of prognostic value in hepatocellular carcinoma after resection? *Arch Surg* 2000;135:1329-1333
 - 43 Tang ZY, Qin LX, Wang XM, Zhou G, Liao Y, Weng Y, Jiang XP, Lin ZY, Liu KD, Ye SL. Alterations of oncogenes, tumor suppressor genes and growth factors in hepatocellular carcinoma: with relation to tumor size and invasiveness. *Chin Med J* 1998;111:313-318
 - 44 Sugo H, Takamori S, Kojima K, Beppu T, Futagawa S. The significance of p53 mutations as an indicator of the biological behavior of recurrent hepatocellular carcinomas. *Surg Today* 1999;29:849-855
 - 45 Heinze T, Jonas S, Karsten A, Neuhaus P. Determination of the oncogenes p53 and C-erb B2 in the tumour cytosols of advanced hepatocellular carcinoma (HCC) and correlation to survival time. *Anticancer Res* 1999;19:2501-2503
 - 46 Qin LX, Tang ZY, Ma ZC, Wu ZQ, Zhou XD, Ye QH, Ji Y, Huang LW, Jia HL, Sun HC, Wang L. P53 immunohistochemistry scoring is an independent prognostic marker of patient with hepatocellular carcinoma resection: A prospective study of 256 formalin-fixed paraffin-embedded tumor samples. *World J Gastroenterol* 2002(in press)
 - 47 Shiota G, Kishimoto Y, Suyama A, Okubo M, Katayama S, Harada K, Ishida M, Hori K, Suou T, Kawasaki H. Prognostic significance of serum anti-p53 antibody in patients with hepatocellular carcinoma. *J Hepatol* 1997;27:661-668
 - 48 Tangkijvanich P, Janchai A, Charuruks N, Kullavanijaya P, Theamboonlers A, Hirsch P, Poovorawan Y. Clinical associations and prognostic significance of serum anti-p53 antibodies in Thai patients with hepatocellular carcinoma. *Asian Pac J Allergy Immunol* 2000;18:237-243
 - 49 Saffroy R, Lelong JC, Azoulay D, Salvucci M, Reynes M, Bismuth H, Debuire B, Lemoine A. Clinical significance of circulating anti-p53 antibodies in European patients with

- hepatocellular carcinoma. *Br J Cancer* 1999;79:604-610
- 50 Endo K, Ueda T, Ohta T, Terada T. Protein expression of MDM2 and its clinicopathological relationships in human hepatocellular carcinoma. *Liver* 2000;20:209-215
 - 51 Chao Y, Shih YL, Chiu JH, Chau GY, Lui WY, Yang WK, Lee SD, Huang TS. Overexpression of cyclin A but not Skp 2 correlates with the tumor relapse of human hepatocellular carcinoma. *Cancer Res* 1998;58:985-990
 - 52 Ohashi R, Gao C, Miyazaki M, Hamazaki K, Tsuji T, Inoue Y, Uemura T, Hirai R, Shimizu N, Namba M. Enhanced expression of cyclin E and cyclin A in human hepatocellular carcinomas. *Anticancer Res* 2001;21:657-662
 - 53 Ito Y, Takeda T, Sakon M, Monden M, Tsujimoto M, Matsuura N. Expression and prognostic role of cyclin-dependent kinase 1 (cdc2) in hepatocellular carcinoma. *Oncology* 2000;59:68-74
 - 54 Philipp-Staheli J, Payne SR, Kemp CJ. p27(Kip1): regulation and function of a haploinsufficient tumor suppressor and its misregulation in cancer. *Exp Cell Res* 2001;264:148-168
 - 55 Fiorentino M, Altamirani A, D'Errico A, Cukor B, Barozzi C, Loda M, Grigioni WF. Acquired expression of p27 is a favorable prognostic indicator in patients with hepatocellular carcinoma. *Clin Cancer Res* 2000;6:3966-3972
 - 56 Ito Y, Matsuura N, Sakon M, Miyoshi E, Noda K, Takeda T, Umeshita K, Nagano H, Nakamori S, Dono K, Tsujimoto M, Nakahara M, Nakao K, Taniguchi N, Monden M. Expression and prognostic roles of the G1-S modulators in hepatocellular carcinoma: p27 independently predicts the recurrence. *Hepatology* 1999;30:90-99
 - 57 Tannapfel A, Wasner M, Krause K, Geissler F, Katalinic A, Hauss J, Mossner J, Engeland K, Wittekind C. Expression of p73 and its relation to histopathology and prognosis in hepatocellular carcinoma. *J Natl Cancer Inst* 1999;91:1154-1158
 - 58 Qin Y, Li B, Tan YS, Sun ZL, Zuo FQ, Sun ZF. Polymorphism of p16INK4a gene and rare mutation of p15INK4b gene exon2 in primary hepatocarcinoma. *World J Gastroenterol* 2000;6:411-414
 - 59 Wang Q, Lin ZY, Feng XL. Alterations in metastatic properties of hepatocellular carcinoma cell following H-ras oncogene transfection. *World J Gastroenterol* 2001;7:335-339
 - 60 Cui J, Yang DH, Bi XJ, Fan ZR. Methylation status of c-fms oncogene in HCC and its relationship with clinical pathology. *World J Gastroenterol* 2001;7:136-139
 - 61 Kawate S, Fukusato T, Ohwada S, Watanuki A, Morishita Y. Amplification of c-myc in hepatocellular carcinoma: correlation with clinicopathologic features, proliferative activity and p53 overexpression. *Oncology* 1999;57:157-163
 - 62 Taviani D, De Petro G, Benetti A, Portolani N, Giulini SM, Barlati S. u-PA and c-MET mRNA expression is coordinately enhanced while hepatocyte growth factor mRNA is down-regulated in human hepatocellular carcinoma. *Int J Cancer* 2000;87:644-649
 - 63 Luo YQ, Wu MC, Cong WM. Gene expression of hepatocyte growth factor and its receptor in HCC and nontumorous liver tissues. *World J Gastroenterol* 1999;5:119-121
 - 64 Prange W, Schirmacher P. Absence of therapeutically relevant c-erbB-2 expression in human hepatocellular carcinomas. *Oncol Rep* 2001;8:727-730
 - 65 Ito Y, Takeda T, Sakon M, Tsujimoto M, Higashiyama S, Noda K, Miyoshi E, Monden M, Matsuura N. Expression and clinical significance of erb-B receptor family in hepatocellular carcinoma. *Br J Cancer* 2001;84:1377-1383
 - 66 Ito Y, Miyoshi E, Takeda T, Sakon M, Noda K, Tsujimoto M, Monden M, Taniguchi N, Matsuura N. Expression and possible role of ets-1 in hepatocellular carcinoma. *Am J Clin Pathol* 2000;114:719-725
 - 67 Ito Y, Monden M, Takeda T, Eguchi H, Umeshita K, Nagano H, Nakamori S, Dono K, Sakon M, Nakamura M, Tsujimoto M, Nakahara M, Nakao K, Yokosaki Y, Matsuura N. The status of Fas and Fas ligand expression can predict recurrence of hepatocellular carcinoma. *Br J Cancer* 2000;82:1211-1217
 - 68 Wang XZ, Chen XC, Yang YH, Chen ZX, Huang YH, Tao QM. Relationship between HBxAg and Fas/FasL in patients with hepatocellular carcinoma. *World J Gastroenterol* 2000;6:S17
 - 69 Kobayashi T, Kubota K, Takayama T, Makuuchi M. Telomerase activity as a predictive marker for recurrence of hepatocellular carcinoma after hepatectomy. *Am J Surg* 2001;181:284-288
 - 70 Tatsuma T, Goto S, Kitano S, Lin YC, Lee CM, Chen CL. Telomerase activity in peripheral blood for diagnosis of hepatoma. *J Gastroenterol Hepatol* 2000;15:1064-1070
 - 71 Suda T, Isokawa O, Aoyagi Y, Nomoto M, Tsukada K, Shimizu T, Suzuki Y, Naito A, Igarashi H, Yanagi M, Takahashi T, Asakura H. Quantitation of telomerase activity in hepatocellular carcinoma: a possible aid for a prediction of recurrent diseases in the remnant liver. *Hepatology* 1998;27:402-406
 - 72 Huang GT, Lee HS, Chen CH, Sheu JC, Chiou LL, Chen DS. Correlation of E-cadherin expression and recurrence of hepatocellular carcinoma. *Hepatogastroenterology* 1999;46:1923-1927
 - 73 Endo K, Ueda T, Ueyama J, Ohta T, Terada T. Immunoreactive E-cadherin, alpha-catenin, beta-catenin, and gamma-catenin proteins in hepatocellular carcinoma: relationships with tumor grade, clinicopathologic parameters, and patients' survival. *Hum Pathol* 2000;31:558-565
 - 74 Wong CM, Fan ST, Ng IO. beta-Catenin mutation and overexpression in hepatocellular carcinoma: clinicopathologic and prognostic significance. *Cancer* 2001;92:136-145
 - 75 Cui J, Zhou XD, Liu YK, Tang ZY, Zile MH. Abnormal Catenin gene expression with invasiveness of primary hepatocellular carcinoma in China. *World J Gastroenterol* 2001;7:542-546
 - 76 Hsu HC, Jeng YM, Mao TL, Chu JS, Lai PL, Peng SY. Beta-catenin mutations are associated with a subset of low-stage hepatocellular carcinoma negative for hepatitis B virus and with favorable prognosis. *Am J Pathol* 2000;157:763-770
 - 77 Sun JJ, Zhou XD, Liu YK, Tang ZY, Feng JX, Zhou G, Xue Q, Chen J. Invasion and metastasis of liver cancer: expression of intercellular adhesion molecule-1. *J Cancer Res Clin Oncol* 1999;125:28-34
 - 78 Mei MH, Xu J, Shi QF, Yang JH, Chen Q, Qin LL. Clinical significance of serum intercellular adhesion molecule-1 detection in patients with hepatocellular carcinoma. *World J Gastroenterol* 2000;6:408-410
 - 79 Xu J, Mei MH, Zeng SE, Shi QF, Liu YM, Qin LL. Expressions of ICAMa21 and its mRNA in sera and tissues of patients with hepatocellular carcinoma. *World J Gastroenterol* 2001;7:120-125
 - 80 Goodison S, Urquidí V, Tarin D. CD44 cell adhesion molecules. *Mol Pathol* 1999;52:189-196
 - 81 Endo K, Terada T. Protein expression of CD44 (standard and variant isoforms) in hepatocellular carcinoma: relationships with tumor grade, clinicopathologic parameters, p53 expression, and patient survival. *J Hepatol* 2000;32:78-84
 - 82 Sakamoto Y, Mafune K, Mori M, Shiraishi T, Imamura H, Mori M, Takayama T, Makuuchi M. Overexpression of MMP-9 correlates with growth of small hepatocellular carcinoma. *Int J Oncol* 2000;17:237-243
 - 83 Jiang YF, Yang ZH, Hu JQ. Recurrence or metastasis of HCC: predictors, early detection and experimental antiangiogenic therapy. *World J Gastroenterol* 2000;6:61-65
 - 84 Bu W, Tang ZY, Ye SL, Liu KD, Huang XW, Gao DM. The association of type IV collagenase with invasion and metastasis of hepatocellular carcinoma. *Zhonghua Xiaohua Zazhi* 1999;19:13-15
 - 85 Fox SB, Taylor M, Grondahl-Hansen J, Kakolyris S, Gatter KC, Harris AL. Plasminogen activator inhibitor-1 as a measure of vascular remodeling in breast cancer. *J Pathol* 2001;195:236-243
 - 86 Zheng Q, Tang ZY, Xue Q, Shi DR, Song HY, Tang HB. Invasion and metastasis of hepatocellular carcinoma in relation to urokinase-type plasminogen activator, its receptor and inhibitor. *J Cancer Res Clin Oncol* 2000;126:641-646
 - 87 Itoh T, Hayashi Y, Kanamaru T, Morita Y, Suzuki S, Wang W,

- Zhou L, Rui JA, Yamamoto M, Kuroda Y, Itoh H. Clinical significance of urokinase-type plasminogen activator activity in hepatocellular carcinoma. *J Gastroenterol Hepatol* 2000;15: 422-430
- 88 Kuroi K, Toi M. Circulating angiogenesis regulators in cancer patients. *Int J Biol Markers* 2001;16:5-26
- 89 Morinaga S, Imada T, Shimizu A, Akaike M, Sugimasa Y, Takemiya S, Takanashi Y. Angiogenesis in hepatocellular carcinoma as evaluated by alpha smooth muscle actin immunohistochemistry. *Hepatogastroenterology* 2001;48:224-228
- 90 El-Assal ON, Yamanoi A, Soda Y, Yamaguchi M, Igarashi M, Yamamoto A, Nabika T, Nagasue N. Clinical significance of microvessel density and vascular endothelial growth factor expression in hepatocellular carcinoma and surrounding liver: possible involvement of vascular endothelial growth factor in the angiogenesis of cirrhotic liver. *Hepatology* 1998;27:1554-1562
- 91 Sun HC, Tang ZY, Li XM, Zhou YN, Sun BR, Ma ZC. Microvessel density of hepatocellular carcinoma: its relationship with prognosis. *J Cancer Res Clin Oncol* 1999;125:419-26
- 92 Poon RT, Fan ST, Wong J. Clinical implications of circulating angiogenic factors in cancer patients. *J Clin Oncol* 2001;19: 1207-1225
- 93 Poon RT, Ng IO, Lau C, Zhu LX, Yu WC, Lo CM, Fan ST, Wong J. Serum vascular endothelial growth factor predicts venous invasion in hepatocellular carcinoma: a prospective study. *Ann Surg* 2001;233:227-235
- 94 Li XM, Tang ZY, Qin LX, Zhou J, Sun HC. Serum vascular endothelial growth factor is a predictor of invasion and metastasis in hepatocellular carcinoma. *J Exp Clin Cancer Res* 1999;18:511-517
- 95 Niu Q, Tang ZY, Ma ZC, Qin LX, Zhang LH. Serum vascular endothelial growth factor is a potential biomarker of metastatic recurrence after curative resection of hepatocellular carcinoma. *World J Gastroenterol* 2000;6: 565-568
- 96 Zhou J, Tang ZY, Fan J, Wu ZQ, Li XM, Liu YK, Liu F, Sun HC, Ye SL. Expression of platelet-derived endothelial cell growth factor and vascular endothelial growth factor in hepatocellular carcinoma and portal vein tumor thrombus. *J Cancer Res Clin Oncol* 2000; 126:57-61
- 97 Tada K, Shiraishi S, Kamiyori T, Nakamura H, Hirano H, Kuratsu J, Kochi M, Saya H, Ushio Y. Analysis of loss of heterozygosity on chromosome 10 in patients with malignant astrocytic tumors: correlation with patient age and survival. *J Neurosurg* 2001;95:651-659
- 98 Bisgaard ML, Jager AC, Dalgaard P, Sondergaard JO, Rehfeld JF, Nielsen FC. Allelic loss of chromosome 2p21-16.3 is associated with reduced survival in sporadic colorectal cancer. *Scand J Gastroenterol* 2001;36:405-409
- 99 Hirano A, Emi M, Tsuneizumi M, Utada Y, Yoshimoto M, Kasumi F, Akiyama F, Sakamoto G, Haga S, Kajiwaru T, Nakamura Y. Allelic losses of loci at 3p25.1, 8p22, 13q12, 17p13.3, and 22q13 correlate with postoperative recurrence in breast cancer. *Clin Cancer Res* 2001;7:876-882
- 100 Simoneau M, LaRue H, Aboukassim TO, Meyer F, Moore L, Fradet Y. Chromosome 9 deletions and recurrence of superficial bladder cancer: identification of four regions of prognostic interest. *Oncogene* 2000;19:6317-6323
- 101 Washburn JG, Wojno KJ, Dey J, Powell JJ, Macoska JA. 8pter-p23 deletion is associated with racial differences in prostate cancer outcome. *Clin Cancer Res* 2000;6:4647-4652
- 102 Wong N, Lai P, Lee SW, Fan S, Pang E, Liew CT, Sheng Z, Lau JW, Johnson PJ. Assessment of genetic changes in hepatocellular carcinoma by comparative genomic hybridization analysis: relationship to disease stage, tumor size, and cirrhosis. *Am J Pathol* 1999;154: 37-43
- 103 Itano O, Ueda M, Kikuchi K, Shimazu M, Kitagawa Y, Aiura K, Kitajima M. A new predictive factor for hepatocellular carcinoma based on two-dimensional electrophoresis of genomic DNA. *Oncogene* 2000;19:1676-1683
- 104 Qin LX, Tang ZY, Sham JST, Ma ZC, Ye SL, Zhou XD. The association of chromosome 8p deletion and tumor metastasis in human hepatocellular carcinoma. *Cancer Res* 1999;59:5662-5665
- 105 Qin LX, Tang ZY, Ye SL, Liu YK, Ma ZC, Zhou XD, Wu ZQ, Lin ZY, Sun FX, Tian J, Guan XY, Pack SD, Zhuang ZP. Chromosome 8p deletion is associated with metastasis of human hepatocellular carcinoma when high and low metastatic models are compared. *J Cancer Res Clin Oncol* 2001;127:482-488
- 106 Zhang LH, Qin LX, Ma ZC, Ye SL, Liu YK, Ye QH, Wu X, Huang W, Tang ZY. Identification of allelic imbalances regions related to metastasis of hepatocellular carcinoma: Comparison between matched primary and metastatic lesions in 22 patients by genome-wide microsatellite Analysis. *Int J Cancer* 2002 (submitted)
- 107 Anker P, Stroun M. Circulating DNA in plasma or serum. *Medicina (B Aires)* 2000;60:699-702
- 108 Taback B, Fujiwara Y, Wang HJ, Foshag LJ, Morton DL, Hoon DS. Prognostic significance of circulating microsatellite markers in the plasma of melanoma patients. *Cancer Res* 2001;61: 5723-5726
- 109 Nunes DN, Kowalski LP, Simpson AJ. Circulating tumor-derived DNA may permit the early diagnosis of head and neck squamous cell carcinomas. *Int J Cancer* 2001;92:214-219
- 110 Kennedy S. Proteomic profiling from human samples: the body fluid alternative. *Toxicol Lett* 2001;120:379-384
- 111 Tsai JF, Chuang LY, Jeng JE, Yang ML, Chang WY, Hsieh MY, Lin ZY, Tsai JH. Clinical relevance of transforming growth factor-beta 1 in the urine of patients with hepatocellular carcinoma. *Medicine (Baltimore)* 1997;76:213-226
- 112 King KL, Li AF, Chau GY, Chi CW, Wu CW, Huang CL, Lui WY. Prognostic significance of heat shock protein-27 expression in hepatocellular carcinoma and its relation to histologic grading and survival. *Cancer* 2000;88:2464-2470
- 113 Osada T, Nagashima I, Tsuno NH, Kitayama J, Nagawa H. Prognostic significance of glutamine synthetase expression in unifocal advanced hepatocellular carcinoma. *J Hepatol* 2000; 33:247-253
- 114 Kondo M, Yamamoto H, Nagano H, Okami J, Ito Y, Shimizu J, Eguchi H, Miyamoto A, Dono K, Umeshita K, Matsuura N, Wakasa K, Nakamori S, Sakon M, Monden M. Increased expression of COX-2 in nontumor liver tissue is associated with shorter disease-free survival in patients with hepatocellular carcinoma. *Clin Cancer Res* 1999;5:4005-4012
- 115 Chau GY, Wu CW, Lui WY, Chang TJ, Kao HL, Wu LH, King KL, Loong CC, Hsia CY, Chi CW. Serum interleukin-10 but not interleukin-6 is related to clinical outcome in patients with resectable hepatocellular carcinoma. *Ann Surg* 2000;231:552-558
- 116 Pirisi M, Toniutto P, Uzzau A, Fabris C, Avellini C, Scott C, Apollonio L, Beltrami CA, Bresadola F. Carriage of HFE mutations and outcome of surgical resection for hepatocellular carcinoma in cirrhotic patients. *Cancer* 2000; 89:297-302
- 117 Yamamoto Y, Sakamoto M, Fujii G, Kanetaka K, Asaka M, Hirohashi S. Cloning and characterization of a novel gene, DRH1, down-regulated in advanced human hepatocellular carcinoma. *Clin Cancer Res* 2001;7:297-303
- 118 Furumoto K, Arii S, Mori A, Furuyama H, Gorris Rivas MJ, Nakao T, Isono N, Murata T, Takahashi C, Noda M, Imamura M. RECK gene expression in hepatocellular carcinoma: correlation with invasion-related clinicopathological factors and its clinical significance. Reverse-inducing-cysteine-rich protein with Kazal motifs. *Hepatology* 2001;33:189-195
- 119 Ye QH, Qin LX, Forgues M, He P, Kim JW, Peng AC, Simon R, Robles A, Chen YD, Ma ZC, Wu ZQ, Ye SL, Liu YK, Tang ZY, Wang XW. Gene expression profiling and supervised machine learning to define metastasis-related genes in human hepatocellular carcinoma. *Nature Med* 2002 (submitted)

Edited by Pagliarini R

Radiofrequency ablation of liver cancers

Lian-Xin Liu, Hong-Chi Jiang, Da-Xun Piao

Lian-Xin Liu, Hong-Chi Jiang, Da-Xun Piao, Department of Surgery, the First Clinical College, Harbin Medical University, Harbin 150001, Heilongjiang Province, China

Supported by Youth Natural Scientific Foundation of Heilongjiang Province; Natural Scientific Foundation of Harbin

Correspondence to: Dr. Lian-Xin Liu, Department of Surgery, the First Clinical College, Harbin Medical University, 23 Youzheng Street, Nangang District, Harbin 150001, Heilongjiang Province, China. scott-lxliu@hotmail.com

Received 2002-05-10 Accepted 2002-05-18

Abstract

Primary and secondary malignant liver cancers are some of most common malignant tumors in the world. Chemotherapy and radiotherapy are not very effective against them. Surgical resection has been considered the only potentially curative option, but the majority of patients are not candidates for resection because of tumor size, location near major intrahepatic blood vessels and bile ducts, precluding a margin-negative resection, cirrhotic, hepatitis virus infection or multifocal. Radiofrequency ablation (RFA), which is a new evolving effective and minimally invasive technique, can produce coagulative necrosis of malignant tumors. RFA should be used percutaneously, laparoscopically, or during the open laparotomy under the guidance of ultrasound, CT scan and MRI. RFA has lots of advantages superior to other local therapies including lower complications, reduced costs and hospital stays, and the possibility of repeated treatment. In general, RFA is a safe, effective treatment for unresectable malignant liver tumors less than 7.0 cm in diameter. We review the principle, mechanism, procedures and experience with RFA for treating malignant liver tumors.

Liu LX, Jiang HC, Piao DX. Radiofrequency ablation of liver cancers. *World J Gastroenterol* 2002;8(3):393-399

INTRODUCTION

Hepatocellular carcinoma (HCC) is one of the most common solid cancers in the world, with an annual incidence estimated to be at least one million new patients^[1]. The mortality was secondary to lung cancer in urban and gastric carcinoma in countryside in China^[2,3]. Furthermore, the liver is second only to lymph nodes as a common site of metastasis from other solid cancers, especially abdominal cancer^[4]. It is not uncommon, particularly in patients with colorectal adenocarcinoma, for the liver to be the only site of metastatic disease^[5]. Patients with liver metastases from colorectal carcinoma or other cancers seldom survive more than 1 year if untreated^[6,7]. Surgical resection of HCC, hepatic metastases of colorectal cancer, and patients with liver-only metastases from other types of primary tumors can result in significant long-term survival benefit in at least 20-40% of patients^[8-12]. Besides these, surgical palliation through tumor cytoreduction in patients with symptomatic neuroendocrine tumor (carcinoid, functioning islet cell) with liver metastases can ameliorate the symptoms related to excess hormone production and release.

Surgical resection has been considered the only potential curative option, but only 5-20% of newly diagnosed HCC or colorectal cancer

liver metastasis patients undergo a potentially curative resection^[13,14]. Patients with disease confined to the liver may not be candidates for resection because of multifocal disease, proximity of tumor to key vascular or biliary structures that precludes a margin-negative resection, potentially unfavorable biology with the presence of multiple liver metastases, or inadequate functional hepatic reserve related to coexistent cirrhosis. Thus, for so few patients with primary or metastatic hepatic malignancies confined to the liver who are not candidates for surgical resection, Surgeons and oncologists have turned to explore novel treatment approaches to control and potentially cure the liver disease. Systemic chemotherapy for HCC and liver metastases results in less than 25% of patients; Complete responses are rare and significant improvements in survival are not sure. Although hepatic artery infusion of chemotherapeutic agents for unresectable disease has led to 40% to 55% response rates in the liver, a survival advantage has been difficult to demonstrate^[15-18].

Localized treatment was used to HCC and colorectal cancer liver metastasis and based on the principle that decreasing the volume of viable tumor or preventing new growth can lead to longer survival and potential cure in selected patients, provided that diffuse micrometastatic disease is not present. These ablative techniques include percutaneous ethanol injection^[19-21], focused ultrasound^[22-24], cryoablation^[25-28], hyperthermia (ie, microwave tumor coagulation^[29-31]), laser photocoagulation^[32-34], and radiofrequency ablation^[35-37] (RFA). Thermal energy produces destruction of tumor cells. When tumor cells are heated above 45-50°C, intracellular proteins are denatured and cell membranes are destroyed through dissolution and melting of lipid bilayers^[38-40]. RFA is a newly developed localized thermal treatment technique which was very useful in HCC and liver metastasis.

THE BACKGROUND AND MECHANISM OF RFA

The early usage of heat to treat tumors was back to early Egyptian and Greek when they used heat to cauterize ulcer and superficial neoplasm. The first experiment in RF ablation of living tissues is credited to d'Arsonval, who demonstrated that an alternating electric current greater than 10kHz could pass through living tissue without causing neuromuscular excitation. Beer and Clark used RF coagulation in human cancers in early 20th century^[41]. Coley suggested that tumors were more sensitive to the effects of hyperthermia than normal cells and that tumors could not dissipate heat by augmenting blood flow as could adjacent normal tissues. RF techniques have gained acceptance as standard method for making well-controlled thermal lesions in the fields of neurology and cardiology since then^[42-44]. It has been used in a variety of neurosurgical procedures aimed at ablating foci of spontaneous neuronal activity, in endoscopic techniques employed in gastroenterology, and in the ablation of aberrant conduction pathways in the heart for the treatment of dysrhythmias. Until the early 1990s, it is the technological modification of RF machine has made it to be used in focal thermal injuries deeper inside the body. More recently, Rossi and McGahan separately pioneered the application of RFA to primary and metastatic lesions in the liver^[45,46].

The so-called RF thermal ablation works by converting RF waves into heat. A high-frequency alternating current (100 to 500kHz), mostly 460kHz, passes from an uninsulated electrode tip into the

surrounding tissues and causes ionic vibration as the ions attempt to follow the change in the direction of the rapidly alternating current. This ionic vibration causes frictional heating of the tissues surrounding the electrode, rather than the heat being generated from the probe itself. The goal of RFA is to achieve local temperatures such that tissue destruction occurs. In general, thermal damage to cells begins at 42°C, with exposure times required for cell death at this temperature ranging from 3 to 50 hours depending on the nature of the tissue. As the temperature is increased, there is an exponential decrease in the exposure time needed for cellular destruction. At temperatures above 60°C, intracellular proteins including collagen denature, the lipid bilayer melts and cell death becomes inevitable. Thermal coagulation begins at 70°C and tissue desiccation at 100°C, producing coagulation necrosis of tumor tissue and surrounding hepatic parenchyma^[46-50]. Tissue heating also drives extracellular and intracellular water out of the tissue and results in further destruction of the tissue due to coagulative necrosis. Besides these, different studies have shown that hyperthermia can cause accelerated emigration and migration of peripheral blood mononuclear cells, activation of effect or cells, induction and secretion of cytokines, expression of heat shock proteins, and increased induction of apoptosis^[51,52].

RFA EQUIPMENT

Three primary RF devices, which worked on the same principles, are available in the world. The differences among the devices are the variations in probes and generator designs.

The device made by RITA Medical Systems consists of a 50W alternating electric current generator and a 15-gauge needle electrode. The needle electrode has a movable hub and 8 retracting curved electrodes from the tip of the needle. Each tip of the needle contains a thermocouple that can register the temperature of the heated tissues.

The device made by Radionics consists of a straight-tip internally cooled needle electrode. The tip of the needle is cooled by perfusing its inner chamber with chilled saline which can prevent scorching of the adjacent tissues and to increase the size of the thermal injury. The device can be operated with not only a single electrode but also with 3 electrodes which are placed in a triangular configuration. The device made by Radiotherapeutic is similar to the RITA device, consists of a needle with a movable hub that can deploy 10 curved needle tips. The multiple prongs are reported to produce a more uniform spherical injury than the devices with fewer prongs. But, this device does not have the temperature surveillance in the tips of the needles.

RFA PROBE

The first RFA probes were single, monopolar needles in the world. Because the RF energy delivered via the monopolar electrode decreases in proportion to the square of the distance from the electrode, coagulative necrosis was restricted to a maximum diameter of 1.6cm in which temperatures reached 80°C. Besides this, the surface temperature of the proximal and distal ends of the probe was higher than that in other parts. Thus, using a monopolar electrode results in an ellipsoid, rather than spherical, zone of necrosis, making evaluation difficult since most tumors are spherical in shape. High temperatures at the surface of the electrode cause a further limitation in size. Once the adjacent tissue reaches a high temperature and desiccates, the resulting tissue coagulum markedly reduces the propagation of RF current and heat through the tissue, yielding a smaller zone of coagulative necrosis^[52].

One method to increase the zone of ablation is to use standard 0.9% saline or hypertonic 5% saline through the needle electrode during RFA. The infused saline solution acts as a liquid electrode to increase the area of RF current conduction around the needle tip^[53]. Miao used 5% saline infusion into swine liver before and during

RFA. Both the electrode tip temperature and tissue impedance decreased and coagulation diameter increased from less than 1.0cm to greater than 5.0cm^[54].

Another technique to improve the volume of ablation involves the use of chilled perfusate into the lumen of electrodes. Lorentzen infused cool (room temperature) water into a specially designed electrode and noted a significant increase in delivered energy and ablation size in the *ex vivo* calf liver^[55]. Goldberg noted that both energy deposition and coagulation necrosis were significantly greater with electrode cooling. This was also the case with *ex vivo* and *in vivo* muscle models. Studies in animals have also suggested that the combination of internally cooled electrodes and interstitial hypertonic saline infusion may result in a larger area of ablation than either technique alone^[51,56].

We can also use a second electrode within a few centimeters of the active electrode to increase the diameter of necrosis. In *ex vivo* experiments, this bipolar arrangement demonstrated that heat was generated not only at the active electrode, but also adjacent to the ground electrode and between the two electrodes. The resulting focus (5cm) was therefore larger than that produced by traditional single monopolar probes. The necrosis area produced by bipolar electrodes is still elliptical rather than spheroid, however, again making evaluation of its effectiveness difficult^[45,57].

Multiple active single probes can be clustered in an attempt to increase the coagulation volume as well. Goldberg *et al*^[60] investigated the effects of RFA via three electrodes placed 0.5cm apart from each other. This resulted in significant increases in the diameter of coagulation necrosis (2.9 to 7.0cm and 1.8 to 3.1cm, respectively) versus standard monopolar techniques. The use of clustered electrodes requires multiple passes and positioning and it is often laborious and difficult to ensure proper configuration. Although at times still used, this method has largely been supplanted by the development of multiprobe array electrodes^[58].

The most promising and currently the most widely used technique for RFA is the multiprobe array system. This system can be placed into the target tissue with the array retracted. Using ultrasound guidance, the array is then deployed and checked for proper positioning of all needles. These deployed multiple array needles create a series of electrodes with an overall diameter ranging up to 3.5 to 7 cm across which RFA current can be passed. Using this multiprobe needle with a standard RFA protocol, a 4-6cm tumor can be completely ablated with the array fully deployed. In general, for lesions less than 2.5cm in diameter, the needle electrode is placed parallel to the plane of the ultrasound probe. For larger tumors, either a larger multiprobe array or multiple deployments of the needle electrode are required. The treatment is planned such that the zones of necrosis overlap, keeping in mind that the entire volume of the tumor plus a margin of uninvolved tissue needs to be ablated.

RFA TECHNIQUES AND PROCEDURES

RFA of liver tumors can be performed percutaneously, using laparoscopic guidance, or as part of an open surgical procedure. The choice of treatment approach is individualized in any given patient. RFA is performed primarily by the liver surgeon and radiologist. The percutaneous approach differs from the laparoscopic and open surgical techniques only by the degree of hepatic exposure.

Patients with one to three small (<3.0cm diameter) cancers located in the periphery of the liver are considered for ultrasound-guided or CT-guided percutaneous RFA. Lesions located high in the dome of the liver near the diaphragm are not always accessible by a percutaneous approach. Furthermore, local anesthesia or monitored sedation is required for most patients treated percutaneously because of pain associated with the heating of tissue near the liver capsule. Patients treated percutaneously are usually discharged within 24h of

their RFA. Sonography is used to localize the lesion to be treated. A percutaneous approach has been used in patients with small, early-stage hepatocellular cancers with coexistent cirrhosis, and in patients with a limited number of small metastases from other organ sites^[59,60].

A laparoscopic approach offers the advantages of laparoscopic ultrasonography, which provides better resolution of the number and location of liver tumors, and a survey of the peritoneal cavity to exclude the presence of extrahepatic disease. Using laparoscopic ultrasound guidance, the RFA needle electrode is advanced percutaneously into the target tumors for treatment. The laparoscopic ultrasound permits more precise positioning of the RF needle multiple array near major blood vessels. Laparoscopic approach was used for patients with no prior history of extensive abdominal operations, and one or two liver tumors <4.0 cm in diameter located centrally in the liver near major intrahepatic blood vessels^[61,62].

The majority of patients underwent RFA of hepatic tumors during an open surgical procedure. This approach is preferred in patients with large tumors (>4.0-5.0 cm diameter), multiple tumors, if tumor locates next to a major intrahepatic blood vessel, or if a laparoscopic approach is impractical because of dense post-surgical adhesions. In contrast to percutaneous RFA treatments, it is possible to perform temporary occlusion of hepatic inflow during the intraoperative RFA procedure. Hepatic inflow occlusion facilitates RFA of large or hypervascular tumors and tumors near blood vessels. The amount of blood flow to a tumor is known to be a critical determinant of temperature response to a given increment of heat. Because heat loss or cooling effect is principally dependent on blood circulation in a given area, temperature response and blood flow are inversely related. By temporarily occluding hepatic inflow during RFA, the cooling effect of blood flow on perivascular tumor cells is minimized^[63]. The inflow occlusion increases the size of the zone of coagulative necrosis and enhances the likelihood of complete tumor cell kill, even if the tumor abuts a major intrahepatic blood vessel^[64].

The RFA needle can be placed under computed tomography (CT) or ultrasound guidance (percutaneous RFA) or ultrasound guidance (percutaneous, laparoscopic, or open RFA). Ultrasound can be used with all techniques of RFA, and offers several other advantages as well, including real-time capabilities, vascular visualization, availability, speed, and low cost. The probes are usually placed at the deep margin of the tumor and subsequently repositioned anteriorly at intervals appropriate to the size of the needle array. Once the needle is localized in the general vicinity of the tumor, the needle tip is placed into the desired portion of the tumor using a freehand technique. The ablation is started with the power setting at 25W, and the setting is automatically advanced to 50W over about 30 seconds. As the temperature at the tips of the deployed prongs exceeds 95°C, the times start to calculate. The temperature should be kept between 95-110°C at least 10 min to get full destroy^[51,65].

IMAGING TECHNIQUES IN RFA

Accurate imaging is essential for successful in situ tumor ablation. Tumors that are not seen can not be targeted, and residual foci of untreated tumor will continue to grow. With respect to tumor detection, and despite remarkable progress in US, CT and MR imaging over the past several years, no currently available imaging technique is perfectly sensitive for the detection of liver tumors, which means that some lesions will undoubtedly be overlooked with all imaging techniques. Generally, these overlooked lesions are small and will grow to a size that allows them to be detected, targeted and treated. Because currently available imaging techniques also may not precisely depict tumor margins, however, small foci of untreated tumor may not be identified. These will continue to grow in size and

result in "local recurrence" after treatments that initially appeared to be successful. Improved imaging techniques should result in not only improved detection of additional lesions but also more accurate determination of tumor margins. Recent and ongoing developments in contrast agents for US and MR imaging coupled with technical innovations in US, CT, and MR imaging may provide the much needed improvements. Additional research will be needed to determine their effect on the efficacy of in situ tumor ablation with RF.

In situ tumor ablation is virtually always performed with imaging guidance. Currently, US is most commonly used for guidance in probe placement, owing to its flexibility, widespread availability, relatively low cost, and real-time imaging capabilities. RF ablation can also be performed with CT or MR imaging guidance; however, until recently, the static nature of CT and the complexity of the MR imaging environment have limited their use. The recent development of CT fluoroscopic systems may result in a larger role for CT in the future. Similarly, the developments of open-architecture MR imaging systems and MR-compatible interventional equipment have resulted in increased interest in the use of this modality to help guide interventional procedures. Preliminary experience now suggests that MR imaging may be useful for in situ ablation procedures with RF^[66-68].

Imaging is used not only to help detect potentially treatable tumors and guide probe placement but also to monitor the effects of therapy. When procedures are performed with US guidance, hyperechogenicity is generally seen surrounding the probe tip during the application of RF energy. This has proved to be only marginally useful for monitoring the effects of therapy because the hyperechoic zones correspond only roughly to the regions of eventual tissue necrosis. Furthermore, these changes evolve rapidly over time and can disappear within minutes of ablation^[69-71]. Acoustic shadowing from more superficial treated areas can also preclude visualization of deeper portions of the tumor if one is not careful to treat deeper areas first. The use of US contrast agents may improve the accuracy of US with respect to monitoring the acute effects of therapy^[72,73]. Contrast-enhanced CT, which is probably the most widely used technique for the follow-up of treated lesions, is less useful for the immediate assessment of treatment results. CT is not particularly helpful for confirming successful treatment or identifying a small focus of untreated tumor. MR imaging appears to be more accurate than US or CT for monitoring the acute effects of^[66-68].

Follow-up imaging is very useful to assess the result of RF and the recurrence of new tumors, although sometimes it is very difficult. CT and MRI were showed more effective than ultrasound for monitoring the RFA ablation in animal studies. If the follow up imaging is performed soon after the procedure, a peripheral hyperemic halo surrounding an area of hypoattenuation devoid of parenchymal enhancement is usually seen with spiral CT or MRI. Occasionally a hyperdense central area corresponding to the needle tract is also seen. The interpretation of the follow-up CT scans required radiologists experience to prevent both diagnosis and underdiagnosis of the residual or recurrent tumor. The ablation process cause a hyperemic response in the liver parenchyma surrounding the ablation. The hyperemic prevents an accurate assessment of the completeness of the ablation in the early post-ablation period. The hyperemia usually resolved within 1 month after the procedure. After this time, persistent or new peritumoral hyperemia is considered an indication of recurrent tumor. Recurrent hypovascular tumors are detected as an enlargement of ablation area, or a subtle double-density halo developing around the margins of the treated area. All areas suspicious for tumor recurrence should be assessed by percutaneous biopsy.

RFA OF PRIMARY LIVER TUMORS

Primary liver cancer is a highly vascular cancer. A vascular sink phenomenon may contribute to the extended ablation times. Most of the

early reports on the use of RFA for HCC came from Rossi *et al*^[74] in Italy in 1995. They reported their results with percutaneous RFA in twenty-four patients (16 men and 8 women; age range, 53 to 79 years) with 36 hepatocellular carcinoma nodules of not more than 3.0cm in diameter underwent radiofrequency interstitial thermal ablation treatment with the intent to achieve a cure. In each patient, the thermal necrosis volume achieved was about double the tumor volume. During the mean follow-up interval of 24.8 months, 13 of 24 patients had recurrences, 9 of whom underwent further radiofrequency thermal ablation treatment. Radiofrequency thermal ablation was again repeated in two patients who showed a second recurrence.

Marone *et al*^[75] reported percutaneous RF results using cooling saline in the tube of 13 cirrhotic patients with 19 hepatocellular carcinoma in 1998. None of the patients had portal thrombosis or extrahepatic spread. They used a radiofrequency generator (100W power) connected to an 18G perfusion electrode needle with an exposed tip of 2-3cm. The circuit is closed through a dispersive electrode positioned under the patient's thighs. A peristaltic pump infuses a chilled (2-5°C) saline solution to guarantee the continuous cooling of the needle tip. The needle was placed into target lesions under US guidance. Complete necrosis as assessed at dynamic CT (no enhancement during the arteriographic phase) was achieved in 16 of 19 nodules (84%). No side-effects occurred. During the follow-up (median: 11 months) no death occurred and five patients had recurrent hepatocellular carcinoma appearing either as single nodule or as multi nodular liver involvement? In a large series from Curley *et al*^[76], 149 discrete HCC tumor nodules in 110 patients had been followed for a minimum of 12 months (median follow-up 19 months) after RF. Percutaneous, laparoscopic or intraoperative RFA was performed in 76 (69%) and 34 (31%) patients, respectively. Median diameter of tumors treated percutaneously (2.8cm) was smaller than lesions treated during laparotomy (4.6cm, $P<0.01$). Local tumor recurrence at the RFA site developed in four patients (3.6%); all four subsequently developed recurrent HCC in other areas of the liver. New liver tumors or extrahepatic metastases developed in 50 patients (45.5%), but 56 patients (50.9%) have no evidence of recurrence. There were no treatment-related deaths, but complications developed in 14 patients (12.7%) after RFA.

RFA OF COLORECTAL CANCER LIVER METASTASES

The liver is the most common site of distant metastasis from colorectal cancer. Colorectal cancer is the fourth most commonly diagnosed cancer and second leading cause of cancer death in the world. Nearly half of patients will develop liver metastases during the course of their disease, with 15-25% having liver metastases at the time of primary diagnosis and another 20% of patients developing metachronous liver metastases^[10,11]. About one-fourth of patients with liver metastases from colorectal cancer have no other sites of metastases and can be treated with regional therapies directed toward their liver tumors. But only a minority of the patients are candidates for surgical resection. RFA, one of the regional therapies, may be offered to patients with unresectable liver metastases.

Most of the early reports on the use of RFA for colorectal cancer liver metastases also came from Rossi *et al*^[74] in Italy. In 1996, they reported their results with percutaneous RFA in 50 patients, in which 11 patients had 13 metastases ranging from 1 to 9cm in diameter. Monopolar and bipolar needles were utilized and multiple probe insertions and treatment sessions were performed. There were no associated complications or deaths. Of the 11 patients with metastases, two underwent subsequent surgical resection, of which one had complete tumor necrosis by histopathologic examination. At a median follow-up of 22.6 months, 10 of 11 patients (90%) were

alive, but two (18%) had a local recurrence and seven (64%) had persistent or distant disease. Only one patient (9%), therefore, was alive without disease. These studies suggested that although RFA was effective in preventing local recurrence of metastases, it may not affect the progressive course of the cancer.

Solbiati *et al*^[77] reported on 117 patients with 179 metastatic lesions undergoing RFA with a mean follow-up of 3 years (range, 6 to 52 months). Computed tomographic follow-up was performed every 4-6 months. Recurrent tumors were retreated when feasible. Estimated median survival was 36 months. Estimated 1, 2, and 3-year survival rates were 93%, 69%, and 46%, respectively. Survival was not significantly related to number of metastases treated. In 77 (66%) of 117 patients, new metastases were observed at follow-up. Estimated median time until new metastases was 12 months. Percentages of patients with no new metastases after initial treatment at 1 and 2 years were 49% and 35%, respectively. Time to new metastases was not significantly related to number of metastases. Seventy (39%) of 179 lesions developed local recurrence after treatment. Of these, 54 were observed by 6 months and 67 by 1 year. This study suggests that at long-term local control can be achieved in a majority of patients, but that the development of new metastases limits improvement in overall survival.

Wood *et al*^[78] reported 231 tumors in 84 patients treated with 91 RFA procedures. The majority of patients had metastatic lesions (213 lesions in 73 patients) and 51 of the 91 treatments consisted of RFA alone. The other 40 included RFA combined with surgical resection, cryoablation, and hepatic artery infusion of chemotherapy. Of the 91 RF treatments, 39 were ablated at laparotomy, 27 by laparoscopy and 25 percutaneously; tumors ranged in size from 0.3 to 9.0cm. There were seven major complications including three deaths, one (1%) of which was directly related to the RFA procedure. Ten patients underwent a second RFA procedure (sequential ablations) and, in one case, a third RFA procedure for large (one patient), progressive (seven patients), and recurrent (three patients) lesions. At a median follow-up of 9 months (range, 1-27 months), 15 patients (18%) had developed a local recurrence. Of the remaining 69 patients, 34 were alive without disease, 14 were alive with disease, and 21 died of their disease; new hepatic tumors or extrahepatic disease therefore had developed in 35 patients. The average hospital stay was 3.6 days overall.

RFA OF OTHER LIVER METASTASES

Most of the papers discussed so far consisted of both primary liver tumors and colorectal cancer liver metastases. RFA for liver tumors has also been evaluated for specific tumor types.

Livraghi *et al*^[79] reported on 24 patients with 64 metastatic breast lesions ranging in size from 1 to 6.6cm. The liver was the only site of disease in 16 patients, while the other eight patients had stable metastatic disease elsewhere. The patients were treated with the percutaneous approach utilizing monopolar or clustered electrodes. Minor complications were noted in two patients and no deaths were reported. Complete necrosis was achieved in 59 (92%) of 64 lesions. Among the 59 lesions, complete necrosis required a single treatment session in 58 lesions (92%) and two treatment sessions in one lesion (2%). In 14 (58%) of 24 patients, new metastases developed during follow-up. Ten (71%) of these 14 patients developed new liver metastases. Currently, 10 (63%) of 16 patients whose lesions were initially confined to the liver are free of disease. One patient died of progressive brain metastases. Although a preliminary study, these results do suggest that RFA for selected patients with metastatic breast carcinoma confined to the liver can be as effective as RFA for colorectal and other metastatic tumors to the liver.

Neuroendocrine tumors metastatic to the liver often produce symptoms secondary to hormone production. Although only a minority are curable by surgical techniques, significant symptomatic relief can be obtained by surgical procedures. For those patients who are not surgical candidates, RFA may provide a viable therapeutic alternative. Siperstein *et al*^[80] reported 18 patients with 115 neuroendocrine tumors were ablated with RFA. The mean lesion size was 3.2cm (range, 1.3 to 10cm) and the average number of lesions ablated per patient was six (range, one to 14). There were two complications consisting of arterial fibrillation in one patient and an upper gastrointestinal bleed in another. Fifteen patients (83%) with 100 lesions were followed for a mean of 12.1 months (range, 3 to 35months). Local recurrence was detected in three patients (20%) and six (6%) lesions and three patients died during follow-up. However, data regarding potential symptom improvement were not reported.

FOLLOW UP OF RFA

Initial imaging serves as an indicator of complete treatment, and provides a basis for subsequent studies. However, the resolution and accuracy of current imaging techniques preclude identification of residual microscopic foci of malignancy at the periphery of a treated lesion. Hence, these viable tumor foci, if present, will grow and result in "local recurrence".

Multiphasic helical CT and contrast-enhanced MR imaging play a central role in the long-term assessment of therapeutic response, allowing confident discrimination between ablated and residual viable tumor. CT and MR studies are obtained at 3-4 months intervals and are combined with tumor marker (serum CEA, AFP, CA19-9) levels to detect local or distant recurrences. In general, sampling error and the histopathologic findings of thermally ablated tissue are too variable to render fine needle aspiration or core biopsy reliable indicators of the presence or absence of residual disease. US has proved valuable for immediate assessment of ablative results during the RF session, still in patients under general anesthesia, allowing for an immediate refinement of the ablation, if needed. US is also valuable for long-term follow-up and detection or confirmation of recurrences; in many patients contrast-guided retreatment has been performed in order to precisely direct RF energy on recurrence areas^[81-83].

ADVANTAGE AND DISADVANTAGE OF RFA

RF thermal ablation has several advantages over other therapies for primary liver cancer and metastasis liver cancer. It can be used as a percutaneous procedure, under the guiding of ultrasound, CT scan and MRI, done in local anesthesia, in out-patient department. The complications and morbidity are lower than hepatic resection and cryosurgery. RFA can be retreated in the patients whose tumors recur at the margin of treatment or have new tumors develop elsewhere in the liver. It has similar results as hepatic resection because it destroyed the tumors completely as taking it out in liver surgery, which is superior to ethanol injection. RF requires less sessions than other ablation procedures such as ethanol injection.

Although RF has a lot of advantages in the treatment of primary and metastasis liver tumors, it still has a few disadvantages and complications. These complications included symptomatic pleural effusion, fever, pain, subcutaneous hematoma, subcapsular liver hematoma, and ventricular fibrillation. The severe complication is treatment-related death. As with all methods related to tumors, the outcome of RF thermal ablation will be related to the skill of physician performing the procedure. Exact placement of the ablation needles require considerable skill and some degree of guesswork by the radiologist and surgeon, which may be the most experienced in interventional procedures. Recurrence at the treatment margin may

result from an inability to adequately kill the tumor the hepatic parenchyma adjacent to the treated tumors. The abundant portal venous blood flow present in normal hepatic parenchyma act as a heat pump, which makes the creation of the thermal injury in normal liver more difficult than that it is in liver tumors. RFA also caused skin burn in percutaneous procedures, hemorrhage, diaphragmatic necrosis, hepatic abscess, hepatic artery injuries, bile ducts injuries, renal failure, coagulopathy and liver failure, which were severe and eventually fatal.

CONCLUSION

Despite the considerable progress that has been made to date, a number of challenges remain for the future. These include the development of techniques that can increase the volume of tissue destroyed at a single treatment session, the development of more suitable and accurate imaging tests, and a better understanding of how to integrate in situ ablation techniques into the overall care of patients with different specific neoplasms.

Although long-term observations are still not available, RFA will definitely give the surgeon a helpful hand and offer the patients a better prognosis. But, RFA is unlikely to be curative for most patients, it can relieve the symptom of patients and improve the quality of life of patients. RFA has been shown to be safer and better tolerated compared to other ablative techniques, such as cryotherapy, laser ablation and microwave ablation, has been associated with fewer local recurrence. However, surgical resection remains the gold standard for treating metastatic and primary liver tumors. RFA of unresectable liver tumors provides a relatively safe, highly effective method to achieve local disease control in some liver cancer patients who are not candidates for liver resection. RFA also shown some better respect in combination with surgical resection, hepatic artery catheter and regional chemotherapy. With the development of RFA equipments and techniques, the treatment of a large primary and secondary liver cancer and malignant tumors at other body sites will be feasible and effective. The most interesting feature of RFA is the minimal-invasiveness with zero mortality rate, significantly lower complications, reduced costs and hospital days compared to surgery and other local therapies. Furthermore, with combination of other procedures, RFA will improve the survival of patients with cancer.

REFERENCES

- Schafer DF, Sorrell MF. Hepatocellular carcinoma. *Lancet* 1999;353: 1253-1257
- Tang ZY. Hepatocellular carcinoma-Cause, treatment and metastasis. *World J Gastroenterol* 2001; 7: 445-454
- Qin LX, Tang ZY. The prognostic significance of clinical and pathological features in hepatocellular carcinoma. *World J Gastroenterol* 2002; 8: 193-199
- Weiss L, Grundmann E, Torhorst J, Hartveit F, Moberg I, Eder M, Fenoglio-Preiser CM, Napier J, Horne CH, Lopez MJ. Haematogenous metastatic patterns in colonic carcinoma: an analysis of 1541 necropsies. *J Pathol* 1986;150:195-203
- Hughes KS, Simon R, Songhorabodi S, Adson MA, Ilstrup DM, Fortner JG, Maclean BJ, Foster JH, Daly JM, Fitzherbert D. Resection of the liver for colorectal carcinoma metastases: a multi-institutional study of patterns of recurrence. *Surgery* 1986; 100: 278-284
- Bengtsson G, Carlsson G, Hafstrom L, Jonsson PE. Natural history of patients with untreated liver metastases from colorectal cancer. *Am J Surg* 1981; 141: 586-589
- Wagner JS, Adson MA, Van Heerden JA, Adson MH, Ilstrup DM. The natural history of hepatic metastases from colorectal cancer. A comparison with resective treatment. *Ann Surg* 1984;199:502-508
- Fong Y, Cohen AM, Fortner JG, Enker WE, Turnbull AD, Coit DG, Marrero AM, Praesad M, Blumgart LH, Brennan MF. Liver resection for colorectal metastases. *J Clin Oncol* 1997; 15: 938-946
- Gayowski TJ, Iwatsuki S, Madariaga JR, Selby R, Todo S, Irish W, Starzl TE. Experience in hepatic resection for metastatic colorectal cancer: analysis of clinical and pathologic risk factors. *Surgery* 1994; 116: 703-710

- 10 Palmer M, Petrelli NJ, Herrera L. No treatment option for liver metastases from colorectal adenocarcinoma. *Dis Colon Rectum* 1989; 32: 698-701
- 11 Wu MC, Shen F. Progress in research of liver surgery in China. *World J Gastroenterol* 2000; 6:773-776
- 12 Nagorney DM, van Heerden JA, Ilstrup DM, Adson MA. Primary hepatic malignancy: surgical management and determinants of survival. *Surgery* 1989; 106: 740-748
- 13 Wanebo HJ, Semoglou C, Attiyeh F, Stearns MJ Jr. Surgical management of patients with primary operable colorectal cancer and synchronous liver metastases. *Am J Surg* 1978; 135:81-85
- 14 Bruinvels DJ, Stiggelbout AM, Kievit J, van Houwelingen HC, Habbema JD, van de Velde CJ. Follow-up of patients with colorectal cancer. A meta-analysis. *Ann Surg* 1994; 219:174-182
- 15 Kemeny N, Huang Y, Cohen AM, Shi W, Conti JA, Brennan MF, Bertino JR, Turnbull AD, Sullivan D, Stockman J, Blumgart LH, Fong Y. Hepatic arterial infusion of chemotherapy after resection of hepatic metastases from colorectal cancer. *N Engl J Med* 1999; 341: 2039-2048
- 16 Fowler WC, Eisenberg BL, Hoffman JP. Hepatic resection following systemic chemotherapy for metastatic colorectal carcinoma. *J Surg Oncol* 1992; 51: 122-125
- 17 Elias D, Lasser P, Rougier P, Ducreux M, Bognel C, Roche A. Frequency, technical aspects, results, and indications of major hepatectomy after prolonged intra-arterial hepatic chemotherapy for initially unresectable hepatic tumors. *J Am Coll Surg* 1995; 180:213-219
- 18 Venook AP. Update on hepatic intra-arterial chemotherapy. *Oncology* 1997; 11: 947-957
- 19 Giovannini M. Percutaneous alcohol ablation for liver metastasis. *Semin Oncol* 2002; 29: 192-195
- 20 Bartolozzi C, Lencioni R. Ethanol injection for the treatment of hepatic tumors. *Eur Radiol* 1996; 6: 682-696
- 21 Lee MJ, Mueller PR, Dawson SL, Gazelle SG, Hahn PF, Goldberg MA, Boland GW. Percutaneous ethanol injection for the treatment of hepatic tumors: indications, mechanism of action, technique, and efficacy. *AJR Am J Roentgenol* 1995; 164: 215-220
- 22 ter Haar GR. High intensity focused ultrasound for the treatment of tumors. *Echocardiography* 2001; 18: 317-322
- 23 Sibille A, Prat F, Chapelon JY, Abou el Fadil F, Henry L, Theillere Y, Ponchon T, Cathignol D. Extracorporeal ablation of liver tissue by high-intensity focused ultrasound. *Oncology* 1993; 50: 375-379
- 24 Yang R, Sanghvi NT, Rescorla FJ, Kopecky KK, Grosfeld JL. Liver cancer ablation with extracorporeal high-intensity focused ultrasound. *Eur Urol* 1993; 23 Suppl 1: 17-22
- 25 Sotsky TK, Ravikumar TS. Cryotherapy in the treatment of liver metastases from colorectal cancer. *Semin Oncol* 2002; 29: 183-191
- 26 Poston G. Cryosurgery for colorectal liver metastases. *Hepatogastroenterology* 2001; 48: 323-324
- 27 Ross WB, Horton M, Bertolino P, Morris DL. Cryotherapy of liver tumors—a practical guide. *HPB Surg* 1995; 8: 167-173
- 28 Seifert JK, Morris DL. Prognostic factors after cryotherapy for hepatic metastases from colorectal cancer. *Ann Surg* 1998; 228: 201-208
- 29 Moroz P, Jones SK, Gray BN. Status of hyperthermia in the treatment of advanced liver cancer. *J Surg Oncol* 2001; 77: 259-269
- 30 Dodd GD 3rd, Soulen MC, Kane RA, Livraghi T, Lees WR, Yamashita Y, Gil lams AR, Karahan OI, Rhim H. Minimally invasive treatment of malignant hepatic tumors: at the threshold of a major breakthrough. *Radiographics* 2000; 20: 9-27
- 31 Greve JW. Alternative techniques for the treatment of colon carcinoma metastases in the liver: current status in The Netherlands. *Scand J Gastroenterol* 2001; 234 (Suppl): 77-81
- 32 Usatoff V, Habib NA. Update of laser-induced thermotherapy for liver tumors. *Hepatogastroenterology* 2001; 48: 330-332
- 33 Heisterkamp J, van Hillegersberg R, Ijzermans JN. Interstitial laser coagulation for hepatic tumors. *Br J Surg* 1999; 86: 293-304
- 34 Schneider PD. Liver resection and laser hyperthermia. *Surg Clin North Am* 1992; 72: 623-639
- 35 Slakey DP. Radiofrequency ablation of recurrent cholangiocarcinoma. *Am Surg* 2002; 68: 395-397
- 36 Yoon SS, Tanabe KK. Surgical treatment and other regional treatments for colorectal cancer liver metastases. *Oncologist* 1999; 4:197-208
- 37 Curley SA. Radiofrequency ablation of malignant liver tumors. *Oncologist* 2001; 6: 14-23
- 38 McGahan JP, Browning PD, Brock JM, Tesluk H. Hepatic ablation using radiofrequency electrocautery. *Invest Radiol* 1990; 25: 267-270
- 39 Buscarini L, Rossi S, Fornari F, Di Stasi M, Buscarini E. Laparoscopic ablation of liver adenoma by radiofrequency electrocautery. *Gastrointest Endosc* 1995; 41: 68-70
- 40 Dickson JA, Calderwood SK. Temperature range and selective sensitivity of tumors to hyperthermia: a critical review. *Ann N Y Acad Sci* 1980; 335:180-205
- 41 Siperstein A, Garland A, Engle K, Rogers S, Berber E, String A, Foroutani A, Ryan T. Laparoscopic radiofrequency ablation of primary and metastatic liver tumors. Technical considerations. *Surg Endosc* 2000; 14:400-405
- 42 Zervas NT, Hamlin H. Stereotactic radiofrequency hypophysectomy. *Appl Neurophysiol* 1978; 41: 219-222
- 43 Cosman ER, Nashold BS, Bedenbaugh P. Stereotactic radiofrequency lesion making. *Appl Neurophysiol* 1983; 46: 160-166
- 44 Rossi S, Fornari F, Pathies C, Buscarini L. Thermal lesions induced by 480 KHz localized current field in guinea pig and pig liver. *Tumori* 1990; 76: 54-57
- 45 McGahan JP, Griffey SM, Budenz RW, Brock JM. Percutaneous ultrasound-guided radiofrequency electrocautery ablation of prostate tissue in dogs. *Acad Radiol* 1995; 2: 61-65
- 46 Wood BJ, Ramkaransingh JR, Fojo T, Walther MM, Libutti SK. Percutaneous tumor ablation with radiofrequency. *Cancer* 2002; 94: 443-451
- 47 Parikh AA, Curley SA, Fornage BD, Ellis LM. Radiofrequency ablation of hepatic metastases. *Semin Oncol* 2002; 29: 168-182
- 48 Choi H, Loyer EM, DuBrow RA, Kaur H, David CL, Huang S, Curley S, Char nsangavej C. Radio-frequency ablation of liver tumors: assessment of therapeutic response and complications. *Radiographics* 2001; 21 Spec No: S41-54
- 49 Goldberg SN. Radiofrequency tumor ablation: Principles and techniques. *Eur J Ultrasound* 2001; 13:129-147
- 50 Liu CL, Fan ST. Nonresectional therapies for hepatocellular carcinoma. *Am J Surg* 1997; 173:358-365
- 51 Buscarini L, Buscarini E, Di Stasi M, Vallisa D, Quaretti P, Rocca A. Percutaneous radiofrequency ablation of small hepatocellular carcinoma: long-term results. *Eur Radiol* 2001; 11:914-921
- 52 Hager ED, Dziambor H, Hohmann D, Gallenbeck D, Stephan M, Popa C. Deep hyperthermia with radiofrequencies in patients with liver metastases from colorectal cancer. *Anticancer Res* 1999; 19: 3403-3408
- 53 Livraghi T, Goldberg SN, Monti F, Bizzini A, Lazzaroni S, Meloni F, Pellicano S, Solbiati L, Gazelle GS. Saline-enhanced radio-frequency tissue ablation in the treatment of liver metastases. *Radiology* 1997; 202:205-210
- 54 Miao Y, Ni Y, Yu J, Marchal G. A comparative study on validation of a novel cooled-wet electrode for radiofrequency liver ablation. *Invest Radiol* 2000; 35: 438-444
- 55 Lorentzen T. A cooled needle electrode for radiofrequency tissue ablation: Thermodynamic aspects of improved performance compared with conventional needle design. *Acad Radiol* 1996; 3: 556-563
- 56 Goldberg SN, Gazelle GS, Solbiati L, Rittman WJ, Mueller PR. Radiofrequency tissue ablation: Increased lesion diameter with a perfusion electrode. *Acad Radiol* 1996; 3: 636-644
- 57 McGahan JP, Gu WZ, Brock JM, Tesluk H, Jones CD. Hepatic ablation using bipolar radiofrequency electrocautery. *Acad Radiol* 1996; 3: 418-422
- 58 Bilchik AJ, Wood TF, Allegra D, Tsioulis GJ, Chung M, Rose DM, Ramming KP, Morton DL. Cryosurgical ablation and radiofrequency ablation for unresectable hepatic malignant neoplasms: A proposed algorithm. *Arch Surg* 2000; 135: 657-662
- 59 Rhim H, Dodd GD 3rd. Radiofrequency thermal ablation of liver tumors. *J Clin Ultrasound* 1999; 27: 221-229
- 60 Goldberg SN, Gazelle GS, Compton CC, Mueller PR, Tanabe KK. Treatment of intrahepatic malignancy with radiofrequency ablation: Radiologic-pathologic correlation. *Cancer* 2000; 88: 2452-2463
- 61 Siperstein AE, Rogers SJ, Hansen PD, Gitomirsky A. Laparoscopic thermal ablation of hepatic neuroendocrine tumor metastases. *Surgery* 1997; 122:1147-1155
- 62 Curley SA, Davidson BS, Fleming RY, Izzo F, Stephens LC, Tinkey P, Croome D. Laparoscopically guided bipolar radiofrequency ablation of areas of portal liver. *Surg Endosc* 1997; 11: 729-733
- 63 Solbiati L, Ierace T, Goldberg SN, Sironi S, Livraghi T, Fiocca R, Ser vadio G, Rizzatto G, Mueller PR, Del Maschio A, Gazelle GS. Percutaneous US-guided radio-frequency tissue ablation of liver metastases: treatment and follow-up in 16 patients. *Radiology* 1997; 202: 195-203
- 64 Stureson C, Liu DL, Stenram U, Andersson-Engels S. Hepatic inflow occlusion increases the efficacy of interstitial laser-induced thermotherapy in rats. *J Surg Res* 1997; 71: 67-72
- 65 Gazelle GS, Goldberg SN, Solbiati L, Livraghi T. Tumor ablation with radio-frequency energy. *Radiology* 2000; 217: 633-646
- 66 Lewin JS, Connell CF, Duerk JL, Chung YC, Clappitt ME, Spisak J, Gazelle GS, Haaga JR. Interactive MR-guided radiofrequency interstitial thermal ablation of abdominal tumors: clinical trial for evaluation of safety and feasibility. *J Magn Reson Imaging* 1998; 8: 40-47

- 67 Steiner P, Botnar R, Dubno B, Zimmermann GG, Gazelle GS, Debatin JF. Radio-frequency-induced thermoablation: monitoring with T1-weighted and proton-frequency-shift MR imaging in an interventional 0.5-T environment. *Radiology* 1998; 206: 803-810
- 68 Goldberg SN, Kruskal JB, Oliver BS, Clouse ME, Gazelle GS. Percutaneous tumor ablation: increased coagulation by combining radio-frequency and ethanol instillation in a rat breast tumor model. *Radiology* 2000; 217:827-831
- 69 Rossi S, Buscarini E, Garbagnati F, Di Stasi M, Quaretti P, Rago M, Zangrandi A, Andreola S, Silverman D, Buscarini L. Percutaneous treatment of small hepatic tumors by an expandable RF needle electrode. *Am J Roentgenol* 1998; 170: 1015-1022
- 70 Solbiati L, Goldberg SN, Ierace T, Livraghi T, Meloni F, Dellanoce M, Sironi S, Gazelle GS. Hepatic metastases: percutaneous radio-frequency ablation with cooled-tip electrodes. *Radiology* 1997; 205:367-373
- 71 Livraghi T, Goldberg SN, Lazzaroni S, Meloni F, Solbiati L, Gazelle GS. Small hepatocellular carcinoma: treatment with radio-frequency ablation versus ethanol injection. *Radiology* 1998; 210:655-661
- 72 Solbiati L, Goldberg SN, Ierace T, Dellanoce M, Livraghi T, Gazelle GS. Radio-frequency ablation of hepatic metastases: postprocedural assessment with a US microbubble contrast agent-early experience. *Radiology* 1999; 211:643-649
- 73 Goldberg SN, Walovitch RC, Straub JA, Shore MT, Gazelle GS. Radio-frequency-induced coagulation in rabbits: immediate detection at US using a synthetic microsphere contrast agent. *Radiology* 1999; 213:438-444
- 74 Rossi S, Di Stasi M, Buscarini E, Quaretti P, Garbagnati F, Squassante L, Paties CT, Silverman DE, Buscarini L. Percutaneous RF interstitial thermal ablation in the treatment of hepatic cancer. *Am J Roentgenol* 1996; 167: 759-768
- 75 Marone G, Francica G, D'Angelo V, Iodice G, Pastore P, Altamura G, Cusati B, Siani A. Echo-guided radiofrequency percutaneous ablation of hepatocellular carcinoma in cirrhosis using a cooled needle. *Radiol Med* 1998; 95: 624-629
- 76 Curley SA, Izzo F, Ellis LM, Nicolas Vauthey J, Vallone P. Radiofrequency ablation of hepatocellular cancer in 110 patients with cirrhosis. *Ann Surg* 2000; 232: 381-391
- 77 Solbiati L, Ierace T, Tonolini M, Osti V, Cova L. Radiofrequency thermal ablation of hepatic metastases. *Eur J Ultrasound* 2001; 13: 149-158
- 78 Wood TF, Rose DM, Chung M, Allegra DP, Foshag LJ, Bilchik AJ. Radiofrequency ablation of 231 unresectable hepatic tumors: Indications, limitations, and complications. *Ann Surg Oncol* 2000; 7: 593-600
- 79 Livraghi T. Guidelines for treatment of liver cancer. *Eur J Ultrasound* 2001; 13:167-176
- 80 Siperstein AE, Berber E. Cryoablation, percutaneous alcohol injection, and radiofrequency ablation for treatment of neuroendocrine liver metastases. *World J Surg* 2001; 25: 693-696
- 81 Fong Y, Blumgart LH, Cohen A, Fortner J, Brennan MF. Repeat hepatic resections for metastatic colorectal cancer. *Ann Surg* 1994;220: 657-662
- 82 Goya T, Miyazawa N, Kondo H, Tsuchiya R, Naruke T, Suemasu K. Surgical resection of pulmonary metastases from colorectal cancer: 10-year follow-up. *Cancer* 1989; 64:1418-1421
- 83 Gough DB, Donohue JH, Trastek VA, Nagorney DM. Resection of hepatic and pulmonary metastases in patients with colorectal cancer. *Br J Surg* 1994; 81: 94-96

Edited by Morris DL

• REVIEW •

Effects of histone acetylation and DNA methylation on p21^{WAF1} regulation

Jing-Yuan Fang, You-Yong Lu

Jing-Yuan Fang, Renji Hospital, Shanghai Institute of Digestive Disease, Shanghai Second Medical University, Shanghai, China
You-Yong Lu, Beijing Cancer Institute, Beijing University, Beijing 100000, China

Correspondence to: Jing-Yuan Fang, M.D., Ph.D., Shanghai Institute of Digestive Disease, Renji Hospital, 145 Shandong Zhong Road, Shanghai 200001, China. jingyuanfang@yahoo.com

Received 2001-12-04 Accepted 2002-02-07

Abstract

Cell cycle progression is regulated by interactions between cyclins and cyclin-dependent kinases (CDKs). p21^{WAF1} is one of the CIP/KIP family which inhibits its CDKs activity. Increased expression of p21^{WAF1} may play an important role in the growth arrest induced in transformed cells. Although the stability of the p21^{WAF1} mRNA could be altered by different signals, cell differentiation and numerous influencing factors. However, recent studies suggest that two known mechanisms of epigenesis, i.e. gene inactivation by methylation in promoter region and changes to an inactive chromatin by histone deacetylation, seem to be the best candidate mechanisms for inactivation of p21^{WAF1}. To date, almost no coding region p21^{WAF1} mutations have been found in tumor cells, despite extensive screening of hundreds of various tumors. Hypermethylation of the p21^{WAF1} promoter region may represent an alternative mechanism by which the p21^{WAF1/CIP1} gene can be inactivated. The reduction of cellular DNMT protein levels also induces a corresponding rapid increase in the cell cycle regulator p21^{WAF1} protein demonstrating a regulatory link between DNMT and p21^{WAF1} which is independent of methylation of DNA. Both histone hyperacetylation and hypoacetylation appear to be important in the carcinoma process, and induction of the p21^{WAF1} gene by histone hyperacetylation may be a mechanism by which dietary fiber prevents carcinogenesis. Here, we review the influence of histone acetylation and DNA methylation on p21^{WAF1} transcription, and effect on pathways or factors associated such as p53, E2A, Sp1 as well as several histone deacetylation inhibitors.

Fang JY, Lu YY. Effects of histone acetylation and DNA methylation on p21^{WAF1} regulation. *World J Gastroenterol* 2002;8(3):400-405

INTRODUCTION

Cell cycle progression is regulated by interactions between cyclins and CDKs^[1,2]. Especially, the transition of G₁ to S phase is known to be regulated by a family of negative cell cycle regulators, CDKIs. The latter includes two families, the CIP/KIP family and the INK4 family^[3-6]. p21^{WAF1} is one of the CIP/KIP family^[7,8]. Increased expression of p21^{WAF1} may play a crucial role in the growth arrest induced in transformed cells^[9].

p21^{WAF1} was first cloned and characterized as an important effector that acted to inhibit cyclin-dependent kinase activity in p53 mediated cell cycle arrest induced by DNA damage^[10,11]. It has been

shown that this is a G C-rich region in the human p21^{WAF1} promoter^[12]. Although the stability of the p21^{WAF1} mRNA could be altered by different signals cell differentiation^[13] and oxidative stress^[14] as well as numerous influencing factors including decorin^[15], Ras/Raf protein^[16], TGF- β ^[17] and Tax of human T cell leukemia virus type 1 (HTLV-1)^[18,19]. However, two known mechanisms of epigenetic modification, gene inactivation by methylation in promoter region and changes to an inactive chromatin by histone deacetylation, seem to be the best candidate mechanisms for the inactivation of CIP/KIP family^[20]. In this review, we focused on the methylation, histone acetylation and some transcription factor, co-transcription factor associated with acetylation.

DNA METHYLATION AND HISTONE ACETYLATION

The post-translational modifications include acetylation, phosphorylation, methylation, ubiquitination and ADP-ribosylation^[21]. In mammals, methylation of the 5' position of cytosine in the CpG dinucleotide sequence is the only naturally occurring covalent modification of the genome. The enzyme DNA 5-cytosine methyltransferase (DNMT) catalyzes the transfer of a methyl group from S-adenosylmethionine to the 5 position of cytosines residing in the dinucleotide sequence CpG^[22]. DNA methylation patterns correlate inversely with gene expression^[23] and, therefore, DNA methylation has been suggested to be an epigenetic determinant of gene expression.

DNA methylation is believed to be an on-off switch in gene expression, CpG islands present in the promoter regions have been shown to be susceptible to hypermethylation in many cancer cells^[24]. CpG islands near promoters and 5' regulatory region are usually unmethylated in normal somatic cells. In contrast, widespread methylation of CpG islands occurs in autosomal genes and leads to the silencing of the genes during oncogenic transformation.

DNA in eukaryotes is packaged with histone and non-histone proteins into chromatin. In general, regions of chromatin that are hyperacetylated are transcriptionally active, whereas regions that are hypoacetylated are silenced. Indeed, a global increase in core histone acetylation does not necessarily induce widespread transcription^[25]. Histone acetylation results in charge neutralization and separation of DNA from the histones allowing nucleosomal DNA to become more accessible to transcription factors. Histone acetylation is believed to stabilize local nucleosomal structure, thereby allowing transcription factors and the basal transcriptional machinery access to DNA. Hyperacetylation of histones has been shown to mark open chromatin and to be required for transcriptional activation^[26].

Histone acetylation is a reversible process: histone acetyltransferases (HATs) transfer the acetyl moiety from acetyl coenzyme A to the lysine neutralizes the positive charge, and histone deacetylases (HDACs) remove the acetyl groups re-establishing the positive charge in the histones. At least six human HDAC enzymes exist, and for higher eukaryotes, HDAC1 was first purified using an affinity matrix based on the deacetylase inhibitor trapoxin^[27]. HDAC inhibitor include trichostatin A (TSA)^[28,29], trapoxin (TPX)^[30], Butyrate^[31,32], MS-27-275 (a synthetic benzamide derivative)^[33] and Apicidin^[9,34]. Due to the inhibitory effects of the compounds of

endogenous genes that plays significant roles in G1-S progression of the cell cycle, HDAC inhibitors have been considered to be a novel class of cancer treatment agent^[34].

Methylation is not genomically uniform, as unmethylated CpG are found preferentially in transcriptionally active chromatin. The highest density of nonmethylated CpG islands, which usually contain promoter or other regulatory DNA that is required for active transcription of a gene. CpG island chromatin is enriched in hyperacetylated histones and deficient in linker histones^[35]. Recent studies have suggested a strong link between histone acetylation, chromatin remodeling, and gene regulation^[26,36,37]. The results from many papers established a link between DNA methylation, histone acetylation and sequence-specific DNA binding activity. In general, CpG island chromatin was found to contain highly acetylated histone H3 and H4. Deacetylation of histone H3 and H4 by the HDACs presumably leads to the formation of a chromatin environment that inhibits transcription^[38]. Hypoacetylated, transcriptionally silenced regions are often methylated^[39]. Furthermore, methylated DNA is

transcriptionally repressed, but only under conditions in which the methylated template is assembled into nucleosomal structures^[40], methylation density defines the level of histone acetylation^[41]. There are the roles of MeCP2, MBD1, MBD2, and MBD3^[35], NuRD (nucleosome-remodeling histone deacetylase)^[42,43] and DMAP1^[44], as well as DNMT1^[44,45] in the linkage of methylation with acetylation.

METHYLATION AND TRANSCRIPTION EXPRESSION OF p21^{WAF1} GENE

Usually, one could propose the negative regulation of p21^{WAF1} on the binding of DNMT1 with PCNA in normal cells^[46], however the loss of p21^{WAF1} from PCNA complexes could cause abnormal gains of methylation during repair of DNA damage^[47]. Moreover, the p21^{WAF1} gene transcription level is regulated by methylation, due to that p21^{WAF1} promoter contains high density of potentially methylatable CpG dinucleotides clustered around the initiation site of transcription (Figure 1).

CpG island
-243

```
CGAGGGACTGGGGAGGAGGGAAGTGCCTCTGCAGCACGCGAGGTTCCGGGACCCGGCTGGCCTGCTGGA
ACTCGGCCAGGCTCAGCTGCTCCGCGCTGGGCAGCCAGGAGCCTGGGC CCCGGGGAGGGCGGTC CCGGG
CGGCGCGGTGGGCCGAGCGCGGGTCCCTCTCTTGAGGCGGGCCCGGGCGGGGCGGTTGTATATCAGGGCCG
CGCTGAGCTGCGCCAGCTGAGGTGTGACAGCT G
-1 | → +1
```

Figure 1 There are more CpG island at the domain near by the transcription start site in the promoter of p21^{WAF1} gene.

Dr. Nass *et al.*^[48] transfected three antisense DNMT1 (pCMV TMH) into human breast cancer MDA231 cell line, and found that the reduced DNMT1 protein and up-regulation of p21^{WAF1} suggesting that DNMT protein levels were inversely correlated with the level of p21^{WAF1} in breast cancer cells.

To date, almost no coding region p21^{WAF1} mutations have been found in tumor cells, despite extensive screening of hundreds of various tumors^[49-51]. Hypermethylation of the p21^{WAF1} promoter region may represent an alternative mechanism by which the p21^{WAF1/CIP1} gene can be inactivated. DNMT and p21^{WAF1} compete for the same binding site on PCNA, an increase in DNMT expression might promote dissociation of p21^{WAF1} from PCNA, perhaps making p21^{WAF1} more susceptible to ubiquitination and proteasome degradation^[52]. A decrease in DNMT expression would then be expected to have an opposite effect on p21^{WAF1} stability^[48]. 5-Azacytidine (5-Aza-C, a demethylating agent) mediated Sp1 expression also up-regulated activities p21^{WAF1}^[53].

Rat-1 is a cell line containing wild-type p53^[54]. Allan and co-workers found which p21^{WAF1} 5'UTR contains a putative CpG island which is methylated in Rat-1 cells that used frequently to assess transformation and for apoptosis studies, the lack of p21^{WAF1} expression appears to be the result of hypermethylation of the p21^{WAF1} promoter region, as p21^{WAF1} protein expression could be induced by growth of Rat-1 cells in the presence of 5-aza-2-deoxycytidine (5-Aza-dC). Furthermore, sequencing analysis of bisulfite-treated DNA demonstrated extensive methylation of cytosine residues in CpG dinucleotides in a CpG-rich island in the promoter region of the p21^{WAF1} gene^[55]. A report showed that altered DNA methylation was present in RMS tumors and that the DNA methyltransferase expression is increased in both embryonal and alveolar subtypes of this cancer^[56,57]. They think that hypermethylation of the p21^{WAF1} gene at the proximal STAT-binding site, correlates with decreased p21^{WAF1} expression. The p21^{WAF1} gene is subjected to methylation regulation at the transcription level and is a target of aberrant methylation in RMS cells.

However, several studies indicated that the hypermethylation of

p21^{WAF1} was not the main machineries of p21^{WAF1} expression regulation. Although Young *et al.*^[58] reported that cells arrested and p21^{WAF1} expressed by DNMT inhibition in normal human fibroblasts. Milutinovic demonstrated that inhibition of DNMT resulted in the rapid induction of the known tumor suppressor and cell cycle regulator p21^{WAF1} by a mechanism that did not involve DNA methylation of the p21^{WAF1} promoter, in human non-small cell lung cancer cell line, A549 cells^[59]. The reduction of cellular DNMT protein levels also induced a corresponding rapid increase in the cell cycle regulator p21^{WAF1} protein demonstrating a regulatory link between DNMT and p21^{WAF1} which was independent of methylation of DNA^[60]. Shin's result showed that the promoter of the p21^{WAF1} gene was not been methylated in gastric cancer cells. This confirmed that methylation was not the mechanism for inactivation of p21^{WAF1} in gastric cancer cells^[20]. In adenomatoid polyps, although DNMT1 expression coincided with the expression of other cell proliferation markers, many DNMT1-expressing cells also expressed p21^{WAF1}. The fidelity of DNMT1 expression was further undetermined in colorectal carcinomas, in which a striking heterogeneity in DNMT1 expression, with some carcinoma cells containing very high DNMT1 levels and others containing very low DNMT1. These results indicate that human colorectal carcinogenesis is accompanied by a progressive dysregulation of DNMT1 expression and suggest that abnormalities in DNMT1 expression may contribute to the abnormal CpG dinucleotide methylation which changes the characteristic of human colorectal carcinoma cell DNA^[61].

HYPERACETYLATION, HDAC INHIBITORS AND OVEREXPRESSION OF p21^{WAF1} GENE

Histone deacetylation is a general mechanism for inactivation of the p21^{WAF1} in gastric cancer cell lines^[20]. Both histone hyperacetylation and hypoacetylation appear to be important in the carcinoma process, and induction of the p21^{WAF1} gene by histone hyperacetylation may be a mechanism by which dietary fiber prevents carcinogenesis^[31].

Regarding the correlation of histone acetylation and p21^{WAF1} gene

expression, that HDAC inhibitor TSA, trapoxin, butyrate and apicidin induce p21^{WAF1} transcriptional activity involved in most studies.

TSA is originally reported to be a fungistatic antibiotic, and it appears to be a promising tool for analyzing the many functions of histone hyperacetylation in cell proliferation and differentiation. TSA can stimulate p21^{WAF1} expression in HT29 cells^[32].

TPX is the microbially derived cyclotetrapeptide^[62], Sambucetti found that it increased the level of chromatin acetylation associated with histone H3 in the trapoxin-responsive region of the p21^{WAF1} promoter, and it activated p21^{WAF1} transcription that led to elevated p21^{WAF1} protein levels in three kinds of human tumor cells. Since the domain of the promoter that is necessary for TPX-mediated activation does not contain p53 binding sites, hence p21^{WAF1} expression upregulation by TPX is independent of p53^[30].

Sodium butyrate is a short chain fatty acid produced in the human colon by bacterial fermentation of carbohydrates^[32], causes hyperacetylation of histone through the inhibition of HDAC. Three years ago, Archer and his coworkers showed firstly the critical importance of p21^{WAF1} in butyrate-mediated growth arrest was able to cause growth arrest in the human colon cancer cell line HT-29^[31]. Siavoshian^[32] suggested that butyrate and TSA stimulated, the p21^{WAF1} expression both at the mRNA and protein levels, whereas they induced histone H4 hyperacetylation. Butyrate sensitivity requires Sp1-3 site in conjunction with the Sp1-5 site and Sp1-6^[29]. Shin *et al*^[20] indicated that the overexpression of p21^{WAF1} gene occurred in human gastric cancer cell lines after butyrate treatment. Butyrate increased histone H4-acetylation in human melanoma cell lines A375 and S91 and up-regulated p21^{WAF1} gene transcription level^[63].

Apicidin is a fungal metabolite shown to exhibit antiparasitic activity by inhibition of HDAC. Han *et al*^[64] indicated that inhibition of HDAC activity by apicidin was closely associated with morphological change and induction of p21^{WAF1}, although the protein levels of cyclin D1, CDK2, HDAC1 and p53 were not affected by the addition of apicidin for 24 hrs, whereas the induction of p21^{WAF1} by apicidin was reversible.

Suberoylanilide hydroxamic acid (SAHA) is a hydroxamic acid-based hybrid polar compound, and it is an inhibitor of HDAC^[65,66]. SAHA causes an accumulation of acetylated histones H3 and H4 in total cellular chromatin by 2h, which is maintained throughout 24h of culture with increased p21^{WAF1} expression, but no change in chromatin associated with the actin and p27 genes, and SAHA also induces up to a 9-fold increase in p21^{WAF1} mRNA and protein in T24 bladder carcinoma cells. p21^{WAF1} by SAHA is regulated, at least in part, by the degree of acetylation of the gene-associated histones and that this induced increase in acetylation is gene selective^[66]. These studies also suggest that p21^{WAF1} is HDAC inhibitor and that the p21^{WAF1} promoter is a useful model for study in histone acetylation regulated transcription.

In addition, MS-27-275 inhibits HDAC and causes hyperacetylation of histones, as well as induces the expression of p21^{WAF1} various tumor cell lines^[33].

The data above indicated that the induction of histone hyperacetylation by HDAC inhibitor is responsible for the antiproliferative activity through the crucial role of p21^{WAF1} in the regulation of cell cycle.

PATHWAY OR FACTORS ASSOCIATED TO ACETYLATION OF p21^{WAF1}

Several genes or transcriptional regulatory proteins including p300/CBP associate to p21^{WAF1} gene regulation.

p53

The p21^{WAF1} expression may be dependent^[11,67] or independent of p53 regulation^[68-70]. Also, the mechanisms of p21^{WAF1} transcription

regulation fall into two general categories: dependent or independent of the p53 gene^[31]. The p21^{WAF1} promoter contains five natural p53 binding sites, at positions 4001, 3764, 2311, 2276, and 1391, respectively (GenBank accession number U24170)^[19].

p53 gene regulates the expression of p21^{WAF1}, and HDAC1,2, and 3 are all capable of downregulating p53 function, i.e., interactions of p53 and HDAC2 likely result in p53 deacetylation, thereby reducing its transcriptional activity^[71]. Clark and co-workers found that loss of the G1/S checkpoint in HIV-1-infected cells may in part be due to Tat's ability to bind p53 and sequester its transactivation activity, as seen in both in vivo and in vitro transcription assays^[72].

p21^{WAF1} overexpression has been seen to inhibit two critical checkpoints in the cell cycle, G1 and G2, through both p53-dependent and -independent^[74].

p300/CBP

Up to now, four families of nuclear proteins including p300/CBP and p300/CBP-associated cofactors contain an intrinsic HAT activity have been confirmed that possess HAT activity^[74-78]. Accumulating evidences suggest that p300 and CBP are adaptors for various DNA-binding transcription factors^[79]. Although the precise mechanism by which p300/CBP stimulates transcription remains unclear, the discovery that p300/CBP and an associated factor P/CAF have histone acetylase activities suggests that these cofactors may regulate transcription through acetylation^[80]. These activities have been proposed to modify the amino-terminal tails of the core histone proteins in a manner that may allow for some as yet uncharacterized modification of nucleosome structure.

p300 has been found to be required for induction of p21^{WAF1} expression in keratinocyte differentiation^[70]. Xiao and coworkers indicated the evidences that p300 is required for TSA-induced, Sp1-mediated p21^{WAF1} transcription: cotransfection of p300 elevated p21^{WAF1} promoter activity, and this elevation was dependent on TSA-responsive GC-box; TSA-induced promoter activation was blocked by the introduction of p300 dominant-negative mutant into cells; Sp1- or Sp3-mediated activation was also suppressed by this p300 dominant-negative mutant^[28]. Owen *et al*^[81] demonstrated the progesterone regulated transcription of the p21^{WAF1} gene through Sp1 and CBP/p300. A report^[82] showed that p21^{WAF1} stimulated trans-activation by p300/CBP, p21^{WAF1} induction of p300 results from the activity of a discrete domain in the amino-terminal half of the protein which functioned to repress transcription. they proposed a model in which p300/CBP activity might switched between promoters following p21^{WAF1} induced cell cycle arrest.

P/CAF and GCN5

Two human homologs of GCN5 have been cloned and shown to have HAT activity^[83,84]. One homolog is human p300/CBP associated factor (hP/CAF), which is a transcriptional co-activator with intrinsic histone acetylase activity, which contributes to transcriptional activation by modifying chromatin and transcriptional factors^[84,95]. The second family member is hGCN5^[85,86]. The ability of hGCN5 to acetylate nucleosomal histones is significantly reduced relative to its activity on free histones, where it predominantly modifies histone H3 at lysine 14.

The co-activator/adaptor protein GCN5 is a conserved histone acetyltransferase, which functions as the catalytic subunit in multiple yeast transcriptional regulatory complexes.

E2A

E2A gene encodes two alternatively spliced products, E12 and E47^[87,88]. The p21^{WAF1} promoter contains eight putative E-box consensus sequences, two of which lie between the TATA box and the transcription starting site, E2 and E1 (as Figure 2). E1 binds E47 hetero- and homodimers and E2 has much less affinity for E47^[89], and

TATA box E Boxes

TATATCAGGGCCG

CGCTGAGCTGCGCCCAGCTGAGGTGTGAGCAGCTGCCGAAGTCAGT

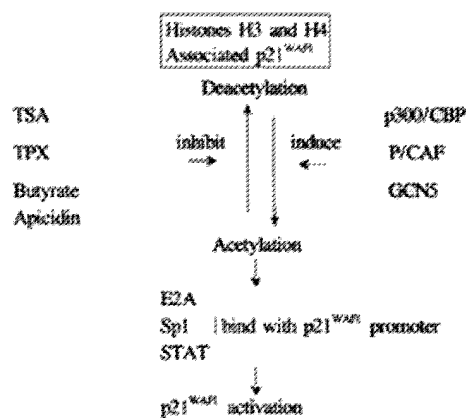
E2 E1 | →+1

The E3 box located 130 bp upstream from the TATA box also contributes to the activation of p21^{WAF1} expression, but the E4 to E8 boxes have no effect on p21^{WAF1} expression^[89]. E2A is shown to be upregulated in HTLV-1 in infected T cells.

The GC-rich region in the six consecutive Sp1 binding sites of the p21^{WAF1} promoter was digested either with methylation-sensitive HpaII or with methylation-insensitive MspI. The resulting DNA was subjected to a PCR reaction. Sp1 binding sites are the common elements that exist in the promoters of both genes^[20]. Using transient reporter gene assays, Pagliuca et al^[94] determined that Sp1 was a strong activator of p21^{WAF1} promoter, whereas Sp3 functioned as a weak transactivator.

In addition to its role in cell cycle regulation, p21^{WAF1} is also believed to inhibit DNA replication through its ability to bind proliferating cell nuclear antigen (PCNA), which is required for both replicative DNA synthesis and DNA repair. However, p21^{WAF1} has no inhibitory effect on the DNA repair function of PCNA^[100,101]. Thus, p21^{WAF1} may play a central role in preventing the replication of mutations incurred after exposure of cells to DNA damage.

Histone acetylation is the major mechanism for regulation of the p21^{WAF1} gene in most cell lines (shown as Figure 3). Both histone hyperacetylation and hypoacetylation appear to be important in the carcinoma process. The influence of methylation on p21^{WAF1} gene expression is dependent on differentiation of cells and tissue. It is our anticipation that induction of the p21^{WAF1} gene by histone hyperacetylation may become a mechanism of dietary prevention of carcinogenesis.



- 1 Norbury C, Nurse P. Animal cell cycles and their control. *Ann Rev Biochem* 1992; 61: 441-470
- 2 Marx J. How cells cycle toward cancer. *Science* 1994; 263: 319-321
- 3 Elledge SJ, Winston J, Harper JW. A question of balance: the role of cyclin-kinase inhibitors in development and tumorigenesis. *Trends Cell Biol* 1996; 6: 388-392
- 4 Sherr CJ, Roberts JM. Inhibitors of mammalian G1 cyclin-dependent kinase. *Genes Dev* 1995; 9: 1149-1163
- 5 Hall M, Bates S, Peters G. Evidence for different mode of action of cyclin-dependent kinase inhibitors: p15 and p16 bind to kinase, p21 and p27 bind to cyclins. *Oncogene* 1995; 11: 1581-1588
- 6 Chen J, Saha P, Kornbluth S, Dynlacht BD, Dutta A. Cyclin-binding motifs are essential for the function of p21CIP1. *Mol Cell Biol* 1996; 16:

- 4673-4682
- 7 Matsuoka S, Edwards MC, Bai C, Parker S, Zhang P, Baldini A, Harper JW, Elledge SJ. p57KIP2, a structurally distinct member of the p21CIP1 Cdk inhibitor family, is a candidate tumor suppressor gene. *Genes Dev* 1995; 9: 650-662
 - 8 Polyak K, Lee MH, Erdjument-Bromage H, Koff A, Roberts JM, Tempst P, Massague J. Cloning of p27Kip1, a cyclin-dependent kinase inhibitor and potential mediator of extracellular antimitogenic signals. *Cell* 1994; 78: 59-66
 - 9 Kim JS, Lee S, Lee T, Lee YW, Trepel JB. Transcriptional activation of p21^{WAF1/CIP1} by apicidin, a novel histone deacetylase inhibitor. *Biochem Biophys Res Comm* 2001; 281: 866-871
 - 10 Gu Y, Turck CW, Morgan DO. Inhibition of CDK2 activity *in vivo* by an associated 20 Kregulatory subunit. *Nature* 1993; 366: 707-710
 - 11 el-Deiry WS, Tokino T, Velculescu VE, Levy DB, Parson R, Trent JM, Li n D, Mercer WE, Kinzler KW, Vogelstein B. WAF1, a potential mediator of p53 tumor suppression. *Cell* 1993; 75: 817-825
 - 12 Prowse DM, Bolgan L, Molnar A, Dotto GP. Involvement of the Sp3 transcription factor in induction of p21Cip1/WAF1 in keratinocyte differentiation. *J Biol Chem* 1997; 272: 1308-1314
 - 13 Schwaller J, Koeffler HP, Niklaus G, Loetscher P, Nagel S, Fey MF, Tobler A. Posttranscriptional stabilization underlies p53-independent induction of p21^{WAF1/CIP1/SDI1} in differentiating human leukemic cells. *J Clin Invest* 1995; 95: 973-979
 - 14 Esposito F, Cuccovillo F, Vanoni M, Cimino F, Anderson CW, Appella E, Russo T. Redox-mediated regulation of p21(waf1/cip1) expression involves a post-transcriptional mechanism and activation of the mitogen-activated protein kinase pathway. *Eur J Biochem* 1997; 245: 730-737
 - 15 Stander M, Naumann U, Wick W, Weller M. Transforming growth factor-(and p21: multiple molecular targets of decorin-mediated suppression of neoplastic growth. *Cell Tissue Res* 1999; 296: 221-227
 - 16 Wang LG, Liu XM, Kreis W, Budman DR. The effect of antimicrotubule agents on signal transduction pathways of apoptosis: a review. *Cancer Chemother Pharmacol* 1999; 44: 355-361
 - 17 Datto MB, Yu Y, Wang XF. Functional analysis of the transforming growth factor beta responsive elements in the WAF1/Cip1/p21 promoter. *J Biol Chem* 1995; 270: 28623-28628
 - 18 Parker SF, Perkins ND, Gitlin SD, Nabel GJ. A cooperative interaction of human T-cell leukemia virus type 1 Tax with the p21 cyclin-dependent kinase inhibitor activates the human immunodeficiency virus type 1 enhancer. *J Virol* 1996; 70: 5731-5734
 - 19 de la Fuente C, Santiago F, Chong SY, Deng L, Mayhoo T, Fu P, Stein D, Denny T, Coffman F, Azimi N, Mahieux R, Kashanchi F. Overexpression of p21^{WAF1} in Human T-Cell Lymphotropic Virus Type 1-Infected Cells and Its Association with Cyclin A/cdk2. *J Virol* 2000; 74: 7270-7283
 - 20 Shin JY, Kim HS, Park J, Park JB, Lee JY. Mechanism for Inactivation of the KIP Family Cyclin-dependent Kinase Inhibitor Genes in Gastric Cancer Cells. *Cancer Res* 2000; 60: 262-265
 - 21 Strahl BD, Allis CD. The language of covalent histone modifications. *Nature* 2000; 403: 41-45
 - 22 Adams RL, McKay EL, Craig LM, Burdon RH. Mouse DNA methylase: methylation of native DNA. *Biochem. Biophys Acta* 1979; 561: 345-357
 - 23 Yeivin A, Razin A. Gene methylation patterns and expression. *EXS* 1993; 64: 523-568
 - 24 Baylin SB, Herman JG, Graff JR, Vertino PM, Issa JP. Alterations in DNA methylation: a fundamental aspect of neoplasia. *Adv Cancer Res* 1998; 72: 141-196
 - 25 Gu W, Roeder RG. Activation of p53 sequence-specific DNA binding by acetylation of the p53 C-terminal domain. *Cell* 1997; 90: 595-606
 - 26 Struhl K. Histone acetylation and transcriptional regulatory mechanism. *Genes Dev* 1998; 12: 599-606
 - 27 Taunton J, Hassig CA, Schreiber SL. A mammalian histone deacetylase related to the yeast transcriptional regulator Rpd3p. *Science* 1996; 272: 408-411
 - 28 Xiao H, Hasegawa T, Isobe K. p300 collaborates with Sp1 and Sp3 in p21^{WAF1/CIP1} promoter activation induced by histone deacetylase inhibitor. *J Biol Chem* 2000; 275: 1371-1376
 - 29 Xiao H, Hasegawa T, Isobe K. Both sp1 and sp3 are responsible for p21waf1 promoter activity induced by histone deacetylase inhibitor in H1H3t3 cells. *J Cell Biochem* 1999; 73: 291-302
 - 30 Sambucetti LC, Fischer DD, Zabudoff S, Kwon PO, Chamberlin H, Trogani N, Xu H, Cohen D. Histone deacetylase inhibition selectively alters the activity and expression of cell cycle proteins leading to specific chromatin acetylation and antiproliferative effects. *J Biol Chem* 1999; 274: 34940-34947
 - 31 Archer SY, Hodin RA. Histone acetylation and cancer. *Current Opin*
 - 32 Siavoshian S, Segain JP, Kornprobst M, Bonnet C, Cherbut C, Galmiche JP, Blottiere HM. Butyrate and trichostatin A effects on the proliferation/differentiation of human intestinal epithelial cells: induction of cyclin D3 and p21 expression. *Gut* 2000; 46: 507-514
 - 33 Saito A, Yamashita T, Mariko Y, Nosaka Y, Tsuchiya K, Ando T, Suzuki T, Tsuruo T, Nakanishi O. A synthetic inhibitor of histone deacetylase, MS-27-2 75, with marked *in vivo* antitumor activity against human tumors. *Proc Natl Acad Sci U S A* 1999; 96: 4592-4597
 - 34 Vettese-Dadey M, Grant PA, Hebbes TR, Crane- Robinson C, Allis CD, Workman JL. Acetylation of histone H4 plays a primary role in enhancing transcription factor binding to nucleosomal DNA *in vitro*. *EMBO J* 1996; 15: 2508-2518
 - 35 Bird AP, Wolffe AP. Methylation-induced repression-belts, braces, and chromatin. *Cell* 1999; 99: 451-454
 - 36 Wade PA, Wolffe AP. Histone acetyltransferases in control. *Curr Biol* 1997; 7: R82-R84
 - 37 Workman JL, Kingston RE. Alteration of nucleosome structure as a mechanism of transcriptional regulation. *Annu Rev Biochem* 1998; 67: 545-579
 - 38 Ng HH, Zhang Y, Hendrick B, Johnson CA, Turner BM, Erdjument-Bromage H, Tempst P, Reinberg D, Bird A. MBD2 is a transcriptional repressor belonging to the MeCP1 histone deacetylase complex. *Nat Genet* 1999; 23: 58-61
 - 39 Jeppesen P, Turner BM. The inactive X chromosome in female mammals is distinguished by a lack of histone H4 acetylation, a cytogenetic marker for gene expression. *Cell* 1993; 74: 281-289
 - 40 Kass SU, Landsberger N, Wolffe AP. DNA methylation directs a time-dependent repression of transcription initiation. *Curr Biol* 1997; 7: 157-165
 - 41 Schubeler D, Lorincz MC, Cimbor DM, Telling A, Feng YQ, Bouhassira EE, Groudine M. Genomic targeting of methylated DNA: influence of methylation on transcription, replication, chromatin structure, and histone acetylation. *Mol Cell Biol* 2000; 20: 9103-9112
 - 42 Zhang Y, Ng HH, Erdjument-Bromage H, Tempst P, Bird A, Reinberg D. An analysis of the NuRD subunits reveals a histone deacetylase core complex and a connection with DNA methylation. *Genes Devel* 1999; 13: 1924-1935
 - 43 Wade PA, Geggion A, Jones PL, Ballestar E, Aubry F, Wolffe AP. Mi-2 complex couples DNA methylation to chromatin remodeling and histone deacetylation. *Nat Genet* 1999; 23: 62-66
 - 44 Rountree MR, Bachman KE, Baylin SB. DNMT1 binds HDAC2 and a new co-repressor, DMAP1, to form a complex at replication foci. *Nat Genet* 2000; 25: 269-276
 - 45 Fuks F, Burgers WA, Brehm A, Hughes-Davies L, Kouzarides T. DNA methyltransferase DNMT1 associates with histone deacetylase activity. *Nat Genet* 2000; 24: 88-91
 - 46 Baylin SB. Tying it all together: epigenetics, genetics, cell cycle, and cancer. *Science* 1997; 277: 1948-1949
 - 47 Chuang LS, Ian HI, Koh TW, Ng HH, Xu G, Li BFL. Human DNA-(Cytosine-5) methyltransferase-PCNA complex as a target for p21^{WAF1}. *Science* 1997; 277: 1996-2000
 - 48 Nass SJ, Ferguson AT, El-Ashry D, Nelson WG, Davidson NE. Expression of DNA methyltransferase (DMT) and the cell cycle in human breast cancer cells. *Oncogene* 1999; 18: 7453-7461
 - 49 Balbin M, Hannon GJ, Pendas AM, Ferrando AA, Vizoso F, Fueyo A, Lopez-Otin C. Functional analysis of a p21^{WAF1}, CIP1, SDI1 mutant (Arg94Trp) identified in a human breast carcinoma. Evidence that the mutation impairs the ability of p21 to inhibit cyclin-dependent kinases. *J Biol Chem* 1996; 271: 15782-15786
 - 50 Malkowicz SB, Tomaszewski JE, Linnenbach AJ, Cangiano TA, Maruta Y, McGarvey TW. Novel p21^{WAF1/CIP1} mutations in superficial and invasive transitional cell carcinomas. *Oncogene* 1996; 13: 1831-1837
 - 51 Shiohara M, el-Deiry WS, Wada M, Nakamaki T, Takeuchi S, Yang R, Chen DL, Vogelstein B, Koeffler HP. Absence of WAF1 mutations in a variety of human malignancies. *Blood* 1994; 84: 3781-3784
 - 52 Maki CG, Howley PM. Ubiquitination of p53 and p21 is differentially affected by ionizing and UV radiation. *Mol Cell Biol* 1997; 17: 355-363
 - 53 Periyasamy S, Ammanamanchi S, Tillekeratne MP, Brattain MG. Repression of transforming growth factor-beta receptor type I promoter expression by Sp1 deficiency. *Oncogene* 2000; 19: 4660-4667
 - 54 Ling CC, Guo M, Chen CH, Deloherey T. Radiation-induced apoptosis: effects of cell age and dose fractionation. *Cancer Res* 1995; 55: 5207-5212
 - 55 Allan LA, Duhig T, Read M, Fried M. The p21^{WAF1/CIP1} Promoter Is Methylated in Rat-1 Cells: Stable Restoration of p53-Dependent p21^{WAF1/CIP1} Expression after Transfection of a Genomic Clone Containing the p21^{WAF1/CIP1} Gene. *Mol Cell Biol* 2000; 20: 1291-1298

- 56 Chen B, He L, Savell VH, Jenkins JJ, Parham DM. Inhibition of the interferon- γ /signal transducers and activators of transcription (STAT) pathway by hypermethylation at a STAT-binding site in the p21^{WAF1} promoter region. *Cancer Res* 2000; 60: 3290-3298
- 57 Chen B, Liu X, Savell VH, Dilday BR, Johnson MW, Jenkins JJ, Parham DM. Increased DNA methyltransferase expression in rhabdomyosarcomas. *Int J Cancer* 1999; 83: 10-140
- 58 Young JJ, Smith JR. DNA methyltransferase inhibition in normal human fibroblasts induces a p21-dependent cell cycle withdrawal. *J Biol Chem* 2001; 276: 19610-19616
- 59 Milutinovic S, Knox JD, Szyf M. DNA methyltransferase inhibition induces the transcription of the tumor suppressor p21^{WAF1/CIP1}/sdi1. *J Biol Chem* 2000; 275: 6353-6359
- 60 Fournel M, Sapieha P, Beaulieu N, Besterman JM, MacLeod AR. Down-regulation of human DNA-(cytosine-5) methyltransferase induces cell cycle regulatory p16ink4A and p21^{WAF1}/Cip1 by distinct mechanisms. *J Biol Chem* 1999; 274: 24250-24256
- 61 De Marzo AM, Marchi VL, Yang ES, Veeraswamy R, Lin X, Nelson WG. Abnormal Regulation of DNA Methyltransferase Expression during Colorectal Carcinogenesis. *Cancer Res* 1999; 59: 3855-3860
- 62 Itazaki H, Nagashima K, Sugita K, Yoshida H, Kawamura Y, Yasuda Y. Isolation and structural elucidation of new cyclotetrapeptides, trapoxins A and B, having detransformation activities as antitumor agents. *J Antibiot* 1990; 12: 1524-1532
- 63 Demary K, Wong L, Spanjaard RA. Effects of retinoic acid and sodium butyrate on gene expression, histone acetylation and inhibitor of proliferation of melanoma cells. *Cancer Lett* 2001; 163:103-107
- 64 Han JW, Ahn SH, Park SH, Wang YS, Bae GU, Seo DW, Kwon HK, Hong S, Lee HY, Lee YW, Lee HW. Apicidin, a Histone deacetylase inhibitor, inhibits proliferation of tumor cells via induction of p21^{WAF1}/Cip1 and Gelsolin. *Cancer Res* 2000;60:6068-6074
- 65 DiGiuseppe JA, Weng LJ, Yu KH, Fu S, Kastan MB, Samid D, Gore SD. Phenylbutyrate-induced G1 arrest and apoptosis in myeloid leukemia cells: structure-function analysis. *Leukemia* 1999; 13: 1243-1253
- 66 Richon VM, Sandhoff TW, Rifkind RA, Marks PA. Histone deacetylase inhibitor selectively induces p21^{WAF1} expression and gene-associated histone acetylation. *Proc Natl Acad Sci U S A* 2000; 97:10014-10019
- 67 el-Deiry WS, Tokino T, Waldman T, Oliner JD, Velculescu VE, Burrell M, Hill DE, Healy E, Rees JL, Hamilton SR. Topological control of p21^{WAF1/CIP1} expression in normal and neoplastic tissues. *Cancer Res* 1995; 55: 2910-2919
- 68 Halevy O, Novitch BG, Spicer DB, Skapek SX, Rhee J, Hannon GJ, Beach D, Lassar ABL. Correlation of terminal cell cycle arrest of skeletal muscle with induction of p21 by MyoD. *Science* 1995; 267: 1018-1021
- 69 Parker SB, Eichele G, Zhang P, Rawla A, Sands AT, Bradley A, Olson EN, Harper JW, Elledge SJ. p53-independent expression of p21Cip1 in muscle and other terminally differentiating cells. *Science* 1995; 67: 1024-1027
- 70 Missero C, Calautti E, Eckner R, Chin J, Tsai LH, Livingston DM, Dotto GP. Involvement of the cell-cycle inhibitor Cip1/WAF1 and the E1A-associated p300 protein in terminal differentiation. *Proc Natl Acad Sci U S A* 1995; 92: 5451-5455
- 71 Juan LJ, Shia WJ, Chen MH, Yang WM, Seto E, Lin YS, Wu CW. Histone deacetylases specifically down-regulate p53-dependent gene activation. *J Biol Chem* 2000; 275: 20436-20443
- 72 Clark E, Santiago F, Deng L, Chong S, de la Fuente C, Wang L, Fu P, Stein D, Denny T, Lanka V, Mozafari F, Okamoto T, Kashanchi F. Loss of G1/S Checkpoint in Human Immunodeficiency Virus Type 1-Infected Cells Is Associated with a Lack of Cyclin-Dependent Kinase Inhibitor p21/Waf1. *J Virol* 2000; 74: 5040-5052
- 73 Macleod KF, Sherry N, Hannon G, Beach D, Tokino T, Kinzler K, Vogelstein B, Jacks T. p53-dependent and independent expression of p21 during cells growth, differentiation, and DNA damage. *Genes Dev* 1995; 9: 935-944
- 74 Bannister AJ, Kouzarides T. The CBP (CREB binding protein) coactivator is a histone acetyltransferase. *Nature* 1996; 384: 641-643
- 75 Parekh BS, Maniatis T. Virus infection leads to localized hyperacetylation of histones H3 and H4 at the IFN- γ promoter. *Mol Cell* 1999; 3: 125-129
- 76 Torchia J, Rose DW, Inostroza J, Kamei Y, Westin S, Glass CK, Rosenfeld MG. The transcriptional co-activator p/CIP binds CBP and mediates nuclear receptor function. *Nature* 1997; 387: 677-684
- 77 Yang X, Herrmann CH, Rice AP. The human immunodeficiency virus Tat proteins specifically associate with TAK in vivo and require the carboxy-terminal domain of RNA polymerase II for function. *J Virol* 1996; 70: 4576-4584
- 78 Ogryzko VV, Schiltz RL, Russanova V, Howard BH, Nakatani Y. The transcriptional coactivators p300 and CBP are histone acetyltransferases. *Cell* 1996; 87: 953-959
- 79 Janknecht R, Hunter T. Transcription. A growing coactivator network. *Nature* 1996; 383: 22-23
- 80 Martinez-Balbas MA, Bauer UM, Nielsen SJ, Brehm A, Kouzarides T. Regulation of E2F1 activity by acetylation. *EMBO J* 2000; 19: 662-671
- 81 Owen GI, Richer JK, Tung L, Takimoto G, Horwitz. Progesterone regulates transcription of the p21^{WAF1} cyclin-dependent kinase inhibitor gene through Sp1 and CBP/p300. *J Biol Chem* 1998; 273: 10696-10701
- 82 Snowden AW, Anderson LA, Webster GA, Perkins ND. A novel transcriptional repression domain mediates p21^{WAF1/CIP1} induction of p300 transactivation. *Mol Cell Biol* 2000; 20: 2676-2686
- 83 Candau R, Moore PA, Wang L, Barlev N, Ying CY, Rosen CA, Berger SL. Identification of human proteins functionally conserved with the yeast putative adaptors ADA2 and GCN5. *Mol Cell Biol* 1996; 16: 593-602
- 84 Yang XJ, Ogryzko VV, Nishikawa J, Howard BH, Nakatani Y. A p300/CBP-associated factor that competes with the adenoviral oncoprotein E1A. *Nature* 1996; 382: 319-324
- 85 Schiltz RL, Nakatani Y. The PCAF acetylase complex as a potential tumor suppressor. *Biochim. Biophys. Acta* 2000; 1470: M37-M53
- 86 Smith ER, Belote JM, Schiltz RL, Yang XJ, Moore PA, Berger SL, Nakatani Y, Allis CD. Cloning of Drosophila GCN5: conserved features among metazoan GCN5 family members. *Nucleic Acids Res* 1998;26:2948-2954
- 87 Mahajan MA, Park ST, Sun XH. Association of a novel GTP-binding protein, DRG, with TAL oncogenic proteins. *Oncogene* 1996; 12: 2343-2350
- 88 Peverali FA, Ramqvist T, Saffrich R, Pepperkok R, Barone MV, Phillipson L. Regulation of G1 progression of E2A and Id helix-loop-helix proteins. *EMBO J* 1994; 13: 4291-4301
- 89 Prabhu S, Ignatova A, Park ST, Sun XH. Regulation of the expression of cyclin-dependent kinase inhibitor p21 by E2A and Id proteins. *Mol Cell Biol* 1997; 17: 5888-5896
- 90 Murre C, McCaw PS, Baltimore D. A new DNA binding and dimerization motif in immunoglobulin enhancer binding, daughterless, MyoD and myc proteins. *Cell* 1989; 56: 777-783
- 91 Lania L, Majello B, De Luca P. Transcriptional regulation of the Sp family proteins. *Int J Biochem Cell Biol* 1997; 29: 1313-1323
- 92 Birnbaum MJ, van Wijnen AJ, Odgren PR, Last TJ, Suske G, Stein GS, Stein JL. Sp1 transactivation of cell cycle regulated promoters is selectively repressed by Sp3. *Biochem* 1995; 34: 16503-16508
- 93 Brandeis M, Frank D, Keshet I, Siegfried Z, Medelsohn M, Nemes A, Tempel V, Razin A, Cedar H. Sp1 elements protect a CpG island from de novo methylation. *Nature* 1994; 371: 435-438
- 94 Pagliuca A, Gallo P, Lania L. Differential role for Sp1/Sp3 transcription factors in the regulation of the promoter activity of multiple cyclin-dependent kinase inhibitor genes. *J Cell Biochem* 2000; 76: 360-367
- 95 Periyasamy S, Ammanamanchi S, Tillekeratne MP, Brattain MG. Repression of transforming growth factor-beta receptor type I promoter expression by Sp1 deficiency. *Oncogene* 2000;19:4660-4667
- 96 Hagen G, Muller S, Beato M, Suske G. Cloning by recognition site screening of two novel GT box binding proteins: A family of Sp1 related genes. *Nuclear Acids Res* 1992; 20: 5519-5525
- 97 Horvath CM, Wen Z, Darnell JE Jr. A STAT protein domain that determines DNA sequence recognition suggests a novel DNA-binding domain. *Genes Dev* 1995; 9: 984-994
- 98 Chin YE, Kitagawa M, Su WC, You ZH, Iwamoto Y, Fu XY. Cell growth arrest and induction of cyclin-dependent kinase inhibitor p21 WAF1/CIP1 mediated by STAT1. *Science* 1996; 272: 719-722
- 99 Darnell JE, Jr. STATs and gene regulation. *Science* 1997; 277: 1630-1635
- 100 Li R, Waga S, Hannon GJ, Beach D, Stillman B. Differential effects by the p21 CDK inhibitor on PCNA-dependent DNA replication and repair. *Nature* 1994; 371: 534-537
- 101 Waga S, Hannon GJ, Beach D, Stillman B. The p21 inhibitor of cyclin-dependent kinases controls DNA replication by interaction with PCNA. *Nature* 1994; 369: 574-578

Edited by Wu XN

• REVIEW •

Influencing factors of pancreatic microcirculatory impairment in acute pancreatitis

Zong-Guang Zhou, You-Dai Chen

Zong-Guang Zhou, You-Dai Chen, Department of Hepato-bilio-pancreatic Surgery & Institute of Microcirculation, West China Hospital, Sichuan University, Chengdu 610041, Sichuan Province, China

Correspondence to: Dr. Zong-Guang Zhou, Department of Hepato-bilio-pancreatic Surgery & Institute of Microcirculation, West China Hospital, Sichuan University, Chengdu 610041, Sichuan Province, China. 258836@mail.guoli.com.cn

Telephone: +86-28-5422484

Received 2001-11-02 Accepted 2001-12-05

Abstract

Pancreatic microcirculatory disturbance plays an important role in the pathogenesis of acute pancreatitis, and it involves a series of changes including vasoconstriction, ischaemia, increased vascular permeability, impairment of nutritive tissue perfusion, ischaemia/reperfusion, leukocyte adherence, hemorrhological changes and impaired lymphatic drainage. Ischaemia possibly acts as an initiating factor of pancreatic microcirculatory injury in acute pancreatitis, or as an aggravating/continuing mechanism. The end-artery feature of the intralobular arterioles suggests that the pancreatic microcirculation is highly susceptible to ischaemia. Various vasoactive mediators, as bradykinin, platelet activating factor, endothelin and nitric oxide participate in the development of microcirculatory failure.

Zhou ZG, Chen YD. Influencing factors of pancreatic microcirculatory impairment in acute pancreatitis. *World J Gastroenterol* 2002;8(3):406-412

INTRODUCTION

Acute pancreatitis remains an important surgical problem with high morbidity and mortality^[1-4]. It is not merely an injury caused by the activated pancreatic enzymes but also involves pancreatic ischaemia. Evidences in basic and clinical research suggest that disturbance of pancreatic microcirculation plays an important role in its pathophysiological processes^[5-14]. The specific local microcirculatory changes cannot be prevented merely by adequate fluid therapy. In recent years, studies with modern molecular biological tools have elucidated that many factors are involved in the development of pancreatic microcirculatory disturbance. Whether the disturbance of pancreatic microcirculation is an initiating factor or as a consequence of progressive pancreatitis is still debatable. The pathophysiological changes of pancreatic microcirculatory disturbance in acute pancreatitis are complex, they include local release of acinar enzymes^[15-25], vasoactive mediators^[26-39], vasoconstriction, increase in vascular permeability, ischaemia^[40-41], ischaemia/reperfusion, leukocyte adherence, intravascular coagulation, capillary stasis, etc., resulting in pancreatic oedema, hemoconcentration, and impaired capillary and venous drainage^[42-44], consequently leading to hemorrhagic pancreatic necrosis^[45].

ROLES OF ISCHAEMIA IN PANCREATIC MICROCIRCULATORY DISTURBANCE DURING ACUTE PANCREATITIS

Ischaemia as an initiating factor

There is a considerable evidence supporting ischaemia as an initiating

factor of pancreatic microcirculatory injury in acute pancreatitis^[46-48]. As long ago as 1862, Panum induced hemorrhagic pancreatitis by injection of wax droplets into pancreatic arteries. Later similar changes were noticed by intra-arterial injection of 8-20µm microspheres, irreversibly obstructing terminal arterioles and occluding the capillaries. While the use of larger particles only results in pancreatic oedema, because there are abundant arcade-like anastomoses between the pancreatic interlobular vessels. There is also evidence suggesting that microvascular injection of microspheres may progress to chronic active pancreatitis.

A clinical report revealed at autopsy that atheromatous thrombi embolized from the aorta into the pancreatic arteries were associated with acute pancreatitis in 10 of 12 cases. The incidence of pancreatitis in 182 patients died after cardiac surgery was 16%. There was also evidence for a high susceptibility of the pancreas to ischaemic injury in patients died of shock. A high incidence of acute pancreatitis shown after cardiopulmonary bypass operations seemed to be associated with intraoperative hypoperfusion in the splanchnic area.

By means of intravital microscopy in conjunction with technique of selected cells-labeling, direct impairments of pancreatic microcirculation in the early phase of acute pancreatitis have been observed in the experimental ischaemia induced by controlled haemorrhage or interruption of arterial blood supply to the pancreas^[49], suggesting the pancreatic microcirculation being highly susceptible to ischaemia. This is closely related to the microvasculature of pancreatic lobule; there is a single centrally-located intralobular artery as the exclusive vascular supply of each lobule, no anastomosis between the intralobular arteries and their branches exists, indicating the cause of its high susceptibility to ischaemia^[50,51].

Ischaemia as an aggravating and continuing mechanism

Temporary complete or partial ischaemia of pancreas would not cause hemorrhagic pancreatic necrosis, the slight histological and functional changes are completely reversible. However, temporary ischaemia has the potential of being transitional from edematous to necrotizing pancreatitis^[52]. While temporary arterial occlusion alone does not injure the pancreas following induction of edematous pancreatitis by duct ligation^[53] with hyperstimulation, arterial occlusion for only 15 min can result in parenchymal necrosis, suggesting that ischaemia as an aggravating factor participates in the development of acute pancreatitis.

Impairment of microcirculatory perfusion of pancreas is the consequence of the effect of various local factors, such as vasoconstriction, free radicals, intravascular coagulation, release of vasoactive mediators taking part in the whole course of acute pancreatitis (see below). Recently, ischaemia/reperfusion is considered one of the important causative factors for development of acute pancreatitis after pancreatic transplantation. It has been repeatedly demonstrated that change of pancreatic perfusion is an early event in experimental acute pancreatitis, and microcirculatory impairment in human pancreas also correlate well with the degree of ischaemic injury. These findings support the hypothesis that the microvasculature is the primary target of reperfusional injury after ischaemia.

CHANGES OF PANCREATIC MICROCIRCULATION IN ACUTE PANCREATITIS

Many indirect methods have been applied to assess the changes of pancreatic microcirculation during acute pancreatitis in previous studies^[54]. Recently, intravital fluorescence microscopy combined with the technique of separate labeled-cells and computerized image analysis system has been successfully used in the studies of pancreatic microcirculation in acute pancreatitis. Many important phenomena as vascular permeability change, vasoconstriction, capillary blood flow, functional capillary density, leukocyte-endothelium interaction, etc., have been continuously and directly observed during the course of acute pancreatitis. It is now believed that microcirculatory changes are important as well as early feature in the pathophysiology of acute pancreatitis^[55].

Vasoconstriction

The first step in the sequence of microcirculatory events in pancreatitis is the constriction of interlobular vessels, especially in the proximal segments of the interlobular arterioles and venules^[56,57]. The vasoconstriction occurring in the early phase of acute pancreatitis may cause ischaemia and stasis of the microcirculation^[58], which can be prevented by the radical scavengers, superoxide dismutase and N-(2-mercaptopropionyl)glycine in sodium taurocholate-induced pancreatitis, suggesting that vasoconstriction might be induced by free radicals. There is also great support for the concept that solutions injected into the pancreatic duct to induce biliary pancreatitis exert their effect via the interstitial route. Even at a low injection pressure of 40 cmH₂O, rupture of the ducto-acinar junction is detectable with subsequent fluid extravasation in the interstitial space, where they gain access to the pancreatic microvasculature precipitating vascular spasm. It has been noticed that segmental constriction of pancreatic arteries occurred in bile-induced pancreatitis, and of mesenteric arteries directly exposed to diluted bile. There is also pronounced damage to the pancreatic vessels resulting in haemorrhage, endothelial detachment and thrombosis, as has been shown with the taurocholate, trypsin, and trypsin-digested blood vessels. The vasotoxic effect of these substances was further substantiated by the demonstration that interstitial injection into the omentum precipitates similar changes at the injection site. The finding that stress and shock can convert oedematous to hemorrhagic experimental pancreatitis suggests that catecholamines mediators might participate in the process. Therefore, pancreatic vasoconstriction in acute pancreatitis might be relevant to a variety of factors.

Changes of permeability

The intravital microscopic findings of immediate leakage of the macromolecular plasma marker (FITC-Dextran 70) from the microvasculature into the interstitial tissue, and the scanning electron microscopic evidence of leakage of the cast material through the capillary membrane in the early phase of acute experimental pancreatitis suggest that presence of increased permeability during the disease process. Further experiments demonstrate that permeability changes precede stasis and stasis precedes leukocyte adherence^[59], suggesting that increased vascular permeability and ischaemia are the initial microcirculatory lesions in acute pancreatitis induced by sodium taurocholate leading to haemorrhagic necrosis. The non-specific detergent effect of sodium taurocholate and bile acids in general seems to be responsible for the initial changes due to the direct dissolution of cellular membranes.

Changes of nutritive tissue perfusion

Acute pancreatitis is characterized by impairment of nutritive tissue perfusion as a consequence of gradually decreased capillary blood flow

and functional capillary density^[60]. Reduction of capillary perfusion volume and of functional capillary density has been observed with intravital microscopy and laser-Doppler flowmetry in the experiments of acute pancreatitis. In such experiments, capillaries are progressively excluded from perfusion starting 30min after the induction of pancreatitis, and with only few capillaries remaining perfused after 3h. At the same time, flow through the preferential pathways is maintained. Measurements of pancreatic blood flow during acute pancreatitis have ever yielded conflicting results. Some found no change or even increased blood flow, but most experiments have repeatedly demonstrated decreased total blood flow in acute pancreatitis. The perfusion values with an initial increase followed by a sharp decrease have been observed. Increased pancreatic blood flow is considered as a consequence of vasodilatation in acute inflammation. Because of the tremendous distributional disturbances of the microcirculation in the pancreas, however, measurements of total blood flow of the pancreatitis do not reflect proportionately the pathological status of different local regional perfusion within the pancreas. The pathological states, both the hyperemia and ischaemia, can be found at the same time in the different regions within the pancreas, thus emphasizing the importance of capillary blood flow measurement for accurate evaluation of microcirculatory blood flow changes. In most of the studies the degree of pancreatic hypoperfusion was found to be disproportionately more severe than the decrease in cardiac output at comparable intervals. Moreover it has been shown that a decrease in pancreatic perfusion cannot be prevented by adequate fluid therapy using Ringer's solution even though cardiovascular parameters are stabilized at the baseline level, proposing a specific mechanism of local microcirculatory ischaemic impairment^[61-63].

Impairment of ischaemia/reperfusion and leukocyte adherence

Ischaemia/reperfusion of the pancreas with impairment of the microcirculation has attracted attention both in experimental and clinical studies of acute pancreatitis^[64-73]. Ischaemia/reperfusion leads to the adherence of leukocytes to the vascular endothelium. In parallel with reduction of functional capillary density, an increase of heterogeneity of capillary perfusion has been noted. Primary capillary perfusion failure after onset of reperfusion is a characteristic microcirculatory feature of ischaemia and is called no-reflow phenomenon. Among various stimuli promoting leukocyte-endothelium interaction are ischaemia/reperfusion and formation of oxygen free radicals leading to rolling and adherence of leukocytes, the latter provoking the "reflow/paradox" phenomenon with loss of endothelial integrity and macromolecular leakage as an end result. Enhanced generation of oxygen radicals elicits ischaemia/reperfusion-induced leukocyte infiltration in the tissue, which is instrumental in the progression of acute pancreatitis. Degree of endothelial cell dysfunction and severity of leukocyte adherence is dependent upon the duration of ischaemia and reperfusion. Complete ischaemia/reperfusion of the pancreas induces extensive capillary stasis, i. e. pancreatic microcirculatory failure.

Effect of hemorrhheological changes

Since blood viscosity is the inherent resistance of blood to flow, it is probable that the hemorrhheological changes might be important to acute necrotizing pancreatitis^[74-84]. 188 Wistar rats were studied by measuring hemorrhheological and stereological parameters of pancreatic microvasculature. The results showed that increased blood viscosity, causing red blood cell aggregation with rouleaux formation, and decreased erythrocyte deformability are responsible for pancreatic microcirculatory disturbances and play an important role in the transition of oedematous pancreatitis to necrosis.

It has been noticed that the time points in the course of

experimental acute pancreatitis are extremely variable. This can be explained as investigators with various pancreatitis models, different infused substance, concentration, volume as well as intraductal pressure, the latter may be more important than the others. The high intraductal injection pressure results in an increased leakage of bile and a more generalized distribution in the interstitial space, even immediate hemorrhagic pancreatic necrosis, thus emphasizing the pathophysiological significance of experimental models in acute pancreatitis. In the low-pressure ductal perfusion model the etiological factor and the pathophysiological course are similar to those associated with the disease clinically.

VASOACTIVE MEDIATORS IN ACUTE PANCREATITIS

Bradykinin

Bradykinin probably exerts its influences upon microvessels via several pathways involving endothelial cells, including stimulating the formation and release of NO, arachidonic acid metabolites and tachykinins. Microcirculatory responses to bradykinin are biphasic: at low concentrations it causes vasodilatation, while at higher concentrations it causes vasoconstriction.

The role which bradykinin plays in microcirculatory impairment of acute pancreatitis is controversial. It was noticed that in sodium taurocholate-induced pancreatitis, the number of perfused capillaries was increased and capillary flow preserved and the mean venular leukocyte adherence decreased and histopathological change improved in icatibant (a B2 receptor antagonist)-treated rats; kinase II inhibitor captopril or exogenous bradykinin in addition to an otherwise effective dosage of icatibant resulted in microcirculatory stasis, extensive venular leukocyte adherence and severe histological damage, indicating that bradykinin may aggravate the microcirculatory disturbance^[85,86]. But another study showed that B2 receptor antagonist increased the severity of acute pancreatitis, while lys-bradykinin substituting bradykinin didn't^[87].

Platelet-activating factor(PAF)

PAF acts on microvascular diameter, permeability and leukocyte rolling, adhesion and migration through different mechanisms, including synthesis and release of NO and arachidonic acid metabolites, and upregulated expressions of ICAM-1 and CD11/CD18. Actions of PAF on microvasculature have the following features: constriction response of venules to PAF is stronger than that of the arterioles; its action on arteriolar diameter is biphasic.

It was observed that treatment with PAF receptor antagonist improved pancreatic capillary blood flow, reduced the severity of pancreatitis-associated endothelial barrier compromise and pancreatic leukocyte recruitment, suggesting that PAF is proinflammatory in pancreatitis^[88-92].

Endothelin(ET)

There are three kinds of endothelins, and endothelin-1 is predominantly expressed by vascular endothelial cells. There are three types of endothelin receptors, and ETA receptor is endothelin-1 selective, and found mainly on vascular smooth muscle cells, mediating vasoconstriction; ETB is nonselective and expressed by endothelial cells; it mediates vasodilatation through the release of NO and prostacyclin. The action of endothelin-1 on microvessels is biphasic: at low concentration, it causes vasodilatation; at higher concentration, it causes sustained vasoconstriction.

Several experiments demonstrated that endothelin-1 was involved in the microcirculatory disturbance and in the development and progression of acute pancreatitis^[93-99]. Administration of endothelin-1 after the caerulein injection decreased pancreatic blood flow significantly, aggravating microcirculatory disturbance. Topically

superfused endothelin-1 induced pancreatic microvascular deterioration and acinar cell injury similar to that induced by intraductal infusion of sodium taurocholate in rats^[100]. Studies also showed that ETA receptor antagonist is protective in microcirculatory disturbance of acute pancreatitis^[101].

Nitric oxide (NO)

NO is formed from L-arginine by NO synthase(NOS). cNOS(constitutive form) catalyzes formation of NO of physiological level. Catalytic activity of iNOS(inducible form) is stronger and lasts longer than that of cNOS, and NO of higher than physiological level is produced by iNOS. NO dilates blood vessels, but at higher concentrations it is cytotoxic.

Pancreatic NO level in acute pancreatitis may be decreased^[102] or significantly elevated in different experiments. Intravenous administration of L-arginine to rats with hemorrhagic pancreatitis improved pancreatic blood flow and a meliorated the severity of pancreatitis in a dose-dependent manner, while nitro-L-arginine infusion to the rats with edematous pancreatitis caused a decrease in pancreatic blood flow and exacerbated pancreatitis, indicating that NO is protective^[103-106]. However, some experiments showed that NO was not involved in the progression from edematous to hemorrhagic pancreatitis. Even microcirculatory changes were significantly alleviated in caerulein-induced pancreatitis pretreated with nitro-L-arginine, suggesting NO may be proinflammatory^[107]; it was found that L-arginine improved the pancreatic microcirculation but worsened the microscopic alterations within the pancreas^[108,109].

Adhesion molecules

Leukocyte-endothelial interaction is an important step in the development of acute pancreatitis. It was demonstrated by experiments that levels of ICAM-1, PECAM-1 and ELAM-1 were upregulated, and expressions of P- and E-selectin enhanced, and leukocytes became CD18-positive in acute pancreatitis^[110,111]. Immunoneutralization of adhesion molecules was proven effective in the treatment of acute pancreatitis^[112]. Administration of monoclonal antibody against ICAM-1 to rats with acute severe pancreatitis significantly enhanced capillary blood flow in the pancreas, reduced leukocyte rolling and stabilized capillary permeability^[113].

PATHOGENESIS OF MICROCIRCULATORY FAILURE IN ACUTE PANCREATITIS

The pancreatic microcirculation is impaired in acute pancreatitis^[114-124]. Capillary stasis may be due to a variety of mechanisms including hemoconcentration and intravascular coagulation, generation of oxygen free radicals in the microenvironment of the pancreatic ducto-acinar complex, increase in interstitial pressure, increase in leukocyte-endothelium interaction^[125], and local reduction of endothelial derived relaxation factor (nitrous oxide)^[126]. An acinar abnormality may be the initiating factor arising from a combination of ductal obstruction and exocrine hypersecretion followed by an increase in intraductal pressure and leakage of enzymes into the pancreatic interstitium with release of zymogen and lysozymes.

Hemoconcentration and intravascular coagulation play an additional role in the development of pancreatic ischaemia in acute pancreatitis. The increased capillary permeability is the initial feature of experimental biliary pancreatitis, resulting in loss of fluid and cells into the pancreatic interstitium induced by osmolarity shifts either in the duct or extracellular fluid^[127]. Local hemoconcentration takes place at the site of plasma sequestration, even if the systemic hematocrit is maintained at the initial level. In conjunction with the impairment of endothelium, intravascular coagulation occurs and causes a further decrease of blood fluidity. These changes are

aggravated by a systemic hypercoagulability in acute pancreatitis, probably due to thromboplastic material and activated trypsin gaining access to the systemic circulation.

The mechanism of oxygen free radical is important in acute pancreatitis of any causes^[128] and is a direct sequel of biliopancreatic reflux at the onset of acute biliary pancreatitis. Besides disintegration of cell membranes by lipid peroxidation, free radicals trigger the extravasation of granulocytes into the surrounding parenchyma representing an early lesion in acute experimental pancreatitis. The initial margination of granulocytes in the capillaries may be a contributing factor in endothelial injury and impairment of capillary perfusion. Oxygen radicals mediate depletion of pancreatic sulphhydryl compounds with changes in both lipid peroxide and oxygen radical scavengers. Serum concentrations of vitamin C, a potent antioxidant, are depleted in acute pancreatitis so that synthetic ascorbic acid derivatives have been used as a free radical scavenger.

Postischemic intensive adherence of leukocytes to the endothelium of the venules and adhesive leukocytes forming plaques partially occluding the lumen of the venules have been observed within the reperfusional period in the experimental acute pancreatitis. This adhesive interaction is largely confined to postcapillary venules. And it is determined by a variety of factors such as expression of adhesion molecules on leukocytes and/or endothelial cells, products of leukocyte (superoxide) and endothelial cell (nitric oxide) activation and physical forces generated by the movement of blood along the vessel wall^[129,130]. The firm adhesion of leukocytes that take place within postcapillary venules may increase the postcapillary pressure more than 200 folds, cause the passive dilatation of the capillaries and microcirculatory stasis. Many studies show that some compounds appear to be effective in reducing or abolishing leukocyte-endothelial cell adhesion, whereas some classical anti-inflammatory drugs such as indomethacin and aspirin actually promote leukocyte adhesion in the venules.

There may also be relation to lymphatic drainage^[131]. Increase in local interstitial pressure as a consequence of obstructed lymph drainage further interferes with pancreatic microperfusion due to the venous outflow impairment. In the early period of acute experimental pancreatitis, dilated lymphatic vessels are visible macroscopically, and further progress of oedema with consequent focal hemorrhagic pancreatic necrosis is possible in case of insufficient lymphatic drainage. Experiment demonstrates that an increase of thoracic duct lymph flow followed by a pronounced and prolonged reduction. Erythrocytes originating from pancreatic interstitial hemorrhages were shown to enter and obstruct the microlymphatics.

CONCLUSIONS

Recent advances in experimental research have helped witness the pathophysiology of acute pancreatitis. The phenomena of microcirculatory changes observed in acute experimental pancreatitis during the past few years gradually underlie the disturbance of the local microcirculation in acute pancreatitis, but several challenges remain. Still some questions remain unexplained concerning the mechanisms: (1) Which is the first event in the pathogenesis of acute pancreatitis? (2) Which factor determines the edematous or hemorrhagic necrotizing pancreatitis in a given experimental or clinical situation? (3) What is the role of impaired distribution of blood supply in early steps of acute pancreatitis? The potential vasoactive mediators responsible for the progression of the disease severity have largely remained subjecting to speculation and debate.

REFERENCES

- Slavin J, Ghaneh P, Sutton R, Hartley M, Rowlands P, Garvey C, Hughes M, Neoptolemos J. Management of necrotizing pancreatitis. *World J Gastroenterol* 2001;7:476-481
- Wu K, Wang BX, Wang XP. Effects of clostridium butyricum on bacterial translocation in rats with acute necrotizing pancreatitis. *Shijie Huaren Xiaohua Zazhi* 2000;8:883-886
- Tu WF, Li JS, Zhu WM, Li ZD, Liu FN, Chen YM, Xu JG, Shao HF, Xiao GX, Li A. Influence of Glutamine and caecostomy/colonic irrigation on gut bacteria/endotoxin translocation in acute severe pancreatitis in pigs. *Shijie Huaren Xiaohua Zazhi* 1999;7:135-138
- Wu CT, Li ZL, Huang XC, Zhang ZL. Effect of Chinese medicine "Qing Yi Tang" and bifidobacterium mixture on intestinal bacterial translocation following acute necrotizing pancreatitis. *Shijie Huaren Xiaohua Zazhi* 1999;7:525-528
- Banks PA. Acute pancreatitis: medical and surgical management. *Am J Gastroenterol* 1994;89(8 Suppl):S78-85
- Kelly DM, McEntee GP, Delaney C, McGeeney KF, Fitzpatrick JM. Temporal relationship of acinar and microvascular changes in caerulein-induced pancreatitis. *Br J Surg* 1993;80:1174-1176
- Bockman DE. Microvasculature of the pancreas. Relation to pancreatitis. *Int J Pancreatol* 1992;12:11-21
- Klar E. Etiology and pathogenesis of acute pancreatitis. *Helv Chir Acta* 1992;59:7-16
- Waldner H. Vascular mechanisms to induce acute pancreatitis. *Eur Surg Res* 1992;24 Suppl 1:62-67
- Wu GD, Wu CW, Xu HB. Qingyitang decoction in treatment of 42 patients with severe acute pancreatitis. *Huaren Xiaohua Zazhi* 1998;6:619-621
- Sweiry JH, Mann GE. Pancreatic microvascular permeability in caerulein-induced acute pancreatitis. *Am J Physiol* 1991;261(4 Pt 1):G685-692
- Kusterer K, Enghofer M, Zendler S, Blochle C, Usadel KH. Microcirculatory changes in sodium taurocholate-induced pancreatitis in rats. *Am J Physiol* 1991;260(2 Pt 1):G346-351
- Klar E, Endrich B, Messmer K. Microcirculation of the pancreas. A quantitative study of physiology and changes in pancreatitis. *Int J Microcirc Clin Exp* 1990;9:85-101
- Wu CT, Li ZL. Anatomy of main pancreatic duct of hybrid dog and acute pancreatitis model. *Shijie Huaren Xiaohua Zazhi* 1999;7:62-63
- Chen HM, Shyr MH, Chen MF. Gabexate mesilate improves pancreatic microcirculation and reduces lung edema in a rat model of acute pancreatitis. *J For mos Med Assoc* 1997;96:704-709
- Gong ZH, Yuan YZ, Lou KX, Tu SP, Zhai ZK, Xu JY. Effects and mechanisms of somatostatin analogues on apoptosis of pancreatic acinar cells in acute pancreatitis in mice. *Shijie Huaren Xiaohua Zazhi* 1999;7:964-966
- Li TZ, Sun SQ, Sun DL. Serological studies on the metabolism of intercellular matrix in human acute pancreatitis. *Huaren Xiaohua Zazhi* 1998;6:1082-1083
- Chen HM, Hwang TL, Chen MF. The effect of gabexate mesilate on pancreatic and hepatic microcirculation in acute experimental pancreatitis in rats. *J Surg Res* 1996;66:147-53
- Huch K, Schmidt J, Schrott W, Sinn HP, Buhr H, Herfarth C, Klar E. Hyperoncotic dextran and systemic aprotinin in necrotizing rodent pancreatitis. *Scand J Gastroenterol* 1995;30:812-816
- Nishiwaki H, Satake K, Hiura A, Umeyama K. Effects of a newly synthesized pancreatic protease inhibitor (PATM) on pancreatic microcirculation in experimental acute pancreatitis. *Gastroenterol Jpn* 1989;24:177-180
- Li ZS, Xu GM, Sun ZX, Jin ZD, Zhou XP, Xie SQ, Li P. Early ERCP and endoscopic treatment in 66 patients with acute pancreatitis. *Huaren Xiaohua Zazhi* 1998;6:150-152
- Li ZS, Qian XD, Xu GM, Sun ZX, Zou XP, Xie SQ. Preventive effect of octreotide on hyperamylasemia and pancreatitis after ERCP. *Huaren Xiaohua Zazhi* 1998;6:617-618
- Kurzanov AN, Titova GP, Vinogradov VA, Aleinik VA, Gerasimov NF. Morphofunctional changes in the pancreas in response to dalargin under normal conditions and in experimental pancreatitis. *Biull Eksp Biol Med* 1988;105:445-447
- Lehtola A, Talja M, Puolakkainen P, Nordling S, Schroder T. Peritoneal lavage combined with volume therapy in porcine hemorrhagic pancreatitis. Effects on hemodynamics, microcirculation, and peritoneal morphology. *Scand J Gastroenterol* 1987;22:559-567
- Yuan YZ, Lou KX, Gong ZH, Tu SP, Zhai ZK, Xu JY. Effects and mechanisms of emodin on pancreatic tissue EGF expression in acute pancreatitis in rats. *Shijie Huaren Xiaohua Zazhi* 2001;9:127-130
- Xia SH, Zhao XY, Guo P, Da SP. Hemocirculatory disorder in dogs with severe acute pancreatitis and intervention of platelet activating factor antagonist. *Shijie Huaren Xiaohua Zazhi* 2001;9:550-554
- Wu CT, Li ZL. Effect of DAO on intestinal damage in acute necrotizing pancreatitis in dogs. *Shijie Huaren Xiaohua Zazhi* 1999;7:64-65

- 28 Zhao HP, Wang WX, Yang CW, Shou NY. Therapeutic effects of naltrexone in plasma endotoxin in experimental acute hemorrhagic necrotizing pancreatitis of rats. *Shijie Huaren Xiaohua Zazhi* 1999;7:400-402
- 29 Qin RY, Zou SQ, Wu ZD, Qiu FZ. Effect of splanchnic vascular perfusion on production of TNF α and OFR in rats with acute hemorrhagic necrotizing pancreatitis. *Huaren Xiaohua Zazhi* 1998; 6:831-833
- 30 Hirano T, Hirano K. Thromboxane A2 receptor antagonist prevents pancreatic microvascular leakage in rats with caerulein-induced acute pancreatitis. *Int J Surg Investig* 1999;1:203-210
- 31 Bhatia M, Saluja AK, Singh VP, Frossard JL, Lee HS, Bhagat L, Gerard C, Steer ML. Complement factor C5a exerts an anti-inflammatory effect in acute pancreatitis and associated lung injury. *Am J Physiol Gastrointest Liver Physiol* 2001;280:G974-978
- 32 Bhatia M, Brady M, Zagorski J, Christmas SE, Campbell F, Neoptolemos JP, Slavin J. Treatment with neutralising antibody against cytokine-induced neutrophil chemoattractant (CINC) protects rats against acute pancreatitis associated lung injury. *Gut* 2000; 47:838-844
- 33 Leung PS, Chan WP, Nobiling R. Regulated expression of pancreatic renin-angiotensin system in experimental pancreatitis. *Mol Cell Endocrinol* 2000;166:121-128
- 34 Gomez-Cambronero L, Camps B, de La Asuncion JG, Cerda M, Pellin A, Pallardo FV, Calvete J, Sweiry JH, Mann GE, Vina J, Sastre J. Pentoxifyline ameliorates cerulein-induced pancreatitis in rats: role of glutathione and nitric oxide. *J Pharmacol Exp Ther* 2000;293: 670-676
- 35 Hirota M, Ogawa M. Shock and its mediators. *Nippon Geka Gakkai Zasshi* 1999;100:667-673
- 36 al-Eryani S, Payer J, Huorka M, Duris I. Etiology and pathogenesis of acute pancreatitis. *Bratisl Lek Listy* 1998;99:303-311
- 37 Plusczyk T, Westermann S, Rathgeb D, Feifel G. Acute pancreatitis in rats: effects of sodium taurocholate, CCK-8, and Sec on pancreatic microcirculation. *Am J Physiol* 1997;272(2 Pt 1):G310-320
- 38 Sakai Y, Hayakawa T, Kondo T, Shibata T, Kitagawa M, Sobajima H, Naruse S, Ohnishi ST. Protective effects of a prostaglandin E1 oligomer on taurocholate-induced rat pancreatitis. *J Gastroenterol Hepatol* 1992;7:591-595
- 39 Vollmar B, Waldner H, Schmand J, Conzen PF, Goetz AE, Habazettl H, Schweiberer L, Brendel W. Oleic acid induced pancreatitis in pigs. *J Surg Res* 1991;50:196-204
- 40 Lehtola A, Kivilaakso E, Puolakkainen P, Karonen SL, Lempinen M, Schroder T. Effects of dextran 70 versus crystalloids in the microcirculation of porcine hemorrhagic pancreatitis. *Surg Gynecol Obstet* 1986; 162:556-562
- 41 Kaplan MH. Pathogenesis of pancreatitis: a unified concept. *Int J Pancreatol* 1986;1:5-8
- 42 Sunamura M, Yamauchi J, Shibuya K, Chen HM, Ding L, Takeda K, Kobari M, Matsuno S. Pancreatic microcirculation in acute pancreatitis. *J Hepatobil Pancreat Surg* 1998;5:62-68
- 43 Plusczyk T, Rathgeb D, Westermann S, Feifel G. Somatostatin attenuates microcirculatory impairment in acute sodium taurocholate-induced pancreatitis. *Dig Dis Sci* 1998;43:575-585
- 44 Schmidt J, Klar E. Etiology and pathophysiology of acute pancreatitis. *Ther Umsch* 1996;53:322-332
- 45 Hoffmann TF, Leiderer R, Waldner H, Arbogast S, Messmer K. Ischemia reperfusion of the pancreas: a new *in vivo* model for acute pancreatitis in rats. *Res Exp Med (Berl)* 1995; 195:125-144
- 46 Sendur R, Pawlik WW. Vascular factors in the mechanism of acute pancreatitis. *Przegl Lek* 1996;53:41-45
- 47 Moolenaar W, Lamers CB. Cholesterol crystal embolization and the digestive system. *Scand J Gastroenterol Suppl* 1991;188:69-72
- 48 Hegewald G, Nikulin A, Gmaz-Nikulin E, Plamenac P, Barenwald G. Ultrastructural changes of the human pancreas in acute shock. *Pathol Res Pract* 1985;179:610-615
- 49 Klar E, Schrott W, Foitzik T, Buhr H, Herfarth C, Messmer K. Impact of microcirculatory flow pattern changes on the development of acute edematous and necrotizing pancreatitis in rabbit pancreas. *Dig Dis Sci* 1994;39:2639-2644
- 50 Zhou ZG, Gao XH. Morphology of pancreatic microcirculation in the monkey: light and scanning electron microscopic study. *Clin Anat* 1995; 8:190-201
- 51 Zhou Z, Zeng Y, Yang P, Cheng Z, Zhao J, Shu Y, Gao X, Yan L, Zhang Z. Structure and function of pancreatic microcirculation. *Shengwu Yiyue Gongchengxue Zazhi* 2001;18:195-200
- 52 Furukawa M, Kimura T, Sumii T, Yamaguchi H, Nawata H. Role of local pancreatic blood flow in development of hemorrhagic pancreatitis induced by stress in rats. *Pancreas* 1993;8:499-505
- 53 Plusczyk T, Westermann S, Bersal B, Menger M, Feifel G. Temporary pancreatic duct occlusion by ethibloc: cause of microcirculatory shutdown, acute inflammation, and pancreas necrosis. *World J Surg* 2001;25:432-437
- 54 Bassi D, Kollias N, Fernandez-del Castillo C, Foitzik T, Warshaw AL, Rattner DW. Impairment of pancreatic microcirculation correlates with the severity of acute experimental pancreatitis. *J Am Coll Surg* 1994;179:257-263
- 55 Banerjee AK, Galloway SW, Kingsnorth AN. Experimental models of acute pancreatitis. *B J Surg* 1994; 81:1096-1103
- 56 Klar E, Werner J. New pathophysiologic knowledge about acute pancreatitis. *Chirurg* 2000;71:253-264
- 57 Onizuka S, Ito M, Sekine I, Tsunoda T, Eto T. Spontaneous pancreatitis in spontaneously hypertensive rats. *Pancreas* 1994;9:54-61
- 58 Skoromnyi AN, Starosek VN. Hemodynamic changes in the liver, kidney, small intestine and pancreas in experimental acute pancreatitis. *Klin Khir* 1998;12:46-48
- 59 Kusterer K, Poschmann T, Friedemann A, Enghofer M, Zendler S, Usadel KH. Arterial constriction, ischemia-reperfusion, and leukocyte adherence in acute pancreatitis. *Am J Physiol* 1993; 265(1 Pt 1): G165-171
- 60 Kerner T, Vollmar B, Menger MD, Waldner H, Messmer K. Determinants of pancreatic microcirculation in acute pancreatitis in rats. *J Surg Res* 1996;62:165-171
- 61 Chen HM, Shyr MH, Ueng SW, Chen MF. Hyperbaric oxygen therapy attenuates pancreatic microcirculatory derangement and lung edema in an acute experimental pancreatitis model in rats. *Pancreas* 1998;17: 44-49
- 62 Klar E, Messmer K, Warshaw AL, Herfarth C. Pancreatic ischaemia in experimental acute pancreatitis: mechanism, significance and therapy. *Br J Surg* 1990;77:1205-1210
- 63 Knol JA, Inman MG, Strodel WE, Eckhauser FE. Pancreatic response to crystalloid resuscitation in experimental pancreatitis. *J Surg Res* 1987;43:387-392
- 64 Obermaier R, Benz S, Kortmann B, Benthues A, Ansoerge N, Hopt UT. Ischemia/reperfusion-induced pancreatitis in rats: a new model of complete normothermic in situ ischemia of a pancreatic tail-segment. *Clin Exp Med* 2001;1:51-59
- 65 Benz S, Bergt S, Obermaier R, Wiessner R, Pfeffer F, Schareck W, Hopt UT. Impairment of microcirculation in the early reperfusion period predicts the degree of graft pancreatitis in clinical pancreas transplantation. *Transplantation* 2001; 27:71:759-763
- 66 Mayer H, Schmidt J, Thies J, Ryschich E, Gebhard MM, Herfarth C, Klar E. Characterization and reduction of ischemia/reperfusion injury after experimental pancreas transplantation. *J Gastrointest Surg* 1999;3:162-166
- 67 von Dobschuetz E, Hoffmann T, Messmer K. Inhibition of neutrophil proteinases by recombinant serpin Lex032 reduces capillary no-reflow in ischemia/reperfusion-induced acute pancreatitis. *J Pharmacol Exp Ther* 1999;290:782-788
- 68 von Dobschuetz E, Hoffmann T, Engelschalk C, Messmer K. Effect of diaspirin cross-linked hemoglobin on normal and postischemic microcirculation of the rat pancreas. *Am J Physiol* 1999;276(6 Pt 1): G1507-1514
- 69 Vollmar B, Janata J, Yamauchi J, Wolf B, Heuser M, Menger MD. Exocrine, but not endocrine, tissue is susceptible to microvascular ischemia/reperfusion injury following pancreas transplantation in the rat. *Transpl Int* 1999;12:50-55
- 70 Benz S, Pfeffer F, Adam U, Schareck W, Hopt UT. Impairment of pancreatic microcirculation in the early reperfusion period during simultaneous pancreas-kidney transplantation. *Transpl Int* 1998;11 Suppl 1:S433-435
- 71 Benz S, Schnabel R, Morgenroth K, Weber H, Pfeffer F, Hopt UT. Ischemia/reperfusion injury of the pancreas: a new animal model. *J Surg Res* 1998;75:109-115
- 72 Hoffmann TF, Leiderer R, Harris AG, Messmer K. Ischemia and reperfusion in pancreas. *Microsc Res Tech* 1997;37:557-571
- 73 Menger MD, Bonkhoff H, Vollmar B. Ischemia-reperfusion-induced pancreatic microvascular injury. An intravital fluorescence microscopic study in rats. *Dig Dis Sci* 1996;41:823-830
- 74 Schmidt J, Huch K, Mithofer K, Hotz HG, Sinn HP, Buhr HJ, Warshaw AL, Herfarth C, Klar E. Benefits of various dextrans after delayed therapy in necrotizing pancreatitis of the rat. *Intensive Care Med* 1996; 22:1207-1213
- 75 Hotz HG, Schmidt J, Ryschich EW, Foitzik T, Buhr HJ, Warshaw AL, Herfarth C, Klar E. Isovolemic hemodilution with dextran prevents contrast medium induced impairment of pancreatic microcirculation in necrotizing pancreatitis of the rat. *Am J Surg* 1995;169:161-166

- 76 Klar E, Foitzik T, Buhr H, Messmer K, Herfarth C. Isovolemic hemodilution with dextran 60 as treatment of pancreatic ischemia in acute pancreatitis. Clinical practicability of an experimental concept. *Ann Surg* 1993;217:369-374
- 77 Yan LN, Lei ZM, Cui XZ, Chen HQ, Yang YT, Li L, Tan JS, Chen LL, Wu HB, Li KL. The role of hemorheologic disturbance in experimental acute pancreatitis. *Huaxi Yike Daxue Xuebao* 1993;24:71-74
- 78 Klar E, Mall G, Messmer K, Herfarth C, Rattner DW, Warshaw AL. Improvement of impaired pancreatic microcirculation by isovolemic hemodilution protects pancreatic morphology in acute biliary pancreatitis. *Surg Gynecol Obstet* 1993;176:144-150
- 79 Schmidt J, Fernandez-del Castillo C, Rattner DW, Lewandowski KB, Messmer K, Warshaw AL. Hyperoncotic ultrahigh molecular weight dextran solutions reduce trypsinogen activation, prevent acinar necrosis, and lower mortality in rodent pancreatitis. *Am J Surg* 1993;165:40-44
- 80 Kusterer K, Enghofer M, Poschmann T, Usadel KH. The effect of somatostatin, gabexate mesilate and dextran 40 on the microcirculation in sodium taurocholate-induced pancreatitis. *Acta Physiol Hung* 1992;80:407-415
- 81 Yan LN, Wei JJ, Wu HG, Chen HQ, Zhong GH, Li L, Chen LL, Li KL, Tan JS. The role of hemorheologic changes in the pathogenesis of acute hemorrhagic necrotizing pancreatitis. *Huaxi Yike Daxue Xuebao* 1990;21:25-29
- 82 Klar E, Herfarth C, Messmer K. Therapeutic effect of isovolemic hemodilution with dextran 60 on the impairment of pancreatic microcirculation in acute biliary pancreatitis. *Ann Surg* 1990;211:346-353
- 83 Aleksandrova NP, Petukhov EB, Riabova SS. Blood rheology and microcirculation in the dynamics of acute experimental pancreatitis. *Biull Eksp Biol Med* 1988;105:106-108
- 84 Becker H, Senninger N. Hemorrhagic pancreatitis: effect of dextran 40 and plasma on microcirculation disorders of the pancreas. *Langenbecks Arch Chir* 1985;365:57-67
- 85 Bloechle C, Kusterer K, Kuehn RM, Schneider C, Knoefel WT, Izbicki JR. Inhibition of bradykinin B2 receptor preserves microcirculation in experimental pancreatitis in rats. *Am J Physiol* 1998; 274(1 Pt 1): G42-51
- 86 Hoffmann T, Kubler J, Messmer K. Bradykinin antagonism in ischemia and reperfusion of the pancreas. *Zentralbl Chir* 1996;121:412-422
- 87 Weidenbach H, Lerch MM, Gress TM, Pfaff D, Turi S, Adler G. Vasoactive mediators and the progression from oedematous to necrotising experimental acute pancreatitis. *Gut* 1995;37:434-440
- 88 Flickinger BD, Olson MS. Localization of the platelet-activating factor receptor to rat pancreatic microvascular endothelial cells. *Am J Pathol* 1999;154:1353-1358
- 89 Foitzik T, Hotz HG, Eibl G, Hotz B, Kirchengast M, Buhr HJ. Therapy for microcirculatory disorders in severe acute pancreatitis: effectiveness of platelet-activating factor receptor blockade vs. endothelin receptor blockade. *J Gastrointest Surg* 1999;3:244-251
- 90 Wang X, Sun Z, Borjesson A, Haraldsen P, Aldman M, Deng X, Leveau P, Andersson R. Treatment with lexipafant ameliorates the severity of pancreatic microvascular endothelial barrier dysfunction in rats with acute hemorrhagic pancreatitis. *Int J Pancreatol* 1999;25: 45-52
- 91 Ji Z, Wang B, Li S. The role of platelet activating factor in mesenterioangial microcirculatory disturbance complicated with acute pancreatitis in rats. *Zhonghua Yixue Zazhi* 1995;75:139-140
- 92 Travis SP, Jewell DP. The role of platelet-activating factor in the pathogenesis of gastrointestinal disease. *Prostagl Leukot Essent Fatty Acids* 1994;50:105-113
- 93 Plusczyk T, Bersal B, Menger MD, Feifel G. Differential effects of ET-1, ET-2, and ET-3 on pancreatic microcirculation, tissue integrity, and inflammation. *Dig Dis Sci* 2001;46:1343-1351
- 94 Foitzik T, Faulhaber J, Hotz HG, Kirchengast M, Buhr HJ. Endothelin mediates local and systemic disease sequelae in severe experimental pancreatitis. *Pancreas* 2001;22:248-254
- 95 Foitzik T, Eibl G, Hotz HG, Faulhaber J, Kirchengast M, Buhr HJ. Endothelin receptor blockade in severe acute pancreatitis leads to systemic enhancement of microcirculation, stabilization of capillary permeability, and improved survival rates. *Surgery* 2000;128:399-407
- 96 Foitzik T, Eibl G, Buhr HJ. Therapy for microcirculatory disorders in severe acute pancreatitis: comparison of delayed therapy with ICAM-1 antibodies and a specific endothelin A receptor antagonist. *J Gastrointest Surg* 2000;4:240-246
- 97 Foitzik T, Hotz HG, Hot B, Kirchengast M, Buhr HJ. Endothelin-1 mediates the alcohol-induced reduction of pancreatic capillary blood flow. *J Gastrointest Surg* 1998;2:379-384
- 98 Foitzik T, Faulhaber J, Hotz HG, Kirchengast M, Buhr HJ. Endothelin receptor blockade improves fluid sequestration, pancreatic capillary blood flow, and survival in severe experimental pancreatitis. *Ann Surg* 1998;228:670-675
- 99 Liu XH, Kimura T, Ishikawa H, Yamaguchi H, Furukawa M, Nakano I, Kinjoh M, Nawata H. Effect of endothelin-1 on the development of hemorrhagic pancreatitis in rats. *Scand J Gastroenterol* 1995;30:276-282
- 100 Plusczyk T, Bersal B, Westermann S, Menger M, Feifel G. ET-1 induces pancreatitis-like microvascular deterioration and acinar cell injury. *J Surg Res* 1999; 85: 301-310
- 101 Liu X, Nakano I, Ito T, Kimura T, Nawata H. Is endothelin-1 an aggravating factor in the development of acute pancreatitis? *Chin Med J (Engl)* 1999;112:603-607
- 102 Shibuya K, Sunamura M, Yamauchi J, Takeda K, Kobari M, Matsuno S. Analysis of the derangement of the pancreatic microcirculation in a rat cerulein pancreatitis model using an intravital microscope system. *Tohoku J Exp Med* 1996; 180: 173-186
- 103 Vollmar B, Janata J, Yamauchi JJ, Menger MD. Attenuation of microvascular reperfusion injury in rat pancreas transplantation by L-arginine. *Transplantation* 1999;67:950-955
- 104 Dobosz M, Hac S, Mionskowska L, Dobrowolski S, Wajda Z. Microcirculatory disturbances of the pancreas in cerulein-induced acute pancreatitis in rats with reference to L-arginine, heparin, and procaine treatment. *Pharmacol Res* 1997;36:123-128
- 105 Dobosz M, Hac S, Wajda Z. Does nitric oxide protect from microcirculatory disturbances in experimental acute pancreatitis in rats? *Int J Microcirc Clin Exp* 1996;16:221-226
- 106 Liu X, Nakano I, Yamaguchi H, Ito T, Goto M, Koyanagi S, Kinjoh M, Nawata H. Protective effect of nitric oxide on development of acute pancreatitis in rats. *Dig Dis Sci* 1995;40:2162-2169
- 107 Dobosz M, Wajda Z, Hac S, Mysliwska J, Mionskowska L, Bryl E, Roszkiewicz A, Mysliwski A. Heparin and nitric oxide treatment in experimental acute pancreatitis in rats. *Forum (Genova)* 1998;8: 303-310
- 108 Dobosz M, Wajda Z, Hac S, Mysliwska J, Bryl E, Mionskowska L, Roszkiewicz A, Mysliwski A. Nitric oxide, heparin and procaine treatment in experimental cerulein-induced acute pancreatitis in rats. *Arch Immunol Ther Exp (Warsz)* 1999;47:155-160
- 109 Hac DS, Mionskowska L, Dobrowolski S, Dymecki D, Makarewicz W, Wajda Z. Microcirculation disorders of the pancreas in cerulein induced acute pancreatitis in rats with regard to nitrogen oxide and heparin. *Wiad Lek* 1997;50(Pt 2):108-114
- 110 Lundberg AH, Granger DN, Russell J, Sabek O, Henry J, Gaber L, Kotb M, Gaber AO. Quantitative measurement of P- and E-selectin adhesion molecules in acute pancreatitis: correlation with distant organ injury. *Ann Surg* 2000; 231: 213-222
- 111 Sunamura M, Shibuya K, Yamauchi J, Matsuno S. Microcirculatory derangement and ischemia of the pancreas. *Nippon Geka Gakkai Zasshi* 1999;100:342-346
- 112 Wang X, Sun Z, Borjesson A, Andersson R. Inhibition of platelet-activating factor, intercellular adhesion molecule 1 and platelet endothelial cell adhesion molecule 1 reduces experimental pancreatitis-associated gut endothelial barrier dysfunction. *Br J Surg* 1999;86: 411-416
- 113 Frossard JL, Saluja A, Bhagat L, Lee HS, Bhatia M, Hofbauer B, Steer ML. The role of intercellular adhesion molecule 1 and neutrophils in acute pancreatitis and pancreatitis-associated lung injury. *Gastroenterology* 1999;116:694-701
- 114 Kaska M, Pospisilova B, Slizova D. Pathomorphological changes in microcirculation of pancreas during experimental acute pancreatitis. *Hepatogastroenterology* 2000;47:1570-1574
- 115 Knoefel WT, Kollias N, Warshaw AL, Waldner H, Nishioka NS, Rattner DW. Pancreatic microcirculatory changes in experimental pancreatitis of graded severity in the rat. *Surgery* 1994;116: 904-913
- 116 Foitzik T, Bassi DG, Fernandez-del Castillo C, Warshaw AL, Rattner DW. Intravenous contrast medium impairs oxygenation of the pancreas in acute necrotizing pancreatitis in the rat. *Arch Surg* 1994;129: 706-711
- 117 Kelly DM, McEntee GP, McGeeney KF, Fitzpatrick JM. Microvasculature of the pancreas, liver, and kidney in cerulein-induced pancreatitis. *Arch Surg* 1993;128:293-295
- 118 Garcia-Cano J, Vazquez Rodriguez de Alba J, Garcia Cabezas J, Diaz-Rubio M. Acute pancreatitis in thrombotic thrombocytopenic purpura. Apropos 2 cases. *An Med Interna* 1992;9:551-553
- 119 Waldner H, Schmand J, Vollmar B, Goetz A, Conzen P, Schweiberer L, Brendel W. Pancreatic circulation in experimental biliary pancreatitis. *Langenbecks Arch Chir* 1990;375:112-118
- 120 Gress TM, Arnold R, Adler G. Structural alterations of pancreatic microvasculature in cerulein-induced pancreatitis in the rat. *Res Exp Med*

- (Berl) 1990;190:401-412
- 121 McEntee G, Leahy A, Cottell D, Dervan P, McGeeney K, Fitzpatrick JM. Three-dimensional morphological study of the pancreatic microvasculature in caerulein-induced experimental pancreatitis. *Br J Surg* 1989;76:853-855
- 122 Nishiwaki H, Satake K, Ko I, Umeyama K. Pancreatic microcirculation in acute pancreatitis of dogs. *Nippon Geka Gakkai Zasshi* 1988;89:238-244
- 123 Nuutinen P, Kivisaari L, Standertskjold-Nordenstam CG, Lempinen M, Schroder T. Microangiography of the pancreas in experimental hemorrhagic pancreatitis. *Eur J Radiol* 1986;6:187-190
- 124 Nuutinen P, Kivisaari L, Standertskjold-Nordenstam CG, Lempinen M, Schroder T. Microangiography of the pancreas in experimental oedemic and haemorrhagic pancreatitis. *Scand J Gastroenterol Suppl* 1986;126:12-17
- 125 Chen HM, Sunamura M, Shibuya K, Yamauchi JI, Sakai Y, Fukuyama S, Mikami Y, Takeda K, Matsuno S. Early microcirculatory derangement in mild and severe pancreatitis models in mice. *Surg Today* 2001;31:634-642
- 126 Menger MD, Plusczyk T, Vollmar B. Microcirculatory derangements in acute pancreatitis. *J Hepatobiliary Pancreat Surg* 2001;8:187-194
- 127 Andre EA, Costa PL, Guarita DR, Meirelles Filho JS, Laudanna AA. Changes in capillary permeability during severe experimental acute pancreatitis in rats. *Rev Hosp Clin Fac Med Sao Paulo* 1996;51:184-188
- 128 Petersson U, Kallen R, Montgomery A, Borgstrom A. Role of oxygen-derived free radicals in protease activation after pancreas transplantation in the pig. *Transplantation* 1998;65:421-426
- 129 Inagaki H, Nakao A, Kurokawa T, Nonami T, Harada A, Takagi H. Neutrophil behavior in pancreas and liver and the role of nitric oxide in rat acute pancreatitis. *Pancreas* 1997;15:304-309
- 130 Toyama MT, Lewis MP, Kusske AM, Reber PU, Ashley SW, Reber HA. Ischaemia-reperfusion mechanisms in acute pancreatitis. *Scand J Gastroenterol Suppl* 1996;219:20-23
- 131 Kul'chitskii KI, Zurnadzhi IN, Blagodarov VN, Bogdanova GI, Shchitov VS, Ponomareva VP. The lymph and blood microcirculatory beds of the pancreas in the early period of experimental acute pancreatitis. *Lik Sprava* 1994;87-89

Edited by Wu XN

Relationship between bilirubin free radical and formation of pigment gallstone

Xiang-Tao Liu, Jian Hu

Xiang-Tao Liu, Jian Hu, Department of Chemical Biology, School of Pharmaceutical Sciences, Peking University, Beijing 100083, China
Supported by the National Natural Science Foundation of China, No. 3880768 and No. 39170719

Correspondence to: Xiang-Tao Liu, Department of Chemical Biology, School of Pharmaceutical Sciences, Peking University, Beijing 100083, China. lxt421@sohu.com

Telephone: +86-010-62091539 Fax: +86-010-62015584

Received 2001-07-19 Accepted 2001-09-04

Abstract

In this paper, we summarize the main progresses made in our group in the field of the mechanism of pigment gallstone formation. It was found that after treatment with free radicals, bilirubin (BR) was changed into free radical itself, and a semiquinone free radical and a superoxide free radical bound with metal were recognized, which was detected by ESR (electron spin resonance). By the means of NMR (nuclear magnetic resonance) and IR (Infra-red spectra), it was postulated that bilirubin polymerized through the reaction between the vinyl group and the hydroxyl group under the attack of free radicals. It was also found that bilirubin free radical were liable to calcify in a kinetic study. Because of its chemical properties, bilirubin free radical was shown to be cytotoxic to hepatocyte, which was demonstrated based on the following facts: induction of phospholipid peroxidation (LPO), leakage of lactate dehydrogenase (LDH) and decrease of glutathione. As to the mechanism of bilirubin-induced cytotoxicity, it was postulated that the main target of bilirubin free radical was the cell membrane, including phospholipid and membrane bound proteins, especially spectrin, a content of cytoskeleton. Based on the results mentioned above, it was deduced that bilirubin free radical is the key factor that initiates and promotes the formation of pigment gallstone, which is consistent with other researches in recent years.

Liu XT, Hu J. Relationship between bilirubin free radical and formation of pigment gallstone. *World J Gastroenterol* 2002;8(3):413-417

INTRODUCTION

For years, gallstone has been nearly the most common illness in digestive system all over the world, especially in China^[1-9], and there are many methods to treat this illness^[10-16], including many Chinese traditional medicines. Although some therapies were successful in the end, the best way to deal with the illness is to prevent it before it occurs. So it is important to clarify the key factors that promote the formation of gallstone. Although there were lots of researches in this field that intended to discover the secrets behind the gallstone^[17-41], there are still lots of phenomena we cannot explain now.

For the mechanism of formation of pigment gallstone, the earliest suggestion came from Maki^[42]. He indicated that bacterial infection induced the hydrolysis of conjugated bilirubin and increased the level of free bilirubin, which was the critical factor for gallstone formation. However, there are many cases of gallstone without bacterial infection. Moreover, the increase of bilirubin concentration

is only an essential condition for the precipitation of bilirubin, but not enough to form stone.

In 1982, Elek *et al*^[43] reported the ESR signal of pigment gallstone. Its intensity varied linearly with quantity of bilirubin. It gave a hint that the formation of pigment gallstone was likely to be linked with free radicals. Recently, a lot of facts indicate that free radicals are the triggers or important links of many diseases. They are relative to cell damages and mutation. In view of the relationship of pigment gallstone with inflammation and accompanying damages of liver, kidney, gastrointestinal system, probably there are certain carriers of free radicals in the circulation and the free radicals cause cell damages. Based on the Elek's experiment, the carrier might be bilirubin. However, we have to illustrate:

Firstly, the attackers during inflammation are superoxide free radicals and hydroxyl radicals, then, how we can link the formation of pigment gallstone to these free radicals.

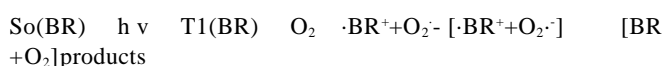
Secondly, whether or not bilirubin free radicals formed in situ during inflammation can induce cell damages and initiate the following pathological processes.

In this report, we demonstrate that bilirubin free radicals can be formed under the attack of other free radicals and induce evident cell damages. Then, the relationship between the formation of pigment gallstone and bilirubin free radicals will be discussed.

FORMATION OF BILIRUBIN FREE RADICAL AND ITS CHEMICAL NATURE

As we find, solid bilirubin absorbs oxygen reversibly when exposed to air, and meanwhile bilirubin free radicals are detectable by ESR^[44]. ESR spectra showed that the free radicals signals of solid bilirubin were composed of a semiquinone signal and a superoxide radical signal (Figure 1). The former may be formed from the carbonyl group, while the latter may be bound with a metal ion, especially the iron that might be released from the haem from which bilirubin was produced. High spin Fe (II) or Fe (III) was found to be coordinated with four tetrapyrrol nitrogens, which was the same as in haem. Various free radical sources, such as FeSO₄+EDTA, XO/XOD and ⁶⁰Co-irradiation were used to generate bilirubin free radicals. The ESR signals obtained were in accordance with those of natural pigment gallstone^[45] (Figure 2). Moreover, the ESR signals of bilirubin became diminished after treatment with free radicals scavengers, such as SOD, mannitol and vitamin C, or ligand of Fe²⁺ or Fe³⁺^[46].

The above results support a mechanism suggested by Foote for photooxidation of bilirubin^[47]: (where BR refers to bilirubin, and T1 represents the transition state of the reaction)



Bilirubin free radicals in solution were showed to be more complex than solid bilirubin free radicals. According to the ESR signals and computer simulation, it was deduced that the signals were composed of three groups of free radicals signals: $\cdot\text{H}_2\text{O}_2^{\cdot-}$, $\text{RCH}_2\cdot$ (Figure 3)^[48]. $\text{O}_2^{\cdot-}$ was from natural bilirubin, and the other two free radicals might be generated during attack of $\text{O}_2^{\cdot-}$ to C-C bond. In

some experiments, only $\cdot\text{OH}$ was trapped by DMPO, which was considered as the dismutation product of $\text{O}_2^{\cdot-}$. In experiment at 77K, semiquinone signal also could be identified just as in solid bilirubin.

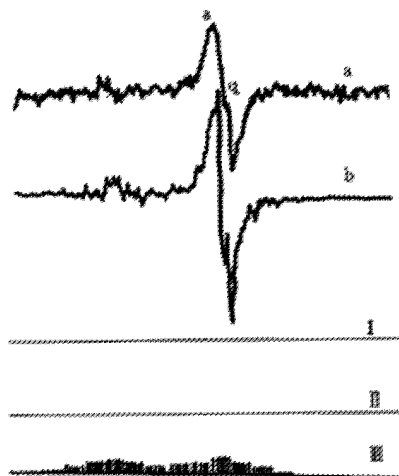


Figure 1 Simulation of ESR spectrum of bilirubin. (a) The experimental spectrum; (b): Simulating spectrum. (I) Superoxide radical; (II) Semiquinone radical; (III) Free electron of superoxideradical delocalized to tetrapyrrole (heterotropism is ignored).

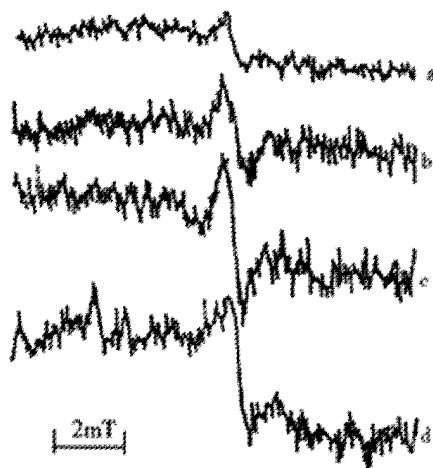


Figure 2 ESR spectra of bilirubin treated with: (a) Bilirubin (from Sigma) as control; (b) ^{60}Co (100Gy); (c) $\cdot\text{OH}$ (Fe(II)+EDTA); (d) $\text{O}_2^{\cdot-}$ (XO/XOD). The relative intensity of ESR peak is: a:b:c:d=1:2.1:2.8:3.9

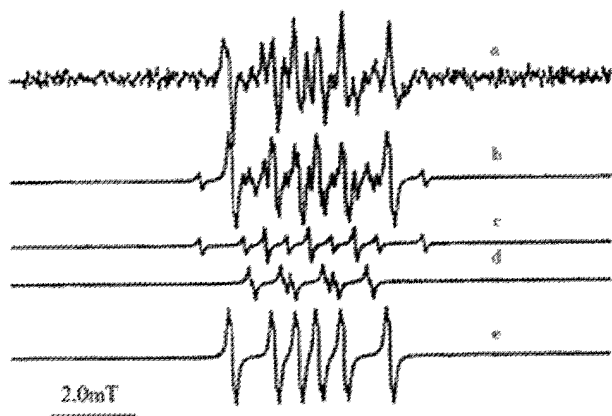


Figure 3 ESR spectra of spin-trapping of bilirubin free radical in solution. (a) DMPO-trapping spectrum of bilirubin; (b) computer simulating spectrum; (c) Simulating spectrum of DMPO-H; (d) Simulating spectrum of DMPO-OOH; (e) simulating spectrum of DMPO-CH₂R.

In conclusion, we proved that bilirubin free radicals consisted of at least semiquinone free radicals and metal bound superoxide free radicals. In solution, $\text{O}_2^{\cdot-}$ attacks bilirubin to generate $\cdot\text{H}$ and RCH_2^{\cdot} , and also dismutates into $\cdot\text{OH}$. Because of the chemical properties of bilirubin free radical, its contributions to the formation of gallstone and its effects on cells discussed below become easier to understand.

PROPERTIES OF BILIRUBIN FREE RADICAL RELEVANT TO FORMATION OF PIGMENT GALLSTONE

To explore the polymerization of bilirubin induced by free radicals, IR and NMR were used to compare the polymerization of original bilirubin or bilirubin treated with free radicals sources. The only significant variation in IR spectra was the decrease of the absorbance at 990cm^{-1} (vinyl group). If the absorbance at 1610cm^{-1} (carboxyl group) was taken as the inner reference^[49], the ratio A_{990}/A_{1610} was found to be 0.6470, 0.5646 and 0.5587 in untreated bilirubin and bilirubin treated with FeSO_4 +EDTA and ^{60}Co irradiation respectively. In NMR spectra, increase of the integral area of the methyl group (1.237ppm) and decrease of that of the vinyl group (above 5ppm) were observed (Figure 4).

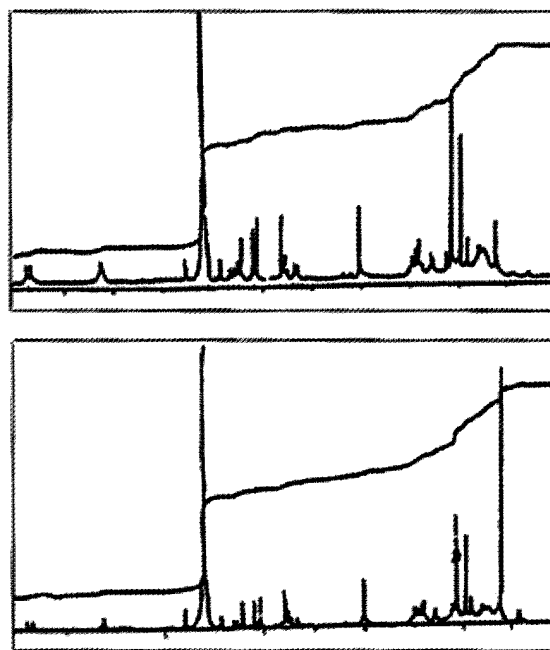


Figure 4 ^1H -NMR spectra of bilirubin. (A) commercial bilirubin (from Sigma); (B) bilirubin treated with ^{60}Co .

Thus, we postulated that bilirubin molecules polymerized through the reaction between the vinyl group and the hydroxyl group by free radicals attack. This hypothesis was consistent with William's suggestion^[50].

By means of the light scattering method, the average molecular weight of the bilirubin free radicals in DMSO solution was determined in the range 60000-80000, which was higher than that of original samples (<20000). The particle size distribution was measured by means of Coulter counter and the result showed that bilirubin free radicals became larger^[51]. A kinetic study showed that the treated bilirubin reacted with calcium ion more rapidly than the untreated sample, and the conditional solubility product was found to be lower. These results suggested that bilirubin free radicals tended to polymerize and deposit, leading to the formation of gallstone.

Based on the above results, we considered that during the gallstone formation bilirubin reacted with the active-oxygen species formed *in vivo* and was changed into free radicals, then polymerized, aggregated and calcified. This might be an important step of formation of pigment gallstone.

CYTOTOXICITY OF BILIRUBIN FREE RADICAL AND ITS CONTRIBUTION TO THE FORMATION OF PIGMENT GALLSTONE

It is well known that bilirubin is cytotoxic. In our experiments, we found that bilirubin free radicals could induce phospholipid peroxidation (LPO), lactate dehydrogenase (LDH) leakage from hepatocytes (Figure 5), and the decrease of intracellular total glutathione (GSH) and oxidized glutathione (GSSG) levels (Figure 6)^[52].

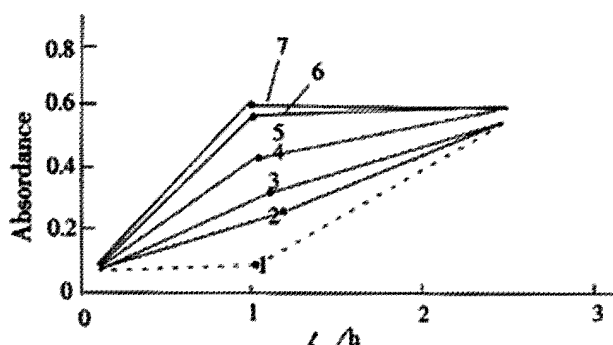


Figure 5 Leakage of lactate dehydrogenase (LDH) of hepatocyte. 1. Control; 2-7. Treated with BR_{VC} , $BR_{comm}+BSA$, BR_{comm} , BR_{Co} , BR_{Fe} , $BR_{XO/XOD}$

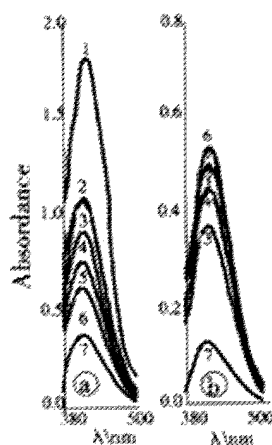


Figure 6 Absorption curve of total and oxidized glutathione level of hepatocyte. (A) Total glutathione; (B) Oxidized glutathione. 1. Control; 2-7. Treated with BR_{VC} , $BR_{comm}+BSA$, BR_{comm} , BR_{Co} , BR_{Fe} , $BR_{XO/XOD}$

The above effects can be diminished when hepatocytes were incubated with bilirubin treated with free radicals scavenger. So cytotoxicity of bilirubin might come from its chemical nature-free radical, just as what had been discussed above. In order to clarify the mechanism of bilirubin-induced cytotoxicity, we investigated effects of bilirubin free radicals on erythrocyte membrane. The SDS-PAGE results showed that after treatment of membrane with bilirubin free radicals, the integral area of band 1 and 2 decreased and some small molecular bands appeared between band 2 and 3 (Figure 7), which indicated that a part of membrane bound proteins, especially the spectrin, were degraded, then the membrane structure might be damaged. The above result was also supported by means of labeling membrane protein with fluorescamine (Figure 8)^[53]. In addition, due to the degradation of membrane bound proteins, the increase of lateral movements of

phospholipids, decrease of polarizability as well as decrease of microviscosity of erythrocyte membrane were observed by means of fluorescence polarization measurement^[54]. The studies on the reaction between membrane and bilirubin free radicals showed that the process comprised three steps: firstly, a rapid formation of an electrostatic complex between bilirubin free radicals and polar groups of phospholipid, then a slow inclusion of bilirubin into hydrophobic core of membrane, and finally an erythrocyte membrane-induced bilirubin aggregation^[55].

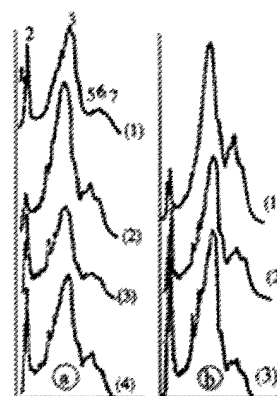


Figure 7 Scans of SDS-PAGE stained with Coomassie blue R-250. (A) 1. control, 2-4 human erythrocyte membrane treated with BR_{Co} , the irradiation doses are 100, 50, 5 (Gy) respectively; (B) human erythrocyte membrane treated with BR_{Fe} , the concentrations of 1-3 are 16.67, 13.3, 6.7 (mmol/L) respectively

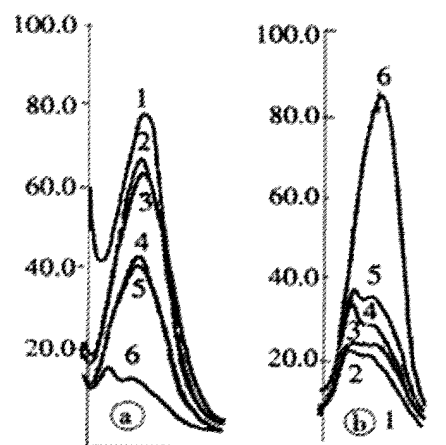


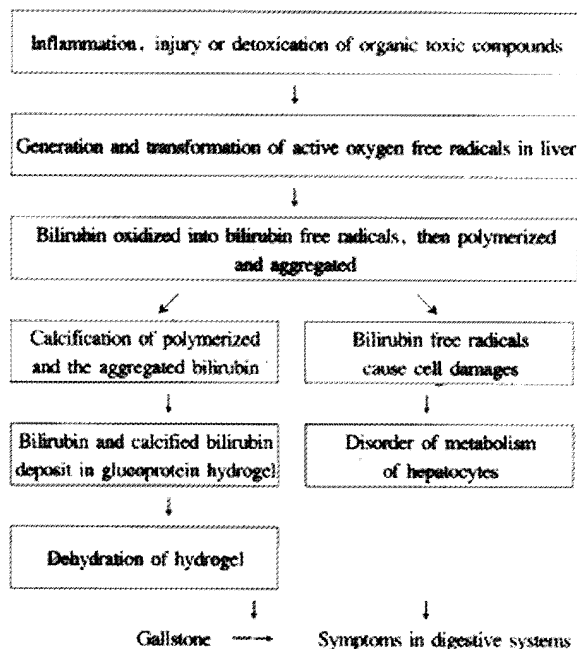
Figure 8 Fluorescence spectrum of erythrocyte proteins labeled with fluorescamine. (A) In the precipitated proteins; (B) In the supernatants. 1. control, 2. BR_{VC} , 3. BR_{comm} , 4-5. BR_{Fe}^{aa} (10 and 20 mmol/L) 6. BR_{Co} (100 Gy)

In summary, bilirubin free radicals can damage the liver cells, which can induce the change of ingredients of the bile, decrease the amount of bile acid. Meanwhile, the abnormal metabolism in hepatocyte can lead to hydrolysis of the conjugated bilirubin, increase the concentration of free bilirubin, thus make bilirubin supersaturated to the bile and promote the formation of pigment gallstone. Moreover, the cell damages caused by free radicals can also promote excretion of glucoprotein, which might act as adhesives and increase the particle size of calcium bilirubinate.

CONCLUSIONS

Based on our results, we considered that there were two ways by which bilirubin free radicals promoted the formation of pigment gallstone. On the one hand, due to the properties of free radicals, bilirubin free radicals formed *in vivo* were more liable to polymerize

and aggregate, then induced the formation of stone. On the other hand, the damages on hepatocytes induced by bilirubin free radicals also impaired the cell function, then led to the disorder of metabolism, which gave rise to the formation of stone indirectly, as well as symptoms in digestive systems. The whole process is illustrated as follows:



REFERENCES

- Zhuang XQ, Sun GH. Analysis of 91 cirrhotic patients complicated by cholelithiasis. *Xin Xiaohuabingxue Zazhi* 1994;2(Suppl 2):20
- Zhang CP, Zhang DX, Han B. The cystic diseases in liver cirrhosis. *Xin Xiaohuabingxue Zazhi* 1994;2(Suppl 2):36
- Hu ZQ, Wu DJ, Wang Y, Wang YH, Xu GN. Clinical analysis of patients with gallstones concomitant gastroduodenal diseases. *Xin Xiaohuabingxue Zazhi* 1996;4:260-261
- Chen G, Wang P, Shi JS, Qin XL. A clinical study of the relationship between gallbladder cancer and gallstone. *Xin Xiaohuabingxue Zazhi* 1997;5:321-322
- Chen P, Wang BS, He LQ. Multifactorial analysis of recurrence of cholecystolithiasis in Shanghai area. *World J Gastroenterol* 1999;5:31-33
- Tandon RK. Prevalence and type of biliary stones in India. *World J Gastroenterol* 2000;6(Suppl 3):4-5
- Jüngst D, Niemeyer A, Müller I, Zündt B, Meyer G, Wilhelm M, del Pozo R. Mucin and phospholipids determine viscosity of gallbladder bile in patients with gallstones. *World J Gastroenterol* 2001;7:203-207
- Shi JS, Ma JY, Zhu LH, Pan BR, Wang ZR, Ma LS. Studies on gallstone in China. *World J Gastroenterol* 2001;7:593-596
- Huang W, Xu BW. Percutaneous cholecystolithocentesis in 552 patients with cholelithiasis. *Xin Xiaohuabingxue Zazhi* 1994;2:96-97
- Zhong J, Wu WY. Experimental study on gandering inhibiting the development of cholesterol stone in guinea pigs. *Xin Xiaohuabingxue Zazhi* 1995;3:69-71
- Yang ZX, Zhu D, Yang YH, Meng YJ, Wang JH. Cholelitholytic effect of Chinese herb rongshiyihao through nasobiliary catheter. *Xin Xiaohuabingxue Zazhi* 1996;4:489-491
- Shi JS, Ren B, Ma QJ, Cheng L, Luo J, Meng QC, Tian HP, Han MR. Experimental study of *Artemisia capillaris* and *Radix curcumae* in preventing gallstone formation in guinea pigs. *Shijie Huaren Xiaohua Zazhi* 1998;6:564-566
- Guo ZW, Wang LF, Shi MY, An X, Deng MJ. Effects of danyihewei granule on stoneforming factors in biliary tract and prevention of postoperative stone formation. *Shijie Huaren Xiaohua Zazhi* 1999;7:132-134
- Xiang RC, Chen F, Wang KM. Synergic effect of erythromycin and CoAA on gallbladder contraction in patients with cholelithiasis. *China Natl J New Gastroenterol* 1996;2:109-111
- Zheng CQ, Li YQ, Zhao SY. Effect of single herb of li dan pai shi tang on motility of gallbladder in normal subjects. *China Natl J New Gastroenterol* 1996;2(Suppl 1):124
- Li ZS. Progress in endoscopic management of pancreas diseases. *World J Gastroenterol* 1998;4:178-180
- Zhao JT, Qi GY, Gao BS, Liang HB, Zhang CQ. Study on motility function of gallbladder in cholelithiasis patients. *Xin Xiaohuabingxue Zazhi* 1996;4:249-250
- Yin QX, Peng LY, Lu RH. Relationship between the bile ingredients and cholelithiasis in patients with liver cirrhosis. *Xin Xiaohuabingxue Zazhi* 1996;4(Suppl 5):81-82
- Shi XS, Huang MK, Wu FL. pH and calcium concentration in gallbladder and hepatic bile. *Xin Xiaohuabingxue Zazhi* 1997;5(Suppl 6):47-48
- Lü HD, Tian MG, Zhang XP, Li HL. Influence of fever on biliary elements of guinea pigs. *Xin Xiaohuabingxue Zazhi* 1997;5:703-704
- Tu XQ, Xiao YQ, Zhu XG, Xu HB, Li WM, Liu YJ. Effects of bile monoconjugated bilirubin on cholesterol nucleation. *Xin Xiaohuabingxue Zazhi* 1997;5:755-756
- Wang XY, Sun XP, Zhou Q, Yang JL, He ZY. Relationship between female hormones, blood lipids and cholelithiasis. *Huaren Xiaohua Zazhi* 1998;6(Suppl 7):216-218
- Wang CY, Yu HZ, Zhang WW. Effect of sex hormones on gallstone formation in rabbits. *Huaren Xiaohua Zazhi* 1998;6(Suppl 7):219-220
- Fang CH, Yang JZ, Kang HG. A PCR study on Hp DNA of bile, mucosa and stone in gallstones patients and its relation to stone nuclear formation. *Shijie Huaren Xiaohua Zazhi* 1999;7:233-235
- Fang CH, Yang J. A study on DNA of aerobic and anaerobic bacteria in bile, mucosa and stone in gallstone patients. *Shijie Huaren Xiaohua Zazhi* 2000;8:66-68
- Zhou LS, Shi JS, Wang ZR, Wang L. Tumor necrosis factor α in gallbladder and gallstone. *Shijie Huaren Xiaohua Zazhi* 2000;8:426-428
- Smout AJPM, vanBerge Henegouwen GP, Samsom M. Normal and disturbed motility of gallbladder and sphincter of oddi. *China Natl J New Gastroenterol* 1996;2(Suppl 1):35-37
- Chen Y, Wang LL, Xiao YX, Ni JH, Yu Y. Analysis of amino acid constituents of gallstones. *China Natl J New Gastroenterol* 1997;3:255-256
- Chen YQ, Cai D, Zhang YL, Hua TF. A comparative study of changing patterns of concanavalin A-binding proteins in early stage of cholesterol gallstone. *China Natl J New Gastroenterol* 1997;3:257-259
- Lü HD, Tian MG, Zhang XP, Li HL. Influence of fever on biliary elements of guinea pigs. *China Natl J New Gastroenterol* 1997;3:265
- Han TQ, Zhang SD, Tang WH, Jiang ZY. Bile acids in serum and bile of patients with cholesterol gallstone. *World J Gastroenterol* 1998;4:82-84
- Wu XT, Xiao LJ, Li XQ, Li JS. Detection of bacterial DNA from cholesterol gallstones by nested primers polymerase chain reaction. *World J Gastroenterol* 1998;4:234-237
- Zhao JC, Xiao LJ, Zhu H, Shu Y, Cheng NS. Changes of lipid metabolism in plasma, liver and bile during cholesterol gallstone formation in rabbit model. *World J Gastroenterol* 1998;4:337-339
- Luo XZ, Wang LS, Lin SZ. An analysis of the relationship between ultrasonography and laparoscopic cholecystectomy. *World J Gastroenterol* 1998;4(Suppl 2):83
- Lin QY, Du JP, Zhang MY, Yao YG, Li L, Cheng NS, Yan LN, Xiao LJ. Effect of apolipoprotein E gene Hha I restricting fragment length polymorphism on serum lipids in cholecystolithiasis. *World J Gastroenterol* 1999;5:228-230
- Wei JG, Wang YC, Du F, Yu HJ. Dynamic and ultrastructural study of sphincter of Oddi in early-stage cholelithiasis in rabbits with hypercholesterolemia. *World J Gastroenterol* 2000;6:102-106
- Jiao XY, Shi JS, Wang JS, Yang YJ, He P. Effects of radical cholecystectomy on nutritional and immune status in patients with gallbladder carcinoma. *World J Gastroenterol* 2000;6:445-447
- Zhou JF, Cai D, Zhu YG, Yang JL, Peng CH, Yu YH. A study on relationship of nitric oxide, oxidation, peroxidation, lipoperoxidation with chronic cholecystitis. *World J Gastroenterol* 2000;6:501-507
- Lammert F, Südfeld S, Busch N, Matern S. Cholesterol crystal binding of biliary immunoglobulin A: visualization by fluorescence light microscopy. *World J Gastroenterol* 2001;7:198-202
- Zhao JT, Qi GY, Gao BS, Liang HB, Zhang CQ. Study on motility function of gallbladder in cholelithiasis patients. *Xin Xiaohuabingxue Zazhi* 1996;4:249-250
- Zhu X. Survey of the relation between fatty liver and gallstone by ultrasonography. *Xin Xiaohuabingxue Zazhi* 1996;4:258-259
- Maki T. Pathogenesis of calcium bilirubinate gallstone. *Ann Surg* 1966;164:90-100
- Elek G, Rockenbauer A. The free radical signal of pigment gallstone. *Klinische Wochenschrift* 1982;60:33-35
- Yang ZH, Wang K, Liu XT. ESR and NMR studies of bilirubin free

- radical. *Sci China B* 1991;8:847-852
- 45 Yang ZH, Wang K, Liu XT. The nature and source of ESR signal in bilirubin. *Advances in free radical and medicine*, Atomic Energy Press, Beijing, 1991;1:309-314
 - 46 Liu XT, Sun FL, Zhao LW, Wang K, Yang ZH, Zhou YH. Polymerization, Aggregation and stable free radical formation of bilirubin induced by activ-oxygen free radical. *Chin BJ* 1990;6:437-443
 - 47 Foote CS. Photosensitized Oxidation and Singlet Oxygen: Consequences in Biological Systems. *Free Radicals in Biology*, Vol.11, Pryor, W.A., Ed., Academic Press, 1976: 3
 - 48 Liu XT, Yang ZH, Wang K, Xiao MF. Some chemical behavior of bilirubin free radical in solution. *Advances in free radical and medicine*, Atomic Energy Press, Beijing, 1991; 3: 35-42
 - 49 Rege RV, Webster CC, Ostrow JD, Carr SH, Ohkubo H. Validation of infrared spectroscopy for assessment of vinyl polymers of bile-pigment gallstones. *Biochem J* 1980;224:871-876
 - 50 William B, Dwyer KR, Kennard CH. Black pigment or polybilirubinate gallstones. *Ann Surg* 1981;193:331-333
 - 51 Liu XT, Tang B, Wang K. The interaction between calcium and bilirubin free radical in the presence of sodium cholate. *Beijing Medi Univer* 1990; 22:285-286
 - 52 Liu XT, Liu HJ, Wang K. Studies on damages of rat hepatocyte induced by bilirubin free radical. *Chin BJ* 1995; 11:71-75
 - 53 Liu XT, Wang K, Xiao MF, Shen LP. Damages of erythrocyte membrane induced by bilirubin free radicals. *Chin BJ* 1992; 8:597-601
 - 54 Liu XT, Shen LP, Wan ZH, Wang K. Effect of bilirubin free radicals on the fluidity of erythrocyte membrane. *Beijing Medi Univer* 1993; 25:369-371
 - 55 Liu XT, Wang K, Xu R. Interaction process of bilirubin free radical with erythrocyte membrane. *Advances in free radical and medicine*, Atomic Energy Press, Beijing, 1991; 3:14-21

Edited by Hu DK

• ESOPHAGEAL CANCER •

Field Population-based blocking treatment of esophageal epithelia dysplasia

Jun Hou, Pei-Zhong Lin, Zhi-Feng Chen, Zhen-Wei Ding, Shao-Sheng Li, Fan-Shu Men, Li-Ping Guo, Yu-Tong He, Chui-Yun Qiao, Chui-Lan Guo, Jian-Ping Duan, Deng-Gui Wen

Jun Hou, Zhi-Feng Chen, Yu-Tong He, Jian-Ping Duan, Deng-Gui Wen, Hebei Cancer Institute, and The Fourth Affiliated Hospital of Hebei Medical University, Shijiazhuang 050011, Hebei Province, China
Pei-Zhong Lin, Zhen-Wei Ding, Li-Ping Guo, Cancer Institute, China Academy of Medical Science, Beijing 100021
Shao-Sheng Li, Fan-Shu Men, Chui-Yun Qiao, Chui-Lan Guo, Cixian Cancer Institute, Cixian County 056500, Hebei Province, China
Supported by The National Eighth-Five-Year Scientific Championship Project No. 85-914-01-02
Correspondence to: Dr. Deng-Gui Wen, Hebei Cancer Institute, Jiankanglu 5, Shijiazhuang 050011, China. dengguiwen@hotmail.com
Telephone: +86-311-6033511 Fax: +86-311-6077634
Received 2001-12-20 Accepted 2002-02-07

Abstract

AIM: To confirm the value of blocking treatment by zenshengping (ZSP), a Chinese herb composite, and Riboflavin for esophageal epithelia dysplasia cases screened out in high risk area in northern china by exfoliative balloon cytology (EBC), so to reduce the incidence rate of esophageal cancer(EC).

METHODS: Esophageal epithelium dysplasia cases including mild esophageal epithelium dysplasia (MEED), stage one severe esophageal epithelium dysplasia (SEEDI), and stage two severe esophageal epithelium dysplasia (SEEDII) were screened out from people aged 40 years and older in the high risk area of Chixian. These cases were randomly divided into a treatment and control group. Subjects in the treatment and control groups took ZSP, riboflavin, and placebo daily for three years. EC cases registered by cancer registry and identified by EBC re-screening in the treatment and control groups were used to calculate incidence and blocking rates to demonstrate the effects of blocking medication.

RESULTS: It was found that 31.92% and 24.15% of people aged 40 years and older in Cixian could be diagnosed as MEED and SEED cases. The severity of dysplasia increased with age. ZSP had blocked EC occurrence by 47.79% after 3 year medication among the SEED cases.

CONCLUSION: ZSP can block the development from SEEDI and SEEDII to EC by 47.79%. Efforts should be made to screen and treat dysplasia cases in people aged 40 years and older in high risk areas to reduce the mortality figures.

Hou J, Lin PZ, Chen ZF, Ding ZW, Li SS, Men FS, Guo LP, He YT, Qiao CY, Guo CL, Duan JP, Wen DG. Field Population-based blocking treatment of esophageal epithelia dysplasia. *World J Gastroenterol* 2002;8(3):418-422

INTRODUCTION

The prognosis of esophageal and cardia cancer is the worst among digestive carcinomas because more than 90% of all its patients are clinically detected at advanced stages, and most of the patients can undergo only non-curative surgery due to either local tumor invasion

into the surrounding tissue or distant metastasis at the time of operation^[1-3]. The five year survival rate for clinically diagnosed EC is below 10%. On the other hand, treatment results for early digestive carcinomas are excellent. Several strategies exist for early treatment, including surgery, endoscopic resection, Chinese herbs, etc. The five year survival of early treated EC and gastric cancer patients can reach 90% or more^[4-16]. Because most EC and gastric patients have no apparent symptoms until the disease develops into advanced stages, early diagnosis at hospitals seems unrealistic presently, and early detection is undergone mostly among high risk populations in area with high incidence by means of exfoliative balloon cytology (EBC) and/or endoscopy^[17-24].

Besides treatment of early ECs such as carcinoma in situ or intramucosal carcinoma, another promising strategy of secondary prevention is receiving great interest presently. A number of researchers have demonstrated that esophageal epithelium dysplasia (EED) is a precancerous lesion which can either develop further into a more severe stage or cancer, stay unchanged, or reverse back to normal again for a period of several years or even a decade. It is therefore very promising to detect patients with EED and treat the precancerous lesions before they transform into the irreversible malignant stage in high risk populations^[25-31]. There are several techniques and chemicals or nutrients that have been reported to be effective in blocking precancerous lesions from transforming into cancer^[32-42]. Linpeizhong reported that an herb composite named Zenshengpin (ZSP) had shown an inhibitory rate of 50% after three years of medication for SEEDI and SEEDII cases^[25]. The present report came from "A Comprehensive Field Prevention and Treatment Study of Esophageal Cancer" carried out in the Chixian county of Hebei Province, which is adjacent to the Linxian county of Henan province, and also has the highest incidence rate of ECs in the world. This study was one of The National Eighth-Five-Year Scientific Championship Project. Its aim was to explore the feasibility of massive screening for EED patients among high risk people and to examine the long term effects of blocking treatment by ZSP and micronutrients in large samples of EED cases.

MATERIALS AND METHODS

Chixian is situated at 36°30" northern latitude, 114°40" eastern longitude, on the east side of the Taihang Mountain, along the Zhanghe River. Across the river to the south is the Anyang City of Henan province. Chixian county occupies an area about 951 square kilometers, and its population is 583611. There is a remarkable variation in the earth stratum of the county, with mountainous, hilly, and level land each constituting about one-third of its total area. The climate is influenced mainly by the warm mainland seasonal wind. The average temperature is 18-25°C and the waterfall is 600-700 millimeters. The major soil there is brown and light colored weed earth. Farm products include wheat, corn, millet, rice, red potato, and beans. Iron and coal are the main minerals, and coal is the main local fuel of the county.

The National Eighth-Five-Year Scientific Championship Project chose people aged 40 years and older in nine rural administrative units in the hilly part of Chixian County as the study population. The hilly

part of the county has a higher incidence rate of EC than the plain part. The nine rural administrative units were further randomly divided into two districts; a treatment and a control district. The number of the study population was 122497. They resided in 101 villages. There was no significant difference in the sex and age distribution of the study population between the treatment and control districts. In preparation for a massive EBC screen of the study population to detect EC, near esophageal cancer (NEC), MEED, SEEDI, and SEEDII cases, a county wide conference was convened by the Chixian County government for local leaders and cancer prevention professionals from the three administrative levels including the county, the rural administration unit, and the villages. At the conference, special committees were set up on each of the three administration level to be responsible for the execution of the EBC massive screen in the areas under their authority. After the conference, a forceful propaganda campaign was carried out countywide to advertise the benefits of massive EBC screenings such as early detection, early treatment and satisfactory survival results. One day prior to the screening, personal contacts with potential examinees were made by local physicians to arrange details for the screening. At the beginning of the screening, physical examination was performed by physicians to exclude persons with serious contraindication to EBC examination, then EBC examination was performed by specialists. Four slides were prepared from specimens obtained by the procedure. The slides were afterwards examined by cytologists with no knowledge about the design of the study. Diagnosis was made according to the five grade cytology classification system including grade I normal, grade II MEED, grade IIIa SEEDI, grade IIIb SEEDII, grade IV NEC, and grade V EC^[28]. A diagnosis of cancer was made only after verification by at least three cytologists. Patients initially diagnosed with grade IIIa, grade IIIb, grade IV, and grade V were reexamined by electronic endoscopy with biopsy.

Finally, 16748 people of the study population in the two districts accepted EBC screening. MEED, SEEDI, and SEEDII patients screened out from the treatment district were pre-chosen as the treatment group; while those of the MEED, SEEDI and SEEDII

cases detected from the control district were chosen to be the control group. There were 1566 cases of MEED and 1396 cases of SEED (including SEEDI and SEEDII) in the treatment group; and 3780 MEED and 2649 SEED cases in the control group. The MEED patients in the treatment group took 8 calcium tablets (CT) which were equivalent to 3 grams of caco3 and 5 milligrams of riboflavin. The SEED patients in the treatment group took 8 ZSP tablets daily. The MEED and SEED cases in the control group took 8 placebo tablets which were the same in color and size as ZSP and CT. The medication of ZSP, CT and placebo continued for three years. Half a year after initiation of the medication, EC cases diagnosed in the treatment and control groups were registered by a cancer registry constructed specifically for the study. At the end of the three year medication, EBC screening was re-initiated to identify EC cases in the treatment and control groups. EC cases registered by the registry and identified by the EBC re-screening were summarized to calculate the incidence rates for the treatment and control groups respectively.

RESULTS

Detection rates of MEED, SEEDI, SEEDII, NEC, and EC

As in Table 1, there were 179 cases of EC, 172 of NEC, 866 of SEEDII, 3179 of SEEDI, and 5346 of MEED as detected by the initial EBC screening from the 16,748 high risk participants aged 40 years and older in the treatment and control districts. The detection rates of MEED, SEEDI, SEEDII, NEC, and EC were 31.92%, 18.98%, 5.17%, 1.03%, and 1.07% respectively. As the age increased by 5 year intervals, the detection rates of MEED, SEEDI, SEEDII, NEC, and EC all increased from the lowest for the 40-year-old group to the highest for the 60-year-old group, but the amount of increase in the detection rates with increase of age was not equal for MEED, SEEDI, SEEDII, NEC, and EC. The increase was the sharpest for EC and the lowest for MEED. An odds ratio (OR) defined as the ratio of the detection rates of the 60-year-old group against that of the 40-year-old group was 5.78 for EC, 2.56 for NEC, 1.80 for SEEDII, 1.61 for SEEDI, and only 1.18 for MEED.

Table 1 Age distribution of detection rates of MEED, SEEDI, SEEDII, NEC, and EC by EBC screening

Histology Grade	Age										Total	OR	
	40-		45-		50-		55-		60-				
	<i>n</i>	Rate%	<i>n</i>	Rate%	<i>n</i>	Rate%	<i>n</i>	Rate%	<i>n</i>	Rate%			
Normal	2703	50.50	1578	43.83	1094	39.10	945	35.59	746	30.09	7021	41.92	0.60
MEED	1574	29.40	1100	31.76	928	33.17	882	33.22	862	34.77	5346	31.92	1.18
SEEDI	820	15.32	626	18.08	550	19.66	572	21.54	611	24.65	3179	19.98	1.61
SEEDII	208	3.89	151	4.36	166	5.93	167	6.29	174	7.02	866	5.17	1.80
NEC	28	0.52	39	1.13	29	1.04	43	1.62	33	1.33	172	1.03	2.56
EC	20	0.37	29	0.84	31	1.11	46	1.73	53	2.14	179	1.07	5.78
Total	5353		3463		2789		2655		2479		16748		

EBC re-screening

EBC re-screening was carried out at the end of the three year medication period to detect EC patients among the MEED, SEEDI, and SEEDII cases in the treatment and control groups. Among the 4045 SEED cases, 77 EC cases had been diagnosed and registered before EBC re-screening (Table 2). With them excluded, there were 3968 SEED cases who should have been re-screened, and in the end 2976 (75.00%) were re-examined. The re-screening completion rate for the treatment and control groups of SEED was 78.4% and 74.2% respectively. As for the 5346 MEED cases, with the 76 EC cases already diagnosed and registered prior to re-screening excluded, 3775 (71.63%) were re-screened. The re-screening rates for the MEED treatment and control groups were 75.6% and 74% respectively.

Registered EC cases and incidence rates

From half a year after initiation of ZSP and CT medication to the time of re-screening, 77 cases of EC were diagnosed and registered among the 4045 SEED cases (Table 2). The three-year incidence rate by registered EC cases alone for all of the SEED cases was 1.90% (77/4045), and for SEED in the treatment and control groups were 0.78% (11/1396) and 2.49% (66/2649) respectively. A significant difference existed between the incidence rates of the two groups ($\chi^2=14.21, P<0.01$). For the 5346 MEED cases, 76 EC patients were registered. The three year incidence rate for all of the MEED cases was 1.42% (76/5346), and was 1.14% (18/1566) and 1.54% (58/3780) for MEED in the treatment and control groups respectively.

There was no significant difference between the incidence rates of the two groups ($\chi^2=1.17, P>0.05$).

Table 2 Effect of blocking treatment of MEED and SEED cases by ZSP, CT, and PLACEBO after three year medication

Group	No. subjects	EC Diagnosed			Incidence Rates (%)	Block Rates (%)
		EBC Re-screening	Registration	Total		
Treatment	1566	10	18	28	1.79	
Control	3780	26	58	84	2.22	
Total	5346	36	76	112	2.10	19.37

SEED

Group	No. subjects	EC Diagnosed			Incidence Rates (%)	Block Rates (%)
		EBC Re-screening	Registration	Total		
Treatment	1396	17	11	28	2.01	
Control	3649	36	66	102	3.85	
Total	4045	53	77	130	3.21	47.79

Re-screened EC cases and prevalence rates

By EBC re-screening, 53 EC cases were detected from the 2976 SEED cases. The prevalence rate was 1.78% (53/2976) for all of the SEED cases combined, and was 1.61% (17/1054) and 1.87% (36/1922) for SEED cases in the treatment and control groups respectively. There was no significant difference between the prevalence rates of the two groups ($\chi^2=0.26, P>0.05$). Among the 3775 MEED cases, 36 EC cases were diagnosed by EBC re-screening, with a prevalence rate of 0.95% (36/3775) for the MEED combined, 0.89% (10/1114) for the treatment group, and 0.97% (26/2661) for the control group. There was no significant difference in the prevalence rates between the two groups ($\chi^2=0.15, P>0.05$).

Combined incidence and blocking rates

During the first three year follow-up, 242 diagnoses of EC were made by registration and re-screening from the 9,391 SEED and MEED cases, yielding a total incidence rate of 2.58% (242/9391) for SEED and MEED combined, 1.89% (56/2962) for the treatment group, and 2.89% (186/6429) for the control group. A significant difference existed between the two groups ($\chi^2=8.12, P<0.01$). A blocking rate of 34.60% calculated as $(2.89-1.89)/2.89 \times 100\%$ was obtained to assess the effects of a three year period of medication by ZSP and CT.

As in Table 2, 112 EC cases were accumulated by three year registration and EBC-re-screening from the 5346 MEED cases (76 registered and 36 screened out). An incidence rate of 2.10% (112/5346) was calculated for the whole MEED group, 1.79% (28/1566) for MEED in the treatment group, and 2.22% (84/3780) for MEED in the control group. The difference between the incidence rates of the two groups did not reach a significant level ($\chi^2=1.02, P>0.05$), and a blocking rate of 19.37% was calculated to demonstrate the effect of CT for MEED cases.

130 EC cases were diagnosed from the 4045 SEED cases by three year registration and EBC re-screening (77 registered and 53 re-screened out). The incidence rate was 3.21% for all of the SEED cases, 2.01% (28/1396) for SEED in the treatment, and 3.85% (102/2649) for SEED in the control group. The difference between the incidence rates of the two groups reached a significant level ($\chi^2=10.00, P<0.01$), and the blocking rate by ZSP for SEED was 47.79%.

Incidence and blocking rates of EC for SEEDI and SEEDII

As in Table 3, 69 EC diagnoses were made during the three year study

period among the 3179 SEEDI cases. The incidence rate was 2.17% (69/3179) for all of the SEEDI cases, 1.66% (20/1206) for SEEDI in the treatment group, and 2.48% (49/1973) for SEEDI in the control group. There was no significant difference between the incidence rates of the treatment and control group ($\chi^2=2.40, P>0.05$), and the corresponding blocking rate was 33.06%.

There were 61 EC cases diagnosed from the 866 SEEDII cases during the same period, yielding an incidence rate of 7.04% (61/866) for all of the SEEDII, 2.87% (8/279) for SEEDII in the treatment group, and 9.03% (53/587) for SEEDII in the control group. A significant difference was observed between the two incidence rates of the two groups ($\chi^2=10.00, P<0.01$), and the blocking rate of ZSP for SEEDII was 68.22%.

Table 3 Results of blocking treatment of SEEDI and SEEDII cases by ZSP and PLACEBO after three years of medication

Group	No. subjects	No. EC Diagnosed	Incidence Rates (%)	Block Rates (%)
Treatment	1206	20	1.66	
Control	1973	49	2.48	
Total	3179	69	2.17	33.06

SEEDII

Group	No. subjects	No. EC Diagnosed	Incidence Rates (%)	Block Rates (%)
Treatment	279	8	2.87	
Control	587	53	9.03	
Total	866	61	7.04	68.22

DISCUSSION

Dysplasia is an atypical state of the epithelium with a basophilic matrix, a high matrix-core ratio, and hyperheterochromatin. It is historically classified into three grades according to the degree of atypical epithelium in comparison with the basal zone as defined by the World Health Organization's International Histological Classification of Tumors^[43]. Atypical cells localized in the basal zone in MEED, while immature cells occupy more than three quadrants of the epithelium in SEEDI and SEEDII.

In this study, we found that 31.92% and 24.15% of people aged 40 years and older in Chixian could be diagnosed as MEED and SEED cases. Qiu and Yang^[44] have reported a similar dysplasia rate of 32.28% in people aged 21 years and older in Linxian, which is a neighboring County to Chixian County situated in the same Taihang Mountain area in northern China where there is the highest incidence of EC. However, the rate of dysplasia in low risk regions was only 4.78%, most of the dysplasia belonged to MEED, and the frequency of dysplasia correlated well with the regional level of ECs.

The severity of dysplasia increased with age. As in Table 1, as patients got older, their chances of being detected as one of the dysplasia states grew higher. This was true with MEED, SEED I, and SEEDII. Moreover, the extent of increase in detection rates with age was small for MEED, large for SEEDI, and still larger for SEEDII. The Odds Ratios of the detection rates of the 60-year-old group versus that of the 40-year-old group for MEED, SEEDI and SEEDII were 1.18, 1.61, and 1.80 respectively. This increase with age is remarkably similar to the increase of incidence or mortality of EC with age^[46-50], but the degree of the latter was much greater. As in Table 1, the Odds Ratio of detection rates of 60-year-olds against that of 40-year-olds grew up to 2.56 and 5.78 for NEC and EC. It may be suggested that the increase of dysplasia rates with age was small and unstable or reversible for the less severe states such as MEED, but

became fixed and remarkably large as the dysplasia progressed into more severe stages or transformed into NEC and EC.

While the chances of dysplasia increased with age, the total detection rates for MEED, SEED and SEEDII decreased from 31.92%, 18.98% to 5.17% in the direction of dysplasia development. It may suggest that although dysplasia may proceed further, only a limited portion proceeds into more severe or malignant.

Our finding and discussion so far support the notion that dysplasia belongs to a early form of carcinoma. The main difference between dysplasia and EC may be that dysplasia is an unstable or unfixed state of existence. It may develop further, but much of it will stay unchanged, or even return to normal or less severe again. Therefore, if we could detect and treat precancerous dysplasia lesions before they develop into carcinomas, then the long-term survival of ECs should dramatically improve.

The present study has focused primarily on the blocking treatment of dysplasia cases in high risk populations. The result was that ZSP blocked EC incidence rate by 47.79% after 3 years of medication for the SEED cases. In a previous National Seventh Five Research Project carried out in Linxian County, Lin found that ZSP reduced the EC transformation rate of SEED cases by 52.2% after 3 year medication^[24]. These consistent findings by a series of population-based prospective cohort studies in the same high risk area enabled us to conclude that EC is preventable on the secondary blocking treatment level, and ZSP is an effective agent to treat precancerous EC lesions in high risk areas^[51-53].

Experimental observations indicate that cancer preventive chemical agents take effect by acting on the promotion stage^[25]. The anticarcinogenicity of certain Chinese herbs is considered to share the same mechanism. In this study, the significant blocking rate of 47.79% by ZSP for the SEED cases resulted mainly from the difference in the registered incidence of EC between the treatment and control groups, as there was no significant difference in the re-screened EC incidence rates between the two groups. As we know, registered EC represents clinically diagnosed late-staged EC, while EC screened out by EBC belonged to the early asymptomatic patients. The finding that ZSP reduced only the registered three year incidence rate, but not the EBC re-screened incidence rate of EC suggests that ZSP may have blocked or delayed the appearance of clinically recognizable EC developed from SEED. In other words, ZSP acted mainly on the late stage of EC development. As in Table 3, the more remarkable blocking rate by ZSP for SEEDII versus SEEDI (68.22% versus 33.06%) also supports the idea that ZSP was effective in blocking or delaying the appearance of EC during the late stages of EC development.

In a previous comprehensive field prevention and treatment study of esophageal cancer carried out in Linxian county, Lin found that Riboflavin had no significant effect on MEED cases at the end of three years of medication, but a blocking rate of 37.0% appeared at the end of 9 year follow up^[24,25]. The result at the end of a three year medication period was the same as in the present study. Further findings will be reported by continuous observation.

In conclusion, we regard dysplasia as a precancerous lesion in people aged 40 years and older in high risk areas. Efforts should be made to screen and treat dysplasia cases before the disease transforms into the irreversible malignant state. Effective screening plus blocking treatment in high risk populations may reduce the mortality rate of EC over the long term. ZSP has been made from natural Chinese herbs which are cheap and share rich resources. Repeated demonstration of its ability will make it a promising agent for secondary prevention of EC.

REFERENCES

- Chen KN, Xu GW. Diagnosis and treatment of esophageal cancer. *Shijie Huaren Xiaohua Zazhi* 2000;8:196-202
- Liu HF, Liu WW, Fang DC. Study of the relationship between apoptosis and proliferation in gastric carcinoma and its precancerous lesion. *Shijie Huaren Xiaohua Zazhi* 1999;7:649-651
- Sherman Jr CD. Digestive carcinomas. In: Union Internationale Contre Le Cancer (UICC). Manual of clinical oncology 5. Beijing: The joint

- publishing house of Beijing Medical University and China Union Medical University, 1992:237-38
- Urba SG, Orriger MB, Tamayo CP, Bromberg J, Forastiere A. Concurrent preoperative chemotherapy and radiation therapy in localized esophageal adenocarcinoma. *Cancer* 1992;69:285-289
- China Ministry Of Public Health. Esophageal cancer. In: China Ministry Of Public Health, ed. Diagnosis and treatment criteria for common malignances in China 2. Beijing: The joint publishing house of Beijing Medical University and China Saint Medical University, 1991:30-31
- Wolfe WG, Anna L, Vaughn RN, Seigler HF, Hathorn JW, Leopold KA, Duhaylongsod FG, Durham NC. Survival of patients with carcinoma of the esophagus treated with combined-modality therapy. *J Thorac Cardiovasc Surg* 1993;105:749-756
- Wang ZQ, He J, Chen W, Chen Y, Zhou TS, Lin YC. Relationship between different sources of drinking water, water quality improvement and gastric cancer mortality in Chang County-A retrospective-cohort study in high incidence area. *World J Gastroenterol* 1998;4:45-47
- Sun JJ, Zhou XD, Zhou G, Liu YK. Expression of intercellular adhesive molecule-1 in liver cancer tissues and liver cancer metastasis. *World J Gastroenterol* 1998;4:202-205
- Yoneda M. Regulation of hepatic function by brain neuropeptides. *World J Gastroenterol* 1998;4:192-196
- Yu JY, Wang LP, Meng YH, Hu M, Wang JL, Bordin C. Classification of gastric neuroendocrine tumors and its clinicopathologic significance. *World J Gastroenterol* 1998;4:158-161
- Deng LY, Zhang YH, Xu P, Yang SM, Yuan XB. Expression of IL-1 β converting enzyme in 5-FU induced apoptosis in esophageal carcinoma cells. *World J Gastroenterol* 1999;5:50-52
- Xiao B, Jing B, Zhang YL, Zhou DY, Zhang WD. Tumor growth inhibition effect of hIL-6 on colon cancer cells transfected with the target gene by retroviral vector. *World J Gastroenterol* 2000;6 :89-92
- Qian SB, Chen SS. Transduction of human hepatocellular carcinoma cells with human Y-interferon gene via retroviral vector. *World J Gastroenterol* 1998;4:210-213
- Shen ZY, Xu LY, Li EM, Cai WJ, Chen MH, Shen J, Zeng Y. Telomere and telomerase in the initial stage of immortalization of esophageal epithelial cell. *World J Gastroenterol* 2002;8:357-362
- Cao WX, Qu JM, Fei XF, Zhu ZG, Yin HR, Yan M, Lin YZ. Methionine-dependence and combination chemotherapy on human gastric cancer cells *in vitro*. *World J Gastroenterol* 2002;8:230-232
- Wu K, Zhao Y, Liu BH, Li Y, Liu F, Guo J, Yu WP. RRR- α -tocopheryl succinate inhibits human gastric cancer SGC-7901 cell growth by inducing apoptosis and DNA synthesis arrest. *World J Gastroenterol* 2002;8:26-30
- Ma LS. Intensify improvement of the diagnosis and treatment level of digestive system diseases in China. *World J Gastroenterol* 1998;4 :287-293
- Gu QL, Li NL, Zhu ZG, Yin HR, Lin YZ. A study on arsenic trioxide inducing *in vitro* apoptosis of gastric cancer cell lines. *World J Gastroenterol* 2000;6 :435-437
- Zou SC, Qiu HS, Zhang CW, Hou QT. A clinical and long term follow up study of perioperative sequential triple therapy for gastric cancer. *World J Gastroenterol* 2000;6:284-287
- Chen GR, Jiang XL, Wang YP. Endoscopic treatment skill on submucosal benign tumors. *Dia Treat Dig Dis* 2001;1:43-45
- Zhang XY. Some recent works on diagnosis and treatment of gastric cancer. *World J Gastroenterol* 1999;5:1-3
- Qiao GB, Han CL, Jiang RC, Sun CS, Wang Y, Wang YJ. Overexpression of P53 and its risk factors in esophageal cancer in urban areas of Xi'an. *World J Gastroenterol* 1998;4:57-60
- Chai L, Yu SZ. Gastric cancer molecular epidemiology in Fujian Changle. *Shijie Huren Xiaohua Zazhi* 1999;7:652-655
- Lin PZ, Chen ZF, Hou J, Liu TG, Wang JX, Ding ZW, Guo LP, Li SS, Men FS, Du CL. Chemical prevention of esophageal cancer. *Zhongguo Yixue Keixue Yuan Xuebao* 1998;20:413-417
- Lin PZ, Zhang JS, Rong ZP, Han R, Xu SP, Gao RQ, Ding ZW, Wang JX, Feng HJ, Cao SG, Guo WS. Medicamentous inhibitory therapy of precancerous lesions of the esophagus-3 and 5 year inhibitory effect of ZSP, Retinamide and Riboflavin. *Zhongguo Yixue Keixue Yuan Xuebao* 1990;12:235-245
- Shen Q, Wang DL, Xiang YY, Wang C, Ren ZC, Yan AH, Ren XH, Chang FJ, Zhang JM, Ye XJ, Zhou YF, Huang M, Zhen HZ, Chai XS, Chen HM, Zhang JQ, Chang YF, Luo DS. A preliminary report of nutritional intervention in dysplasia of the esophagus. *Zhongguo Zhongliu Lichuang* 1991;18:31-35
- Hou J, Yuan FR, Li SS, Li ZY, Chen ZF. A clinical study on the treatment results of esophageal dysplasia by composite Dangsheng pill. *Zhongguo Yixue Xuebao* 1992;7:11-13
- Kitamura K, Kuwano H, Yasuda M, Sonoda K, Sumiyoshi K, Tsutsui S, Kitamura M, Sugimachi K. What is the earliest malignant lesion in the esophagus? *Cancer* 1996;77:1614-1618

- 29 Xia HK. Association between *Helicobacter pylori* and gastric cancer: current knowledge and future research. *World J Gastroenterol* 1998;4: 93-96
- 30 Tian XJ, Wu J, Meng L, Dong ZW, Shou CC. Expression of VEGF 121 in gastric carcinoma MGC803 cell line. *World J Gastroenterol* 2000;6:281-283
- 31 Assy N, Paizi M, Gaitini D, Baruch Y, Spira G. Clinical implication of VEGF serum levels in cirrhotic patients with or without portal hypertension. *World J Gastroenterol* 1999;5:296-300
- 32 Xiao ZF, Yang ZY, Zhou ZM, Yin WB, Gu XZ. Radiotherapy of double primary esophageal carcinoma. *World J Gastroenterol* 2000;6:145-146
- 33 Xiao B, Shi YQ, Zhao YQ, You H, Wang ZY, Liu XL, Yin F, Qiao TD, Fan DM. Transduction of Fas gene or Bcl-2 antisense RNA sensitizes cultured drug resistant gastric cancer cells to chemotherapeutic drugs. *World J Gastroenterol* 1998;4:421-425
- 34 Zhang QX, Dou YL, Shi XY, Ding YI. Expression of somatostatin mRNA in various differentiated types of gastric carcinoma. *World J Gastroenterol* 1998;4:48-51
- 35 Hou J, Chen ZF, Li SS, Li ZY, Yan HR. Clinical study on treatment of esophageal precancerous lesion with Cangdouwan Pill. *Zhongguo Zonglun Lingchuang* 1996;23:117-119
- 36 Wu QM, Li SB, Wang Q, Wang DH, Li XB, Liu CZ. The expression of COX-2 in esophageal carcinoma and its relation to clinicopathologic characteristic. *Shijie Huaren Xiaohua Zazhi* 2001;9:11-14
- 37 Hou J, Yan FR, Li SS, Li ZY, Chen ZF. Clinical study on the effect of Cangdouwan on esophageal precancerous lesion. *Zhongguo Zhongxiyi Jiehe Zhazhi* 1992;12:604-606
- 38 Abe M, Takahashi M. Intraoperative radiotherapy: the Japanese experience. *Int J Radiat Oncol Biol Phys* 1981;7:863-868
- 39 Swisher SG, Hunt KK, Holmes C, Zinner MJ, McFadden DW. Changes in the surgical management of esophageal cancer from 1970-1993. *The American J. Surgery* 1995;169:609-615
- 40 Tao DM, Xu YZ, Wang XH, Gu YK, Wang DY, Wang TX. Follow up of 417 cases of severe esophageal dysplasia. *Henan Zhongliuxue Zhazhi* 1997;10:38-43
- 41 Li JY, Blot LI B, Tailor, Guo WD, Wang W, Liu PQ, Zhen SF, Yang ZS, Liu FS, Sun YH, LIU SF, Wang GQ, Wang ZY, Zhang YH, Lu SX, Wu YP, Zhou XN, Shen Q, Zhang DH, Lian GT, Hu TS, Wang ZQ, Liu Y, Greenwood, Flawmeine. Preliminary reports of population-based nutritional preventive experiment of cancer and other common diseases. *Zhonghua Zhongliu Zhazhi* 1993;15:165-181
- 42 Semba S, Yokozaki H, Yamamoto S, Yasui W, Tahara E. Microsatellite instability in precancerous lesions and adenocarcinomas of the stomach. *Cancer* 1996;77:1620-1627
- 43 Correa P. Precursors of gastric and esophageal cancer. *Cancer* 1982; 50:2554-2565
- 44 Qiu SL, Yang GR. Precursor lesions of esophageal cancer in high-risk population in Henan province. *Cancer* 1988;62:551-557
- 45 Mimori K, Mori M, Tanaka S, Akiyoshi T, Sugimachi K. The overexpression of elongation factor 1 Gamma mRNA in gastric carcinoma. *Cancer* 1995;75:1446-1449
- 46 Forastiere AA, Orringer MB, Perez-Tamayo C, Urba SG, Husted S, Takasugi BJ, Zahurak M. Concurrent chemotherapy and radiation therapy followed by transhiatal esophagectomy for local-regional cancer of the esophagus. *J Clinical Oncology* 1990;8:119-127
- 47 Cao GH, Yan SM, Yuan ZK, Wu L, Liu YF. A study of the relationship between trace element Mo and gastric cancer. *World J Gastroenterol* 1998;4:55-56
- 48 Jiang YF, Yang ZH, Hu JQ. Recurrence or metastasis of HCC: Predictors, early detection and experimental antiangiogenic therapy. *World J Gastroenterol* 2000;6:61-65
- 49 Qiao YL, Hou J, Yang L, He YT, Liu YY, Li LD, Li SS, Lian SY, Ding ZW. Trend of esophageal cancer in the high risk area of Taihang mountain and prevention strategy. *Zhongguo Yixue Kei Xueyuan Xuebao* 2001;23:10-14
- 50 Inoue H, Takeshita K, Hori H, Muraoka Y, Yoneshita H, Endo M. Endoscopic mucosal resection with a cap-fitted panendoscope for esophagus, stomach, and colon mucosal lesions. *Gastrointestinal Endoscopy* 1993;39:58-64
- 51 Dong ZW, Tang PZ, Li LD. Control strategy in high risk area of esophageal cancer in China. *Zhongguo Zhongliu* 2000;9:71-73
- 52 Shen Q, Zhen HZ, Cai XS, Chen HM, Zhang JQ, Wang DL, Xiang YY, Chang YF, Luo DS, Wang C, Chang FJ. Compound riboflavin used in nutritional intervention of esophageal dysplasia- A long-term study. *Henan Zhongliuxue Zhazhi* 1991;4:1-5
- 53 Ding ZW, Gao F, Lin PZ, Wang JX, Guo LP. Long term effect of block treatment for esophageal dysplasia cases. *Zhonghua Zhongliu Zhazhi* 1999; 21:275-277

Edited by Pagliarini R

• ESOPHAGEAL CANCER •

Tumor suppressor gene p16 and Rb expression in gastric cardia precancerous lesions from subjects at a high incidence area in northern China

Yun Zhou, Shan-Shan Gao, Yong-Xin Li, Zong-Min Fan, Xin Zhao, Yi-Jun Qi, Jun-Ping Wei, Jian-Xiang Zou, Gang Liu, Li-Huo Jiao, Yong-Min Bai, Li-Dong Wang

Yun Zhou, Department of Oncology, the First Affiliated Hospital, Zhengzhou University, Zhengzhou 450052, Henan Province, China
Shan-Shan Gao, Yong-Xin Li, Zong-Min Fan, Xin Zhao, Yi-Jun Qi, Jun-Ping Wei, Jian-Xiang Zou, Gang Liu, Li-Huo Jiao, Yong-Min Bai, Li-Dong Wang, Laboratory for Cancer Research, College of Medicine, Zhengzhou University (Formerly Henan Medical University), Zhengzhou 450052, Henan Province, China
Supported by the National Natural Science Foundation of China, No. 39770296

Correspondence to: Li-Dong Wang, M.D., Laboratory for Cancer Research, College of Medicine, Zhengzhou University, Zhengzhou 450052, Henan Province China. ldwang@371.net
Telephone: +86-371-6970165 Fax: +86-371-6970165
Received 2001-07-05 Accepted 2001-07-16

Abstract

AIM: To further understand the molecular basis for gastric cardia carcinogenesis and to provide etiological clues.

METHODS: Endoscopic mucosa biopsy and histopathological examinations were made on 37 subjects from a high incidence area for both esophageal and gastric cardia carcinomas in northern China. All the biopsy samples were fixed in 850ml⁻¹ alcohol and embedded in paraffin. Each block contained one piece of tissue and was serially sectioned at 5 μ m. Immunohistochemistry (ABC) was carried out on these gastric cardia samples to determine the alterations of p16 and Rb.

RESULTS: Based on the histopathological examination there were 11 cases of chronic superficial gastritis, 12 cases of chronic atrophic gastritis and 14 cases of dysplasia. The immunostaining demonstrated different levels of unclear immunostaining of p16 and Rb in normal gastric cardia tissue and the tissues with different severity of lesions. With the lesions progressing, the positive immunostaining rates for p16 protein had a decreasing tendency. In contrast, the positive immunostaining rate for Rb protein had an increasing tendency. There was a significant negative relationship between the two parameters. Changes of p16 was CSG 11(100%), CAG 7 (58%), DYS 4(29%) and changes of Rb was CSG 2(18%), CAG 8(67%) and DYS 12(86%), ($P<0.05$).

CONCLUSION: The alterations of p16 and Rb protein may play a role in the early stages of gastric cardia carcinogenesis.

Zhou Y, Gao SS, Li YX, Fan ZM, Zhao X, Qi YJ, Wei JP, Zou JX, Liu G, Jiao LH, Bai YM, Wang LD. Tumor suppressor gene p16 and Rb expression in gastric cardia precancerous lesions from subjects at a high incidence area in northern China. *World J Gastroenterol* 2002;8(3):423-425

INTRODUCTION

Gastric cardia cancer is subject being studied. An interesting observation is that gastric cardia cancer and esophageal cancer seem to

occur together in many high-incidence areas in China, and both were referred to as esophageal cancer (EC) by the public because of the common syndrome of dysphagia^[1,2]. Histologically, esophageal and gastric cardia cancers have been considered as single clinical entity for incidence and mortality calculation in China. The molecular changes in the early stage of gastric cardia carcinogenesis have not been characterized^[3-5]. In the present study, we investigated the roles of p16 and Rb alteration in gastric cardia carcinogenesis by measuring the expression rates of p16 and Rb in normal gastric cardia tissues and the tissues with different severity of lesions from the symptom-free subjects at a high incidence area of gastric cardia cancers in Henan, northern China.

MATERIALS AND METHODS

Tissue collection and processing

Gastric cardia biopsies were taken from 37 symptom-free subjects at Huixian County and Linxian County, Henan Province, China, the high-risk areas for esophageal and gastric cardia cancers during the mass survey. All the biopsy specimens were fixed with 850ml⁻¹ alcohol, embedded with paraffin, and serially sectioned at 5 μ m. The sections were mounted onto histostick-coated slides. Three or four adjacent ribbons were collected for histopathological analysis (HE stain), and immunohistochemical staining. Histopathological diagnosis for gastric cardia epithelia was made using the previously established criteria. Based on the cellular morphological changes and tissue architecture, the gastric cardia epithelia were graded as chronic superficial gastritis (CSG), chronic atrophic gastritis (CGT) and dysplasia (DYS)^[6-9]. The polyclonal p16 antibody is rabbit antiserum against human p16 protein (Dakoco, USA). The polyclonal Rb antibody is rabbit antiserum against man Rb protein (Oncogene Science Inc., USA). After dewaxing, inactivating endogenous peroxidase activity, and blocking cross-reactivity with normal serum, we incubated the sections with a diluted solution of the primary antibodies overnight at 4°C (1:100 for p16, 1:100 for Rb). Location of the primary antibodies was achieved by subsequent application of a biotinylated anti-primary antibody, an avidin biotin complex conjugated to horseradish peroxidase, and diaminobenzidine (Vectastain Elite Kit, Dako, USA). Normal serum blocking and omission of the primary antibody were used as negative controls^[10,15].

Statistical analysis

The data were expressed as the mean \pm SD unless otherwise stated. The χ^2 test was used for histopathological and immunostaining rate evaluation ($P<0.05$ considered significant).

RESULTS

Histopathology findings

Histopathological examination showed that there were 11 cases of chronic superficial gastritis, 12 cases of chronic atrophic gastritis and 14 cases of dysplasia (Table 1). Both p16 and Rb immunostaining-positive cells were observed in different severity of lesions of gastric

cardia epithelia. In CSG, the positive immunostaining rates of p16 was much higher than that of Rb. An interesting observation is that the positive immunostaining rate of p16 was much lower than that of Rb in DYS. As the lesions of gastric cardia epithelia progressed from CSG to DYS, the positive immunostaining rates of p16 decreased significantly ($P < 0.05$), especially from CSG to CAG. However, the positive immunostaining rates of Rb increased significantly ($P < 0.05$). Correlation analysis showed significantly negative correlation between the decreasing tendency of P16 and the increasing tendency of Rb with the lesions progressing from CSG, CAG to DYS.

Table 1 Changes of p16 and Rb in gastric cardia precancerous lesions

Histological types	Number examined	P16 IHC positive ^a n (%)	Rb IHC positive ^b n (%)
CSG	11	11(100)	2(18)
CAG	12	7(58)	8(67)
DYS	14	4(29)	12(86)

^a $P < 0.05$, CSG vs CAG, CAG vs DYS; ^b $P < 0.05$, DYS vs CAG, CAG vs. CSG

DISCUSSION

Gastric cardia carcinoma (GCC) is one of the most frequent digestive malignant diseases in northern China. A remarkable epidemiological characteristic for GCC is the occurring together with esophageal cancer in the same high-incidence area (HIA). In contrast with the strikingly decreasing of incidence rate of distal gastric cancer around the world in the past two decades, especially in America and Europe, the incidence of GCC increased dramatically; the incidence of esophageal-gastric-junction cancer increased to 6 folds with a speed of 4% yearly, which was one of the fastest increasing malignant diseases, the mechanism in unclear. There are several distinct differences between GCC and distal gastric cancer with respect to epidemiology, etiological factors, histogenesis and clinical characteristics, and therefore GCC should be categorized as a distinct clinical disease. Lacking of sensitive and diagnostic biomarker and technique in early stage of GCC as well as the deficiency of effective and specific reagents for its treatment and prevention leads to its poor prognosis and higher mortality. An interesting observation in this study was that the alterations of tumor suppressor gene p16 and Rb products occurred in the early stage of gastric cardia carcinogenesis, even in CSG. With the lesions progressing from CSG, CAG to DYS, the positive immunostaining rates of p16 decreased significantly, especially from CSG to CAG. However, the positive immunostaining rates of Rb increased significantly. The positive immunostaining rate of p16 was much higher than of Rb in CSG. But, in DYS, the positive immunostaining rates of p16 was much lower than that of Rb. These results suggested that the tumor suppressor gene p16 and Rb may play different roles in the different stages of gastric cardia epithelia carcinogenesis. CAG and GYS have been considered as precancerous lesions of stomach cancer. Although the role of CSG is not clear during the gastric cardia carcinogenesis, it may provide a favorable macroenvironment for gastric carcinogenesis. The significance of CSG in the development of stomach cancer remains to be further characterized.

P16 gene, located at chromosome 9p21, is a new tumor suppressor gene, which was identified by an American molecular geneticist in 1995 and is also called multiple tumor suppressor 1 (MTS1) for its suppressing function to multiple tumors. Recent studies showed that the changes of p16 gene and its products were found in many primary tumors and cell lines^[9,11-15]. Rb gene is the first tumor suppressor gene identified by the location cloning method, located at chromosome 13p. The product of Rb is a nuclear phosphoprotein, which is distributed extensively in different kinds of tissues^[16-22]. It was considered that the cell-cycle progression normally depends on regulation by cyclins and cyclin inhibiting proteins. The overexpression of cyclins and/or the deletion of inhibiting protein could result in overworking of cell-cycle dependent kinetics (cdk),

which makes cells enter into proliferative stage. The p16 could functionally inhibit cdk activity specifically and make Rb unphosphorylated, thus preventing the cell cycle progression from G1 phase to S phase^[22-26].

Tam *et al* found that inactive Rb and/or Rb protein exist in all of the p16 over-expression cell lines, and inactive Rb protein could act directly on p16, suggesting that Rb can inhibit p16 protein expression. P16, Rb and cdk may constitute a feedback regulation circle. In the present study, a significant negative relationship between p16 and Rb protein expression was observed, which is consistent with Tam's observation^[26-33].

REFERENCES

- Zhou Q, Zou JX, Chen YL, Yu HZ, Wang LD, Li YX, Guo HQ, Gao SS, Qiu SL. Alteration of tumor suppressor gene p16 and Rb in gastric carcinogenesis. *Xin Xiaohuabingxue Zazhi* 1997;5:705-706
- Wang Y, Yang SQ, Wang ZG, Pu XD, Sun WG, Liu GZ. Significance of P16 protein expression in hepaticocellular carcinoma tissues. *Huaren Xiaohua Zazhi* 1998;6:412-414
- Quan J, Fan XG. Progress in experimental research of *Helicobacter pylori* infection and gastric carcinoma. *Shijie Huaren Xiaohua Zazhi* 1999;7:1068-1069
- Lu JG, Huang ZQ, Wu JS, Wang Q, Ma QJ, Yao X. Significance of tumor suppressor gene p16 expression in primary biliary cancer. *Shijie Huaren Xiaohua Zazhi* 2000;8:638-610
- Xiao WH, Liu WW, Lu YY, Li Z. Mutation of suppressor gene p53 in hepatocellular carcinoma. *Xin Xiaohuabingxue Zazhi* 1997;5:573-574
- Jiang HH, Liu ZM, Zuang YQ, Yang DH, Jiang YQ, Li JQ. Homozygous deletion of p16 in human gastric adenocarcinoma. *Huaren Xiaohua Zazhi* 1998;6:934-935
- Wu SH, Ma LP, Lin W, Sui YF. The relation between suppressor gene p16, p21, PRB and gastric cancer. *Shijie Huaren Xiaohua Zazhi* 1999;7:551
- Qi YJ, Wang LD, Nie Y, Cai C, Yang GY, Xing EP, Yang CS. Alteration of p16 mRNA expression in esophageal cancer tissue from patients at high incidence area in northern China. *World J Gastroenterol* 1998;4(Suppl 2):108
- Luo F, Kan B, Lei S, Yan LN, Mao YQ, Zou LQ, Yang YX, Wei YQ. Study on p53 protein and C-erbB2 protein expression in primary hepatic cancer and colorectal cancer by flow cytometry. *World J Gastroenterol* 1998;4(Suppl 2):87
- Jiao LH, Wang LD, Xing EP, Yang GY, Yang CS. Frequent inactivation of p16 and p15 expression in human esophageal squamous cell carcinoma detected by RT-PCR. *World J Gastroenterol* 1998;4(Suppl 2):105
- Tian XJ, Wu J, Meng L, Dong ZW, Shou CC. Expression of VEGF-121 in gastric carcinoma MGC803 cell line. *World J Gastroenterol* 2000;6:281-283
- Liu HF, Liu WW, Fang DC, Men RP. Expression of bcl-2 protein in gastric carcinoma and its significance. *World J Gastroenterol* 1998;4:228-230
- He SW, Shen KQ, He YJ, Xie B, Zhao YM. Regulatory effect and mechanism of gastric and its antagonists on colorectal carcinoma. *World J Gastroenterol* 1999;5:408-416
- Huang PL, Zhu SN, Lu SL, Dai SZ, Jin YL. Inhibitor of fatty acid synthase induced apoptosis in human colonic cancer cells. *World J Gastroenterol* 2000;6:295-297
- Zhou Q, Zou JX, Chen YL, Yu HZ, Wang LD, Li YX, Guo HQ, Gao SS, Qiu SL. Alteration of tumor suppressor gene p16 and Rb in gastric carcinogenesis. *China Nat J New Gastroenterol* 1997;3:265
- Yang JM, Wang RQ, Bu BG, Zhou ZC, Fang DC and Luo YH. Effect of HCV infection on expression of several cancer-associated gene products in HCC. *World J Gastroenterol* 1999;5:25-27
- Qin Y, Li B, Tan YS, Sun ZL, Zuo FQ, Sun ZF. Polymorphism of p16INK4a gene and rare mutation of p15INK4b gene exon2 in primary hepatocarcinoma. *World J Gastroenterol* 2000;6:411-414
- Li J, Yang XK, Yu XX, Ge ML, Wang WL, Zhang J, Hou YD. Overexpression of p27KIP1 induced cell cycle arrest in G1 phase and subsequent apoptosis in HCC-9204 cell line. *World J Gastroenterol* 2000;6:513-521
- Favrot M, Coll JL, Louis N, Negoescu A. Cell death and cancer: replacement of apoptotic genes and inactivation of death suppressor genes in the rapy. *Gene Ther* 1998;5:728-739
- Gao HJ, Yu LZ, Bai JF, Peng YS, Sun G, Zhao HL, Miu K, Lu XZ, Zhang XY, Zhao ZQ. Multiple genetic alterations and behavior of cellular biology in gastric cancer and other gastric mucosal lesion: *H. pylori* infection, histological types and staging. *World J Gastroenterol* 2000;6:848-854
- Huang ZM. Modern research in traditional herbal medicine Oenanthe

- Javanica. *Shijie Huaren Xiaohua Zazhi* 2001;9:1-5
- 22 Quigley EMM. Is there a pathologic basis for gastrointestinal dysotility? *World J Gastroenterol* 1998;4(Suppl 2):10-17
- 23 Zhou YA, Gu ZP, Wang XX, Ma QF, Huang LJ. Reexpression of p16-INK4a gene suppresses growth of human esophageal cercinoma cells. *Shijie Huaren Zazhi* 2001;9:877-881
- 24 Chino O, Kijima H, Nishi T, Tanaka H, Oshiba G, Kise Y, Kajiware H, Tsuchida T, Tanaka M, Tajima T, Makuuchi H. Clinicopathological studies of esophageal carcinoma on achalasia: analysis of carcinogenesis using histological and immunohistochemical procedures. *Anticancer Res* 2000;20 :3717-3722
- 25 Jin S, Peng Q, Lu S. Deletion of MTS1/p16 gene in human esophageal carcinoma. *Zhonghua Zhongliu Zazhi* 1998;20:9-11
- 26 Chiang PW, Beer DG, Wei WL, Orringer MB, Kurnit DM. Detection of erbB-2 amplifications in tumors and sera from esophageal carcinoma patients. *Clin Cancer Res* 1999;5:1381-1386
- 27 Schrupp DS, Matthews W, Chen GA, Mixon A, Altirki NK. Flavopiridol mediates cell cycle arrest and apoptosis in esophageal cancer cells. *Clin Cancer Res* 1998;4:2885-2890
- 28 Tang YC, Li Y, Qian GX. Reduction of tumorigenicity of SMMC27721 hepatoma cells by vascular endothelial growth factor antisense gene therapy. *World J Gastroenterol* 2001;7:22-27
- 29 Chen QP. Enteral nutrition and acute panceratitis. *World J Gastroenterol* 2001;7:185-192
- 30 Niu WX, Qin XY, Liu H, Wang CP. Clinicopathological analysis of patients with gastric cancer in 1200 cases. *World J Gastroenterol* 2001;7:281-284
- 31 Yuan P, Sun MH, Zhang JS, Zhu XZ, Shi DR. APC and K ras gene mutation in aberrant crypt foci of human colon. *World J Gastroenterol* 2001;7:352-356
- 32 He XS, Su Q, Chen ZC, He XT, Long ZF, Ling H, Zhang LR. Expression, deletion and mutation of p16 gene in human gastric cancer. *World J Gastroenterol* 2001;7:515-521
- 33 Zhang XL, Quan QZ, Wang YJ, Jiang XL, Wang D, Li WB. Protective effects of cyclosporine A on T cell dependent ConA induced liver injury in Kunming mice. *World J Gastroenterol* 2001;7:569-571

Edited by Ma JY

• GASTRIC CANCER •

Rapid screening mitochondrial DNA mutation by using denaturing high-performance liquid chromatography

Man-Ran Liu, Kai-Feng Pan, Zhen-Fu Li, Yi Wang, Da-Jun Deng, Lian Zhang, You-Yong Lu

Man-Ran Liu, Kai-Feng Pan, Zhen-Fu Li, Yi Wang, Da-Jun Deng, Lian Zhang, You-Yong Lu, Beijing Institute for Cancer Research, Beijing Laboratory of Molecular Oncology, School of Oncology, Peking University, Beijing 100034, China
Supported by the National Key Basic Science Research Program, No. G1998051203 and National Science Foundation of China (NSFC), No. 39602526.

Correspondence to: Dr. You-Yong Lu, Peking University, School of Oncology, Beijing Institute for Cancer Research, Beijing Laboratory of Molecular Oncology, 1 Da-Hong-Luo-Chang Street, Western District, Beijing 100034, China. yongylu@public.bta.net.cn
Telephone: +86-10-66163061 Fax: +86-10-66175832
Received 2002-01-28 Accepted 2002-03-14

Abstract

AIM: To optimize conditions of DHPLC and analyze the effectiveness of various DNA polymerases on DHPLC resolution, and evaluate the sensitivity of DHPLC in the mutation screening of mitochondrial DNA (mtDNA).

METHODS: Two fragments of 16s gene of mitochondrial DNA (one of them F2 is a mutant fragment) and an A3243G mutated fragment were used to analyze the UV detection limit and determine the minimum percentage of mutant PCR products for DHPLC and evaluate effects of DNA polymerases on resolution of DHPLC. Under the optimal conditions, we analyzed the mtDNA mutations from muscle tissues of mitochondrial encephalomyopathy with lactic acidosis and stroke-like episodes (MELAS) and screened blindly for variances in D-loop region of mtDNA from human gastric tumor specimen.

RESULTS: Ten A3243G variants were detected in 12 cases of MELAS, no alterations were detected in controls and these results were consistent with the results obtained by analysis of RFLP with ApaI. We also identified 26 D-loop variances in 46 cases of human gastric cancer tissues and 38 alterations in 13 gastric cancer cell lines. The mutation of mtDNA at 80ng PCR products containing a minimum of 5% mutant sequences could be detected by using DHPLC with UV detector. Moreover, Ampli-Taq Gold polymerase was equally as good as the proofreading DNA polymerase (e.g., Pfu) in eliminating the false positive produced by Taq DNA polymerases.

CONCLUSION: DHPLC is a powerful, rapid and sensitive mutation screening method for mtDNA. Proofreading DNA polymerase is more suitable for DHPLC analysis than Taq polymerase.

Liu MR, Pan KF, Li ZF, Wang Y, Deng DJ, Zhang L, Lu YY. Rapid screening of mitochondrial DNA mutation by using denaturing high-performance liquid chromatography. *World J Gastroenterol* 2002;8(3):426-430

INTRODUCTION

A number of methods, such as PCR-SSCP, DGGE and CSGE, have been developed to screen the gene mutation. PCR-SSCP is a common method in mutation detection^[1-16]. The low resolution and reproducibility or time-cost limit their application for mutation

screening^[17-23]. Recently, a more accurate and rapid DNA screening strategy^[24-29]—Denaturing High-performance Liquid Chromatography (DHPLC) has been applied to mutation screening in human disease-related gene^[30-42] and prenatal diagnosis^[43,44].

However, there are few published data on detection of mitochondrial DNA (mtDNA) variation by DHPLC, especially in cancer. In order to detect effectively the mtDNA mutation, the optimizations of DHPLC for mtDNA mutation screening have been evaluated. The evaluation included the ultraviolet (UV) detection limit for PCR products with variant ingredients, minimal detected ratio of variant to wild type in PCR mixture. In addition, small peak was often observed preceding the chromatography profile in both amplimers of nucleus and mitochondrial genes when Taq DNA polymerases were used in PCR amplification. It may result in failure of DHPLC analysis. Therefore, we also evaluated the effect of DNA polymerases on the resolution of DHPLC in detection of heteroduplex. Basing on those analyses, we identified the mutation of A3243G substitute for patients with mitochondrial encephalomyopathy with lactic acidosis and stroke-like episodes (MELAS). Finally, the variances of D-loop in mtDNA were blindly screened by DHPLC for patients with gastric carcinoma and gastric cancer cell lines.

MATERIALS AND METHODS

Samples and DNA preparation

The specimen in this study included: (1) 12 cases of MELAS, 72 cases of other mitochondrial encephalomyopathies and 30 cases of controls. (2) 46 paired samples of gastric tumor tissues and non-tumor tissues, and 13 gastric cancer cell lines. (3) A randomly selected fragment (fragment 6: from 2616 to 2884nt) within 16s gene was selected to evaluate effect of 11 brands of DNA polymerases on resolution of DHPLC. (4) Another variant fragment (fragment 2: from 1777 to 2069nt) in 16s gene of gastric cancer cell line MKN45 was used to analyze the UV detection limit of PCR products for DHPLC. A variant sample of MELAS, whose ratio of mutant type (G) to wild type (A) at 3243 allele site was about 60 percent, was employed to determine the minimum percentage of mutant PCR products for DHPLC. The genome DNA was isolated following standard phenol/chloroform and ethanol precipitation extraction procedures.

PCR conditions and quantification of PCR products

Fragment containing A3243G mutation in mtDNA of MELAS was amplified by using one pair of oligonucleotide primers. Fragments of D-loop were amplified by using four pairs of overlapping primers described by Levin *et al*^[45]. Another pair of primers was used to amplify fragment 6 (F6) within 16s gene for assessing effect of DNA polymerases on DHPLC (Table 1). 20μL standard PCR reactive system contain genome DNA 15ng, forward and reverse primer 125nmol·L⁻¹ each, 1×buffer (Mg²⁺ 1.6μmol·L⁻¹), dNTP 37.5μmol·L⁻¹, Pfu DNA polymerase 1.5units (or Taq DNA polymerase 1 unit). PCR was performed with 32 cycles consisting of a denaturing step of 94°C for 35s, primer annealing for 50s and an elongation step of 72°C for 90s. The final step at 72°C was extended to 10min. Annealing temperature of each fragment was showed in table 1. In addition, one mutated fragment (F2), harboring in mitochondrial 16s

gene of gastric cancer cell line MKN45, was used to analyze the UV detection limit of PCR products for DHPLC and amplified by PCR protocol for 19, 21, 24, 27, 30 cycles at annealing temperature of 53°C with Pfu polymerase.

Table 1 Primer sequence, PCR Conditions and DHPLC oven temperature used in this study

Fragments	Size (bp)	Primer Sequence	Annealing temp. (°C)	DHPLC temp. (°C)	DHPLC start gradient
A3243G	494	F: cctcccttaggaaaggaca R: gcctagggttgaggttgacca	59	58	55% B ^a
D-loop F1	505	F: gctggaagatct ttaactccaccattagcacc R: ctacgcgtcgac gcgaggagtagcactcttg	65	58	58%B
D-loop F2	515	F: gctggaagatct aatcaatatccgcacaag R: ctacgcgtcgac ttaagtctgtggccagaag	65	58	58%B
D-loop F3	494	F: gctggaagatct caccctattaaccactcacg R: ctacgcgtcgac tgagattagtagtatggag	58	57	58%B
D-loop F4	585	F: gctggaagatct acaagaacccataaccaccagc R: ctacgcgtcgac acttggttaacgtgtgacc	65	58	59%B
16s-F2	292	F: atatgtaccgcaagggaaga R: ggggttctgtggcacaat	53	56	49%B
16s-G6	268	F: aataggacactgtatgaatgg R: tagttcgttgactgggtg	53	60	51 %B

^aEluent buffer B was 0.1mmol·L⁻¹ TAE, 25% acetonitrile, pH7.0.

The PCR products of mutant fragment (F2) amplified with 19-30 cycles were electrophoresed by 2% agarose gel. The agarose gel was exposed to Kodak Image Station 440CF, and the resulting signal qualified by using the Kodak 1d Image Analysis software. Values were normalized against pUC18 message. A variant sample which ratio of mutant type (G) to wild type (A) at 3243 allele site was about 60 percent and a normal blood sample were amplified respectively. Both PCR products were mixed according to ratio of mutant: wild type to be 50%, 40%, 30%, 20%, 10%, 5% and 0%.

DHPLC analysis

PCR products from gastric cancer cell lines were mixed with about 30 percent of PCR ingredients of normal blood in order to detect homozygous mutation in cell lines. Prior to DHPLC analysis, all fragments were heated to 95°C for 3min, followed by slow cooling to 45°C over 50min to form a mixture of hetero- and homoduplex. The melting temperature and optimal gradient for each fragment (Table 1) can be obtained with WAVEMAKER4.0 software with some empirical optimization. Aliquots of 3μL PCR products were automatically loaded on the DNasep column and eluted on a linear acetonitrile gradient in a 0.1mol·L⁻¹ triethylamine acetate buffer (pH 7.0) with a constant flow rate of 0.9mL·min⁻¹. Elution of DNA from the column was detected by absorbing at 260nm.

DNA sequencing

PCR products were purified by 4% PAGE gel. Direct sequencing of the PCR products was performed by use of the fluorescent terminators on an ABI Prism 377 sequencer (PE Biosystems, USA). The sequence data were checked with MITOMAP Human mtDNA "Cambridge" Sequences (<http://www.gen.emory.edu/MITOMAP/mitoseq.html>).

RESULTS

Optimization of DHPLC for mtDNA mutation detection

The UV detection limit was analyzed for PCR products with variants. The concentration of PCR products of 16s gene containing a variance from gastric cancer cell line MKN45 was about 8, 20, 40, 85 and 110ng·μL⁻¹ after amplification with 19, 21, 24, 27, 30 cycles respectively. The UV detection limit was about 80ng for the PCR products whose mutated ingredients were efficiently detected by DHPLC.

The minimal ratio of heteroduplex detected by DHPLC was studied. To investigate the sensitivity of DHPLC in detection of mtDNA variants, we used PCR products from the mutated MELAS sample to mix with normal blood amplimers based on ratio of mutant to wild type to be 50%, 40%, 30%, 20%, 10%, 5%, 1% and 0%. Our results showed that heteroduplexes were sensitively

detected by DHPLC, when the ratio (mutant:wild) range from 5% to 50% in the mixture of PCR products (Figure 1). Moreover, the chromatography profiles of DHPLC were similar when mutant products in mixture were about 10-40%. It suggested that homozygous mutation could be easily identified if 20-30% wild PCR products were added.

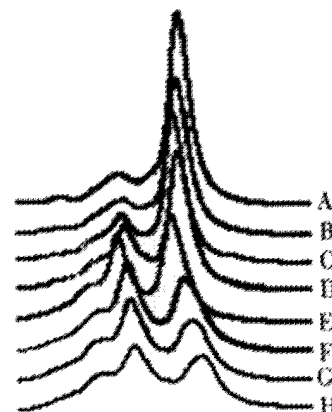


Figure 1 The minimal ratio of hetero-: homoduplex in mixture were identified by DHPLC. The composition of mutant type in PCR product mixture are 0% (A, wild type), 1% (B), 5% (C), 10% (D), 20% (E), 30% (F), 40% (G) and 50% (H) respectively. Chromatogram B has no difference to chromatogram A. Heteroduplex peak start to change in sample containing 5% variant (C). The heteroduplex can be obviously discerned in sample with 10% variant (D). Chromatogram E to H is almost similar. It indicates that about 5% mutant composition in PCR product mixture can be detected by DHPLC.

The effect of DNA polymerases on DHPLC was evaluated. A small peak was often observed preceding the main peak in most of fragments amplified by Taq DNA polymerases. In order to understand whether this was an universality or DHPLC resolution induced by Taq polymerase, we chose 6 brands of Taq, 1 type of Taq Gold and 4 kinds proofreading DNA polymerases to amplify a randomly selected fragment (F6) for DHPLC analysis. Our findings displayed that all in this study gave a broadened peak proceeding the main peak, but Taq Gold and proofreading DNA polymerases (such as Pfu and Vent) had no or tiny peak before the main peak (Figure 2). To exclude the results that were induced by polymerase buffer, we further amplified the fragment using Taq polymerase to match with Taq Gold and proofreading polymerase buffer, or Taq Gold and proofreading polymerase with Taq polymerase buffer. The results indicated that the particular small peak was only related to Taq DNA polymerase itself.

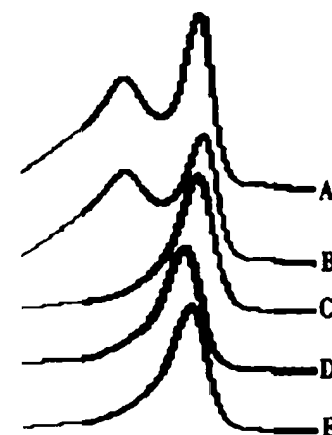


Figure 2 The universality of a broad small peak proceeding the main peak induced by Taq DNA polymerase. An extra small peak is observed preceding the eluted chromatography profile of A and B but not in chromatogram of C, D and E. Chromatogram A is a representative of products amplified by Taq DNA

polymerase. B is typical chromatography profile when Taq DNA polymerase matched with Pfu DNA polymerase buffer in PCR reaction. C and D respectively comes from amplimers amplified by Ampli-Taq Gold and Vent DNA polymerase. E is one of chromatograms coming from PCR amplification by using Pfu DNA polymerase.

Mutation screening of mtDNA

Patients with MELAS have been suggested to associate with mutation of A3243G in tRNA^{Leu}[46,47]. 10 variant cases out of 12 MELAS patients were successfully identified by DHPLC. No alterations were detected in 72 cases with other mitochondrial encephalomyopathies and 30 controls at this allele site. These results were completely consistent with results obtained by restriction endonuclease Apa I.

Basing on above results, we further screened blindly the variants of non-coding D-loop region of mtDNA in gastric cancer using 4 pairs of overlapping primers. In the primary scanning, 28 heteroduplexes were identified in gastric tumor tissues and 38 variances were distinguished in cell lines. The typical chromatograms of heteroduplexes in each fragment were showed in Figure 3. To prove the results, all of positive samples were detected repeatedly. 26 heteroduplexes in tumor group were confirmed, 2 cases were checked to be negative. The two samples were distinguished to be positive due to change of retention time in contrast with other samples, but their chromatograms were similar with wild type. The detected variant frequency of mtDNA by DHPLC was listed in table 2. Ten variant fragments were randomly chosen for direct DNA sequencing, and all of mutated fragments were confirmed.

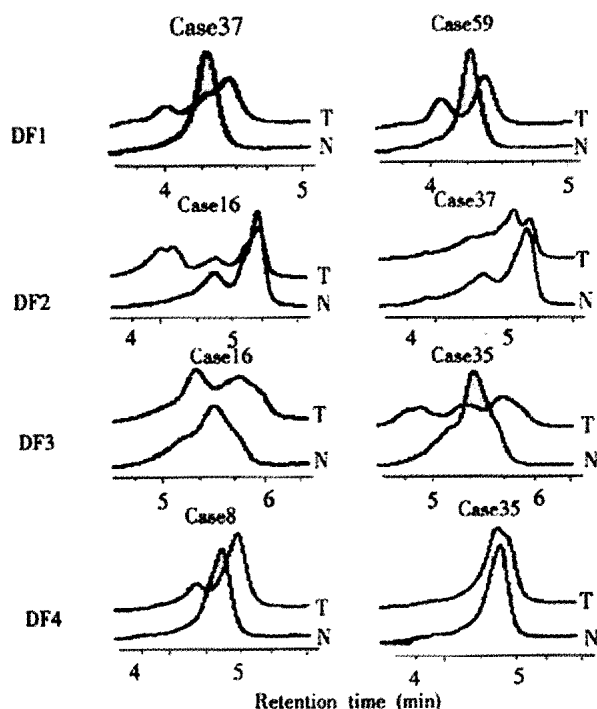


Figure 3 The representative DHPLC chromatograms of variant fragments detected blindly for patients with gastric carcinoma in D-loop of mtDNA. The chromatogram of tumor tissue is visibly different to that of its counterpart non-tumor tissue. The variant cases are listed on the top of each DHPLC chromatogram. DF1, DF2, DF3 and DF4 represent the tested fragments of D-loop respectively. T: tumor tissues; N: non-tumor tissues.

Table 2 The detected frequency of variance of mtDNA by using DHPLC

Fragments Samples	A3243G			D-loop	
	MELAS	Other Encephal ^a	Normal blood	Tumor	Cell line
Positive/total fragments	10/12	0/72	0/30	26/184	38/52
Percent (%)	83.3	0	0	14.1	73.1

DISCUSSION

Mutation detection by DHPLC is performed at a temperature sufficient to partially denature the DNA heteroduplexes. The different retention times of hetero- and homoduplex on the DNASEp matrix allow for high sensitivity and rapid detection[48,49]. In generally, the heteroduplex profile is easily distinguished from homoduplex peak.

Although the present data have showed that DHPLC is a convenient and sensitive method in mutation screening[17,22,24-26,28]. It may be a challenge to mutation detection of mtDNA because of complicated heteroplasmy in mitochondria[50,51] and various types of variances in mtDNA molecule. Due to hundreds to thousands mtDNA copies in a cell[52], the ratio of a special mutant to normal mtDNA is relatively low. However, a number of various variants may co-existence in a sample. For these reasons, sensitive and rapid detecting method is needed to distinguish different types of variances in large sets of mtDNA copies. We applied DHPLC to screen the mtDNA mutation in this study. Our data showed that DHPLC was a powerful screening strategy for mtDNA mutation. Firstly, about 80ng of PCR products with variant that could be identified by DHPLC were enough to UV detection limit. The heteroduplex peak was not visible when total PCR products were less than 50ng each injection. But the homoduplex peak could be satisfactorily detected. Next, about 5 percent of mutant products in PCR mixture were effectively discerned. These results indicated that DHPLC was sensitive to distinguish those minimal special variants from a large normal mtDNA. Finally, the results were reproducible.

In detection of A3243G mutation for MELAS patients, we proved our collaborators research. Ten variant samples identified by using restriction endonuclease ApaI were all distinguished by DHPLC. Heteroduplexes of tumor tissues obtained by DHPLC were also visibly different to that of non-tumor counterpart, when DHPLC was used to screen blindly the variances of D-loop of mtDNA in gastric cancer. These results also demonstrated that DHPLC, as same as research for nuclear DNA[25-27,29,34], was a sensitive method for mtDNA mutation screening.

As mutation detection of nucleus genes, several factors must be addressed when DHPLC is employed in mtDNA screening. These factors include primer design, PCR optimization, choice of optimal melting temperature or reverse-phase gradient[29,49,53] and DNA polymerase in this study. We find Taq polymerase may influence identification of mutation for DHPLC screening. Taq DNA polymerase tends to add a deoxyribonucleotide, preferentially dATP, to the 3'-hydroxyl terminus of a blunt-ended substrate, and the high-sensitivity of the WAVE system makes it capable of registering these A-tailed products to form an extra peak. In particular, the GC-rich small fragment with high T_m is easy to be influenced. Because the selected temperature of column oven is high, the retention time of heteroduplex will be reduced and the extra small peak is prone to form a false heteroduplex peak.

The concentration of dNTP in PCR reaction is factor of DHPLC resolution for heteroduplex detection. DNA molecules bind with the DNASEp cartridge via the triethylammonium acetate (TEAA). The dNTP contends with DNA in interaction with TEAA and decrease DNASEp cartridge's binding sites to TEAA-DNA complex. Therefore, ability of cartridge to bind with DNA and resolution of DHPLC will be reduced. In order to obtain improved resolution of DHPLC, it is necessary to elute the cartridge by 75% acetonitrile regularly.

In conclusion, DHPLC is a powerful screening method for mtDNA mutation because of its high-throughput, automation, sensitivity and high reproducibility.

ACKNOWLEDGMENT

We thank Dr. Z.X. Wan and J.J.Zhang for kindly providing of

mtDNA from MELAS and other known mutated samples. We also thank Dr. W.G. Liu, Assistant professor, Mayo Clinic, Rochester USA, for comments on the manuscript. This work was supported by the National Key Basic Science Research Program, No. G1998051203, and National Science Foundation of China (NSFC), No. 39602526.

REFERENCES

- Deng ZL, Ma Y. Aflatoxin sufferer and p53 gene mutation in hepatocellular carcinoma. *World J Gastroenterol* 1998; 4: 28-29
- Luo D, Liu QF, Gove C, Naomov NV, Su JJ, Williams R. Analysis of N-ras gene mutation and p53 gene expression in human hepatocellular carcinomas. *World J Gastroenterol* 1998; 4: 97-99
- Peng XM, Peng WW, Yao JL. Codon 249 mutations of p53 gene in development of hepatocellular carcinoma. *World J Gastroenterol* 1998; 4:125-127
- Zhao X, Cai YY, Xie DW, Wang LD, Yang CS. Multiplex PCR SSCP: a highly effective and efficient method of mutation detection and analysis. *World J Gastroenterol* 1998; 4:106
- Peng XM, Yao CL, Chen XJ, Peng WW, Gao ZL. Codon 249 mutations of p53 gene in non-neoplastic liver tissues. *World J Gastroenterol* 1999; 5:324-326
- Weng ML, Li JG, Gao F, Zhang XY, Wang PS, Jiang XC. The mutation induced by space conditions in *Escherichia coli*. *World J Gastroenterol* 1999; 5:445-447
- Ji CY, Smith DR, Goh HS. The role and prognostic significance of p53 mutation in colorectal carcinomas. *World J Gastroenterol* 2000; 6:78
- Liu WD, Hada T, Cheng JD, Higashino K. Point mutations in E2, NS3 and NS5A of hepatitis G virus. *World J Gastroenterol* 2000; 6:41
- Qin Y, Li B, Tan YS, Sun ZL, Zuo FQ, Sun ZF. Polymorphism of p16INK4a gene and rare mutation of p15INK4b gene exon2 in primary hepatocarcinoma. *World J Gastroenterol* 2000; 6:411-414
- Wang Y, Liu H, Zhou Q, Li X. Analysis of point mutation in site 1896 of HBV precore and its detection in the tissues and serum of HCC patients. *World J Gastroenterol* 2000; 6:395-397
- Wang XJ, Yuan SL, Li CP, Iida N, Oda H, Aiso S, Ishikawa T. Infrequent p53 gene mutation and expression of the cardia adenocarcinomas from a high-incidence area of Southwest China. *World J Gastroenterol* 2000; 6:750-753
- Liu J, Chen SL, Zhang W, Su Q. P21-WAF1 gene expression with p53 mutation in esophageal carcinoma. *Shijie Huaren Xiaohua Zazhi* 2000; 8:1350-1353
- Cui J, Yang DH, Qin HR. Mutation and clinical significance of c-fms oncogene in hepatocellular carcinoma. *Shijie Huaren Xiaohua Zazhi* 2001; 9:392-395
- Fan RY, Li SR, Wu ZT, Wu X. Detection of P53 protein, K-ras and APC gene mutation in sporadic colorectal cancer tissue and exfoliative epithelial cells in stool. *Shijie Huaren Xiaohua Zazhi* 2001; 9:771-775
- He XS, Su Q, Chen ZC, He XT, Long ZF, Ling H, Zhang LR. Expression, deletion and mutation of p16 gene in human gastric cancer. *World J Gastroenterol* 2001; 7:515-521
- Yuan P, Sun MH, Zhang JS, Zhu XZ, Shi DR. APC and K-ras gene mutation in aberrant crypt foci of human colon. *World J Gastroenterol* 2001; 7:352-356
- Choy YS, Dabora SL, Hall F, Ramesh V, Niida Y, Franz D, Kasprzyk-Obara J, Reeve MP, Kwiatkowski DJ. Superiority of denaturing high performance liquid chromatography over single-stranded conformation and conformation-sensitive gel electrophoresis for mutation detection in TSC2. *Ann Hum Genet* 1999; 63:383-391
- Gross E, Arnold N, Goette J, Schwarz-Boeger U, Kiechle M. A comparison of BRCA1 mutation analysis by direct sequencing, SSCP and DHPLC. *Hum Genet* 1999; 105:72-78
- Boutin P, Vasseur F, Samson C, Wahl C, Froguel P. Routine mutation screening of HNF-1alpha and GCK genes in MODY diagnosis: how effective are the techniques of DHPLC and direct sequencing used in combination? *Diabetologia* 2001; 44:775-778
- Eng C, Brody LC, Wagner TM, Devilee P, Vijg J, Szabo C, Tavtigian SV, Nathanson KL, Ostrander E, Frank TS. Interpreting epidemiological research: blinded comparison of methods used to estimate the prevalence of inherited mutations in BRCA1. *J Med Genet* 2001; 38: 824-833
- Klein B, Weirich G, Brauch H. DHPLC-based germline mutation screening in the analysis of the VHL tumor suppressor gene: usefulness and limitations. *Hum Genet* 2001; 108:376-384
- Kristensen VN, Kelefiotis D, Kristensen T, Borresen-Dale AL. High-throughput methods for detection of genetic variation. *Biotechniques* 2001; 30:318-322
- Xiao WZ, Oefner PJ. Denaturing high-performance liquid chromatography: A review. *Hum Mutat* 2001;17:439-474
- O'Donovan MC, Oefner PJ, Roberts SC, Austin J, Hoogendoorn B, Guy C, Speight G, Upadhyaya M, Sommer SS, McGuffin P. Blind analysis of denaturing high-performance liquid chromatography as a tool for mutation detection. *Genomics* 1998; 52:44-49
- Arnold N, Gross E, Schwarz-Boeger U, Pfisterer J, Jonat W, Kiechle M. A highly sensitive, fast, and economical technique for mutation analysis in hereditary breast and ovarian cancers. *Hum Mutat* 1999; 14:333-339
- Hoogendoorn B, Norton N, Kirov G, Williams N, Hamshire ML, Spurlock G, Austin J, Stephens MK, Buckland PR, Owen MJ, O'Donovan MC. Cheap, accurate and rapid allele frequency estimation of single nucleotide polymorphisms by primer extension and DHPLC in DNA pools. *Hum Genet* 2000; 107:488-493
- Spiegelman JL, Mindrinos MN, Oefner PJ. High-accuracy DNA sequence variation screening by DHPLC. *Biotechniques* 2000; 29:1084-1090
- Roberts PS, Jozwiak S, Kwiatkowski DJ, Dabora SL. Denaturing high-performance liquid chromatography (DHPLC) is a highly sensitive, semi-automated method for identifying mutations in the TSC1 gene. *J Biochem Biophys Methods* 2001; 47:33-37
- Taliani MR, Roberts SC, Dukek BA, Pruthi RK, Nichols WL, Heit JA. Sensitivity and specificity of denaturing high-pressure liquid chromatography for unknown protein C gene mutations. *Genet Test* 2001; 5:39-44
- Yokomizo A, Tindall DJ, Drabkin H, Gemmill R, Franklin W, Yang P, Sugio K, Smith DI, Liu W. PTEN/MMAC1 mutations identified in small cell, but not in non-small cell lung cancers. *Oncogene* 1998; 17:475-479
- Benit P, Kara-Mostefa A, Berthelon M, Sengmany K, Munnich A, Bonnefont JP. Mutation analysis of the hamartin gene using denaturing high performance liquid chromatography. *Hum Mutat* 2000; 16: 417-421
- Gross E, Arnold N, Pfeifer K, Bandick K, Kiechle M. Identification of specific BRCA1 and BRCA2 variants by DHPLC. *Hum Mutat* 2000; 16:345-353
- Nickerson ML, Weirich G, Zbar B, Schmidt LS. Signature-based analysis of MET proto-oncogene mutations using DHPLC. *Hum Mutat* 2000; 16:68-76
- van Den Bosch BJ, de Coe RF, Scholte HR, Nijland JG, van Den Bogaard R, de Visser M, de Die-Smulders CE, Smeets HJ. Mutation analysis of the entire mitochondrial genome using denaturing high performance liquid chromatography. *Nucleic Acids Res* 2000;28:E89
- Cohn D, Mutch D, Elbendary A, Rader J, Herzog T, Goodfellow P. No evidence for BCL10 mutation in endometrial cancers with microsatellite instability. *Hum Mutat* 2001; 17:117-121
- Gross E, Kiechle M, Arnold N. Mutation analysis of p53 in ovarian tumors by DHPLC. *J Biochem Biophys Methods* 2001; 47:73-81
- Han SS, Cooper DN, Upadhyaya MN. Evaluation of denaturing high performance liquid chromatography (DHPLC) for the mutational analysis of the neurofibromatosis type 1 (NF1) gene. *Hum Genet* 2001; 109:487-497
- Kleymenova E, Walker CL. Determination of loss of heterozygosity in frozen and paraffin embedded tumors by denaturing high-performance liquid chromatography (DHPLC). *J Biochem Biophys Methods* 2001; 47:83-90
- Le Gac G, Mura C, Ferec C. Complete scanning of the hereditary hemochromatosis gene (HFE) by use of denaturing HPLC. *Clin Chem* 2001; 47:1633-1640
- Lin D, Goldstein JA, Mhatre AN, Lustig LR, Pfister M, Lalwani AK. Assessment of denaturing high-performance liquid chromatography (DHPLC) in screening for mutations in connexin 26 (GJB2). *Hum Mutat* 2001; 18:42-51
- Nicolao P, Carella M, Giometto B, Tavolato B, Cattin R, Giovannucci-Uzielli ML, Vacca M, Regione FD, Piva S, Bortoluzzi S, Gasparini P. DHPLC analysis of the MECP2 gene in Italian Rett patients. *Hum Mutat* 2001; 18:132-140
- zur Stadt U, Rischewski J, Schneppenheim R, Kabisch H. Denaturing HPLC for identification of clonal T-cell receptor gamma rearrangements in newly diagnosed acute lymphoblastic leukemia. *Clin Chem* 2001; 47:2003-2011
- Lam CW, Sin SY, Lau ET, Lam YY, Poon P, Tong SF. Prenatal diagnosis of glycogen storage disease type 1b using denaturing high performance liquid chromatography. *Prenat Diagn* 2000; 20:765-768
- Benit P, Bonnefont JP, Kara Mostefa A, Francannet C, Munnich A, Ray PF. Denaturing high-performance liquid chromatography (DHPLC)-based prenatal diagnosis for tuberous sclerosis. *Prenat Diagn* 2001; 21:279-283
- Levin BC, Cheng HY, Reeder DJ. A human mitochondrial DNA standard reference material for quality control in forensic identification, medical diagnosis, and mutation detection. *Genomics* 1999; 55:135-146
- Dubeau F, De Stefano N, Zifkin BG, Arnold DL, Shoubridge EA. Oxidative phosphorylation defect in the brains of carriers of the tRNA^{Leu} (UUR) A3243G mutation in a MELAS pedigree. *Ann Neurol* 2000; 47:

- 179-185
- 47 Sternberg D, Chatzoglou E, Laforet P, Fayet G, Jardel C, Blondy P, Fardeau M, Amselem S, Eymard B, Lombes A. Mitochondrial DNA transfer RNA gene sequence variations in patients with mitochondrial disorders. *Brain* 2001; 124:984-994
- 48 Kuklin A, Davis AP, Haefele R, Alianell G, Gjerde D, Taylor P. New paradigms in NDA polymorphism detection. *Biomed Prod* 1998; 7:90-92
- 49 Kuklin A, Munson K, Gjerde D, Haefele R, Taylor P. Detection of single-Nucleotide Polymorphisms with the WAVETM DNA fragment Analysis System. *Genet Test* 1997/98; 1:201-206
- 50 Battersby BJ, Shoubridge EA. Selection of a mtDNA sequence variant in hepatocytes of heteroplasmic mice is not due to differences in respiratory chain function or efficiency of replication. *Hum Mol Genet* 2001; 10: 2469-2479
- 51 Srivastava S, Moraes CT. Manipulating mitochondrial DNA heteroplasmy by a mitochondrially targeted restriction endonuclease. *Hum Mol Genet* 2001; 10:3093-3099
- 52 Chinnery PF, Turnbull DM. Mitochondrial DNA and disease. *Lancet* 1999; 354:17-21
- 53 Narayanaswami G, Taylor P. Improved efficiency of mutation detection by denaturing high-performance liquid chromatography using modified primers and hybridization procedure. *Genet Test* 2001; 5:9-16

Edited by Pagliarini R

• GASTRIC CANCER •

Changes of NF- κ B, p53, Bcl-2 and caspase in apoptosis induced by JTE-522 in human gastric adenocarcinoma cell line AGS cells: role of reactive oxygen species

Hong-Liang Li, Dan-Dan Chen, Xiao-Hong Li, Hai-Wei Zhang, Yan-Qing Lü, Chun-Ling Ye, Xian-Da Ren

Hong-Liang Li, Xiao-Hong Li, Yan-Qing Lü, Chun-Ling Ye, Xian-Da Ren, Department of Pharmacology, Jinan University Pharmacy College, Guangzhou 510632, Guangdong, China
Dan-Dan Chen, Department of Cardiology, First Affiliated Hospital, Zhongshan University, Guangzhou 510089, Guangdong, China
Hai-Wei Zhang, Department of Pathology, Jinan University Medical College, Guangzhou 510632, Guangdong, China

Supported by National Natural Science Foundation of China, No. 39770300, 30070873, and the Overseas Chinese Affairs Office of the State Council Foundation, No. 98-33

Correspondence to: Prof. Xian-Da Ren, Department of Pharmacology, Jinan University Pharmacy College, Guangzhou 510632, Guangdong, China. tsam@jnu.edu.cn

Telephone: +86-20-85220261

Received 2002-01-28 Accepted 2002-03-05

Abstract

AIM: To identify whether JTE-522 can induce apoptosis in AGS cells and ROS also involved in the process, and to investigate the changes in NF- κ B, p53, bcl-2 and caspase in the apoptosis process.

METHODS: Cell culture, MTT, Electromicroscopy, agarose gel electrophoresis, lucigenin, Western blot and electrophoretic mobility shift assay (EMSA) analysis were employed to investigate the effect of JTE-522 on cell proliferation and apoptosis in AGS cells and related molecular mechanisms.

RESULTS: JTE-522 inhibited the growth of AGS cells and induced the apoptosis. Lucigenin assay showed the generation of ROS in cells under incubation with JTE-522. The increased ROS generation might contribute to the induction of AGS cells to apoptosis. EMSA and Western blot revealed that NF- κ B activity was almost completely inhibited by preventing the degradation of I κ B α . Additionally, by using Western blot we confirmed that the level of bcl-2 was decreased, whereas p53 showed a great increase following JTE-522 treatment. Their changes were in a dose-dependent manner.

CONCLUSION: These findings suggest that reactive oxygen species, NF- κ B, p53, bcl-2 and caspase-3 may play an important role in the induction of apoptosis in AGS cells after treatment with JTE-522.

Li HL, Chen DD, Li XH, Zhang HW, Lü YQ, Ye CL, Ren XD. Changes of NF- κ B, p53, Bcl-2 and caspase in apoptosis induced by JTE-522 in human gastric adenocarcinoma cell line AGS cells: role of reactive oxygen species. *World J Gastroenterol* 2002;8(3):431-435

INTRODUCTION

Apoptosis is an active cell death process, which requires specific gene regulation. A critical role for p53 in the execution of some forms of apoptosis has been suggested^[1-6]. This protein is a sequence-specific DNA-binding protein, active as a transcription factor. It has been proposed that p53 may be involved in the cellular response to DNA

damage, producing arrest in the G₁ phase of the cell cycle to allow efficient repair of DNA before entry to S phase, or cell death if the damage is too large to be repaired^[7,8]. Another gene implicated in apoptosis is bcl-2. The bcl-2 gene product functions as an anti-apoptotic signal, suppressing apoptosis induced by a wide variety of stimuli, including chemotherapeutic drugs and γ radiation^[9-13]. The exact mechanism of bcl-2 in preventing apoptosis is still not clear. However, bcl-2 has been implicated in cellular control of their redox state^[14].

Previous studies have demonstrated that non-steroidal anti-inflammatory drugs (NSAIDs) given *in vivo* to rodents and human can inhibit tumor growth^[15,16]. JTE-522 is a novel NSAIDs, which is a specific inhibitor of cyclooxygenase-2 (COX-2) with significant anti-inflammatory and analgesic properties^[17]. Some reported that JTE-522 possesses strong chemopreventive activity against colon carcinogenesis^[18], but the precise mechanism by which JTE-522 inhibits colon carcinogenesis is not clear. It is often attributed to specific inhibition of arachidonic acid metabolism via coxenzymes. However, recent studies showed that the antitumor effect had little connection with NSAIDs inhibitory activity against cyclooxygenase, and was not prevented by exogenous supplementation of 16,16-dimethyl prostaglandin E₂. Several groups have shown that certain NSAIDs induce apoptosis of tumor cell line, which is associated with the generation of reactive oxygen species (ROS)^[19,20]. However, the signaling pathway leading to apoptotic cell death remains unclear.

ROS can play a central role in regulating cell proliferation and cell death. Evidence has been obtained that ROS such as superoxide and hydrogen peroxide can influence cell death triggered by internal cues (p53-mediated), external cues (TGF- β -mediated) and immunogenic signals (TNF- α)^[21,22]. In other instances, however, generation of ROS can inhibit apoptosis. Although the mechanism involved is still controversial, redox status and/or hydrogen peroxide have both been proposed as critical factors^[19]. Therefore it is possible that ROS may play a role in regulating apoptosis in gastric epithelium.

The purpose of the present study is to identify whether JTE-522 can induce apoptosis in AGS cells and ROS are also involved in the process, and to investigate the changes in NF- κ B, p53, bcl-2 and caspase in the apoptosis process.

MATERIALS AND METHODS

Cell line and reagents

Human gastric adenocarcinoma cell line AGS was provided by Cancer Institute, Zhongshan University. Cells were grown in RPMI-1640 medium and supplemented with 10% new bovine serum, penicillin G (100kU.L⁻¹) and kanamycin (0.1g.L⁻¹) at 37°C in a 5% CO₂-95% air atmosphere. Antibodies used in this study included p53, bcl-2, I κ B α and Beta actin were obtained from Santa Cruz. All other chemicals were purchased from Sigma Chemical Co (St. Louis, MO, USA).

MTT assay

AGS cells growing on 96-well plates were treated with JTE-522 (0.1 mmol/L - 1 mmol/L) for 72h, untreated cells served as a control. 10 μ L of the 2.5g.L⁻¹ stock solution of 3-[4, 5-dimethylthiaolyl]-2,

5-diphenyl-tetrazolium bromide (MTT) was added to each well. After 1h of incubation at 37°C, the medium was removed, 50µl of the extraction buffer (10% Triton-X100; 0.1mol/L HCl) was added, and plates were gently shaken for 30min at room temperature. The optical densities were measured at 570nm.

Morphological and biochemical analysis of apoptosis

Morphological changes in the nuclear chromatin of cells undergoing apoptosis were detected by electron microscopy (EM). Cells were pelleted and fixed with 30mL/L glutaraldehyde in PBS. EM analysis was performed as described previously^[23]. Oligonucleosomal cleavage of genomic DNA was detected by agarose gel electrophoresis. In brief, genomic DNA isolated as previously described^[24] was subjected to 1.5% agarose gel electrophoresis, followed by ethidium bromide staining.

Assay for reactive oxygen species production

Generation of ROS was assessed using lucigenin. AGS cells grown in 75cm² culture flasks were incubated for 6h with JTE-522 (0.1-1mmol/L) in the presence or absence of 100µmol/L pyrrolidine dithiocarbamate (PDTTC). The cells were then scraped off and washed in cold Hank's buffer. An aliquot containing 1×10^6 cells in 100µL of Hank's buffer was mixed in microtiter wells with 100µl of lucigenin prepared at a concentration of 40µmol/L. Light emission was detected using a Berthold LB96V luminometer for 3min.

Assessment of caspase activity

Caspase-3 activity was measured using a caspase assay kit according to the supplier's instruction. In brief, caspase-3 fluorogenic substrates (Ac-DEVD-AMC or Ac-IETD-AMC) were incubated with JTE-522-treated with cell lysates for 1h at 37°C, then AMC liberated from Ac-DEVD-AMC or Ac-IETD-AMC was measured using a fluorometric plate reader with an excitation wavelength of 380nm and an emission wavelength of 420-460nm.

Western blot analysis

The cells were lysed in lysis buffer (25mmol/L hepes, 1.5% Triton X-100, 1% sodium deoxycholate, 0.1% SDS, 0.5mol/L NaCl, 5mmol/L EDTA, 50mmol/L NaF, 0.1mmol/L sodium vanadate, 1mmol/L phenylmethylsulfonyl fluoride (PMSF), and 0.1g.L⁻¹ leupeptin (pH7.8) at 4°C with sonication. The lysates were centrifuged at 15000g for 15min and the concentration of the protein in each lysate was determined with Coomassie brilliant blue G-250. Loading buffer (42mmol/L Tris-HCl, 10% glycerol, 2.3% SDS, 5% 2-mercaptoethanol and 0.002% bromophenol blue) was then added to each lysate, which was subsequently boiled for 3min and then electrophoresed on a SDS-polyacrylamide gel. Proteins were transferred to nitrocellulose and incubated sequentially with antibodies against IκBα, p53 and bcl-2 and then with peroxidase-conjugated secondary antibodies in the second reaction. Detection was performed with enhanced chemiluminescence reagent.

Electrophoretic mobility shift assay (EMSA)

Nuclear extracts were prepared from AGS cells treated with JTE-522. Synthetic double-strand oligonucleotides of consensus NF-κB binding sequence, GATCCCAACGGCAGGGGA, were end-labeled with [γ^{32}]ATP using T4 polynucleotide kinase. Nuclear extract was incubated with the labeled probe in the presence of poly (dI-dC) in a binding buffer containing 20mM N-2-hydroxyethylpiperazine-N'-2-ethanesulfonic acid at room temperature for 30min. For supershift assays, a total of 0.2µg of antibodies against p65 subunit of NF-κB were included in the reaction. DNA-protein complexes were resolved by electrophoresis in a 5% non-denaturing polyacrylamide gel, which was dried and visualized by autoradiography.

RESULTS

Effect of JTE-522 on cell proliferation and apoptosis

AGS cells were incubated with various doses of JTE-522 for 72h. Analysis of cell viability using MTT assay showed that JTE-522 significantly inhibited cell viability. The inhibition of cell viability was dependent on the dose of JTE-522 used (Figure 1).

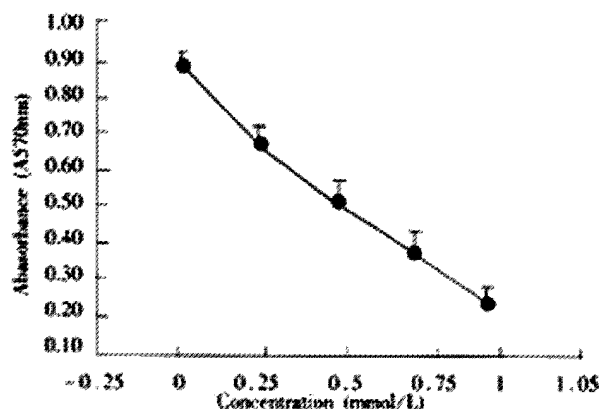


Figure 1 Effect of JTE-522 on cell growth in AGS cells. The cells were treated with various concentrations of JTE-522 for 72h. The antiproliferative effect was measured by MTT assay. Results are the means±SD from three independent determinations.

The effect was due to apoptosis as demonstrated by EM and electrophoresis of genomic DNA. JTE-522-treated cells showed compacted nuclear chromatin with finely granular masses margined against the nuclear envelope and condensed cytoplasm, the nuclear outline was convoluted and the organelles were preserved (Figure 2) and led to oligonucleosomal cleavage of genomic DNA (Figure 3), which were hallmarks of apoptosis.

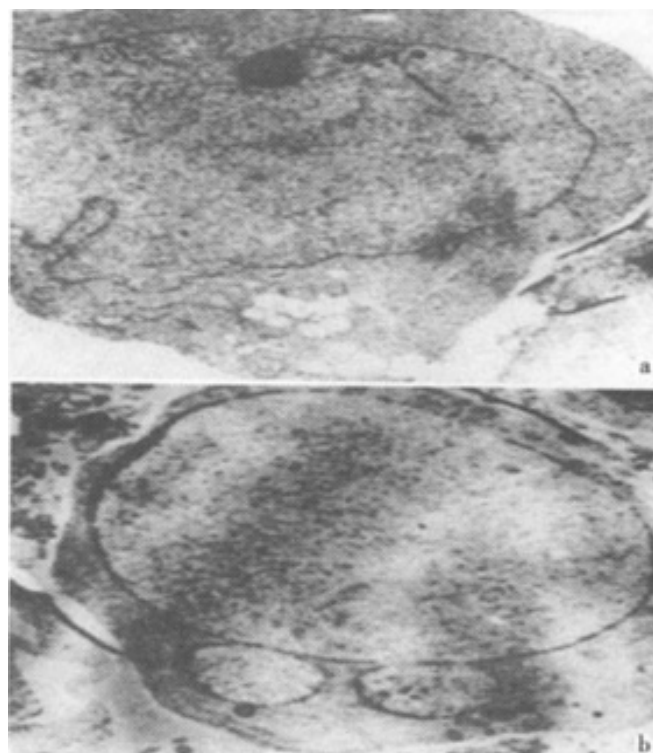


Figure 2 Electro micrographs of JTE-522-treated AGS cells. Control AGS cells (A), or treated with 1mmol/L (B) JTE-522 for 72h, were examined by EM as in "Materials and Methods". Magnification: $\times 4000$

We next investigated whether the activation of caspase was involved in JTE-522-induced apoptosis of AGS cells. JTE-522-induced apoptosis of AGS cells was accompanied by the induction of caspases activity as demonstrated by the cleavage of Ac-DEVD-AMC and Ac-IETD-AMC, respectively (Figure 4). These results indicated that JTE-522-induced cell death of AGS cells was a typical apoptosis associated with caspase activation.

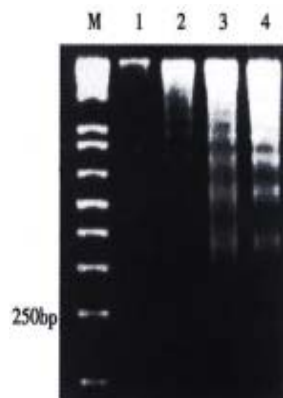


Figure 3 DNA ladder pattern formation of AGS cells. Cells treated with different concentrations of JTE-522 for 72h and the formation of oligonucleosomal fragments was determined by 1.5% agarose gel electrophoresis. M, DNA markers; lanes 1-4, AGS cells treated with 0, 0.25, 0.50, 1mmol/L of JTE-522

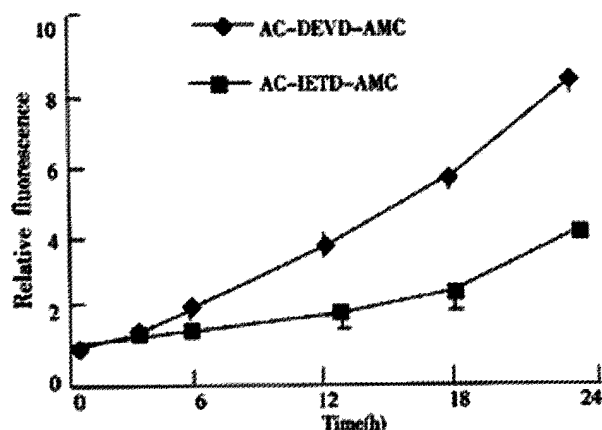


Figure 4 Activation of caspase-3 activities by JTE-522 in AGS cells for indicated time period. JTE-522 treatment (0.75mmol/L) induced cleavage of Ac-DEVD-AMC and Ac-IETD-AMC, indicating activation of caspase-3 activity, respectively

Effect of JTE-522 on the production of ROS in AGS cells

The effect of JTE-522 on the production of ROS in AGS cells, as assessed with lucigenin chemiluminescence, was shown in Figure 5. Chemiluminescence was significantly enhanced by incubation with various doses of JTE-522. This enhancement was prevented by co-incubation with PDTC at 100μmol/L. These results demonstrated the generation of reactive oxygen species in cells under incubation with JTE-522.

Effect of JTE-522 on the expression of p53, bcl-2, IκBα and the activation of NF-κB

NF-κB plays a complex role in regulating programmed cell death. In many instances the inhibition of NF-κB activity can sensitize cells to death inducers^[25]. In other instances, however, NF-κB activation has been found to play an important role in the induction of apoptosis. To determine whether the treatment with JTE-522 have any effect in the NF-κB transcriptional factors. We performed EMSA with nuclear extracts prepared from control or treated cells exposed to JTE-522 for various concentrations for 6h. The NF-κB specific complexes found in this cell line were almost complete inhibited in comparison with untreated

cells (Figure 6A). In accordance with result, an analysis of IκBα proteins level by Western blot demonstrated that the degradation of this protein was greatly inhibited during the apoptotic process(Figure 6B).

Additionally, by using Western blot we confirmed that the level of bcl-2 was decreased, whereas p53 showed a great increase following JTE-522 treatment. Their changes were in a dose-dependent manner (Figure 7).

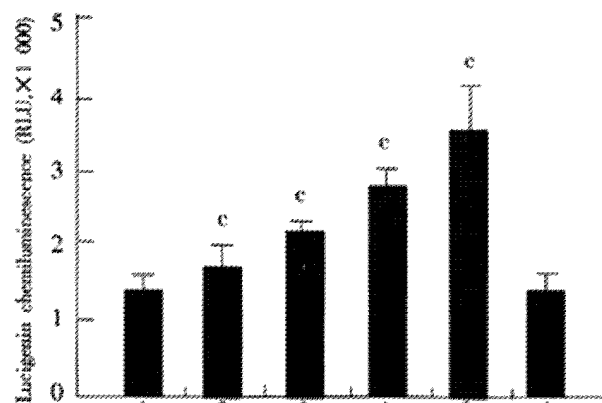


Figure 5 Effect of JTE-522 on the generation of ROS. AGS cells were incubated for 6h with JTE-522 (0.25-1mmol/L) in the presence or absence of PDTC at 100μmol/L. Lucigenin-associated chemiluminescence was measured for 3min with a lumirometer. (A). Lane 1: control; lane 2-5: AGS cells treated with 0.25, 0.5, 0.75, 1mmol/L of JTE-522; lane 6: JTE-522 (1mmol/L) +PDTC (100μmol/L) **P*<0.01 vs control. Results are the means±SD from three independent determinations.

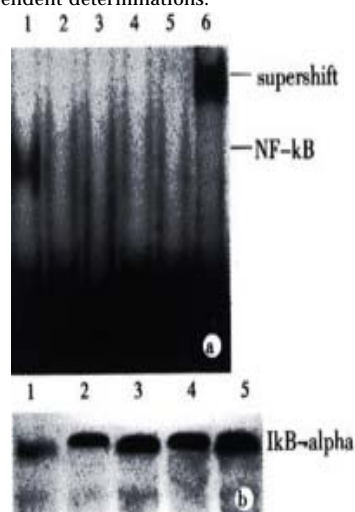


Figure 6 Effect of JTE-522 on NF-κB binding activity and IκBα degradation. Cells were treated with JTE-522 for 6h. Cells were harvested and EMSA was performed as described (A). Lane 1: control; lane 2-5: AGS cells treated with 0.25, 0.50, 0.75, 1mmol/L of JTE-522. The identity of DNA-complexed proteins was confirmed by supershift assays using antibodies against p65 subunit of NF-κB (lane 6). Immunoblot analysis of IκBα of corresponding cytosolic supernatant (B). Representative results from four independent experiments.

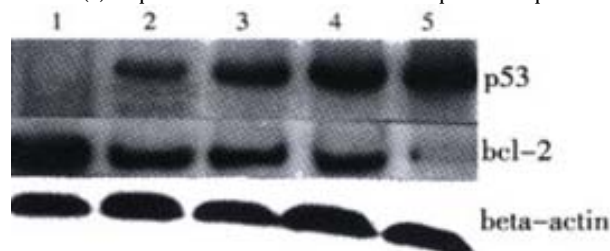


Figure 7 P53, bcl-2 protein levels in AGS cells treated with JTE-522. Cell lysates were collected and processed at 6h. The whole cellular protein was electrophoresed in SDS-PAGE gel. Western blot was performed using antibodies against p53, bcl-2. Beta actin was used as a lane-loading control. (1) control; (2) 0.25mmol/L; (3) 0.5mmol/L; (4) 0.75mmol/L; (5) 1 mmol/L. Representative results from three independent experiments.

DISCUSSION

Using cultured AGS human gastric adenocarcinoma cells, the observations described in this study demonstrate that JTE-522, a novel NSAIDs inhibits the growth of AGS cells and induces apoptosis in a concentration-dependent manner.

The onset of apoptosis is associated with the proteolytic activation of caspases. Caspases, a family of cysteine proteases, play a critical role in the execution of apoptosis^[26-31]. They are synthesized as proenzymes that are processed by self-proteolysis and/or cleavage by another protease to their active forms in cells undergoing apoptosis. Caspase-3 is a major executioner of apoptosis. It is promoted during the early stage of apoptosis and the activated form is a marker for cells undergoing apoptosis^[32]. After activation by initiators, the proform (p32) is cleaved to the active forms p20, p17, or p11, respectively^[33]. Therefore, activation of caspase-3 in AGS cells in this study not only indicated the occurrence of apoptosis, but also implied the involvement of caspase-3 in JTE-522-induced apoptosis.

ROS have been found to play a central role in regulating apoptosis in numerous instances. Given that reduced rates of apoptosis may contribute to carcinogenesis, the regulation of cellular ROS production may be an important variable in the development of neoplasias. Other studies have also suggested a potential role for ROS in cancer suppression. For example, the p53 tumor suppressor protein activates the expression of ROS-generating proteins that increase cellular ROS production and eventually trigger apoptosis^[34,35]. Increased ROS generation by chemopreventive agents may serve to compensate the lower levels of ROS generation in p53 null cells (AGS cells are p53 null)^[36,37]. Animal studies have also implicated ROS in regulating carcinogenesis. Mice with elevated levels of glutathione peroxidase are more sensitive to skin carcinogenesis than their wild type counterpart^[32]. A similar correlation has been made in the colon, where strains with higher levels of glutathione peroxidase activity have a higher cancer risk. The role of ROS in carcinogenesis is however likely to be complex given the potential mutagenicity of ROS. For example, the NSAIDs inhibition of cyclooxygenase has been proposed to suppress carcinogenesis by suppressing the production of peroxy radicals and the subsequent formation of mutagenic lipid peroxidation breakdown products^[38]. The role of ROS in carcinogenesis may depend on the relative levels of different ROS generated, and where and when they are present. However, as demonstrated in this paper, we showed that JTE-522 increased ROS generation in AGS cells, and this increased ROS generation might contribute to the induction of AGS cells to apoptosis.

The bcl-2 protooncogene is unique among cellular genes for its ability in many contexts to block apoptotic cell death. A mechanism has been proposed in which bcl-2 regulates antioxidant pathways at sites of free radical generation^[39]. The protein of bcl-2 also protects against apoptosis by blocking cytochrome C release hence this protein may have an antioxidant function^[40]. In our experiment, the expression of bcl-2 decreased, and the p53 protein upregulated following JTE-522 treatment, these changes may implies that intracellular ROS may interfere with the expression of bcl-2 and p53, thereby contributing to inducing apoptosis in AGS cells.

In studying the mechanism by which the NSAIDs influenced cell death, common effects on the transcription factor NF- κ B were noted. The NF- κ B transcription factor is ubiquitous and can be detected under its inactive form in the cytoplasm of almost all cell types^[41,42]. It suppresses the expression of cytokines, chemokines, growth factors, cell adhesion molecules, and some acute phase proteins in health and various pathological states^[43,44]. Experimental data clearly indicate that NF- κ B is a major regulator of the inflammatory reaction by controlling the expression of pro-inflammatory molecules in response to cytokines oxidative stress and infectious agents^[45,46]. NF- κ B is maintained under such an inactive cytoplasmic form by virtue of its association with an inhibitory molecule named I κ B. I κ B α is the best

characterized member of this family. In our current work, EMSA revealed that JTE-522 inhibited NF- κ B activation. Western blot experiments demonstrated that this effect was mediated by inhibition of I κ B α degradation. Determining the role of NF- κ B in gastric carcinogenesis could help to guide the development of improved chemoprevention and treatment strategies.

In summary, JTE-522 inhibited cell growth and induced apoptosis in AGS cells. Increased ROS may play an important role in this caspase-3 mediated apoptotic process. The inhibition of NF- κ B by JTE-522 may be mediated by preventing I κ B α degradation. The precise relationship and importance of each of these factors in the apoptotic process should be established by more direct and profound analysis.

ACKNOWLEDGMENTS

We gratefully acknowledge Prof Geng-Tao Lui, Institute of Material Medica, Chinese Academy of Medical Sciences for the many helpful discussion and suggestions relating to this work; Special thanks to Chris Simmet and Pasricha Jerriment for proofreading the manuscript and for useful suggestions; Dr Cheng-Wei He for technical advice and helpful discussion; Dr Gang-Fei Peng for FCM; Dr Tao Wang for Western blot; Dr Guo-Qing Xie and Mr Hai-Nan Wang for photo processing.

REFERENCES

- 1 Peng XM, Peng MM, Chen Q, Yao JL. Apoptosis, Bcl-2 and p53 protein expression in tissues from hepatocellular carcinoma. *Huaren Xiaohua Zazhi* 1998; 6: 834-836
- 2 Hua JS. Effect of Hp: cell proliferation and apoptosis on stomach cancer. *Shijie Huaren Xiaohua Zazhi* 1999;7: 647-648
- 3 Xue XC, Fang GE, Hua JD. Gastric cancer and apoptosis. *Shijie Huaren Xiaohua Zazhi* 1999;7: 359-361
- 4 Qin LF, Wang RN. Prognostic significance of FCM DNA analysis in carcinoma of stomach. *Shanghai Dier Yike Daxue Xuebao* 1992; 12: 198-202
- 5 Yu GQ, Zhou Q, Ding Ivan, Gao SS, Zhang ZY, Zou JX, Li YX, Wang LD. Changes of p53 protein blood level in esophageal cancer patients and normal subjects from a high incidence area in Henan, China. *World J Gastroenterol* 1998; 4: 218
- 6 Luo D, Liu QF, Gove V, Namov NV, Su JJ, Williams R. Analysis of N-ras gene mutation and p53 gene expression in human hepatocellular carcinomas. *World J Gastroenterol* 1998; 4: 97-99
- 7 Li HL, Zhang HW, Ren XD. Synergism between heparin and adriamycin on cell proliferation and apoptosis in human nasopharyngeal carcinoma CNE2 cells. *Acta Pharmacol sin* 2002;23:167-172
- 8 Li HL, Ye KH, Ren XD. Heparin induced apoptosis in human nasopharyngeal carcinoma CNE2 cells. *Cell Research* 2001;11:311-315
- 9 Qiao Q, Wu JS, Zhang J, Ma QJ, Lai DN. Expression and significance of apoptosis related gene bcl-2, bax in human large intestine adenocarcinoma. *Shijie Huaren Xiaohua Zazhi* 1999; 7: 936-938
- 10 Yuan RW, Ding Q, Jiang HY, Qin XF, Zou SQ, Xia SS. Bcl-2, p53 protein expression and apoptosis in pancreatic cancer. *Shijie Huaren Xiaohua Zazhi* 1999; 7: 851-854
- 11 Jiang YG, Li QF, Wang YM, Gu CH. Bcl-2/bax expression and hepatocyte apoptosis on liver tissue in tupaia with HDV/HBV infection. *Shijie Huaren Xiaohua Zazhi* 2000; 8: 625-628
- 12 Fan XQ, Ya JG. Apoptosis in oncology. *Cell Research* 2001;11:1-7
- 13 Zhang MH, Zhang Q, Shao BX. Effect of Bcl-2 and caspase-3 on calcium distribution in apoptosis of HL-60 cell. *Cell Research* 2000; 10: 213-20
- 14 Kane DJ, Sarafian TA, Anton R, Hahh H, Bntler E. Bcl-2, inhibition of neural death: decreased generation of reactive oxygen species. *Science* 1993; 262: 1274-1277
- 15 Reddy BS, Rao CV, Seibert K. Evaluation of COX-2 inhibitor for potential chemopreventive properties in colon carcinogenesis. *Cancer Res* 1996; 56: 4566-4569
- 16 Shibata MA, Hasegawa R, Imaida K, Hagiwara A. Chemoprevention by dehydroepiandrosterone and indomethacin in a rat model of multiorgan carcinogenesis model. *Cancer Res* 1995; 55: 4870-4874
- 17 Tomozawa S, Nagawa H, Tsuno N. Inhibition of haematogenous metastasis of colon cancer in mice by a selective COX-2 inhibitor, JTE-522. *Br J Cancer* 1999; 81: 1274-1279
- 18 Yang ZY, Rorison KA. Cyclooxygenase-2-selective antagonists do not inhibit growth of colorectal carcinoma cell lines. *Cancer letters* 1998; 122: 25-30

- 19 Kusuvara H, Komatsu H, Sugahara K. Reactive oxygen species are involved in the apoptosis induced by NSAIDs in cultured gastric cells. *Eur J Pharmacol* 1999; 383: 331-337
- 20 Tanaka K, Pracyk JB, Takeda K, Yu ZX, Finkel T. Expression of Id1 results in apoptosis of cardiac myocytes through a redox-dependent mechanism. *J Biol Chem* 1998; 273: 25922-25828
- 21 Fridovich I. Superoxide radical and superoxide dismutases. *Annu Rev Biochem* 1995; 64: 97-112
- 22 Manna SK, Zhang HJ, Yan T, Oberley LW, Aggarwal BB. Overexpression of manganese superoxide dismutase suppress tumor necrosis factor-induced apoptosis and activation of nuclear transcription factor- κ B and AP-1. *J Biol Chem* 1998; 273: 13245-13254
- 23 Qiao L, Hanif R, Sphical E, Steven J, Rigas B. Effect of aspirin on induction of apoptosis in AGS human colon adenocarcinoma cells. *Biochem Pharmacol* 1998; 55: 53-64
- 24 Jiang ZF, Zhao Y, Hong X, Zhai ZH. Nuclear apoptosis induced by isolated mitochondria. *Cell Research* 2000; 10: 221-232
- 25 Beg AA, Baltimore D. An essential role for NF- κ B in preventing TNF- α induced cell death. *Science* 1996; 274: 787-789
- 26 Cohen GM. Caspases: the executioners of apoptosis. *Biochem J* 1997; 326: 1-6
- 27 Kumar S, Lavin MF. The ICE family of cysteine proteases as effectors of cell death. *Cell Death Differ* 1996; 3: 255-267
- 28 Salvesen GS and Dixit VM. Caspases: intracellular signaling by proteolysis. *Cell* 1997; 91: 443-446
- 29 Shen ZY, Shen J, Li QS, Chen CY, Chen JY, Zeng Y. Morphological and functional changes of mitochondria in apoptosis esophageal carcinoma cells induced by arsenic trioxide. *World J Gastroenterol* 2002;8:31-35
- 30 Du C, Fang M, Li Y, Wang X, Smac A. Mitochondrial protein that promotes cytochrome c dependent caspase activation by eliminating IAP inhibition. *Cell* 2000; 102: 43-53
- 31 Desagher S, OsenSand A, Nichols A, Eskes R, Montessuit S, Lauper S, Maundrell K, Antonsson B, Martinou JC. Bid-induced conformational cytochrome c release during apoptosis. *J Cell Biol* 1999; 144: 891-901
- 32 Schlegel J, Peters I, Orrenius S, Miller DK. Cpp32/apopain is a key interleukin 1 beta converting enzyme-like protease involved in Fas-mediated apoptosis. *J Biol Chem* 1996; 271: 1841-1844
- 33 Stennicke HR, Salvesen GS. Properties of the caspases. *Biochim Biophys Acta* 1998; 1387: 17-31
- 34 Polyak K, Xia Y, Zweier JL, Kinzler KW. A model for p53-mediated apoptosis. *Nature* 1997; 389: 300-305
- 35 Johnson TM, Yu ZX, Ferrans RA. Relative oxygen species are downstream mediators of p53-dependent apoptosis. *Proc Natl Acad Sci USA* 1996; 93: 11848-11852
- 36 Ossina NK, Cannas A, Powers VC, Gilbert EM, Tomei SR. Interferon- γ modulates a p53-independent apoptotic pathway and apoptosis-related gene expression. *J Biol Chem* 1997; 272: 16351-16357
- 37 Xu CT, Huang LT, Pan BK. Current gene therapy for stomach carcinoma. *World J Gastroenterol* 2001;7:752-759
- 38 Lu YP, Lou YR, Newmark HL, Huang MT. Enhanced skin carcinogenesis in transgenic mice with high expression of glutathione peroxidase or both glutathione peroxidase and superoxide dismutase. *Cancer Res* 1997; 57: 1468-1474
- 39 Hockenbery OM, Oltvai ZN, Yin XM, Korsmeyer SJ. Bcl-2 functions in an antioxidant pathway to prevent apoptosis. *Cell* 1993; 75: 241-251
- 40 Cai J, Jones DP. Superoxide in apoptosis: mitochondrial generation triggered by cytochrome C loss. *J Biol Chem* 1998; 273: 11401-1144
- 41 Barnes PJ, Karin M. Nuclear factor- κ B, a pivotal transcription factor in chronic inflammatory disease. *New Eng J Med* 1997; 336: 1066-1071
- 42 Huang S, Li JY, Wu J, Meng L, Shou CC. Mycoplasma infections and different human carcinomas. *World J Gastroenterol* 2001;7:266-269
- 43 Baeuerle PA, Baltimore D. NF- κ B: ten years after. *Cell* 1996; 87: 13-20
- 44 Wu YL, Sun B, Zhang XJ, Wang SN, He HY, Qiao MM, Zhong J, Xu JY. Growth inhibition and apoptosis induction of Sulindac on human gastric cancer cells. *World J Gastroenterol* 2001;7:796-800
- 45 Kipp E, Ghosh S. Inhibition of NF- κ B by sodium salicylate and aspirin. *Science* 1994; 265: 956-959
- 46 Giardina C, Boulares H, Inan MS. NSAIDs and butyrate sensitize a human colorectal cancer cell line to TNF and Fas ligation: the role of reactive oxygen species. *Biochim Biophys Acta* 1999; 1448: 425-438

Edited by Zhang JZ

• GASTRIC CANCER •

Inhibition of human telomerase in MKN-45 cell line by antisense hTR expression vector induces cell apoptosis and growth arrest

Run-Hua Feng, Zheng-Gang Zhu, Jian-Fang Li, Bin-Ya Liu, Min Yan, Hao-Ran Yin, Yan-Zhen Lin

Run-Hua Feng, Zheng-Gang Zhu, Jian-Fang Li, Bin-Ya Liu, Min Yan, Hao-Ran Yin, Yan-Zhen Lin, Shanghai Institute of Digestive Surgery, Ruijin Hospital, Shanghai Second Medical University, Shanghai 200025, China
Supported by the National Natural Science Foundation of China, No. 39770725

Correspondence to: Dr. Zheng-Gang Zhu, Shanghai Institute of Digestive Surgery, Ruijin Hospital, Shanghai Second Medical University, Shanghai 200025, China. digsur@online.sh.cn
Telephone: +86-21-64373909 Fax: +86-21-64373909
Received 2002-01-14 Accepted 2002-02-07

Abstract

AIM: To investigate the effects of antisense human telomerase RNA (hTR) on the biologic behavior of human gastric cancer cell line: MKN-45 by gene transfection and its potential role in the gene therapy of gastric cancer.

METHODS: The hTR cDNA fragment was cloned from MKN-45 through RT-PCR and subcloned into eukaryotic expression vector (pEF6/V5-His-TOPO) in cis-direction or trans-direction by DNA recombinant methods. The constructed sense, antisense and empty vectors were transfected into MKN-45 cell lines separately by lipofectin-mediated DNA transfection technology. After drug selection, the expression of antisense hTR gene in stable transfectants and normal MKN-45 cells was detected by RT-PCR, the telomerase activity by TRAP, the apoptotic features by PI and Hoechst 33258 staining, the cell cycle distribution by flow cytometry and the population doubling time by cell counting. Comparison among the stable transfectants and normal MKN-45 cells was made.

RESULTS: The sense, antisense hTR eukaryotic expression vectors and empty vector were successfully constructed and proved to be the same as original design by restriction endonuclease analysis and sequencing. Then, they were successfully transfected into MKN-45 cell lines separately with lipofectin. The expression of antisense hTR gene was only detected in MKN-45 cells stably transfected with antisense hTR vector (named as MKN-45-ahTR) but not in the control cells. In MKN-45-ahTR, the telomerase activity was inhibited by 75%, the apoptotic rate was increased to 25.3%, the percentage of cells in the G0/G1 phase was increased to 65%, the proliferation index was decreased to 35% and the population doubling time was prolonged to 35.3 hours. However, the telomerase activity, the apoptotic rate, the distribution of cell cycle, the proliferation index and the population doubling time were not different among the control cells.

CONCLUSION: Antisense hTR can significantly inhibit telomerase activity and proliferation of MKN-45 cells and induce cell apoptosis. Antisense gene therapy based on telomerase inhibition can be a potential therapeutic approach to the treatment of gastric cancer.

Feng RH, Zhu ZG, Li JF, Liu BY, Yan M, Yin HR, Lin YZ. Inhibition of human telomerase in MKN-45 cell line by antisense hTR expression vector induces cell apoptosis and growth arrest. *World J Gastroenterol* 2002;8(3):436-440

INTRODUCTION

Gastric cancer is a very common tumor in China. More and more patients with gastric cancer can now be found in early stage because of the improvement of the technology of diagnosis^[1]. Although surgery and chemotherapy are effective for these patients with localized tumors, the prognosis of patients having advanced or metastatic tumors is not ideal^[2-6]. As a result, it is absolutely necessary to explore a novel modality of treatment. Fortunately, with the development of molecular biology, medicine is on the brink of a new era—that of molecular genetic medicine. People are now equipped with a new and powerful weapon: gene therapy which was previously only the stuff of dreams and scientific fantasy to fight against disease. Just like other kinds of cancer, the gastric cancer is now recognized as a genetic disease. The gastric cancer cells contain many genetic alterations (caused by some pathogenic agents such as *Helicobacter pylori*) which accumulate as tumor develop^[7-28]. This makes it possible to treat cancer with gene therapy^[29,30]. Because the target aimed by the gene therapy is undoubtedly the abnormal gene, thus, the task to find an effective target gene directed against by the gene therapy is becoming increasingly important and urgent. Human telomerase is a ribonucleoprotein which can add the telomeric repeats (TTAGGG) to the ends of the chromosome to maintain the telomere length using its integral RNA component (hTR) as a template^[31,32]. Initially identified in HeLa cell extracts, human telomerase has been detected in immortalised cell lines and more than 85% of tumors while normally quiescent in normal somatic cells (except for proliferative cells of renewable tissues such as activated lymphocytes)^[33-35]. It is suggested that cancer cells maybe achieve cellular immortality, an important characteristic of cancer cell, through the reactivation of telomerase^[36,37]. The seemingly essential roles of telomerase in maintaining telomere length, ensuring chromosome integrity and its nearly ubiquitous reactivation in human cancers have made telomerase a new therapeutic target for anticancer therapy^[38,39]. It was reported that HeLa cells transfected with an antisense hTR lost telomeric DNA and began to die after 23 to 26 doublings. According to a recent review, telomerase activity was also detected in 85-88% of gastric carcinomatous tissues. To gastric cancer, hTR was expressed at a higher level in the tumor than that in the corresponding mucosa and tumors with telomerase activity were generally large in size with a high frequency of lymph node metastasis. Moreover, the patients with telomerase-positive tumors shared poorer prognosis than those with telomerase-negative tumors^[40-45]. However, whether antisense gene therapy directed against telomerase will be useful in gastric cancer is so far unknown. We describe here the biologic behavior changes in MKN-45 cell line, a human gastric cell line, after transfected with antisense hTR expression vector and investigate the potential value of telomerase as a target for antisense gene therapy in gastric cancer.

MATERIALS AND METHODS

Cell Culture

MKN-45 cell, a human gastric cancer cell line, was obtained from Shanghai institute of Cell Biology, Chinese Academy of Sciences. The cells were routinely cultured in RPMI-1640 media (Gibco BRL) supplemented with 10% heat-inactivated fetal bovine serum (Gibco BRL), 100u/ml penicillin and 100u/ml streptomycin in an atmosphere consisting of 5% CO₂ in air at 37°C in a humidified incubator.

Construction of sense and antisense hTR eukaryotic expression vector

The hTR cDNA fragment was cloned from MKN-45 cell line through RT-PCR and subcloned into eukaryotic expression vector: pEF6/V5-His-TOPO vector (Invitrogen) in cis-direction or trans-direction by using DNA recombinant methods as described previously^[46]. They were all proved to be the same as original design by restriction endonuclease analysis and sequencing. The sense, antisense and empty vectors were named as pEF-hTR, pEF-ahTR and pEF-empty correspondingly.

Transfection of eukaryotic expression vector

Stable transfection of pEF-hTR, pEF-ahTR and pEF-empty was carried out by standard lipofection mediated DNA transfection method. In brief, approximately 1.5×10⁵ MKN-45 cells were transfected with 2μg vector DNA that had been complexed with 20μl lipofectin reagent (Gibco BRL). Two days after the transfection, the stable transfectants were selected by 2μg/ml blasticidin (Invitrogen) in the culture media. They were named as MKN-45-hTR, MKN-45-ahTR and MKN-45-empty correspondingly.

In addition, the pEF6/V5-His-TOPO/lacZ vector (pEF6/V5-His-TOPO vector carrying the reporter gene: lacZ gene in its multi cloning sites, provided by Invitrogen) was transfected into MKN-45 cells and selected by the same method as described above. It was named as MKN-45-lac correspondingly.

RT-PCR for detecting antisense hTR expression

Total RNA was extracted from the transfectants and normal MKN-45 cells using Trizol reagent (Gibco BRL). One microgram of total RNA was reversetranscribed with ahTR specific primer1 (5'-gaacgggccagcagctgacat-3') using THERMOSCRIPT RT-PCR system for first-strand cDNA synthesis (Gibco BRL). The RT condition was set for 65°C, 30min→85°C, 5min. Then, the cDNA was amplified with the PCR using PLATINUM Taq DNA polymerase (Gibco BRL) and employing ahTR specific primer1 and primer2 (5'-gggtgcggagggtggcct-3'). The PCR conditions were set for 94°C, 2min→94°C, 20s; 69°C, 20s; 72°C, 20s; 30 cycles→72°C, 2min. The product length is 196bp. The G6PDH was co-reversetranscribed employing G6PDH specific primer1 (5'-cgcccccttctctccctctgct-3') and co-amplified with PCR using G6PDH specific primer1 and primer2 (5'-cccgcctctgctgctactac-3') as internal control. The product length is 247bp. Each RT-PCR product was electrophoretically separated in 2% agarose with EtBr.

β-Gal staining

The MKN-45 cells stably transfected with pEF6/V5-His-TOPO/lacZ vector were subjected to β-Gal staining by using β-Gal Staining Kit (Invitrogen) to detect whether the vector could effectively express lacZ gene.

Apoptotic features

To determine whether MKN-45-ahTR transfected with the pEF-ahTR vector displayed an apoptotic morphology, it was stained with the DNA binding fluorochrome bis (benzimidazole) trihydro-chloride, Hoechst 33258 (provided by Shanghai institute of Immunology) and observed under UV fluorescence microscope.

To determine the apoptotic rate and cell cycle distribution, the MKN-45-ahTR and control cells were stained with PI and analysed by flow cytometry.

Telomerase activity assay

Telomerase activity was measured using the commercially available TRAP_{EZE} Telomerase Detection Kit (Intergen). In brief, the cell extract was made according to the protocol provided, then 2μl of the cell extract was added to 48μl of the reaction mixture containing 10× TRAP Reaction Buffer, 50× dNTP Mix, TS Primer, TRAP Primer Mix, Taq Polymerase and dH₂O in amounts and types specified by the TRAP_{EZE} Telomerase Detection Kit. After centrifuged briefly, this mixture was incubated at 30°C for 30min to allow telomerase elongation of the TS primer and then subjected to PCR amplification in a thermal cycler for 35 cycles: 94°C for 30s; 59°C for 30s and 72°C for 30s. The product was then electrophoresed on a 12.5% non-denaturing PAGE (without urea). After electrophoresis, the gel was stained with SYBR Green I (Molecular Probes) according to the manufacturer's instructions.

Quantification of telomerase product was calculated using BIO-RAD Fluor-STM MultiImager and the formula (discussed in detail in the TRAP_{EZE} Telomerase Detection Kit instruction booklet).

$$\text{TPG}(\text{units}) = \frac{(\chi - \chi_0) / c}{(\gamma - \gamma_0) / c_R} \times 100$$

Abbreviation in the above formular is as follows: TPG, total product generated; χ , sample signal; χ_0 , heat-inactivated control; γ , 0.1 amole quantitation TSR8 control; γ_0 , 1× CHAPS Lysis Buffer only control; c , sample internal standard band; c_R , 0.1 amole quantitation TSR8 internal standard band.

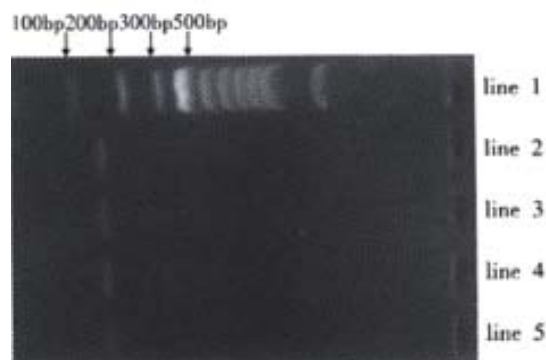
Cell growth curve and population doubling time

Cells were seeded at a density of 2×10⁵ per 25ml flask in 1.5ml of cell culture media. The number of cells per flask was counted every day for 6 days. The population doubling time of cells transfected with pEF-hTR, pEF-ahTR and pEF-empty and normal MKN-45 cells were calculated and the cell growth curve was drawn.

RESULTS

Expression of antisense hTR gene in MKN-45 cells

We transfected MKN-45 cells with pEF-hTR, pEF-ahTR and pEF-empty vector respectively, following the blasticidin selection, the drug resistant cells were collected and RT-PCR was performed with antisense hTR specific primers. We detected the ahTR specific product only in the pEF-ahTR vector transfected cells but not in the pEF-hTR, pEF-empty vector transfected cells and parental cells. However, steady state expression of G6PDH (as internal control) was observed in all cells.



Line 1: 100bp DNA Ladder (Promega), Lane 2: normal MKN-45, Lane 3: MKN-45-hTR, Lane 4: MKN-45-empty, Lane 5: MKN-45-ahTR

Figure 1 The expression of antisense hTR gene.

Only the cells transfected with pEF-ahTR expressed the antisense hTR, however, the G6PDH was detected in all samples that indicated an appropriate RT-PCR reaction.

β-Gal staining

After drug selection, nearly all MKN-45 cells stably transfected with pEF6/V5-His-TOPO/lacZ vector were stained blue by β-Gal Staining Kit while parental cells were not.

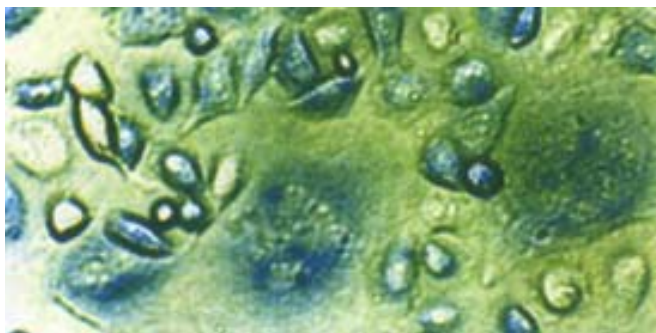
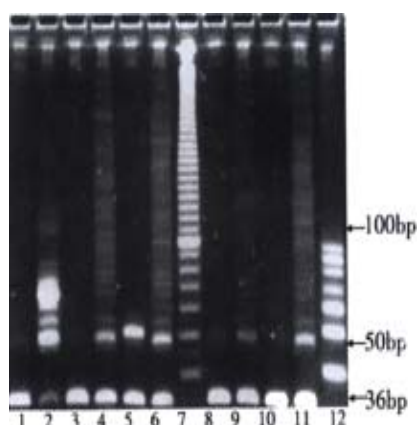


Figure 2 The result of β-Gal staining of MKN-45-lac. (×600)

Telomerase activity

We measured telomerase activity of the pEF-hTR, pEF-ahTR and pEF-empty transfected MKN-45 cells and parental cells through TRAP method described above. It was found that the level of telomerase activity in the pEF-ahTR transfected MKN-45 cells was greatly inhibited, compared with that in the parental MKN-45 cells. However, there was no difference between the level of telomerase activity in the pEF-hTR, pEF-empty transfected MKN-45 cells and parental MKN-45 cells.



Line 1: 1× CHAPS Lysis Buffer only control; Line 2: 0.1 amole quantitation TSR8 control; Line 3: MKN-45-empty heat-inactivated control; Line 4: MKN-45-empty; Line 5: MKN-45 heat-inactivated control; Line 6: MKN-45; Line 7: 10bp DNA Ladder (Gibco BRL); Line 8: MKN-45-ahTR heat-inactivated control; Line 9: MKN-45-ahTR; Line 10: MKN-45-hTR heat-inactivated control; Line 11: MKN-45-hTR; Line 12: 10bp DNA Step Ladder (Promega). **Figure 3A** Detection of telomerase activity with the telomeric repeat amplification protocol (TRAP) assay. A 36bp internal control band present in all samples indicated an appropriate polymerase chain reaction (PCR).

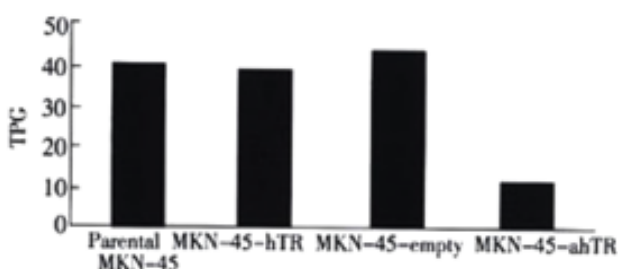


Figure 3B Comparison of telomerase activity in MKN-45-ahTR and control cells. Compared with control cells, the telomerase activity in MKN-45-ahTR was inhibited by about 75%.

Cellular effects of telomerase inhibition

As Figures 4, 5 and Table 1 showed, compared with controls cells, the MKN-45-ahTR cell displayed a longer population doubling time, an increased percentage of cells in the G0/G1 phase, a lower cell proliferation index and a higher apoptotic rate, which demonstrated that, through inhibiting telomerase activity, antisense hTR gene transfection could inhibit the proliferative capacity of NKN-45 and induce cell apoptosis.



Figure 4 Hoechst 33258 staining of MKN-45-ahTR. (×600) The cells undergoing apoptosis demonstrated apoptotic chromatin changes: blebbing, fragmentation and condensation under fluorescence microscope.

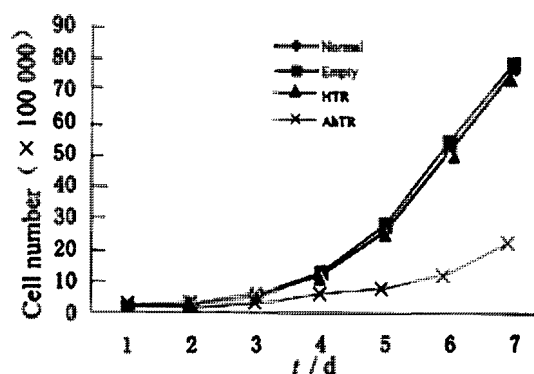


Figure 5 Cell growth curve.

Table 1 Comparison of distribution of cell cycle, cellular proliferation index, apoptotic rate, population doubling time of MKN-45-ahTR and those of control cells

	Distribution of cell cycle (%)			cell proliferation index (%)	Apoptotic rate (%)	population doubling time (hours)
	G0/G1	S	G2/M			
MKN-45-ahTR	65	34.2	0.8	35	25.3	35.3
MKN-45-hTR	55.7	37.5	6.8	44.3	0	23.2
MKN-45-empty	54.1	38.4	7.5	45.9	0	22.7
normal MKN-45	54.7	37.8	7.5	45.3	0	22.9

DISCUSSION

Compared with normal somatic cells, which reach the end of their replicative capacity after a limited number of population doubling and enter a senescence phase, the cancer cells have an unlimited replicative capacity. This important characteristic of cancer, named immortality, is gaining more and more attention, seeing that cancer cells may achieve cellular immortality through only a major pathway: activation of the telomerase^[47].

Telomerase is a unique ribonucleoprotein that can synthesize telomeric DNA onto chromosomal ends using a segment of its RNA component (hTR) as a template to compensate for the lose of telomeric repeats (TTAGGG) caused by the so-called “end-replication” problem. Recent Study demonstrated that 758 of 895 (85 %) of malignant tumors but none of 70 normal somatic tissues

expressed telomerase activity. In addition, the level of telomerase activity influences the prognosis of patient to a certain degree. For example, high level of telomerase correlates with poor clinical outcome in neuroblastoma, while patients with metastatic IV-S neuroblastoma without telomerase activity experiences spontaneous regression of tumors. These findings indicate that telomerase plays an important role in carcinogenesis and therefore undoubtedly become the basis of the widely held view of telomerase as a highly selective target for antisense gene therapy of cancer^[48].

The RNA component of telomerase (hTR) is crucial to the telomerase activity^[49-51]. Human cell lines that expressed hTR mutated in the template region generated the predicted mutant telomerase activity. In addition, recent experiments have shown that antisense gene therapy directed against telomerase RNA component (hTR) could effectively inhibit telomerase activity and induce apoptotic cell death in ovarian cancer, prostate cancer, bladder cancer, malignant gliomas and human breast epithelial cells^[52-56]. However, whether such anti-cancer effect can be obtained in human gastric cancer is still unknown. Therefore, we examined the effect of antisense hTR (ahTR) expression on the growth of human gastric cancer cell line: MKN-45 through transfection of an ahTR expression vector.

Given that whether the vector can effectively and stably express the exogenous gene it carries will directly influence the effect of antisense gene therapy. Firstly, we adopted two different methods to detect the expression of exogenous gene by the pEF6/V5-His-TOPO vector before conducting other experimental items. The first one was to detect the expression of reporter gene. pEF6/V5-His-TOPO/lacZ vector is the same as the pEF6/V5-His-TOPO vector except that the former carrying lacZ gene, a kind of widely used reporter gene, in its multi cloning sites. Usually by using β -Gal staining method, the researchers can easily detect the expression of lacZ gene through which they further evaluate the ability of the vector's promoter to express the exogenous gene. We found that nearly all cells stably transfected with pEF6/V5-His-TOPO/lacZ vector were stained blue while control cells were not. Therefore, we believed that pEF6/V5-His-TOPO/lacZ vector could effectively express the exogenous gene (lacZ gene) it carried, so did the pEF6/V5-His-TOPO vector. The second one was to detect the expression of antisense hTR gene directly through RT-PCR method. Only the cells transfected with pEF-ahTR expressing the antisense hTR gene were found. Both the results proved that pEF6/V5-His-TOPO vector could effectively express the exogenous gene, thus laying the solid fundament for the study of following experimental items.

As the results showed, the most significant conclusions we could draw from this study were that telomerase in human gastric cancer cell line: MKN-45 could be inhibited by a vector expressing mRNA complementary to the template region of hTR and that the growth of cancer cells was retarded and cell apoptosis was induced after telomerase was inhibited by this method. Therefore, our experiment clearly demonstrated that blocking the RNA component of telomerase with antisense hTR expression vector appeared to be a rational approach to the treatment of gastric cancer. The telomerase may become an ideal target for antisense gene therapy in human gastric cancer.

However, it is noticeable that not all cells transfected with antisense hTR gene underwent apoptosis, and underlying mechanism is still unknown. The possible reason is that the carcinogenesis process is complicated and the reactivation of telomerase may play an important but by no means the sole role during this process. Many oncogenes and tumor suppressor genes are also involved in tumorigenesis^[57,58]. While believed to be necessary for cancer cells to grow without limit, telomerase is not sufficient to transform a normal cell into a tumor cell. Thus, anti-cancer effect of antisense gene therapy will be more satisfactory if multitargets are aimed. For example, a recent report showed that the combination of 2-5A-anti-hTR and Ad5CMV-p53 had greater anti-tumor efficacy against all

p53-mutant glioma cells than each treatment alone^[59]. Seeing that telomerase activity and p53 dysfunction are also detected in gastric cancer^[60,61], this approach may be effective in treating gastric cancer patients too and the similar investigation is being conducted in our laboratory now.

REFERENCES

- Zhang XY. Some recent works on diagnosis and treatment of gastric cancer. *World J Gastroenterol* 1999;5:1-3
- Lin YZ, Yin HR, Zhu ZG, Lu W, Li DL, Zhang J. The surgical treatment of gastric cancer in Shanghai. *Asian J Surg* 2001;24:258-262
- Maehara Y, Kakeji Y, Oda S, Takahashi I, Akazawa K, Sugimachi K. Time trends of surgical treatment and the prognosis for Japanese patients with gastric cancer. *Br J Cancer* 2000;83: 986-991
- Borie F, Millat B, Fingerhut A, Hay JM, Fagniez PL, De Saxce B. Lymphatic involvement in early gastric cancer: prevalence and prognosis in France. *Arch Surg* 2000;135:1218-1223
- Cascinu S, Graziano F, Barni S, Labianca R, Comella G, Casaretti R, Frontini L, Catalano V, Baldelli AM, Catalano G. A phase II study of sequential chemotherapy with docetaxel after the weekly PELF regimen in advanced gastric cancer. A report from the Italian group for the study of digestive tract cancer. *Br J Cancer* 2001;84:470-474
- Valle JW. Adjuvant therapy for gastric cancer-has the standard changed? *Br J Cancer* 2001; 84: 875-877
- Liu HF, Liu WW, Fang DC, Yang SM, Wang RQ. Bax gene expression and its relationship with apoptosis in human gastric carcinoma and precancerous lesions. *Shijie Huaren Xiaohua Zazhi* 2000;8:665-668
- Fang DC, Zhou XD, Luo YH, Wang DX, Lu R, Yang SM, Liu WW. Microsatellite instability and loss of heterozygosity of suppressor gene in gastric cancer. *Shijie Huaren Xiaohua Zazhi* 1999;7:479-481
- Wang YK, Ma NX, Lou HL, Li Y, Wang L, Pan H, Zhang ZB. Relationship between P53, nm23 protein expression and lymphatic hyperplasia in gastric cancer. *Shijie Huaren Xiaohua Zazhi* 1999;7:34-36
- Takano Y, Kato Y, van Diest PJ, Masuda M, Mitomi H, Okayasu I. Cyclin D2 overexpression and lack of p27 correlate positively and cyclin E inversely with a poor prognosis in gastric cancer cases. *Am J Pathol* 2000;156:585-594
- Cui DX, Yan XJ, Su CZ. Differentially expressed genes were isolated in gastric carcinoma by optimised differential display PCR. *Shijie Huaren Xiaohua Zazhi* 1999;7:139-144
- Zhao Y, Zhang XY, Shi XJ, Hu PZ, Zhang CS, Ma FC. Clinical significance of expressions of P16, P53 proteins and PCNA in gastric cancer. *Shijie Huaren Xiaohua Zazhi* 1999;7:246-248
- Noguchi T, Muller W, Wirtz HC, Willers R, Gabbert HE. FHIT gene in gastric cancer: association with tumour progression and prognosis. *J Pathol* 1999;188:378-381
- Cui DX, Yan XJ, Zhang L, Zhao JR, Jiang M, Guo YH, Zhang LX, Bai XP, Su CZ. Screening and its clinical significance of 6 fragments of highly expressing genes in gastric cancer and precancerous mucosa. *Shijie Huaren Xiaohua Zazhi* 1999;7:770-772
- He XS, Su Q, Chen ZC, He XT, Long ZF, Ling H, Zhang LR. Expression, deletion and mutation of p16 gene in human gastric cancer. *World J Gastroenterol* 2001;7:515-521
- Liu HF, Liu WW, Fang DC, Men RP. Expression and significance of proapoptotic gene Bax in gastric carcinoma. *World J Gastroenterol* 1999; 5:15-17
- Wang B, Shi LC, Zhang WB, Xiao CM, Wu JF, Dong YM. Expression and significance of P16 gene in gastric cancer and its precancerous lesions. *Shijie Huaren Xiaohua Zazhi* 2001;9:39-42
- Ji F, Peng QB, Zhan JB, Li YM. Study of differential polymerase chain reaction of C-erbB-2 oncogene amplification in gastric cancer. *World J Gastroenterol* 1999;5:152-155
- Guo CQ, Wang YP, Liu GY, Ma SW, Ding GY, Li JC. Study on *Helicobacter pylori* infection and -p53, c-erbB-2 gene expression in carcinogenesis of gastric mucosa. *Shijie Huaren Xiaohua Zazhi* 1999;7:313-315
- Chen SY, Wang JY, Ji Y, Zhang XD, Zhu CW. Effects of *Helicobacter pylori* and protein kinase C on gene mutation in gastric cancer and precancerous lesions. *Shijie Huaren Xiaohua Zazhi* 2001;9:302-307
- Zhang Z, Yuan Y, Gao H, Dong M, Wang L, Gong YH. Apoptosis, proliferation and p53 gene expression of H. pylori associated gastric epithelial lesions. *World J Gastroenterol* 2001;7:779-782
- Wang DX, Fang DC, Li W, Du QX, Liu WW. A study on relationship between infection of *Helicobacter pylori* and inactivation of antioncogenes in cancer and pre-cancerous lesion. *Shijie Huaren Xiaohua Zazhi* 2001; 9:984-987
- Xue FB, Xu YY, Wan Y, Pan BR, Ren J, Fan DM. Association of *H. pylori* infection with gastric carcinoma: a Meta analysis. *World J Gastroenterol* 2001;7:801-804

- 24 Miehlik S, Kirsch C, Dragosics B, Gschwandler M, Oberhuber G, Antos D, Dite P, Luter J, Labenz J, Leodolter A, Malfertheiner P, Neubauer A, Ehninger G, Stolte M, Bayerdorfer E. *Helicobacter pylori* and gastric cancer: current status of the Austrian Czech German gastric cancer prevention trial (PRISMA Study). *World J Gastroenterol* 2001;7:243-247
- 25 Liu HF, Liu WW, Fang DC, Yang SM, Zhao L. Gastric epithelial apoptosis induced by *Helicobacter pylori* and its relationship with Bax protein expression. *Shijie Huaren Xiaohua Zazhi* 2000;8:860-862
- 26 Yamagata H, Kiyohara Y, Aoyagi K, Kato I, Iwamoto H, Nakayama K, Shimizu H, Tanizaki Y, Arima H, Shinohara N, Kondo H, Matsumoto T, Fujishima M. Impact of *Helicobacter pylori* infection on gastric cancer incidence in a general Japanese population: the Hisayama study. *Arch Intern Med* 2000;160:1962-1968
- 27 Zhang ZW, Farthing MJG. Molecular mechanisms of *H. pylori* associated gastric carcinogenesis. *World J Gastroenterol* 1999;5:369-374
- 28 Yao YL, Xu B, Song YG, Zhang WD. Overexpression of cyclin E in Mongolian gerbil with *Helicobacter pylori*-induced gastric precancerosis. *World J Gastroenterol* 2002;8:60-63
- 29 Yu WL, Huang ZH. Progress in studies on gene therapy for gastric cancer. *Shijie Huaren Xiaohua Zazhi* 1999;7:887-889
- 30 Xu CT, Huang LT, Pan BR. Current gene therapy for stomach carcinoma. *World J Gastroenterol* 2001;7:752-759
- 31 Chen B, Liu WW, Fang DC. An overview of current studies on telomerase. *Shijie Huaren Xiaohua Zazhi* 2001;9:441-446
- 32 Chen JL, Blasco MA, Greider CW. Secondary structure of vertebrate telomerase RNA. *Cell* 2000;100:503-514
- 33 Vasef MA, Ross JS, Cohen MB. Telomerase activity in human solid tumors. Diagnostic utility and clinical applications. *Am J Clin Pathol* 1999;112:S68-75
- 34 Feng DY, Zheng H, Fu CY, Cheng RX. An improvement method for the detection of *in situ* telomerase activity: *in situ* telomerase activity labeling. *World J Gastroenterol* 1999;5:535-537
- 35 He XX, Wang JL, Wu JL, Yuan SY, Ai L. Telomerase expression, *Hp* infection and gastric mucosal carcinogenesis. *Shijie Huaren Xiaohua Zazhi* 2000;8:505-508
- 36 Fu W, Begley JG, Killen MW, Mattson MP. Anti-apoptotic role of telomerase in pheochromocytoma cells. *J Biol Chem* 1999;274:7264-7271
- 37 Hahn WC, Stewart SA, Brooks MW, York SG, Eaton E, Kurachi A, Beijersbergen RL, Knoll JH, Meyerson M, Weinberg RA. Inhibition of telomerase limits the growth of human cancer cells. *Nat Med* 1999;5:1164-1170
- 38 Lichtsteiner SP, Lebkowski JS, Vasserot AP. Telomerase, a target for anticancer therapy. *Ann N Y Acad Sci* 1999;886:1-11
- 39 Guo Z, Yang SM. A new anti-cancer target point: progress in the studies of telomere and its inhibitors. *Shijie Huaren Xiaohua Zazhi* 1999;7:607-609
- 40 Ma JP, Zhan WH, Cai SR, Peng JS, Wang JP. Telomerase activity in gastric cancer. *Chin J Dig* 2000;1:13-16
- 41 He XX, Wang JL, Wu JL, Yuan SY, Ai L. Telomere, cellular DNA content and gastric mucosal carcinogenesis. *Shijie Huaren Xiaohua Zazhi* 2000;8:509-512
- 42 Okusa Y, Ichikura T, Mochizuki H, Shinomiya N. Clinical significance of telomerase activity in biopsy specimens of gastric cancer. *J Clin Gastroenterol* 2000;30:61-63
- 43 Zhang FX, Deng ZY, Zhang XY, Kang SC, Wang Y, Yu XL, Wang H, Bian XH. Telomeric length associated with prognosis in human primary and metastatic gastric cancer. *Shijie Huaren Xiaohua Zazhi* 2000;8:153-155
- 44 Kakeji Y, Maehara Y, Koga T, Shibahara K, Kabashima A, Tokunaga E, Sugimachi K. Gastric cancer with high telomerase activity shows rapid development and invasiveness. *Oncol Rep* 2001;8:107-110
- 45 Yakoob J, Hu GL, Fan XG, Zhang Z. Telomere, telomerase and digestive cancer. *World J Gastroenterol* 1999;5:334-337
- 46 Feng RH, Li JF, Liu BY, Zhu ZG, Yin HR. hTR gene cloning from human gastric cancer cells and the construction of its sense and antisense eukaryotic expression vector. *Shijie Huaren Xiaohua Zazhi* 2001;9:1409-1414
- 47 Shammas MA, Simmons CG, Corey DR, Reis RJS. Telomerase inhibition by peptide nucleic acids reverses "immortality" of transformed human cells. *Oncogene* 1999;18:6191-6200
- 48 Neidle S, Kelland LR. Telomerase as an anti-cancer target: current status and future prospects. *Anti-cancer drug des* 1999;14:341-347
- 49 Weilbaecher RG, Lundblad V. Assembly and regulation of telomerase. *Curr Opin Chem Biol* 1999;3:573-577
- 50 Gilley D, Blackburn EH. The telomerase RNA pseudoknot is critical for the stable assembly of a catalytically active ribonucleoprotein. *Proc Natl Acad Sci USA* 1999;96:6621-6625
- 51 Liu JP. Studies of the molecular mechanisms in the regulation of telomerase activity. *FASEB J* 1999;13:2091-2104
- 52 Kushner DM, Paranjape JM, Bandyopadhyay B, Cramer H, Leaman DW, Kennedy AW, Silverman RH, Cowell JK. 2-5A antisense directed against telomerase RNA produces apoptosis in ovarian cancer cells. *Gynecol Oncol* 2000;76:183-192
- 53 Kondo Y, Koga S, Komata T, Kondo S. Treatment of prostate cancer *in vitro* and *in vivo* with 2-5-A-anti-telomerase RNA component. *Oncogene* 2000;19:2205-2211
- 54 Koga S, Kondo Y, Komata T, Kondo S. Treatment of bladder cancer cells *in vitro* and *in vivo* with 2-5A antisense telomerase RNA. *Gene Ther* 2001;8:654-658
- 55 Mukai S, Kondo Y, Koga S, Komata T, Barna BP, Kondo S. 2-5A antisense telomerase RNA therapy for intracranial malignant gliomas. *Cancer Res* 2000;60:4461-4467
- 56 Herbert BS, Pitts AE, Baker SI, Hamilton SE, Wright WE, Shay JW, Corey DR. Inhibition of human telomerase in immortal human cells leads to progressive telomere shortening and cell death. *Proc Natl Acad Sci USA* 1999;96:14276-14281
- 57 Wu SH, Ma LP, Jin W, Sui YF. Tumor suppressor gene: P16, p21, PRB and gastric cancer. *Shijie Huaren Xiaohua Zazhi* 1999;7:551
- 58 Wang DX, Fang DC, Liu WW. Study on alteration of multiple genes in intestinal metaplasia, atypical hyperplasia and gastric cancer. *Shijie Huaren Xiaohua Zazhi* 2000;8:855-859
- 59 Komata T, Kondo Y, Koga S, Ko SC, Chung LWK, Kondo S. Combination therapy of malignant glioma cells with 2-5-A-antisense telomerase RNA and recombinant adenovirus p53. *Gene Ther* 2000;7:2071-2079
- 60 Qin LJ. *In situ* hybridization of P53 tumor suppressor gene in human gastric precancerous lesions and gastric cancer. *Shijie Huaren Xiaohua Zazhi* 1999;7:494-497
- 61 Zhang L, Fu HM, Jin SZ, Huang R, Zhou CG. Overexpression of P53 and relationship between extracellular matrix and differentiation, invasion and metastasis of gastric carcinoma. *Shijie Huaren Xiaohua Zazhi* 2001;9:992-996

Edited by Zhang JZ

• GASTRIC CANCER •

Expression and function of classical protein kinase C isoenzymes in gastric cancer cell line and its drug-resistant sublines

Ying Han, Zhe-Yi Han, Xin-Min Zhou, Ru Shi, Yue Zheng, Yong-Quan Shi, Ji-Yan Miao, Bo-Rong Pan, Dai-Ming Fan

Ying Han, Zhe-Yi Han, Xin-Min Zhou, Yong-Quan Shi, Ji-Yan Miao, Dai-Ming Fan, Institute of Digestive Disease, Xijing Hospital, Fourth Military Medical University, Xi'an 710032, Shaanxi Province, China
Ru Shi, Department of Pharmacology and Reagents, Xijing Hospital, Fourth Military Medical University, Xi'an 710032, Shaanxi Province, China
Yue Zheng, the 6th Undergraduate Section, Fourth Military Medical University, Xi'an 710032, Shaanxi Province, China

Bo-Rong Pan, Oncology Center of Xijing Hospital, Fourth Military Medical University, Xi'an 710032, Shaanxi Province, China

Supported by the National Nature Science Foundation of China, No. 30030140 and No. 30000066.

Correspondence to: Dai-Ming Fan, Institute of Digestive Disease, Xijing Hospital, Fourth Military Medical University, Xi'an 710032, Shaanxi Province, China. fandaim@fmmu.edu.cn

Telephone: +86-29-3375221 Fax: +86-29-2539041

Received 2001-11-02 Accepted 2001-12-06

Abstract

AIM: To investigate the expression and function of classical protein kinase C (PKC) isoenzymes in inducing MDR phenotype in gastric cancer cells.

METHODS: Two cell lines were used in the study: gastric cancer cell SGC7901 and its drug-resistant cell SGC7901/VCR stepwise-selected by vincristine 0.3, 0.7 and 1.0 mg·L⁻¹, respectively. The expression of classical PKC (cPKC) isoenzymes in SGC7901 cells and SGC7901/VCR cells were detected using immunofluorescent cytochemistry, laser confocal scanning microscope and Western blot. The effects of anti-PKC isoenzymes antibody on adriamycin accumulation in SGC7901/VCR cells were determined using flow cytometric analysis.

RESULTS: (1) SGC7901 cells exhibited positive staining of PKC- α . SGC7901/VCR cells exhibited stronger staining of PKC- α than SGC7901 cells. The higher dosage vincristine selected, the much stronger staining of PKC- α was observed on SGC7901/VCR cells. (2) Both SGC7901 and SGC7901/VCR cells exhibited positive staining of PKC- β I and PKC- β II with no significant difference. (3) Compared with SGC7901, SGC7901/VCR cells had decreased adriamycin accumulation and retention. Accumulation of adriamycin in SGC7901 was 5.21 \pm 2.56 mg·L⁻¹, in SGC7901/VCR 0.3 was 0.85 \pm 0.29 mg·L⁻¹, in SGC7901/VCR 0.7 was 0.81 \pm 0.32 mg·L⁻¹, and in SGC7901/VCR 1.0 was 0.80 \pm 0.33 mg·L⁻¹; Retention of adriamycin in SGC 7901 was 2.51 \pm 1.23 mg·L⁻¹, in SGC7901/VCR 0.3 was 0.47 \pm 0.14 mg·L⁻¹, in SGC7901/VCR 0.7 was 0.44 \pm 0.15 mg·L⁻¹, and in SGC 7901/VCR 1.0 was 0.41 \pm 0.11 mg·L⁻¹. (4) Fluorescence intensity presented adriamycin accumulation in SGC7901/VCR cells was increased from 1.14 \pm 0.36 to 2.71 \pm 0.94 when cells were co-incubated with anti-PKC- α but not with anti-PKC- β I, PKC- α II and PKC γ antibodies.

CONCLUSION: PKC- α , but not PKC- β I, PKC- β II or PKC γ , may play a role in multidrug resistance of gastric cancer cells SGC7901/VCR.

Han Y, Han ZY, Zhou XM, Shi R, Zheng Y, Shi YQ, Miao JY, Pan BR, Fan DM. Expression and function of classical protein kinase C isoenzymes in gastric cancer cell line and its drug-resistant sublines. *World J Gastroenterol* 2002;8(3):441-445

INTRODUCTION

Multi-drug resistance (MDR), the principal mechanism by which many cancers develop resistance to a variety of chemotherapeutic drugs, is a major factor in the failure of many forms of chemotherapy^[1-4]. It affects patients with numerous blood cancers and solid tumors. Cellular drug resistance is mediated by different mechanisms operating at different steps of the cytotoxic action of the drug from a decrease of drug accumulation in the cell to the abrogation of apoptosis induced by the chemical substance. Several different mechanisms will switch on in the MDR cells, but usually one major mechanism is operating. The most investigated mechanisms with known clinical significance are: (1) activation of transmembrane proteins effluxing different chemical substances from the cells, in which P-glycoprotein (P-gp) is the most known efflux pump; (2) activation of the enzymes of the glutathione detoxification system; (3) alterations of the genes and the proteins involved into the control of apoptosis (especially p53 and Bcl-2)^[5-12]. PKC comprises a family of at least 13 distinct serine/threonine kinase isoenzymes involved in signal transduction pathways that govern a wide range of physiological processes including differentiation, proliferation, gene expression, brain function, membrane transport and the organization of cytoskeletal and extracellular matrix proteins^[13-26]. Recently accumulated evidence indicates that PKC activity, especially cPKC, plays a significant role in the formation of tumor MDR. The isoenzymes possess distinct differences in localization in different cells. Within a single cell, PKC isoforms also exhibit differences in expression and function, so research on distinct function in tumor MDR of isoenzymes has important significance in screening drugs with high specificity that could reverse MDR and in disclosing the mechanism of MDR formation and its regularity of the reversion.

MATERIALS AND METHODS

Materials

Human gastric cancer cell line SGC7901 was reserved by our institute and its drug-resistant sublines SGC7901/VCR were stepwise-selected by vincristine 0.3, 0.7 and 1.0 mg·L⁻¹, respectively. RPMI 1640 medium was the product of Gibco (U.S.A.). Newborn bovine serum was purchased from Hyclone (U.S.A.). Chemical drugs vincristine and adriamycin were purchased from Farmitalia Carlo Erba

(U.S.A.) and Minsheng (Hangzhou, China). Rabbit-anti-human polyclonal antibody PKC- α , PKC- β I, PKC- β II and PKC γ were the products of Santa Cruz Biotechnology. SABC immunohistochemistry kit and the HRP labeled goat-anti-rabbit IgG was purchased from Boste (Wuhan, China). FITC labeled goat-anti-rabbit IgG was purchased from Zhongshan (China).

Methods

Immunofluorescent cytochemistry The expression of PKC isoenzymes were detected by routine immunocytochemical fluorescence method^[27,28]. The procedures were as follows. Cells were maintained at 37°C in a 50mL·L⁻¹ CO₂-humidified incubator in RPMI 1640 medium supplemented with 25mmol·L⁻¹ HEPES buffer and 100mL·L⁻¹ new born bovine serum. SGC7901/VCR cells were cultured in the medium with extra adding vincristine at the concentration of 0.3, 0.7 and 1.0mg·L⁻¹, respectively. Cells at exponential phase were harvested, digested by 2.5g·L⁻¹ trypsin and then cultured on the slides in the medium described above at 37°C for further 24h; RPMI 1640 medium was then washed by PBS and cells were fixed in cold acetone for 5min; 50mL·L⁻¹ H₂O₂ was added and incubated at room temperature for 10-15min and added 3g·L⁻¹ TritonX-100 for another 15min; normal goat serum (1:10) was added and incubated at room temperature for 30min; rabbit-anti-human polyclonal antibody PKC- α , PKC- β I, PKC- β II and PKC γ (1:100) were added respectively and incubated at 4°C over night; FITC labeled goat-anti-rabbit IgG was added and incubated at 37°C for 1h; the slides were sealed by 500mL·L⁻¹ glycerin buffer and observed with a fluorescence microscope. Unrelated monoclonal antibody and PBS were used as negative controls.

Laser confocal scanning microscope The laser confocal scanning microscope protocols used were as described^[29,30]. Methods of cell culture and stain with Ab were carried out as described in immunocytochemical fluorescence method. FITC labeled goat-anti-rabbit IgG was added in the darkness and incubated at room temperature for 3h; the slides were sealed by 500mL·L⁻¹ glycerin buffer and observed with a laser confocal scanning fluorescence microscope. Unrelated monoclonal antibody and PBS were used as negative controls.

SDS-PAGE According to Chen et al and Xiao *et al*^[31-33], cells at exponential phase were harvested and washed by cold PBS and suspended in extraction buffer (50mmol·L⁻¹ Tris-Cl (pH7.5), 150mmol·L⁻¹ NaCl, 0.2mmol·L⁻¹ EDTA, 1mmol·L⁻¹ PMSF and 10g·L⁻¹ NP-40). The homogenate was heated for 5min in a boiling water bath and then centrifuged. The supernatants were harvested and the protein concentrations were assayed by Bradford method. 150 μ g total protein were electrophoresed on SDS-polyacrylamide gels with the stacking and the separating gels containing 50 and 100g·L⁻¹ acrylamide, respectively, and the gels were stained with Coomassie brilliant blue dye.

Western blot analysis According to She *et al*^[34], after SDS-PAGE, proteins were transferred onto nitrocellulose membrane under a constant current of mA for 1h. Non-specific binding sites were blocked by PBS with 50mL·L⁻¹ milk plus 1g·L⁻¹ Tween-20 at room temperature. Primary and secondary antibodies were rabbit-anti-human polyclonal antibody PKC and HRP labeled goat-anti-rabbit IgG, respectively. Films were exposed in DAB detection reagent to develop color of bands.

Flow cytometric analysis According to Jiang *et al*^[35] and Feng *et al*^[36], cells were cultured in 6-well culture plates at 37°C for 48h, adriamycin was added to the final concentration of 5mg·L⁻¹. After further culture for 1h, rabbit-anti-human polyclonal antibody against different cPKC isoenzymes was added and incubated for 40min, PBS and normal rabbit serum were used as negative controls. And then,

cells were harvested or cultured in drug-free medium for another 30 min and harvested. The harvested cells of the phases were suspended in cold PBS, intracellular adriamycin fluorescence intensity was determined by flow cytometric analysis with the stimulative and acceptant wave length at 488nm and 575nm, respectively.

Statistical analysis Data were presented as $\bar{x} \pm s$. Significant differences were determined by using ANOVA in statistical software SPSS10.0.

RESULTS

Immunofluorescent cytochemistry

To investigate the expression of PKC isoenzymes of SGC7901 cells and its drug-resistant cell subline SGC7901/VCR, immunofluorescent cytochemistry was performed. The positive signals were of fluorescent signals. Both SGC7901 cells and SGC7901/VCR cells expressed PKC- α , PKC- β I, PKC- β II and PKC γ . The expression of PKC- α was stronger in SGC7901/VCR cells than that in SGC7901 cells. There was no significant difference in the expression of PKC- β I and PKC- β II between SGC7901/VCR cells and SGC7901 cells. And the expression of PKC γ in SGC7901/VCR cells was positive as strongly as that in SGC7901 cells, and also no significant difference was found.

Laser confocal microscope analysis

PKC- α expressed in both SGC7901 cells and SGC7901/VCR cells. The positive signals were localized in cytoplasm and membrane. Compared with SGC7901 cells, the intensity of fluorescence in SGC7901/VCR cells was increased significantly when analysed by the intensity of pixel by using computer, which was 100 in SGC7901/VCR cells and 80 in SGC7901 cells.

Western blot

The expression of PKC- α was significantly higher in SGC7901/VCR cells than that in SGC7901 cells, in which expression increased with the increase of drug-dose-resistance of SGC7901/VCR cells. No significant difference was found in the expression of PKC- β I, PKC- β II and PKC γ between SGC7901/VCR cells and SGC7901 cells (Figure 1).

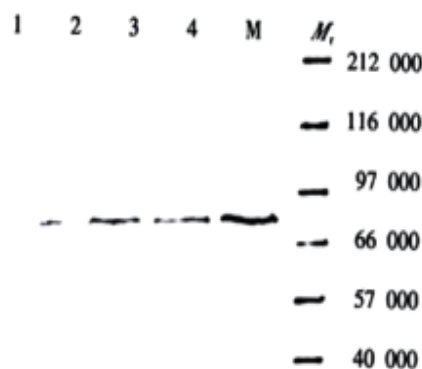


Figure 1 Western blot (detected with anti-PKC- α antibody)

Flow cytometric analysis

The effects of anti-PKC- α or β I antibody on adriamycin accumulation and retention in SGC7901/VCR cells were determined by flow cytometric analysis. When cells were cultured in drug-RPM1640, intracellular drug concentration would increase and finally stabilised at the highest plateau value, which was called adriamycin accumulation. When cells were cultured in drug-free medium, drug was effluxed from cells and subsequently, drug concentration stabilised at a lower plateau value, which was still higher than the

initial value and so called adriamycin retention. The results presented by the values of fluorescence intensity showed that adriamycin accumulation and retention decreased in SGC7901/VCR cells than that in SGC7901 cells. When co-incubated with anti-PKC- α antibody, the accumulation of adriamycin in MDR cells increased and showed partly dose-dependent effect, while PKC- β I, PKC- β II and PKC γ could not influence the ADR accumulation in SGC7901/VCR cells (Table 1,2).

Table 1 Adriamycin accumulation and retention in cells by flow cytometric analysis ($\bar{x} \pm s$ fluorescence intensity)

Adriamycin	SGC7901	SGC7901/VCR in different resistant drug dose (VCR.mg.L ⁻¹)		
		0.3	0.7	1.0
Accumulation	5.21 \pm 2.56	0.85 \pm 0.29 ^b	0.81 \pm 0.32 ^b	0.80 \pm 0.33 ^b
Retention	2.51 \pm 1.23	0.47 \pm 0.14 ^b	0.44 \pm 0.15 ^b	0.41 \pm 0.11 ^b

^bP<0.01, vs SGC7901.

Table 2 Effects of adriamycin accumulation in SGC7901/VCR cells by anti-PKC isoenzymes Ab ($\bar{x} \pm s$ fluorescence intensity)

Group	ρ (anti-PKC isoenzymes Ab)/(μ g.L ⁻¹)			
	0	25	250	500
Anti-PKC- α Ab	1.14 \pm 0.36	1.09 \pm 0.32	2.49 \pm 0.84 ^b	2.71 \pm 0.94 ^b
Anti-PKC- β IAb	1.14 \pm 0.36	1.13 \pm 0.38	1.14 \pm 0.39	1.14 \pm 0.39
Anti-PKC- α IIAb	1.14 \pm 0.36	1.14 \pm 0.38	1.14 \pm 0.40	1.14 \pm 0.39
Anti-PKC- γ Ab	1.14 \pm 0.36	1.14 \pm 0.39	1.14 \pm 0.40	1.14 \pm 0.39

^bP<0.01, vs 0 μ g.L⁻¹ anti-PKC isoenzymes Ab

DISCUSSION

The development of resistance to chemotherapeutic agents remains one of the major obstacles for successful cure of cancer patients. Tumor cells may acquire MDR in the course of exposure to various compounds that are used in modern anticancer therapy, including cytotoxic drugs and differentiating agents. Therefore, the recurrence of the disease after the initial treatment may be associated with establishment of secondary MDR in the residual tumor. Research on resistance to cancer treatment was mainly focused for 20 years on MDR. No useful method of reversing MDR, suitable for clinical use, has yet emerged from this large quantity of work. The reason could be an complicated mechanism involved in it. There are several ways for cancer cells to develop resistance or defense mechanisms against cytotoxic drugs^[37-43].

Resistance to therapy has been correlated to the presence of at least two molecular “pumps” that actively expel chemotherapeutic drugs from the tumor cells. This action thus spares tumor cells from the effects of the drug, which has to act inside the cells at the nucleus or the cytoplasm. The two pumps commonly found to confer MDR in cancer are P-gp and multidrug resistance-associated protein (MRP). But they can not explicate the phenomenon of MDR fully. It also reported that some cancer cells are resistant to signal of apoptosis and so making cell life longer might confer to the MDR phenotype.

Recent studies have indicated that the signal of phosphorylation might be an important part of MDR mechanisms. PKC isoforms are often overexpressed in disease states such as cancer and play a critical role in regulation of long term cellular events such as proliferation, differentiation and tumorigenesis. An increase in PKC activity might result in an oncogenic role and in MDR. Several studies indicate a role for PKC in the regulation of the MDR phenotype, since several PKC inhibitors are able to partially reverse MDR and inhibit P-gp phosphorylation.

The PKC family consists of several isoforms comprising three groups: classical, novel and atypical. PKC isoforms are widely

distributed in mammalian tissues and have many important physiological functions^[44-47]. cPKC subfamily shows significant specificity in tissue distribution. The isoenzymes possess distinct differences in localization in different cells. Within a single cell, PKC isoforms also exhibit differences in their distribution before and after their translocation following activation. For example, thymus cells express PKC- α and PKC- β I but not PKC- β II and PKC γ ; Cortical and medullary cells of suprarenal gland express PKC- α , while the cortical cells also express PKC- β I and PKC γ .

To date in recent years, the MDR phenotype is also associated with variation in content of PKC isoenzymes. Different isoforms possess distinct differences in expression and function in different MDR cells. It has been confirmed that sensitive cells show the phenotype of MDR when transfected with cDNA encoding PKC- α , which indicates the effect of PKC on MDR. Resistance to ADR of mouse leukemia MDR cell-line could be reversed by anti-PKC- β mAb when it was incubated with anti-PKC- α or anti-PKC- β mAb^[48-60].

This study confirmed that PKC- α , PKC- β I, PKC- β II and PKC γ were expressed in both SGC7901 cells and SGC7901/VCR cells. Our results showed that the expression of PKC- α was significantly higher in SGC7901/VCR cells than that in SGC7901 cells and the expression increased with the increase of drug-dose-resistance of SGC7901/VCR cells. There was no significant difference in the expression of PKC- β I, PKC- β II and PKC γ between SGC7901/VCR cells and SGC7901 cells. The result of flow cytometric analysis showed that ADR accumulation decreased in SGC7901/VCR cells much than that in SGC7901 cells, together with increase of the expression of PKC- α . Further study confirmed that anti-PKC- α antibody could reverse ADR accumulation in MDR cells to some degree and showed partly dose-dependent effect, while PKC- β I, PKC- β II and PKC γ could not influence the ADR accumulation in SGC7901/VCR cells. The results suggested that the formation of MDR in SGC7901/VCR cells was associated with over expression of PKC- α but not with PKC- β I, PKC- α II and PKC γ . Since isoenzymes of PKC possess only 1-10 amino acid in there pseudo substrate action site in C1 domain, research on distinct function in tumor MDR of isoenzymes has important significance in screening effective drugs with high specificity that could reverse MDR and in disclosing the mechanism of MDR formation and its regularity of the reversion. Because gastric cancer is common in China and some areas in the world^[61-80], this results may be important for further study.

REFERENCES

- 1 Yao XQ, Qing SH. Detection of multidrug resistance gene in progressive colon cancer and its significance. *Shijie Huaren Xiaohua Zazhi* 1999;7:535-536
- 2 Tu SP, Jiang SH, Qiao MM, Cheng SD, Wang LF, Wu YL, Yuan YZ, Wu YX. Effect of trichosanthin on cytotoxicity and induction of apoptosis of multiple drugs resistance cells in gastric cancer. *Shijie Huaren Xiaohua Zazhi* 2000;8:150-152
- 3 Cheng SD, Wu YL, Zhang YP, Qiao MM, Guo QS. Abnormal drug accumulation in multidrug resistant gastric carcinoma cells. *Shijie Huaren Xiaohua Zazhi* 2001;9:131-134
- 4 Zhang LJ, Chen KN, Xu GW, Xing HP, Shi XT. Congenital expression of Mdr-1 gene in tissues of carcinoma and its relation with pathomorphology and prognosis. *World J Gastroenterol* 1999;5:53-56
- 5 Zhan M, Yu D, Lang A, Li L, Pollock RE. Wild type p53 sensitizes soft tissue sarcoma cells to doxorubicin by down-regulating multidrug resistance-1 expression. *Cancer* 2001;92:1556-1566
- 6 Liu B, Staren E, Iwamura T, Appert H, Howard J. Effects of Taxotere on invasive potential and multidrug resistance phenotype in pancreatic carcinoma cell line SUIT-2. *World J Gastroenterol* 2001;7:143-148
- 7 Chen B, Zhang XY, Zhang YJ, Zhou P, Gu Y, Fan DM. Antisense to cyclin D1 reverses the transformed phenotype of human gastric cancer cells. *World J Gastroenterol* 1999;5:18-21
- 8 Liu XL, Xiao B, Yu ZC, Guo JC, Zhao QC, Xu L, Shi YQ, Fan DM. Down regulation of Hsp90 could change cell cycle distribution and increase drug sensitivity of tumor cells. *World J Gastroenterol* 1999;5:199-208

- 9 You H, Xiao B, Cui DX, Shi YQ, Fan DM. Two novel gastric cancer associated genes identified by differential display. *World J Gastroenterol* 1998;4:334-336
- 10 Xiao B, Shi YQ, Zhao YQ, You H, Wang ZY, Liu XL, Yin F, Qiao TD, Fan DM. Transduction of Fas gene or Bcl-2 antisense RNA sensitizes cultured drug resistant gastric cancer cells to chemotherapeutic drugs. *World J Gastroenterol* 1998;4:421-425
- 11 Warr JR, Bamford A, Quinn DM. The preferential induction of apoptosis in multidrug-resistant KB cells by 5-fluorouracil. *Cancer Lett* 2002;175:39-44
- 12 Roepe PD. pH and multidrug resistance. *Novartis Found Symp* 2001;240:232-247
- 13 Caruso-Neves C, Silva IV, Morales MM, Lopes AG. Cytoskeleton elements mediate the inhibition of the (Na⁺)+K⁺)atpase activity by PKC in *Rhodnius prolixus* malpighian tubules during hyperosmotic shock. *Arch Insect Biochem Physiol* 2001;48:81-88
- 14 Suga S, Wu J, Ogawa Y, Takeo T, Kanno T, Wakui M. Phorbol ester impairs electrical excitation of rat pancreatic beta-cells through PKC-independent activation of KATP channels. *BMC Pharmacol* 2001;1:3
- 15 MacDonald JF, Kotecha SA, Lu WY, Jackson MF. Convergence of PKC-dependent kinase signal cascades on NMDA receptors. *Curr Drug Targets* 2001;2:299-312
- 16 Chen L, Hahn H, Wu G, Chen CH, Liron T, Schechtman D, Cavallaro G, Banci L, Guo Y, Bolli R, Dorn GW 2nd, Mochly-Rosen D. Opposing cardioprotective actions and parallel hypertrophic effects of delta PKC and varepsilon PKC. *Proc Natl Acad Sci U S A* 2001;98:11114-11119
- 17 Kumar A, Hawkins KS, Hannan MA, Ganz MB. Activation of PKC-beta(I) in glomerular mesangial cells is associated with specific NF-kappaB subunit translocation. *Am J Physiol Renal Physiol* 2001;281:F613-619
- 18 Rivedal E, Opsahl H. Role of PKC and MAP kinase in EGF- and TPA-induced connexin43 phosphorylation and inhibition of gap junction intercellular communication in rat liver epithelial cells. *Carcinogenesis* 2001;22:1543-1550
- 19 Smith J, Yu R, Hinkle PM. Activation of MAPK by TRH Requires Clathrin-Dependent Endocytosis and PKC but Not Receptor Interaction with beta-Arrestin or Receptor Endocytosis. *Mol Endocrinol* 2001;15:1539-1548
- 20 Banan A, Fields JZ, Talmage DA, Zhang Y, Keshavarzian A. PKC-beta1 mediates EGF protection of microtubules and barrier of intestinal monolayers against oxidants. *Am J Physiol Gastrointest Liver Physiol* 2001;281:G833-847
- 21 Manier DH, Shelton RC, Sulser F. Cross-talk between PKA and PKC in human fibroblasts: what are the pharmacotherapeutic implications? *J Affect Disord* 2001;65:275-279
- 22 Boesch DM, Garvin JL. Age-dependent activation of PKC isoforms by angiotensin II in the proximal nephron. *Am J Physiol Regul Integr Comp Physiol* 2001;281:R861-867
- 23 Lum H, Podolski JL, Gurnack ME, Schulz IT, Huang F, Holian O. Protein phosphatase 2B inhibitor potentiates endothelial PKC activity and barrier dysfunction. *Am J Physiol Lung Cell Mol Physiol* 2001;281:L546-555
- 24 Shindo M, Irie K, Nakahara A, Ohigashi H, Konishi H, Kikkawa U, Fukuda H, Wender PA. Toward the identification of selective modulators of protein kinase C (PKC) isozymes: establishment of a binding assay for PKC isozymes using synthetic C1 peptide receptors and identification of the critical residues involved in the phorbol ester binding. *Bioorg Med Chem* 2001;9:2073-2081
- 25 Kim MS, Lim WK, Cha JG, An NH, Yoo SJ, Park JH, Kim HM, Lee YM. The activation of PI 3-K and PKC zeta in PMA-induced differentiation of HL-60 cells. *Cancer Lett* 2001;171:79-85
- 26 Radeff JM, Nagy Z, Stern PH. Involvement of PKC-beta in PTH, TNF-alpha, and IL-1 beta effects on IL-6 promoter in osteoblastic cells and on PTH-stimulated bone resorption. *Exp Cell Res* 2001;268:179-188
- 27 Ma X, Qiu DK, Xu J, Zeng MD. Effects of Cordyceps polysaccharides in patients with chronic hepatitis C. *Huaren Xiaohua Zazhi* 1998;6:582-584
- 28 Zhao LF, Han DW. Clinical significance of endotoxemia in liver diseases. *Shijie Huaren Xiaohua Zazhi* 1999;7:391-393
- 29 Wang CM, Huang XF, Pan BR, Dai XW, Ma FC, Zhao YM. Expression of chromogranin C/secretogranin II and pancreastatin in the pancreatic ductal carcinoma. *Huaren Xiaohua Zazhi* 1998;6:470-473
- 30 Huang XF, Wang CM, Dai XW, Pan BR, Yu LB, Fang L, Qian B, Zhao YL. Significance of cathepsin D and chromogranin A expression in human primary hepatocellular carcinomas. *Huaren Xiaohua Zazhi* 1998;6:474-478
- 31 Chen YK, Wu XB, Zhang ZY. Study on causes of serum anti-HBs positive patients with chronic liver diseases. *Huaren Xiaohua Zazhi* 1998;6:49-50
- 32 Xiao B, Shi YQ, Zhao YQ, You H, Liu XL, Fan DM. Expression of Fas gene in gastric cancer cells transduced with Fas gene. *Huaren Xiaohua Zazhi* 1998;6:400-403
- 33 Yang LJ, Sui YF, Chen ZN. Preparation and activity of conjugate of monoclonal antibody HAb18 against hepatoma F(ab')₂ fragment and staphylococcal enterotoxin A. *World J Gastroenterol* 2001;7:216-221
- 34 She FF, Su DH, Lin JY. Virulence and potential pathogenicity of coccoid *Helicobacter pylori* induced antibiotics. *World J Gastroenterol* 2001;7:254-258
- 35 Jiang XL, Quan QZ, Sun ZQ, Wang YJ, Qi F. Expression of adhesion molecules in tissues and peripheral lymphocyte of patients with ulcerative colitis. *Huaren Xiaohua Zazhi* 1998;6:54-55
- 36 Feng S, Song JD, Tian XR. Significance of proliferating cell nuclear antigen expression in colorectal carcinomas. *Huaren Xiaohua Zazhi* 1998;6:146-147
- 37 Gu SQ, Liang YY, Fan LR, Li BY, Wang DS. Co-regulative effects of the cAMP/PKA and DAG/PKC signal pathways on human gastric cancer cells during differentiation induced by traditional Chinese medicines. *China Natl J New Gastroenterol* 1997;3:50-53
- 38 Liu B, Staren E, Iwamura T, Appert H, Howard J. Effects of Taxotere on invasive potential and multidrug resistance phenotype in pancreatic carcinoma cell line SUIT-2. *World J Gastroenterol* 2001;7:143-148
- 39 Xu BH, Zhang RJ, Lu DD, Chen XD, Wang NJ. Expression of mdrl gene coded Pglycoprotein in hepatocellular carcinoma and its clinical significance. *Huaren Xiaohua Zazhi* 1998;6:783-785
- 40 Liu ZM, Shou NH. Expression significance of mdrl gene in gastric carcinoma tissue. *Shijie Huaren Xiaohua Zazhi* 1999;7:145-146
- 41 Shi YQ, Xiao B, Miao JY, Zhao YQ, You H, Fan DM. Construction of eukaryotic expression vector pBK fas and MDR reversal test of drug-resistant gastric cancer cells. *Shijie Huaren Xiaohua Zazhi* 1999;7:309-312
- 42 Liu Y, Lu MZ, Li QM, Wang YL. The expression of p53 C-myc and P-gp proteins in gastric cancer. *Xin Xiaohuabingxue Zazhi* 1997;5:585-586
- 43 Yin F, Shi YQ, Zhao WP, Xiao B, Miao JY, Fan DM. Suppression of P-gp induced multiple drug resistance in a drug resistant gastric cancer cell line by overexpression of Fas. *World J Gastroenterol* 2000;6:664-670
- 44 Kato A, Miyazaki M, Ambiru S, Yoshitomi H, Ito H, Nakagawa K, Shimizu H, Yokosuka O, Nakajima N. Multidrug resistance gene (MDR-1) expression as a useful prognostic factor in patients with human hepatocellular carcinoma after surgical resection. *J Surg Oncol* 2001;78:110-115
- 45 Kaminski MS, Zelenetz AD, Press OW, Saleh M, Leonard J, Fehrenbacher L, Lister TA, Stagg RJ, Tidmarsh GF, Kroll S, Wahl RL, Knox SJ, Vose JM. Pivotal Study of Iodine I 131 Tositumomab for Chemotherapy-Refractory Low-Grade or Transformed Low-Grade B-Cell Non-Hodgkin's Lymphomas. *J Clin Oncol* 2001;19:3918-3928
- 46 Ahlman H, Khorram-Manesh A, Jansson S, Wangberg B, Nilsson O, Jacobsson CE, Lindstedt S. Cytotoxic treatment of adrenocortical carcinoma. *World J Surg* 2001;25:927-933
- 47 Dei S, Teodori E, Garnier-Suillerot A, Gualtieri F, Scapecchi S, Budriesi R, Chiarini A. Structure-activity relationships and optimisation of the selective MDR modulator 2-(3,4-dimethoxyphenyl)-5-(9-fluorenylamino)-2-(methylethyl) pentanenitrile and its N-methyl derivative. *Bioorg Med Chem* 2001;9:2673-2682
- 48 Mansson E, Paul A, Lofgren C, Ullberg K, Paul C, Eriksson S, Albertioni F. Cross-resistance to cytosine arabinoside in a multidrug-resistant human promyelocytic cell line selected for resistance to doxorubicin: implications for combination chemotherapy. *Br J Haematol* 2001;114:557-565
- 49 Meng LH, Zhang JS, Ding J. Salvicine, a novel DNA topoisomerase II inhibitor, exerting its effects by trapping enzyme-DNA cleavage complexes. *Biochem Pharmacol* 2001;62:733-741
- 50 Chang G, Roth CB. Structure of MsbA from *E. coli*: A Homolog of the Multidrug Resistance ATP Binding Cassette (ABC) Transporters. *Science* 2001;293:1793-1800
- 51 Gill PK, Gescher A, Gant TW. Regulation of MDR1 promoter activity in human breast carcinoma cells by protein kinase C isozymes alpha and theta. *Eur J Biochem* 2001;268:4151-4157
- 52 Shtil AA, Ktitorova OV, Kakpakova ES, Holian O. Differential effects of the MDR1 (multidrug resistance) gene-activating agents on protein kinase C: evidence for redundancy of mechanisms of acquired MDR in leukemia cells. *Leuk Lymphoma* 2000;40:191-195
- 53 Matsumoto Y, Kunishio K, Nagao S. Increased phosphorylation of DNA topoisomerase II in etoposide resistant mutants of human glioma cell line. *J Neurooncol* 1999;45:37-46
- 54 Pallares-Trujillo J, Lopez-Soriano FJ, Argiles JM. Lipids: A key role in multidrug resistance? *Int J Oncol* 2000;16:783-798
- 55 van Gijn R, van Tellingen O, Haverkate E, Kettenes-van den Bosch JJ, Bult A, Beijnen JH. Pharmacokinetics and metabolism of the staurosporine

- analogue CGP 41 251 in mice. *Invest New Drugs* 1999;17:29-41
- 56 Merritt JE, Sullivan JA, Drew L, Khan A, Wilson K, Mulqueen M, Harris W, Bradshaw D, Hill CH, Rumsby M, Warr R. The bisindolylmaleimide protein kinase C inhibitor, Ro 32-2241, reverses multidrug resistance in KB tumour cells. *Cancer Chemother Pharmacol* 1999;43:371-378
- 57 Han Y, Cao YX, Shi YQ, Fan DM. Expression of P-gp and PKC isoenzymes in multidrug resistance gastric cancer cell-line SGC7901/VCR. *Disi Junyi Daxue Xuebao* 2000;21:1454-1456
- 58 Han Y, Shi YQ, Li L, Fan DM. Expression and function of PKC isoenzymes PKC- α and PKC- β I in gastric cancer cell-line SGC 7901 and its subline SGC7901/VCR. *Zhonghua Zhongliu Zazhi* 2001;23:103-106
- 59 Han Y, Shi YQ, Zheng Y, Nie YZ, Zhang HB, Zhang ML, Pan BR, Fan DM. Protein kinase C is related to multidrug resistance by MGr1-Ag. *Shijie Huaren Xiaohua Zazhi* 2001;9:517-521
- 60 Han Y, Shi YQ, Zheng Y, Zhang HB, Zhang ML, Wang CM, Fan DM. Expression and distribution of PKC isoenzymes in swelling activated multidrug resistance gastric cancer cell-line. *Zhonghua Yixue Zazhi* 2001; 81: 328-331
- 61 Xu L, Zhang SM, Wang YP, Zhao FK, Wu DY, Xin Y. Relationship between DNA ploidy, expression of ki 67 antigen and gastric cancer metastasis. *World J Gastroenterol* 1999;5:10-11
- 62 Wu YA, Lu B, Liu J, Li J, Chen JR, Hu SX. Consequence alimentary reconstruction in nutritional status after total gastrectomy for gastric cancer. *World J Gastroenterol* 1999;5:34-37
- 63 Ji F, Peng QB, Zhan JB, Li YM. Study of differential polymerase chain reaction of C-erbB 2 oncogene amplification in gastric cancer. *World J Gastroenterol* 1999;5:152-155
- 64 Zhan WH, Ma JP, Peng JS, Gao JS, Cai SR, Wang JP, Zheng ZQ, Wang L. Telomerase activity in gastric cancer and its clinical implications. *World J Gastroenterol* 1999;5:316-319
- 65 Ji F, Wang WL, Yang ZL, Li YM, Huang HD, Chen WD. Study on the expression of matrix metallo proteinase 2Mrna in human gastric cancer. *World J Gastroenterol* 1999;5:455-457
- 66 Wang H, Zheng MH, Zhang HB, Zhu J, He JR, Lu AG, Ji YB, Zhang MJ, Jiang Y, Yu BM, Li HW. Study on incisional implantation of tumor cells by carbon dioxide pneumo peritoneum in gastric cancer of a murine model. *World J Gastroenterol* 1999;5:544-546
- 67 Zou SC, Qiu HS, Zhang CW, Tao HQ. A clinical and long term follow up study of peri operative sequential triple therapy for gastric cancer. *World J Gastroenterol* 2000;6:284-286
- 68 Cai L, Yu SZ, Zhang ZF. Helicobacter pylori infection and risk of gastric cancer in Changle County, Fujian Province, China. *World J Gastroenterol* 2000;6:374-376
- 69 Zhang FX, Zhang XY, Fan DM, Deng ZY, Yan Y, Wu HP, Fan JJ. Antisense telomerase RNA induced human gastric cancer cell apoptosis. *World J Gastroenterol* 2000;6:430-432
- 70 Gu QL, Li NL, Zhu ZG, Yin HR, Lin YZ. A study on arsenic trioxide inducing in vitro apoptosis of gastric cancer cell lines. *World J Gastroenterol* 2000;6:435-437
- 71 Wang ZN, Xu HM. Relationship between collagen c α expression and biological behavior of gastric cancer. *World J Gastroenterol* 2000;6:438-439
- 72 Tu SP, Zhong J, Tan JH, Jiang XH, Qiao MM, Wu YX, Jiang SH. Induction of apoptosis by arsenic trioxide and hydroxy camptothecin in gastric cancer cells *in vitro*. *World J Gastroenterol* 2000;6:532-539
- 73 Jiang BJ, Sun RX, Lin H, Gao YF. Study on the risk factors of lymphatic metastasis and the indications of less invasive operations in early gastric cancer. *World J Gastroenterol* 2000;6:553-556
- 74 Deng DJ. Progress of gastric cancer etiology: Nnitrosamides in the 1990s. *World J Gastroenterol* 2000;6:613-618
- 75 Gao HJ, Yu LZ, Bai JF, Peng YS, Sun G, Zhao HL, Miu K, Lü XZ, Zhan g XY, Zhao ZQ. Multiple genetic alterations and behavior of cellular biology in gastric cancer and other gastric mucosal lesions: *H. pylori* infection, histological types and staging. *World J Gastroenterol* 2000;6:848-854
- 76 Miehke S, Kirsch C, Dragosics B, Gschwantler M, Oberhuber G, Antos D, Dite P, Lc]uter J, Labenz J, Leodolter A, Malfertheiner P, Neubauer A, Ehninger G, Stolte M, Bayerd rffer E. Helicobacter pylori and gastric cancer: current status of the Austrian-Czech-German gastric cancer prevention trial (PRISMA Study). *World J Gastroenterol* 2001;7:243-247
- 77 Xu AG, Li SG, Liu JH, Gan AH. Function of apoptosis and expression of the proteins Bcl-2, p53 and C-myc in the development of gastric cancer. *World J Gastroenterol* 2001; 7:403-406
- 78 Cai L, Yu SZ, Zhang ZF. Glutathione S-transferases M1, T1 genotypes and the risk of gastric cancer: A case control study. *World J Gastroenterol* 2001;7:506-509
- 79 He XS, Su Q, Chen ZC, He XT, Long ZF, Ling H, Zhang LR. Expression, deletion and mutation of p16 gene in human gastric cancer. *World J Gastroenterol* 2001;7:515-521
- 80 Fang DC, Yang SM, Zhou XD, Wang DX, Luo YH. Telomere erosion is independent of microsatellite instability but related to loss of heterozygosity in gastric cancer. *World J Gastroenterol* 2001;7:522-526

Edited by Zhang JZ

• GASTRIC CANCER •

Induction of apoptosis by TPA and VP-16 is through translocation of TR3

Su Liu, Qiao Wu, Xiao-Feng Ye, Jian-Huai Cai, Zhi-Wei Huang, Wen-Jin Su

Su Liu, Qiao Wu, Xiao-Feng Ye, Jian-Huai Cai, Zhi-Wei Huang, Wen-Jin Su, Key Laboratory of the Ministry of Education for Cell Biology and Tumor Cell Engineering, School of Life Sciences, Xiamen University, Xiamen 361005, Fujian Province, China
Supported by the National Outstanding Youth Science foundation of China (B type, 39825502); the National Natural Science Foundation of China (39880015, 30170477); the Natural Science Foundation of Fujian Province (C0110004).

Correspondence to: Dr. Qiao Wu, Key Laboratory of the Ministry of Education for Cell Biology and Tumor Cell Engineering, School of Life Sciences, Xiamen University, Xiamen 361005, Fujian Province, China. xgwu@xmu.edu.cn
Telephone: +86-592-2182542 Fax: +86-592-2086630

Received 2001-11-02 Accepted 2001-12-20

Abstract

AIM: To investigate the role of TR3 in induction of apoptosis in gastric cancer cells.

METHODS: Human gastric cancer cell line, MGC80-3, was used. Expression of TR3 mRNA and its protein was detected by Northern blot and Western blot. Localization of TR3 protein was showed by immunofluorescence analysis under laser-scanning confocal microscope. Apoptotic morphology was observed by DAPI fluorescence staining, and apoptotic index was counted among 1000 cells randomly. Stable transfection assay was carried out by Lipofectamine.

RESULTS: Treatment of MGC80-3 cells with TPA and VP-16 resulted in apoptosis, accompanied by the repression of Bcl-2 protein in a time-dependent manner. At the same time, TPA and VP-16 also up-regulated expression level of TR3 mRNA in MGC80-3 cells that expressed TR3 mRNA. When antisense-TR3 expression vector was transfected into the cells, expression of TR3 protein was repressed. In this case, TPA and VP-16 did not induce apoptosis. In addition, TPA and VP-16-induced apoptosis involved in translocation of TR3. In MGC80-3 cells, TR3 localized concentrative in nucleus, after treatment of cells with TPA and VP-16, TR3 translocated from nucleus to cytosol obviously. However, when this nuclear translocation was blocked by LMB, apoptosis was not occurred in MGC80-3 cells even in the presence of TPA and VP-16.

CONCLUSION: Induction of apoptosis by TPA and VP-16 is through induction of TR3 expression and translocation of TR3 from nucleus to cytosol, which may be a novel signal pathway for TR3, and represent the new biological function of TR3 to exert its effect on apoptosis in gastric cancer cells.

Liu S, Wu Q, Ye XF, Cai JH, Huang ZW, Su WJ. Induction of apoptosis by TPA and VP-16 is through translocation of TR3. *World J Gastroenterol* 2002;8(3):446-450

INTRODUCTION

TR3 (also termed as NGFI-B and Nur77) is an orphan receptor that belongs to the member of the steroid/thyroid/retinoid receptor superfamily^[1-3]. It is an immediate-early response gene, and its expression is rapidly induced by a variety of growth stimuli, including

growth factors, phorbol ester and cAMP-dependent pathways^[1,3-5]. Similar to other members of the superfamily, TR3 functions in nucleus as a transcriptional factor to positively or negatively regulate gene expression necessary to alter the cellular phenotype in response to the growth stimuli^[6]. We found recently that TR3 heterodimerizes with retinoid X receptor (RXR) that binds to retinoic acid receptor α (RAR α) promoter, and regulates RAR α expression that is critical to inducing apoptosis^[7]. In addition, TR3 also heterodimerizes with chicken ovalbumin upstream promoter transcription factor (COUP-TF) to inhibit COUP-TF binding to retinoic acid responsive element (RARE) through direct protein-protein interaction^[8]. These evidences suggest that TR3 can mediate diverse signals through its ability either to bind to a variety of response elements or to interact with different protein factors. However, the mechanism by which TR3 exerts its biological functions remains largely unknown.

Apoptosis, as a distinct form of cell death, is an important process that can lead to tumor regression, and suppression of apoptosis is often associated with abnormal cell survival and malignant growth^[9-15]. The involvement of TR3 in apoptosis was first demonstrated by showing that TR3 was rapidly induced by T-cell antigen receptor (TCR) signaling in immature thymocytes and T-cell hybridomas^[16,17]. Overexpression of a dominant-negative TR3 protein or inhibition of TR3 expression by antisense-TR3 inhibited TCR-induced apoptosis, whereas constitutive expression of TR3 led to massive apoptosis^[16,17]. These evidences clearly indicate that TR3 plays an important role in TCR-mediated apoptosis. The involvement of TR3 in apoptosis process is also observed in many cancer cell lines. Treatment of lung cancer cells with AHPN/CD437 strongly induced apoptosis, which was accompanied by a rapid induction of TR3. Inhibition of TR3 by antisense-TR3 effectively abolished apoptosis induction by AHPN/CD437^[18]. Rapid induction of TR3 was also found in other cancer cells after stimulation of apoptosis by a variety of apoptosis-inducing agents^[19-21]. Therefore, these observations suggest that expression of TR3 is required for induction of cell apoptosis.

How TR3 functions to regulate apoptosis in gastric cancer cells is less understood. In this study, we investigated the role of TR3 in inducing apoptosis in gastric cancer cells. The results showed that 12-O-tetradecanoylphorbol-13-acetate (TPA) and VP-16 (also called etoposide) induced apoptosis, accompanied by TR3 expression. More importantly, TR3 protein translocated from nucleus to cytosol, when apoptosis occurred by TPA or VP-16 induction. However, when the translocation was blocked by leptomycin B (LMB), apoptosis was not detected, even in the presence of apoptotic stimuli. Our findings, therefore, have drawn an inspiration that translocation of TR3 from nucleus to cytosol may be one of the essential links involved in the mechanism of apoptosis by apoptotic stimuli in gastric cancer cells.

MATERIALS AND METHODS

Cell line and culture condition

Human gastric cancer cell line, MGC80-3, was established by Cancer Research Center in Xiamen University^[22]. The cells were maintained in RPMI-1640 medium, supplemented with 10% FCS, 1 mM glutamine, and 100u/ml penicillin.

Agents

TPA and VP-16 (Sigma) are used as apoptosis stimuli that can induce apoptosis in a variety of cells, including breast cancer cells, lung cancer cells, prostate cancer cells^[23-30]. LMB is an antibiotic with anti-fungal and anti-tumor activity that was first discovered and purified from the fermentation broth and mycelia of streptomyces^[31-33]. Recently, this antibiotic has become an important tool for studying nuclear localization^[34-36].

Apoptosis analysis^[37]

MGC80-3 cells were treated with TPA and VP-16 for different time indicated in figures, trypsinized, washed with PBS, fixed in 3.7% paraformaldehyde, and then stained with 50 μ g/mL of 4,6-diamidino-2-phenylindole (DAPI, Sigma) containing 100 μ g/mL of DNase-free RNase A to facilitate the examination of nuclei under fluorescence microscope. Apoptotic cells were counted among 1000 cells randomly. The apoptotic index was a mean of three independent experiments.

Immunofluorescence analysis^[38]

MGC80-3 cells were cultured on cover glass overnight, and then treated with TPA and VP-16 as required. After washed with PBS, cells were fixed in 4% paraformaldehyde. After fixation, the cells were incubated firstly with anti-TR3 antibody (Santa Cruz), and then reacted with corresponding FITC-conjugated anti-IgG (Pharmlingen) as secondary antibody. Fluorescent images were observed and analyzed under laser-scanning confocal microscope (Bio-Rad MRC-1024ES).

Western blot analysis^[38,39]

Total 50 μ g of nuclear extract was electrophoresed on 8% denaturing gel and electroblotted onto a nitrocellulose membrane. The membrane was probed with anti-TR3 antibody followed by corresponding secondary antibody. The antibody reactivity was detected with an Amersham ECL kit according to the manufacturer's instruction. For the cytosolic and nuclear fractions, the cells were suspended in 500 μ l of 10mM Tris-Cl (pH 7.8), 1% Nonidet P-40, 10mM mercaptoethanol, 0.5mM phenylmethylsulfonyl fluoride, 1 μ g/ml leupeptin and aprotinin for 2 min at 0°C, then 500 μ l of DDW was added, and the cells were allowed to swell for 2min. The cells were sheared by 10 passages through 22 gauge needle. Nuclei were recovered by centrifugation at 400Xg for 6min, and the low-speed supernatant was centrifuged at 100000g for 30min. The high-speed supernatant constituted the cytosolic fraction.

Stable transfection

Antisense-TR3 expression vector (provided kindly by Dr. Uemura, and Dr. Chang^[40]) was stably transfected into MGC80-3 cells by LipofectamineTM (Gibco/BRL) as described previously^[41], then screened with 600 μ g of G418. Expression of endogenous TR3 protein was determined by Western blot.

RESULTS

Expression of TR3 mRNA in response to apoptotic stimuli

TPA and VP-16 were both known as the apoptotic stimuli which induced apoptosis in many kinds of cancer cell lines, including the cancer cells of prostate, breast and lung^[23-30]. To determine whether these apoptotic stimuli also functioned in gastric cancer cells, a specific, DAPT staining for display of apoptotic nuclear morphology was adopted under fluorescence microscope^[38]. The observation indicated that treatment of MGC80-3 cells with TPA and VP-16 caused the classical morphological characteristics of apoptosis, including nuclear condensation and fragmentation (Figure 1A). The apoptotic index was further determined by counting 1000 cells randomly. In MGC80-3 cells, the apoptotic index was merely 3.89

%. However, the apoptotic index induced by TPA and VP-16 increased in a time-dependent manner (Figure 1B). The highest apoptotic index reached 44.33% (for TPA induction) and 32.16% (for VP-16 induction), respectively. Thus, the data demonstrated that TPA and VP-16 indeed induced apoptosis in gastric cancer cells.

Members of the Bcl-2 family were involved in the regulation of apoptotic process^[42,43]. Since TPA and VP-16 induced apoptosis significantly in MGC80-3 cells shown above, it should be interrelated with some proteins that were associated with apoptosis initiation. To investigate this possibility, expression of Bcl-2 was detected. Western blot showed that when TPA treated with cells for different time, the expression of BCL-2 protein was repressed in a time-dependent manner (Figure 1C), which was consistent with the result shown in Figure 1A and B. Similar result was seen in the cells treated with VP-16 (data not shown). This result suggested that inhibition of Bcl-2 might render MGC80-3 cells more susceptible to the apoptosis-inducing effect of TPA and VP-16.

Several evidences showed that TR3 was involved in the regulation of apoptosis in different cell types^[16,44,45]. We investigated the role of TR3 in apoptosis of MGC80-3 cells induced by TPA and VP-16. Treatment of cells with TPA and VP-16 not only induced MGC80-3 cell apoptosis and repressed its relative protein, Bcl-2 (Figure 1A-C), but also enhanced expression of TR3 mRNA obviously that was expressed at relative low level in MGC80-3 cells (Figure 1D). Taken together, these results revealed a possible link between expression of TR3 and induction of apoptosis in gastric cancer cells.

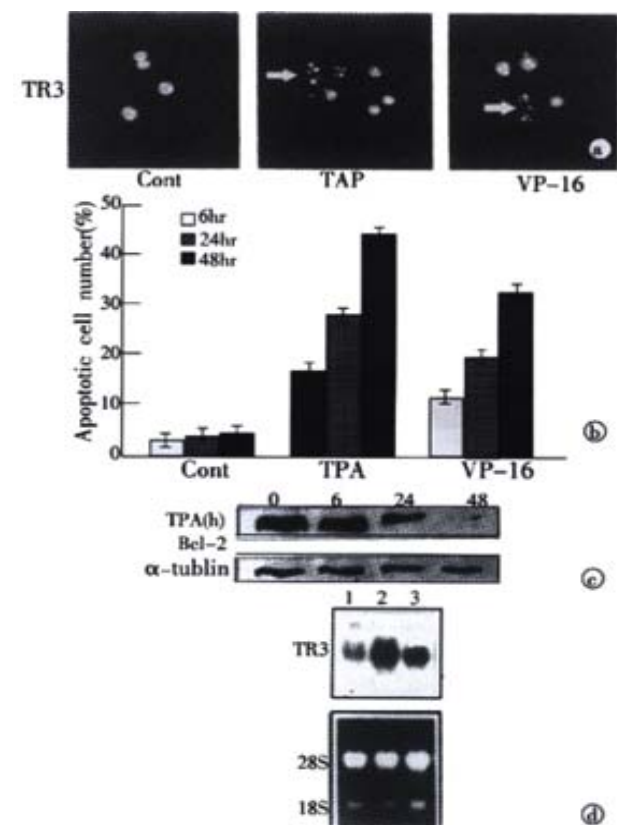


Figure 1 Induction of apoptosis and TR3 expression induced by TPA and VP-16 in MGC80-3 cells. (A) Morphological analysis of apoptotic cells. Cells treated with TPA and VP-16 for 24 hr, and then stained with DAPI. Nuclear morphology was visualized under fluorescence microscope. (B) Measure of apoptotic index by counting 1000 cells stained with DAPI under fluorescence microscope. The data shown represents mean of three independent experiments (\pm SE). (C) Analysis of Bcl-2 protein expression. Cells were treated with TPA for indicated time, and Western blot was performed as described in

materials and methods. α -tubulin was used to quantify the amount of protein used in each lane. (D) Detection of TR3 mRNA expression. Cells were treated with TPA and VP-16 for 24 hr. Preparation of total RNA and Northern blot were carried out as described in materials and methods. 18S and 28S were shown to quantify the loading RNA. Lane 1: control; Lane 2: TPA treatment; Lane 3: VP-16 treatment.

Translocation of nuclear TR3 to cytosol induced by apoptotic stimuli

It was reported recently that translocation of protein was closely associated with its biological function^[24,38,47]. To determine whether the apoptotic stimuli could cause translocation of TR3 in MGC80-3 cells, the immunofluorescent localization of TR3 protein was conducted by using correspondent TR3-specific antibody and laser-scanning confocal microscope observation. The results illustrated that in MGC80-3 cells, TR3 protein was concentrative in nucleus (Figure 2A). When treatment of TPA for 6 hr, the majority of TR3 protein was still remained in nucleus, little in cytosol. However, after 24 hr of TPA treatment, the majority of TR3 protein translocated from nucleus to cytosol, little in nucleus (Figure 2A). Similar result was also seen in the cells treated with VP-16. After treatment of 24 hr, TR3 protein almost translocated to cytosol (data not shown).

To further verify this protein translocation, the cytosolic and nuclear fractions were isolated respectively, and TR3 protein level was detected by Western blot. As shown in Figure 2B, TR3 protein was expressed in MGC80-3 cells, which located in nucleus (Figure 2B). TPA and VP-16 treatment led to down-regulation of TR3 protein in nuclear and up-regulation in cytosol with a time-dependent manner. After treatment of the cells for 6 hr with TPA and VP-16, respectively, TR3 protein was distributed both in nucleus and cytosol. However, after 24 hr treatment of TPA and VP-16, TR3 protein appeared more in cytosol and little in nucleus clearly (Figure 2B). This result was in accordance with the result shown in Fig. 2A, suggesting that translocation of TR3 protein might be associated with induction of apoptosis, which was a novel signal pathway for TPA and VP-16 to exert their biological functions.

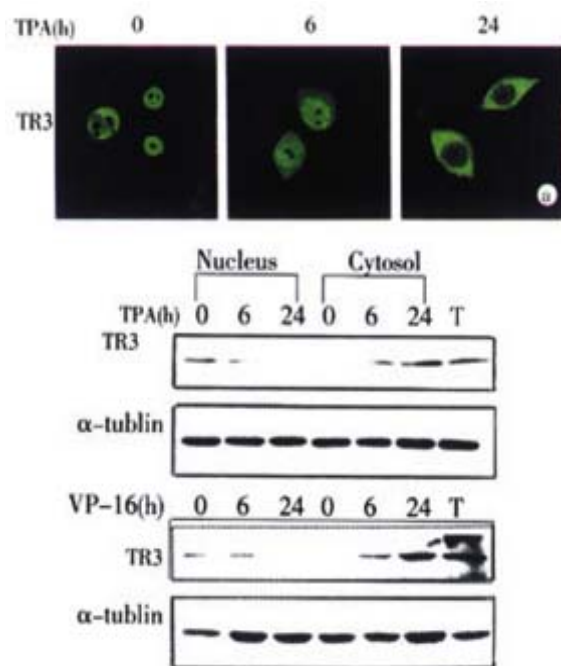


Figure 2 Translocation of TR3 protein from nucleus to cytosol in MGC80-3 cells. The cells treated with TPA for indicated time. (A) Translocation of TR3 protein observed by laser-scanning confocal microscope. TR3 protein was immunostained with anti-TR3 antibody and corresponding FITC-conjugated secondary antibody. (B) Western blot showed the translocation of TR3 protein. Nuclear and cytosolic fractions were prepared as described in materials and methods. α -tubulin was shown to quantify the loading protein. T: total protein.

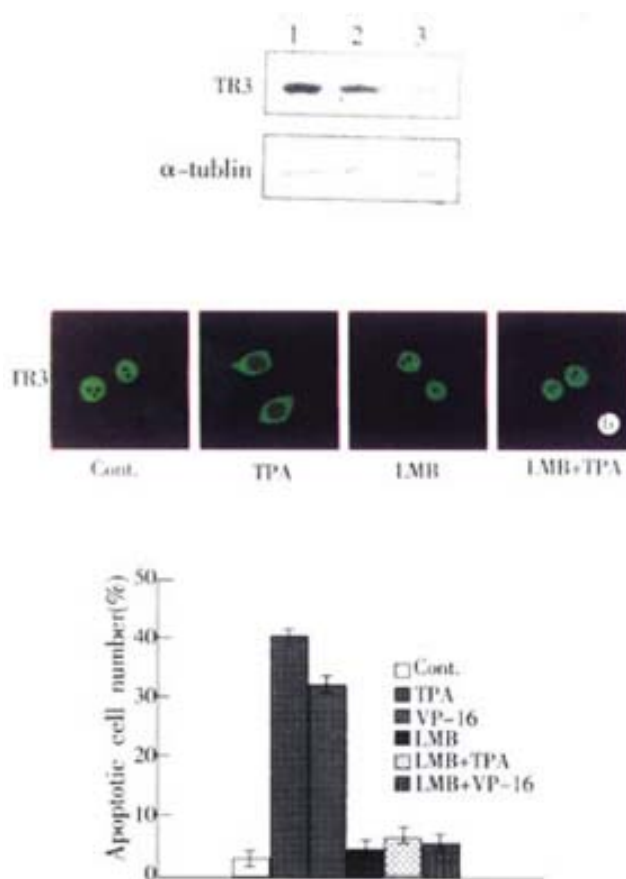


Figure 3 Inhibition of TR3 protein expression and its translocation in MGC80-3 cells. (A) Repression of TR3 protein expression by transfection of antisense-TR3 expression vector into MGC80-3 cells. Endogenous TR3 protein was determined by Western blot. Empty vector was also transfected into cells as a positive control. α -tubulin was shown to quantify the loading protein. Lane 1: protein from MGC80-3 cells; Lane 2: protein from the cells transfected with empty vector; Lane 3: protein from the cells transfected with antisense-TR3 expression vector. Inhibitory effect of LMB on TR3 protein translocation induced by TPA. The cells treated with different agents indicated as in the figure. The reaction with antibody was similar to the description in Fig. 2A. (C) Inhibitory effect of LMB on apoptosis induction by TPA and VP-16. Cells treated with different agents indicated as in the figure. Apoptotic index was measured as described in Fig. 1B.

Inhibition of both TR3 protein expression and its translocation

Since TR3 protein was expressed in MGC80-3 cells (Figure 2A, B), we transfected antisense-TR3 expression vector into the cells to determine whether inhibition of TR3 protein expression caused TPA and VP-16 fail to induce apoptosis. The stable transfection result was showed in Figure. 3A. Expression of TR3 protein was almost repressed in transfected cells, whereas TR3 protein still expressed in the cells transfected with empty vector, compared to MGC80-3 cells. In this transfected cells, TPA and VP-16 could not induce apoptosis. The apoptotic index only reached 5.14% (for TPA induction) and 4.62% (for VP-16 induction), which were less than that in MGC80-3 cells treated with TPA and VP-16 (Figure 1B) and those transfected with empty vector (apoptotic index amounted to 39.78% for TPA induction and 27.56% for VP-16 induction).

It was then necessary to probe into the intrinsic mechanism of whether there was some inevitable linkage between TR3 protein translocation and apoptosis induction. Since LMB has been used in many systems to demonstrate the nuclear localization and inhibited the export of a number of proteins, including actin, transcription factors, kinases and cell cycle regulators^[48-54], we used LMB as inhibitor to block nuclear protein TR3 export from nucleus to cytosol. In MGC80-3 cells, TR3 protein was mainly located in nucleus, after treatment of

24 hr with TPA, the most of TR3 protein was translocated from nucleus to cytosol in the absence of LMB (Figure 3B). However, in the presence of LMB, TR3 protein was remained in nucleus, although MGC80-3 cells were treated by TPA for 24 hr (Figure 3B). The similar result was also observed in VP-16 treated-cells (data not shown). According to this inhibitory result, we detected the apoptotic index to determine the relationship between translocation of TR3 protein and apoptosis induction. As shown in Figure 3C, in the presence of LMB, TPA and VP-16 did not induced apoptosis, compared with that TPA and VP-16 induced apoptosis of MGC80-3 cells obviously in the absence of LMB. Thus, preventing the nuclear TR3 protein export from nucleus to cytosol repressed TPA and VP-16's ability to induce apoptosis. The result again confirmed that translocation of TR3 protein was associated with induction of apoptosis.

DISCUSSION

The TR3 orphan receptor is required for activation-induced apoptosis of T-cell hybridomas^[16]. To gain insight into its function during apoptosis, we, in this study, analyzed the relationship between TR3 expression and its translocation and apoptosis induction in gastric cancer cells.

TR3 is an early response gene whose expression is induced by a variety of stimuli, including signals for cell survival, such as growth factors, and signals for cell death, such as TCR^[1,3-5]. To study the role of TR3 in gastric cancer cells, we used TPA and VP-16 to induce apoptosis, and found that when apoptosis occurred and its related protein Bcl-2 was inhibited by TPA and VP-16 in MGC80-3 cells, TR3 mRNA was indeed up-regulated. After transfection of antisense-TR3 expression vector into MGC80-3 cells that expressed TR3 at protein level resulted in the inhibition of TR3 protein expression. In the transfected cells, we could not detect marked apoptosis, even in the presence of TPA and VP-16 induction. The apoptotic index was only 5.14% (for TPA induction) and 4.62% (for VP-16 induction), similar to the control MGC80-3 cells with 3.89% and less than the TPA and VP-16 treated-cells with 44.33% (for TPA induction) and 32.16% (for VP-16 induction). These results indicated that TPA and VP-16 regulated apoptosis through induction of TR3 expression at both mRNA and protein levels.

TR3 functions as a nuclear transcription factor in the regulation of target gene expression^[6]. The movement of transcription factors between nucleus and cytoplasm is important in regulating its activity^[24,47]. Our observation showed that TPA and VP-16-induced apoptosis involved in translocation of TR3 protein. In MGC80-3 cells, TR3 protein localized mainly in the nucleus in which it might be associated with other nuclear proteins related to stimulation of cell proliferation, such as PKB/AKT, cFos, and AP-1^[18,55-58]. However, when cells were treated with TPA and VP-16 for 24 hours, respectively, translocation of TR3 from nucleus to cytosol was observed, with an increase protein expression of TR3 in cytosol and a decrease in nucleus in a time-dependent manner. In this case, apoptosis induced by TPA and VP-16 did happened, also in a time-dependent manner, and during this process, Bcl-2 protein, known to induce cell survival in variety of cell types^[59,60], was strongly inhibited by TPA and VP-16. In addition, when this nuclear export was blocked by LMB, apoptosis was not detected, regardless of the presence of TPA and VP-16. As a comparison, all-trans retinoic acid that could not induce TR3 translocation from nucleus to cytosol failed to induction of apoptosis in MGC80-3 cells although it could also induce TR3 expression (data not shown). Taken together, these data clearly demonstrated that induction of apoptosis by TPA and VP-16 was through the translocation of TR3 from nucleus to cytosol, which might be a novel signal pathway for apoptosis and the new function for TR3 to exert its effect on apoptosis induction. Bcl-2 may play an important role in the regulation of TPA and VP-16 -induced apoptosis.

Of course, the link between the mechanism of TR3 function and the apoptosis induction in gastric cancer cells should be studied further from other aspects.

REFERENCES

- 1 Milbrandt J. Nerve growth factor induces a gene homologous to the glucocorticoid receptor gene. *Neuron* 1998;1:183-188
- 2 Chang C, Kokontis J. Identification of a new member of the steroid receptor super-family by cloning and sequence analysis. *Biochem Biophys Res Commun* 1988;155:971-977
- 3 Hazel TG, Nathans D, Lau LF. A gene inducible by serum growth factors encodes a member of the steroid and thyroid hormone receptor superfamily. *Proc Natl Acad Sci USA* 1988;85:8444-8448
- 4 Williams GT, Lau LF. Activation of the inducible orphan receptor gene nur77 by serum growth factors: dissociation of immediate - early responses. *Mol Cell Biol* 1993;13:6124-6136
- 5 Lim RW, Zhu CY, Stringer B. Differential regulation of primary response gene expression in skeletal muscle cell through multiple signal transduction pathways. *Biochim Biophys Acta* 1995; 126:91-100
- 6 Williams TE, Fahrner TJ, Johnston M, Milbrandt J. Identification of the DNA binding site for NGFI-B by genetic selection in yeast. *Science* 1991;252:277-281
- 7 Wu Q, Dawson M, Zheng Y, Hobbs PD, Agadir A, Jong L, Li Y, Liu R, Zhang XK. Inhibition of trans-retinoic acid-resistant human breast cancer cell growth by retinoid x receptor-selective retinoids. *Mol Cell Biol* 1997;17:6598-6608
- 8 Wu Q, Li Y, Liu R, Agadir A, Lee OK, Liu Y, Zhang XK. Modulation of retinoic acid sensitivity in lung cancer cells through dynamic balance of orphan receptors nur77 and COUP-TF and their heterodimerization. *EMBO J* 1997;16:1656-1669
- 9 Fisher DE. Apoptosis in cancer therapy: crossing the threshold. *Cell* 1994;78:539-542
- 10 Jacobson MD, Burne JF, King MP. Bcl-2 blocks apoptosis in cells lacking mitochondrial DNA. *Nature* 1993;361:365-369
- 11 Douglas RG, John CR. Mitochondrial and Apoptosis. *Science* 1998;8: 1309-1312
- 12 Boldin MP, Goncharov TM, Goltsev YV. Involvement of MACH, a novel MORT1/FADD-interacting protease, in Fas/Apo1- and TNF receptor induced cell death. *Cell* 1996;85:803-815
- 13 Enari M, Sakahira H, Yokoyama H. A caspase-activated Dnase that degrades DNA during apoptosis and its inhibitor ICAD. *Nature* 1998; 391:43-50
- 14 Zhuang XQ, Yuan SZ, Wang XH, Lai RQ, Luo ZQ. Oncoprotein expression and inhibition of apoptosis during colorectal tumorigenesis. *China Natl J New Gastroentero* 1996; 2:3-5
- 15 Xue XC, Fang GE, Hua JD. Gastric cancer and apoptosis. *Shijie Huaren Xiaohua Zazhi* 1999;7:359-361
- 16 Woronicz JD, Calnan B, Ngo V, Winoto A. Requirement for the orphan steroid receptor nur77 in apoptosis of T-cell hybridomas. *Nature* 1994;367:277-280
- 17 Liu ZG, Smith SW, McLaughlin KA, Schwartz LM, Osborne BA. Apoptotic signals delivered through the T-cell hybrid require the immediate-early gene nur77. *Nature* 1994;367:281-284
- 18 Li Y, Agadir A, Liu R, Dawson M, John CR, Fontana JA, Bost F, Hobbs PD, Zheng Y, Chen GQ, Shroot B, Mercola D, Zhang XK. Molecular determinants of AHPN(CD437)-induced growth arrest and apoptosis in human lung cancer cell lines. *Mol Cell Biol* 1998;18:4719-4731
- 19 Maruyama K, Tsukada T, Bandoh S, Sasaki K, Ohkura N, Yamaguchi K. Retinoic acids differentially regulate NOR-1 and its closely related orphan nuclear receptor genes in breast cancer cell line MCF-7. *Biochem Biophys Res Comm* 1997;231:417-420
- 20 Gregg TW, Lau LF. Activation of the inducible orphan receptor gene nur77 by serum growth factors: dissociation of immediate-early and delayed-early responses. *Mol Cell Biol* 1993;13: 6124-6136
- 21 Jeong KY, Lau LF. Involvement of JunD in transcription activation of the orphan receptor gene nur77 by nerve growth factor and membrane depolarization in PC12 cells. *Mol Cell Biol* 1994; 14:7731-7743
- 22 Wang KH. Establishment of gastric carcinoma cell line MGC80-3 cells. *Exp Biol Sinica* 1983; 16:257-267
- 23 Yang XJ, Chen SB, Bao JZ, Wang Y, Zhang ZB, Zhang XK, Zhang XR. Effect of HGF on etoposide-induced apoptosis. *Chin J New Gastroenterol* 1997; 5: 518-519
- 24 Li H, Kolluri SK, Gu J, Dawson M, Cao XH, Hobbs PD, Chen GQ, Lu JS, Lin F, Xie ZH, Fontana JA, Reed JC, Zhang XK. Cytochrome C release and apoptosis induced by mitochondrial targeting of nuclear orphan receptor TR3. *Science* 2000;289:1159-1164
- 25 Agadir A, Shealy YF, Hill DH, Zhang XK. Retinyl methyl ether down-regulates transcriptional activation by tumor promoter TPA and nuclear protooncogenes cJun and cFos. *Cancer Res* 1997; 57:3444-3450

- 26 Jia L, Patwari Y, Srinivasula SM, Neland AC, Fernandes-alnemri T, Alnemri ES, Kelsey SM. Bax translocation is crucial for the sensitivity of leukaemic cells to etoposide-induced apoptosis. *Oncogene* 2001;20: 4817-4826
- 27 Custodio BA, Cardoso MP, Madeira MC, Almeida LM. Mitochondrial permeability transition induced by the anticancer drug etoposide. *Toxicology in vitro* 2001;15:265-270
- 28 Godlewski MM, Motyl MA, Gajkowska B, Wareski P, Koronkiewicz M, Motyl T. Subcellular redistribution of BAX during apoptosis induced by anticancer drugs. *Anti-cancer drugs* 2001;12: 607-617
- 29 Kim R, Inoue H, Tanabe K, Toge T. Effect of inhibitors of cysteine and serine proteases in anticancer drug-induced apoptosis in gastric cancer cells. *Int J Oncology* 2001;18:1227-1232
- 30 Friedrich K, Wieder T, Von Haefen C, Radetzki S, Janicke R, Schulze-Osthoff K, Dorken B, Daniel PT. Overexpression of caspase-3 restores sensitivity for drug-induced apoptosis in breast cancer cell lines with acquired drug resistance. *Oncogene* 2001;20:2749-2760
- 31 Hamamoto T. Leptomycins A and B, new antifungal antibiotics. II. Structural elucidation. *J Antibiot (Tokyo)* 1983;36:646-650
- 32 Hamamoto T. Leptomycins A and B, new antifungal antibiotics. III. Mode of action on *Schizosaccharomyces pombe*. *J Antibiot (Tokyo)* 1985;38:1573-1580
- 33 Yoshida M. Effects of Leptomycin B on the cell cycle of fibroblasts and fission yeast cells. *Exp Cell Res* 1990;187:150-156
- 34 Fornerod M, Ohno M, Yoshida M, Mattaj JW. CRM1 is an export receptor for leucine-rich nuclear export signals. *Cell* 1997;90:1051-1060
- 35 Ossareh NB, Bachelier F, Dargemont C. Evidence for a role of CRM1 in signal-mediated nuclear protein export. *Science* 1997;278:141-144
- 36 Fukuda M, Asano S, Nakamura T, Adachi M, Yoshida M, Yanagida M, Nishida E. CRM1 is responsible for intracellular transport mediated by the nuclear export signal. *Nature* 1997;390:308-311
- 37 Liu Y, Lee MO, Wang HG, Li Y, Hashimoto Y, Klaus M, John CR, Zhang XK. Retinoic acid receptor (mediates the growth-inhibitory effect of retinoic acid by promoting apoptosis in human breast cancer cells. *Mol Cell Biol* 1996;16:1138-1149
- 38 Wu Q, Liu S, Ding L, Ye XF, Su WJ. PKC (translocation from mitochondria to nucleus is closely related to induction of apoptosis in gastric cancer cells. Science in China 2001, in press
- 39 Wu Q. Distinct Ways of Retinoic Acid Receptors on Inhibition of AP-1 Activity in Gastric Cancer Cells. *Chin J Biochem Mol Biol* 2001;17: 430-435
- 40 Uemura H, Chang C. Antisense TR3 orphan receptor can increase prostate cancer cell viability with etoposide. *Treatment Endocrinol* 1997;139:2329-2334
- 41 Liu S, Wu Q, Chen ZM, Su WJ. The effect pathway of retinoic acid is through regulation of retinoic acid receptor α in gastric cancer cells. *World J Gastroenterol* 2001;7:662-666
- 42 Xu AG, Li SG, Liu JH, Gan AH. The function of apoptosis and protein expression of bcl-2, p53 and C-myc in the development of gastric cancer. *World J Gastroenterol* 2000; 6(Suppl 3):27
- 43 Wang XW, Xie H. Presence of Fas and Bcl-s proteins in BEL-7404 human hepatoma cells. *World J Gastroenterol* 1998; 4:540-543
- 44 Woronicz JD, Lina A, Calnan BJ, Szychowski S, Cheng L, Winoto A. Regulation of the Nur77 orphan steroid receptor in activation-induced apoptosis. *Mol Cell Biol* 1995;15:6364-6376
- 45 Lin W, Youn HD, Liu J. Thapsigargin-induced apoptosis involves Cabin1-MEF2-mediated induction of Nur77. *Eur J Immunol* 2001;31: 1757-1764
- 46 Steff AM, Trop S, Maira M, Drouin J, Hugo P. Opposite ability of pre-TCR and alpha beta TCR to induce apoptosis. *J Immunol* 2001;166: 5044-5050
- 47 Katagiri Y, Takeda K, Yu ZX, Ferans VJ, Ozato K, Guroff G. Modulation of retinoid signaling through NGF-induced nuclear export of NGFI-B. *Nat Cell Biol* 2000;2:435-440
- 48 Wada A, Fukuda M, Mishima M, Nishida E. Nuclear export of actin novel mechanism regulating the subcellular localization of a major cytoskeletal protein. *EMBO J* 1998;17:1635-1641
- 49 Sachdev S, Hannink M. Loss of Ik(a-mediated control over nuclear import and DNA binding enables oncogenic activation of c-Rel. *Mol Cell Biol* 1998;18:5445-5456
- 50 Kudo N, Taoka H, Toda T, Yoshida M, Horinouchi S. A novel nuclear export signal sensitive to oxidative stress in the fission yeast transcription factor Pap 1. *J Biol Chem* 1999; 274:15151-15158
- 51 Huang TT, Kudo N, Yoshida M, Miyamoto S. A nuclear export signal in the N-terminal regulatory domain of Ik α controls cytoplasmic localization of inactive NF- κ B/IkBa complexes. *Proc Natl Acad Sci USA* 2000;97:1014-1019
- 52 Fukuda M, Gotoh Y, Nishida E. Interaction of MAP kinase with MAP kinase kinase: its possible role in control of nucleocytoplasmic transport of MAP kinase. *EMBO J* 1997;16:1901-1908
- 53 Engel K, Kotlyarov A, Gaestel M. Leptomycin B-sensitive nuclear export of MAPKAP kinase 2 is regulated by phosphorylation. *EMBO J* 1998;17:3363-3371
- 54 Taagepera S, McDonald D, Loeb JE, Whitaker LL, McElroy AK, Wang JYJ, Hope TJ. Nuclear-cytoplasmic shuttling of C-ABL tyrosine kinase. *Proc Natl Acad Sci USA* 1999; 95:7457-7562
- 55 Fernandez PM, Brunel F, Jimenez MA, Saez JM, Cereghini S, Zakin MM. Nuclear receptors Nor1 and NGFI-B/Nur77 play similar, albeit distinct, roles in the hypothalamo-pituitary-adrenal axis. *Endocrinology* 2000;141:2392-2400
- 56 Pekarsky Y, Hallas C, Palamarchuk A, Koval A, Bullrich F, Hirata Y, Bichi R, Letofsky J, Croce CM. AKT phosphorylates and regulates the orphan nuclear receptor Nur77. *Proc Natl Acad Sci USA* 2001;98:3690-3694
- 57 Kang HJ, Song MJ, Choung SY, Kim SJ, Lee MO. Transcriptional induction of Nur77 by indomethacin that results in apoptosis of colon cancer cells. *Biol Pharm Bull* 2000; 23:815-819
- 58 Meng AH, Ling YL, Zhang XP, Zhao XY, Zhang JL. CCCK-8 inhibits expression of TNF-alpha in the spleen of endotoxic shock rats and signal transduction mechanism of p38 MAPK. *World J Gastroenterol* 2002; 8:139-143
- 59 Dai J, Yu SX, Qi XL, Bo AH, Xu YL, Guo ZY. Expression of bcl-2 and c-myc protein in gastric carcinoma and precancerous lesions. *World J Gastroenterol* 1998; 4 (Suppl 2): 84-85
- 60 Liu HF, Liu WW, Fang DC, Men RP. Expression of bcl-2 protein in gastric carcinoma and its significance. *World J Gastroenterol* 1998; 4: 228-230

Edited by Zhang JZ

• GASTRIC CANCER •

Effect of preoperative regional artery chemotherapy on proliferation and apoptosis of gastric carcinoma cells

Hou-Quan Tao, Shou-Chun Zou

Hou-Quan Tao, Shou-Chun Zou, Department of Surgery, Zhejiang Provincial People's Hospital, Hangzhou 310014, Zhejiang Province, China
Correspondence to: Dr. Hou-quan Tao, Department of Surgery, Zhejiang Provincial People's Hospital, Hangzhou 310014, Zhejiang Province, China. houquantao@yahoo.com

Telephone: +86-571-85236842 Fax: +86-571-85131448

Received 2001-12-20 Accepted 2002-02-23

Abstract

AIM: To study the effects of preoperative regional artery chemotherapy (PRACT) in inducing growth inhibition and apoptosis of gastric carcinoma (GC) cells.

METHODS: TUNEL (terminal-deoxynucleotidyl-transferase TdT-mediated dUTP-fluorescein and labeling) method and immunohistochemical techniques were used to detect the state of apoptosis and proliferation of GC cells in histopathologic sections. A total of 110 cases of GC and 68 cases of metastatic lymph node with or without PRACT were adopted. Correlations between apoptosis index (AI), proliferation index (PI) and PRACT and prognosis were analysed.

RESULTS: The apoptosis index (AI) was significantly higher in the PRACT group ($12.5\% \pm 4.33\%$) than in the untreated group ($7.1\% \pm 3.43\%$, $P < 0.001$), whereas the proliferation index (PI) in the PRACT group ($33.8\% \pm 8.8\%$) was significantly lower than that in untreated group ($43.6\% \pm 12.8\%$, $P < 0.01$). Both AI and PI were correlated to the differentiation degree of GC in PRACT group, the AI in the differentiated group was higher than that in undifferentiated group ($P < 0.001$), but the PI was lower in the differentiated group than that of the undifferentiated group ($P < 0.01$). The AI of GC cells in metastatic lymph node was also significantly higher in the PRACT group ($7.9\% \pm 3.41\%$) than in the untreated group ($3.6\% \pm 2.93\%$, $P < 0.01$), though the PI of GC cells in metastatic lymph nodes in the PRACT group ($17.2\% \pm 6.8\%$) was significantly lower than that in the untreated group ($26.7\% \pm 9.3\%$, $P < 0.01$). The severity of histopathologic changes was significantly higher in the PRACT group than in the untreated group ($P < 0.05$). In addition, postoperative surveys demonstrated that the 5-year survival rate of GC patients in the PRACT group was significantly higher than that of patients in the untreated group ($P < 0.01$).

CONCLUSION: Preoperative regional artery chemotherapy (PRACT) showed inhibitory action on the growth of GC cells mainly through inhibiting proliferation and inducing the apoptosis of tumor cells. PRACT can improve the prognosis of GC patients also.

Tao HQ, Zou SC. Effect of preoperative regional artery chemotherapy on proliferation and apoptosis of gastric carcinoma cells. *World J Gastroenterol* 2002;8(3):451-454

INTRODUCTION

Human gastric carcinogenesis is a multistep and multifactorial process^[1-8]. In this process, the state of apoptosis and proliferation of gastric epithelium will change^[9,10]. The loss of balance between cell proliferation and apoptosis may result in tumor development and progression^[11-16]. Cell necrosis and apoptosis are two fundamental processes of tumor cell death. Apoptosis is the biological process of tumor cell death regulated by genes^[17-28]. Many (and perhaps all) agents of cancer chemotherapy effect tumor cell killing *in vitro* and *in vivo* through inducing the mechanisms of apoptosis. Many chemotherapy-induced side-effects and mass shrinkage may result from the increase of tumor cell apoptosis and the inhibition of tumor cell proliferation^[17, 29-34].

To clarify the relationship between the effects of preoperative regional artery chemotherapy (PRACT) on inhibition and killing of GC cells with apoptosis, methods of terminal-deoxynucleotidyl-transferase (TdT)-mediated dUTP-fluorescein and labeling (TUNEL) and immunohistochemical techniques were used to detect the apoptosis and proliferation of GC cells in 110 cases of GC with or without PRACT. Histopathologic changes and prognosis were also observed and compared between the two groups.

MATERIALS AND METHODS

Clinical data

110 patients with GC who underwent curative resections at Zhejiang Provincial Peoples' Hospital from Dec. 1988 to July 1996 were studied, including 68 cases with PRACT and 42 cases without PRACT. No significant difference was found in the age, sex, and TNM staging between the two groups. The surgical specimens were fixed in 10% formaldehyde solution, and paraffin embedded tissue blocks were cut into 6 μ m sections and mounted on glass slides. All patients had been followed up at least 5 years after operation.

Scheme of preoperative chemotherapy

Celiac arteriography was performed by precutaneous transfemoral-artery catheters according to Seldinger's method and superselective catheterization proceeded to the supplying artery of focus of lesion. Antineoplastic agents of FAP(5-FU 1.0g/m², MMC 10mg/m², CDDP 80mg/m²) or FMP(5-FU 1.0g/m², ADR 20mg/m², CDDP 80mg/m²) scheme was infused into regional artery by a single administration and thereafter surgical operation was performed in 10-14 days.

Main reagents

Terminal-deoxynucleotidyl-transferase(TdT)-mediated dUTP-fluorescein and labeling(TUNEL) kits were purchased from Boehringer Inc. and stored in -20°C for use. SP kits and PCNA monoclonal antibody were produced by Maixin Inc.(Fujian).

Histochemical detection of apoptosis

Tumor cell apoptosis was identified by the TUNEL method^[35,36]. Briefly, deparaffinized and rehydrated sections were treated with proteinase K (20mg/L in 10mmol/L Tris, pH 8.0) for 20min at room temperature and washed with 1 \times TBS (20mmol/L Tris, pH 7.6,

140mmol/L NaCl). After, endogenous peroxidase was inactivated by using 30ml/L hydrogen for 5min and washing with 1×TBS. Equilibration buffer was added to each section and samples were incubated at room temperature for 20min. Terminal deoxynucleotidyl transferase (TdT) enzyme in TdT labeling reaction mixture at 1:20 dilution was piped onto the sections, followed by 2h incubation at 37°C. After terminating the reaction by immersing sections into stop solution and washing with blocking buffer for 10min at room temperature, the anti-digoxigenin-peroxidase was added to the sections. NBT/BCIP solution was used for color development. Sections were counterstained by fast red. A positive control was generated by covering a specimen with DNase I(1mg/L) as the first step of the procedure. Specific positive tissue sections were used for negative controls by substituting distilled water for the TdT in the reaction mixture. Positively stained tumor cells were identified as nuclei that were blue-brown in color, and were counted in ten randomly selected fields under high power of microscope to determine the rate of apoptosis cell among all tumor cells. Apoptotic index (AI)=(the number of apoptosis cells/total number of tumor cells)×1000%.

Immunohistochemical staining for PCNA

SP immunohistochemical staining techniques were used. The primary antibody was PCNA monoclonal antibody (diluted 1:50). Before staining, the sections were microwave heated in 0.05mol·L⁻¹ citric acid solution for antigen retrieval. PBS was substituted for primary antibodies as negative control. PCNA-positive cells (proliferative cells) were observed. The proliferative index (PI) was obtained by calculating the percentage of positively stained cells evaluated for each tissue section after counting 1000 cells at ten high power fields randomly.

Comparison of pathologic histology change

In H&E staining sections, tumor cell necrosis and degeneration, endothelium change, and the degree of fibrosis were observed and compared between the PRACT group and untreated group. The degree of histopathologic change was divided into four grades from 0 to III.

Statistical analysis

Data were expressed as $\bar{x} \pm s$, and the t test or Wilcoxin test were used for statistical analysis. Survival rate was calculated by using Kaplan-Meier method and analyzed by the log-rank test. The level of significance was $P < 0.05$.

RESULTS

Comparison of tumor cell proliferation and apoptosis between PRACT and untreated groups

The main morphological characteristics of apoptosis cell consist of cell shrinkage, cytoplasmic condensation, nuclear pyknosis, cytomembrane blebbing or fragmentation, and formation of apoptotic bodies. More apoptosis and less proliferation were detected in the patients in the PRACT group. The apoptosis index (AI) of the PRACT group and untreated group was (12.5%±4.33%) and (7.1%±3.43%), respectively. The t test showed that the AI of the PRACT group was significantly higher than that of the untreated group ($P < 0.001$), whereas the proliferation index (PI) in the PRACT group (33.8%±8.8%) was significantly lower than that in untreated group (43.6%±12.8%, $P < 0.01$).

Relationship between tumor cell proliferation, apoptosis and the tumor differentiation degree in PRACT group

The pathologic diagnosis and grading of GC was determined according to the Histopathologic Standard of the Chinese National Gastric Cancer Association. GC was divided mainly into two histologic subtypes: a

differentiated type which consists of papillary and tubular adenocarcinomas, and an undifferentiated type which consists of poorly differentiated adenocarcinomas, signet ring-cell carcinomas and mucinous adenocarcinomas. Among the 68 patients with PRACT, AI of 32 tumors of the differentiated type was (14.8%±4.99%), while that of undifferentiated type tumor was only (6.6%±3.31%), AI was significantly different between the two groups ($P < 0.001$). However, the PI of 32 tumors of the differentiated type (29.6%±7.4%) was lower than that in the undifferentiated group (38.5%±11.2%, $P < 0.01$).

Effect of PRACT on proliferation and apoptosis of metastatic lymph node GC cells

Among the 62 cases with lymph node metastasis, AI of metastatic lymph node GC cells in 34 cases with PRACT was (7.9%±3.41%), and that of 28 cases without PRACT was (7.9%±2.93%). The t test indicated that there was a significant difference between two groups ($P < 0.01$). On the contrary, the PI in the metastatic lymph node GC cells in 34 cases with PRACT (17.2%±6.8%) was significantly lower than that of 28 untreated cases (26.7%±9.3%, $P < 0.01$).

Comparison of histopathologic changes between PRACT and untreated groups (Table 1)

The data are shown in Table 1. No change was marked as grade 0, I to III grade was defined change. The Wilcoxin test showed a significance difference between the two groups.

Table 1 Comparison of histopathologic changes between the PRACT group and the untreated group

Histopathologic grade	PRACT group (n=68)	Untreated group (n=42)
0	26	26 ^a
I	22	12
II	16	4
III	4	0

^a $P < 0.05$, vs I+II+III

Effect of PRACT on the survival rate of GC patients

All patients underwent curative resection and had been followed up for at least 5 years, 49 died of tumor recurrence. A postoperative survey demonstrated that the 5-year survival rate of patients with PRACT (63.2%, 43/68) was significantly higher than that of patients without PRACT (42.8%, 18/42, $P < 0.01$).

DISCUSSION

PRACT can effectively inhibit or kill cancer cells by a single administration of high concentration antineoplastic agent into the main supplying artery of the cancer focus. It can not only limit and reduced the tumor mass and improve the curative rate, but it can also act on the peri-operative area by means of drug infiltration to kill subclinical tumor foci which may exist before the operation as well as the invisible micrometastatic foci so as to increase the opportunity of curative resection^[33,37]. Many *in vitro* and *in vivo* experiments indicated that the induction of apoptosis and inhibition of proliferation are the main mechanisms of eliminating tumor cells by most chemotherapeutic agents^[17,29-34,38]. To explore the effect of PRACT on human GC cell apoptosis, TUNEL, a combined molecular biological and morphological technique, was used to investigate and compare the number of apoptotic cells in GC tissue sections as well as that in metastatic lymph node sections of the PRACT and untreated groups. This method, using an *in situ* staining technique, demonstrates not only the distribution pattern of apoptotic cells, but also the

sensitivity of the technique: it can detect very small amount of apoptotic cells, so it is widely used in cell apoptosis studies^[35,36]. Moreover, PCNA expression was detected by using an immunohistochemical technique in order to count the proliferation index.

Cell apoptosis is different from cell necrosis; the latter is a pathological form of extensive cell death under strong cell damage and it is not under gene regulation, while cell apoptosis is a normal physiological phenomenon for the active elimination of surplus cells or defective cells under strict genetic control^[29]. It plays an important role in regulating total cell amount and also in malignant disease. After gene mutation and formation of malignancy, the rate of cell apoptosis lowers significantly. It is this depletion of cell apoptosis contributing to the expansion of tumor mass; hence it is possible to treat the cancer by means of increasing the proportion of tumor cell apoptosis. Recent studies have shown that 5-Fu, MMC, CDDP, ADR and many other chemotherapeutic drugs treat cancer by inhibiting proliferation and inducing apoptosis^[29-34,39-41]. So induction of tumor cell apoptosis has already been used as an important indicator to detect the ability of chemotherapeutic drugs to inhibit tumor growth. FMC or FAP schemes composed of the aforementioned drugs are now frequently used for pre-operative chemotherapy of GC.

Our results demonstrate that: (1) The apoptosis index of GC cells in the PRACT group is significantly higher than that of the untreated group, and PI of GC cells in the PRACT group is significantly lower than that of the untreated group, indicating that PRACT has an obvious inhibition effect on GC cells. We also found that no significant necrosis was found in the rich blood supply area around the blood vessels, but instead much apoptosis was observed there, indicating that induction of apoptosis by PRACT is the main mechanism of inhibition of tumor growth. (2) Apoptosis rate is correlated with tumor differentiation degree in the PRACT group. AI of differentiated type of GC is significantly higher than that of undifferentiated type, but PI of differentiated type of GC is significantly lower than that of undifferentiated type. This may be due to the better blood supply of the differentiated type of GC^[42], allowing more chemotherapeutic drugs to be delivered to the tumor tissue to increase the induction of tumor cell apoptosis so it is more sensitive to chemotherapy. (3) AI of GC cells in metastatic lymph nodes is significantly higher in the PRACT group than that of the untreated group, and PI of GC cells in metastatic lymph nodes is significantly lower in the PRACT group than that of the untreated group, suggesting that PRACT is able to inhibit proliferation and induce apoptosis of metastatic tumor cells. This is very interesting, because lymph node metastasis and recurrence of GC are main factors influencing the overall postoperative survival rate. If the apoptotic cell proportion in metastatic lymph nodes can be increased by effective measures, the prognosis of postoperative GC patients can be improved. Our results suggest that PRACT may approach this goal. (4) With respect to the histopathologic change of GC, including cancer cell reactions, endothelium changes, and the degree of fibrosis, the degree of severity is higher in PRACT group than that in untreated group, suggesting that PRACT can lead to more structural changes of GC tissue so as to enhance the killing effect of cancer cells by chemotherapy drugs. (5) With regard to prognosis, we have showed that PRACT can increase the relapse-free survival rate of GC patients^[37]. In fact, altering the balance between apoptosis and proliferation may contribute to improving the prognosis of cancer^[43-49]. The results of this paper indicate that PRACT can induce apoptosis and inhibit proliferation of GC cells. So we suggest that PRACT is a useful therapeutic scheme for GC.

In conclusion, this study of detecting the proliferation and apoptosis of GC with or without PRACT showed significant inhibition of GC cell growth by PRACT, with its mechanism mainly through

inducing tumor cell apoptosis. PRACT can increase the survival rate of GC patients after operation.

REFERENCES

- 1 Ma JL, Liu WD, Zhang ZZ, Zhang L, You WC, Chang YS. Relationship between gastric cancer and precancerous lesions. *Huaren Xiaohua Zazhi* 1998;6:222-223
- 2 Liu WZ, Zheng X, Shi Y, Dong QJ, Xiao SD. Effect of *Helicobacter pylori* infection on gastric epithelial proliferation in progression from normal mucosa to gastric carcinoma. *World J Gastroenterol* 1998;4:246-248
- 3 Badov D, Lambert JR, Finlay M, Balazs ND. *Helicobacter pylori* as a pathogenic factor in Menetrier's disease. *Am J Gastroenterol* 1998;93:1976-1979
- 4 Tucci A, Poli L, Tosetti C, Biasco G, Grigioni W, Varoli O, Mazzoni C, Paparo GF, Stanghellini V, Caletti G. Reversal of fundic atrophy after eradication of *Helicobacter pylori*. *Am J Gastroenterol* 1998;93:1425-1431
- 5 Pan CJ, Zhong P, Huang XR, Liu KY, Wang SX. Study on the correlation between proliferation and apoptosis in atrophy and intestinal metaplasia of gastric mucosa. *Shijie Huaren Xiaohua Zazhi* 2000;8:143-146
- 6 Xia HX, Zhang GS. Apoptosis and proliferation in gastric cancer caused by *Hp* infection. *Shijie Huaren Xiaohua Zazhi* 1999;7:740-742
- 7 Lu W, Chen LY, Gong HS. PCNA and c-erbB-2 expression in gastric mucosal intestinal metaplasia with *Helicobacter pylori* infection. *Shijie Huaren Xiaohua Zazhi* 1999;7:111-113
- 8 Ishida M, Gomyo Y, Tatebe S, Ohfuji S, Ito H. Apoptosis in human gastric mucosa, chronic gastritis, dysplasia, and carcinoma: analysis by terminal deoxynucleotidyl transferase-mediated dUTP-biotin nick end labeling. *Virchows Arch* 1996;428:229-235
- 9 Wang YK, Ji XL, Ma NX. Expressions of p53 bcl-2 and c-erbB-2 proteins in precarcinomatous gastric mucosa. *Shijie Huaren Xiaohua Zazhi* 1999;7:114-116
- 10 Tu SP, Jiang SH, Tan JH, Jiang XH, Qiao MM, Zhang YP, Wu YL, Wu YX. Proliferation inhibition and apoptosis induced by arsenic trioxide on gastric cancer cell SGC-7901. *Shijie Huaren Xiaohua Zazhi* 1999;7:18-21
- 11 Anti M, Armuzzi A, Gasbarrini A, Gasbarrini G. Importance of changes in epithelial cell turnover during *Helicobacter pylori* infection in gastric carcinogenesis. *Gut* 1998;43:S27-S32
- 12 Akira K, Yoshihiko M, Tadashi K, Yoshihiro K, Keizo S. The biologic features of intramucosal gastric carcinoma with lymph node metastasis. *Surgery* 2002;131:S71-77
- 13 Martin SJ, Green DR. Apoptosis and cancer: the failure of controls on cell death and cell survival. *Crit Rev Oncol/Hematol* 1995;18:137-153
- 14 Guo YQ, Zhu ZH, Li JF. Flow cytometric analysis of apoptosis and proliferation in gastric cancer and precancerous lesion. *Shijie Huaren Xiaohua Zazhi* 2000;8:983-915
- 15 Shen YF, Zhuang H, Shen JW, Chen SB. Cell apoptosis and neoplasms. *Shijie Huaren Xiaohua Zazhi* 1999;7:267-268
- 16 Hale AJ, Smith CA, Satherland LC, Stomeman VEA, Longthorne VL, Culhane AL. Apoptosis: molecular regulation of cell death. *Eur J Biochem* 1996;236:1-26
- 17 Kimura H, Konishi K, Kaji M, Maeda K, Yabushita K, Tsuji M, Ogino H, Satomura Y, Unoura M, Miwa A. Apoptosis, cell proliferation and expression of oncogenes in gastric carcinomas induced by preoperative administration of 5-fluorouracil. *Oncol Rep* 2000;7:971-976
- 18 Liu HF, Liu WW, Fang DC, Men RP. Expression and significance of proapoptotic gene Bax in gastric carcinoma. *World J Gastroenterol* 1999;5:15-17
- 19 Liu HF, Liu WW, Fang DC, Men RP. Expression of bcl-2 protein in gastric carcinoma and its significance. *World J Gastroenterol* 1998;4:228-230
- 20 Xu AG, Li SG, Liu JH, Gan AH. Function of apoptosis and expression of the proteins Bcl-2, p53 and C-myc in the development of gastric cancer. *World J Gastroenterol* 2001;7:403-406
- 21 Guo CQ, Wang YP, Liu GY, Ma SW, Ding GY, Li JC. Study on *Helicobacter pylori* infection and -p53, c-erbB-2 gene expression in carcinogenesis of gastric mucosa. *Shijie Huaren Xiaohua Zazhi* 1999;7:313-315
- 22 Qin LJ. In situ hybridization of P53 tumor suppressor gene in human gastric precancerous lesions and gastric cancer. *Shijie Huaren Xiaohua Zazhi* 1999;7:494-497
- 23 Zhang ZW, Farthing MJG. Molecular mechanisms of *H. pylori* associated gastric carcinogenesis. *World J Gastroenterol* 1999;5:369-374
- 24 Mao LZ, Wang SX, Ji WF, Ren JP, Du HZ, He RZ. Comparative studies on p53 and PCNA expressions in gastric carcinoma between young and aged patients. *Huaren Xiaohua Zazhi* 1998;6:397-399
- 25 Wang XH, Zhang WD, Zhang YL, Zheng JZ, Sun Y. Relationship between

- Hp* infection and oncogene and tumor suppressor gene expressions in gastric cancer and precancerosis. *Huaren Xiaohua Zazhi* 1998;6:516-518
- 26 Sun YX, Chen CJ, Zhou HG, Shi YQ, Pan BR, Feng WY. Expression of c-myc and p53 in colorectal adenoma and adenocarcinoma. *Huaren Xiaohua Zazhi* 1998;6:1054-1056
- 27 Xu QW, Li YS, Zhu HG. Relationship between expression P53 protein, PCNA and CEA in colorectal cancer and lymph node metastasis. *World J Gastroenterol* 1998;4:218
- 28 Lin GY, Chen ZL, Lu CM, Li Y, Ping XJ, Huang R. Immunohistochemical study on p53, H-rasp21, c-erbB-2 protein and PCNA expression in HCC tissues of Han and minority ethnic patients. *World J Gastroenterol* 2000;6:234-238
- 29 Yusuf AH. Apoptosis and the dilemma of cancer chemotherapy. *Blood* 1997;89:1845-1853
- 30 Zain J, Huang YQ, Feng X, nierodzik ML, Li JJ, Karparkin S. Concentration-dependent dual effect of thrombin on impaired growth/apoptosis or mitogenesis in tumor cells. *Blood* 2000;95:3133-3138
- 31 Kelly JD, Williamson KE, Weir HP, McManus DT, Hamilton PW, Keane PF, Johnston SR. Induction of apoptosis by mitomycin-C in an ex vivo model of bladder cancer. *Bju Int* 2000;85:911-917
- 32 Shah SA, Potter MW, McDade TP, Ricciardi R, Perugini RA, Elliott PT, Adams J, Callery MP. 26S proteasome inhibition induces apoptosis and limits growth of human pancreatic cancer. *J Cell Biochem* 2001;82:110-122
- 33 Huang j, He X, Lin X, Zhang C, Li J. Effect of preoperative transcatheter arterial chemoembolization on tumor cell activity in hepatocellular carcinoma. *Zhonghua Yixue Zazhi* 2000;113:446-448
- 34 Wu YL, Sun B, Zhang XJ, Wang SN, He HY, Qiao MM, Zhong J, Xu JY. Growth inhibition and apoptosis induction of Sulindac on Human gastric cancer cells. *World J Gastroenterol* 2001;7:796-800
- 35 Wijsmal JH, Jonker RR, Keijzer R, van de Velde CJ, Cornelisse CJ. A new method to detect apoptosis in paraffin sections in situ end labeling of fragmented DNA. *J Histochem Cytochem* 1993;41:7-12
- 36 Kiyozuka Y, Akamatsu T, Singh Y, Ichiyoshi H, Senzaki H, Tsubura A. Optimal prefiration of cells to demonstrate apoptosis by the TUNEL method. *Acta Cytol* 1999;43:393-399
- 37 Zou SC, Qiu HS, Zhang CW, Tao HQ. A clinical and long-term follow-up study of perioperative sequential triple therapy for gastric cancer. *World J Gastroenterol* 2000;6:284-286
- 38 Hickman JA. Apoptosis induced by anticancer drugs. *Cancer metasis Rev* 1992;11:121-139
- 39 Dive C, Hickman JA. Drug-target interactive: only first step in the comitment to a programmed cell death? *Br J Cancer* 1991;64:192-196
- 40 Inada T, Ichikawa A, Igarashi S, Kubota T, Ogata Y. Effect of preoperative 5-fluorouracial on apoptosis of advanced gastric cancer. *J Surg Oncol* 1997;65:106-110
- 41 Inada T, Ichikawa A, Kubota T, Ogata Y, Moossa AR, Hoffman RM. 5-Fu-induced apoptosis correlates with efficacy against human gastric and colon cancer xenografts in nude mice. *Anticancer Res* 1997;17:1965-1971
- 42 Tao HQ, Lin YZ, Wang RN. Significance of microvessel count and vascular endotjelial growth factor expression in intestinal-type gastric carcinoma. *Zhongguo Zhongliu Linchuang* 1998;25:786-789
- 43 Shen XB, Zhao XM, Hu JG, Jin XP, Wang J. Significance of cell apoptosis and proliferation in gastric cancer. *Shejie Huaren Xiaohua Zazhi* 2000;8:1050-1052
- 44 Zhang M, Cai S, Shi D. Prognostic value of cell proliferation and apoptosis in uterine cervical cancer treated with radiation. *Zhonghua Zhongliu Zazhi* 1999;21:290-292
- 45 Xie X, Clausen OPF, De Angelis P, Boysen M. Bax expression has prognostic significance that is enhanced when combined with AgNOR counts in glottic carcinoma. *Br J Cancer* 1998;78:100-105
- 46 Rieger L, Weller M, Bornemann A, Schabet M, Dichgans J, Meyermann R. Bcl-2 family protein expression in human malignant glioma: a clinical-pathological correlative study. *J Neurol Sci* 1998;155:68-75
- 47 Re GG, Hazen-Martin DJ, EL-Bahtimi R, Brownlee NA, Willingham MC, Garvin AJ. Prognostic significance of Bcl-2 in Wilm's tumors and oncogenic protential of Bcl-Xl in rare tumor cases. *Int J Cancer* 1999;84:192-200
- 48 Ghanem MA, van der Kwast TH, Den Hollander JC, Sudaryo MK, Van den Heuvel MM, Noordzij MA, Nijman RJM, Soliman EH, van Steenbrugge GJ. The prognostic significance of apoptosis-associated protein Bcl-2, BAX, and Bcl-X in clinical nephroblastoma. *Br J Cancer* 2001;85:1557-1563
- 49 Apolinario RM, van der Valk P, de Jong JS, Deville W, van Art-Otte J, Dingemans AM, van Mourik JC, Postmus PE, Pinedo HM, Giaccone G. Prognostic value of the expression of p53, bcl-2, and bax oncoproteins, and neovascularization in patient with radically resected non-small-cell lung cancer. *J Clin Oncol* 1997;15:2456-2466

Edited by Pagliarini R

• GASTRIC CANCER •

Effects of epidermal growth factor on the growth of human gastric cancer cell and the implanted tumor of nude mice

Lu Xia, Yao-Zong Yuan, Chun-Di Xu, Yong-Pin Zhang, Ming-Ming Qiao, Jia-Xu Xu

Lu Xia, Yao-Zong Yuan, Chun-Di Xu, Yong-Pin Zhang, Ming-Ming Qiao, Jia-Xu Xu, Department of Gastroenterology, Ruijin Hospital, Shanghai Second Medical University, Shanghai 200025, China
Correspondence to: Dr. Lu Xia, Department of Gastroenterology, Ruijin Hospital, Shanghai Second Medical University, Shanghai 200025, China. xialu@126.com
Telephone: +86-21-64370045-665242 Fax: +86-21-64150773
Received 2001-09-26 Accepted 2001-10-29

Abstract

AIM: Epidermal growth factor (EGF) plays an important role in the regulation of gastrointestinal tissue growth and development, and it can stimulate epithelial proliferation, cell differentiation and growth. It has been established that the EGF can promote gastric cytoprotection and ulcer healing. But the potential ability of EGF to regulate the gastric cancer growth is unknown. This study is to investigate the influence of EGF on human gastric cancer cell and the implanted tumor growth of nude mice.

METHODS: The cell growth rates of human gastric adenocarcinoma cell lines MKN-28, MKN-45, SGC-7901 and normal human gastric epithelial cells 3T3 were assessed when incubated with recombinant human EGF (rhEGF, 0.05, 0.1, 0.5, 1.0, 10, 50, 100mg.L⁻¹) using MTT method. The cells of MKN-28, MKN-45, SGC-7901 (gastric cancer tissue 1.5mm³) were implanted in the BALB/cA nude mice for 10 days. The EGF was given intraperitoneally (15, 30, 60μg.kg⁻¹) for 3 weeks. The body weights of the tumor-bearing animals and their tumor mass were measured afterwards to assess the mitogenic effect of rhEGF in the nude mice.

RESULTS: Within the concentration range of 0.05-100mg.L⁻¹, rhEGF could increase the cell growth of normal 3T3 cells (cell growth rate 100% vs 102.8%, $P < 0.05$), but partially restrain the gastric cancer cell growth. The latter effect was related to cell differentiation. In 15-60μg/kg rhEGF groups, the mean implanted tumor mass of MKN-28 cell were 1.75g, 1.91g, 2.08g/NS group 1.97g ($P > 0.05$), the mean tumor mass of SGC-7901 cell were 1.53g, 1.07g, 1.20g/NS group 1.07g ($P > 0.05$), and for MKN-45 cell, the tumor mass were respectively 1.92g, 1.29g, 1.77g/NS group 1.82g ($P > 0.05$). So rhEGF had no obvious effect on implanted MKN-28, SGC-7901 and MKN-45 tumor growth.

CONCLUSION: EGF has no stimulating effect on the human gastric cancer cell growth neither *in vitro* nor *in vivo*.

Xia L, Yuan YZ, Xu CD, Zhang YP, Qiao MM, Xu JX. Effects of epidermal growth factor on the growth of human gastric cancer cell and the implanted tumor of nude mice. World J Gastroenterol 2002;8(3):455-458

INTRODUCTION

Growth factors are found in a variety of adult and embryonic tissues. They are important regulators of cell differentiation and proliferation,

and play an important role in maintaining the integrity of the epithelium. They have also been implicated in malignancy. Epidermal growth factor (EGF), a single-chain polypeptide of 53 amino acid residues, is found mainly in the submandibular glands and Brunner's gland of the gastrointestinal tract. It can be combined with the specific receptor (EGF-R) of the target cell membrane^[1]. Some studies suggested that the expression of EGF-R was increased in gastric cancer tissue. It was also reported that EGF can increase the mitosis *in vitro*^[2]. Patients with EGF receptor-positive gastric cancer may have a poorer prognosis than those with EGF receptor-negative cancers. So, EGF has the function to influence the tumor cell growth. At present, the effect of EGF in this process has been unclear yet.

In this report, we seek to determine the effect of EGF on the growth of human gastric cancer cell (MKN-28, SGC-7901 and MKN-45) *in vitro*. In nude mice which underwent surgical implantation of the same gastric cancer cells, EGF was injected intraperitoneally to investigate the influence of EGF on tumor cell growth, so as to confirm the safety of EGF in the treatment of peptic ulcer^[3-14].

MATERIALS AND METHODS

Materials

Gastric cancer cell lines, MKN-28, SGC-7901 and MKN-45, are well-differentiated, moderate-differentiated and low-differentiated human adenocarcinoma cell lines respectively. 3T3 cell is normal human gastric epithelium. They are all established and characterized in our laboratory. rhEGF was obtained from Institute of Biochemistry and Cell Biology, Shanghai Institute for Biological Science, Chinese Academy of Science (100μg/amp). 3-(4,5-dimethylthiazol-2-yl) and 5-diphenyltetrazolium bromide were the product of Fluka Chemie AG. Balb/cA nude mice: were obtained from Institute of Pharmaceutics, Shanghai Institute for Biological Science, Chinese Academy of Science. 35-40 day old, 18-20g, female. Mitomycin C (MMC) was the product of Kyowa Hakko, Japan, 2mg/Amp.

Methods

Cell cultures Human gastric cancer cells were propagated as adherent monolayers and removed from culture surfaces by treatment with trypsin, then seeded in microwells at 1×10^8 .L⁻¹ in complete medium composed of RPMI 1640 and 200mL.L⁻¹ fetal bovine serum (FBS). The cells were grown in 96-well microplates of RPMI1640 tissue culture medium supplemented with 200mL.L⁻¹ FBS at 37°C in a humidified atmosphere of 50mL.L⁻¹ CO₂ in air. After 24h incubation, the cells were then added by rhEGF at the concentration of 0.05, 0.1, 0.5, 1.0, 10, 50, 100mg.L⁻¹ for further incubation of 72 hours. Uninoculated RPMI 1640 medium was used as a control under otherwise identical experimental procedures. At the end of cell incubation, cell numbers and their viability were determined by MTT method. Add MTT(1g.L⁻¹) in each microwell for 4h in 37°C air. After centrifugation, 100μL dimethyl sulfoxide (DMSO) was added into each well for 30 minutes. Absorption rate of treated and control cells was measured at 570nm (A value) for quantitative measurement of cell growth. Each test kit contained a positive control and an additional

positive control. Experimental controls were treated with DMSO only.

Tumor implantation into nude mice Gastric cancer tissue (1.5mm³) were implanted s.c. in the right dorsal area of 4-6wk old male nude mice. Animals were fed with an autoclaved diet and tap water (acidified to pH 2.5). After 10d, the animals were assigned into the rhEGF treatment groups (15,30,60µg.kg⁻¹, intraperitoneally, 5 times per week for 3wk), negative control group (saline, 2mL intraperitoneum) and positive control group(MMC, 2mg.kg⁻¹, twice every week, 6 times altogether). The body mass of Balb/cA tumor-bearing animals and their tumor weights were measured using anesthesia with ether.

Inhibitory rate (IR) of tumor growth = m(tumor)_c- m(tumor)_T/m(tumor)_c
(m(tumor)_c: mean tumor weight of negetive control group; m(tumor)_T: mean tumor weight of rhEGF treatment group).

Statistical analysis

Student's *t* test was performed to assess potentially significant differences between individual groups of observations. The test statistics were then compared with values obtained from standard two-tailed tables. A *P* value of <5% was accepted as indicating probable significance when comparing the various groups.

RESULTS

Mitogenic effects of EGF in vitro

We found that EGF had no significant growth-stimulatory effects on gastric cancer cells in a dose-dependent manner (Figure 1). The lowest cell growth rates in MKN-28, S-7901 and MKN-45 cell lines were 81.7%, 80.7% and 86.1% respectively, compared with the control at the 0.05,50,100mg.L⁻¹ of rhEGF. EGF could inhibit the cancer cell growth within the level of 0.05 to 100mg.L⁻¹. But there was no probable significance within the same group. In contrast, for the normal 3T3 cells, EGF could increase the cell growth significantly after the coinubation (*P*=0.0008). We also found that the influence of EGF on the gastric cancer cell growth was dependent on the differentiation of the cell. Under the same concentration, the inhibition was greater in well-differentiated cells.

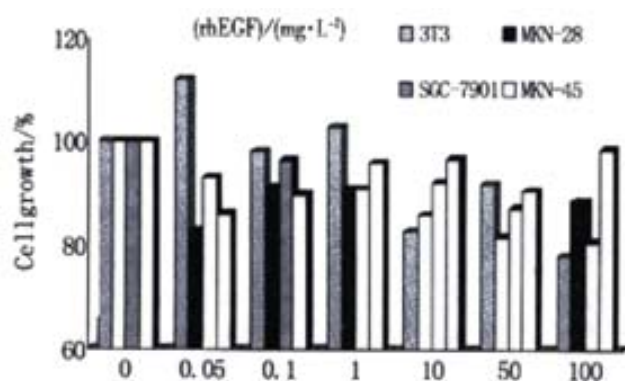


Figure 1 The effect of rhEGF on the growth of gastric cancer

Effect of EGF on the implanted tumor in nude mice

The mean tumor weight of negative control group after the study was 1.97g in MKN-28 nude mice. In MMC treatment group, the tumor weight was 0.47g (*P*<0.05). In rhEGF groups (15,30,60µg.kg⁻¹), the tumor weights were 1.75, 1.91 and 2.08g respectively. The inhibitory rate were -5.3% to 11.1%, compared with negative control group. In rhEGF60µg.kg⁻¹ group, the positive data suggested that the weight was higher than control, but the difference was not

significant. There were no significant difference compared with the negative control group (Table 1). In S-7901 and MKN-45 cell lines, the same results found indicated that intraperitoneal rhEGF treatment could not stimulate the tumor growth in nude mice within the concentration 15-30µg.kg⁻¹ (Table 2,3).

Table 1 The effect of rhEGF i.p. on the growth of MKN-28 tumor in nude mice

Group	Dosage	n	Body mass/g		Tumor mass $\bar{x} \pm s$ /g	Inhibitory rate/%	P value
			Beginning	End			
NS	0.2mL	16	17.6	22.6	1.97±0.94	—	—
MMC	2µg.kg ⁻¹	8	17.8	20.0	0.47±0.61	76.2	<0.05
RhEGF	15µg.kg ⁻¹	8	17.4	22.0	1.75±0.81	11.1	<0.05
RhEGF	30µg.kg ⁻¹	8	17.9	23.8	1.91±0.98	3.0	<0.05
RhEGF	60µg.kg ⁻¹	8	17.9	22.9	2.08±1.56	-5.3	<0.05

P value: compared with the NS group.

Table 2 The effect of rhEGF i.p. on the growth of SGC-7901 tumor in nude mice

Group	Dosage	n	Body mass/g		Tumor mass $\bar{x} \pm s$ /g	Inhibitory rate/%	P value
			Beginning	End			
NS	0.2mL	16	14.4	25.2	1.07±0.60	—	—
MMC	2µg.kg ⁻¹	8	15.2	21.7	0.66±0.29	38.6	<0.05
RhEGF	15µg.kg ⁻¹	8	15.9	25.3	1.53±0.29	-43.8	<0.05
RhEGF	30µg.kg ⁻¹	8	14.1	23.8	1.07±0.63	-0.7	<0.05
RhEGF	60µg.kg ⁻¹	8	13.4	23.9	1.20±0.47	-12.5	<0.05

P value: compared with the NS group.

Table 3 The effect of rhEGF i.p. on the growth of MKN-45 tumor in nude mice

Group	Dosage	n	Body mass/g		Tumor mass $\bar{x} \pm s$ /g	Inhibitory rate/%	P value
			Beginning	End			
NS	0.2mL	20	16.1	19.8	1.82±0.95	—	—
MMC	2µg.kg ⁻¹	10	16.2	19.7	1.07±0.42	41.1	<0.05
RhEGF	15µg.kg ⁻¹	10	16.0	20.3	1.92±1.04	-5.5	<0.05
RhEGF	30µg.kg ⁻¹	10	16.5	19.8	1.29±0.83	8.0	<0.05
RhEGF	60µg.kg ⁻¹	8	16.1	20.4	1.77±1.04	3.1	<0.05

DISCUSSION

We have examined the effect of EGF on the established cell line, MKN-28, SGC-7901 and MKN-45, derived from human gastric adenocarcinoma, both *in vitro* and *in vivo*. The results may be somewhat controversy to those formerly reported, that EGF had no obviously effect on the gastric cancer growth^[15,16]. Growth factors are components of signal transduction pathways that have a considerable spectrum of biological activity, such as control of cell proliferation, differentiation, apoptosis and transformation^[17,18]. Of these growth factors, EGF family are important agents for gastric mucosa. The EGF family include at least seven mammalian polypeptides: EGF, TGF-α, amphiregulin (AR), crypto heregulin, betacellulin and heparin-binding epidermal growth factor (HB-EGF). Except crypto and heregulin, all of these proteins have been shown to bind and activate the 170-kilodalton EGF receptor tyrosine kinase^[19,20]. They share a similar spectrum of biological activities exerted through interaction with EGF-R. EGF-R is a transmembrane glycoprotein, which can stimulate cell proliferation mainly through induction of the proto-oncogenes c-fos and c-myc, and of molecules such as polyamines. The TGF can cause morphological transformation and promote anchorage independent growth *in vitro*. Although there is no evidence of TGF secretion from nonneoplastic adult tissue, it is synthesized during fetal development and produced by many tumor tissues^[21,22]. TGF-α is frequently produced by malignant as well as normal cells and may stimulate their own proliferation. However, less is known about the role of EGF in oncogenesis^[23-25]. The importance of growth factors in the healing and oncogenesis of gastrointestinal diseases has recently received much attention. In inflamed mucosa, EGF is found predominantly in the cytoplasm of the superficial epithelial and isthmus

cells, as in the normal mucosa^[26]. In addition to providing a mitogenic stimulus, EGF may also help the proliferating cells to migrate into the superficial epithelium during the process of "cytoprotective" epithelial repair^[27].

The development of monoclonal and polyclonal antibodies against EGF has allowed studies of the localization of EGF in normal and neoplastic tissues to be performed^[28-31]. Immunocytochemical staining has shown distribution of epidermal growth factor and transforming growth factor α (TGF- α) in the gastrointestinal tract with high levels^[32-35]. Normal epithelial cells secrete such growth factors to regulate cell replacement by autocrine or paracrine mechanisms. It is speculated that these growth factors may regulate the transition rate between G2-phase and mitosis of the cell cycle^[36]. It has reported that HB-EGF is mitogenic for some types of cells, such as fibroblasts, vascular smooth muscle cells, keratinocytes and rat hepatocytes, but not endothelial cells^[37].

The mitogenic action of EGF and TGF- α *in vitro* has been reported in many gastrointestinal tissues, including esophagus, stomach and intestine, and there is little information about the association between the mucosal expression of these peptides and indices of cellular proliferation *in vivo*^[38]. It was reported that EGF immunoreactivity was present in 26-37% of gastric cancers, and the presence of EGF in gastric cancer correlated with the degree of gastric wall invasion, lymph node metastasis and disease progression^[39-42]. Although the epidermal growth factor/receptor system has been found abnormal in intestinal type gastric cancer, overexpression of EGF-R, erbB-2 and erbB-3 receptor genes was mainly found. There has been some controversy in the literature whether EGF-R overexpression related to tumor progression or to early stages of gastric carcinogenesis^[43-46]. The study had shown that overexpression of the EGF-R gene was infrequent in the metaplastic gastric mucosa. A major problem in gastric carcinogenesis is to determine the changing point from benign pre-neoplastic lesions to malignancy. There is a general agreement that this process involves different steps in cellular changes, requiring both activation and inhibition of specific genes, but there is still no evidence to support EGF or EGF-R overexpression to be a reliable marker of increased cancer risk in patients^[47-50]. The present study has sought to clarify their effect on the growth of gastric cancer cell *in vitro* and *in vivo*. In this study, we have found that there was no effect of EGF on the growth of established cell lines, MKN-28, SGC-7901, MKN-45, derived from human gastric adenocarcinoma, both *in vitro* and *in vivo*. Further study is headed to elucidate whether EGF could cause abnormal differentiation of the cells during the treatment of peptic ulcer for a long period.

REFERENCES

- 1 Playford RJ, Wright NA. Why is epidermal growth factor present in the gut lumen. *Gut* 1996;38:303-305
- 2 Maehiro K, Watanabe S, Hirose M, Iwazaki R, Miwa H, Sato N. Effects of epidermal growth factor and insulin on migration and proliferation of primary cultured rabbit gastric epithelial cells. *Gastroenterology* 1997;32:573-578
- 3 Chen BW, Wang HT, Liu ZX, Jie BQ, Ma QJ. Effect of exogenous EGF on proto-oncogene expression in experimental gastric ulcer in rats. *Shijie Huaren Xiaohua Zazhi* 1999;7:504-509
- 4 Fiorucci S, Lanfrancone L, Santucci L, Calabro A, Orsini B, Federici B, Morelli A. Epidermal growth factor modulates pepsinogen secretion in guinea pig gastric chief cells. *Gastroenterology* 1996;111:945-958
- 5 Konturek PC, Brzozowski T, Konturek SJ, Ernst H, Drozdowicz D, Pajdo R, Hahn EG. Expression of epidermal growth factor alpha during ulcer healing. *Scand J Gastroenterol* 1997; 32:6-15
- 6 Konturek PC, Ernst H, Brzozowski T. Expression of epidermal growth factor and transforming growth factor α after exposure of rat gastric mucosa to stress. *Scand J Gastroenterol* 1996;31:209-216
- 7 Hu YT, Zhen CE, Xing GZ, Zhang ML, Zhang JS, Wang DX, Lu YM. Relationship between transforming growth factor alpha, epidermal growth factor and prostaglandin E2 in patients with peptic ulcer. *Shijie Huaren Xiaohua Zazhi* 2002;10:43-47
- 8 Konturek JW, Hengst K, Konturek SJ, Domschke W. Epidermal growth factor in gastric ulcer healing by nocolprost, a stable prostaglandin E2 derivative. *Scand J Gastroenterol* 1997;32:980-984
- 9 Kang JY, Teng CH, Chen FC. Effect of capsaicin and cimetidine on the healing of acetic acid induced gastric ulceration in the rat. *Gut* 1996;38:832-836
- 10 Furukawa O, Okabe S. Cytoprotective effect of epidermal growth factor on acid- and pepsin-induced damage to rat gastric epithelial cells: roles of Na⁺/H⁺ exchangers. *J Gastroenterol Hepatol* 1997;12:353-359
- 11 Arakawa T, Watanabe T, Fukuda T, Higuchi K, Takaishi O, Yamasaki K, Kobayashi K, Tarnawski A. Indomethacin treatment during initial period of acetic acid-induced rat gastric ulcer healing promotes persistent polymorphonuclear cell-infiltration and increases future ulcer recurrence. *Dig Dis Sci* 1996;41:2055-2061
- 12 Qiu BS, Pfeiffer CJ, Wu W, Cho CH. Tungstic acid reduction of cold-resistant stress-induced ulceration in rats. *J Gastroenterol Hepatol* 1997; 12:19-23
- 13 Blandizzi C, Gherardi G, Marveggio C, Lazzeri G, Natale G, Carignani D, Colucci R, Tacca MD. Suramin enhances ethanol-induced injury to gastric mucosa in rats. *Dig Dis Sci* 1997;42:1233-1241
- 14 Miyazaki Y, Hiraoka S, Tsutsui S, Kitamura S, Shinomura Y, Matsuzawa Y. Epidermal growth factor receptor mediates stress induced expression of its ligands in rat gastric epithelial cells. *Gastroenterol* 2001;120:108-116
- 15 Ross JS, McKenna BJ. The HER-2/neu oncogene in tumors of the gastrointestinal tract. *Cancer Invest* 2001;19:554-568
- 16 Wang LD, Wilson EJ, Osburn J, Delvalle J. Epidermal growth factor inhibits carbachol-stimulated canine parietal cell function via protein kinase C. *Gastroenterology* 1996;110:469-477
- 17 Wagner S, Beil W, Westermann J, Logan R, Bock CT, Trautwein C, Bleck JS, Manns MP. Regulation of gastric epithelial cell growth by *Helicobacter pylori*: evidence for a major role of apoptosis. *Gastroenterology* 1997;113:1836-1847
- 18 Messa C, Russo F, Pricci M, Di Leo A. Epidermal growth factor and 17beta-estradiol effects on proliferation of a human gastric cancer cell line (AGS). *Scand J Gastroenterol* 2000;35:753-758
- 19 Granelli P, Fichera G, Zennaro F, Siadi C, Ruberto FD, Fregoni F, Appierto V, Buffa R, Ferrero S, Biunno I. Expression of the epidermal growth factor receptor gene in human intestinal metaplasia: a preliminary report. *Scand J Gastroenterol* 1997;32:485-489
- 20 Naef M, Yokoyama M, Friess H, Buchler MW, Korc M. Co-expression of heparin-binding EGF-like growth factor and related peptides in human gastric carcinoma. *Int J Cancer* 1996;66:315-321
- 21 Chen DL, Wang WZ, Wang JY. Epidermal growth factor prevents gut atrophy and maintains intestinal integrity in rats with acute pancreatitis. *World J Gastroenterol* 2000;6:762-765
- 22 Seno M, Tada H, Kosaka M, Sasada R, Igarashi K, Shing Y, Folkman J, Ueda M, Yamada H. Human beatcellulin, a member of the EGF family dominantly expressed in pancreas and small intestine, is fully active in a monomeric form. *Growth Factors* 1996;13:181-191
- 23 Becker KF, Keller G, Hoefler H. The use of molecular biology in diagnosis and prognosis of gastric cancer. *Surg Oncol* 2000;9:5-11
- 24 Werner M, Becker KF, Keller G, Hofler H. Gastric adenocarcinoma: pathomorphology and molecular pathology. *J Cancer Res Clin Oncol* 2001;127:207-216
- 25 Masaki T, Hatanaka Y, Nishioka M, Tokuda M, Shiratori Y, Reginfo W, Omata M. Activation of epidermal growth factor receptor kinase in gastric carcinoma: a preliminary study. *Am J Gastroenterol* 2000;95:2135-2136
- 26 Sanz-Ortega J, Steinberg SM, Moro E, Saez M, Lopez JA, Sierra E, Sanz-Espenera J, Merino MJ. Comparative study of tumor angiogenesis and immunohistochemistry for p53, c-ErbB2, c-myc and EGFR as prognostic factors in gastric cancer. *Histol Histopathol* 2000;15:455-462
- 27 Ma L, Liu ES, Chow JY, Wang JY, Cho CH. Interactions of EGF and ornithine decarboxylase activity in the regulation of gastric mucus synthesis in cigarette smoke exposed rats. *Zhonghua Binglixue Zazhi* 1999;42:137-143
- 28 Pelaez BM, Ruibal MA, Aza GJ. Gastric carcinoma: expression of c-erbB-2/neu oncoprotein, epidermal growth factor receptor, cathepsin D, progesterone receptor and tumor associated glycoprotein-72 in different histological types. *Rev Esp Enferm Dig* 1999;91:826-837
- 29 Choi JH, Kim HC, Lim HY, Nam DK, Kim HS, Yi SY, Shim KS, Han WS. Detection of transforming growth factor-alpha in the serum of gastric carcinoma patients. *Oncology* 1999;57:236-241
- 30 Hirao T, Sawada H, Koyama F, Watanabe A, Yamada Y, Sakaguchi T, Tatsumi T, Fujimoto H, Emoto K, Narikiyo M, Oridate N, Nakano H. Antisense epidermal growth factor receptor delivered by adenoviral vector blocks tumor growth in human gastric cancer. *Cancer Gene Ther* 1999;6:423-427
- 31 Hosokawa N, Yamamoto S, Uehara Y, Hori M, Tsuchiya KS. Effect of thiazinotrienomycin B, an ansamycin antibiotic, on the function of epidermal growth factor receptor in human stomach tumor cells. *J Antibiot* 1999;52:485-490

- 32 Luan F, Wang M, You W. The correlation of TGF- α , EGFR in precancerous lesions and carcinoma of stomach with PCNA expression. *Zhonghua Binglixue Zazhi* 1997;26:31-34
- 33 Koyama S, Maruyama Y, Adachi S. Expression of epidermal growth factor receptor and CD44 splicing variants sharing exons 6 and 9 on gastric and esophageal carcinomas: a two-color flow-cytometric analysis. *J Cancer Res Clin Oncol* 1999;125:47-54
- 34 Wang Q, Wu JS, Gao DM, Lai DN, Ma QJ. Expression significance of epidermal growth factor receptor and transforming growth factor α mRNA in human colorectal carcinoma. *Shijie Huaren Xiaohua Zazhi* 1999;7:590-592
- 35 Hu X, Gao J, Li Y. The amounts of inositol 1,4,5-triphosphate and its response to epidermal growth factor and laminin of carcinoma substrains with high or low metastatic potentials. *Zhonghua Yixue Zazhi* 1997;77:665-667
- 36 Tsugawa K, Yonemura Y, Hirono Y, Fushida S, Kaji M, Miwa K, Miyazaki I, Yamamoto H. Amplification of the c-met, c-erbB-2 and epidermal growth factor receptor gene in human gastric cancers: correlation to clinical features. *Oncology* 1998;55:475-481
- 37 Slesak B, Harlozinska A, Porebska I, Bojarowski T, Lapinska J, Rzeszutko M, Wojnar A. Expression of epidermal growth factor receptor family proteins (EGFR, c-erbB-2 and c-erbB-3) in gastric cancer and chronic gastritis. *Anticancer Res* 1998;18:2727-2732
- 38 Murakami N, Fukuchi S, Takeuchi K, Hori T, Shibamoto S, Ito F. Antagonistic regulation of cell migration by epidermal growth factor and glucocorticoid in human gastric carcinoma cells. *J Cell Physiol* 1998;176:127-137
- 39 Romano M, Ricci V, Popolo AD, Sommi P, Blanco CD, Bruni CB, Ventura U, Cover TL, Blaser MJ, Coffey RJ, Zarrilli R. *Helicobacter pylori* upregulates expression of epidermal growth factor-related peptides, but inhibits their proliferative effect in MKN 28 gastric mucosal cells. *J Clin Invest* 1998; 101:1604-1613
- 40 Ishikawa T, Ichikawa Y, Tarnawski A, Fujiwara Y, Fukuda T, Arakawa T, Mitsuhashi M, Shimada H. Indomethacin interferes with EGF-induced activation of ornithine decarboxylase in gastric cancer cells. *Digestion* 1998;59:47-52
- 41 Gao JH, Liang HJ, Liu WW, Fang DC, Wang ZH. Expression of C-myc gene protein and epidermal growth factor receptor in gastric mucosa pre-and post- *Helicobacter pylori* clearance. *Shijie Huaren Xiaohua Zazhi* 1999;7:1018-1019
- 42 Zarrilli R, Ricci V, Romano M. Molecular response of gastric epithelial cells to *Helicobacter pylori*-induced cell damage. *Cell Microbiol* 1999;1:93-99
- 43 He Y, Zhou J, Wu JS, Dou KF. Inhibitory effects of EGFR antisense oligodeoxynucleotide in human colorectal cancer cell line. *World J Gastroenterol* 2000;6:747-749
- 44 Masaki T, Hatanaka Y, Nishioka M, Tokuda M, Shiratori Y, Reginfo W, Omata M. Activation of epidermal growth factor receptor kinase in gastric carcinoma: a preliminary study. *Am J Gastroenterol* 2000;95: 2135-2136
- 45 Uribe JM, Barrett KE. Nonmitogenic actions of growth factors: An integrated view of their role in intestinal physiology and pathophysiology. *Gastroenterology* 1997;112:225-268
- 46 Murayama Y, Miyagawa JI, Higashiyama S, Kondo S, Yabu M, Isozaki K, Kayanoki Y, Kanayama S, Shinomura Y, Taniguchi N, Matsuzawa Y. Localization of heparin-binding epidermal growth factor in human gastric mucosa. *Gastroenterology* 1995;109:1051-1059
- 47 Filipe MJ, Osborn M, Linehan J, Sanidas E, Brito MJ, Jankowski J. Expression of transforming growth factor alpha, epidermal growth factor receptor and epidermal growth factor in precursor lesions to gastric carcinoma. *British J Cancer* 1995;71:30-36
- 48 Yashi W, Oue N, Kuniyasu H, Ito R, Tahara E, Yokozaki H. Molecular diagnosis of gastric cancer: present and future. *Gastric Cancer* 2001; 4:113-121
- 49 Saikawa Y, Kubota T, Otani Y, Kitajima M, Modlin IM. Cyclin D1 antisense oligonucleotide inhibits cell growth stimulated by epidermal growth factor and induces apoptosis of gastric cancer cells. *Jpn J Cancer Res* 2001;92:1102-1109
- 50 Garcia I, Vizoso F, Andicoechea A, Raigoso P, Verez P, Alexandre E, Garcia-Muniz JL, Allende MT. Clinical significance of epidermal growth factor receptor content in gastric cancer. *Int J Biol Markers* 2001;16:183-188

Edited by Zhang JZ

• LIVER CANCER •

P53 immunohistochemical scoring: an independent prognostic marker for patients after hepatocellular carcinoma resection

Lun-Xiu Qin, Zhao-You Tang, Zeng-Chen Ma, Zhi-Quan Wu, Xin-Da Zhou, Qing-Hai Ye, Yuan Ji, Li-Wen Huang, Hu-Liang Jia, Hui-Chuan Sun, Lu Wang

Lun-Xiu Qin, Zhao-You Tang, Zeng-Chen Ma, Zhi-Quan Wu, Xin-Da Zhou, Qing-Hai Ye, Yuan Ji, Li-Wen Huang, Hu-Liang Jia, Hui-Chuan Sun, Lu Wang, Liver Cancer Institute and Zhongshan Hospital, Fudan University, Shanghai, China

Supported by the Key Project of Medical Development in Shanghai, the National Science Funding for Young Scientists (No. 30000075), and Fund for Leading Specialty of Shanghai Metropolitan Bureau of Public Health
Correspondence to: Zhao-You Tang, M.D., Professor & Chairman, Liver Cancer Institute & Zhongshan Hospital, Fudan University, 136 Yi Xue Yuan Road, Shanghai 200032, China. zytang@srcap.stc.sh.cn
Telephone: +86-21-64037181

Received 2001-09-26 Accepted 2001-10-29

Abstract

AIM: To confirm if p53 mutation could be a routine predictive marker for the prognosis of hepatocellular carcinoma (HCC) patients.

METHODS: Two hundreds and forty-four formalin-fixed paraffin-embedded tumor samples of the patients with HCC receiving liver resection were detected for nuclear accumulation of p53. The percent of P53 immunoreactive tumor cells was scored as 0 to 3+ in P53 positive region (<10% -, 10-30% +, 31-50% ++, >50% +++). Proliferating cell nuclear antigen (PCNA) and some clinicopathological characteristics, including patients' sex, preoperative serum AFP level, tumor size, capsule, vascular invasion (both visual and microscopic), and Edmondson grade were also evaluated.

RESULTS: In univariate COX hazard regression model analysis, tumor size, capsule status, vascular invasion, and p53 expression were independent factors that were closely related to the overall survival (OS) rates of HCC patients. The survival rates of patients with 3+ for p53 expression were much lower than those with 2+ or + for p53 expression. Only vascular invasion ($P<0.05$) and capsule ($P<0.01$) were closely related to the disease-free survival (DFS) of HCC patients. In multivariate analysis, p53 overexpression (RI 0.5456, $P<0.01$) was the most significant factor associated with the OS rates of patients after HCC resection, while tumor size (RI 0.5209, $P<0.01$), vascular invasion (RI 0.5271, $P<0.01$) and capsule (RI-0.8691, $P<0.01$) were also related to the OS. However, only tumor capsular status was an independent predictive factor ($P<0.05$) for the DFS. No significant prognostic value was found in PCNA-I, Edmondson's grade, patients' sex and preoperative serum AFP level.

CONCLUSION: Accumulation of p53 expression, as well as tumor size, capsule and vascular invasion, could be valuable markers for predicting the prognosis of HCC patients after resection. The quantitative immunohistochemical scoring for P53 nuclear accumulation

might be more valuable for predicting prognosis of patients after HCC resection than the common qualitative analysis.

Qin LX, Tang ZY, Ma ZC, Wu ZQ, Zhou XD, Ye QH, Ji Y, Huang LW, Jia HL, Sun HC, Wang L. P53 immunohistochemical scoring: an independent prognostic marker for patients after hepatocellular carcinoma resection. *World J Gastroenterol* 2002;8(3):459-463

INTRODUCTION

Liver cancer has been ranked the 2nd cancer killer in China since 1990s. The age-standardized mortality rate in China is as high as 34.7/10⁵, which accounts for 53% of all liver cancer deaths worldwide^[1]. Although many advances in its clinical study have been made, a definitive subset is cured by surgery only, and encouraging long-term survival of patients have been obtained in some clinical centers, the overall dismal outcome of patients with hepatocellular carcinoma (HCC) have not been completely changed^[2,3]. Lack of control of metastatic foci and recurrence is the most prevalent cause of death in patients with HCC, and it is important to identify the factors that predispose patients to death. Much effort has been made to predict HCC behavior, but there is still lack of specific prognostic indicators.

Prognostic factors in HCC conventionally consist of staging with the tumor node metastasis system (TNM) and grading by tumor cellular differentiation. With new discoveries in the cancer biology, pathological and biological factors of HCC in relation to prognosis have been studied quite extensively. Morphological features of the tumor, both gross and histological, are found to be significantly associated with tumor recurrence and patient survival. A complementary approach is to analyze the HCC for molecular markers with prognostic significance with reference to the recurring possibility and survival time. A large number of molecular biological factors have been shown to be associated with the invasiveness of HCC, and have potential prognostic significance, e.g. c-erbB-2, uPA, PAI-I, VEGF, CDKN2 and p53 mutations, p53 antibody, H-ras, mdm-2, TGF α , EGFR, VEGF, bFGF, PD-ECGF, MMP-2, ICAM-1 are positively related to HCC invasiveness, whereas nm23-H1, Kai-1, TIMP-2, Integrin α 5 and E-cadherin are negatively relative factors^[4]. Although a great amount of markers have been tried, a routine biomarker for prediction of prognosis of HCC is not yet available.

As early as in 1995, we found that p53 mutations were related to the invasiveness of HCC. Thereafter, we performed immunohistochemical staining for p53 overexpression in the surgical specimen of HCC patients treated in our institute, to see if p53 mutation could be a routine predictive marker for the prognosis of HCC patients. In the present study, we reviewed the results of the studies over the past 5 years, and evaluated whether nuclear accumulation of p53 would be a feasible prognostic marker in the routine diagnostic evaluation of HCC, in particular, to analyze the relationship between p53 overexpression and survival of patients with HCC.

MATERIALS AND METHODS

Tumor samples and HCC patients

Totally, 256 consecutive patients with HCC were enrolled in this study. All of them were surgically treated in the Liver Cancer Institute of Fudan University (former Liver Cancer Institute of Shanghai Medical University), Shanghai, China in the years 1996-1999. Except for 12 cases without informative follow-up data, 244 cases were reviewed, which included 197 male (80.7%) and 47 female (19.3%). The mean age was 50.4 (15-76) years. All specimens were formalin-fixed, paraffin-embedded, which were proved to be hepatocellular carcinoma (HCC). Some histological characteristics including the states of capsule, vascular invasion (both visual and microscopic), cell differentiation were reviewed by one pathologist. The mean tumor size was 5.9 (1-16)cm, ≤ 5 cm in 131 cases (53.7%), >5 cm but ≤ 8 cm 56 cases (23.0%), and >8 cm 57 cases (23.3%). The tumor of 128 cases (52.5%) had no capsule, and 116 cases (47.5%) were well-capsulated. The Edmondson grade distribution was grade I in 7 (2.9%) cases, Grade II-III in 235 (96.3%) cases, and grade IV in 2 (0.8%) cases. Vascular invasion was found in 69 cases (28.3%), which included visual tumor thrombi in portal vein in 31 cases and microvascular invasion in 38 cases. Obvious evidence of liver cirrhosis was found in 217 (88.9%) cases, no cirrhosis in 27 (11.1%) cases. Two hundred and twenty-two cases (91%, 222/244) were followed up. The mean follow-up time was 21.6 (2.2-49) months.

Immunohistochemistry

A standard indirect immunoperoxidase protocol was used for immunohistochemistry (ABC-Elite; Vector Laboratories, Inc., Burlingame, CA). Monoclonal anti-p53, PCNA antibodies (Dako) were used for detection of p53 and PCNA, respectively (1:200 dilution in PBS containing 1% bovine serum albumin and 0.1% Triton X-100). A high-temperature (20 minutes in a pressure cooker) treatment procedure with antigen unmasking solution (Vector Laboratories, Inc.) was used to enhance the staining. The primary antibody was omitted for negative controls.

We used the percentage of p53-positive tumor nuclei in all major foci of cancer as p53 immunohistochemical scoring system. The percent of p53 immunoreactive tumor cells was scored as 0 to 3+ in p53 positive regions. Nuclear p53 expression in $\geq 10\%$ of tumor cells was scored as aberrant overexpression, $<10\%$ -, 10%-30% +, 31%-50% ++, and $>50\%$ +++.

The patients' sex, serum AFP level, and the pathological characteristics of tumor, including tumor size, capsule, vascular invasion (both visual and microscopic), Edmondson grade, etc. were also evaluated.

Statistical analyses

The log-rank test, Kaplan-Meier analysis and univariate and multivariate Cox regression modeling were used for evaluation of contribution of the variables to relapse and disease-specific survival. Overall and disease-free survival rates were calculated with the Life-Table method, and the survival time was calculated from the operative date. The survival curves were estimated by Kaplan-Meier analysis. The prognostic significance of these markers was analyzed using the log-rank test. A Cox regression analysis was performed to show the relationship of the markers studied with the overall and disease-free survival rates of the HCC patients, and to identify the prognostic factors of the HCC patient after operation. The results were correlated with clinicopathological parameters and the prognosis evaluated by uni- and multi-variate analysis using local control, freedom from distant metastasis, disease-free survival, and overall survival as endpoints.

RESULTS

The 1-, 3- and 5-year overall survival rates of the 244 cases of HCC patients studied were 81.9%, 57.6% and 48.7%, respectively. And, the 1-, 3- and 5-year disease-free survival rates were 55.2%, 38.3%, and 32.2%, respectively. p53 immunohistochemical staining was heterogeneous in the HCC tissues, and nuclear staining for p53 were found in 112 of the 222 (50.5%) cases. The 1-, 3- and 5-year overall survival rates of the HCC patients with positive p53 nuclear accumulation were 81.2% (91/112), 50.9% (57/112), and 33.0% (37/112), while those of the HCC patients with negative p53 expression were 88.8%, 66.3% and 60.6%, respectively. Furthermore, among the patients with positive P53 expression, those with 3+ ($>50\%$) for P53 immunohistochemical scoring had a poorest prognosis, their 1-, and 3-year overall survival rates were only 38.5%, and 12.3%, which were much lower than those with 2+ (60.0% and 46.7%, respectively) and those with + (83.5% and 57.3%, respectively). Therefore, the score of P53 overexpression was adversely related to the survival rates of HCC patients (Table 1).

Table 1 Relationship between some clinicopathological parameters and overall survival rates of HCC patients (a univariate analysis)

Parameters	n	Overall survival rates %		
		1-year	3-year	5-year
P53 expression				
-	110	88.8	66.3	60.6
+	86	83.5	57.3	42.9
++	13	60.0	46.7	
+++ ^b	13	38.5	12.3	
Tumors size (cm)				
<=5cm	122	92.6	69.0	55.8
>5, <=8cm	50	78.0	63.0	55.1
>8cm ^b	50	60.0	23.9	
Vascular invasion				
No	160	88.7	68.5	60.7
Microscopic	36	80.6	47.0	
Visual	26	42.3	7.5	
Capsule				
No	112	74.0	42.0	26.4
Well ^b	110	90.5	75.9	75.9

^bP<0.01

The overall survival rates of patients after radical resection of small HCC (≤ 5 cm) were higher than those >5 cm and ≤ 8 cm in diameter. The 3-year survival rate of those with tumor >8 cm in diameter (23.9%) was much lower than those with tumor ≤ 8 cm in diameter (63.0%) (Table 1). The 1- and 3-year overall survival rates of the HCC patients with vascular invasion (both visual and microscopic) were 64.5% (42/62) and 30.6% (19/62), respectively. The patients with visual tumor thrombi in portal vein had a poorer prognosis, their 1- and 3-year overall survival rates were only 42.3% (11/26) and 7.5% (2/26), respectively. No 5-year survival was found. The 1-year, 3-year, and 5-year overall survival rates of patients without vascular invasion were 88.7%, 68.5%, and 60.7%, respectively, which were much higher than those with vascular invasion (P<0.01). A similar situation was also found with disease-free survival (Table 1). The 1-, 3-, and 5-year overall survival rates of patients with well-capsulated HCC were 90.5%, 75.9%, and 75.9%, respectively, while those of the patients without tumor capsule were 74.0%, 42.0%, and 26.4% Table. No significant relationship

between the PCNA-LI, Edmondson grade, patients' sex, or serum AFP level, and overall or disease-free survival rates was found ($P>0.05$).

In univariate Cox hazard regression model analysis, tumor size, capsule status, vascular invasion, p53 expression were independent factors that were closely related to the overall survival rates of HCC patients, while no obvious relationship was found between the PCNA ($P>0.05$) expression and the overall survival. Only vascular invasion ($P=0.0187$) and tumor capsule ($P=0.0059$) were closely related to the disease-free survival of HCC patients, no obvious relationship was found between p53, PCNA status and the disease-free survival (Tables 1, 2).

Similarly, in multivariate analysis, the p53 (RI 0.5456, $P<0.01$) was the most significant factor associated with the overall survival rates of HCC patients after resection. Tumor size (RI 0.5209, $P<0.01$), vessel invasion (RI 0.5271, $P<0.01$) and capsule (RI-0.8691, $P<0.01$) were also related to the overall survival. For the disease-free survival, tumor capsule status remained the only independent predictive factor ($P<0.05$, Table 3). No significant prognostic value was found in the PCNA-LI, Edmondson grade, or patients' sex, serum AFP level for the overall or disease-free survival both in univariate and multivariate Cox analyses.

Table 2 Parameters affecting the disease-free survival rates of HCC patients (a univariate analysis)

Patients (a univariate analysis)				
Parameters	n	Disease-free survival rates (%)		
		1-year	3-year	5-year
Vascular invasion				
No	116	93.9	64.6	54.2
Yes ^a	22	72.7	37.0	
Capsule				
No	57	82.3	44.9	44.9
Yes ^b	81	96.3	73.2	

^a $P<0.05$, ^b $P<0.01$, vs No.

Table 3 Relationship between some clinicopathological parameters and overall survival rates of HCC patients (a multivariate analysis)

	Correlation coefficient	Wald	Standard error	P
P53 expression	0.55	18.88	0.13	<0.01
Tumor size	0.52	14.97	0.13	<0.01
Vascular invasion	0.53	11.85	0.15	<0.01
Tumor capsule	-0.87	10.30	-0.10	<0.01

DISCUSSION

It is difficult to predict the prognosis of patients with HCC, because so far, there is no any specific marker for that yet. Assessment of the clinicopathological and biological malignancy of HCC may help predict outcome. Some pathological features, such as size of the tumor, vascular invasion, fibrous capsule infiltration, and intrahepatic metastasis are thought as prognostic factors for HCC^[5]. New invasiveness scoring system has been proposed based on the items such as venous invasion, tumor capsule, intrahepatic spreading, etc. In our previous report, tumor size was the most important factor for the prognosis of HCC patients and postoperative recurrence possibility^[3]. In this study, in univariate Cox hazard regression model analysis, tumor size, capsule status, and vascular invasion were independent factors which were closely related to both of the overall and disease-free survival rates of HCC patients. Similarly, in multivariate analysis, they were also independent prognostic factors for the overall survival, and the tumor capsule status and vascular invasion were predictive factors for disease-free survival. All these further confirmed

the significance of pathological characteristics of tumor itself in the survival of HCC patients, and the importance of early detection, early diagnosis and early treatment of HCC.

Some biomarkers such as the tumor DNA content, P53 protein expression, proliferating cell nuclear antigen (PCNA) labeling index, and argyrophilic proteins of nuclear organizer regions were used as markers of biological malignancy. P53 protein plays a central role in cellular responses, including cell-cycle arrest and cell death in response to DNA damage. p53 dysfunction can induce abnormal cell growth, increased cell survival, genetic instability, and drug resistance. p53 mutations occur in approximately half of human cancers. Associations of p53 mutation or positive immunohistochemical stain with higher grade and more advanced stage are common. p53 mutation has been found related to advanced tumor stage in cancers of endometrium, cervix, ovary, liver, prostate and bladder, indicating that for these tumors p53 mutation may be a late event contributing to tumor progression^[6]. And p53 mutation has been reported to be a strong marker predicting an increased risk of local relapse, treatment failure, and overall and disease-free survival in many kinds of human carcinomas, such as breast^[7-11], colon-recta^[12,13], esophagus^[14], head and neck^[15], lung^[16-18], ovarian^[19], as well as sarcoma^[20]. An increased intracellular concentration of the P53 protein, although not identical to, is sometimes seen in tumors with p53 mutation and correlated with poor prognosis in some tumors. Several studies have shown a relationship between the nuclear accumulation of p53 protein and poor disease-free and overall survival of prostate cancer^[21,22], and oral cancer^[23]. Detection of micrometastasis of the regional lymph nodes of ovarian cancer by immunohistochemical staining of P53 protein may be useful in predicting the prognosis of patients with stage I or II epithelial ovarian cancer^[24]. The presence of serum anti-p53 antibody has also been found to be associated with survival of patients with breast cancer, ovarian cancer, and hepatocellular carcinoma, and colorectal cancer^[25,26]. However, there is still a great controversy as to whether alteration of the p53 gene adversely affects the survival of cancer patients. Many reports failed to show the independent prognostic value of p53 in the carcinomas of tongue^[27], breast^[28-30], stomach^[31], lung^[32], ovarian^[33], bladder^[34,35], colorectal^[36], and non-Hodgkin's lymphoma^[37].

In a similar situation, there are controversial results about the relationship between the p53 overexpression or p53 gene mutation and the prognosis of HCC patients. It was shown that p53 mutation was involved in determining the dedifferentiation, the proliferative activity, tumor progression^[38], and closely related to the invasiveness of HCC^[4], which might also influence the postoperative course. Mutations of p53 gene or positive immunostaining for mutant P53 protein expression could be used as a significant indicator of poor prognosis^[39-41]. Serum anti-p53 antibody could also be a useful prognostic factor for patients with HCC^[42]. However, many studies showed that neither the immunohistochemical detection of p53 expression, nor the serum anti-p53 antibodies had a significant prognostic value for outcome of patients with HCC^[43-45].

In this study, nuclear staining for P53 was found in 112 of the 222 (50.5%) cases, which was similar to the previous study. The 3-year and 5-year overall survival rates of the HCC patients with positive P53 nuclear accumulation were much lower than those of the HCC patients with negative P53 expression. Its significance was even better than that of the factors such as tumor size, vascular invasion and tumor capsule, though they were also related to the overall survival. Therefore, the score of P53 overexpression was adversely related to the survival rates of HCC patients. These indicated that p53 mutation or nuclear accumulation of p53 expression could be a valuable marker for predicting the prognosis of HCC patients after resection. Among the patients with positive P53 expression, those

with 3+ (>50%) for P53 immunohistochemical scoring had a poorest prognosis, their 1-, and 3-year overall survival rates were only 38.5% and 12.3%, respectively, which were much lower than those with 2+ (60.0% and 46.7%) and those with + (83.5% and 57.3%). Therefore, the quantitative immunohistochemical scoring for P53 expression might be more valuable than the common qualitative analysis for P53 expression for predicting the prognosis of HCC patients.

Proliferating cell nuclear antigen (PCNA) labeling index has been thought as another marker of biological malignancy. A correlation between PCNA-LI and recurrent time and rate was reported. PCNA-LI could be a valuable prognostic marker for HCC. However, in this study, no correlation between PCNA-LI and overall or disease-free survival was found.

In summary, HCC is one of the most common cancers in China. Although great advances in its clinical study have been made, metastatic recurrence is the most prevalent cause of death in patients with HCC. Over the past few years, much effort has been made on this target, including predicting HCC behavior^[46-60]. In this study, through the retrospective review of the 244 HCC patients, we found that accumulation of p53 expression as well as tumor size, capsule or vascular invasion could be a valuable marker for predicting the prognosis of HCC patients after resection. The quantitative immunohistochemical scoring for P53 nuclear accumulation might be more valuable than the common qualitative analysis for P53 expression for predicting prognosis of patients after HCC resection.

REFERENCES

- Pisani P, Parkin M, Bray F, Ferlay J. Estimates of the worldwide mortality from 25 cancers in 25 cancers in 1990. *Int J Cancer* 1999;83: 18-29
- Greenlee RT, Hill-Harmon MB, Murray T, Thun M. Cancer Statistics, 2001. *CA Cancer J Clin* 2001;51:15-36
- Tang ZY. Hepatocellular carcinoma-Cause, treatment and metastasis. *World J Gastroenterol* 2001;7:445-454
- Tang ZY, Qin LX, Wang XM, Zhou G, Liao Y, Weng Y, Jiang XP, Lin ZY, Liu KD, Ye SL. Alterations of oncogenes, tumor suppressor genes and growth factors in hepatocellular carcinoma: with relation to tumor size and invasiveness. *Chin Med J* 1998;111:313-318
- Poon RT, Fan ST, Ng IO, Lo CM, Liu CL, Wong J. Different risk factors and prognosis for early and late intrahepatic recurrence after resection of hepatocellular carcinoma. *Cancer* 2000;89:500-507
- Greenblatt MS, Bennett WP, Hollstein M, Harris CC. Mutations in the p53 tumor suppressor gene: Clues to cancer etiology and molecular pathogenesis. *Cancer Res* 1994;54:4855-4878
- Overgaard J, Yilmaz M, Guldberg P, Hansen LL, Alsner J. TP53 mutation is an independent prognostic marker for poor outcome in both node-negative and node-positive breast cancer. *Acta Oncol* 2000; 39:327-333
- Zellars RC, Hilsenbeck SG, Clark GM, Allred DC, Herman TS, Chamness GC, Elledge RM. Prognostic value of p53 for local failure in mastectomy-treated breast cancer patients. *J Clin Oncol* 2000;18: 1906-1913
- Takahashi M, Tonoki H, Tada M, Kashiwazaki H, Furuuchi K, Hamada J, Fujioka Y, Sato Y, Takahashi H, Todo S, Sakuragi N, Moriuchi T. Distinct prognostic values of p53 mutations and loss of estrogen receptor and their cumulative effect in primary breast cancers. *Int J Cancer* 2000;89:92-99
- Blaszyk H, Hartmann A, Cunningham JM, Schaid D, Wold LE, Kovach JS, Sommer SS. A prospective trial of midwest breast cancer patients: a p53 gene mutation is the most important predictor of adverse outcome. *Int J Cancer* 2000;89:32-38
- Sirvent JJ, Fortuno-Mar A, Olona M, Orti A. Prognostic value of p53 protein expression and clinicopathological factors in infiltrating ductal carcinoma of the breast. A study of 192 patients. *Histol Histopathol* 2001;16:99-106
- Bouzourene H, Gervaz P, Cerottini JP, Benhattar J, Chaubert P, Saraga E, Pampallona S, Bosman FT, Givel JC. p53 and Ki-ras as prognostic factors for Dukes' stage B colorectal cancer. *Eur J Cancer* 2000;36:1008-1015
- Kahlenberg MS, Stoler DL, Rodriguez-Bigas MA, Weber TK, Driscoll DL, Anderson GR, Petrelli NJ. p53 tumor suppressor gene mutations predict decreased survival of patients with sporadic colorectal carcinoma. *Cancer* 2000;88:1814-1819
- Ireland AP, Shibata DK, Chandrasoma P, Lord RV, Peters JH, DeMeester TR. Clinical significance of p53 mutations in adenocarcinoma of the esophagus and cardia. *Ann Surg* 2000;231:179-187
- Tamas L, Kraxner H, Mechtler L, Repassy G, Ribari O, Hirschberg A, Szentkuti G, Jaray B, Szentirmay Z. Prognostic significance of P53 histochemistry and DNA histogram parameters in head and neck malignancies. *Anticancer Res* 2000;20:4031-4037
- Gemba K, Ueoka H, Kiura K, Tabata M, Harada M. Immunohistochemical detection of mutant p53 protein in small-cell lung cancer: relationship to treatment outcome. *Lung Cancer* 2000;29:23-31
- Murakami I, Hiyama K, Ishioka S, Yamakido M, Kasagi F, Yokosaki Y. p53 gene mutations are associated with shortened survival in patients with advanced non-small cell lung cancer: an analysis of medically managed patients. *Clin Cancer Res* 2000;6:526-530
- Mitsudomi T, Hamajima N, Ogawa M, Takahashi T. Prognostic significance of p53 alterations in patients with non-small cell lung cancer: a meta-analysis. *Clin Cancer Res* 2000;6:4055-4063
- Shahin MS, Hughes JH, Sood AK, Buller RE. The prognostic significance of p53 tumor suppressor gene alterations in ovarian carcinoma. *Cancer* 2000;89:2006-2017
- de Alava E, Antonescu CR, Panizo A, Leung D, Meyers PA, Huvos AG, Pardo-Mindan FJ, Healey JH, Ladanyi M. Prognostic impact of P53 status in Ewing sarcoma. *Cancer* 2000;89:783-792
- Borre M, Stausbol-Gron B, Overgaard J. p53 accumulation associated with bcl-2, the proliferation marker MIB-1 and survival in patients with prostate cancer subjected to watchful waiting. *J Urol* 2000;164:716-721
- Leibovich BC, Cheng L, Weaver AL, Myers RP, Bostwick DG. Outcome prediction with p53 immunostaining after radical prostatectomy in patients with locally advanced prostate cancer. *J Urol* 2000; 163:1756-1760
- Osaki T, Kimura T, Tatemoto Y, Dapeng L, Yoneda K, Yamamoto T. Diffuse mode of tumor cell invasion and expression of mutant p53 protein but not of p21 protein are correlated with treatment failure in oral carcinomas and their metastatic foci. *Oncology* 2000;59:36-43
- Suzuki M, Ohwada M, Saga Y, Kohno T, Takei Y, Sato I. Micrometastatic p53-positive cells in the lymph nodes of early stage epithelial ovarian cancer: prognostic significance. *Oncology* 2001;60: 170-175
- Shiota G, Ishida M, Noguchi N, Oyama K, Takano Y, Okubo M, Katayama S, Tomie Y, Harada K, Hori K, Ashida K, Kishimoto Y, Hosoda A, Suou T, Kanbe T, Tanaka K, Nosaka K, Tanida O, Kojo H, Miura K, Ito H, Kaibara N, Kawasaki H. Circulating p53 antibody in patients with colorectal cancer: relation to clinicopathologic features and survival. *Dig Dis Sci* 2000;45:122-128
- Vogl FD, Frey M, Kreienberg R, Runnebaum IB. Autoimmunity against p53 predicts invasive cancer with poor survival in patients with an ovarian mass. *Br J Cancer* 2000;83:1338-1343
- Kantola S, Parikka M, Jokinen K, Hyrynkangs K, Soini Y, Alho OP, Salo T. Prognostic factors in tongue cancer - relative importance of demographic, clinical and histopathological factors. *Br J Cancer* 2000; 83:614-619
- Ferrero JM, Ramaioli A, Formento JL, Francoual M, Etienne MC, Peyrottes I, Ettore F, Leblanc-Talent P, Namer M, Milano G. P53 determination alongside classical prognostic factors in node-negative breast cancer: an evaluation at more than 10-year follow-up. *Ann Oncol* 2000;11:393-397
- Bergh J. Clinical studies of p53 in treatment and benefit of breast cancer patients. *Endocr Relat Cancer* 1999;6:51-59
- Reed W, Hannisdal E, Boehler PJ, Gundersen S, Host H, Marthin J. The prognostic value of p53 and c-erb B-2 immunostaining is over-rated for patients with lymph node negative breast carcinoma: a multivariate analysis of prognostic factors in 613 patients with a follow-up of 14-30 years. *Cancer* 2000;88:804-813
- Kaye PV, Radebold K, Isaacs S, Dent DM. Expression of p53 and p21waf1/cip1 in gastric carcinoma: lack of inter-relationship or correlation with prognosis. *Eur J Surg Oncol* 2000;26:39-43
- Schiller JH, Adak S, Feins RH, Keller SM, Fry WA, Livingston RB, Hammond ME, Wolf B, Sabatini L, Jett J, Kohman L, Johnson DH. Lack of prognostic significance of p53 and K-ras mutations in primary resected non-small-cell lung cancer on E4592: a Laboratory Ancillary Study on an Eastern Cooperative Oncology Group Prospective Randomized Trial of Postoperative Adjuvant Therapy. *J Clin Oncol* 2001;19:448-457
- Gadducci A, Cianci C, Cosio S, Carnino F, Fanucchi A, Buttitta F, Conte PF, Genazzani AR. p53 status is neither a predictive nor a prognostic variable in patients with advanced ovarian cancer treated with a paclitaxel-based regimen. *Anticancer Res* 2000;20:4793-4799
- Gontero P, Casetta G, Zitella A, Ballario R, Pacchioni D, Magnani C, Muir GH, Tizzani A. Evaluation of P53 protein overexpression, Ki67 proliferative activity and mitotic index as markers of tumour recurrence in superficial transitional cell carcinoma of the bladder. *Eur Urol* 2000;38:

- 287-296
- 35 Fleshner N, Kapusta L, Ezer D, Herschorn S, Klotz L. p53 nuclear accumulation is not associated with decreased disease-free survival in patients with node positive transitional cell carcinoma of the bladder. *J Urol* 2000;164:1177-182
- 36 Gallego MG, Acenero MJ, Ortega S, Delgado AA, Cantero JL. Prognostic influence of p53 nuclear overexpression in colorectal carcinoma. *Colon Rectum* 2000;43:971-975
- 37 Nieder C, Petersen S, Petersen C, Thames HD. The challenge of p53 as prognostic and predictive factor in Hodgkin's or non-Hodgkin's lymphoma. *Ann Hematol* 2001;80:2-8
- 38 Itoh T, Shiro T, Seki T, Nakagawa T, Wakabayashi M, Inoue K, Okamura A. Relationship between p53 overexpression and the proliferative activity in hepatocellular carcinoma. *Int J Mol Med* 2000;6:137-142
- 39 Jeng KS, Sheen IS, Chen BF, Wu JY. Is the p53 gene mutation of prognostic value in hepatocellular carcinoma after resection? *Arch Surg* 2000;135:1329-1333
- 40 Sugo H, Takamori S, Kojima K, Beppu T, Futagawa S. The significance of p53 mutations as an indicator of the biological behavior of recurrent hepatocellular carcinomas. *Surg Today* 1999;29:849-855
- 41 Hayashi H, Sugio K, Matsumata T, Adachi E, Takenaka K, Sugimachi K. The clinical significance of p53 gene mutation in hepatocellular carcinomas from Japan. *Hepatology* 1995;22:1702-1707
- 42 Shiota G, Kishimoto Y, Suyama A, Okubo M, Katayama S, Harada K, Ishida M, Hori K, Suou T, Kawasaki H. Prognostic significance of serum anti-p53 antibody in patients with hepatocellular carcinoma. *J Hepatol* 1997;27:661-668
- 43 Tangkijvanich P, Janchai A, Charuruks N, Kullavanijaya P, Theamboonlers A, Hirsch P, Poovorawan Y. Clinical associations and prognostic significance of serum anti-p53 antibodies in Thai patients with hepatocellular carcinoma. *Asian Pac J Allergy Immunol* 2000;18:237-243
- 44 Saffroy R, Lelong JC, Azoulay D, Salvucci M, Reynes M, Bismuth H, Debuire B, Lemoine A. Clinical significance of circulating anti-p53 antibodies in European patients with hepatocellular carcinoma. *Br J Cancer* 1999;79:604-610
- 45 Terris B, Laurent-Puig P, Belghitti J, Degott C, Henin D, Flejou JF. Prognostic influence of clinicopathologic features, DNA-ploidy, CD44H and p53 expression in a large series of resected hepatocellular carcinoma in France. *Int J Cancer* 1997;74:614-619
- 46 Tang ZY, Sun FX, Tian J, Ye SL, Liu YK, Liu KD, Xue Q, Chen J, Xia JL, Qin LX, Sun HC, Wang L, Zhou J, Li Y, Ma ZC, Zhou XD, Wu ZQ, Lin ZY, Yang BH. Metastatic human hepatocellular carcinoma models in nude mice and cell line with metastatic potential. *World J Gastroenterol* 2001;7:597-601
- 47 Li Y, Tang ZY, Ye SL, Liu YK, Chen J, Xue Q, Chen J, Gao DM, Bao WH. Establishment of cell clones with different metastatic potential from the metastatic hepatocellular carcinoma cell line MHCC97. *World J Gastroenterol* 2001;7:630-636
- 48 Niu Q, Tang ZY, Ma ZC, Qin LX, Zhang LH. Serum vascular endothelial growth factor is a potential biomarker of metastatic recurrence after curative resection of hepatocellular carcinoma. *World J Gastroenterol* 2000;6:565-568
- 49 Wu ZQ, Fan J, Qiu SJ, Zhou J, Tang ZY. The value of postoperative hepatic regional chemotherapy in prevention of recurrence after radical resection of primary liver cancer. *World J Gastroenterol* 2000;6:131-133
- 50 Wang Q, Lin ZY, Feng XL. Alterations in metastatic properties of hepatocellular carcinoma cell following H-ras oncogene transfection. *World J Gastroenterol* 2001;7:335-339
- 51 Jiang YF, Yang ZH, Hu JQ. Recurrence or metastasis of HCC: predictors, early detection and experimental antiangiogenic therapy. *World J Gastroenterol* 2000;6:61-65
- 52 Cao XY, Liu J, Lian ZR, Clayton M, Hu JL, Zhu MH, Fan DM, Feitelson M. Cloning of differentially expressed genes in human hepatocellular carcinoma and nontumor liver. *World J Gastroenterol* 2001;7:579-582
- 53 Hou L, Li Y, Jia YH, Wang B, Xin Y, Ling MY. Molecular mechanism about lymphogenous metastasis of hepatocarcinoma cells in mice. *World J Gastroenterol* 2001;7:532-536
- 54 Fan ZR, Yang DH, Cui J, Qin HR, Huang CC. Expression of insulin-like growth factor II and its receptor in hepatocellular carcinogenesis. *World J Gastroenterol* 2001;7:285-288
- 55 Xu J, Mei MH, Zeng SE, Shi QF, Liu YM, Qin LL. Expressions of ICAM and its mRNA in sera and tissues of patients with hepatocellular carcinoma. *World J Gastroenterol* 2001;7:120-125
- 56 Huang XF, Wang CM, Dai XW, Li ZJ, Pan BR, Yu LB, Qian B, Fang L. Expressions of chromogranin: A and cathepsin D in human primary hepatocellular carcinoma. *World J Gastroenterol* 2000;6:693-698
- 57 Mei MH, Xu J, Shi QF, Yang JH, Chen Q, Qin LL. Clinical significance of serum intercellular adhesion molecule 1 detection in patients with hepatocellular carcinoma. *World J Gastroenterol* 2000;6:408-410
- 58 Qin Y, Li B, Tan YS, Sun ZL, Zuo FQ, Sun ZF. Polymorphism of p16INK4a gene and rare mutation of p15INK4b gene exon2 in primary hepatocarcinoma. *World J Gastroenterol* 2000;6:411-414
- 59 Kong XB, Yang ZK, Liang LJ, Huang JF, Lin HL. Overexpression of Pglycoprotein in hepatocellular carcinoma and its clinical implication. *World J Gastroenterol* 2000;6:134-135
- 60 Lin GY, Chen ZL, Lu CM, Li Y, Ping XJ, Huang R. Immunohistochemical study on p53, H-ras/p21, c-erbB2 protein and PCNA expression in HCC tissues of Han and minority ethnic patients. *World J Gastroenterol* 2000;6:234-238

Edited by Ma JY

• LIVER CANCER •

Antitumor activities of human autologous cytokine-induced killer (CIK) cells against hepatocellular carcinoma cells *in vitro* and *in vivo*

Fu-Sheng Wang, Ming-Xu Liu, Bing Zhang, Ming Shi, Zhou-Yun Lei, Wen-Bing Sun, Qing-You Du, Ju-Mei Chen

Fu-Sheng Wang, Ming-Xu Liu, Bing Zhang, Ming Shi, Zhou-Yun Lei, Wen-Bing Sun, Qing-You Du, Ju-Mei Chen, Division of Biological Engineering, Beijing Institute of Infectious Diseases, Beijing 100039, China
Wen-Bing Sun, Department of Surgery, Beijing Hospital of Infectious Diseases, Beijing 100039, China

Supported by Science and Technology Development Foundation of Beijing Institute of Infectious Diseases, No.01Z094

Correspondence to: Dr. Fu-Sheng Wang, Division of Biological Engineering, Beijing Institute of Infectious Diseases, 26 Fengtai Road, Beijing 100039, China. fswang@public.bta.net.cn

Telephone: +86-10-66933332 Fax: +86-10-63831870

Received 2001-04-11 Accepted 2002-02-25

Abstract

AIM: To characterize the anticancer function of cytokine-induced killer cells (CIK) and develop an adoptive immunotherapy for the patients with primary hepatocellular carcinoma (HCC), we evaluated the proliferation rate, phenotype and the antitumor activity of human CIK cells from healthy donors and HCC patients *in vitro* and *in vivo*.

METHODS: Peripheral blood mononuclear cells (PBMC) from healthy donors and patients with primary HCC were incubated *in vitro* and induced into CIK cells in the presence of various cytokines such as interferon-gamma (IFN- γ), interleukin-1 (IL-1), IL-2, and monoclonal antibody (mAb) against CD3. The phenotype and characterization of CIK cells were identified by flow cytometric analysis. The cytotoxicity of CIK cells was determined by ^{51}Cr release assay.

RESULTS: The CIK cells were shown to be a heterogeneous population with different cellular phenotypes. The percentage of CD3 $^{+}$ /CD56 $^{+}$ positive cells, the dominant effector cells, in total CIK cells from healthy donors and HCC patients, significantly increased from 0.1-0.13% at day 0 to 19.0-20.5% at day 21 incubation, which suggested that the CD3 $^{+}$ CD56 $^{+}$ positive cells proliferated faster than other cell populations of CIK cells in the protocol used in this study. After 28 day *in vitro* incubation, the CIK cells from patients with HCC and healthy donors increased by more than 300-fold and 500-fold in proliferation cell number, respectively. CIK cells originated from HCC patients possessed a higher *in vitro* antitumor cytotoxic activity on autologous HCC cells than the autologous lymphokine-activated killer (LAK) cells and PBMC cells. In *in vivo* animal experiment, CIK cells had stronger effects on the inhibition of tumor growth in Balb/c nude mice bearing BEL-7402-producing tumor than LAK cells (mean inhibitory rate, 84.7% vs 52.8%, $P < 0.05$) or PBMC (mean inhibitory rate, 84.7% vs 37.1%, $P < 0.01$).

CONCLUSION: Autologous CIK cells are of highly efficient cytotoxic effector cells against primary hepatocellular carcinoma cells and might serve as an alternative adoptive therapeutic strategy for HCC patients.

Wang FS, Liu MX, Zhang B, Shi M, Lei ZY, Sun WB, Du QY, Chen JM. Antitumor activities of human autologous cytokine-induced killer (CIK) cells against hepatocellular carcinoma cells *in vitro* and *in vivo*. *World J Gastroenterol* 2002;8(3):464-468

INTRODUCTION

Cytokine-induced killer (CIK) cells are the major histocompatibility complex-unrestricted cytotoxic lymphocytes and generated by incubation of peripheral blood monocytes (PBMC) in the presence of various types of cytokines such as CD3 monoclonal antibody, interleukin-2 (IL-2), interleukin-1 (IL-1) and interferon-gamma^[1]. CIK cells are the population of heterogeneous effector cells possessing enhanced cytotoxicity and a higher proliferation rate as compared with lymphokine-activated killer (LAK) and tumor infiltrating lymphocytes (TIL) cells. The high anti-tumor activity of CIK cells is mainly due to the high proliferation of double CD3 $^{+}$ and CD56 $^{+}$ positive cells^[2-5]. Some reports indicated that CIK cells, other than LAK and TIL cells, can be efficiently employed as an adjuvant in anticancer immunotherapeutic strategy for the eradication of residual cancer cells and prevention or delay of tumor relapse^[6-9].

Hepatocellular carcinoma (HCC) is the malignant transformation of hepatocytes and is a common complication of chronic hepatitis mainly caused by hepatitis B virus (HBV) and hepatitis C virus (HCV) infection in China^[10]. The mechanisms underlying the malignant transformation of hepatocytes are not well defined. Many driving factors including the persistent hepatitis B or C virus infections, host immunological and genetic factors might have been involved in the process. For example, a failure to mount an efficient immune response to HCC cells, either because of selective defects or immune tolerance in the host immune system or because of tumor interference with a function(s) of immune cells, could account for the inability of HCC patients to block the pathogenesis of HCC occurrence^[11-18]. In attempt to characterize the anticancer function of CIK cells and develop an alternative adoptive immunotherapy for the patients with primary HCC, we evaluated the proliferation rate and phenotype of CIK cells from healthy donors and primary HCC patients. Furthermore, we compared the cytotoxic activity and antitumor effects of major effector CIK cells with double CD3 $^{+}$ and CD56 $^{+}$ positive markers against the primary and secondary HCC *in vitro* cell culture system and *in vivo* tumor-bearing mice model.

MATERIALS AND METHODS

Reagents and cell lines

RPMI1640 and DMEM medium, recombinant human IL-1 α , IL-2, interferon gamma (IFN- γ), TNF- α and monoclonal antibody against the CD3 surface antigen (mAb CD3) were all purchased from Gibco Co. The Flt-3 ligand, mouse anti-human FITC-conjugated CD3 and CD56 monoclonal antibodies were obtained from BD-Pharmingen and Fetal calf serum (FCS) from Hyclone. BEL7402 is human HCC cell line kept in liquid nitrogen in our laboratory.

Cell separation

The patients with primary HCC and healthy donors were submitted to cytophoresis after their writing contents were signed. An enriched peripheral blood mononuclear cells (PBMC) product was collected using the specific program of the Cobe Spectra blood separator. Cells were resuspended in phosphate buffered saline (PBS) without calcium and magnesium. The separation of PBMC was performed as previously described^[2,19-21]. The concentrated PBMC cells were used immediately for CIK cell culture.

Generation of cytokine-induced killer (CIK) cells

CIK cells were generated as described previously^[2,3,22,23]. Briefly, non-adherent Ficoll-separated human peripheral blood mononuclear cells were prepared and incubated in RPMI1640 medium containing 100ml·L⁻¹ FCS and various types of cytokines added according to the reported protocol with minor modifications^[23]. The final concentrations of the cytokines and antibody added were as follows: IL-2, 1000×10³U·L⁻¹; IL-1, 100×10³U·L⁻¹; IFN-γ, 100×10³U·L⁻¹; mAb CD3, 50μg·L⁻¹. Cells were incubated at 37°C in a humidified atmosphere of 50ml·L⁻¹ CO₂ and fed every 3 days in fresh complete medium with 100ml·L⁻¹ FCS and various types of cytokines at 0.5×10⁶cells·L⁻¹.

Immunofluorescent staining of effector cells

Starting PBMC, LAK or CIK effector cells were stained with various types of FITC- or PE-conjugated mouse mAb's against human surface antigens. Antibodies used included anti-CD3, anti-CD4, anti-CD16, anti-CD56 and anti-TCR-α/β, anti-TCR-γ/δ (all from Becton Dickinson, Beijing, China). Five ×10⁵ of cells were incubated with a optimal amount of antibody at 4°C for 30min. To remove excessive antibody, the incubation mixture was centrifuged at 250×g for 10min. The pellet was resuspended in PBS containing 2ml·L⁻¹ of human AB serum and treated as described before^[21]. Stained cells were washed and analyzed with FACScaliber (Becton Dickinson) in our laboratory.

Isolation of primary HCC cells from patients

Fresh liver cancer tissues were obtained from the HCC patients at the department of Surgery in our hospital and immediately immersed in sterilized PBS (pH 7.0) solution containing penicillin, 100×10³U·L⁻¹; streptomycin, 100×10³U·L⁻¹ and gentamycin, 500×10³U·L⁻¹ for 1h at room temperature, then washed with PBS for three times. The liver cancer tissues were cut into small pieces (1-2mm³ in size), and digested with 37°C-rewarm serum-free medium with 1.25g·L⁻¹ of collagenase-V for 2h. In order to separate them into single cell suspension, all the digested pieces of tissues were filtered through the 200 mesh of sterilized copper wire bag. The single cell suspension was further isolated by Percoll gradient centrifugation. Finally, the resuspended cells in DMEM medium with 200ml·L⁻¹ FCS were the primary HCC cells.

Cytotoxic effects of CIK cells by ⁵¹Cr release assay

⁵¹Cr release cytotoxic assays were performed as reported previously^[24]. Briefly, one ×10⁶ of human primary HCC cells were incubated with culture medium containing 7.4MBq of ⁵¹Cr solution at 37°C for one hour. The labeling cells were washed with PBS solution for three times and added to 96-well culture plates at 2×10⁴cells/well. CIK cells were incubated with tumor cells at various ratios of effector cells to target cells as 6.25 : 1, 12.5 : 1, 25 : 1 and 50 : 1. After 4h incubation, all cells were collected by centrifugation and an aliquot of supernatant was counted in a gamma counter. The percentage of specific release was calculated as described^[25].

Inhibitory Effects of CIK cells on HCC in tumor-bearing nude mice models

In pilot experiments, 1.5×10⁶ of BEL-7402 cells injected subscapularly could produce solid tumor in Balb/c nude mice at the tenth day with 100% of incidence rate. The Balb/c nude mice used in the study were randomly divided into four groups treated with physical solution, PBMC, LAK and CIK cells, respectively. The nude mice received 3.0Gy of whole body irradiation and injected subscapularly with 5×10⁶ BEL-7402 cells, which were at the stage of exponential growth (designated as day 0). On day 1, 0.25mL of 1×10⁷ effector cells such as CIK, PBMC or LAK cells were injected locally where tumor cells were inoculated for 6 consecutive days. In controls, the nude mice received 0.25mL physical solution. The size of tumor was recorded every other day. The solid tumors were peeled off after the nude mice were dislocated by killing them on the 35th day.

Statistical analysis

The Wilcoxon matched-pairs test was used to analyze for statistical significance. The P value less than 0.05 was considered as significant difference.

RESULTS

Proliferation and phenotype of CIK cells

Figure 1A and B show the proliferation of CIK cells from healthy donors and patients with primary HCC at different incubation days. During cell generation, there was a steady increase in both the absolute number and the percentage of CD3⁺/CD56⁺ cells, e.g. the percentage of CD3⁺/CD56⁺ cells was 7.5% on 14d and 51.3% on 56d of in vitro incubation, respectively. After 14d in vitro incubation, the number of total incubated CIK cells increased significantly (500 fold from 8.07×10⁵ to 1.02×10⁸). The majority (as high as 82%±6.4%) of these cells were positive for TCR-α/β. Cells expressing TCR-γ/δ were relatively rare (4.5%±2.6%). The proliferation capability of PBMC obtained from normal donors was slightly higher than that of PBMC obtained from the HCC patients. The percentage of double CD3⁺/CD56⁺ positive cells varied during CIK cell generation. The percentage of CD3⁺/CD56⁺ positive cells in total CIK cells from healthy donors and HCC patients significantly increased from 0.1-0.13% at day 0 to 18.95-20.5% at day 21, which suggested that the CD3⁺ CD56⁺ positive cells proliferated faster than other populations of CIK cells in the protocol used in this study.

In peripheral blood, 24.2% of CD56⁺ cells coexpressed CD3⁺ as compared to 36.2% in LAK cell cultures and 76% in CIK cell cultures (Figure 2). Conversely, only 17.8% and 42.1% of CD3⁺ cells in peripheral blood and LAK cells coexpressed CD56⁺, whereas 76.6% of CIK CD3⁺ cells coexpressed CD56⁺. At d 28 of CIK cell generation, the percentage of CD3⁺ cells coexpressing CD56⁺ increased to 82.4%.

Table 1 Phenotype of CIK cells and cytotoxic activity of CIK subsets

Subset	Percentage positively of CIK	LU/10 ⁶ cell stained cells	Cell number ×10 ⁶	Total LU per culture
CIK		43.6±4.8	712±24.3	29,074
TCR-α/β	82.0±6.4	20.6±3.8	583±41.6	12,088
CD56	30.4±5.6	78.4±6.9	214±70.3	13,948
CD16	15.8±5.4	60.4±6.0	89±40.9	4106

Note: Total LU per culture was calculated by multiplying the number of LU per million cells by the total number of cells.

Effect of different sera on CIK proliferation

When CIK cells were incubated in RPMI1640 medium containing 100 ml·L⁻¹ of fetal calf serum or 100ml·L⁻¹ human AB serum or free-

serum medium, respectively, they exhibited different growth curves (Figure 3). CIK cells had the highest proliferation rate in human AB serum-containing medium, the lowest in serum-free medium. The proliferated numbers of CIK cells increased by 500 fold in human AB serum-containing medium, 450 fold increase in fetal calf serum-containing medium, and 50-60 fold in free-serum medium, respectively.

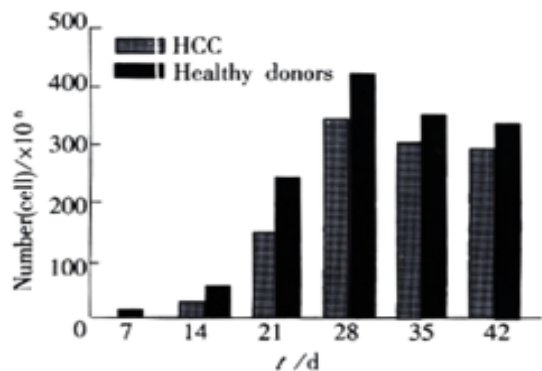


Figure 1A Proliferation of CIK cells *in vitro* culture system

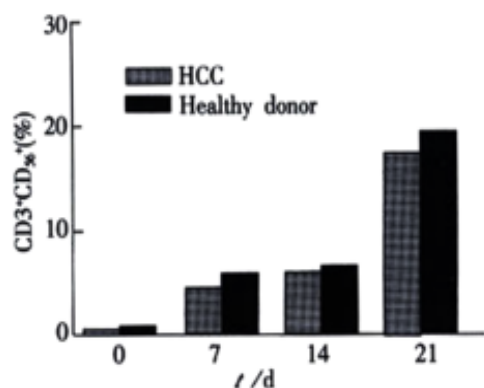


Figure 1B The percentages of double CD3⁺ CD56⁺ positive cells at various incubation time *in vitro* culture system

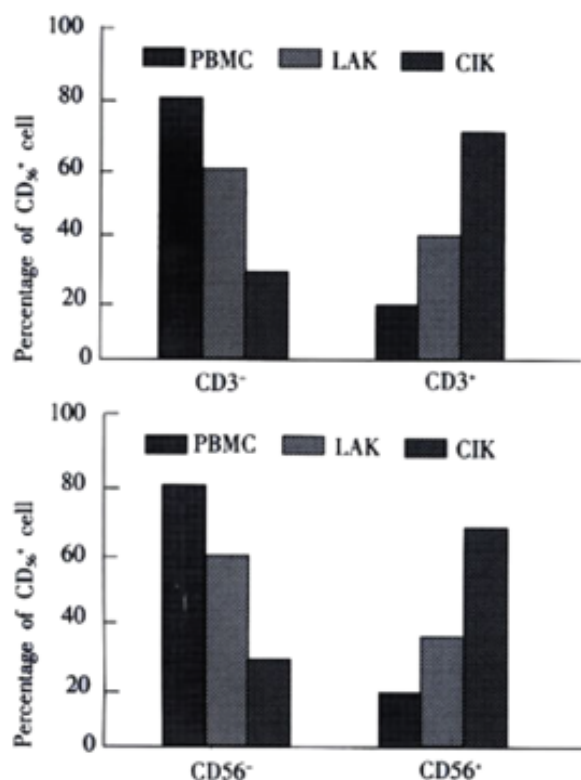


Figure 2 Subsets of CIK cells from patients with primary HCC. CIK cells were

counterstained for CD3 and CD56 at day 12 of CIK generation and the percentage of positively stained cells was determined by flow cytometry. PBMC and LAK were stained like CIK cells. LAK cells were used at day 6 of generation. Upper. CD56⁺ subsets of CIK cells, LAK, PBMC. Subsets of CD56⁺ cells were compared to the total number of CD56⁺ cells. The figure represents data from three different experiments. Results are presented as mean value ± SEM. Lower. CD3⁺ subsets of CIK cells, LAK, PBMC. Subsets of CD3⁺ cells were compared to the total number of CD3⁺ cells. The figure represents data from three different experiments. Results are presented as mean value ± SEM.

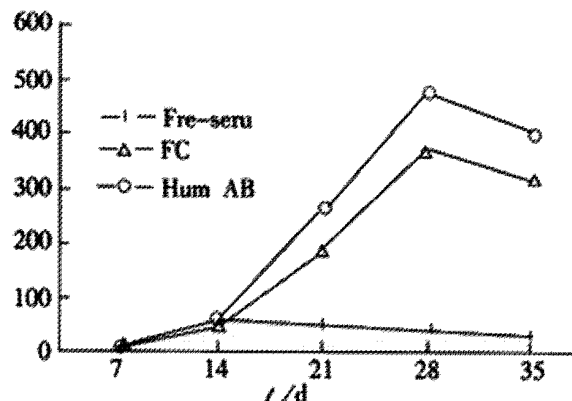


Figure 3 Effects of different culture system on growth of CIK cells

Cytotoxic activity of CIK cells on primary HCC cells

The CIK cell subpopulations were tested for cytotoxicity against the HCC cells as measured by ⁵¹Cr release. The primary HCC cells were used as the target cells and the CIK cells from the same patients with HCC as the effector cells. Both of them at various ratios of effector cells to target cells were mixed together for evaluation of the cytotoxic activity of CIK cells. CD3⁺/CD56⁺ T cells were identified to be the major cytolytic effectors, as previously reported, the CD3⁺/CD56⁺ subpopulation of CIK cells exhibited maximum ⁵¹Cr release cytotoxicity toward target cells (Figure 4) with the increased ratio of effector and target cells, the cytotoxic effects of CIK cells correspondingly became stronger. In controls, PBMC cells only showed a weaker cytotoxic effect on primary HCC cells compared with CIK cells, and maintained at a lower platform level even if the ratio of effector and target cells increased.

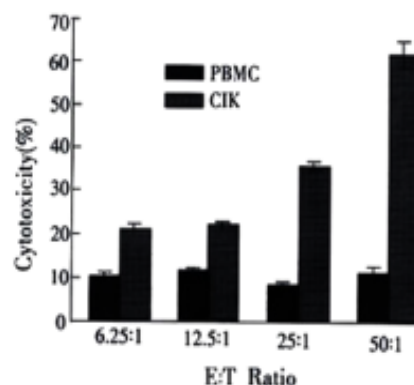


Figure 4 Cytotoxic activity of CIK, PBMC cells against primary HCC cells

Inhibitory effects of CIK cells on HCC in tumor-bearing nude mice

Inhibitory effects of CIK cells on HCC cells in tumor-bearing nude mice are summarized in Table 2. In CIK-treated group, 15 nude mice were inoculated with tumor cells and received treatment of CIK cells for six day consecutively. Tumorigenesis was found in ten of fifteen (66.7%) nude mice. However, tumorigenesis was formed in all the mice in PBMC and LAK treated groups. Furthermore, the tumor size was smaller and limited in the mice of CIK-treated group as compared with those in the mice of PBMC- and LAK-treated groups. There was an obvious difference between the CIK group and LAK group

($P<0.05$), and between CIK group and PBMC group ($P<0.01$), which suggest that CIK cells have a great priority of inhibitory effects on tumorigenesis in tumor-bearing nude mice as compared with LAK cells.

Table 2 Inhibitory effects of CIK, PBMC and LAK cells on HCC cells in tumor-bearing nude mice

Group	n	Tumor/g	Tumorigenesis (%)	Inhibitory rate (%)
Control	9	2.10±0.41	100	0
PBMC	11	1.32±0.27	100	37.1
LAK	11	0.99±0.33	100	52.8
CIK	15	0.32±0.31	66.7	84.7 ^{ab}

^a $P<0.05$ vs LAK group, ^b $P<0.01$ vs PBMC group.

DISCUSSION

In this study, we found that autologous CIK cells had a higher proliferation rate and enhanced cytotoxic activity compared with lymphokine-activated killer cells^[5,26,27]. The CIK cells from the primary HCC patients had a lower proliferation ability than that from the healthy donors though no obvious difference was found in the phenotype and components of CIK cells between the two groups. Interestingly, the cytotoxic activity of CIK cells from healthy donors was proved to be stronger than that from the patients with primary HCC. This results might reflect the functions of CIK cells in HCC patients is probably inhibited to some content by itself, which is consistent with the fact that there is a decreased function of peripheral blood dendritic cells in patients with primary HCC^[28,29]. Whether the dysfunctional dendritic cells led to the decreased proliferation and function of CIK cells? Martin et al reported that CIK cells significantly increased the cytotoxic activity after co-cultured with autologous dendritic cells, and they considered this phenomenon to be induced by IL-12 cytokine secretion from dendritic cells and cell-cell interactions between the two population^[5].

Though LAK cells recognize and kill target cells by a non-MHC restricted mechanism in the same way like CIK cells, the CIK cells were found to have the greatest lytic activity^[5]. Our results suggested that the CIK effector cells are the subpopulation coexpressing CD3⁺/CD56⁺ phenotypes, which supported the facts that CIK cells possessed a higher proliferation rate and higher antitumor cytotoxic activity in vitro than LAK cells^[26,30,31].

Immunological effector cells involved in cell-mediated cytotoxicity, such as CIK cells, cytotoxic T lymphocytes (CTLs) and natural killer (NK) cells, possess cytoplasmic granules that are involved in target cell death. These granules contain a pore-forming protein called perforin or cytolytic, a family of serine esterases (granzymes), lysosomal enzymes, and proteoglycan molecules. The cytolysis of tumor cells produced by CIK effector cells might be mediated by the local direct exocytosis of cytoplasmic granules that penetrate the cell membrane of the bound target cell. Stimulation of CIK cells with tumor cells or anti-CD3 mAb is sufficient for exocytosis of cytotoxic material. The detailed mechanism by which these effector cells recognize tumor cell targets has remained elusive. However, leukocyte function associated antigen-1 (LFA-1) and intercellular adhesion molecule-1 (ICAM-1) appears to be involved. CIK cells do not express the CD16 (Fc receptor) surface molecule, and therefore do not participate in antibody-dependent cellular cytotoxicity (ADCC). The CD3⁺/CD56⁺ cell subpopulation is derived from T cells. The cytotoxic effects of CIK cells against tumor cell targets are blocked by antibodies against the adhesion receptor LFA-1 and its counter receptor, ICAM-1, indicating that the adhesion molecule LFA-1 responsible for cellular interaction is necessary for CIK cell-mediated cytotoxicity. Cognate tumor cell targets could also induce BLT esterase release from CIK cells. These observations showed that the cellular interaction involving LFA-1 is important for cytolysis of target cells by the CIK cells. The mechanism of exocytosis of cytoplasmic granules leading to cytolysis of the target

cell is still unclear. Based on the previous reports, the pathway by which CIK cells can kill target cells, is probably dependent on LFA-1, which probably leads to a granule-dependent cytolysis and is usually the dominant one and accounts for CIK cell cytotoxicity against HCC target cells mediated by CIK recognition structures. Identification of the putative CIK receptors for tumor cell targets as well as other cell surface molecules involved in these cytotoxicity mechanisms will be extremely useful for further understanding of non-MHC-restricted lymphocyte cytotoxicity against tumor cells^[5,21,32, 33].

Our study showed that the human CIK cells could eradicate 84.7% of the established human hepatoma tumor in nude mice and had no toxic side effects, which is consistent with the reports described before^[5,30,31]. In addition, CIK cells have an important property of efficiently killing the resistant tumor cells with overexpression of p-glycoprotein^[33,34]. Recent studies proved that the activity of CIK cells killing tumor cells in a non-MHC restricted way could be enhanced by co-culture with dendritic cells or by using the bispecific antibody. In summary, CIK cells may have a major impact on the adoptive immunotherapeutic protocols for patients with primary HCC^[35,36].

REFERENCES

- Zoll B, Lefterova P, Csapai M, Finke S, Trojanek B, Ebert O, Micka B, Roigk K, Fehlinger M, Schmidt-Wolf GD, Huhn D, Schmidt-Wolf IG. Generation of cytokine-induced killer cells using exogenous interleukin-2, -7, or -12. *Cancer Immunol Immunother* 1998; 47: 221-226
- Du QY, Wang FS, Xu DP, Liu H, Lei ZY, Liu MX, Wang YD, Chen JM and Wu CT. Cytotoxic effects of CIK against hepatocellular carcinoma cells in vitro. *Shijie Huaren Xiaohua Zazhi* 2000; 8: 863-866
- Maki G. Ex vivo purging of stem cell autografts using cytotoxic cells. *J Hematother Stem Cell Res* 2001;10:545-551
- Lu PH, Negrin RS. A novel population of expanded human CD3⁺CD56⁺ cells derived from T cells with potent in vivo anti-tumor activity in mice with potent severe combined immunodeficiency. *J Immunol* 1994; 153: 1687-1696
- Marten A, Renoth S, von Lilienfeld-Toal M, Buttgerit P, Schakowski F, Glasmacher A, Sauerbruch T, Schmidt-Wolf IG. Enhanced lytic activity of cytokine-induced killer cells against multiple myeloma cells after co-culture with idiotype-pulsed dendritic cells. *Haematologica* 2001; 86:1029-1037
- Shi Y, Yu J, Cen X, Zhu P, Ma M. Large-capacity expanded cytotoxic-induced killer cells and its cytotoxic activity. *Shengwu Yixue Gongchengxue Zazhi* 2001; 18:94-96
- Alvarnas JC, Linn YC, Hope EG, Negrin RS. Expansion of cytotoxic CD3⁺ CD56⁺ cells from peripheral blood progenitor cells of patients undergoing autologous hematopoietic cell transplantation. *Biol Blood Marrow Transplant* 2001; 7:216-222
- Hoffman DM, Gitlitz BJ, Belldgrun A, Figlin RA. Adoptive cellular therapy. *Semin Oncol* 2000; 27: 221-233
- Andreesen R, Hennemann B, Krause SW. Adoptive immunotherapy of cancer using monocyte-derived macrophages: rationale, current status, perspectives. *J Leukoc Biol* 1998; 64: 419-426
- Zhou HG, Gu GW. Study of molecular epidemiology in hepatocellular carcinoma in China. *Shijie Huaren Xiaohua Zazhi* 1998; 6:432-434
- Chen HB, Zhang JK, Huang ZL, Sun JL, Zhou YQ. Effects of cytokines on dendritic cells against human hepatoma cell line. *Shijie Huaren Xiaohua Zazhi* 1999;7:191-193
- Li MS, Yuan AL, Zhang WD, Liu SD, Lu AM, Zhou DY. Dendritic cells induce the enhancement of immune reactions against hepatocellular carcinoma cells in vitro. *Shijie Huaren Xiaohua Zazhi* 1999;7:161-163
- Ma CH, Sun WS, Cao YL, Zhang LN, Song J. Coinhibitory effect of recombinant tumor necrosis factor α and mutant interleukin-2 on H7402. *Huaren Xiaohua Zazhi* 1998;6:97-98
- He P, Tang ZY, Ye SL, Liu BB. Relationship between expression of α fetoprotein messenger RNA and some clinical parameters of human hepatocellular carcinoma. *World J Gastroenterol* 1999;5:111-115
- Lee JH, Ku JL, Park YJ, Lee KU, Kim WH, Park JG. Establishment and characterization of four human hepatocellular carcinoma cell lines containing hepatitis B virus DNA. *World J Gastroenterol* 1999;5:289-295
- Kong XB, Yang ZK, Liang LJ, Huang JF, Lin HL. Overexpression of P-glycoprotein in hepatocellular carcinoma and its clinical implication. *World J Gastroenterol* 2000; 6:134-135
- Yang DH, Zhang MQ, Du J, Xu C, Liang QM, Mao JF, Qin HR, Fan ZR. Inhibitory effect of IGF- α antisense RNA on malignant phenotype of hepatocellular carcinoma. *World J Gastroenterol* 2000;6:266-267
- Bian HJ, Chen ZN, Deng JL. Direct technetium-99m labeling of anti-hepatoma monoclonal antibody fragment: a radioimmunoconjugate for hepatocellular carcinoma imaging. *World J Gastroenterol* 2000;6:348-352

- 19 Schmidt-Wolf GD, Negrin RS, Schmidt-Wolf IG. Activated T cells and cytokine-induced CD3+CD56+ killer cells. *Ann Hematol* 1997; 74: 51-56
- 20 Finke S, Trojanek B, Lefterova P, Csipai M, Wagner E, Kircheis R, Neubauer A, Huhn D, Wittig B, Schmidt-Wolf IG. Increase of proliferation rate and enhancement of antitumor cytotoxicity of expanded human CD3⁺ CD56⁺ immunologic effector cells by receptor-mediated transfection with the interleukin-7 gene. *Gene Ther* 1998; 5: 31-39
- 21 Ren H, Xing SX, Xu HW, Song YH, Shang XZ, Zhou GS, Tian JX, Li DJ. Initial Study on proliferation of CIK cells and their antitumor activity *in vitro* and *in vivo*. *Zhongguo Zhongliu Shengwu Zhiliao Zazhi* 1999; 6: 17-21
- 22 Zoll B, Lefterova P, Ebert O, Huhn D, Von Ruecker A, Schmidt-Wolf IG. Modulation of cell surface markers on NK-like T lymphocytes by using IL-2, IL-7 or IL-12 *in vitro* stimulation. *Cytokine* 2000;12:1385-1390
- 23 Schmidt-Wolf IG, Finke S, Trojanek B, Denkena A, Lefterova P, Schwella N, Heuft HG, Prange G, Korte M, Takeya M, Dorbic T, Neubauer A, Wittig B, Huhn D. Phase I clinical study applying autologous immunological effector cells transfected with the interleukin-2 gene in patients with metastatic renal cancer, colorectal cancer and lymphoma. *Br J Cancer* 1999; 81:1009-1016
- 24 Carlens S, Gilljam M, Chambers BJ, Aschan J, Guven H, Ljunggren HG, Christensson B, Dilber MS. A new method for *in vitro* expansion of cytotoxic human CD3-CD56⁺ natural killer cells. *Hum Immunol* 2001;62:1092-1098
- 25 Hoyle C, Bangs CD, Chang P, Kamel O, Mehta B, Negrin RS. Expansion of Philadelphia chromosome-negative CD3⁺CD56⁺ cytotoxic cells from chronic myeloid leukemia patients: *in vitro* and *in vivo* efficacy in severe combined immunodeficiency disease mice. *Blood* 1998; 92: 3318-3327
- 26 Zhang JK, Chen HB, Sun JL, Zhou YQ. Effect of dendritic cells on LPAK cells induced at different times in killing hepatoma cells. *Shijie Huaren Xiaohua Zazhi* 1999;7:673-675
- 27 Xiao LF, Luo LQ, Zou Y, Huang SL. Study of the phenotype of PBLs activated by CD28/CD80 and CD2/CD58 and acting with hepatoma cells and the restricted usage of TCR V α gene subfamily. *Shijie Huaren Xiaohua Zazhi* 1999;7:1044-1046
- 28 Kakumu S, Ito S, Ishikawa T, Mita Y, Tagaya T, Fukuzawa Y, Yoshioka K. Decreased function of peripheral blood dendritic cells in patients with hepatocellular carcinoma with hepatitis B and C virus infection. *J Gastroenterol Hepatol* 2000; 15:431-436
- 29 Ninomiya T, Akbar SM, Masumoto T, Horiike N, Onji M. Dendritic cells with immature phenotype and defective function in the peripheral blood from patients with hepatocellular carcinoma. *J Hepatol* 1999;31:323-331
- 30 Flieger D, Kufer P, Beier I, Sauerbruch T, Schmidt-Wolf IG. A bispecific single-chain antibody directed against EpCAM/CD3 in combination with the cytokines interferon alpha and interleukin-2 efficiently re-targets T and CD3+CD56⁺ natural-killer-like T lymphocytes to EpCAM-expressing tumor cells. *Cancer Immunol Immunother* 2000; 49:441-448
- 31 Muller M, Scheffold C, Lefterova P, Huhn D, Neubauer A, Schmidt-Wolf IG. Potential of autologous immunologic effector cells for prediction of progression of disease in patients with chronic myelogenous leukemia. *Leuk Lymphoma* 1998; 31:335-341
- 32 Verneris MR, Kornacker M, Mailander V, Negrin RS. Resistance of *ex vivo* expanded CD3+CD56⁺ T cells to Fas-mediated apoptosis. *Cancer Immunol Immunother* 2000; 49:335-345
- 33 Schmidt-Wolf IG, Lefterova P, Johnston V, Scheffold C, Csipai M, Mehta BA, Tsuruo T, Huhn D, Negrin RS. Sensitivity of multidrug-resistant tumor cell lines to immunologic effector cells. *Cell Immunol* 1996; 169: 85-90
- 34 Wang FS, Kobayashi H, Liang KW, Ohnuma T, Holland FJ. Retrovirus-mediated transfer of anti-MDR1 ribozymes fully restores chemosensitivity of P-glycoprotein-expressing human lymphoma cells. *Human Gene Therapy* 1999; 10: 1185-1195
- 35 Toporski J, Gorczynska E, Kalwak K, Turkiewicz D, Nowakowska B, Ryczan R, Boguslawska-Jaworska J. Double haploidentical transplantation of hematopoietic progenitor cells in a boy with myelodysplastic syndrome. *Pediatr Hematol Oncol* 1999;16:257-261
- 36 Lefterova P, Marten A, Buttgerit P, Weineck S, Scheffold C, Huhn D, Schmidt-Wolf IG. Targeting of natural killer-like T immunologic effector cells against leukemia and lymphoma cells by reverse antibody-dependent cellular cytotoxicity. *J Immunother* 2000; 23:304-310

Edited by Ma JY

• LIVER CANCER •

The promoting molecular mechanism of alpha-fetoprotein on the growth of human hepatoma Bel7402 cell line

Meng-Sen Li, Ping-Feng Li, Shi-Peng He, Guo-Guang Du, Gang Li

Meng-Sen Li, Department of Biochemistry, Hainan Medical College, Haikou 571101, Hainan Province, China

Ping-Feng Li, Guo-Guang Du, Gang Li, Department of Biochemistry and Molecular Biology, Health Science Center, Peking University, Beijing 100083, China

Shi-Peng He, Department of Biophysics, Health Science Center, Peking University, Beijing 100083, China

Supported by National Natural Science Foundation of China, No. 39760077

Correspondence to: Gang Li and Ping-Feng Li, Department of Biochemistry and Molecular Biology, Health Science Center, Peking University, Beijing 100083, China. ligang55@263.net or 55ligang@163.com
Telephone: +86-10-62092454

Received 2002-01-26 Accepted 2002-03-05

Abstract

AIM: The goal of this study was to characterize the AFP receptor, its possible signal transduction pathway and its proliferative functions in human hepatoma cell line Bel 7402.

METHODS: Cell proliferation enhanced by AFP was detected by MTT assay, ^3H -thymidine incorporation and S-stage percentage of cell cycle analysis. With radioactive labeled ^{125}I -AFP for receptor binding assay; cAMP accumulation, protein kinase A activity were detected by radioactive immunosorbent assay and the change of intracellular free calcium ($[\text{Ca}^{2+}]_i$) was monitored by scanning fluorescence intensity under TCS-NT confocal microscope. The expression of oncogenes N-ras, p53, and p21^{ras} in the cultured cells *in vitro* were detected by Northern blotting and Western blotting respectively.

RESULTS: It was demonstrated that AFP enhanced the proliferation of human hepatoma Bel 7402 cell in a dose dependent fashion as shown in MTT assay, ^3H -thymidine incorporation and S-phase percentage up to 2-fold. Two subtypes of AFP receptors were identified in the cells with Kds of $1.3 \times 10^{-9} \text{ mol.L}^{-1}$ and $9.9 \times 10^{-8} \text{ mol.L}^{-1}$ respectively. Pretreatment of cells with AFP resulted in a significant increase (625%) in cAMP accumulation. The activity of protein kinase A activity were increased up to 37.5, 122.6, 73.7 and 61.2% at treatment time point 2, 6, 12 and 24 hours. The level of intracellular calcium were elevated after the treatment of alpha-fetoprotein and achieved to 204% at 4min. The results also showed that AFP (20 mg.L^{-1}) could upregulate the expression of N-ras oncogenes and p53 and p21^{ras} in Bel 7402 cells. In the later case, the alteration were 81.1%(12h) and 97.3%(12h) respectively compared with control.

CONCLUSION: These results demonstrate that AFP is a potential growth factor to promote the proliferation of human hepatoma Bel 7402 cells. Its growth-regulatory effects are mediated by its specific plasma membrane receptors coupled with its transmembrane signaling transduction through the pathway of cAMP-PKA and intracellular calcium to regulate the expression of oncogenes.

Li MS, Li PF, He SP, Du GG, Li G. The promoting molecular mechanism of alpha-fetoprotein on the growth of human hepatoma Bel7402 cell line. *World J Gastroenterol* 2002;8(3):469-475

INTRODUCTION

Alpha-fetoprotein (AFP) is an oncofetal protein normally produced in the fetal liver and yolk sac, whose higher serum level is a useful marker for hepatocellular carcinoma and yolk sac tumors. Although the physicochemical and structural properties of this 70-kDa glycoprotein have been largely documented, its pathophysiological functions were limited in *in vitro* studies. In the last decade, the growth regulatory properties of AFP have aroused interest as a result of studies involving ontogenetic and oncogenic growth in both cell culture and animal models^[1-3]. A myriad of studies has now described that AFP is capable of regulating growth in ovarian, placental, uterine, hepatic phagocyte, bone marrow, and lymphatic cells^[4] in addition to various neoplastic cells^[5]. This suggests that AFP is not merely a fetal form of albumin-like carrier protein and a marker for cancer and fetal disorders, but should rather now be considered as a potential factor associated with the regulation of growth, differentiation, regeneration, apoptosis and transformation in both ontogenetic and oncogenic growth processes. Although it is currently thought that a 62- to 67-kDa membrane protein on the surface of monocytes and phagocytes is specific for AFP binding^[6,7], the properties of the binding sites were still unknown in most tumor cell lines. Furthermore, few studies have focused on its intracellular signaling events and gene expression. The goal of this study is to characterize the AFP receptor, its possible signal transduction pathway and its proliferative functions in human hepatoma Bel 7402 cells.

MATERIALS AND METHODS

Reagents

Purified AFP was from Sigma (USA). Monoclonal antibody against AFP (anti-AFP) was prepared in this laboratory and used to block AFP. The cAMP kit and Na^[125I] were purchased from Amersham, UK. Fluo-3 AM was from BIORAD (USA). Monoclonal antibodies for p53 and p21 were purchased from MBI (USA).

Purification of human AFP Human AFP was prepared as previously described^[8]. Briefly, human cord blood AFP was precipitated by ammonium sulphate and passed through an anti-AFP affinity chromatography column. AFP-positive fractions were collected and concentrated. The purity of prepared AFP was 92.7% as determined by sodium dodecyl sulfate-polyacrylamide gel electrophoresis. The protein was stored at -80°C until use.

Effect of AFP on the cell proliferation Total 1.5×10^4 cells per well of Bel 7402 cells were plated into 96-well plates and cultured in RPMI 1640 medium supplemented with 10% fetal calf serum (FCS) at 37°C in a humidified atmosphere of 5% CO₂ for 48h. The cultures were replaced with medium without FCS for another 24h, and treated with different concentration of AFP ($1-80 \text{ mg.L}^{-1}$) for 48h. The effects of AFP on the proliferation of cells were measured by MTT assay and ^3H -Thymidine incorporation, which were performed following a regular procedure.

Effect of AFP on the cell cycle First, 3×10^4 cells per well of Bel 7402 cells were plated into 6-well plates. Culture and AFP treatment were then performed as described above. After being treated

for 24h, the cells were digested with 0.25% trypsin/0.02% EDTA and washed three times with PBS. A final density of 1×10^6 cells in 1ml was added 20 μ l (10mg.mL⁻¹) RNase (Promega USA) solution and incubated at 37°C for 30min. The effects of AFP on the cell cycle were detected with flow cytometry.

AFP receptor binding assay Bel-7402 cells were maintained in a humidified atmosphere of 5% CO₂ at 37°C in RPMI-1640 medium supplemented with 10% FCS. The cells were initially depleted of serum for 12h and then washed with cold medium. Resuspended cells were passed through a 300-mesh screen and adjusted to 1×10^6 cells per ml. ¹²⁵I-AFP was radioiodinated by the iodogen method and run through a column of Sephadex-G25 to remove free ¹²⁵I. The specific activity of ¹²⁵I-AFP was 2715 Ci per mmol and the purity of radioactivity ratio was 99.4%. Each reaction contained 7 $\times 10^5$ cells, ¹²⁵I-AFP of 5 $\times 10^4$ cpm and different concentrations of non-labeled AFP (0.25-64.5ng). The reaction was triplicated and performed at 4°C for 2h. All samples were collected onto glassfiber membrane (presaturated with 0.5% albumin) and washed three times with 15ml of PBS. The radioactivity of ¹²⁵I was detected by a γ -counter. Human serum albumin (HSA) as a non-labeled ligand was utilized for measuring IC₅₀. The parameters of binding were ed using a program of Radioligand Binding Assay of Receptors (RBA).

Extraction and measurement of cAMP The cells were adjusted to 4 $\times 10^4$ cells per ml and cultured in 24 well plates. After 24h incubation, the cells were collected and resuspended in the medium supplemented with 0.1% egg albumin and 25mmol.L⁻¹ of HEPES (pH 7.4) and 2mmol.L⁻¹ IBMX (3-methyl-1-isobutyl-xanthine) at 37°C for 15min. AFP (20mg.L⁻¹) and/or anti-AFP (40mg.L⁻¹) was added into each well respectively for 4h. Extraction of cAMP was performed according to the method described by Iwashia^[9]. In short, the supernatant was removed and replaced with 1ml of cold PBS per well. After wash, the pellet was frozen in -80°C for 30min and then 0.5ml of HCl (0.05N) was added into each well for another 30min. The samples were thawed and spun at 10000g for 5min. The supernatants were lyophilized, and the content of cAMP was measured by the radio immunoassay following the instruction of cAMP assay kit.

Determination of protein kinase A activity Total 4 $\times 10^5$ cells per well were cultured in 24-well plates for 48h, changed to fresh medium without FCS for another 24h, and then treated with either AFP (20mg.L⁻¹), anti-AFP (40mg.L⁻¹) or AFP (20mg.L⁻¹) plus anti-AFP (40mg.L⁻¹) respectively. After 2, 6, 12 and 24h treatment, the cells were washed and resuspended in 1ml PBS. The measurement of PKA activity has been described by Plet^[10]. Briefly, 40 μ l of cell extract was mixed with 160 μ l of the reaction mixture at the final concentration of 20mmol.L⁻¹ Tris-HCl (pH 7.5), 5mmol.L⁻¹ MgCl₂, 0.25g.L⁻¹ BSA, 0.5g.L⁻¹ histone, 2 $\times 10^{-7}$ mol.L⁻¹ ATP (γ -³²P ATP, 3.7 $\times 10^4$ Bq) and 8.0 μ mol.L⁻¹ cAMP at 37°C for 10min. Followed by incubation on ice for 5min, the reaction mixture was filtered through Whatmen GF/C filter, washed with 10% TCA-2% phosphoric acid and 5% TCA for 30min. The radioactivities were measured by a liquid scintillation counter, and PKA activity was expressed as pmol value of ³²P in histone catalyzed by per mg protein per min.

Determination of intracellular calcium concentration The cell suspension was dispensed into specific culture plates at a density of 2 $\times 10^4$ cells per ml and incubated at 37°C in a humidified atmosphere of 5% CO₂ for 48h. The supernatant was removed and replaced with medium without FCS for 6h, followed by washing three times with Hank's solution. The measurement of intracellular calcium concentration has been described by Tsugorka and Petti *et al*^[11,12]. Briefly, the cells were loaded with 10ml of Fluo-3AM in Hank's solution at a final concentration of 5 μ mol.L⁻¹ and incubated at 37°C

for 30min. After washing 3 times with Hank's solution, either AFP (20mg.L⁻¹) or anti-AFP (40mg.L⁻¹) was loaded into each well. The change of intracellular free calcium ([Ca²⁺]_i) was monitored by scanning fluorescence intensity under TCS-NT confocal microscopy every 10s.

RNA isolation and Northern blotting Cells were treated with either AFP (20mg.L⁻¹), anti-AFP (40mg.L⁻¹) or AFP (20mg.L⁻¹) plus anti-AFP(40mg.L⁻¹) for 24h. Total cellular RNA was isolated from cell lines with TRIzol reagent(Promega, Madison,WI, U.S.A) according to the manufacturer's protocol. RNA (10-20 μ g/lane),quantitated by absorbance at 260nm, and fractionated by eletrophoresis through a 1% formaldehyde agarose gel, and the fractionated RNA was transferred(in 20 \times SSC) to nitrocellulose membranes(Millipore corporation Bedford, MA; U.S.A), by standard procedure^[13] These membranes were hybridized with a ³²P labeled probe and washed using standard protocol. The membranes were then exposed to X-ray film at -70°C for varying periods of time.

Western blot analysis Cells were treated with either AFP (20mg.L⁻¹), anti-AFP (40mg.L⁻¹) or AFP (20mg.L⁻¹) plus anti-AFP(40mg.L⁻¹) for 24h. After three times wash, the cells in each reaction were lysed in 10 μ l of lysis buffer containing 0.2% Triton X-100, 500mmol.L⁻¹ NaCl, 500mmol.L⁻¹ sucrose, 1mmol.L⁻¹ EDTA, 0.15mmol.L⁻¹ spermine, 0.5mmol.L⁻¹ spermidine, 10mmol.L⁻¹ HEPES (pH 8.0), 200 μ mol.L⁻¹ phenylmethylsulfonyl fluoride, 2mg leupeptin.L⁻¹, 2mg pepstatin.L⁻¹, 24 IU aprotinin.ml⁻¹ and 7mmol.L⁻¹ γ -mercaptoethanol. 40 μ g proteins were subjected to sodium dodecyl sulfate-polyacrylamide gel electrophoresis (SDS-PAGE) and transferred to PVDF membrane for immunodetection. SDS- PAGE molecular weight markers (Bio-Rad) verified the correct location of the visualized bands. The membranes were blocked in 5% nonfat milk (w/v) in PBS-Tween, then probed with anti-p53 or anti-p21 and followed by secondary antibodies (goat anti-mouse Ig-alkaline phosphatase). Immunoreactive proteins were detected using color development system (NBT/BCIP).

Statistical analysis Data were analyzed by t test and expressed as mean \pm SD based on 3 or 4 independent experiments.

RESULTS

Effect of AFP on the cell proliferation

Pretreating Bel 7402 cells with AFP (1-80mg.L⁻¹) resulted in a dose-dependent increase in cell proliferation (Figure 1). The increase was about 2-fold at a dose of 80mg.L⁻¹ as compared to the control (0mg.L⁻¹). The effects of AFP (20mg.L⁻¹) on cell proliferation could be blocked by anti-AFP (40mg.L⁻¹) which was observed both in MTT assay and ³H-Thymidine incorporation (Figure 2). The increase was not observed in the HSA-treated group and non-treatment control. Flow cytometric analysis showed that AFP (20mg.L⁻¹) pretreatment increased the S phase cell population by 59.3% of Bel 7402 cells (Table 1).

Table 1 The effects of AFP on the cell cycle progression. Bel 7402 cells maintained in RPMI 1640 medium were respectively treated with either AFP (20mg.L⁻¹), anti-AFP (40mg.L⁻¹), AFP (20mg.L⁻¹) + anti-AFP (40mg.L⁻¹) or HSA (20mg.L⁻¹) for 24 hours. The effects of AFP on the cell cycle progression were analyzed by flow cytometry. The data represented the mean values of four independent experiments performed each in triplicate

Groups	G ₁ (%)	S (%)	G ₂ +M (%)
Conrtol	37.0 \pm 3.0	42.7 \pm 2.8	19.2 \pm 1.8
AFP	20.3 \pm 1.6 ^a	68.0 \pm 4.2 ^a	12.7 \pm 1.3 ^a
AFP+anti-AFP	32.0 \pm 2.1	48.8 \pm 2.51	9.2 \pm 1.3
anti-AFP	34.61 \pm 1.9	45.8 \pm 2.5	19.6 \pm 1.9
HSA	36.9 \pm 4.3	43.2 \pm 2.6	19.9 \pm 2.4

^aP<0.05 vs control group

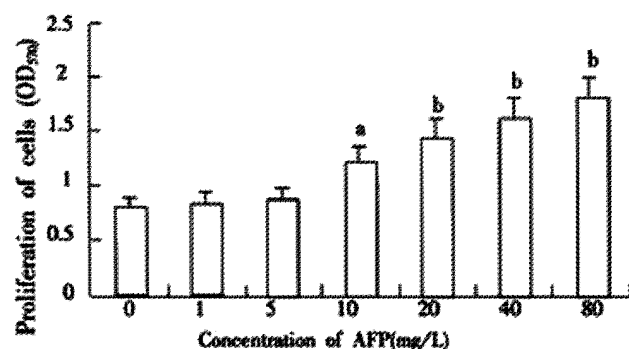


Figure 1 The effects of different concentration of AFP on the proliferation of cells. Bel 7402 cells were incubated with different concentrations of AFP for 48h and the cell proliferation was measured by MTT assay. The data represented the mean values of six independent experiments performed each in triplicate. ^a $P < 0.05$ and ^b $P < 0.01$ vs control (0mol.L⁻¹).

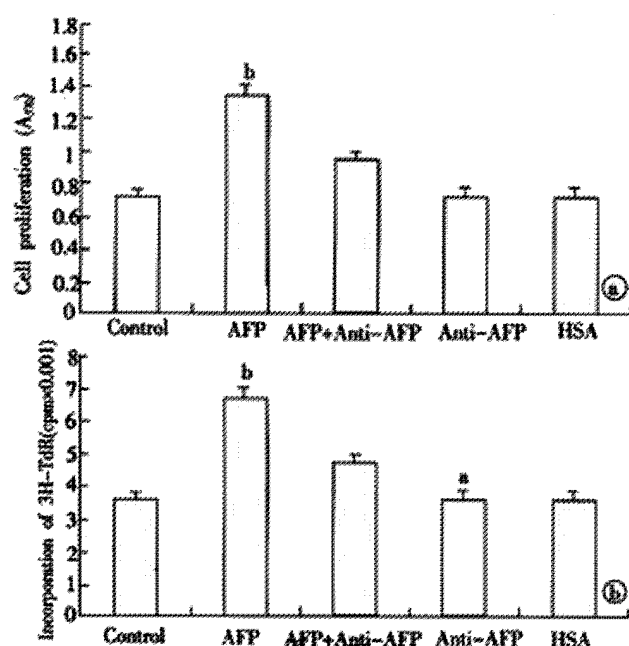


Figure 2 The blockage of anti-AFP to the effect of AFP on the proliferation of cells. A. The data of MTT assay. B. The data of ³H-TdR incorporation. The cells were respectively treated with either AFP (20mg.L⁻¹), anti-AFP (40mg.L⁻¹), AFP (20mg.L⁻¹) + anti-AFP (40mg.L⁻¹) or HSA (20mg.L⁻¹) for 48h. (MTT assay) or 18h (³H-TdR incorporation). The data represented the mean value of four independent experiments performed each in triplicate. ^a $P < 0.05$ and ^b $P < 0.01$ vs control (0mol.L⁻¹).

Distribution of AFP receptor on the membranes of Bel 7402 cells

The binding sites of AFP on the surface of the cells and K_d values were calculated based on Scatchard plot analysis of ¹²⁵I-AFP. Scatchard analysis showed that there were two classes of receptors with different affinities on Bel 7402 cells. As for Bel 7402 cells, K_{D1} with 89400 sites per cell was 1.3×10^{-9} mol.L⁻¹ and K_{D2} with 582000 sites per cell was 9.9×10^{-8} mol.L⁻¹ (Figure 3). To indicate a higher affinity of the binding sites for AFP, IC₅₀ was calculated to achieve 50% inhibition. More than two fold of HSA were needed compared with AFP (data not shown), which indicated a higher affinity for the binding sites on the surface of cells to AFP.

Effect of AFP on intracellular camp

AFP markedly elevated the concentration of cAMP up to 625% in Bel 7402 cells (Figure 4). Anti-AFP could not alter the concentrations of

cAMP when added alone, but it reversed the effect of AFP. As a control, HSA did not influence the content of cAMP.

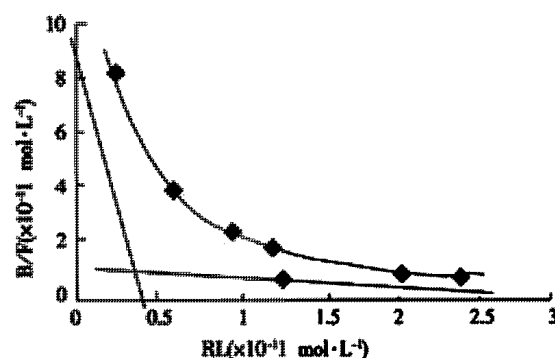


Figure 3 Scatchard analysis of ¹²⁵I-AFP binding to Bel 7402 cells. The properties of AFP receptor in Bel 7402 cells was detected with receptor binding assay and analyzed by a program of Radioligand Binding Assay of Receptor. The data were selected from three independent experiments.

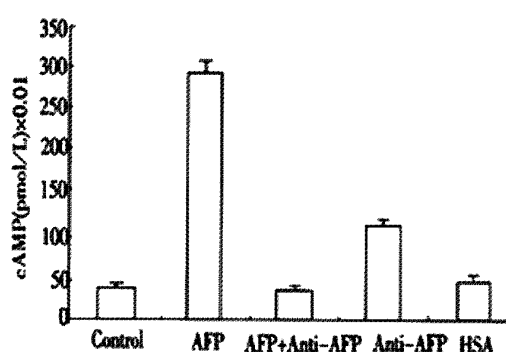


Figure 4 The effects of AFP on the cAMP concentration in cytosol of human hepatoma Bel 7402 cells. 4×10^4 cells were respectively treated with AFP (20mg.L⁻¹), anti-AFP (40mg.L⁻¹), AFP (20mg.L⁻¹) + anti-AFP (40mg.L⁻¹) or HSA (20mg.L⁻¹). The data represented the mean values of four independent experiments performed each in triplicate. ^b $P < 0.01$ vs control (0mol.L⁻¹).

Effect of AFP on PKA activity

The activities of PKA in the cytosol of Bel 7402 cells were obviously elevated after being treated with AFP (20mg.L⁻¹) for 2, 6, 12 or 24h (Figure 5). The activities of PKA were increased up to 37.5, 122.6, 73.7 and 61.2% in Bel 7402 cells at each time point. The peak value was achieved at 6h and then declined gradually, but still maintained a higher activity for several hours. Anti-AFP or HSA alone did not affect the activity of PKA in Bel 7402 cells, but anti-AFP could block the effects of AFP on the activity of PKA.

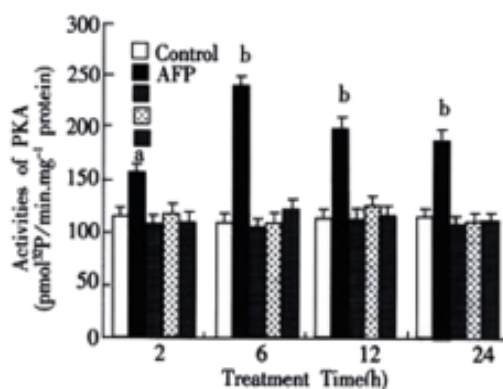


Figure 5 The effects of AFP on the activity of PKA in Bel 7402 cells. 4×10^5 cells per ml were respectively treated with either AFP (20mg.L⁻¹), anti-AFP (40mg.L⁻¹), AFP (20mg.L⁻¹) + anti-AFP (40mg.L⁻¹) or HAS (20mg.L⁻¹) for different time and the activities of intracellular PKA were then detected. The data represented the mean values of four independent experiments performed each in triplicate. ^a $P < 0.05$ and ^b $P < 0.01$ vs control (0mol.L⁻¹).

Determination of intracellular $[Ca^{2+}]_i$ release

Figures 6A1-5 and figure 6B showed that AFP increased the intracellular $[Ca^{2+}]_i$ after treatment of 2, 4, 6, 8 and 10 min in Bel 7402 cells. The

peak was achieved at treatment time 4 min (increment 204.1% in Bel 7402 cells). Anti-AFP and HSA did not change the content of $[Ca^{2+}]_i$ in either cell type. However, anti-AFP could reverse the effect of AFP.

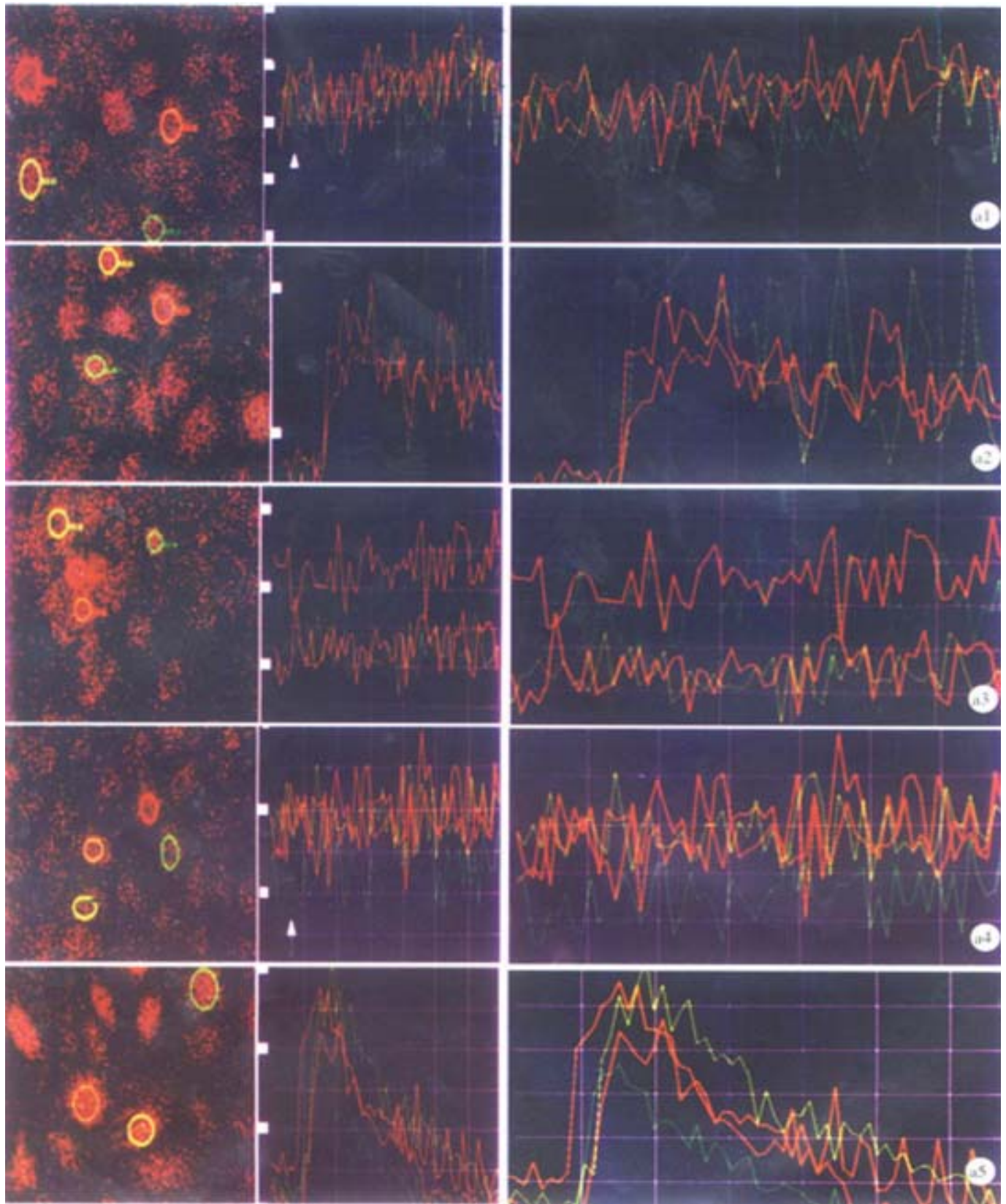


Figure 6A The change of Ca^{2+} concentration in human hepatoma Bel7402 cells was measured by confocal microscopic scanning. Cells were incubated with $5\mu\text{mol.L}^{-1}$ fluo-3/AM at 37°C for 30min and then stimulated with Hank's. (1) AFP(20mg.L^{-1}); (2) HSA(20mg.L^{-1}); (3) Anti-AFP; (40mg.L^{-1}); (4) or AFP(20mg.L^{-1}) + Anti-AFP(40mg.L^{-1}); (5) The arrow indicate the stimulated time point.

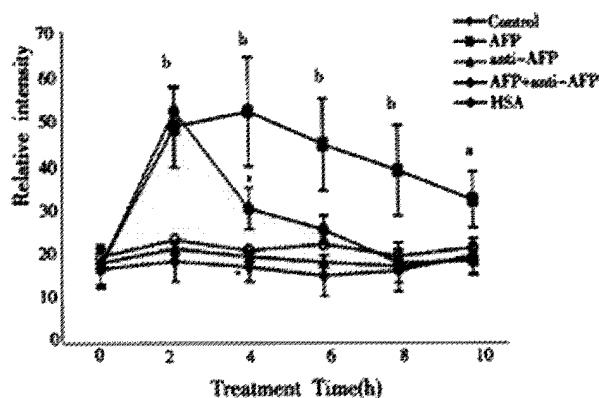


Figure 6B The graph shows the scanning results. The data represented as the mean value of 10 cells \pm s. ^a $P < 0.05$ and ^b $P < 0.01$ vs control (0mol.L⁻¹)

Expression of p53 and p21 proteins

The results in Figure 8 demonstrated the overexpression of mutant p53 and p21 protein in AFP-treated group in Bel 7402 cells. Anti-AFP could reverse the upregulated effects of AFP on the expression of p53 and p21 genes. HSA could not influence the amount of these proteins. Each graph was selected from 3 similar results.

Expression of N-ras mRNA

The results in Figure 7 demonstrated the overexpression of N-ras mRNA in AFP-treated group in the Bel 7402 cells. Anti-AFP could reverse the upregulated effects of AFP on the expression of N-ras mRNA. HSA could not influence the mRNA amount of the oncogene. Each graph was selected from 3 similar results.

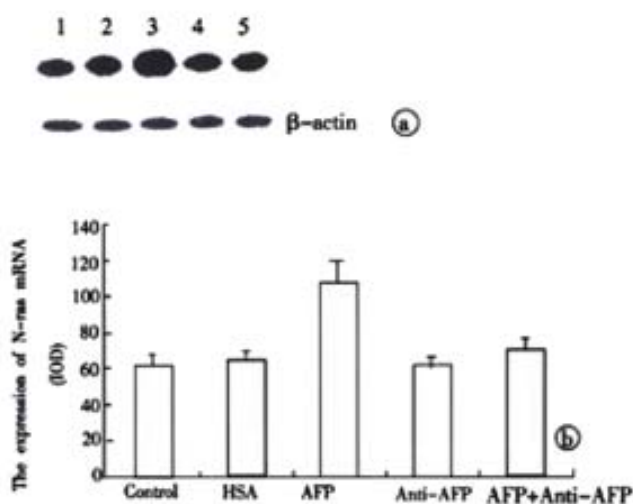


Figure 7 The effects of AFP on the expression of N-ras mRNA in Bel 7402 cells. 1×10^5 cells were respectively treated with AFP (20mg.L⁻¹), anti-AFP (40mg.L⁻¹), AFP (20mg.L⁻¹) + anti-AFP (40mg.L⁻¹) or HSA (20mg.L⁻¹) for 12 hours and expression of N-ras mRNA was detected by Northern blot assay. Lane 1: control group; Lane 2: HSA treated group; Lane 3: AFP treated group; Lane 4: anti-AFP treated group; Lane 5: AFP plus anti-AFP treated group. The data was selected from 3 independent experiments. A: Autoradiograph of Northern blot. B: Quantitated by densitometric scanning of N-ras mRNA expression blot in Bel7402 cells (relative IOD units). The columns represent the means of triplicate determinations \pm s.

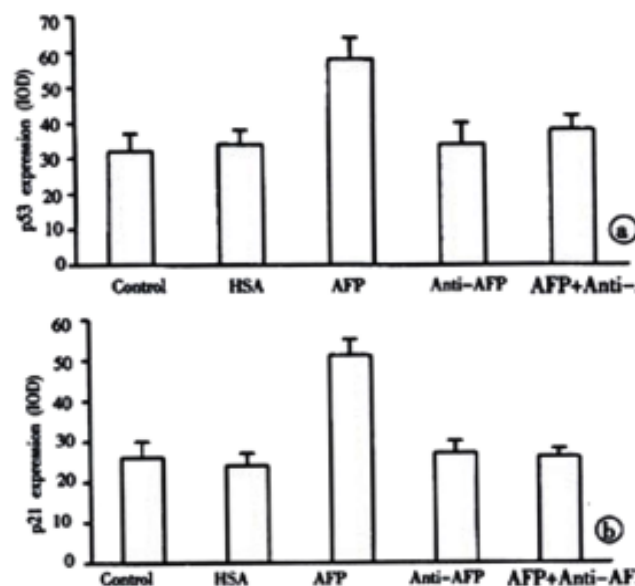
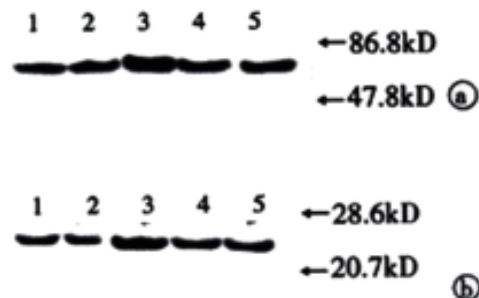


Figure 8 The effects of AFP on the expression of p53 (A) and p21 (B) proteins in Bel 7402 cells. 1×10^5 cells were respectively treated with AFP (20mg.L⁻¹), anti-AFP (40mg.L⁻¹), AFP (20mg.L⁻¹) + anti-AFP (40mg.L⁻¹) or HSA (20mg.L⁻¹) for 24 hours and the expression of p53 and p21 protein were detected by Western blot assay. Lane 1: control group; lane 2: HSA treated group; lane 3: AFP treated group; lane 4: anti-AFP treated group; lane 5: AFP plus anti-AFP treated group. The data was selected from 3 independent experiments. A: p53; B: p21. The columns represent the means of triplicate determinations \pm s.

DISCUSSION

AFP is an onco-developmental gene product. In the adult, AFP is highly expressed during liver regeneration and hepatocarcinogenesis and used as a marker for the diagnosis of hepatocellular carcinoma^[14-16]. The regulation and activation on the expression of the AFP gene have been extensively investigated^[17-21]. Although less data indicated AFP could causes apoptosis in tumor cells^[22,23], the data from most current research demonstrate that AFP is enhancer in tumor growth. The downregulation of expression of alpha-fetoprotein is able to induce the suppression of growth of malignant hepatocyte cell^[24-26]. Although the biological role of AFP in cell growth has been reported^[27-29], the properties of the AFP receptor as well as the subsequent events after AFP binding were still undefined. Our data indicate that a specific AFP receptor does exist in a human tumor cell line, Bel 7402 cells. There were two kinds of receptors with different affinities in Bel 7402 cells ($K_D: 10^{-9}$ and 10^{-8} mol.L⁻¹), which was consistent with similar experiments that characterized the K_D of binding protein in monocytes in the range of 10^{-11} - 10^{-7} mol.L⁻¹^[6,30]. The AFP-binding protein possibly containing the AFP-receptor has been isolated from human

embryos and human breast cancer tissue^[31].

Based on the results of MTT assay, ³H-thymidine incorporation and flow cytometry analysis, as well as the enhanced expression of mutant p53 and p21 and expression of protooncogenes N-ras mRNA, AFP appears to be a potential growth promoting factor.

Since the albumin and AFP genes are similar in structure, they are believed to be derived from a common ancestral gene, even in the same albuminoid gene family. In all our AFP studies, none of the results showed that human serum albumin (HSA) as a control was able to alter the parameters of cell proliferation although it can non-specifically bind to the cell surface.

Little information on the effect of AFP on signal transduction was available. The present experiments demonstrated that intracellular cAMP was significantly elevated 7 fold in Bel 7402 cells. PKA activities were also increased. This indicates that a cAMP-dependent protein kinase pathway is involved in the effects of AFP on the tumor cells, even though some data from other laboratory indicated that the alteration of activity of PKC affected only liver gene expression rather than cell growth in fetal hepatocytes^[32]. Other experiments for the relationship between AFP and message has been tested^[33].

In addition, the results of intracellular calcium showed that AFP markedly increased intracellular [Ca²⁺]_i. It has been reported that Bcl-2 suppresses apoptosis by inhibiting calcium activation of the permeability transition of mitochondria^[34] and the inhibition of calcium influx was related to the suppression of lymphoma cell-line proliferation^[35]. Furthermore, a reciprocal regulation between calcium signaling and hypertrophic growth has been identified^[36]. According to these findings, a higher intracellular [Ca²⁺]_i elicited by AFP may play a role in tumorigenesis.

Although growing evidence has confirmed the effects of AFP on the growth of tumor cells, little work has focused on the subsequent events in the nucleus. The impacts of overexpression of protooncogenes N-ras, mutant p53, p21 and other genes on tumor growth have been largely documented^[37-41]. In the present experiment, mutant p53 and p21 protein were over produced under the treatment of AFP, which was consistent with similar work^[42,43]. It suggested that the mechanism by which elevated levels of mutant p53 and p21 proteins might be involved in AFP-induced oncogenesis.

The pattern inducing the hepatocarcinogenesis is multimodal^[44,45], but the effect of AFP on the growth of tumor has been confirmed. Based on our experiments, the functional mechanism of AFP on the growth of tumors may be attributed, at least in part, to receptor-mediated cAMP pathway and/or calcium signaling resulting in overexpression of certain genes. The clarification of the mechanism will provide a possibility for the gene therapy of liver tumor^[46-48]. Further investigations on the function of AFP may shed further light on the mechanism of AFP action.

ACKNOWLEDGMENT

This work was supported by National Natural Science Foundation of China (1.39760077). We wish to thank Lei Hu, M.D., PhD, Northwestern University, Chicago, USA, for critical reading of the manuscript.

REFERENCES

- Mizejewski GJ, Warner AS. Alpha-fetoprotein can regulate in the uterus of the immature and adult ovariectomized mouse. *J Reprod Fert* 1989; 85: 177-185
- Keel BA, Eddy KB, Cho S, May JV. Synergistic action of purified alpha-fetoprotein and growth factors on the proliferation of porcine granulosa cells in monolayer culture. *Endocrinology* 1991; 129: 217-225
- Wang W, Alpert E. Downregulation of phorbol 12-myristate 13-acetate-induced tumor necrosis factor-alpha and interleukin-1 beta production and gene expression in human monocytic cells by human alpha-fetoprotein. *Hepatology* 1995; 22: 921-928
- Mizejewski GJ. Alpha-fetoprotein as a biologic response modifier: relevance to domain and subdomain structure. *Proc Soc Exp Biol Med* 1997; 215: 333-362
- Dudich E, Semenkova L, Gorbatoeva E, Dudich I, Khromykh L, Tatulov E, Grechko G, Sukhikh G. Growth-regulative activity of human alpha-fetoprotein for different types of tumor and normal cells. *Tumour Biol* 1998; 19: 30-40
- Suzuki Y, Zeng CQ, Alpert E. Isolation and characterization of a specific alpha-fetoprotein receptor on human monocytes. *J Clin Invest* 1992; 90: 1530-1536
- Moro R, Tamaoki T, Wegmann TG, Longnecker BM, Laderoute MP. Monoclonal antibodies directed against a widespread oncofetal antigen: The alpha-fetoprotein receptor. *Tumor Biol* 1993; 14: 116-130
- Nish S, Hiral H. Purification of human, dog and rabbit α -fetoprotein by immunoabsorbents of sepharose couple with anti- human α -fetoprotein. *Biochem et Biophysica ACTA* 1972; 278: 293-298
- Iwashita S, Mitsui KI, Shoji-kasai Y. cAMP-mediated modulation of signal transduction of epidermal growth factor (EGF) receptor system in human epidermoid carcinoma A431 cells. *J Biol Chem* 1990; 265: 10702-10708
- Plet A, Evain-Brion D, Gerbaud P, Anderson WB. Retinoic acid-induced rapid loss of nuclear cyclic AMP-dependent protein kinase in teratocarcinoma cells. *Cancer Res* 1987; 47: 5831-5834
- Tsugorka A, Roise E, Blatter LA. Imaging elementary events of calcium release in skeletal cells. *Science* 1995; 269: 1723-1726
- Petti EJ, Hallett MB. Early Ca²⁺ signaling events in neutrophils detected by rapid confocal laser scanning. *Biochem J* 1995; 310: 445-448
- Sambrook J, Fritsch EF, Maniatis T. Molecular cloning: A laboratory manual, 2nd edition. *Cold spring harbor* 1989; 18:60-75
- Tu DG, Wang ST, Chang TT, Chiu NT, Yao WJ. The value of serum tissue polypeptide specific antigen in the diagnosis of hepatocellular carcinoma. *Cancer* 1999; 85: 1039-1043
- Sell S, Xu KL, Huff WE, Kabena LF, Harvery RB, Dunsford HA. Aflatoxin exposure produces serum alphafetoprotein elevations and marked oval cell proliferation in young male Pekin ducklings. *Pathology* 1998; 30: 34-39
- Yuasa T, Yoshiki T, Ogawa O, Tanaka T, Isono T, Mishima M, Higuchi K, Okada Y, Yoshida O. Detection of alpha-fetoprotein mRNA in seminoma. *J Androl* 1999; 20: 336-340
- Chen H, Egan JO, Chiu JF. Regulation and activities of alpha-fetoprotein. *Crit Rev Eukaryot Gene Expr* 1997; 7: 11-41
- Ohguchi S, Nakatsukasa H, Higashi T, Ashida K, Nouse K, Ishizaki M, Hino N, Kobayashi Y, Uematsu S, Tsuji T. Expression of alpha-fetoprotein and albumin genes in human hepatocellular carcinomas: limitations in the application of the genes for targeting human hepatocellular carcinoma in gene therapy. *Hepatology* 1998; 27: 599-607
- Ishikawa H, Nakata K, Tsuruta S, Nakao K, Kato Y, Tamaoki T, Eguchi K. Differential regulation of albumin gene expression by heparin-binding epidermal growth factor-like growth factor in alpha-fetoprotein-producing and -nonproducing human hepatoma cells. *Tumour Biol* 1999; 20: 130-138
- Abeleu GI, Eraisier TL. Cellular aspects of alpha-fetoprotein reexpression in tumors. *Semin Cancer Biol* 1999; 9: 95-107
- Magge TR, Cai Y, El-Houseini ME, Locker J, Wan YJ. Retinoic acid mediates down-regulation of the alpha-fetoprotein gene through decreased expression of hepatocyte nuclear factors. *J Biol Chem* 1998; 273: 30024-30032
- Dudich I, Tokhtamysheva N, Semenkova L, Dudich E, Hellman J, Korpela T. Isolation and structural and functional characterization of two stable peptic fragments of human alpha-fetoprotein. *Biochemistry* 1999; 38: 10406-10414
- Dudich E, Semenkova L, Dudich I, Gorbatoeva E, Tokhtamysheva N, Tatulov E, Nikolaeva M, Sukhikh G. alpha-fetoprotein causes apoptosis in tumor cells via a pathway independent of CD95, TNFR1 and TNFR2 through activation of caspase-3-like proteases. *Eur J Biochem* 1999; 266: 750-761
- Zhang M, Gong Y, Assy N, Minuk GY. Increased GABAergic activity inhibits alpha-fetoprotein mRNA expression and the proliferative activity of the HepG2 human hepatocellular carcinoma cell line. *J Hepatol* 2000; 32:85-91
- Hamamoto R, Kamihira M, Iijima S. Growth and differentiation of cultured fetal hepatocytes isolated various developmental stages. *Biosci Biotechnol Biochem* 1999; 63: 395-401
- Gruppiso PA, Bienieki TC, Faris RA. The relationship between differentiation and proliferation in late gestation fetal rat hepatocytes. *Pediatr Res* 1999; 46: 14-19
- Wang XW, Xie H. Alpha-fetoprotein enhances the proliferation of human hepatoma cell in vitro. *Life Science* 1999; 64: 17-23
- Wang XW, Xu B. Stimulation of tumor-cell growth by alpha-fetoprotein. *Int J Cancer* 1998; 75: 596-599
- Koide N, Nishio A, Igarashi J, Kajikawa S, Adachi W, Amano J. Alpha-fetoprotein-producing gastric cancer: histochemical analysis of cell proliferation, apoptosis, and angiogenesis. *Am J Gastroenterol* 1999; 94: 1658-1663
- Torres JM, Geuskens M, Uriel J. Activated human T lymphocytes express albumin binding proteins which cross-react with alpha-fetoprotein. *Eur J*

- Cell Biol* 1992; 57: 222-228
- 31 Kanevsky VY, Pozdnyakova LP, Aksenova OA, Severin SE, Katukov VY, Severin ES. Isolation and characterization of AFP-binding proteins from tumor and fetal human tissues. *Biochem Mol Biol Int* 1997; 41: 1143-1151
 - 32 Roncero C, Ventura JJ, Sanchez A, Bois JB, Mesa ML, Thomassin H, Danan JL, Benito M, Fabregat I. Phorbol esters down-regulate alpha-fetoprotein gene expression without affecting growth in fetal hepatocytes in primary culture. *Biochim Biophys Acta* 1998; 1402: 151-164
 - 33 Benassayag C, Rigourd V, Mignot TM, Hassid J, Leroy MJ, Robert B, Civel C, Grange G, Dallot E, Tanguy J, Nunez EA, Ferre F. Does high polyunsaturated free fatty acid level at the feto-maternal interface alter steroid hormone message during pregnancy? *Prostagl Leukot Essent Fatty-Acids* 1999; 60: 393-399
 - 34 Murphy RC, Schneider E, Kinnally KW. Overexpression of Bcl-2 suppresses the calcium activation of a mitochondrial megachannel. *FEBS Lett* 2001; 497: 73-76
 - 35 Anesini C, Ferraro G, Lopez P, Borda E. Different intracellular signals coupled to the antiproliferative action of aqueous crude extract from *Larrea divaricata* Cav. and nor-dihydroguaiaretic acid on a lymphoma cell line. *Phytomedicine* 2001; 8: 1-7
 - 36 Kline R, Jiang T, Xu X, Rybin VO, Steinberg SF. Abnormal calcium and protein kinase C-epsilon signaling in hypertrophied atrial tumor myocytes (AT-1 cells). *Am J Physiol Heart Circ Physiol* 2001; 280: H2761-2769
 - 37 Kirla R, Salminen E, Huhtala S, Nuutinen J, Talve L, Haapasalo H, Kalim H. Prognostic value of the expression of tumor suppressor genes p53, p21, p16 and prb, and Ki-67 labelling in high grade astrocytomas treated with radiotherapy. *J Neurooncol* 2000; 46: 71-80
 - 38 Yuen PW, Lam KY, Choy JT, Ho WK, Wei WI. Clinicopathological significance of p53 and p21 expression in the surgical treatment of laryngeal carcinoma. *Anticancer Res* 2000; 20: 4863-4866
 - 39 Komarova EA, Christov K, Faerman AI, Gudkov AV. Different impact of p53 and p21 on the radiation response of mouse tissues. *Oncogene* 2000; 19: 1791-1798
 - 40 Kumar DD, Kubota H, Tabara H, Kotoh T, Monden N, Igarashi M, Kohno H, Nagasue N. nm23 in the primary and metastatic sites of gastric carcinoma. Relation to AFP-producing carcinoma. *Oncology* 1999; 56: 122-128
 - 41 Yamamoto H, Fujimoto J, Okamoto E, Furuyama J, Tamaoki T, Hashimoto TT. Suppression of growth of hepatocellular carcinoma by sodium butyrate *in vitro* and *in vivo*. *Int J Cancer* 1998; 76: 897-902
 - 42 Liu Z, Liu G, Zhang S. Reversing effect of dimethyl-4,4'-dimethoxy-5,6,5',6'-dimethylenedioxybiphenyl-2,2'-dicarboxylate (DDB) on the phenotypes of human hepatocarcinoma cells line. *Cancer Lett* 1996; 108: 67-72
 - 43 Mazume H, Nakata K, Hida D, Hamasaki K, Tsuruta S, Nakao K, Kato Y, Eguchi K. Effect of simvastatin, a 3-hydroxy-3-methylglutaryl coenzyme A reductase inhibitor, on alpha-fetoprotein gene expression through interaction with the ras-mediated pathway. *J Hepatol* 1999; 30: 904-910
 - 44 Feng DY, Zheng H, Tan Y, Cheng XR. Effect of phosphorylation of MAPK and Stat3 and expression of c-fos and c-jun proteins on hepatocarcinogenesis and their clinical significance. *World J Gastroenterol* 2001; 7: 33-36
 - 45 Sun BH, Zhang J, Wang BJ, Zhao XP, Wang YK, Yu ZQ, Yang DL, Hao LJ. Analysis of *in vivo* patterns of caspase 3 gene expression in primary hepatocellular carcinoma and its relationship to p21^{WAF1} expression and hepatic apoptosis. *World J Gastroenterol* 2000; 6: 356-360
 - 46 Ishikawa H, Nakata K, Mawatari F, Ueki T, Tsuruta S, Ido A, Nakao K, Kato Y, Ishii N, Eguchi K. Utilization of variant-type of human alpha-fetoprotein promoter in gene therapy targeting for hepatocellular carcinoma. *Gene Ther* 1999; 6: 465-470
 - 47 Ohguchi S, Nakatsukasa H, Higashi T, Ashida K, Nouse K, Ishizaki M, Hino N, Kobayashi Y, Uematsu S, Tsuji T. Expression of alpha-fetoprotein and albumin genes in human hepatocellular carcinomas: limitations in the application of the genes for targeting human hepatocellular carcinoma in gene therapy. *Hepatology* 1998; 27: 599-607
 - 48 Moskaleva EY, Posypanova GA, Shmyrev II, Rodina AV, Muizhnek EL, Severin ES, Katukov VY, Luzhkov YM, Severin SE. Alpha-fetoprotein-mediated targeting-a new strategy to overcome multidrug resistance of tumour cells *in vitro*. *Cell Biol Int* 1997; 21: 793-799

Edited by Pagliarini R and Zhang JZ

• LIVER CANCER •

Influence of hepatic arterial blockage on blood perfusion and VEGF, MMP-1 expression of implanted liver cancer in rats

Wei-Jian Guo, Jie Li, Wan-Long Ling, Yong-Rui Bai, Wen-Zhu Zhang, Yu-Fan Cheng, Wen-Hua Gu, Jun-Yan Zhuang

Wei-Jian Guo, Jie Li, Wan-Long Ling, Wen-Hua Gu, Jun-Yan Zhuang, Department of Oncology, Xinhua Hospital of Shanghai Second Medical University, Shanghai 200092, China
Yong-Rui Bai, Department of Radiotherapy, Xinhua Hospital of Shanghai Second Medical University, Shanghai 200092, China
Wen-Zhu Zhang, Yu-Fan Cheng, Department of Pathology, Xinhua Hospital of Shanghai Second Medical University, Shanghai 200092, China
Supported by Science and Technology Development Fund of Shanghai Municipality, No. 004119086
Correspondence to: Wei-Jian Guo, Department of Oncology, Xinhua Hospital of Shanghai Second Medical University, 1665 Kongjiang Road, Shanghai 200092, China. guoweijian1@sohu.com
Received 2001-08-09 Accepted 2001-10-22

Abstract

AIM: To investigate the influence of hepatic arterial blockage on blood perfusion of transplanted cancer in rat liver and the expression of vascular endothelial growth factor (VEGF) and matrix metalloproteinase-1 (MMP-1), and to explore the mechanisms involved in transarterial embolization (TAE)-induced metastasis of liver cancer preliminarily.

METHODS: Walker 256 carcinosarcoma was transplanted into rat liver to establish the liver cancer model. Hepatic arterial ligation (HAL) was used to block the hepatic arterial blood supply and simulate TAE. Blood perfusion of tumor in control, laparotomy control, and HAL group was analyzed by Hoechst 33342 labeling assay, the serum VEGF level was assayed by ELISA, the expression of VEGF and MMP-1 mRNA was detected by in situ hybridization.

RESULTS: Two days after HAL, the number of Hoechst 33342 labeled cells which represent the blood perfusion of tumor directly and hypoxia of tumor indirectly in HAL group decreased significantly compared with that in control group (329 ± 29 vs 384 ± 19 , $P < 0.01$). The serum VEGF level in the HAL group increased significantly as against that of the control group ($93 \text{ ng} \cdot \text{L}^{-1} \pm 44 \text{ ng} \cdot \text{L}^{-1}$ vs $55 \text{ ng} \cdot \text{L}^{-1} \pm 19 \text{ ng} \cdot \text{L}^{-1}$, $P < 0.05$). The expression of VEGF and MMP-1 mRNA in the tumor tissue of the HAL group increased significantly compared with that of the control and the laparotomy control groups ($P < 0.05$). The blood perfusion data of the tumor, represented by the number of Hoechst 33342 labeled cells, showed a good linear inverse correlation with the serum VEGF level ($r = -0.606$, $P < 0.05$) and the expression of VEGF mRNA in the tumor tissue ($r = -0.338$, $P < 0.01$).

CONCLUSION: Blockage of hepatic arterial blood supply results in decreased blood perfusion and increased expression of metastasis-associated genes VEGF and MMP-1 of transplanted liver cancer in rats. Decreased blood perfusion and hypoxia may be the major cause of up-regulated expression of VEGF.

Guo WJ, Li J, Ling WL, Bai YR, Zhang WZ, Cheng YF, Gu WH, Zhuang JY. Influence of hepatic arterial blockage on blood perfusion and VEGF, MMP-1 expression of implanted liver cancer in rats. *World J Gastroenterol* 2002;8(3):476-479

INTRODUCTION

Primary liver cancer (PLC) is one of the most common cancers in Asia. Patients with PLC usually have very poor prognoses, and the overall 5-year survival rate was not more than 5% worldwide^[1-3]. Surgery is considered as the only potential cure. However, the resection rate for PLC is only 10%-30%. Transarterial embolization (TAE) is one of the main non-surgical treatments for liver cancer in Asia via selectively blocking of the hepatic arterial blood supply of the tumor. However, a prospective controlled study showed that TAE enhanced the rate of lung metastases and accelerated metastases in patients with PLC^[4]. Other reports also showed that preoperative TAE for resectable PLC or TAE after curative resection of PLC could result in intrahepatic recurrence or extrahepatic metastasis, and a shorter survival^[5,6]. Metastases induced by TAE will undoubtedly reduce the long-term efficacy of TAE for PLC, but the mechanisms responsible for that have not been previously reported and there is no good method to inhibit metastasis.

In the present study, we have observed the influence of hepatic arterial ligation (HAL) which simulate TAE on metastasis related genes expression in Walker 256 tumor transplanted in rat liver to explore the mechanisms involved in TAE-induced metastasis of liver cancer preliminarily.

MATERIALS AND METHODS

Tumor model and treatment schedule

An implanted liver cancer model was obtained from Shanghai Medical Industry Research Institute, China. Male pathogen-free Wistar rats, weighing 100-120g, were anesthetized with pentobarbital sodium (40mg/kg). Following midline laparotomy, Walker 256 carcinosarcoma (about 1 mm^3) was implanted into one hepatic lobe of the rat. Seven days later, the rats that developed tumors were divided randomly into 3 groups: a control group without any treatment ($n=8$), a laparotomy control group ($n=4$) which underwent laparotomy only, and a HAL group ($n=8$). In the HAL group, after anesthesia and laparotomy, the proper hepatic artery was ligated by a sewing line.

Staining of perfused vessels with Hoechst 33342

The perfusion marker Hoechst 33342 (Sigma, USA) was dissolved in sterile saline immediately before use. Two days after HAL, all rats from all three groups were anesthetized and then their abdominal cavity was opened. The inferior vena cava was punctured to collect 0.5mL blood and to inject 0.2mL Hoechst 33342 (at a concentration of $6.25 \text{ g} \cdot \text{L}^{-1}$). The hepatic lobes bearing tumor were excised 1min after injection of Hoechst 33342 to prevent diffusion of Hoechst 33342 into adjacent non-perfused vascular structures. Hoechst 33342 is removed very rapidly from the circulation (half-time of 2min) and is very stable, once bound to DNA. Thus, Hoechst 33342 specifically labels the nuclei of endothelial cells and nuclei of the cells adjacent to the vessel walls, thereby delineating the perfused vessels^[7-9]. The tumors were excised and frozen in liquid nitrogen and then stored at -80°C until tumors were sectioned. Frozen sections ($5 \mu\text{m}$) were cut and Hoechst 33342 labeled cells were visualized and photographed

under a fluorescence microscope equipped with a camera with 365nm excitation and 420nm emission filters showing blue fluorescence. Four high power fields under the fluorescence microscope were photographed and Hoechst 33342 labeled cells were counted. The mean number of labeled cells reflected the blood perfusion of tumor and has been shown to be inversely related to the level of hypoxia in tumor^[7].

In situ hybridization (ISH) detection

ISH kits (Boster, China) were used to detect vascular endothelial growth factor (VEGF) and matrix metalloproteinase-1 (MMP-1) mRNA expression. Experiments were performed following the manufacturer's instructions. Briefly, frozen sections (5 μ m) were taken from the tumor and fixed with 40g·L⁻¹ polyformaldehyde in PBS (0.1mol·L⁻¹) for 30min, then digested in pepsin for 3min at 37°C. The material was prehybridized for 2h and then hybridized with Digoxin labeled probe overnight at 40°C. After hybridization, sections were washed with 2 \times SSC, 0.2 \times SSC, and then incubated with rabbit anti-Digoxin antibody, biotinylated secondary antibody IgG, SABC. Slides were stained with DAB and studied under a light microscope equipped with a camera. A positive stain should be present as intracytoplasmic. The level of mRNA expression was evaluated by two of the authors on blinded sections and was expressed as a positive staining rate.

Serum VEGF assay with ELISA

Blood samples collected from the inferior vena cava of rats were pooled, coagulated, and centrifuged at 1000 \times g for 10min. After the serum was aspirated, the VEGF level was assayed with an ELISA kit (MEGA, USA). Experiments were performed following the manufacturer's instructions.

Statistical analysis

The number of Hoechst 33342 labeled cells, the percentage of positive staining cells of ISH detection, and the serum VEGF level were expressed as mean \pm SD. The difference between mean values were compared by Student's *t* test. A *P* value less than 0.05 was considered to be statistically significant. Linear regression was used for the correlation assessment. Statistical analyses were performed using SPSS software.

RESULTS

Blood perfusion of tumor

The mean number of Hoechst 33342 labeled cells represents the blood perfusion of tumor, and indirectly represents the level of hypoxia in tumor. The lower number of labeled cells suggests an impaired blood perfusion and a higher level of hypoxia in tumor. The mean number of Hoechst 33342 labeled cells in the control, the laparotomy control, and the HAL groups were 384 \pm 19, 369 \pm 27, and 329 \pm 29, respectively. The number of labeled cells in the HAL group decreased significantly compared with that in the control and the laparotomy control groups (*P*<0.05, Table 1 and Figure 1). This suggests a decreased blood perfusion and a more serious hypoxia of tumor after HAL.

VEGF and MMP-1 mRNA expression

ISH showed both VEGF and MMP-1 mRNA expressed in the implanted tumor of control and laparotomy control groups. There was no significant difference between these two groups (*P*>0.05). The expression of VEGF and MMP-1 in the HAL group was elevated significantly compared with values in the control and the laparotomy control groups (*P*<0.05). Results of their expression in the different groups are shown in Table 1, and Figures 2 and 3.

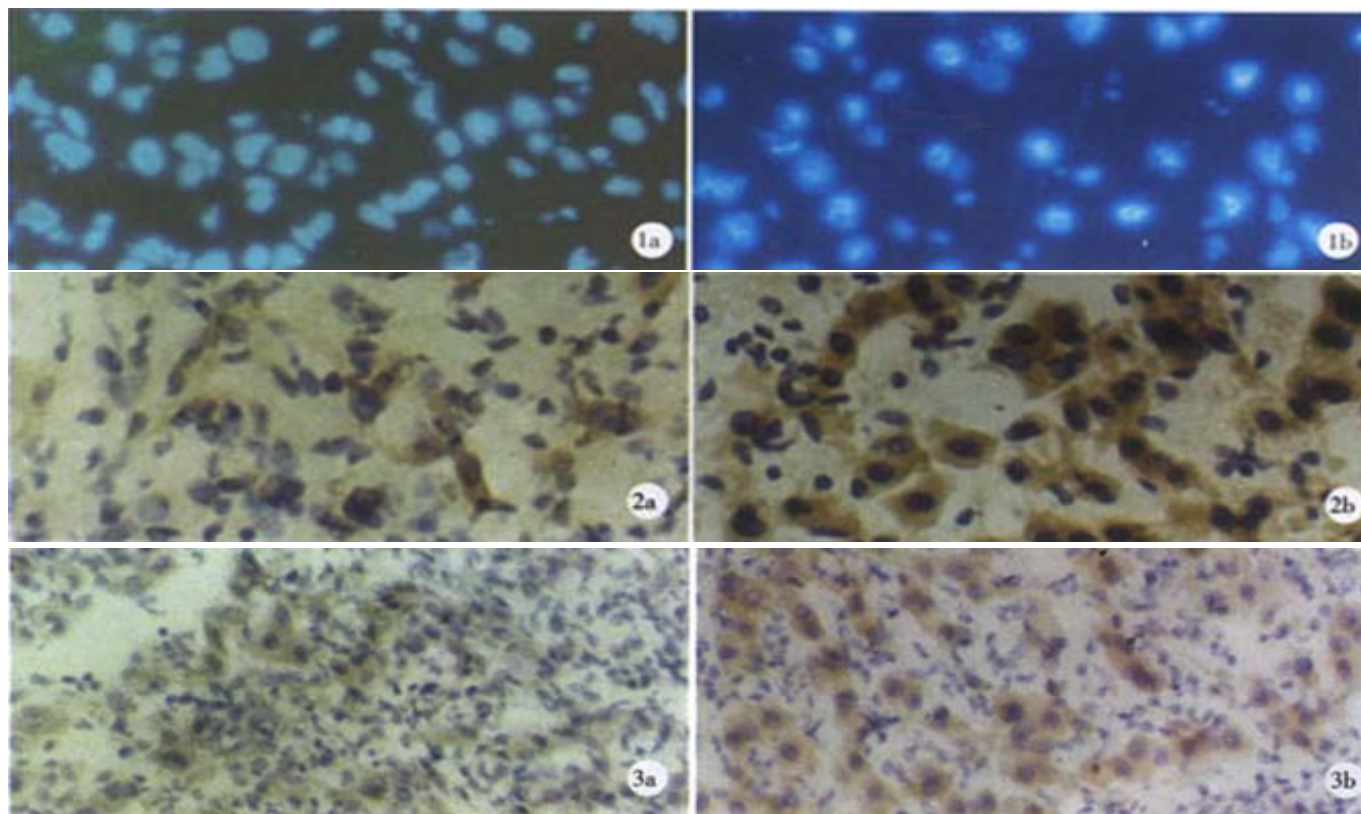


Figure 1 Hoechst 33342 labeled cells. A: Control animals; B: HAL group, decreased number of labeled cells means decreased vascular supply.
Figure 2 VEGF mRNA in hybridization. A: Low expression in tumor of control animals; B: HAL group, a higher VEGF expression.
Figure 3 MMP-1 mRNA in hybridization. A: Low expression in tumor of control animals; B: HAL group, a higher MMP-1 expression.

Serum VEGF level

The serum VEGF level was $55\text{ng}\cdot\text{L}^{-1}\pm 19\text{ng}\cdot\text{L}^{-1}$ in the control group, and $70\text{ng}\cdot\text{L}^{-1}\pm 40\text{ng}\cdot\text{L}^{-1}$ in the laparotomy control group, which was elevated slightly, but not significantly, as compared to the control group. While in the HAL group, the level of serum VEGF was $93\text{ng}\cdot\text{L}^{-1}\pm 44\text{ng}\cdot\text{L}^{-1}$, which was elevated significantly when compared with the control group ($P<0.05$, Table 1).

Table 1 Number of Hoechst labeled cells, serum VEGF, and VEGF, MMP-1 mRNA expression in tumor ($\bar{x}\pm s$)

Groups	n	Hoechst 33342 labeled cells	Serum VEGF ($\text{ng}\cdot\text{L}^{-1}$)	VEGF mRNA	MMP-1 mRNA
Control	8	384 ± 19	55 ± 19	0.34 ± 0.14	0.24 ± 0.17
Laparotomy control	4	369 ± 27	70 ± 40	0.19 ± 0.17	0.30 ± 0.02
HAL	8	$329\pm 29^{\text{bc}}$	$93\pm 44^{\text{a}}$	$0.51\pm 0.15^{\text{ad}}$	$0.47\pm 0.11^{\text{bc}}$

^a $P<0.05$, ^b $P<0.01$ vs control group; ^c $P<0.05$, ^d $P<0.01$ vs laparotomy control group.

Correlation between blood perfusion and VEGF, MMP-1 expression

There was a positive correlation between the serum VEGF level and the expression level of VEGF mRNA in tumor tissue ($r=0.206$, $P<0.05$). The blood perfusion data of tumor, represented by number of Hoechst 33342 labeled cells, showed a good linear inverse correlation with the serum VEGF level ($r=-0.606$, $P<0.05$) and VEGF mRNA expression in tumor tissue ($r=-0.338$, $P<0.01$). These data suggest that deteriorating blood perfusion and increased hypoxia of tumor correlated with a higher level of VEGF expression. There was no linear correlation between the number of Hoechst 33342 labeled cells and MMP-1 mRNA expression in tumor tissue.

DISCUSSION

TAE is an excellent debulking procedure and destroys malignant cells by selectively blocking the blood perfusion of the liver cancer. However, TAE can not block the blood supply of liver cancer and eliminate tumor cells completely, because the liver cancer receives the blood supply not only from the hepatic artery, but also from the port vein. Besides, it has been found that TAE could promote metastases of liver cancer^[4-6]. Thus, the long-term efficacy of TAE was disappointing: the 5-year survival rate was not above 20%^[10-14]. Even in several prospective randomized trials, TAE failed to improve significantly the survival of patients with PLC^[15,16]. Currently, the mechanisms involved in TAE-induced metastases of PLC are unknown. Understanding the mechanisms will facilitate the development of methods for blocking metastases and promoting long-term efficacy of TAE for treatment of liver cancer.

In recent years, many *in vitro* studies showed that hypoxia could enhance the metastatic ability of cancer cells by different mechanisms. It was reported that hypoxia stimulated carcinoma cell invasiveness by way of up-regulation of urokinase receptor expression^[17,18]. Hypoxia is the most important stimulus for the up-regulation of VEGF, one of the key cytokines for angiogenesis^[19-21]. Hypoxia could also induce the expression of other genes that promote angiogenesis and metastasis, such as basic fibroblast growth factor (bFGF) and angiogenin in tumor cells^[22-24]. Rofstad *et al*^[25] found that hypoxia could induce metastasis of human melanoma cells via VEGF-mediated angiogenesis. *In vivo* research also suggested that hypoxia may be one of the important stimuli of metastases. Hypoxia of tumor correlated with the expression of VEGF^[26-29], which was found to be correlated with metastases of the tumor and poor prognosis^[30-34]. Hypoxia in the squamous cell carcinoma of the uterine cervix with lymph node metastases was more serious than that in the carcinoma without lymph node metastases^[35]. Thus, we hypothesized that the inefficient vascular supply after TAE would result in hypoxia of some of the liver cancer cells, as it blocks the blood supply incompletely. We also suggest that hypoxia caused by

TAE may induce metastasis-associated factors, such as VEGF mediated metastases of liver cancer. It was found that the serum VEGF level in patients with liver cancer elevated 7 days after TAE therapy^[36]. In the present study, we blocked the hepatic arterial blood supply of implanted cancer in rat liver by HAL to simulate TAE therapy, and found that the blood perfusion decreased. This appears to suggest a more serious hypoxia. The expression of VEGF, both in serum and in tumor tissue, increased 2 days after the blockage of the arterial blood supply. Furthermore, we found that there was an inverse correlation between the blood perfusion of tumor and the serum VEGF level or VEGF mRNA expression in tumor tissues. These data indicate that hypoxia after HAL may be the major cause of the elevated expression of VEGF. The results of our study provide evidence for our hypothesis preliminarily. The hypoxia after TAE should be detected directly by hypoxyprobe-1^[37,38], and if the hypoxia and expression of VEGF play a direct role in the mechanisms involved in TAE-induced metastases of liver cancer requires further studies. MMP is a secreted or transmembrane protein that is capable of digesting extracellular matrix and basement membrane and was associated with invasion and metastases of human tumor, such as hepatocellular carcinoma and colon cancer^[39-46]. It has been found that hypoxia could increase cellular invasiveness by inducing the expression of MMP^[47-50]; but there was no report about the change of MMP expression in liver cancer after TAE or HAL therapy. In the present study, we found that the expression of MMP-1 in tumor tissue increased 2 days after the blockage of the arterial blood supply, but there was no linear correlation between the blood perfusion of the tumor and MMP-1 mRNA expression in tumor tissue. Which is the cause of elevated MMP-1 expression and whether it played a direct role in the mechanisms involved in TAE-induced metastasis need further study.

In conclusion, the blood perfusion of implanted liver cancer in rats decreases and the expression of metastases-associated genes VEGF and MMP-1 increases after blockage therapy of the hepatic arterial blood supply. Decreased blood supply and hypoxia may be the main cause of VEGF expression. A more complete understanding of the mechanisms involved in TAE-induced metastasis may lead to an enhancement of the long-term effects of TAE on liver cancer.

ACKNOWLEDGMENT

We would like to thank Mrs. Margaret-Hiatt Rosen, Director of Admission, the Mead School, Stamford, USA, for her correction of the English translation of the paper.

REFERENCES

- 1 Faivre J, Forman D, Esteve J, Obradovic M, Sant M. Survival of patients with primary liver cancer, pancreatic cancer and biliary tract cancer in Europe. EUROCARE Working Group. *Eur J Cancer* 1998; 34: 2184-2190
- 2 Chen J, Sankaranarayanan R, Li W. Population-based survival analysis of primary liver cancer in a high-incidence area-Qidong, China during 1972-1991. *Zhonghua Yufang Yixue Zazhi* 1997; 31: 149-152
- 3 El-Serag HB, Mason AC, Key C. Trends in survival of patients with hepatocellular carcinoma between 1977 and 1996 in the United States. *Hepatology* 2001; 33: 62-65
- 4 Lion TC, Shih SC, Kao CR. Pulmonary metastasis of hepatocellular carcinoma associated with transarterial chemoembolization. *J Hepatol* 1995; 23: 563-568
- 5 Hanazaki K, Kajikawa S, Shimozaawa N, Mihara M, Shimada K, Hiraguri M, Koide N, Adachi W, Amano J. Survival and recurrence after hepatic resection of 386 consecutive patients with hepatocellular carcinoma. *J Am Coll Surg* 2000; 191: 381-388
- 6 Lai EC, Lo CM, Fan ST, Liu CL, Wong J. Postoperative adjuvant chemotherapy after curative resection of hepatocellular carcinoma: a randomized controlled trial. *Arch Surg* 1998; 133: 183-188
- 7 Rijken PF, Bernsen HJ, Peters JP, Hodgkiss RJ, Raleigh JA, van der Kogel AJ. Spatial relationship between hypoxia and the (perfused) vascular network in a human glioma xenograft: a quantitative multi-parameter analysis. *Int J Radiat Oncol Biol Phys* 2000; 48: 571-582
- 8 Bernsen HJ, Rijken PF, Hagemeier NE, van der Kogel AJ. A quantitative analysis of vascularization and perfusion of human glioma xenografts at different implantation sites. *Microvasc Res* 1999; 57: 244-257
- 9 Durand RE, Raleigh JA. Identification of nonproliferating but viable

- hypoxic tumor cells *in vivo*. *Cancer Res* 1998; 58: 3547-3550
- 10 Ueno K, Miyazono N, Inoue H, Nishida H, Kanetsuki I, Nakajo M. Transcatheter arterial chemoembolization therapy using iodized oil for patients with unresectable hepatocellular carcinoma: evaluation of three kinds of regimens and analysis of prognostic factors. *Cancer* 2000; 88: 1574-1581
 - 11 Poon RT, Ngan H, Lo CM, Liu CL, Fan ST, Wong J. Transarterial chemoembolization for inoperable hepatocellular carcinoma and postresection intrahepatic recurrence. *J Surg Oncol* 2000; 73: 109-114
 - 12 Savastano S, Miotto D, Casarrubea G, Teso S, Chiesura-Corona M, Feltrin GP. Transcatheter arterial chemoembolization for hepatocellular carcinoma in patients with Child's grade A or B cirrhosis: a multivariate analysis of prognostic factors. *J Clin Gastroenterol* 1999; 28: 334-340
 - 13 Sithinamsuwan P, Piratvisuth T, Tanomkiat W, Apakupakul N, Tongyoo S. Review of 336 patients with hepatocellular carcinoma at songklanagarind hospital. *World J Gastroenterol* 2000; 6: 339-343
 - 14 Guo WJ, Yu EX. Evaluation of combined therapy with chemoembolization and irradiation for large hepatocellular carcinoma. *Br J Radiol* 2000; 73: 1091-1097
 - 15 Pelletier G, Ducreux M, Gay F, Lubinski M, Hagege H, Dao T, Van Steenberghe W, Buffet C, Rougier P, Adler M, Pignon JP, Roche A. Treatment of unresectable hepatocellular carcinoma with lipiodol chemoembolization: a multicenter randomized trial. *Groupe CHC. J Hepatol* 1998; 29: 129-134
 - 16 Bruix J, Llovet JM, Castells A, Montana X, Bru C, Ayuso MDC, Vilana R, Rodes J. Transarterial embolization versus symptomatic treatment in patients with advanced hepatocellular: results of a randomized, controlled trial in a single institution. *Hepatology* 1998; 27: 1578-1583
 - 17 Graham CH, Forsdike J, Fitzgerald CJ, Macdonald-Goodfellow S. Hypoxia-mediated stimulation of carcinoma cell invasiveness via up-regulation of urokinase receptor expression. *Int J Cancer* 1999; 80: 617-623
 - 18 Kroon ME, Koolwijk P, van der Vecht B, van Hinsbergh VW. Urokinase receptor expression on human microvascular endothelial cells is increased by hypoxia: implications for capillary-like tube formation in a fibrin matrix. *Blood* 2000; 96: 2775-2783
 - 19 Gunningham SP, Currie MJ, Han C, Turner K, Scott PA, Robinson BA, Harris AL, Fox SB. Vascular endothelial growth factor-B and vascular endothelial growth factor-C expression in renal cell carcinomas: regulation by the von Hippel-Lindau gene and hypoxia. *Cancer Res* 2001; 61: 3206-3211
 - 20 Rossler J, Breit S, Havers W, Schweigerer L. Vascular endothelial growth factor expression in human neuroblastoma: up-regulation by hypoxia. *Int J Cancer* 1999; 81: 113-117
 - 21 Vasir B, Aiello LP, Yoon KH, Quickel RR, Bonner-Weir S, Weir GC. Hypoxia induces vascular endothelial growth factor gene and protein expression in cultured rat islet cells. *Diabetes* 1998; 47: 1894-1903
 - 22 Le YJ, Corry PM. Hypoxia-induced bFGF gene expression is mediated through the JNK signal transduction pathway. *Mol Cell Biochem* 1999; 202: 1-8
 - 23 Hartmann A, Kunz M, Kstlin S, Gillitzer R, Toksoy A, Brcker EB, Klein CE. Hypoxia-induced up-regulation of angiogenin in human malignant melanoma. *Cancer Res* 1999; 59: 1578-1583
 - 24 Brahimi-Horn C, Berra E, Pouyssegur J. Hypoxia: the tumor's gateway to progression along the angiogenic pathway. *Trends Cell Biol* 2001; 11: S32-36
 - 25 Rofstad EK, Danielsen T. Hypoxia-induced metastasis of human melanoma cells: involvement of vascular endothelial growth factor-mediated angiogenesis. *Br J Cancer* 1999; 80: 1697-1707
 - 26 Fukumura D, Xu L, Chen Y, Gohongi T, Seed B, Jain RK. Hypoxia and acidosis independently up-regulate vascular endothelial growth factor transcription in brain tumors *in vivo*. *Cancer Res* 2001; 61: 6020-6024
 - 27 Cvetkovic D, Movsas B, Dicker AP, Hanlon AL, Greenberg RE, Chapman JD, Hanks GE, Tricoli JV. Increased hypoxia correlates with increased expression of the angiogenesis marker vascular endothelial growth factor in human prostate cancer. *Urology* 2001; 57: 821-825
 - 28 Dunst J, Stadler P, Becker A, Kuhn T, Lautenschlager C, Molls M, Haensgen G. Tumor hypoxia and systemic levels of vascular endothelial growth factor (VEGF) in head and neck cancers. *Strahlenther Onkol* 2001; 177: 469-473
 - 29 Laderoute KR, Alarcon RM, Brody MD, Calaoagan JM, Chen EY, Knapp AM, Yun Z, Denko NC, Giaccia AJ. Opposing effects of hypoxia on expression of the angiogenic inhibitor thrombospondin 1 and the angiogenic inducer vascular endothelial growth factor. *Clin Cancer Res* 2000; 6: 2941-2950
 - 30 Ishigami SI. Predictive value of vascular endothelial growth factor in metastasis and prognosis of human colonrectal cancer. *Br J Cancer* 1998; 78: 1379-1384
 - 31 O-charoenrat P, Rhys-Evans P, Eccles SA. Expression of vascular endothelial growth factor family members in head and neck squamous cell carcinoma correlates with lymph node metastasis. *Cancer* 2001; 92: 556-568
 - 32 Fujimoto J, Sakaguchi H, Aoki I, Khatun S, Tamaya T. Clinical implications of expression of vascular endothelial growth factor in metastatic lesions of ovarian cancers. *Br J Cancer* 2001; 85: 313-316
 - 33 Niu Q, Tang ZY, Ma ZC, Qin LX, Zhang LH. Serum vascular endothelial growth factor is a potential biomarker of metastatic recurrence after curative resection of hepatocellular carcinoma. *World J Gastroenterol* 2000; 6: 565-568
 - 34 Harada Y, Ogata Y, Shirouzu K. Expression of vascular endothelial growth factor and its receptor KDR (kinase domain-containing receptor)/Flk-1 (fetal liver kinase-1) as prognostic factors in human colorectal cancer. *Int J Clin Oncol* 2001; 6: 221-228
 - 35 Sundfor K, Lyng H, Rofstad EK. Tumour hypoxia and vascular density as predictors of metastasis in squamous cell carcinoma of the uterine cervix. *Br J Cancer* 1998; 78: 822-827
 - 36 Suzuki H, Mori M, Kawaguchi C, Adachi M, Miura S, Ishii H. Serum vascular endothelial growth factor in the course of transcatheter arterial embolization of hepatocellular carcinoma. *Int J Oncol* 1999; 14: 1087-1090
 - 37 Raleigh JA, Chou SC, Bono EL, Thrall DE, Varia MA. Semiquantitative immunohistochemical analysis for hypoxia in human tumors. *Int J Radiat Oncol Biol Phys* 2001; 49: 569-574
 - 38 Shabsigh A, Ghafar MA, de la Taille A, Burchardt M, Kaplan SA, Anastasiadis AG, Buttyan R. Biomarker analysis demonstrates a hypoxic environment in the castrated rat ventral prostate gland. *J Cell Biochem* 2001; 81: 437-444
 - 39 Jiang YF, Yang ZH, Hu JQ. Recurrence or metastasis of HCC, predictors, early detection and experimental antiangiogenic therapy. *World J Gastroenterol* 2000; 6: 61-65
 - 40 Ogata Y, Miura K, Ohkita A, Nagase H, Shirouzu K. Imbalance between matrix metalloproteinase 9 and tissue inhibitor of metalloproteinases 1 expression by tumor cells implicated in liver metastasis from colorectal carcinoma. *Kurume Med J* 2001; 48: 211-218
 - 41 Ohnishi Y, Tajima S, Ishibashi A. Coordinate expression of membrane type-matrix metalloproteinases-2 and 3 (MT2-MMP and MT3-MMP) and matrix metalloproteinase-2 (MMP-2) in primary and metastatic melanoma cells. *Eur J Dermatol* 2001; 11: 420-423
 - 42 Ghilardi G, Biondi ML, Mangoni J, Leviti S, DeMonti M, Guagnellini E, Scorza R. Matrix metalloproteinase-1 promoter polymorphism 1G/2G is correlated with colorectal cancer invasiveness. *Clin Cancer Res* 2001; 7: 2344-2346
 - 43 O-Charoenrat P, Rhys-Evans PH, Eccles SA. Expression of matrix metalloproteinases and their inhibitors correlates with invasion and metastasis in squamous cell carcinoma of the head and neck. *Arch Otolaryngol Head Neck Surg* 2001; 127: 813-820
 - 44 Nordqvist AC, Smurawa H, Mathiesen T. Expression of matrix metalloproteinases 2 and 9 in meningiomas associated with different degrees of brain invasiveness and edema. *J Neurosurg* 2001; 95: 839-844
 - 45 Ye S, Dhillon S, Turner SJ, Bateman AC, Theaker JM, Pickering RM, Day I, Howell WM. Invasiveness of cutaneous malignant melanoma is influenced by matrix metalloproteinase 1 gene polymorphism. *Cancer Res* 2001; 61: 1296-1298
 - 46 Yamamoto H, Itoh F, Iku S, Adachi Y, Fukushima H, Sasaki S, Mukaiya M, Hirata K, Imai K. Expression of matrix metalloproteinases and tissue inhibitors of metalloproteinases in human pancreatic adenocarcinomas: clinicopathologic and prognostic significance of matrilysin expression. *J Clin Oncol* 2001; 19: 1118-1127
 - 47 Yamanaka M, Ishikawa O. Hypoxic conditions decrease the mRNA expression of proalpha1(I) and (III) collagens and increase matrix metalloproteinases-1 of dermal fibroblasts in three-dimensional cultures. *J Dermatol Sci* 2000; 24: 99-104
 - 48 Canning MT, Postovit LM, Clarke SH, Graham CH. Oxygen-mediated regulation of gelatinase and tissue inhibitor of metalloproteinases-1 expression by invasive cells. *Exp Cell Res* 2001; 267: 88-94
 - 49 Koong AC, Denko NC, Hudson KM, Schindler C, Swiersz L, Koch C, Evans S, Ibrahim H, Le QT, Terris DJ, Giaccia AJ. Candidate genes for the hypoxic tumor phenotype. *Cancer Res* 2000; 60: 883-887
 - 50 Himelstein BP, Koch CJ. Studies of type IV collagenase regulation by hypoxia. *Cancer Lett* 1998; 124: 127-133

• LIVER CANCER •

The point mutation of p53 gene exon7 in hepatocellular carcinoma from Anhui Province, a non HCC prevalent area in China

Hu Liu, Yuan Wang, Qing Zhou, Shu-Yu Gui, Xu Li

Hu Liu, Yuan Wang, Qing Zhou, Laboratory of Molecular Biology and Department of Biochemistry, Anhui Medical University, Hefe 230032i, Anhui Province, China

Shu-Yu Gui, Department of Respiratory Disease, the First Affiliated Hospital of Anhui Medical University, Hefe 230022, Anhui Province, China

Xu Li, Department of Infectious Disease, the First Affiliated Hospital of Anhui Medical University, Hefe 230022, Anhui Province, China

Supported by the Natural Science Foundation of Anhui Province, No. 99044312(WY) and No.9741006(LX) and Natural Science Foundation of Anhui Educational Commission, No.JL-97-077(WY).

Correspondence to: Yuan Wang, Laboratory of Molecular Biology, Anhui Medical University, Hefe 230032, Anhui Province, China. wangyuan@mail.hf.ah.cn

Telephone: +86-551-5161140

Received 2001-12-20 Accepted 2002-01-24

Abstract

AIM: In hepatocellular carcinoma (HCC) prevalent areas of China, the point mutation of p53 exon7 is highly correlated with Hepatitis B virus(HBV) infection and aflatoxin B intake. While in non-HCC-prevalent areas of China, these factors are not so important in the etiology of HCC. Therefore, the point mutation of p53 exon7 may also be different than that in HCC-prevalent areas of China. The aim of this study is to investigate the status and carcinogenic role of the point mutation of p53 gene exon7 in hepatocellular carcinoma from Anhui Province, a non-HCC-prevalent area in China.

METHODS: PCR,PCR-SSCP and PCR-RFLP were applied to analyze the homozygous deletion and point mutation of p53 exon7 in HCC samples from Anhui, which were confirmed by DNA sequencing and Genbank comparison.

RESULTS: In the 38 samples of hepatocellular carcinoma, no homozygous deletion of p53 exon7 was detected and point mutations of p53 exon7 were found in 4 cases, which were found to be heterozygous mutation of codon 249 with a mutation rate of 10.53%(4/38). The third base mutation(GiúT) of p53 codon 249 was found by DNA sequencing and Genbank comparison.

CONCLUSION: The incidence of point mutation of p53 codon 249 is lower in hepatocellular carcinoma and the heterozygous mutation of p53 exon7 found in these patients only indicate that they have genetic susceptibility to HCC. p53 codon 249 is a hotspot of p53 exon7 point mutation, suggesting that the point mutation of p53 exon 7 may not play a major role in the carcinogenesis of HCC in Anhui Province, a non-HCC-prevalent area in China.

Liu H, Wang Y, Zhou Q, Gui SY, Li X. The point mutation of p53 gene exon7 in hepatocellular carcinoma from Anhui Province, a non HCC prevalent area in China. *World J Gastroenterol* 2002;8(3):480-482

INTRODUCTION

Hepatocellular carcinoma is one of the most common cancers in the world. Abnormalities of p53 are the most frequent genetic alterations in human cancers, and the role and mechanism of p53 gene mutations have been well studied in many types of cancer^[1-3]. Genetic analysis of 26 HCC samples from North America and Europe revealed a high incidence of an AGG→AGT transversional changes in codon 249 of the p53 gene; and recently exon7 has been proven a hotspot of p53 gene mutation^[4-6]. Zhang *et al*^[4] reported the high relationship between HBVx gene and codon 249 mutation of the p53 gene in HCC-prevalence areas in China. Our previous studies have also indicated that hepatitis B virus infection is an important risk factor for HCC^[7]. These data indicate that p53 mutations generally occur in the process of HCC carcinogenesis in HCC-prevalent area in China. However, further mutation analyses will be necessary to clarify the status of p53 mutations for HCC in non-HCC-prevalent areas in China.

In this study, we analyzed p53 exon 7 point mutation in HCCs from non-HCC-prevalent areas in China using the polymerase chain reaction(PCR), PCR-single-strand conformational polymorphism (PCR-SSCP), PCR-restriction fragment length polymorphism (PCR-RFLP) and DNA sequencing analysis.

MATERIALS AND METHODS

Specimens

The surgical specimens of HCC were collected from the First Affiliated Hospital of Anhui Medical University, which were confirmed by pathological diagnosis and stored at -80°C. The patients were born in and permanent residents of different places of the Anhui Province, China.

PCR of p53 exon7

DNA was extracted from tissues with standard proteinase K-phenol/chloroform methods^[9]. The primers for p53 gene exon7 amplification were designed according to the sequence of p53 exon7 published^[4,5]. 3'primer(GW-XI-1C): 5'CTT GCC ACA GGT CTC CCC AA,5'primer (GW-XI-1D): 5' TGT GCA GGG TGG CAA GTG GC; CDK4 as a control, 3'primer(GW-IV-1K): 5'GGA GGT CGG TAC CAG AGT G,5'primer(GW-IV-1J): 5'CAT GTA GAC CAG GAC AGG. Into 100ng of DNA template of each sample was added PCR reaction solution (10mmol/L Tris, 50mmol/L KCl, 2mmol/L MgCl₂, 0.001% Gelatin, 200mmol/L dNTPs, 6% DMSO and 0.5mmol/L primers). Hotstart was performed: 97°C 5min; chilled on ice at once. 0.9U of Taq polymerase was added, which was diluted with 1×PCR buffer for each sample. Ran PCR: 94°C 30s, 60°C 30s, 72°C 30s, 35 cycles in all and checked with 2% agarose gel electrophoresis stained with ethidium bromide. The result of homozygous deletion should be the one with no specific band of p53 exon7 while its counterpart of CDK4 appeared.

PCR-SSCP of p53 exon7^[1]

8μl of PCR products were aspirated, into which was added equal volumes of deionized formamide and 4μl of DNA loading buffer (0.25% bromophenol blue, 0.25% xylene cyanol FF, 30% glycerol).

They were mixed well, boiled for 5min, and then chilled on ice for 3min. The samples (20 μ l in volume) were loaded into separate wells. Samples were run in an 8% non-denaturing polyacrylamide gel at 80V for 5 hrs. The gel was taken off from the electrophoresis apparatus and readied for silver staining. The gel was submerged in 5% ethanol for 5min; 3min in 1% HNO₃; 20min in 0.012mol·L⁻¹ AgNO₃; washed with dd-H₂O for about 10 sec; developed with 0.28mol·L⁻¹ Na₂CO₃; fixed with 10% acetic acid; and finally washed with dd-H₂O. When the bands appeared, photos were taken and the gel was dried with Slab Gel Dryer or wrapped with a membrane and air dried for several days. Na₂CO₃ was changed 2-4 times when the developing solution turned black.

Restrictive endonuclease digestion of p53 exon7 and Restrictive enzyme mapping

Into each restrictive endonuclease system was added 2 μ l of 10 \times Buffer C, 2 μ l of DTT(1%), 2 μ l of BSA(1%) and 0.25 μ l of HaeIII(20U· μ l⁻¹). The total volume was brought up to 20 μ l with PCR products. They were incubated at 37°C for 3hrs and checked with an 8% non-denaturation polyacrylamide gel, electrophoresed at 40V for 4hrs and developed with silver staining^[8] as described above.

DNA sequencing of PCR products

The sample of p53 exon7 mutation was confirmed by PCR-SSCP and RFLP and PCR products of p53 exon7 were sent the to Bioasia Biotechnololy Company, Shanghai, China for DNA sequencing with ABI 377 automatic DNA sequencer.

RESULTS

PCR of p53 exon7

With 100ng of genomic DNA extracted from surgical HCC tissue as template, p53 exon7 and CDK4 genes were amplified with different specific primers in separate tubes. The products were checked with 2% agarose gel electrophoresis. The results showed that the products amplified with each pair of specific pairs were of the same length with that reported in the literature(Figure 1). No homozygous deletion of p53 exon7 was found in any HCC surgical sample.



Figure 1 Agarose gel electrophoresis of PCR products of p53 exon7. A: 1-6. PCR products of p53 exon7 amplified from HCC genomic DNA 710bp DNA ladder; B: 1-6. PCR products of CDK4 gene amplified from HCC genomic DNA as control

PCR-SSCP of p53 exon7

Point mutations of p53 exon7 were found in 4 cases out of the 38 samples of HCC examined. No.1, 6 and 9 sample had point mutations of p53 exon7 (Figure 2).

PCR-RFLP of the codon 249 of p53 exon7

With PCR-RFLP, we found that 4 samples have heterozygous point mutation of p53 codon 249, which has a band of 150bp in addition to wild type bands(40, 60, and 90bp) as shown by agarose/EB gel electrophoresis(Figure 3). However, no homozygous point mutation was found among these samples, which would have had bands of 40bp and 150bp. We found that those samples which have point mutation of p53 codon 249 was the same samples that were found to have point mutation of p53 exon 7 by PCR-SSCP.

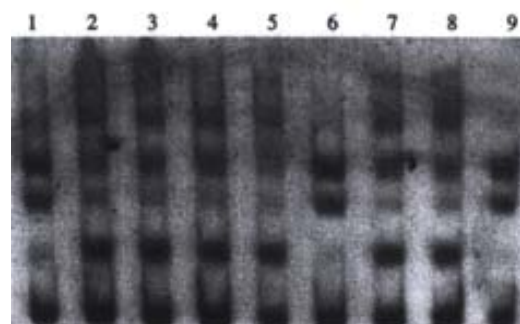


Figure 2 PCR-SSCP of p53 exon7 Samples of 1,6,9 have point mutations of p53 exon7 Samples of 2,3,4,5,7,8 don't have point mutations of p53 exon7

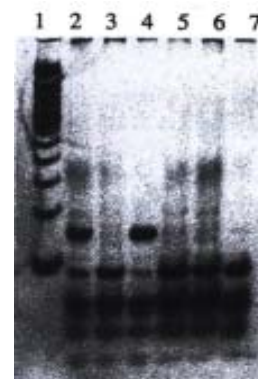


Figure 3 PCR-RFLP of p53 codon249. 1. 100bp DNA ladder; 2 and 4: heterozygous point mutation of p53 codon249; 3, 5, 6 and 7: p53 Exon7 wild type.

DNA sequencing

One sample that has been found by PCR-SSCP to have point mutation of p53 exon7 was randomly chosen for DNA sequencing. The DNA sequencing result is shown in the following graph. The sequence was compared with that published by the Genbank (gbAF136270.1 HOMOTSP1), which shows that a point mutation exists in p53 codon 249 with ggAc taken place of ggCc (Figure 4,5).

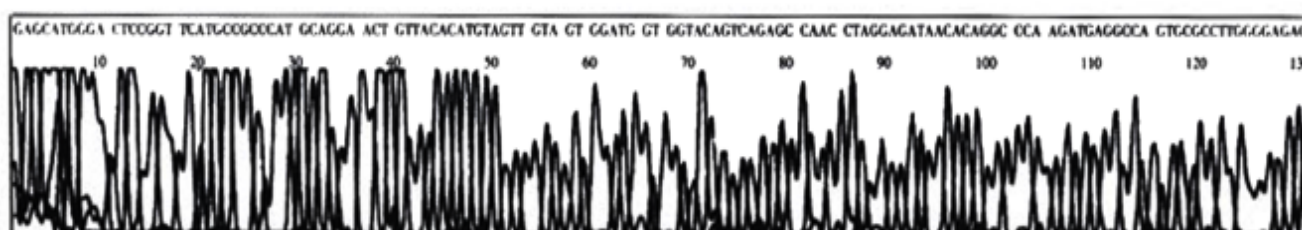


Figure 4 Sequencing of p53 exon 7 PCR product

• LIVER CANCER •

Effect of Nimesulide on proliferation and apoptosis of human hepatoma SMMC-7721 cells

Geng Tian, Jie-Ping Yu, He-Sheng Luo, Bao-Ping Yu, Hui Yue, Jian-Ying Li, Qiao Mei

Geng Tian, Jie-Ping Yu, He-Sheng Luo, Bao-Ping Yu, Hui Yue, Jian-Ying Li, Qiao Mei, Gastroenterology department, Renmin hospital of Wuhan university, Wuhan 430060, Hubei Province, China

Correspondence to: Jie-Ping Yu, Gastroenterology department, Renmin hospital of Wuhan university, 238Jie-fang Road, Wuhan 430060, Hubei Province, China. tg3030330@sina.com

Telephone: +86-27-88077184

Received 2001-11-15 Accepted 2002-01-15

Abstract

AIM: Cyclooxygenase-2 (COX-2) has been suggested to be associated with carcinogenesis. We sought to investigate the effect of the selective COX-2 inhibitor, Nimesulide on proliferation and apoptosis of SMMC-7721 human hepatoma cells.

METHODS: This study was carried out on the culture of hepatic carcinoma SMMC-7721 cell line. Various concentrations of Nimesulide (0, 200 μ mol/L, 300 μ mol/L, 400 μ mol/L) were added and incubated. Cell proliferation was detected with MTT colorimetric assay, cell apoptosis by electron microscopy, flow cytometry and TUNEL.

RESULTS: Nimesulide could significantly inhibit SMMC-7721 cells proliferation dose-dependent and in a dependent manner compared with that of the control group. The duration lowest inhibition rate produced by Nimesulide in SMMC-7721 cells was 19.06%, the highest inhibition rate was 58.49%. After incubation with Nimesulide for 72h, the most highest apoptosis rate and apoptosis index of SMMC-7721 cells comparing with those of the control were $21.20\% \pm 1.62\%$ vs $2.24\% \pm 0.26\%$ and 21.23 ± 1.78 vs 2.01 ± 0.23 ($P < 0.05$).

CONCLUSION: The selective COX-2 inhibitor, Nimesulide can inhibit the proliferation of SMMC-7721 cells and increase apoptosis rate and apoptosis index of SMMC-7721 cells. The apoptosis rate and the apoptosis index are dose-dependent. Under electron microscope SMMC-7721 cells incubated with 300 μ mol and 400 μ mol Nimesulide show apoptotic characteristics. With the clarification of the mechanism of selective COX-2 inhibitors, These COX-2 selective inhibitors can become the choice of prevention and treatment of cancers.

Tian G, Yu JP, Luo HS, Yu BP, Yue H, Li JY, Mei Q. Effect of Nimesulide on proliferation and apoptosis of human hepatoma SMMC-7721 cells. *World J Gastroenterol* 2002;8(3):483-487

INTRODUCTION

Hepatic carcinoma was one of most common malignant tumors in China. Its death rate was the third among all cancers, second to gastric carcinoma and lung carcinoma. Although there is a progress in diagnosis and treatment of hepatic carcinoma, its prognosis is still poor. Investigating its pathogenesis and finding new diagnostic and treatment methods is important. Recent epidemiological studies indicate an inverse relationship between the risk of colorectal cancer

and intake of NSAIDs. NSAIDs could reduce the incidence of gastric carcinoma and pancreatic carcinoma. It could inhibit tumor cells proliferation and induce apoptosis^[1-4]. Cyclooxygenases (COXS) are key enzymes in the conversion of arachidonic acid to prostaglandins and other eicosanoids. Recently two isoforms of the enzyme have been identified. COX-1 is constitutively expressed in a number of cell types, whereas the isoform designated COX-2 is inducible by a variety of factors, as cytokines, growth factors, and tumor promoters. Some studies have suggested that COX-2, but not COX-1, was involved in colon carcinogenesis and might thus be the target of chemopreventive effect by the COX inhibitor, nonsteroidal anti-inflammatory drugs. The effects of COX-2 on inflammation, precancerous conditions and cancers have been delineated^[42-47]. To date the effects of Nimesulide on the growth and apoptosis of human hepatoma cell line SMMC-7721 in vitro have not been analyzed, and that is the aim of this study.

MATERIALS AND METHODS

RPMI 1640 medium is a product of CIBCO; Nimesulide and MTT were from Sigma; In situ cell death detection kit was from Boehringer Mannheim, Germany; 96-well plates were from Costar.

Cell lines and culture

Human hepatoma SMMC-7721 cells were obtained from the Wuhan University Center for type culture collection. The cells were grown as monolayers in RPMI1640 medium supplemented with 10% fetal calf serum (FCS, Gibco) and incubated at 37°C in the humidified incubator with 5% CO₂ in air.

Assay of cell proliferation

The SMMC-7721 cells were seeded at 5×10^4 /ml density in 96-well plates 200 μ l cell suspension per well. Each group had four wells with a non-treated group as control. When the cells anchored to the plates, various concentrations (0, 200 μ mol/L, 300 μ mol/L, 400 μ mol/L) of Nimesulide were added and the slides were incubated at 37°C, 5% CO₂ for 5 days. In order to maintain Nimesulide concentrations, we changed the culture medium (included various concentrations of Nimesulide) every day. When the cells described above were cultured for 48h, 72h, 96h, 120h, 0.5% MTT 20 μ l was added to each well and cultured for another 4h. The supernatant was discarded and dimethyl sulfoxide (DMSO) 200 μ l added. When the crystals were dissolved, the optical density (OD) value of the slides was read on an enzyme-labeled Minireader II at 492nm. Cellular proliferation inhibition rate (CPIR) was calculated using the following equation: $CPIR = (1 - \text{average OD value of experimental group} / \text{average OD value of control group}) \times 100\%$

Electron microscopic observation

The SMMC-7721 cells were seeded in culture flasks. Four culture bottles were divided into normal group and control group. When the cells were anchored to the plates, various concentrations (0, 200 μ mol/L, 300 μ mol/L, 400 μ mol/L) of Nimesulide were added and the cells incubated at 37°C, 5% CO₂ for 3 days. Then hepatoma cells were

digested by 0.25% trypsinase and collected. After rinsing with PBS, the cells were fixed with 2.5% glutaraldehyde for 30min and washed with PBS. After routine embedding and sectioning, the cells were observed by Hitachi H-600 electronic microscope.

Flow cytometric analysis

The SMMC-7721 cells were seeded in culture flasks. The culture bottles were divided into normal and three control groups. Each group had three culture bottles. When the cells were anchored to the plates, various concentrations (0,200 μ mol/L,300 μ mol/L,400 μ mol/L) of Nimesulide were added and the cells incubated at 37°C, 5% CO₂ for 3 days. Then each group of cells were washed with PBS, trypsinized and fixed with 70% ethanol at -20°C for 30 minutes. Fixed cells were incubated with IP/Rnase solution for 15 minutes and 10⁶ cells of each culture bottle were harvested and analyzed with FACScan Becton Dickeyson Flow Cytometer.

In situ apoptotic cell death detection by TUNEL

A TUNEL kit (Boehringer Mannheim, IN) was used to detect DNA fragmentation, the characteristic of apoptotic cell death. The SMMC-7721 cells were seeded in culture flasks. Culture bottles were divided into normal and three control groups. Each group had three culture bottles. When the cells were anchored to the plates, various concentrations (0,200 μ mol/L,300 μ mol/L,400 μ mol/L) of Nimesulide were added and the cells incubated at 37°C, 5% CO₂ for 3 days. In order to maintain Nimesulide concentrations, we changed the culture medium (including various concentrations of Nimesulide) every day. After having been cultured for 3 days, each culture bottle cells were scraped and centrifuged 800r/min for 5 minutes. Then the deposited cells were smeared and air-dried. Following the manufacturer's directions, smears were incubated with the TUNEL reaction mixture for 60min at 37°C and then with converter-POD for 30min. The DAB-substrate solution was added to the smears and kept at room temperature until positive signal appeared. Then they were dried and analyzed under light microscope.

Under light microscope, the TUNEL positive nuclei were stained brown. Selecting 5 fields randomly (the number of cells in each field >1000).

Apoptosis index (AI)=(number of apoptotic cells/ the number of cells in each field) ×100%.

Statistical analysis

Statistical analysis was performed using the student's t test and analysis of variance. $P<0.05$ was considered significant.

RESULTS

Effect of Nimesulide in various concentrations on the growth of SMMC-7721

We analyzed the effects of Nimesulide on cell proliferation in cultured human hepatoma cell line SMMC-7721 after 5 days of treatment. Nimesulide, a selective COX inhibitor, produced a dose-dependent inhibition of cells growth (Table 1 and Figure 1). The lowest inhibition rate produced by Nimesulide in SMMC-7721 cells was 19.06%, the highest being 58.49%.

Morphology observation

Under the electron microscope, SMMC-7721 cells exhibited characteristics of apoptosis including plasma membrane blebbing, cytoplasmic condensation, pyknotic nuclei, condensed chromatin and apoptotic bodies. Compared with control groups, 300 μ mol/L and 400 μ mol/L groups cells had many more cells with apoptotic characteristics (Figure 2).

Table 1 Inhibition effect of Nimesulide on proliferation and growth in hepatic carcinoma cell line SMMC-7721

Nimesulide Concentrations (μ mol/L)	OD Value			
	the 2 nd day	the 3 rd day	the 4 th day	the 5 th day
0	1.039±0.066	1.516±0.117	2.142±0.072	2.467±0.080
200	0.841±0.027 ^a	1.109±0.231 ^a	1.416±0.080 ^a	1.341±0.021 ^a
300	0.796±0.019 ^a	1.002±0.274 ^a	1.101±0.028 ^a	1.243±0.168 ^a
400	0.581±0.164 ^a	0.825±0.016 ^a	0.943±0.032 ^a	1.024±0.026 ^a

^a $P<0.05$ vs control group

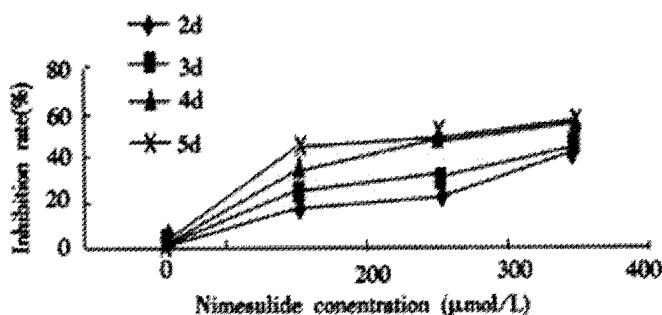


Figure 1 Inhibition rate of Nimesulide on proliferation of SMMC-7721 cells. Cells were incubated with 200 μ mol/L,300 μ mol/L,400 μ mol/L Nimesulide for 2d,3d,4d,5d respectively.



Figure 2 Transmission electron micrograph of SMMC-7721 cells treated with Nimesulide at the concentration of 300 μ mol/L for 72h. The picture showed early change of apoptosis, the nuclear chromatin condensation.

Flow-cytometry analysis of cell apoptosis

The peak value appearing before the G₁ peak is called apoptotic peak. As shown in Figure 3 and Table 2, the apoptotic peak and rate increased with increasing concentrations of Nimesulide. Furthermore, Nimesulide induced cells apoptosis in a dose and time-dependent manner ($P<0.01$).

Table 2 Apoptosis rate of SMMC-7721 cells induced by Nimesulide

Nimesulide concentration (μ mol/L)	Apoptosis rate (%)
0	2.24±0.26
200	7.42±0.43 ^b
300	9.84±1.54 ^b
400	21.20±1.62 ^b

^b $P<0.01$ vs control group

Analysis of apoptosis by TUNEL

As shown in Figure 4 and Table 3, the apoptotic index increased with increase of Nimesulide concentrations which what appeared to be dose-dependent relationship in the alone groups ($P<0.05$).

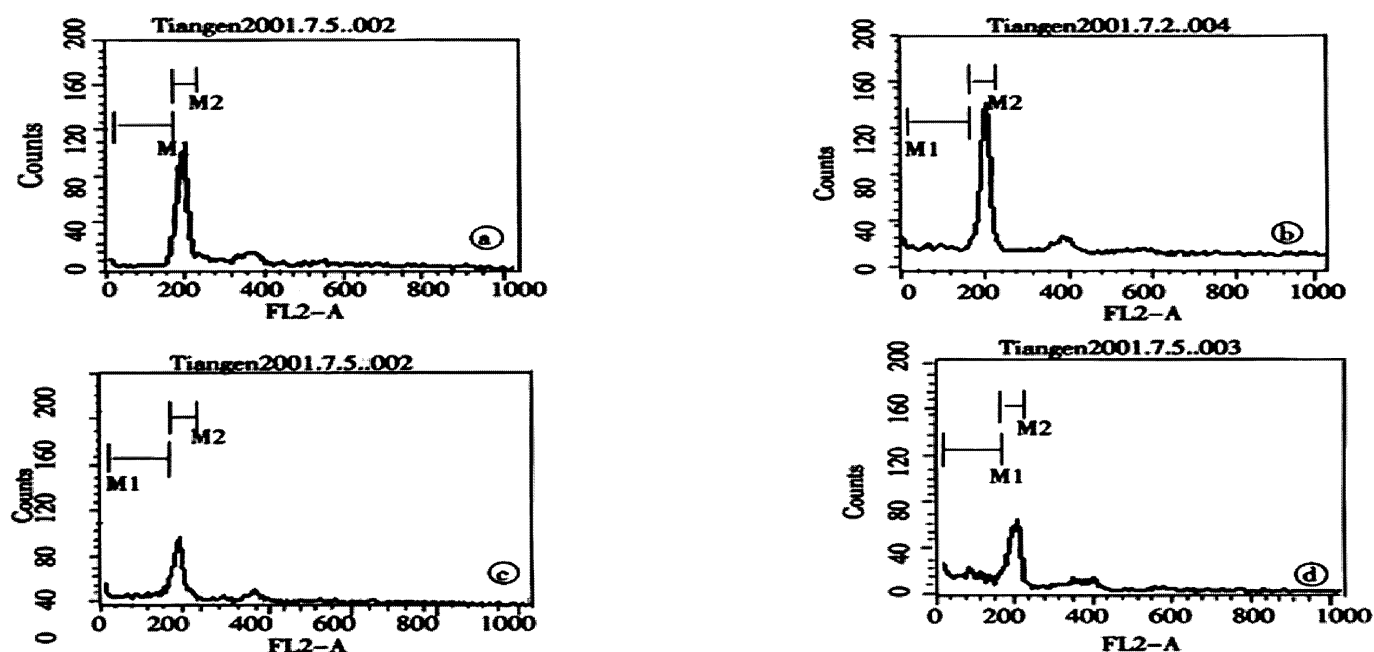


Figure 3 Cell apoptosis was determined by flow-cytometry, SMMC-7721 cells were treated with Nimesulide at various concentrations (0, 200, 300, 400 $\mu\text{mol/L}$ respectively A to D).

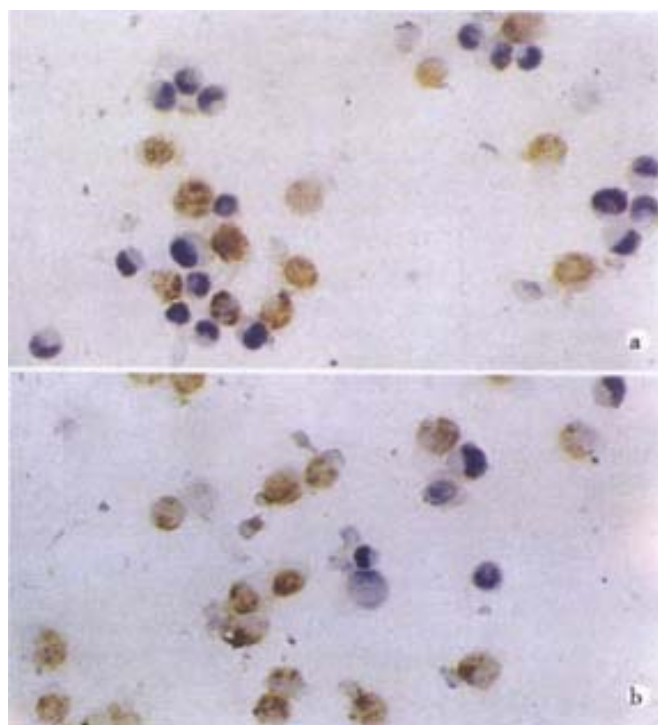


Figure 4 TUNEL stain showed SMMC-7721 cells apoptosis. SMMC-7721 cells were treated with Nimesulide at various concentrations (300, 400 $\mu\text{mol/L}$ A and B).

Table 3 Apoptosis index of SMMC-7721 cells induced by Nimesulide

Nimesulide concentration ($\mu\text{mol/L}$)	Apoptosis index (%)
0	2.016 \pm 0.23
200	7.64 \pm 0.34 ^a
300	10.14 \pm 1.42 ^a
400	21.23 \pm 1.78 ^a

^a $P < 0.05$ vs control group

DISCUSSION

It had been shown that selective COX-2 inhibitors inhibited tumor cells proliferation and induced tumor cells apoptosis, in colon and prostate carcinoma cell lines^[48,49]. To date, their effects on human hepatoma SMMC-7721 cell lines have not yet been studied. The aim of this study was to investigate the effect of Nimesulide, a selective COX inhibitor, on the proliferation and apoptosis of SMMC-7721 cell lines. The results indicated that various concentrations of Nimesulide could change the morphology of SMMC-7721 cells and inhibit SMMC-7721 cells proliferation obviously in a dose and time-dependent manner. Nimesulide could induce SMMC-7721 cells apoptosis and cause death in a dose-dependent manner. The precise mechanism by which selective COX-2 inhibitors inhibit tumor cells growth and induce tumor cells apoptosis was not been clearfield. The available data supported the two hypotheses.

Some studies indicate that COX-2 is a key enzyme in the conversion of arachidonic acid to prostaglandins. Selective COX-2 inhibitors can decrease prostaglandins biosynthesis, and prostaglandins can inhibit cell-mediated immunity, which enables the tumor cells escaping the host-immunity^[50,51]; PGs also can conjugate with PPAR α and activate cell proliferation passage of signal conduction, promote cells proliferation^[52]; PGs can also inhibit cells apoptosis and cause cells division uncontrollable, thus accelerating tumor genesis^[53,54]; the effects of COX-2 inhibitors might involve prostaglandin biosynthesis. Some studies indicated that the effects of COX-2 were not related to COX-2 expression and PGs. Hanif *et al.*^[55] verified that NASIDs (nonselective COX inhibitors) could induce apoptosis of colon carcinoma cell line HCT-15. HCT-15 cells have no COX gene transcription, and does not produce PGs. When adding exogenous PGs to the HCT-15 cells, it could not reverse the induction of HCT-15 cells apoptosis by NASIDs.

On the whole, Nimesulide, a selective COX-2 inhibitor, can inhibit the growth of hepatoma cells and induce tumor cells apoptosis. With the clarification of the mechanism of selective COX-2 inhibitors, These COX-2 selective inhibitors can become the choice of prevention and treatment of cancers.

ACKNOWLEDGMENT

I would like to thank my wife and all those who provided assistance for this study.

REFERENCES

- Gao HJ, Yu LZ, Sun G, Miu K, Bai JF, Zhang XY, Lü XZ, Zhao ZQ. The expression of COX-2 in gastric carcinoma and paracancerous tissues. *Shijie Huaren Xiaohua Zazhi* 2000;8:578-579
- Wu HP, Wu KCH, Li L, Yao LP, Lan M, Wang X, Fan DM. Cloning of human cyclooxygenase-2 (Hcox-2) encoded gene and the study of gastric cancer cell transfected with its antisense vector. *Shijie Huaren Xiaohua Zazhi* 2000;8: 1211-1217
- Gao HJ, Yu LZ, Bai JF, Peng YS, Sun G, Zhao HL, Miu K, Lü XZ, Zhang XY, Zhao ZQ. Multiple genetic alterations and behavior of cellular biology in gastric cancer and other gastric mucosal lesions: *H. pylori* infection, histological types and staging. *World J Gastroenterol* 2000;6:848-854
- Wu QM, Li SB, Wang Q, Wang DH, Li XB, Liu CZ. The expression of COX-2 in esophageal carcinoma and its relationship to clinicopathologic characteristic. *Shijie Huaren Xiaohua Zazhi* 2001; 9: 11-14
- Sun B, Wu YL, Zhang XJ, Wang SN, He HY, Qiao MM, Zhang YP, Zhong J. Effects of Sulindac on growth inhibition and apoptosis induction in human gastric cancer cells. *Shijie Huaren Xiaohua Zazhi* 2001; 9:997-1002
- Zhuang ZH, Wang LD. Non-steroidal anti-inflammatory drug and digestive tract tumors. *Shijie Huaren Xiaohua Zazhi* 2001;9:1050-1053
- Shen ZX, Cao G, Sun J. The effect of COX-2 mRNA expression in colorectal cancer tissues. *Shijie Huaren Xiaohua Zazhi* 2001;9:1082-1084
- Mann M, Sheng H, Shao J, Williams CS, Pisacane PI, Sliwowski MX, DuBois RN. Targeting cyclooxygenase 2 and HER-2/neu pathways inhibit colorectal carcinoma growth. *Gastroenterology* 2001; 120: 1713-1739
- Glinghammar B, Rafter J. Colonic luminal contents induce cyclooxygenase 2 transcription in human colon carcinoma cells. *Gastroenterology* 2001; 120: 401-410
- Wallace JL, McKnight W, Reuter BK, Vergnolle N. NSAID-induced gastric damage in rats: requirement for inhibition of both cyclooxygenase 1 and 2. *Gastroenterology* 2000; 119: 706-714
- Callejas NA, Bosca L, Williams CS, DuBOIS RN, Martin-Sanz P. Regulation of cyclooxygenase 2 expression in hepatocytes by CCAAT/enhancer-binding proteins. *Gastroenterology* 2000; 119: 493-501
- Zhang Z, DuBois RN. Par-4, a proapoptotic gene is regulated by NSAIDs in human colon carcinoma cells. *Gastroenterology* 2000; 118: 1012-1017
- Shirvani VN, Ouatu-Lascar R, Kaur BS, Omary MB, Triadafilopoulos G. Cyclooxygenase 2 expression in Barrett's esophagus and adenocarcinoma: Ex vivo induction by bile salts and acid exposure. *Gastroenterology* 2000;118:487-496
- Shattuck-Brandt RL, Varilek GW, Radhika A, Yang F, Washington MK, DuBois RN. Cyclooxygenase 2 expression is increased in the stroma of colon carcinomas from IL-10(-/-) mice. *Gastroenterology* 2000; 118:337-345
- Sinicropo FA, Lemoine M, Xi L, Lynch PM, Cleary KR, Shen Y, Frazier ML. Reduced expression of cyclooxygenase 2 proteins in hereditary nonpolyposis colorectal cancers relative to sporadic cancers. *Gastroenterology* 1999; 117: 350-358
- Fu S, Ramanujam KS, Wong A, Fantry GT, Drachenberg CB, James SP, Meltzer SJ, Wilson KT. Increased expression and cellular localization of inducible nitric oxide synthase and cyclooxygenase 2 in *Helicobacter pylori* gastritis. *Gastroenterology* 1999; 116: 1319-1329
- Bosch-Marce M, Claria J, Titos E, Masferrer JL, Altuna R, Poo JL, Jimenez W, Arroyo V, Rivera F, Rodes J. Selective inhibition of cyclooxygenase 2 spares renal function and prostaglandin synthesis in cirrhotic rats with ascites. *Gastroenterology* 1999; 116: 1167-1175
- Klimp AH, Hollema H, Kempinga C, van der Zee AG, de Vries EG, Daemen T. Expression of cyclooxygenase-2 and inducible nitric oxide synthase in human ovarian tumors and tumor-associated macrophages. *Cancer Res* 2001; 61: 7305-7309
- Lal G, Ash C, Hay K, Redston M, Kwong E, Hancock B, Mak T, Kargman S, Evans JF, Gallinger S. Suppression of intestinal polyps in Msh2-deficient and non-Msh2-deficient multiple intestinal neoplasia mice by a specific cyclooxygenase-2 inhibitor and by a dual cyclooxygenase-1/2 inhibitor. *Cancer Res* 2001; 61: 6131-6136
- Subbarayan V, Sabichi AL, Llansa N, Lippman SM, Menter DG. Differential expression of cyclooxygenase-2 and its regulation by tumor necrosis factor-alpha in normal and malignant prostate cells. *Cancer Res* 2001; 61: 2720-2726
- Oshima M, Murai N, Kargman S, Arguello M, Luk P, Kwong E, Taketo MM, Evans JF. Chemoprevention of intestinal polyposis in the Apcdelta716 mouse by rofecoxib, a specific cyclooxygenase-2 inhibitor. *Cancer Res* 2001; 61: 1733-1740
- Shiotani H, Denda A, Yamamoto K, Kitayama W, Endoh T, Sasaki Y, Tsutsumi N, Sugimura M, Konishi Y. Increased expression of cyclooxygenase-2 protein in 4-nitroquinoline-1-oxide-induced rat tongue carcinomas and chemopreventive efficacy of a specific inhibitor, nimesulide. *Cancer Res* 2001; 61: 1451-1456
- Boudreau MD, Sohn KH, Rhee SH, Lee SW, Hunt JD, Hwang DH. Suppression of tumor cell growth both in nude mice and in culture by n-3 polyunsaturated fatty acids: mediation through cyclooxygenase-independent pathways. *Cancer Res* 2001; 61: 1386-1391
- Denkert C, Kobel M, Berger S, Siegert A, Leclere A, Trefzer U, Hauptmann S. Expression of cyclooxygenase 2 in human malignant melanoma. *Cancer Res* 2001; 61: 303-308
- Taylor MT, Lawson KR, Ignatenko NA, Marek SE, Stringer DE, Skovan BA, Gerner EW. Sulindac sulfone inhibits K-ras-dependent cyclooxygenase-2 expression in human colon cancer cells. *Cancer Res* 2000; 60: 6607-6610
- Williams CS, Watson AJ, Sheng H, Helou R, Shao J, DuBois RN. Celecoxib prevents tumor growth *in vivo* without toxicity to normal gut: lack of correlation between *in vitro* and *in vivo* models. *Cancer Res* 2000; 60: 6045-6051
- Souza RF, Shewmake K, Beer DG, Cryer B, Spechler SJ. Selective inhibition of cyclooxygenase-2 suppresses growth and induces apoptosis in human esophageal adenocarcinoma cells. *Cancer Res* 2000; 60: 5767-5772
- Grubbs CJ, Lubet RA, Koki AT, Leahy KM, Masferrer JL, Steele VE, Kelloff GJ, Hill DL, Seibert K. Celecoxib inhibits N-butyl-N-(4-hydroxybutyl)-nitrosamine-induced urinary bladder cancers in male B6D2F1 mice and female Fischer-344 rats. *Cancer Res* 2000; 60: 5599-5602
- Jacoby RF, Seibert K, Cole CE, Kelloff G, Lubet RA. The cyclooxygenase-2 inhibitor celecoxib is a potent preventive and therapeutic agent in the min mouse model of adenomatous polyposis. *Cancer Res* 2000; 60: 5040-5044
- Joki T, Heese O, Nikas DC, Bello L, Zhang J, Kraeft SK, Seyfried NT, Abe T, Chen LB, Carroll RS, Black PM. Expression of cyclooxygenase 2 (COX-2) in human glioma and *in vitro* inhibition by a specific COX-2 inhibitor, NS-398. *Cancer Res* 2000; 60: 4926-4931
- Attiga FA, Fernandez PM, Weeraratna AT, Manyak MJ, Patierno SR. Inhibitors of prostaglandin synthesis inhibit human prostate tumor cell invasiveness and reduce the release of matrix metalloproteinases. *Cancer Res* 2000; 60: 4629-4637
- Marrogi A, Pass HI, Khan M, Metheny-Barlow LJ, Harris CC, Gerwin BI. Human mesothelioma samples overexpress both cyclooxygenase-2 (COX-2) and inducible nitric oxide synthase (NOS2): *in vitro* antiproliferative effects of a COX-2 inhibitor. *Cancer Res* 2000; 60: 3696-3700
- Cahlin C, Gelin J, Delbro D, Lonnroth C, Doi C, Lundholm K. Effect of cyclooxygenase and nitric oxide synthase inhibitors on tumor growth in mouse tumor models with and without cancer cachexia related to prostanoids. *Cancer Res* 2000; 60: 1742-1749
- Masferrer JL, Leahy KM, Koki AT, Zweifel BS, Settle SL, Woerner BM, Edwards DA, Flickinger AG, Moore RJ, Seibert K. Antiangiogenic and antitumor activities of cyclooxygenase-2 inhibitors. *Cancer Res* 2000; 60: 1306-1311
- Reddy BS, Hirose Y, Lubet R, Steele V, Kelloff G, Paulson S, Seibert K, Rao CV. Chemoprevention of colon cancer by specific cyclooxygenase-2 inhibitor, celecoxib, administered during different stages of carcinogenesis. *Cancer Res* 2000; 60: 293-297
- Mohammed SI, Knapp DW, Bostwick DG, Foster RS, Khan KN, Masferrer JL, Woerner BM, Snyder PW, Koki AT. Expression of cyclooxygenase-2 (COX-2) in human invasive transitional cell carcinoma (TCC) of the urinary bladder. *Cancer Res* 1999; 59: 5647-5650
- Molina MA, Sitja-Arnau M, Lemoine MG, Frazier ML, Sinicropo FA. Increased cyclooxygenase-2 expression in human pancreatic carcinomas and cell lines: growth inhibition by nonsteroidal anti-inflammatory drugs. *Cancer Res* 1999; 59: 4356-4362
- Tucker ON, Dannenberg AJ, Yang EK, Zhang F, Teng L, Daly JM, Soslow RA, Masferrer JL, Woerner BM, Koki AT, Fahey TJ 3rd. Cyclooxygenase-2 expression is up-regulated in human pancreatic cancer. *Cancer Res* 1999; 59: 987-990
- Chan G, Boyle JO, Yang EK, Zhang F, Sacks PG, Shah JP, Edelstein D, Soslow RA, Koki AT, Woerner BM, Masferrer JL, Dannenberg AJ. Cyclooxygenase-2 expression is up-regulated in squamous cell carcinoma of the head and neck. *Cancer Res* 1999; 59: 991-994
- Zimmermann KC, Sarbia M, Weber AA, Borchard F, Gabbert HE, Schror K. Cyclooxygenase-2 expression in human esophageal carcinoma. *Cancer Res* 1999;59:198-204
- Koga H, Sakisaka S, Ohishi M, Kawaguchi T, Taniguchi E, Sasatomi K, Harada M, Kusaba T, Tanaka M, Kimura R, Nakashima Y, Nakashima

- O, Kojiro M, Kurohiji T, Sata M. Expression of cyclooxygenase-2 in human hepatocellular carcinoma: relevance to tumor dedifferentiation. *Hepatology* 1999; 29: 688-696
- 42 Nanji AA, Jokelainen K, Fotouhinia M, Rahemtulla A, Thomas P, Tipoe GL, Su GL, Dannenberg AJ. Increased severity of alcoholic liver injury in female rats: role of oxidative stress, endotoxin, and chemokines. *Am J Physiol Gastrointest Liver Physiol* 2001; 281: G1348-1356
- 43 Ganey PE, Barton YW, Kinser S, Sneed RA, Barton CC, Roth RA. Involvement of cyclooxygenase-2 in the potentiation of allyl alcohol-induced liver injury by bacterial lipopolysaccharide. *Toxicol Appl Pharmacol* 2001; 174: 113-121
- 44 Miyamoto T, Ogino N, Yamamoto S, Hayaishi O. Purification of prostaglandin endoperoxide synthetase from bovine vesicular gland microsomes. *J Bio Chem* 1976; 251:2629-2636
- 45 Simmons DL, Levy DB, Yannoni Y, Erikson RL. Identification of Phorbol ester-repressible v-src- inducible gene. *Proc Natl Acad Sci USA* 1989;86:1178-1182
- 46 Tian G, Yu JP, Luo HS, Yu BP, Li JY. The expression and effect of cyclo oxygenases-2 in acute hepatic injury. *Shijie Huaren Xiaohua Zazhi* 2002;10:24-27
- 47 Tian G, Yu JP, Luo HS, Yu BP, Li JY. The effect of COX-2 and oxidant stress in acute hepatic injury. *Yixue Yanjiusheng Xuebao* 2002; 6; 165-169
- 48 Elder DJE, Halton DE, Hague A, Paraskeva C. Induction of apoptotic cell death in human colorectal carcinoma cell lines by a cyclooxygenase-2 (COX-2) selective nonsteroidal anti-inflammatory drug: independence from COX-2 protein expression. *Clin Cancer Res* 1997; 3:1679-1683
- 49 Liu X H, Yao S, Kirschenbaum A, Levine AC. NS398, a selective cyclooxygenase inhibitor induces apoptosis and downregulates bcl-2 expression in LNCap cells. *Cancer Res* 1998; 58:4245-4249
- 50 Yang VW, Shields JM, Hamilton SR, Spannhake EW, Hubbard WC, Hyind LM, Robinson R, Giardiello FM. Size-dependent increased in prostanoid levels in adenomas of patients with familial adenomatous polyposis. *Cancer Res* 1998;58:1750-1753
- 51 Votila P. The role of cyclic AMP and oxygen intermediates in the inhibition of cellular immunity in cancer. *Cancer Immunot Immunother* 1996;43: 1-9
- 52 Parker J, Kaplon MK, Alvarez CJ, Krishnaswamy G. Prostaglandin H synthase expression is variable in human colorectal adenocarcinoma cell lines. *Exp cell Res* 1997;236: 321-329
- 53 Sheng H, Shao JY, Morrow JD, Beauchamp RD, Dubois RN. Modulation of apoptosis and BCL-2 expression by prostaglandin E2 in human colon cancer cells. *Cancer Res* 1998;58: 362-366
- 54 Orlov SN, Thorin-Trescases N, Dulin No. Activation of cAMP signaling transiently inhibits apoptosis in vascular smooth muscle cell in a site upstream of caspase-1. *Cell Death Differ* 1999;6:661-672
- 55 Hanif R, Pittas A, Feng Y, Koutsos MI, Qiao L, Staiano-Coico L, Shiff SI, Rigas B. Effects of nonsteroidal anti-inflammatory drugs on proliferation and on induction of apoptosis in colon cancer cells by prostaglandin-independent pathway. *Biochem Pharmacol* 1996; 52:237-245

Edited by Wu XN

• LARGE INTESTINAL CANCER •

Reduction of the incidence and mortality of rectal cancer by polypectomy: a prospective cohort study in Haining County

Shu Zheng, Xi-Yong Liu, Ke-Feng Ding, Lin-Bo Wang, Pei-Lin Qiu, Xin-Feng Ding, Yong-Zhou Shen, Gao-Fei Shen, Qi-Rong Sun, Wei-Dong Li, Qi Dong, Su-Zhan Zhang

Shu Zheng, Xi-Yong Liu, Qi Dong, Cancer Institute, Zhejiang University, 88 Jiefang Road, HangZhou 310009, Zhejiang Province, China
Ke-feng Ding, Lin-Bo Wang, Pei-Lin Qiu, Su-Zhan Zhang, The 2nd affiliated Hospital, Medical School of Zhejiang University, 88 Jiefang Road, HangZhou 310009, Zhejiang Province, China
Xin-Feng Ding, Yong-Zhou Shen, Gao-Fei Shen, Qi-Rong Sun, Wei-Dong Li, Haining Cancer Institute, Haining 314400, Zhejiang Province, China
Supported by The 7th 5-year National Medical Strategic Science and Technology Plan, No. 75-61-02-17; The 8th 5-year National Medical Strategic Science and Technology Plan, No. 85-914-01-09
Correspondence to: Shu Zheng, Cancer Institute, Zhejiang University, 88 Jiefang Road, HangZhou 310009, Zhejiang Province, China. zhengshu@mail.hz.zj.cn
Telephone: +86-571-87783868 Fax: +86-571-87214404
Received 2001-12-20 Accepted 2002-02-07

Abstract

AIM: To reduce the incidence and mortality of rectal cancer and address the hypothesis that colorectal cancer often arise from precursor lesion(s), either adenomas or non-adenomatous polyps, by conducting a population-based mass screening for colorectal cancer in Haining County, Zhejiang, PRC.

METHODS: From 1977 to 1980, physicians screened the population of Haining County using 15cm rigid endoscopy. Of over 240000 participants, 4076 of them were diagnosed with precursor lesions, either adenomas or non-adenomatous polyps, which were then removed surgically. All individuals with precursor lesions were followed up and reexamined by endoscopy every two to five years up to 1998.

RESULTS: After the initial screening, 953 metachronous adenomas and 417 non-adenomatous polyps were detected and removed from the members of this cohort. Further, 27 cases of colorectal cancer were detected and treated. Log-rank tests showed that the survival time among those cancer patients who underwent mass screening increased significantly compared to that of other colorectal cancer patients ($P < 0.0001$). According to the population-based cancer registry in Haining County, age-adjusted incidence and mortality of rectal cancer decreased by 41% and 29% from 1977-1981 to 1992-1996, respectively. Observed cumulative 20-year rectal cancer incidence was 31% lower than the expected in the screened group; the mortality due to rectal cancer was 18% lower than the expected in the screened group.

CONCLUSION: Mass screening for rectal cancer and precursor lesions with proctoscopy in the general population and periodical following-up with routine endoscopy for high-risk patients may decrease both the incidence and mortality of rectal cancer.

Zheng S, Liu XY, Ding KF, Wang LB, Qiu PL, Ding X, Shen YZ, Shen GF, Sun QR, Li WD, Dong Q, Zhang SZ. Reduction of the incidence and mortality of rectal cancer by polypectomy: a prospective cohort study in Haining County. *World J Gastroenterol* 2002;8(3):488-492

INTRODUCTION

Colorectal cancer is the second most common cause of death from cancer in the United States^[1,2] and the fifth in mainland of China^[3]. Dietary modification and non-steroidal anti-inflammatory drugs (NSAID) may reduce the risk of colorectal cancer^[4-6]. Nevertheless, few of the Chinese people have benefited from these chemoprevention strategies so far. Recently, the results of several randomized controlled trial showed that fecal occult blood testing (FOBT) based on mass screening might reduce the mortality caused by colorectal cancer in general population^[7-9]. Unfortunately, the incidence of colorectal cancer could not be reduced by this protocol.

As reviewed by Potter^[10-13], colorectal cancer is a result of accumulation of multiple genetic alterations within the epithelial cells. The concept of the adenoma-to-carcinoma is well accepted, and describes a stepwise progression from normal colorectal epithelium to adenoma, and to carcinoma^[14-16]. The adenomatous polyps, the precursor lesion resulted from epithelial cell hyperproliferation and crypt dysplasia, have malignant potential. Progression from precursor lesions to colorectal cancer is a multi-step process that requires ten to fifteen years^[15]. Approximately 30-60% of patients with a history of adenomas will develop a metachronous adenoma within three to five years after their initial polypectomy^[17,18]. Therefore, it has been hypothesized that removing colorectal polyps might change the natural history of colorectal cancer; mass screening and following up with endoscopy might reduce the incidence and mortality of colorectal cancer. Nevertheless, evidence for the effectiveness of colonoscopy is indirect, since no large trials with mortality endpoints have been conducted to evaluate the efficacy of screening for colorectal cancer with colonoscopy^[19-21].

According to census survey of death causes in 1970 in China, more than 66% of colorectal cancers were found in the rectum^[22-24]. It is suggested that about 60% of colorectal cancer could be effective by screening with proctoscopy in China. To prove above hypothesis, we conducted a population-based mass screening with 15cm rigid endoscopy in Haining County, PRC from 1977 to 1980. Results presented herein are based on findings at the initial screening as well as 20 years of follow-up examinations in those individuals with precursor lesions.

MATERIALS AND METHODS

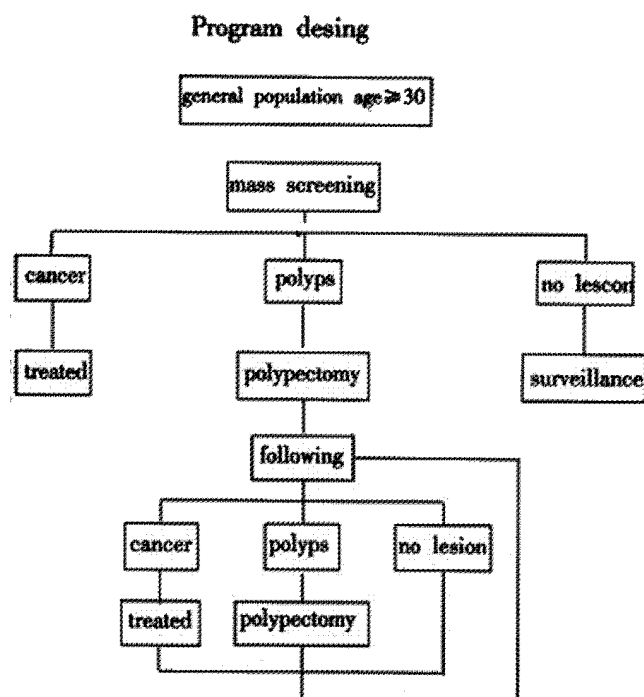
Study design was described in Figure 1. The high-risk population with rectal polyps was identified by proctoscopy through a general population-based mass-screening program, and followed with endoscopy periodically. All detectable polyps including adenomatous or non-adenomatous polyps were removed.

As previously described in detail^[25,26], population-based screenings with 15cm rigid endoscopy was conducted from 1977 to 1978 in Haining County, a rural community located in the eastern part of China. Only residents in Haining County who were at least 30 years old were eligible for the screenings. The screening team includes

epidemiologist, physician, pathologist, surgeon and investigators, who had been trained before starting the program. We screened 186234 of the 223866 eligible individuals (83% response rate), of which 2815 were found carrying polyps and/or adenomas. The detectable adenoma and/or polyp were surgically removed thereafter. All individuals with precursor lesions were eligible for follow-up endoscopic screenings, which were performed in the years of 1979-1980, 1981, 1983, 1987, 1993 and 1998. In addition, of the 53987 volunteers who aged 30 or over screened during 1979-1980's following-up, polyps and/or adenomas were detected and removed in 1,261 individuals. These patients were eligible for follow-up endoscopic screenings in 1982, 1984, 1988, 1994 and 1998. Due to technological advances in screening methods during this time period, all screenings after 1985 were performed with 60cm flexible sigmoidoscopy rather than 15cm rigid endoscopy.

Pathologic material was reviewed independently by three senior pathologists using standard criteria developed by the World Health Organization (WHO). A final diagnosis was made when at least two of the pathologists agreed on the patient's diagnosis. The age distribution of patients from both screenings is presented in Table 1. Table 2 lists the pathologic features of the initial polyp or adenoma for each patient; for patients with more than one adenoma or polyp, the most advanced lesion is listed.

Cancer mortality data was collected since 1974, and Cancer incidence data was available since 1977 by the population-based cancer registry in Haining County. The International Classification of Disease (ICD-9) was employed by the registry for site-specific histologic classification. Population estimates were based on the periodic censuses, with age- and sex-specific annual estimates derived by linear inter- and extrapolation for the remaining years. Rates for each period are age-adjusted to the world standard population using the direct method for each 5-year age group. From 1974 to 1976, before mass screening program carried out, the adjusted mortality of colon and rectum cancer was 2.66 and 4.20 per 100000 respectively. From 1977 to 1996, histologic confirmation was available for 94.4% of the 1005 incident colorectal cancer cases and 92.3% of the 735 deaths due to colorectal cancer.



Note: Polyps include adenomatous polyps and non-adenomatous polyps. All polyps would be removed when detected by endoscopy examiner.

Figure 1 Design for mass screening and following-up with endoscopy

Table 1 Age distribution of two groups of high-risk populations with polyps

Age Group	1 ^a		2 ^b		Total(%)
	Male(%)	Female(%)	Male(%)	Female(%)	
30-	644(36.6)	440(41.6)	287(34.4)	181(37.2)	1 552(38.1)
40-	452(25.7)	270(25.6)	226(27.1)	100(23.7)	1 049(25.8)
50-	434(24.7)	237(22.4)	204(24.4)	99(23.5)	974(23.9)
60-	164(9.3)	89(8.4)	99(11.9)	37(27.2)	389(9.6)
70-	64(3.7)	21(2.0)	19(2.3)	5(1.2)	109(2.7)
Total	1758	1057	835	422	4072

^a1: high-risk population with history of polyps identified during 1977-1978; ^b2: High-risk population identified in 1980. The age of 4 participants is unknown

Table 2 Pathologic features of initial polyps of two groups of high-risk populations

Pathologic Diagnosis	First group		Second group		Total	
	n	%	n	%	n	%
Adenoma	1485	52.88	876	69.47	2361	58.02
Tubular	1352	48.15	843	66.85	2195	53.94
Tubulovillous	104	3.70	31	2.46	135	3.32
Villous	19	0.68	2	0.16	21	0.52
Non-adenomatous	1326	47.22	382	30.29	1708	41.98
Mucosal	596	21.23	95	7.53	691	16.98
Juvenile	183	6.52	95	7.53	278	6.83
Hyperplastic	113	4.02	72	5.71	185	4.55
Inflammatory	90	3.21	4	0.32	94	2.31
Schistosomiasis	326	11.61	115	9.12	441	10.84
Lymphoid	10	0.36	1	0.08	11	0.27
Other	8	0.28	0	0.00	8	0.20
No pathologic diag	7	0.25	3	0.24	10	0.25
Total	2815		1261		4076	

RESULTS

From 1979 to 1998, patients diagnosed with adenomas and/or polyps during the first screening have been followed up six times. Of 2815 cases with polyps, 20.5% of them participated whole six times endoscopy examination, and 89.6% finished at least three times. While those patients diagnosed at the group of volunteers have been re-screened five times, and 82.5% of them were re-examined at least two times. Table 3 summarizes the expected and observed incidence rates of adenomas, polyps and colorectal cancer for both groups. After the initial screening, 953 metachronous adenomas and 417 non-adenomatous polyps were detected and removed from members of this cohort. Further, 27 cases of colorectal cancer were detected and treated, we analyzed data collected by the cancer registry of Haining County, Zhejiang Province, PR China. Both rectum cancer incidence and mortality were decreased steadily from 1977 to 1996 (Table 3). The age and sex adjusted incidence rates of rectal cancer decreased from 7.27 per 100000 (1977-1981) to 3.71 per 100000 (1992-1996), and mortality was decreased from 4.20 per 100000 (1974-1976) to 2.98 per 100 000 (1992-1996). Thus, age-adjusted incidence and mortality of rectal cancer decreased by 41% and 29% respectively. Nevertheless, both adjusted incidence rates and mortality of colon cancer increased slightly at the same period.

Table 3 Output of following with endoscopy among high-risk population with history of polyps

Year	Expected n	Observed n (%)	Adenoma n (%)	Non-adenomatous n (%)	Colorectal cancer (1/100000)
1st group					
1979	2803	2197(78.38)	178(8.10)	104(4.73)	6(273.10)
1981	2763	1592(57.62)	61(3.83)	27(1.70)	4(251.26)
1983	2719	2147(78.96)	108(5.03)	33(1.54)	2(93.15)
1987	2689	2408(89.52)	191(7.93)	96(4.00)	4(166.11)
1993	2388	1475(61.77)	121(8.20)	52(3.53)	4(271.19)
1998	2207	1020(46.22)	95(9.31)	17(1.67)	4(392.16)
2nd group					
1982	1253	461(36.79)	17(3.69)	6(1.30)	0(0.00)
1984	1235	1056(85.51)	49(4.64)	26(2.46)	0(0.00)
1988	1183	931(78.70)	64(6.87)	20(2.15)	0(0.00)
1994	1097	479(43.66)	33(6.68)	17(3.55)	3(626.30)
1998	1040	486(46.73)	36(7.41)	17(3.50)	0(0.00)
Total		1425	2953(6.68)	417(2.93)	27(189.45)

^aFollowing with 60cm flexible sigmoidoscopy since 1987

Cumulative 20-year incidence and mortality caused by colon and rectal cancers are presented in Figures 2,3 and table 4. Figure 2 shows the incidence of colon and rectal cancers in those individuals aged 30 years and older in the mass screening in 1977. Figure 3 shows mortality caused by colon and rectal cancer in the screened population (those aged 30 years and older in 1977). According to incidence and mortality of age and sex sub-group during 1977 to 1981, we calculated the annual expected rate of sub-group for this cohort population from 1977 to 1996, and then 20-year cumulative incidence and mortality. Observed cumulative 20-year rectal cancer incidence was 31% lower than expected in the screened group; mortality caused by rectal cancer was 18% lower than expected in the screened group. There is no significant difference of incidence and mortality of colon cancer almost between observed and expected. Results showed incidence and mortality were only reduced in the rectal cancer, but not colon cancer.

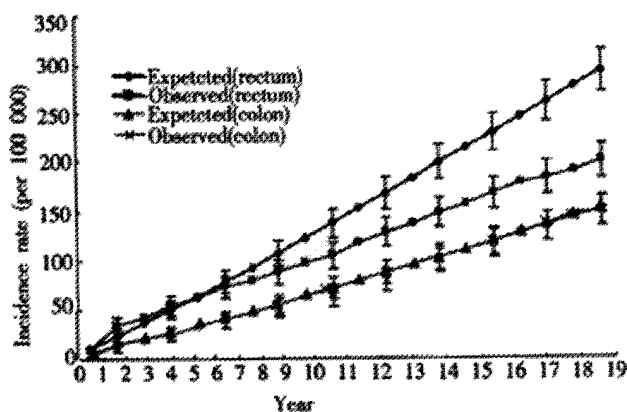


Figure 2 The Expected and Observed Twenty-year Cumulative Incidence of Colon and Rectum Cancer

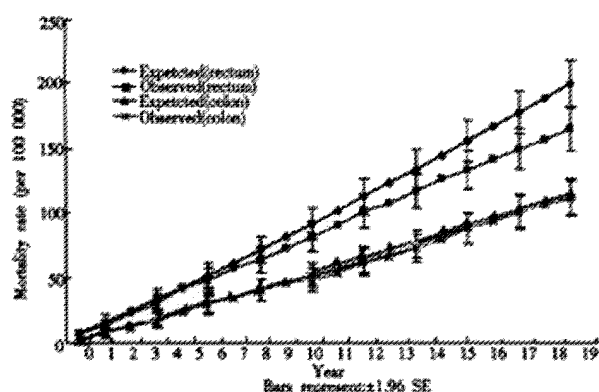


Figure 3 The Expected and Observed Twenty-year Cumulative mortality of Colon and Rectum Cancer

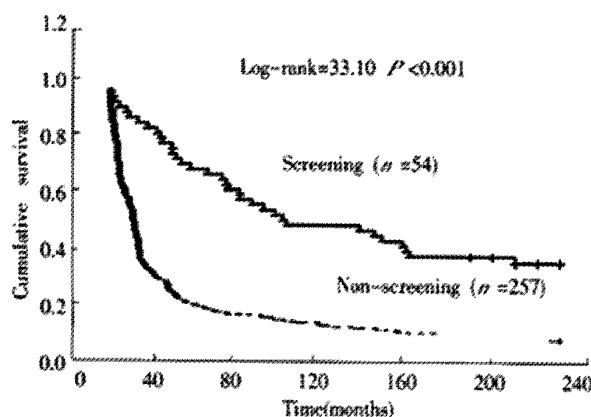


Figure 4 Survival curve (Kaplan-Meier) of rectal cancer diagnosed during 1977-1982

During the initial screenings, 54 cases of colorectal adenocarcinomas were detected and treated. Survival analyses showed that patients with rectal cancers detected during the screenings had significantly longer survival time than rectal cancers identified in patients who were not included in the mass screenings at the same period (log-rank=27.12; $P<0.001$) (See Figure 4). The mean age of screened rectal cancer patients was 57 years (SD=12.8) while the mean age of non-screened rectal cancer patients was 59 years (SD=12.1). The median survival time of screened patients was 133 months (95% CI=56-210mos.) compared with only 14 months (95% CI=11-15 mos.) in non-screened patients. Excluded the leading time bias, the median survival time for screened patients was prolonged by 7.9 years.

DISCUSSION

In the 1980's, it was suggested that population-wide screening with fecal occult blood test (FOBT) was not cost-effective^[27,28]. However, more recent analyses suggest that FOBT-based screening can reduce colorectal cancer mortality^[29-32]. Mandel and colleagues at the Mayo Clinic in Minnesota conducted a randomized screening of over 46,000 individuals^[33,34]. Participants were randomized to annual or biannual FOB test group and a control group. The cumulative 18-year colorectal cancer mortality was reduced by 33% in the annually screened group and 21% in the biennially screened group compared to the control group. It is important to note that although FOBT may be important in early detection of colorectal cancer, this test does not affect the underlying process of neoplastic transformation in the large bowel. In addition, the use of a rehydrated hemoccult test instead of an unrehydrated hemoccult test increased test sensitivity but decreased test specificity resulting in over 10% of participants undergoing colonoscopy exam at each screening. Moreover, a total of 38% of the screened group had at least one colonoscopy during the entire study period. It was proposed by Lang and colleagues that approximately one third to one half of the observed reduction in mortality found in Mandel's study was the result of chance selection for colonoscopy rather than the FOBT itself^[35-37]. Another two randomized screening trials using unrehydrated hemoccult test every two years resulted in only 4% of the test group requiring colonoscopy, yet reduced colorectal cancer mortality by 15-18%^[39-43]. However, no evidence showed incidence rate has been reduced from colorectal cancer by FOBT-based mass screening.

The population-wide mass screenings were conducted from 1977-1980 among 246252 residents of Haining County aged 30 years or older. The overall participation rates were 83%. A total of 54 cases of rectal cancer were detected and treated. Overall survival in these patients was significantly increased compared to non-screened rectal cancer patients (log-rank=33.4; $P<0.0001$). Excluding leading time bias, the survival time was prolonged by almost 8 years in screened patients. In addition, 4076 patients with newly discovered adenomas and/or nonadenomatous polyps were treated by polypectomy and followed with periodic examinations through 1998. During follow-up, 953 metachronous adenomas and 417 nonadenomatous polyps were detected and removed; an additional 27 colorectal cancers, 12 of which were carcinoma in situ, were diagnosed and treated. According to the Haining County Cancer Registry, from 1977 to 1996 both age- and sex-adjusted colorectal cancer incidence and mortality decreased by 41% and 29% respectively. Further, cumulative 20-year observed incidence and mortality from rectal cancer in the screened population decreased by 31% and 18%, respectively. If interest, incidence rates of rectal cancer in Shanghai, PRC (located 120km from Haining) increased by 11.3% in males and 6.0% in females from 1972 to 1994^[44,45]. Chinese official data showed from 1973-1975 to 1990-1992, age and sex adjusted mortality caused by colorectal cancer increase by 3.61% in urban and decrease by 5.22% in rural population of China^[3]. Above evidence supported that

both incidence and mortality of rectal cancer decreased in Haining due to the population-wide mass screening and following-up with endoscopy to high-risk population.

Winawer and colleagues reported a 76-90% reduction in colorectal cancer incidence in 1418 adenoma patients who underwent periodic colonoscopy after initial polypectomy compared to age-, sex-, and polyp-size-adjusted control groups. Further, follow-up colonoscopy performed three years after initial colonoscopy detection and removal was found to be as effective as follow-up colonoscopy performed after only one or two years. Thus, it is suggested that a screening interval of three years is sufficient following colonoscopic removal of newly diagnosed adenomas^[15,16]. Anyway, our results showed only 31% reduction of incidence of rectal cancer through population-wide mass screening with proctoscopy. It is suggested that there are other pathways besides except of adenoma pathway.

These results suggest that colorectal cancer may be prevented by mass screening with FOBT or endoscopy. Further, removal of precursor lesions may slow or halt the natural history of rectal neoplasms. Our data suggest that mass screening by endoscopy can reduce the incidence and mortality of colorectal cancer. Screening guidelines for asymptomatic individuals suggest that all individuals aged 50 years or older may be benefited by periodic digital rectal examinations, stool guaiac and/or colonoscopy. For patients without adenomas or polyps, these exams should be repeated every three to five years, while patients with precursor lesions should be re-examined for new lesions after one year^[46-48]. Data from cancer statistics of United States indicated that approximately 60% of colorectal cancers are found in the distal colon or rectum^[49,50]. However, according to 1980's report by the Research Team in China, 80% of colorectal cancers are found in the distal colon or rectum, with up to 66% in the rectum alone^[24]. Therefore, it was suggested that mass screening and following up with sigmoidoscopy periodically might be more cost-effective than colonoscopy in China.

REFERENCES

- Landis SH, Murray T, Bolden S, Wingo PA. Cancer Statistics, 1999. *CA Cancer J Clin* 1999;49:8-31
- Landis SH, Murray T, Bolden S, Wingo PA. Cancer statistics, 1998. *CA Cancer J Clin* 1998;48:6-29
- Li LD, Lu FZ, Zhang SW, Mu R, Sun Xd, Wangpu XM, Sun J, Zhou YS, Ouyang NH, Rao KQ, Chen YD, Sun AM, Sun AM, Xue ZF, Xia Y. Analyses of variation trend and short term detection of Chinese malignant tumor mortality during twenty years. *Zhong guo Zhongliu* 1997;19:3-9
- Gupta RA, Dubois RN. Colorectal cancer prevention and treatment by inhibition of cyclooxygenase-2. *Nature Rev Cancer* 2001;1:11-21
- Cruz-Correa M, Hyland LM, Romans KE, Booker SV, Giardiello FM. Long-term treatment with sulindac in familial adenomatous polyposis: a prospective cohort study. *Gastroenterology* 2002;122:641-645
- Gwyn K, Sinicrope FA. Chemoprevention of colorectal cancer. *Am J Gastroenterol* 2002;97:13-21
- Mandel JS, Church TR, Bond JH, Ederer F, Geisser MS, Mongin SJ, Snover DC, Schuman LM. The effect of fecal occult-blood screening on the incidence of colorectal cancer. *N Engl J Med* 2000;343:1603-1607
- Robinson MH, Rodrigues VC, Hardcastle JD, Chamberlain JO, Mangham CM, Moss SM. Faecal occult blood screening for colorectal cancer at Nottingham: details of the verification process. *J Med Screen* 2000;7:97-98
- Jorgensen OD, Kronborg O, Fenger C. A randomised study of screening for colorectal cancer using faecal occult blood testing: results after 13 years and seven biennial screening rounds. *Gut* 2002;50:29-32
- Potter JD. Colorectal cancer: Molecules and Populations. *J Natl Cancer Inst* 1999;91:916-932
- Slattery ML, Potter JD, Ma KN, Caan BJ, Leppert M, Samowitz W. Western diet, family history of colorectal cancer, NAT2, GSTM-1 and risk of colon cancer. *Cancer Causes Control* 2000;11:1-8
- Borugian MJ, Sheps SB, Whittemore AS, Wu AH, Potter JD, Gallagher RP. Carbohydrates and colorectal cancer risk among Chinese in North America. *Cancer Epidemiol Biomarkers Prev* 2002;11:187-193
- Ulrich CM, Kampman E, Bigler J, Schwartz SM, Chen C, Bostick R, Fosdick L, Beresford SA, Yasui Y, Potter JD. Colorectal adenomas and the C677T MTHFR polymorphism: evidence for gene-environment interaction? *Cancer Epidemiol Biomarkers Prev* 1999;8:659-668
- Markowitz AJ, Winawer SJ. Screening and surveillance for colorectal cancer. *Semin Oncol* 1999;26:485-498
- Winawer SJ. Natural history of Colorectal Cancer. *Am J Med* 1999;106:3S-6S
- Winawer SJ, Zauber AG. The advanced adenoma as the primary target of screening. *Gastrointest Endosc Clin N Am* 2002;12:1-9
- Bedenne L, Faiver J, Boutron MC. Adenoma-carcinoma sequence or "de novo" carcinogenesis? A study of adenoma remnants in a population-based series of large bowel cancer. *Cancer* 1992;69:833-838
- Bedenne L, Jouve JL. Monitoring colorectal cancer after surgical resection. *Presse Med* 1999;28:651-656
- Smith RA, Cokkinides V, von E, Levin B, Cohen C, Runowicz CD, Sener S, Saslow D, Eyre HJ. American Cancer Society. American Cancer Society guidelines for the early detection of cancer. *CA Cancer J Clin* 2002;52:8-22
- Smith RA, von Eschenbach AC, Wender R, Levin B, Byers T, Rothenberger D, Brooks D, Creasman W, Cohen C, Runowicz C, Saslow D, Cokkinides V, Eyre H. ACS Prostate Cancer Advisory Committee, ACS Colorectal Cancer Advisory Committee, ACS Endometrial Cancer Advisory Committee. American Cancer Society guidelines for the early detection of cancer: update of early detection guidelines for prostate, colorectal, and endometrial cancers. Also: update 2001—testing for early lung cancer detection. *CA Cancer J Clin* 2001;51:38-75;77-80
- Byers T, Levin B, Rothenberger D, Dodd GD, Smith RA. American Cancer Society guidelines for screening and surveillance for early detection of colorectal polyps and cancer: update 1997. American Cancer Society Detection and Treatment Advisory Group on Colorectal Cancer. *CA Cancer J Clin* 1997;47:154-160
- Zheng S. Early detection and early diagnosis for colorectal cancer. *Shiyong Zhongliu* 1987;4:129-131
- Yu H, Zheng S, Cai XH, Wu JM, Qiu PL, Zhu WX. Evaluation of RPHA fecal occult blood test in screening for colorectal cancer. *Zhonghua Zhongliu Zazhi* 1990;12:108-111
- Zheng S, Yu H, Zhang SZ, Yong G, Sun QR, Zhou L, Liu XY, Li WD. Evaluation of digestive malignant tumor screening methods. *Shiyong Zhongliu Zazhi* 1996; 11:188-189
- Yang G, Zheng W, Sun QR, Shu XO, Li WD, Yu H, Shen GF, Shen YZ, Potter JD, Zheng S. Pathologic Features of Initial Adenoma as Predictors for Metachronous adenomas of the rectum. *J Natl Cancer Inst* 1998;9:1661-1665
- Sun QR. Dynamic Observation on 2815 cases of recto-anal adenoma and polyps for 10 years. *Zhonghua Waikexue Zazhi* 1992;9:561-566
- Eddy DM, Nugent FW, Eddy JF, Collier J, Gilbertsen V, Gottlieb LS, Rice R, Sherlock P, Winawer S. Screening for colorectal cancer in a high-risk population: result of a mathematical model. *Gastroenterology* 1987;92:682-692
- Bat L, Pines A, Ron E, Niv Y, Arditi E, Shemesh E. A community-based program of colorectal screening in an asymptomatic population: evaluation of screening tests and compliance. *Am J Gastroenterol* 1986;81:647-651
- Bond JH. Fecal occult blood test screening for colorectal cancer. *Gastrointest Endosc Clin N Am* 2002;12:11-21
- La VC. Fecal occult blood screening for colorectal cancer: open issues. *Ann Oncol* 2002;13:31-34
- Burke CA, Tadikonda L, Machicao V. Fecal occult blood testing for colorectal cancer screening: use the finger. *Am J Gastroenterol* 2001;96:3175-3177
- Bolin TD, Lapsley HM, Korman MG. Screening for colorectal cancer: what is the most cost-effective approach? *Med J Aust* 2001;174:298-301
- Mandel JS, Church TR, Bond JH, Ederer F, Geisser MS, Mongin SJ, Snover DC, Schuman LM. The effect of fecal occult-blood screening on the incidence of colorectal cancer. *N Engl J Med* 2000;343:1603-1607
- Mandel JS. Colorectal cancer screening. *Cancer Metastasis Rev* 1997;16:263-279
- Lang CA, Ransohoff DF. What can we conclude from the randomized controlled trials of fecal occult blood test screening? *Eur J Gastroenterol Hepatol* 1998;10:199-204
- Lang CA, Ransohoff DF. Fecal occult blood screening for colorectal cancer. Is mortality reduced by chance selection for screening colonoscopy? *JAMA* 1994;271:1011-1013
- Ransohoff DF, Lang CA. Using colonoscopy to screen for colorectal cancer. *Am J Gastroenterol* 1994;89:1765-1766
- Mapp TJ, Hardcastle JD, Moss SM, Robinson MH. Survival of patients with colorectal cancer diagnosed in a randomized controlled trial of faecal occult blood screening. *Br J Surg* 1999;86:1286-1291
- Robinson MH, Hardcastle JD, Moss SM, Amar SS, Chamberlain JO, Armitage NC, Scholefield JH, Mangham CM. The risks of screening: data from the Nottingham randomised controlled trial of faecal occult blood screening for colorectal cancer. *Gut* 1999;45:588-592
- Moss SM, Hardcastle JD, Coleman DA, Robinson MH, Rodrigues VC.

- Interval cancers in a randomized controlled trial of screening for colorectal cancer using a faecal occult blood test. *Int J Epidemiol* 1999;28:386-390
- 41 Rasmussen M, Kronborg O, Fenger C, Jorgensen OD. Possible advantages and drawbacks of adding flexible sigmoidoscopy to hemoccult-II in screening for colorectal cancer. A randomized study. *Scand J Gastroenterol* 1999;34:73-78
- 42 Kjeldsen BJ, Kronborg O, Fenger C, Jorgensen OD. The pattern of recurrent colorectal cancer in a prospective randomised study and the characteristics of diagnostic tests. *Int J Colorectal Dis* 1997;12:329-334
- 43 Kronborg O, Fenger C, Olsen J, Jorgensen OD, Sondergaard O. Randomized population study of screening for intestinal cancer with Hemoccult-II. *Ugeskr Laeger* 1997;159:4977-4981
- 44 Ji BT, Devesa SS, Chow WH, Jin F, Gao YT. Colorectal cancer incidence trends by subsite in urban Shanghai, 1972-1994. *Ca Epid Bio Prev* 1998; 7: 661-666
- 45 Jin F, Devesa SS, Chow WH, Zheng W, Ji BT, Fraumeni JF Jr, Gao YT. Cancer incidence trends in urban Shanghai, 1972-1994: an update. *Int J Cancer* 1999; 83: 435-440
- 46 Liu XY, Zheng S, Yang G, YU H, Zhou L, Zhang X, Sun QR, Shen GF, Shen YZ, Ding XF. Evaluation of the application of the optimized colorectal cancer screening protocol in high-risk population. *Zhongliu Fangzhi Yanjiu* 1997;24:197-199
- 47 Zheng S. Progress in colorectal cancer research in China. *Zhongguo Zhongliu Linchuang* 1998;25:225-228
- 48 Zheng S. Recent study on colorectal cancer in China. *Chin Med J* 1996; 109:179-192
- 49 Greenlee RT, Murray T, Bolden S, Wingo PA. Cancer statistics, 2000. *CA Cancer J Clin* 2000;50:7-33
- 50 Ries LA, Wingo PA, Miller DS, Howe HL, Weir HK, Rosenberg HM, Vernon SW, Cronin K, Edwards BK. The annual report to the nation on the status of cancer, 1973-1997, with a special section on colorectal cancer. *Cancer* 2000;88:2398-2424

Edited by Pagliarini R

• LARGE INTESTINAL CANCER •

Effects of ursolic acid and oleanolic acid on human colon carcinoma cell line HCT15

Jie Li, Wei-Jian Guo, Qing-Yao Yang

Jie Li, Wei-Jian Guo, Department of Oncology, Cancer Center, Xin Hua Hospital, Shanghai Second Medical University, Shanghai 200092, China
Qing-Yao Yang, Department of Biology, Shanghai Teachers University, Shanghai 200234, China

Correspondence to: Dr. Jie Li, Department of Oncology, Cancer Center, Xin Hua Hospital, Shanghai Second Medical University, Shanghai 200092, China. ljee@citic.net

Telephone: +86-21-65010796 Fax: +86-21-65010796

Received 2001-12-20 Accepted 2002-02-07

Abstract

AIM: Ursolic acid (UA) and oleanolic acid (OA) are triterpene acids having a similar chemical structure and are distributed widely in plants all over the world. In recent years, it was found that they had marked anti-tumor effects. There is little literature currently available regarding their effects on colon carcinoma cells. The present study was designed to investigate their inhibitory effects on human colon carcinoma cell line HCT15.

METHODS: HCT15 cells were cultured with different drugs. The treated cells were stained with hematoxylin-eosin and their morphologic changes observed under a light microscope. The cytotoxicity of these drugs was evaluated by tetrazolium dye assay. Cell cycle analysis was performed by flow cytometry (FCM). Data were expressed as means \pm SEM and Analysis of variance and Student's *t*-test for individual comparisons.

RESULTS: Twenty-four to 72h after UA or OA 60 μ mol/L treatment, the numbers of dead cells and cell fragments were increased and most cells were dead at the 72nd hour. The cytotoxicity of UA was stronger than that of OA. Seventy-eight hours after 30 μ mol/L of UA or OA treatment, a number of cells were degenerated, but cell fragments were rarely seen. The IC_{50} values for UA and OA were 30 and 60 μ mol/L, respectively. Proliferation assay showed that proliferation of UA and OA-treated cells was slightly increased at 24h and significantly decreased at 48h and 60h, whereas untreated control cells maintained an exponential growth curve. Cell cycle analysis by FCM showed HCT15 cells treated with UA 30 and OA 60 for 36h and 72h gradually accumulated in G_0/G_1 phase (both drugs $P < 0.05$ for 72h), with a concomitant decrease of cell populations in S phase (both drugs $P < 0.01$ for 72h) and no detectable apoptotic fraction.

CONCLUSION: UA and OA have significant anti-tumor activity. The effect of UA is stronger than that of OA. The possible mechanism of action is that both drugs have an inhibitory effect on tumor cell proliferation through cell-cycle arrest.

Li J, Guo WJ, Yang QY. Effects of ursolic acid and oleanolic acid on human colon carcinoma cell line HCT15. *World J Gastroenterol* 2002;8(3):493-495

INTRODUCTION

Ursolic acid (UA) and oleanolic acid (OA) are triterpene acids having a similar chemical structure and are distributed widely in plants

all over the world^[1-20]. They are of interest to scientists because of their biological activities. OA has antifungal^[21,22], insecticidal^[23], anti-HIV^[24,25], diuretic^[26], complement inhibitory^[27], blood sugar depression^[28] and gastrointestinal transit modulating^[29] activities. UA and OA also possess liver-protection^[30-33] and anti-inflammatory effects^[34-37]. In recent years, it was found that they had marked anti-tumor effects and exhibited cytotoxic activity toward many cancer cell line in culture^[38-44]. Concerning their effects on colon carcinoma cells, there is little available so far in the current literature. The present study was designed to investigate their inhibitory effects on the human colon carcinoma cell line HCT15.

MATERIALS AND METHODS

Drugs and reagents

UA and OA were gifts from Professor Qing-Yao Yang, Department of Biology, Shanghai Teachers University. UA was extracted from *Catharantus roseus* L. with purity 99%, and OA from *Ziziphus jujuba* Mill. with purity 98%. The drugs were dissolved in 100% ethanol and then diluted 10 times with RPMI-1640 as the working solution, the final concentration of ethanol being less than 2%. Me^a-2SO was purchased from the Sigma Company (USA).

Cell line and culture medium

HCT15 had been introduced from the NCI (USA) and was cultured and kept in this laboratory. The culture medium used was RPMI-1640 with 10% BSA (Huamei BG, Co Ltd, China).

Cell morphology observation

The morphology of the live cells was observed with an inverted microscope and the live and dead cells were identified after 1% Trypan blue staining^[45]. Cell smear was stained with hematoxylin-eosin (HE). Cytotoxicity identification with tetrazolium dye assay (MTT) 1.8×10^4 cells were inoculated to each of the 3 parallel wells on a 96-well plate and cultured overnight. Different concentrations of UA and OA were added with a final volume of 0.2mL and cultured for 72 more hours. MTT 20 μ L (5g/L) was added to each well. 4h later samples were centrifuged and the supernatant was discarded. 180 μ L Me₂SO was added and the 570nm absorbance was read. The mean value of each concentration (3 well) was obtained. Experiments were repeated three times^[46].

The inhibition rate (%) = (1 - average rate of the treated/average of the control) \times 100

Flowcytometric detection of cell cycle

Cell cycle was determined by flowcytometric assays^[47]. To 1ml of cell suspension with a concentration of 1×10^8 /L, 30 μ mol/L UA and OA 60 μ mol/L were added. The cells were collected after being cultured for 36h and 72h, respectively. Collected cells were treated with absolute alcohol, then with 1% Triton X-100 (Sigma, USA) for 10min at room temperature. The samples were centrifuged, and the supernatant discarded. 0.01% Rnase was added and samples were shaken for 10min in a 37°C water bath. Samples were stained with 0.05% propidium iodide for 10min in 4°C in darkness. The cell cycle distribution was detected with flowcytometer (Model FACSCALIBAR, B.D., USA) and 10000 cells were analyzed with MODFIT software.

Data analysis

Data are displayed as percentage of control condition. Data were expressed as means \pm SEM and Analysis of variance and Student's *t*-test for individual comparisons. $P < 0.05$ was considered statistically significant.

RESULTS

Changes in cell morphology

When HCT15 cells were treated with UA 60 μ mol/L for 24 hours, a number of cells were found dead with a lot of cellular fragments. Among the intact cells, the dead ones accounted for more than 30%. Seventy-two hours later, the number of cells decreased significantly and the remaining cells became shrunken with disappearance of cellular refraction. On the smear stained with HE, a large amount of cellular fragments could be found. When treated with OA 60 μ mol/L for 24 hours, a few cells were dead. There were relatively large amounts of cellular fragments and the dead cells accounted for about 15% at 72 h. Within 72 hours of either UA or OA treatment at a concentration of 30 μ mol/L, a percentage of the cells became rugate at the periphery with blurred cellular borders. There was no obvious cell fragmentation. Relatively large amount of degenerated cells could be seen on HE stained smear, but degenerated cells with OA were markedly less than that with UA.

The cytotoxicity

Cell viability was significantly decreased by treatment of UA and OA for 72 h in a dose-dependent manner. Their IC_{50} were 30 μ mol/L for UA and 60 μ mol/L for OA (Figure 1). Proliferation assay showed that proliferation of UA and OA-treated cells slightly increased at 24 h and significantly decreased at 48 h and 60 h, whereas untreated control cells maintained exponential growth curves (Figure 2).

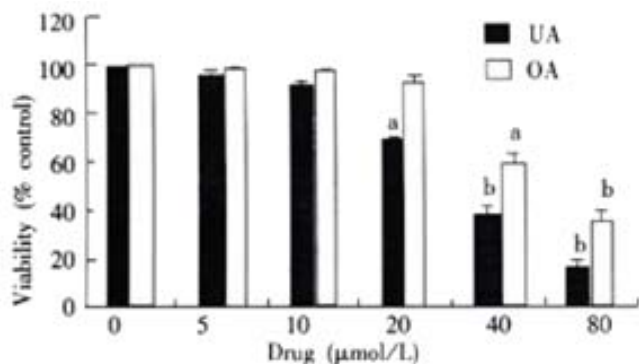


Figure 1 Effects of UA and OA on viability of colon carcinoma cell line. Relative cell viability was assessed by MTT assays. HCT15 cells were treated with various concentrations of UA and OA, respectively for 48 h. Data points represent mean values of 3 replicates, with bar indicating SEM. ^a $P < 0.05$, ^b $P < 0.01$ vs control.

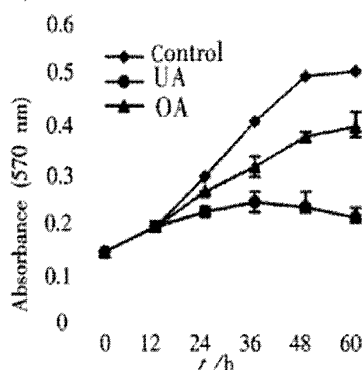


Figure 2 Effects of UA and OA on proliferation of HCT15 cells. HCT15 cells were treated with 30 μ mol/L UA and OA, respectively. The absorbance of 570 nm means the amount of living cells. Data points represent mean values of 3 replicates, with bar indicating SEM. $P < 0.05$, $P < 0.01$ vs control.

Change in cell cycle

When treated the HCT15 cells with different doses of UA and OA for different times, the cell cycle obtained by FCM were as shown in Table 1. HCT15 cells treated with UA 30 μ mol/L and OA 60 μ mol/L for 12 h and 48 h gradually accumulated in G_0/G_1 phase, with a concomitant decrease of cell population in S phase and no detectable apoptotic fraction.

Table 1 The cell cycle distribution of colon carcinoma cell line HCT15 treated with UA and OA ($n=3$ $\bar{x} \pm s$)

Cell cycle	Control		UA (30 μ mol/L)		OA (60 μ mol/L)	
	36h	72h	36h	72h	36h	72h
G_0+G_1	62 \pm 7	50 \pm 7	70 \pm 6	81 \pm 10 ^a	68 \pm 9	76 \pm 6 ^a
S	31 \pm 5	42 \pm 8	22 \pm 4 ^a	9 \pm 3 ^b	26 \pm 4	12 \pm 3 ^b
G_2+M	7 \pm 2	8 \pm 2	8 \pm 3	10 \pm 2	6 \pm 1	12 \pm 2

^a $P < 0.05$, ^b $P < 0.01$ vs control.

DISCUSSION

UA and OA both belong to pentacyclic triterpenoid acids. They have a similar molecular structure, but have different sites of the methyl group on the E loop: if the methyl group at C_{19} of UA is moved to C_{20} , it becomes OA. They are distributed widely in plants. In Korean traditional medicine, UA was used in anti-tumor therapy for a long time. Recently, it has been indicated in and outside China that UA and OA have a definitive antitumor activity by various routes^[48-50].

This paper observed the anti-tumor activity of UA and OA on the HCT15 cells with some preliminary studies on their mechanism of action. With concentrations higher than their IC_{50} , there was obvious cell death and fragmentation. With the IC_{50} concentration, a few cell fragments were found, but cell death was also obvious. To investigate the effects of UA and OA on the viability of HCT15 cells, HCT15 viability was assessed by MTT assay. In addition, we performed a proliferation assay to identify the anti-proliferation effect of UA and OA. The results showed that cell viability was significantly decreased in a concentration-dependent manner and proliferation was markedly inhibited by both drugs. It was shown that both drugs possessed an inhibitory effect on HCT15 cells. The activity was significantly stronger with UA than with OA. According to changes in HCT15 cell morphology, UA and OA have a direct cytotoxic effect on HCT15 cells. Also it has been reported that UA exhibited both cytotoxic and cytostatic activity in A431 human epidermoid carcinoma cells^[48] and OA has a cytotoxic activity against many cancer cell lines^[43]. After incubation of the HCT15 cells with UA or OA for different times, the cell cycle was notably changed. When treated with IC_{50} concentration for 36 and 72 hours, the G_0/G_1 phase cells were gradually increased, with a concomitant decrease of cell population in S phase and no detectable apoptotic fraction. This result was in accordance with an inhibitory effect of UA and OA on HCT15 cells proliferation. These observations suggest that UA and OA may be involved in the action of the G_0/G_1 checkpoint and inhibition of DNA replication. Some studies have supported this inference. They have found that oleanane-type triterpenoids had inhibitory effects on DNA polymerase beta and DNA topoisomerases^[51,52]. Many papers have demonstrated that UA can induce apoptosis^[53,54]. But in the present study FCM assays showed that no apoptotic fraction in treated HCT15 cells. It is worth studying this further by using other methods of detecting apoptosis.

In conclusion, UA and OA have a definite anti-tumor activity on HCT15 cells. The effect of UA is stronger than that of OA. The possible mechanism of action is that both drugs have an inhibitory effect on tumor cell proliferation through cell-cycle arrest.

The toxicity of UA and OA is low and their distribution in plants is extensive. Besides their anti-tumor activity, they also possess immuno-regulatory and liver-protective effects. Therefore, they have

a bright future in clinical application. Further investigation to explore their potential in tumor treatment may prove to be worthwhile.

REFERENCES

- Zhu N, Sheng S, Sang S, Jhoo JW, Bai N, Karwe MV, Rosen RT, Ho CT. Triterpene Saponins from Debittered Quinoa (Chenopodium quinoa) Seeds. *J Agric Food Chem* 2002;50:865-867
- Takeoka G, Dao L, Teranishi R, Wong R, Flessa S, Harden L, Edwards R. Identification of three triterpenoids in almond hulls. *J Agric Food Chem* 2000;48:3437-3439
- Upadhyay RK, Pandey MB, Jha RN, Singh VP, Pandey VB. Triterpene glycoside from Terminalia arjuna. *J Asian Nat Prod Res* 2001;3:207-212
- Si J, Gao G, Chen D. Chemical constituents of the leaves of Crataegus scabrifolia (Franch.) Rehd. *Zhongguo Zhongyao Zazhi* 1998;23:422-432
- Guo XM, Zhang L, Quan SC, Hong YH, Sun LN, Liu MZ. Isolation and identification of Triterpenoid compounds in the fruits of Chaenomeles lagenaria (Loisel.) Koidz. *Zhongguo Zhongyao Zazhi* 1998;23:546-547
- Wang YP, Zhu ZY, Wang CF, Yang JS. Determination of oleanolic acid and total saponins in Aralia L. *Zhongguo Zhongyao Zazhi* 1998;23:518-521
- Shi LF, Cai Z, Wu GT, Yang ST, Ma Y. RP-HPLC determination of water-soluble active constituents and oleanolic acid in the fruits of Ligustrum lucidum Ait. collected from various areas. *Zhongguo Zhongyao Zazhi* 1998;23:77-79
- Ding H, Wang Y, Wang SY, You WY. Quantitative determination of ursolic acid in Herba cynomorii by ultraviolet spectrophotometry. *Zhongguo Zhongyao Zazhi* 1998 ;23:102-103, inside back cover
- Zhou FX, Liang PY, Zhou Q, Qin ZQ. Chemical constituents of the stem and root of Syzygium buxifolium Hook. Et Arn. *Zhongguo Zhongyao Zazhi* 1998;23:164-165
- Kamel MS, Mohamed KM, Hassanean HA, Ohtani K, Kasai R, Yamasaki K. Acylated flavonoid glycosides from Bassia muricata. *Phytochemistry* 2001;57:1259-1262
- Akbar E, Riaz M, Malik A. Ursene type nortriterpene from Debregeasia salicifolia. *Fitoterapia* 2001;72:382-385
- Siddiqui BS, Sultana I, Begum S. Triterpenoidal constituents from Eucalyptus camaldulensis var. obtusa leaves. *Phytochemistry* 2000;54:861-865
- Prasad D, Juyal V, Singh R, Singh V, Pant G, Rawat MSM. A new secoiridoid glycoside from Lonicera angustifolia. *Fitoterapia* 2000;71:420-424
- Hou AJ, Yang H, Jiang B, Zhao QS, Lin ZW, Sun HD. A new ent-kaurane diterpenoid from Isodon phyllostachys. *Fitoterapia* 2000;71:417-419
- Ye WC, Zhang QW, Liu X, Che CT, Zhao SX. Oleanane saponins from Gymnema sylvestre. *Phytochemistry* 2000;53:893-899
- Setzer WN, Setzer MC, Bates RB, Jackes BR. Biologically active triterpenoids of Syncarpia glomulifera bark extract from Paluma, north Queensland, Australia. *Planta Med* 2000;66:176-177
- Nguyen LH, Harrison LJ. Xanthones and triterpenoids from the bark of Garcinia vilseniana. *Phytochemistry* 2000;53:111-114
- Perez-Camino MC, Cert A. Quantitative determination of hydroxy pentacyclic triterpene acids in vegetable oils. *J Agric Food Chem* 1999; 47:1558-1562
- Chang CW, Wu TS, Hsieh YS, Kuo SC, Chao PD. Terpenoids of Syzygium formosanum. *J Nat Prod* 1999;62:327-328
- Vo DH, Yamamura S, Ohtani K, Kasai R, Yamasaki K, Nguyen TN, Hoang MC. Oleanane saponins from Polyscias fruticosa. *Phytochemistry* 1998;47:451-457
- Tang HQ, Hu J, Yang L, Tan RX. Terpenoids and flavonoids from Artemisia species. *Planta Med* 2000;66:391-393
- Jeong TS, Hwang EI, Lee HB, Lee ES, Kim YK, Min BS, Bae KH, Bok SH, Kim SU. Chitin synthase II inhibitory activity of ursolic acid, isolated from Crataegus pinnatifida. *Planta Med* 1999;65:261-263
- Marquina S, Maldonado N, Garduno-Ramirez ML, Aranda E, Villarreal ML, Navarro V, Bye R, Delgado G, Alvarez L. Bioactive oleanolic acid saponins and other constituents from the roots of Viguiera decurrens. *Phytochemistry* 2001;56:93-97
- Kashiwada Y, Nagao T, Hashimoto A, Ikeshiro Y, Okabe H, Cosentino LM, Lee KH. Anti-AIDS agents 38. Anti-HIV activity of 3-O-acyl ursolic acid derivatives. *J Nat Prod* 2000;63:1619-1622
- Ma C, Nakamura N, Hattori M, Kakuda H, Qiao J, Yu H. Inhibitory effects on HIV-1 protease of constituents from the wood of Xanthoceras sorbifolia. *J Nat Prod* 2000;63:238-242
- Alvarez ME, Maria AO, Saad JR. Diuretic activity of Fabiana patagonica in rats. *Phytother Res* 2002;16:71-73
- Assefa H, Nimrod A, Walker L, Sindelar R. Enantioselective synthesis and complement inhibitory assay of A/B-ring partial analogues of oleanolic acid. *Bioorg Med Chem Lett* 2001;11:1619-1623
- Yoshikawa M, Matsuda H. Antidiabetogenic activity of oleanolic acid glycosides from medicinal foodstuffs. *Biofactors* 2000;13:231-237
- Li Y, Matsuda H, Yoshikawa M. Effects of oleanolic acid glycosides on gastrointestinal transit and ileus in mice. *Bioorg Med Chem* 1999;7:1201-1205
- Yim TK, Wu WK, Pak WF, Ko KM. Hepatoprotective action of an oleanolic acid-enriched extract of Ligustrum lucidum fruits is mediated through an enhancement on hepatic glutathione regeneration capacity in mice. *Phytother Res* 2001;15:589-592
- Saraswat B, Visen PK, Agarwal DP. Ursolic acid isolated from Eucalyptus tereticornis protects against ethanol toxicity in isolated rat hepatocytes. *Phytother Res* 2000;14:163-166
- Latha PG, Panikkar KR. Modulatory effects of ixora coccinea flower on cyclophosphamide-induced toxicity in mice. *Phytother Res* 1999;13: 517-520
- Jeong HG. Inhibition of cytochrome P450 2E1 expression by oleanolic acid: hepatoprotective effects against carbon tetrachloride-induced hepatic injury. *Toxicol Lett* 1999;105:215-222
- Ismaili H, Tortora S, Sosa S, Fkih-Tetouani S, Ildirissi A, Della Loggia R, Tubaro A, Aquino R. Topical anti-inflammatory activity of Thymus wilddenowii. *J Pharm Pharmacol* 2001;53:1645-1652
- Giner-Larza EM, Manez S, Recio MC, Giner RM, Prieto JM, Cerda-Nicolas M, Rios JL. Oleanonic acid, a 3-oxotriterpene from Pistacia, inhibits leukotriene synthesis and has anti-inflammatory activity. *Eur J Pharmacol* 2001;428:137-143
- Ryu SY, Oak MH, Yoon SK, Cho DI, Yoo GS, Kim TS, Kim KM. Anti-allergic and anti-inflammatory triterpenes from the herb of Prunella vulgaris. *Planta Med* 2000;66:358-360
- Baricevic D, Sosa S, Della Loggia R, Tubaro A, Simonovska B, Krasna A, Zupancic Topical anti-inflammatory activity of Salvia officinalis L. leaves: the relevance of ursolic acid. *J Ethnopharmacol* 2001;75:125-132
- Li J, Xu LZ, Zhu WP, Zhang TM, Li XM, Jin AP, Huang KM, Li DL, Yang QY. Effects of ursolic acid and oleanolic acid on Jurkat lymphoma cell line in vitro. *Zhongguo Aizheng Zazhi* 1999; 9:395-397
- Hollosy F, Idei M, Csorba G, Szabo E, Bokonyi G, Seprodi A, Meszaros G, Szende B, Keri G. Activation of caspase-3 protease during the process of ursolic acid and its derivative-induced apoptosis. *Anticancer Res* 2001;21:3485-3491
- Rios MY, Gonzalez-Morales A, Villarreal ML. Sterols, triterpenes and biflavonoids of Viburnum juncundum and cytotoxic activity of ursolic acid. *Planta Med* 2001;67:683-684
- Martin-Cordero C, Reyes M, Ayuso MJ, Toro MV. Cytotoxic triterpenoids from Erica andevalensis. *Z Naturforsch [C]* 2001;56:45-48
- Lauthier F, Taillet L, Trouillas P, Delage C, Simon A. Ursolic acid triggers calcium-dependent apoptosis in human Daudi cells. *Anticancer Drugs* 2000;11:737-745
- Ko HH, Yen MH, Wu RR, Won SJ, Lin CN. Cytotoxic isoprenylated flavans of Broussonetia kazinoki. *J Nat Prod* 1999;62:164-166
- Cha HJ, Park MT, Chung HY, Kim ND, Sato H, Seiki M, Kim KW. Ursolic acid-induced down-regulation of MMP-9 gene is mediated through the nuclear translocation of glucocorticoid receptor in HT1080 human fibrosarcoma cells. *Oncogene* 1998;16:771-778
- Mascotti K, McCullough J, Burger SR. HPC viability measurement: trypan blue versus acridine orange and propidium iodide. *Transfusion* 2000; 40:693-696
- Li J, Xu LZ, He KL, Guo WJ, Zheng YH, Xia P, Chen H. Reversal effects of norgestrol acetate on multidrug resistance in adriamycin-resistant MCF7 breast cancer cell line. *Breast Cancer Res* 2001; 3:253-263
- Cao WX, Cheng QM, Fei XF, Li SF, Yin HR, Lin YZ. A study of preoperative methionine-depleting parenteral nutrition plus chemotherapy in gastric cancer patients. *World J Gastroenterol* 2000; 6:255-258
- Hollosy F, Meszaros G, Bokonyi G, Idei M, Seprodi A, Szende B, Keri G. Cytostatic, cytotoxic and protein tyrosine kinase inhibitory activity of ursolic acid in A431 human tumor cells. *Anticancer Res* 2000;20:4563-4570
- Choi CY, You HJ, Jeong HG. Nitric oxide and tumor necrosis factor-alpha production by oleanolic acid via nuclear factor-kappaB activation in macrophages. *Biochem Biophys Res Commun* 2001;288:49-55
- Subbaramaiah K, Michaluart P, Sporn MB, Dannenberg AJ. Ursolic acid inhibits cyclooxygenase-2 transcription in human mammary epithelial cells. *Cancer Res* 2000;60:2399-2404
- Wada S, Iida A, Tanaka R. Screening of triterpenoids isolated from Phyllanthus flexuosus for DNA topoisomerase inhibitory activity. *J Nat Prod* 2001;64:1545-1547
- Deng JZ, Starck SR, Hecht SM. DNA polymerase beta inhibitors from Baeckea gunniana. *J Nat Prod* 1999;62:1624-1626
- Choi BM, Park R, Pae HO, Yoo JC, Kim YC, Jun CD, Jung BH, Oh GS, So HS, Kim YM, Chung HT. Cyclic adenosine monophosphate inhibits ursolic acid-induced apoptosis via activation of protein kinase A in human leukaemic HL-60 cells. *Pharmacol Toxicol* 2000;86:53-58
- Kim DK, Baek JH, Kang CM, Yoo MA, Sung JW, Chung HY, Kim ND, Choi YH, Lee SH, Kim KW. Apoptotic activity of ursolic acid may correlate with the inhibition of initiation of DNA replication. *Int J Cancer* 2000;87:629-636

• LARGE INTESTINAL CANCER •

TGF β_1 expression and angiogenesis in colorectal cancer tissue

Bin Xiong, Ling-Ling Gong, Feng Zhang, Ming-Bo Hu, Hong-Yin Yuan

Bin Xiong, Ling-Ling Gong, Feng Zhang, Ming-Bo Hu, Hong-Yin Yuan, Department of Oncology, Affiliated Zhongnan Hospital of Wuhan University, Wuhan 430071, Hubei Province, China
Supported by Hubei province Natural Science Foundation, No.2000J054
Correspondence to: Dr. Bin Xiong, Department of Oncology, Affiliated Zhongnan Hospital of Wuhan University, Wuhan 430071, Hubei, Province, China. xbxh@public.wh.hb.cn
Telephone: +86-27-87325716
Received 2001-07-19 Accepted 2001-08-23

Abstract

AIM: Transforming growth factor(TGF) β_1 is involved in a variety of important cellular functions, including cell growth and differentiation, angiogenesis, immune function and extracellular matrix formation. However, the role of TGF β_1 as an angiogenic factor in colorectal cancer is still unclear. We investigate the relationship between transforming growth factor β_1 and angiogenesis by analyzing the expression of transforming growth factor(TGF) β_1 in colorectal cancer, as well as its association with VEGF and MVD.

METHODS: The expression of TGF β_1 , VEGF, as well as MVD were detected in 98 colorectal cancer by immunohistochemical staining. The relationship between the TGF β_1 expression and VEGF expression, MVD was evaluated. To evaluate the effect of TGF β_1 on the angiogenesis of colorectal cancers.

RESULTS: Among 98 cases of colorectal cancer, 37 were positive for TGF β_1 (37.8%), 36 for VEGF (36.7%), respectively. The microvessel counts ranged from 19 to 139.8, with a mean of 48.7 (standard deviation, 21.8). The expression of TGF β_1 was correlated significantly with the depth of invasion, stage of disease, lymph node metastasis, VEGF expression and MVD. Patients in T3-T4, stage III-IV and with lymph node metastasis had much higher expression of TGF β_1 than patients in T1-T2, stage I-II and without lymph node metastasis ($P < 0.05$). The positive expression rate of VEGF (58.3%) in the TGF- β_1 positive group is higher than that in the TGF- β_1 negative group (41.7%, $P < 0.05$). Also, the microvessel count (54 ± 18) in TGF- β_1 positive group is significantly higher than that in TGF- β_1 negative group (46 ± 15 , $P < 0.05$). The microvessel count in tumors with both TGF- β_1 and VEGF positive were the highest (58 ± 20 , 36-140, $P < 0.05$). Whereas that in tumors with both TGF- β_1 and VEGF negative were the lowest (38 ± 16 , 19-60, $P < 0.05$).

CONCLUSION: TGF β_1 might be associated with tumor progression by modulating the angiogenesis in colorectal cancer and TGF β_1 may be used as a possible biomarker.

Xiong B, Gong LL, Zhang F, Hu MB, Yuan HY. TGF β_1 expression and angiogenesis in colorectal cancer tissue. *World J Gastroenterol* 2002;8(3):496-498

INTRODUCTION

Angiogenesis is essential for tumor growth and metastasis^[1-6]. An association between poor prognosis and increase in microvascular

density (MVD) of tumor has been reported in certain tumors^[5-10]. This neoangiogenesis depends on the production of angiogenic factors by tumor cells and normal cells^[7-15]. Vascular endothelial growth factor (VEGF) also plays a key role in angiogenesis of tumor^[3-20], but the role of transforming growth factor- β_1 is not clear yet. Now the expression of TGF- β_1 and VEGF, MVD were detected in 98 colorectal cancer by immunohistochemical staining, in order to investigate the correlation of TGF- β_1 and angiogenesis in colorectal cancer.

MATERIALS AND METHODS

Patients

All total of 98 colorectal adenocarcinoma patients who had undergone surgical resection in the Affiliated Zhongnan Hospital of Wuhan University (Wuhan) from July 1998 to December 2000 were included. There were 53 male and 45 female, with an age range from 23 to 74 years (mean, 56 ± 11.2 years). Among the 98 adenocarcinoma patients, 17 were well differentiated, 47 moderately differentiated and 34 poorly differentiated. According to Dukes stage criteria, 34 cases were stage I, 29 stage II, 30 stage III and 5 stage IV.

Methods

Immunohistochemistry All the tissue specimens were fixed in 100 mL L⁻¹ neutral formalin and embedded in paraffin. Five-micrometer-thick sections were treated with xylene, dehydrated in ethanol. Tissue sections were washed three times in 0.05 mol L⁻¹ PBS, incubated in endogenous peroxidase blocking solution. Non-specific antibody binding was blocked by pretreatment with PBS containing 5 g L⁻¹ bovine serum albumin. Sections were then rinsed in PBS and incubated overnight at 4°C with diluted anti-TGF β_1 protein polyclonal antibody, anti-VEGF protein polyclonal antibody and anti-CD34 protein monoclonal antibody. These steps were performed using immunostain kit according to the manufacturers instructions. PBS was used as substitutes of protein antibody for negative control groups. The sections were examined under light microscopy. Anti-TGF β_1 protein polyclonal antibody were purchased from Bosden Co (Wuhan). Anti-VEGF protein polyclonal antibody, anti-CD34 protein monoclonal antibody, and S-P detection kit were purchased from Fuzhou Maixin Co. Anti-TGF β_1 protein polyclonal antibody was diluted to 1:100. Anti-VEGF protein polyclonal antibody and anti-CD34 protein monoclonal antibody were impromptu type.

Results Positive signal was located in the cytoplasm or/and cell membrane. Immunoreactivity was graded as follows: +, $\geq 10\%$ stained tumor cells; -, $< 10\%$ stained tumor cells^[21-23]. The microvessel counting procedures have been described in the published studies^[21-24]. Briefly, the stained sections were screened at a magnification of $\times 100$ ($\times 10$ objective and $\times 10$ ocular lens) under a light microscope to identify the 3 regions of the section with the highest microvessel density. Microvessels were counted in these areas at a magnification of $\times 200$, and the average numbers of microvessels were recorded. The average number is known as MVD of the tumor.

Statistical analysis The difference between each group was analyzed by Chi-square test and correlativity. Significant difference was taken of $P < 0.05$.

RESULTS

TGF β_1 expression in colorectal cancer and clinicopathologic findings

TGF β_1 was localized mainly in the cytoplasm and cell membrane of the tumor cells (Figure 1). TGF β_1 expression was detected in 37 tumors (37.8%). The correlation between TGF β_1 expression and the clinicopathologic findings was shown in Table 1. The expression of TGF β_1 was correlated significantly with the depth of invasion, stage of disease and lymph node metastasis. Patients in T3-T4, stage III-IV and with lymph node metastasis had much higher TGF β_1 than patients in T1-T2, stage I-II and without lymph node metastasis ($P < 0.05$). The expression of TGF β_1 was not correlated with age, gender and differentiation degree of the tumor.

Relationship between TGF β_1 expression, VEGF expression and MVD

VEGF was localized mainly in the cytoplasm and cell membrane of the tumor cells (Figure 2). VEGF expression was detected in 36 tumors (36.7%), and TGF- β_1 expression was correlated closely with VEGF expression (Table 1). The positive expression rate of VEGF (58.3%) in the positive TGF- β_1 group was higher than that in the negative TGF- β_1 group (41.7%, $P < 0.05$).

The number of the microvessel counts in all cases were 19-140 (\pm s, 49 ± 22). Moreover, the microvessel counts were 54 ± 18 in TGF- β_1 positive tumors and 46 ± 15 in TGF- β_1 negative tumors ($P < 0.05$, Table 1). TGF- β_1 expression, VEGF expression and MVD were significantly correlated one another ($r = 0.5816$, 0.2619 and 0.5182 , respectively, $P < 0.05$). The microvessel counts in tumors with both positive TGF- β_1 and VEGF were the highest (58 ± 20 , 36-140; $P < 0.05$). The microvessel counts in tumors with both negative TGF- β_1 and VEGF were the lowest (38 ± 16 , 19-60; $P < 0.05$). The microvessel counts in tumors with positive TGF β_1 and negative VEGF were 25-128 (49 ± 18), and that in tumors with negative TGF β_1 and positive VEGF were 31-133 (50 ± 20), lower than that in tumors with both positive TGF- β_1 and VEGF ($P < 0.05$).

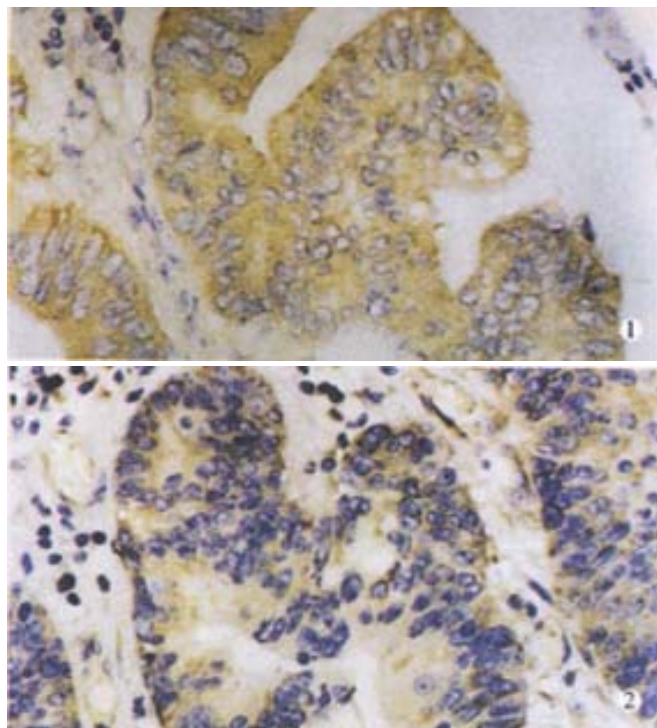


Figure 1 TGF β_1 mainly in cytoplasm and membrane of tumor cells, $\times 400$
Figure 2 VEGF expression mainly in cytoplasm and membrane of tumor cell, $\times 400$

Table 1 Relationship between expression of TGF β_1 and clinicopathologic findings

Clinic-pathologic parameters	TGF β_1 expression(%)	
	Positive(n=37)	Negative(n=61)
Male	20 (37.8)	33 (62.3)
Female	17 (37.8)	28 (62.2)
Age (y)	55 \pm 13	57 \pm 12
Histology: differentiation		
Well	9(52.9)	8 (47.1)
Moderate	15 (31.9)	32 (68.1)
Poor	13 (38.2)	21 (61.8)
Depth of invasion		
T1-T2	17 (28.3)	43 (71.7)
T3-T4	20 (52.6)	18 (47.4) ^a
Lymph node metastasis		
Present	18 (51.4)	17 (48.6)
Absent	19 (30.2)	44 (69.8) ^a
Dukes Stage		
I	8 (23.5)	26 (76.5)
II	9 (31.1)	20 (68.9)
III+IV	20 (57.1)	15 (42.9) ^a
VEGF expression		
Positive	21 (58.3)	15 (41.7)
Negative	16 (25.8)	46 (74.2) ^a
MVD ($\bar{x} \pm s$)	54 \pm 18	46 \pm 15 ^a

^a $P < 0.05$, vs positive

DISCUSSION

The process of angiogenesis is the outcome of an imbalance between positive and negative angiogenic factors produced by both tumor cells and normal cells. Numerous angiogenic factors have been described. Of these, VEGF play a key role in the angiogenesis in the colorectal cancer^[3-25]. VEGF is a multi-functional cytokine, and has direct relationship with angiogenesis. The factors that regulate VEGF expression in tumor and non-tumor cells have now been elucidated^[20-31]. The TGF β s represent a family of multifunctional cytokines that modulate the growth and function of many cells, including those with malignant transformation. The over-expression of TGF β_1 has been reported in tissue from patients with different carcinoma, and is believed to play a role in tumor transformation and progression, as well as in tumor regression^[23-33]. Studied the correlation of TGF β_1 and angiogenesis of gastric cancer, and found TGF β_1 might regulate angiogenesis through an up-regulation of the expression of VEGF. A direct correlation between TGF β_1 expression and microvessel counts had not been identified in the current study^[20-30]. TGF β_1 has no relationship with VEGF expression in breast cancer tissue, but is correlated with the expression of platelet-derived growth factor, and co-regulate angiogenesis^[20-24]. The modulating mechanisms of TGF β_1 in angiogenesis are not entirely the same in different type of tumor.

The role of TGF β_1 in angiogenesis of colorectal cancer is not identified yet. This study found that the expression of VEGF and MVD in positive TGF β_1 group are significantly higher than that in TGF β_1 negative group. The expression of TGF β_1 is significantly positively correlated with the expression of VEGF. It demonstrated that TGF β_1 may be correlated indirectly with angiogenesis through an up-regulation of the expression of VEGF. The expression of TGF β_1 is also significantly positively correlated with MVD in colorectal cancer.

It demonstrates that TGF β_1 may modulate angiogenesis directly or indirectly through up-regulating the expression of other angiogenic factors. The microvessel counts in tumors that were both positive TGF- β_1 and VEGF were the highest of all. It demonstrates that TGF- β_1 and VEGF may co-modulate the angiogenesis.

TGF β_1 expression was detected in 37 tumors (37.8%). The expression of TGF β_1 was correlated significantly with the depth of invasion, stage of disease and lymph node metastasis. Patients in T3-T4, stage III-IV and with lymph node metastasis had much higher expression of TGF β_1 than patients in T1-T2, stage I-II and without lymph node metastasis ($P < 0.05$).

REFERENCES

- 1 Grunstein J, Roberts WG, Mathieu-Costello O, Hanahan D, Johnson RS. Tumor-derived expression of vascular endothelial growth factor is a critical factor in tumor expansion and vascular function. *Cancer Res* 1999; 59:1592-1598
- 2 Karpanen T, Egeblad M, Karkkainen MJ, Kubo H, Yla-Herttuala S, Jaattela M, Alitalo K. Vascular endothelial growth factor C promotes tumor lymphangiogenesis and intralymphatic tumor growth. *Cancer Res* 2001;61:1786-1790
- 3 Siemeister G, Schirner M, Weindel K, Reusch P, Menrad A, Marme D, Martiny-Baron G. Two independent mechanisms essential for tumor angiogenesis: inhibition of human melanoma xenograft growth by interfering with either the vascular endothelial growth factor receptor pathway or the tie-2 pathway. *Cancer Res* 1999; 59: 3185-3191
- 4 Masood R, Ca J, Zheng T, Smith DL, Hinton DR, Gill PS. Vascular endothelial growth factor(VEGF) is an autocrine growth factor for VEGF receptor-positive human tumors. *Blood* 2001;98:1904-1913
- 5 Leenders W, Altena MV, Lubsen N, Rutter D, Waa RDI. *In vivo* activities of mutants of vascular endothelial growth factor(VEGF) with differential *in vitro* activities. *Int J Cancer* 2001;91: 327-333
- 6 Veikkola T, Karkkainen M, Claesson-Welsh L, Alitalo K. Regulation of angiogenesis via vascular endothelial growth factor receptors. *Cancer Res* 2000;60: 203-212
- 7 Teraoka H, Sawada T, Nishihara T, Yashiro M, Ohira M, Ishikawa T, Nishini H, Hirakawa K. Enhanced VEGF production and decreased immunogenicity induced by TGF β_1 promote liver metastasis of pancreatic cancer. *British J Cancer* 2001;85:612-617
- 8 Wu RS, Meade-Tollin L, Besselse D, Seftor E, Katsanis E, McEarchern JA, Koble JJ, Mack V, Arteaga CL, Dumout N, Mary JC, Akporiaye ET. Invasion and metastasis of a mammary tumor involve TGF β signaling. *Int J Cancer* 2001; 91: 76-82
- 9 Ying YQ, Zhou X, Wu P, Huang WB. Significance of TGF- α and TGF- β_1 expressions in the tissue of colorectal cancer. *Shijie Huaren Xiaohua Zazhi* 2001;9:223-225
- 10 Wang SM, Wu JS, Yao X, He ZS, Pan BR. Effect of TGF α , EGFR anti-sense oligodeoxynucleotides on colon cancer cell line. *Shijie Huaren Xiaohua Zazhi* 1999;7:522-524
- 11 Wang CH, Zhang XM, Zhan M, Tang FX. TGF- β and its receptor expression in human colorectal cancer. *Shijie Huaren Xiaohua Zazhi* 2001;9:462-463
- 12 Yu BM, Zhao R. Molecular biology of colorectal carcinoma. *Shijie Huaren Xiaohua Zazhi* 1999;7:173-175
- 13 Yang JH, Rao BJ, Wang Y, Tu XH, Zhang LY. Clinical significance of detecting the circulating cancer cells in peripheral blood from colorectal cancer. *Shijie Huaren Xiaohua Zazhi* 2000;8:187-189
- 14 Jia L, Chen TX, Sun JW, Na ZM, Zhang HH. Relationship between microvessel density and proliferating cell nuclear antigen and prognosis in colorectal cancer. *Shijie Huaren Xiaohua Zazhi* 2000;8:74-76
- 15 Maehara YB, Kakeji Y, Kabashima A, Emi Y, Watanabe A, Akazawa K, Baba H, Kohnoe S, Sugimachi K. Role of transforming growth factor- β_1 in invasion and metastasis in gastric carcinoma. *J Clin Oncol* 1999;17:607-614
- 16 Rodeck V, Nishiyama J, Mauriel A. Independent regulation of growth and Smad-mediated transcription by TGF- β in human melanoma cells. *Cancer Res* 1999;59:547-550
- 17 Shyr M, Sheen C, Han SC, Chin WS, Hock CE, Wei JC. Serum levels of TGF- β_1 in patients with breast cancer. *Arch Surg* 2001;13:937-940
- 18 Shim KS, Kim KH, Han WS, Park EB. Elevated serum levels of transforming growth factor- β_1 in patients with colorectal carcinoma. *Cancer* 1999;85:554-561
- 19 Kadambi A, Carreira CM, Yun CO, Padera TP, Dolmans DE, Carmeliet P, Fukumura D, Jain RK. Vascular endothelial growth factor (VEGF)-C differentially affects tumor vascular function and leukocyte recruitment: role of VEGF-receptor 2 and host VEGF-A. *Cancer Res* 2001; 61: 2404-2408
- 20 Saito H, Tsujitani S, Oka S, Kondo A, Lkeguchi M, Maeta M, Kaibara N. The expression of transforming growth factor- β_1 is significantly correlated with the expression of vascular endothelial growth factor and poor prognosis of patients with advanced gastric carcinoma. *Cancer* 1999;86:1455-1462
- 21 Zhuang ZH, Chen YL, Wang CD, Chen YG. Expression of TGF β_1 and TGF β receptor in gastric carcinoma and precancerous lesions. *Shijie Huaren Xiaohua Zazhi* 1999;7: 507-509
- 22 Xiong B, Yuan HY, Hu MB, Zhang F. Serum levels of transforming growth factor- β_1 correlating with T cell subsets and natural killer cell activity in colorectal cancer. *Shijie Huaren Xiaohua Zazhi* 2001;9:1194-1195
- 23 Ariazi EA, Satomi Y, Ellis MJ, Haag JD, Shi W, Sattler CA, Gould MN. Activation of the transforming growth factor β signaling pathway and induction of cytostasis and apoptosis in mammary carcinomas treated with the anticancer agent perillyl alcohol. *Cancer Res* 1999;59:1917-1928
- 24 Liu DH, Zhang W, Su YP, Zhang XY, Huang YX. Constructions of eukaryotic expression vector of sense and antisense VEGF165 and its expression regulation. *Shijie Huaren Xiaohua Zazhi* 2001; 9:886-891
- 25 Wan SM, Sun SH, Deng MD, Ge QL, Yang YJ. TGF- β_1 and PDGF-A expression in gastric cancer tissue and prognosis. *Shijie Huaren Xiaohua Zazhi* 2002;10: 36-39
- 26 Si XH, Yang LJ. Extraction and purification of TGF β and its effect on the induction of apoptosis of hepatocytes. *World J Gastroenterol* 2001; 7: 527-531
- 27 Wu K, Liu BH, Zhao DY, Zhao Y. Effect of vitamin E succinate on expression of TGF- β_1 , C-Jun and JNK1 in human gastric cancer SGC-7901 cells. *World J Gastroenterol* 2001;7:83-87
- 28 Liu F, Liu JX, Cao ZC, Li BS, Zhao CY, Kong L, Zhen Z. Relationship between TGF- β_1 , serum indexes of liver fibrosis and hepatic tissue pathology in patients with chronic liver diseases. *Shijie Huaren Xiaohua Zazhi* 1999; 7: 519-521
- 29 Liu XP, Song SB, Li G, Wang DJ, Zhao HL, Wei LX. Correlations of microvessel quantitation in colorectal tumors and clinicopathology. *Shijie Huaren Xiaohua Zazhi* 1999; 7: 37-39
- 30 Huang YX, Zhang GX, Lu MS, Fan GR, Chen NL, Wu GH. Increased expression of transforming growth factor- β_1 in hepatocellular carcinoma. *Huaren Xiaohua Zazhi* 1999; 7: 150-152
- 31 Yan JC, Chen WB, Ma Y, Shun XH. Expression of vascular endothelial growth factor in liver tissues of hepatitis B. *Huaren Xiaohua Zazhi* 1999; 7: 837-840
- 32 Xiang DD, Wei YL, Li JF. Molecular mechanism of TGF- β_1 on Ito cell. *Huaren Xiaohua Zazhi* 1999; 7: 980-981
- 33 Ma XM, Wang YL, Pan BR. Progress in VEGF studies. *Huaren Xiaohua Zazhi* 1999; 7: 895-896

Edited by Wu XN

• VIRAL LIVER DISEASES •

Full-length core sequence dependent complex-type glycosylation of hepatitis C virus E2 glycoprotein

Li-Xin Zhu, Jing Liu, Ying-Chun Li, Yu-Ying Kong, Caroline Staib, Gerd Sutter, Yuan Wang, Guang-Di Li

Li-Xin Zhu, Jing Liu, Ying-Chun Li, Yu-Ying Kong, Yuan Wang, Guang-Di Li, Institute of Biochemistry and Cell Biology, Shanghai Institutes for Biological Sciences, Chinese Academy of Sciences, Shanghai 200031, China Caroline Staib, Gerd Sutter, GSF-Institut für Molekulare Virologie, Trogerstr. 4b, 81675 München, Germany. The first two authors contributed equally to this paper.

Supported by the National 863 High Technology Foundation of China, No.863-102-07-02-02, No.2001AA215171 and the project CHN 98/112 (WTZ-Internationales Büro des BMBF).

Correspondence to: Yuan Wang and Guang-Di Li, Institute of Biochemistry and Cell Biology, Shanghai Institutes for Biological Sciences, Chinese Academy of Sciences, 320 Yue-Yang Road, Shanghai 200031, China. wangyuan@server.shcnc.ac.cn

Telephone: +86-21-64374430 Fax: +86-21-64338357

Received 2001-12-05 Accepted 2002-01-23

Abstract

AIM: To study HCV polyprotein processing is important for the understanding of the natural history of HCV and the design of vaccines against HCV. The purpose of this study is to investigate the affection of context sequences on hepatitis C virus (HCV) E2 processing.

METHODS: HCV genes of different lengths were expressed and compared in vaccinia virus/T7 system with homologous patient serum S94 and mouse anti-serum M_{E2116} raised against *E.coli*-derived E2 peptide, respectively. Deglycosylation analysis and GNA (*Galanthus nivalus*) lectin binding assay were performed to study the post-translational processing of the expressed products.

RESULTS: E2 glycoproteins with different molecular weights (~75kDa and ~60kDa) were detected using S94 and M_{E2116}, respectively. Deglycosylation analysis showed that this difference was mainly due to different glycosylation. Endo H resistance and its failure to bind to GNA lectin demonstrated that the higher molecular weight form (75kDa) of E2 was complex-type glycosylated, which was readily recognized by homologous patient serum S94. Expression of complex-type glycosylated E2 could not be detected in all of the core-truncated constructs tested, but readily detected in constructs encoding full-length core sequences.

CONCLUSION: The upstream conserved full-length core coding sequence was required for the production of E2 glycoproteins carrying complex-type N-glycans which reacted strongly with homologous patient serum and therefore possibly represented more mature forms of E2. As complex-type N-glycans indicated modification by Golgi enzymes, the results suggest that the presence of full-length core might be critical for E1/E2 complex to leave ER. Our data may contribute to a better understanding of the processing of HCV structural proteins as well as HCV morphogenesis.

Zhu LX, Liu J, Li YC, Kong YY, Staib C, Sutter G, Wang Y, Li GD. Full-length core sequence dependent complex-type glycosylation of hepatitis C virus E2 glycoprotein. *World J Gastroenterol* 2002;8(3):499-504

INTRODUCTION

Hepatitis C virus (HCV), the major cause of post-transfusion and community-acquired non-A, non-B hepatitis^[1,2], is a member of the Flaviviridae family^[3]. This virus has a positive-sense, single stranded RNA genome of about 9.6 kb, which encodes a polyprotein precursor of about 3000 amino acids. The polyprotein is further processed into various precursors and mature viral proteins^[4,5]. The structural proteins are encoded in the order NH₂-core-E1-E2-P7, which are processed into core (C), E1, E2, and P7 by host membrane-associated signal peptidase(s)^[6-11]. The downstream nonstructural region is processed by a viral metalloprotease and a viral serine protease located at the N-terminus of NS3^[12-17]. The core protein is thought to constitute the viral capsid with E1 and E2 being the virus envelope proteins. Numerous studies have shown that E1 and E2 are heavily glycosylated and associate to form a noncovalent heterodimeric complex^[9,10,18,19]. E1 and E2 are believed to be type I transmembrane proteins with an N-terminal glycosylated ectodomain and a C-terminal hydrophobic anchor.

The lack of an efficient *in vitro* cell culture system for productive HCV propagation^[20-27] and low levels of HCV particles in the liver tissues or blood of infected patients^[28,29] have hampered the study of native viral proteins. Fortunately, a variety of prokaryotic and eukaryotic expression systems have proved useful for the production and characterization of HCV encoded proteins^[8,9,11,30-32]. However, diverse findings have been reported, regarding the molecular weights of E2, which most likely is a reflection of the differences in efficiency of HCV polyprotein processing and post-translational modification achieved in the particular systems^[7-9,11,17-19,30]. In this study, the E2 expression of recombinant plasmids carrying various length of HCV C-E1-E2 coding sequences was analyzed in the vaccinia virus/bacteriophage T7 RNA polymerase expression system^[33]. The results suggest that the upstream conserved core coding sequence is required for the production of E2 glycoproteins carrying complex-type N-glycans which react strongly with homologous patient serum and therefore possibly represent more mature forms of E2.

MATERIALS AND METHODS

Cells and viruses

Human HeLa (ATCC #CCL-2) and monkey BS-C-1 (ATCC #CCL-26) cells were maintained in Dulbecco's modified essential medium (DMEM/HG) supplemented with 5% heat inactivated fetal calf serum (FCS) at 37°C in a 5% CO₂ atmosphere. Recombinant vaccinia virus vTT7 that expresses the bacteriophage T7 RNA polymerase gene under the control of vaccinia virus early/late promoter P7.5 was generated and propagated as previously described^[34]. PFU (plaque forming unit) titration was performed on BS-C-1 cell monolayers.

Plasmid constructions

The vaccinia virus/T7 promoter expression vector pTM1 was kindly provided by Bernard Moss (NIH, Bethesda, USA) and all of the expression plasmids carrying HCV cDNA encoding structural proteins described below were derived from pTM1. Figure 1 depicts the HCV gene fragment in the expression plasmids. Plasmids pCEH-2 (1-730)

and pEH containing HCV C, E1 and E2 gene of subtype 1b^[35] (GENBANK accession #D10934) were described previously^[34]. Briefly, cDNA sequences encoding HCV polyprotein amino acids 192 to 730 were inserted into pTM1 to obtain pEH. HCV sequences encoding complete C were fused with the E1/E2 sequences of pEH to result in plasmid pCEH-2(1-730). The latter plasmid served as basis for PCR cloning to generate plasmids pCE1(1-341), pCEH-2(108-730), pCEH-2(120-730), pCEH-2(137-730), pCEH-2(156-730), pCEH-2(167-730), pCEH-2(1-661) and pTM1/EH(192-661) for the expression of 5' or/and 3' truncated HCV sequences encoding HCV polyprotein amino acids as indicated by numbers in parenthesis. Plasmid pC-E2H(1-195/394-661) was generated by deleting E1 coding sequences from pCEH-2(1-661) and linking polyprotein amino acids aa194 and aa394 together. Authenticity of HCV cDNA sequences in all constructed plasmids was confirmed by automatic sequencing.

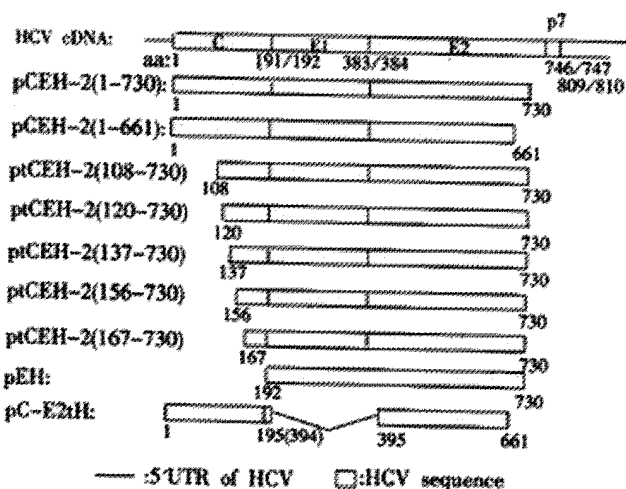


Figure 1 Schematic maps of HCV coding sequences inserted into the plasmid pTM1 and expressed under transcriptional control of the bacteriophage T7 pol promoter. Numbers refer to amino acids of the HCV polyprotein.

Transient expression of recombinant genes using vaccinia virus/T7 RNA polymerase (VV-T7pol)

HeLa cells grown to 80% confluency were infected with recombinant vaccinia virus vTT7 at a multiplicity of infection (MOI) of 10 PFU per cell to allow for production of recombinant T7 RNA polymerase. At 2h post-infection, the inoculum was removed and DNA of pTM1 based expression plasmids was transfected using DOTAP liposomal transfection reagent as described by the manufacturer (Roche Molecular Biochemicals, Mannheim). After 24 hours of incubation, infected/transfected cells were washed twice with PBS, harvested by scraping, pelleted upon brief centrifugation, and resuspended in a small volume of PBS. Cell lysates were prepared by adding SDS-PAGE sample loading buffer and stored at -80°C until further analysis.

Western blot analysis

Cell lysates were separated by reductive SDS-PAGE and then transferred onto nitrocellulose membranes (Schleicher & Schuell). Blocking was done using 5% fat-free milk powder. For immunodetection of HCV proteins, blots were incubated with primary antibodies, washed, and incubated with 1000 fold diluted HRP-protein A (Sigma). The membranes were then washed again and reactive proteins were detected using the ECL system (Amersham Pharmacia Biotech) according to the manufacturers' instructions. The primary antibodies used in this study include: anti-HCV human serum S94 at a dilution of 1:500 (kindly provided by Wang, Y., Beijing

University, China), anti-HCV human serum S268 at a dilution of 1:500 (kindly provided by Lu Z., Shanghai Ruijin Hospital, China), anti-E2 mouse polyclonal antibody M_{E2116}^[36] at a dilution of 1:300 (raised against E. Coli-derived HCV E2 polypeptide aa450 to 565), and anti-E1 rabbit polyclonal antibody R_{E1135-C} at a dilution of 1:250 (raised against an E. coli-derived C-terminally truncated HCV E1 fragment).

Characterization of N-glycans on expressed E2 glycoproteins

For deglycosylation analysis, cell pellets were directly lysed in denaturing buffer provided by the manufacturer and digested with PNGase F (NEB) or Endo H (NEB) for 2 hours at 37°C.

The type of N-glycans on expressed E2 glycoproteins was also analyzed by testing its ability to bind to GNA (Galanthus nivalus) lectin. HeLa cells infected with vTT7 and transfected with pCEH-2(1-730) were collected by scraping, washed in cold PBS, and then lysed with lysis buffer (50mM Tris-HCl [pH8.0], 150mM NaCl, 0.5% Nonidet P-40, 1mM PMSF). After centrifugation at 10000g, the supernatant was allowed to bind to GNA-agarose (Sigma). The flow-through fraction was collected and the gel matrices were washed with lysis buffer. Bound proteins were eluted with 1M α -D-mannopyranoside (Sigma) in lysis buffer. Samples were then analyzed by Western-blotting.

RESULTS

Detection of E2 glycoproteins of different Molecular Weights using antibodies of distinct origins

The hybrid vaccinia virus/T7 bacteriophage RNA polymerase expression system was used to study the expression of the HCV structural proteins. The transient expression products of plasmids pCEH-2(1-730) and pCEH-2(1-661), which contain HCV cDNA encoding the structural region terminating at amino acid 730 and 661 of the polyprotein respectively, were analyzed by Western blot using polyclonal mouse serum M_{E2116} raised against E.coli-derived E2 protein^[36]. E2 products with apparent molecular weights (MWs) of ~60kDa and ~50kDa were detected for pCEH-2(1-730) and pCEH-2(1-661) respectively (Figure 2, lane 1, 3). The apparent molecular weights were higher than calculated values, which, along with the heterogeneous appearance of the detected bands, suggested that these were glycosylated expression products. The lower molecular weight of the E2 species obtained from expression of pCEH-2(1-661) in comparison to pCEH-2(1-730) was consistent with the introduced truncation at the 3' end of the E2 coding sequences leading to the loss of 70 amino acids in the recombinant polypeptide backbone.

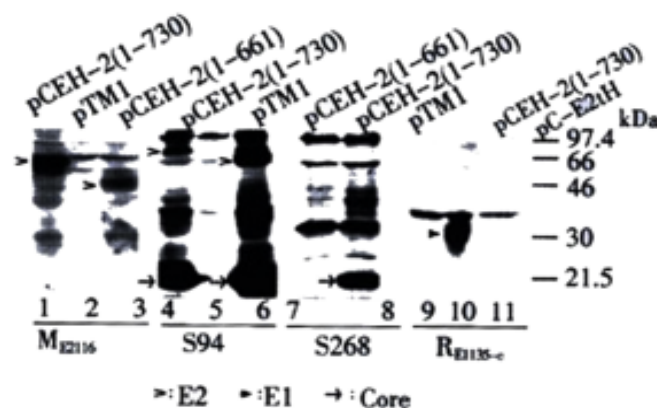


Figure 2 Detection of E2 glycoprotein species of different molecular masses. Transient expression products were analyzed by Western blot with antibodies of distinct origin: mouse polyclonal antibody M_{E2116} (lane 1, 2, 3); HCV patient serum S94 (lane 4, 5, 6); HCV patient serum S268 (lane 7, 8); rabbit polyclonal antibody R_{E1135-C} (lane 9, 10, 11). Empty vector pTM1 was used as the negative control. HCV-specific protein bands are indicated by arrowheads. The plasmids used for transfection are indicated at the top of the lanes.

The expression products were also analyzed with HCV patient serum S94. Multiple prominent bands were detected for pCEH-2(1-730) and pCEH-2(1-661), but not for vector plasmid pTM1, representing expressed HCV structure proteins and possibly some precursors. The bands of ~75 kDa and ~66 kDa (Figure 2, lane 4, 6), which again consistent with the different length of E2 coding sequence in both plasmids, should represented the E2 proteins, although their MWs were higher than that detected by M_{E2116} . It is worth noting that the analyzed HCV cDNA originated from the same patient from whom S94 was collected. The core antigen and some precursors of expression products could also be detected by another HCV patient serum S268, but we could not detect the E2-specific 75kDa band (Figure 2, lane 8), which could be attributed to the high variability of the E2 glycoprotein^[37, 38].

The antibody dependent detection of different E2 glycoprotein species was surprising. To rule out that the E2 bands of higher MW is the uncleaved E1-E2 precursors, the expression products from pCEH-2(1-730) were analyzed with anti-E1 rabbit sera. A heavy band of about 30kDa was detected, possibly representing multiple forms of E1 proteins (Figure 2, lane 10), while no E1-specific band with higher MW was detected. Another possible explanation could be that E2 polypeptides of varying sizes were synthesized due to incomplete or irregular processing of the polyprotein. This hypothesis was abandoned when we subjected recombinant proteins to deglycosylation with PNGase F prior to Western blot analysis with mouse polyclonal antibody M_{E2116} . After PNGase F treatment, only one E2-specific band with apparent molecular weight of 30 kDa was detected for pCEH-2(1-661) expression products, while an E2-specific doublet band of 33/34 kDa was detected for pCEH-2(1-730) expression products (Figure 3), which is consistent with the MWs of calculated E2 polypeptide backbones. It suggests that difference of the MWs of E2 species detected by M_{E2116} and S94 from the same transient expression products (pCEH-2(1-730): ~60kDa and ~75kDa, pCEH-2(1-661): ~50kDa and ~66kDa) is mainly due to different N-glycosylation. The detection of a E2 peptide doublet with pCEH-2(1-730) but not with pCEH-2(1-661) is in agreement with the fact that E2 contains a PKR-eIF2 α phosphorylation site (PKR: RNA-activated protein kinase) at aa659-670^[39], which is largely deleted in the pCEH-2(1-661) construct.

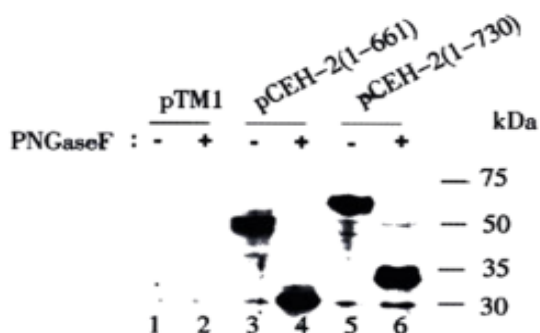


Figure 3 Deglycosylation analysis of the expressed HCV E2 proteins with PNGase F. Transient expression products were subjected to Western blot analysis with M_{E2116} as the primary antibody. pTM1 transfected cells were used as control. The plasmids used for transfection are indicated at the top of the lanes. Samples incubated with deglycosylation buffer were run in parallel. +: samples digested with PNGase F, -: samples incubated with PNGase F reaction buffer.

Altogether, the above results suggest that the 75kDa and 66kDa bands detected by S94 are HCV E2 glycoproteins of heavier glycosylation and thus higher molecular weight.

M_{E2116} - and S94-reactive E2 glycoproteins carried different types of N-glycans

Since M_{E2116} - and S94-reactive E2 species had polypeptide backbones

of the same size, the difference in apparent molecular weight and antibody reactivity could only be attributed to differences in the degree and/or type of glycosylation. The glycan type on different E2 species expressed from pCEH-2(1-730) was then analyzed by testing their sensitivity to PNGase F and Endo H. PNGase F hydrolyzes all types of N-glycan chains from glycopeptides and glycoproteins unless they carry α -1-3 linked core fucose residues present in insect and plant glycoproteins^[40], while Endo H cleaves only high mannose structures and hybrid structures on N-linked oligosaccharides of glycoproteins^[41]. Figure 4A shows that the M_{E2116} -reactive E2 species was sensitive to both PNGase F and Endo H digestion. The S94-reactive E2 species disappeared after PNGase F digestion (Figure 4B). It was difficult to detect the deglycosylated E2 with S94 after PNGase F treatment, because there were multiple HCV polyprotein precursor proteins of about 30000 reacted strongly with S94 and unglycosylated E2 seemed to react weakly with S94 (unpublished data). However, the highly glycosylated, S94-reactive E2 band remained after Endo H digestion (Figure 4B). The glycan type of different E2 species expressed from pCEH-2(1-730) were also analyzed by testing their ability to bind to GNA lectin. GNA is specific for the non-reducing end of α -D-mannosyl residue of glycoconjugate and therefore can be used to probe the presence of high mannose type or hybrid type glycans on glycoproteins^[42, 43]. The M_{E2116} -reactive E2 species could quantitatively bind to and be eluted from GNA-agarose, whereas no obvious binding could be demonstrated for S94-reactive E2 species (Figure 5).

The resistance of S94-reactive E2 glycoprotein species to Endo H digestion together with the fact that it could not bind to GNA indicates that the S94-reactive E2 protein carries complex-type glycans.

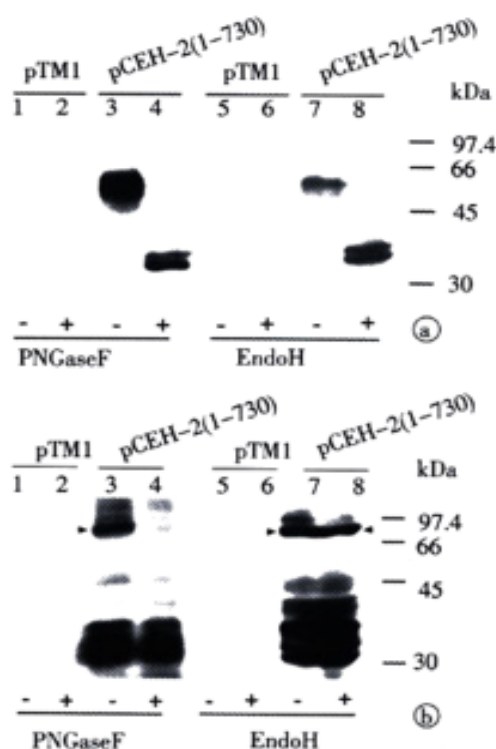


Figure 4 Different sensitivities of two glycosylated E2 species to PNGase F and Endo H. Transient expression products of pCEH-2(1-730) were digested with PNGase F or Endo H, respectively. The digested samples were analyzed by Western blot with M_{E2116} (A) and S94 (B). Empty vector pTM1 was used as negative control.

Samples incubated with deglycosylation buffer were run in parallel. +: samples digested with Endoglycosidase, -: samples incubated with Endoglycosidase reaction buffer. The plasmids used for transfection are indicated at the top of the lanes. Endoglycosidases used in this study are indicated at the bottom of the lanes. S94-reactive E2 proteins are indicated by arrowheads.

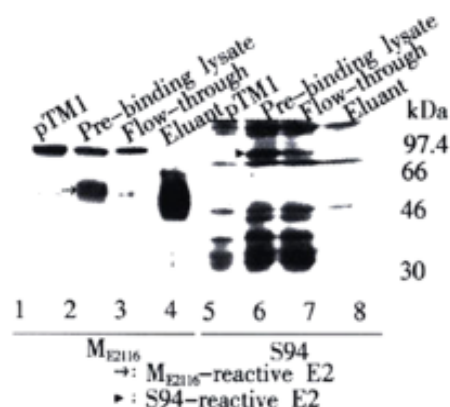


Figure 5 Different ability of differently glycosylated E2 species to bind to GNA-agarose. HeLa cells infected with vT7 and transfected with pCEH-2(1-730) were collected, washed and lysed with lysis buffer. The cleared supernatant was then allowed to bind to GNA-agarose. The gel beads were washed and eluted with 1M α -D-mannopyranoside in lysis buffer. Pre-binding lysate, flow-through and eluate fractions were analyzed by Western blot analysis. HeLa cells infected with vT7 and transfected with pTM1 were served as negative control. The sera used as primary antibodies are indicated at the bottom of the lanes. E2 proteins are indicated by arrowheads.

HCV core sequence dependent formation of complex-glycosylated E2

We also assessed if co-expression of core or E1 coding sequences had any effect on the production of the E2 proteins, which was readily recognized by homologous patient serum S94. A set of expression plasmids containing HCV cDNAs with various deletions in the core sequence (ORF starting at aa108, aa120, aa137, aa151, or aa167, respectively) were constructed. The lysates from vT7-infected and plasmid DNA transfected HeLa cells were analyzed by Western blot with either the mouse anti-serum M_{E2116} or the patient serum S94 (Figure 6).

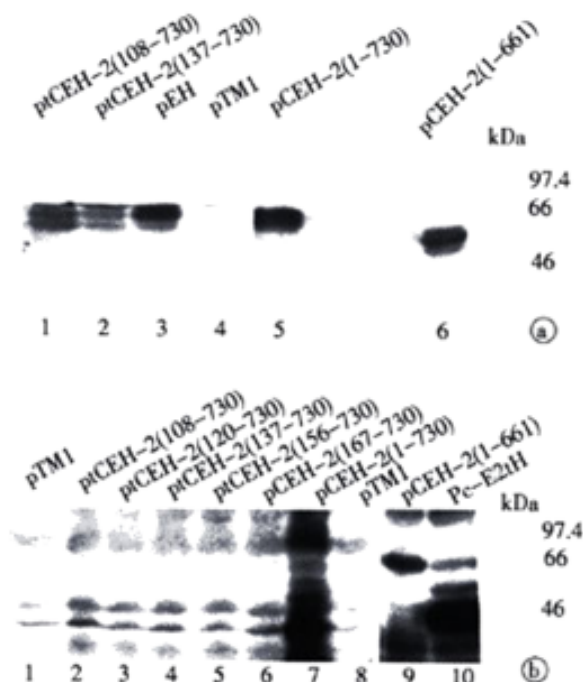


Figure 6 Requirement of the core sequence for the expression of complex-type glycosylated E2. Expression products of differently truncated HCV structural genes were analyzed by Western blot analysis. Blots were probed with M_{E2116} (A) or with S94 (B). Empty vector pTM1 was used as negative control. The plasmids used for transfection are indicated at the top of the lanes.

When using mouse antibody M_{E2116}, recombinant E2 of \sim 60kDa and \sim 50kDa could be detected upon expression of all constructs tested (Figure 6A). Patient serum S94 allowed detection of E2 for pCEH-2(1-730) and pCEH-2(1-661) with full-length core coding sequences (Figure 6B, lanes 7, 9), similar to that described in Figure 2. In contrast, no E2 products could be visualized after expression of constructs containing no or only partial core sequences (Figure 6B, lanes 1-6). Interestingly, deletion of E1 coding sequences had no significant effect on the synthesis of S94 detectable E2 protein (Figure 6B, lane 10). These results suggest that the presence of complete HCV core sequence is crucial for the expression and/or post-translational processing of the complex-type glycosylated form of E2.

DISCUSSION

In this study, various constructs of HCV cDNAs placed under transcriptional control of the bacteriophage T7 promoter were transiently expressed using vaccinia virus/T7 system. Upon characterization of the HCV gene products with different antibodies, two species of E2 with different MWs were identified in the expression products of the same plasmid. The high molecular weight forms of E2 were readily recognized by a patient serum, but displayed weak reactivity with antibodies raised against E. coli derived E2. These high molecular weight forms of E2 were not likely produced from inefficient proteolytical processing at the E1/E2 boundary as these proteins were not stained with E1-specific antibodies. Efficient processing at E1/E2 was confirmed by deglycosylation analysis. The difference of the MWs of E2 species detected by S94 and by M_{E2116} was therefore mainly due to different N-glycosylation. The S94-reactive E2 glycoproteins, which were resistant to Endo H digestion and could not bind to GNA, carry complex-type glycans.

The specific recognition of the complex-type glycosylated E2 but not the high-mannose-type glycosylated E2 by homologous patient serum S94 suggested that the former could be a better representation of native E2 proteins on HCV virions. Similar results were also reported by Inudoh *et al*^[44]. By comparing the reactivity of complex-type glycosylated E2 and the high-mannose-type glycosylated E2 with different patient sera, they demonstrated that the former is superior in diagnosing HCV infection. Their results and our results reported here are in concordance with the finding that E2 protein on patient derived virions contained complex-type sugars indicating Golgi-specific modification^[45].

Expression of full-length or C-terminally truncated envelop proteins in eukaryotic cells has demonstrated that E1 and E2 are retained within the ER membrane system due to the presence of ER-retention signals in the C-termini of both envelope proteins^[46-50]. However, recent study indicates that HCV E2 proteins could also present in the Golgi apparatus of the stably transfected cell line expressing HCV C-E1-E2-NS2 fragment. A possible explanation could be that Martire *et al*^[51] used an HCV gene fragment including full-length core sequences in their study while structural protein sequences without full-length core sequences were used to study the localization of envelop proteins. The results reported here demonstrated that the complex-type glycosylated, possibly more mature form of E2 is only detectable upon co-expression of the complete HCV core coding sequence. Deletion of the first 107 N-terminal core amino acid residues was obviously sufficient to abrogate production of complex-glycosylated E2. This result suggest that the core protein might allow for targeting the envelope glycoproteins to Golgi-specific modification, which could be a key step in the morphogenesis of HCV virions. HCV-like particles were observed when HCV cDNA encoding whole core, E1 and E2 was expressed in baculovirus-insect expression system^[52]. After binding of core to the E1-E2 complex statically located on the ER membrane, virus-like particles might be formed and the conformation of E1-E2 complex changed, which could result in the abrogation of the ER-retention

signal for the E1-E2 complex. Then the virus-like particles might migrate along the secretion pathway, where E2 (and E1) proteins undergo more complex glycosylation by the Golgi enzymes.

In summary, upon expression of recombinant HCV core, E1, and E2 sequences, the E2 proteins of different glycosylations could be identified. The complex-glycosylated E2 protein might represent a more mature form of E2 and its formation required the conserved core coding sequences. Our data may contribute to a better understanding of the processing of HCV structural proteins as well as HCV morphogenesis.

ACKNOWLEDGMENT

We thank Wang, Y. and Lu, Z. for providing the HCV clones and the HCV specific patient sera.

REFERENCES

- Choo QL, Kuo G, Weiner AJ, Overby LR, Bradley DW, Houghton M. Isolation of a cDNA clone derived from a blood-borne non-A, non-B viral hepatitis genome. *Science* 1989; 244: 359-362
- Kuo G, Choo QL, Alter HJ, Gitnick GL, Redeker AG, Purcell RH, Miyamura T, Dienstag JL, Alter MJ, Stevens CE, Tegtmeier GE, Bonino F, Colombo M, Lee WS, Kuo C, Berger K, Shuster JR, Overby LR, Bradley DW, Houghton M. An assay for circulating antibodies to a major etiologic virus of human non-A, non-B hepatitis. *Science* 1989; 244: 362-364
- Major ME, Feinstone SM. The molecular virology of hepatitis C. *Hepatology* 1997; 25: 1527-1538
- Choo QL, Richman KH, Han JH, Berger K, Lee C, Dong C, Gallegos C, Coit D, Medina-Selby A, Barr PJ, Weiner AJ, Bradley DW, Kuo G, Houghton M. Genetic organization and diversity of the hepatitis C virus. *Proc Natl Acad Sci USA* 1991; 88: 2451-2455
- Houghton M, Weiner A, Han J, Kuo G, and Choo QL. Molecular biology of hepatitis viruses: implications for diagnosis, development and control of viral disease. *Hepatology* 1991; 14: 381-388
- Harada S, Watanabe Y, Takeuchi K, Suzuki T, Katayama T, Takebe Y, Saito I, Miyamura T. Expression of processed core protein of hepatitis C virus in mammalian cells. *J Virol* 1991; 65: 3015-3021
- Hijikata M, Kato N, Ootsuyama Y, Nakagawa M, Shimotohno K. Gene mapping of the putative structural region of the hepatitis C virus genome by *in vitro* processing analysis. *Proc Natl Acad Sci USA* 1991; 88: 5547-5551
- Lanford RE, Notvall L, Chavez D, White R, Frenzel G, Simonsen C, Kim J. Analysis of hepatitis C virus capsid, E1 and E2/NS1 proteins expressed in insect cells. *Virology* 1993; 197: 225-235
- Ralston R, Thudium K, Berger K, Kuo C, Gervase B, Hall J, Selby M, Kuo G, Houghton M, Choo QL. Characterization of hepatitis C virus envelop glycoprotein complexes expressed by recombinant vaccinia viruses. *J Virol* 1993; 67: 6753-6761
- Selby MJ, Choo QL, Berger K, Kuo G, Glazer E, Eckart M, Lee C, Chien D, Kuo C, Houghton M. Expression, identification and subcellular localization of the proteins encoded by the hepatitis C viral genome. *J Gen Virol* 1993; 74:1103-1113
- Spaete RR, Alexander D, Rugroden ME, Choo QL, Berger K, Crawford K, Kuo C, Leng S, Lee C, Ralston R, Thudium K, Tung JW, Kuo G, Houghton M. Characterization of the hepatitis C virus E2/NS1 gene product expressed in mammalian cells. *Virology* 1992; 188: 819-830
- Grakoui A, McCourt DW, Wychowski C, Feinstone SM, Rice CM. A second hepatitis C virus-encoded proteinase. *Proc Natl Acad Sci USA* 1993; 90: 10583-10587
- Hijikata M, Mizushima H, Akagi T, Mori S, Kakiuchi N, Kato N, Tanaka T, Kimura K, Shimotohno K. Two distinct proteinase activities required for the processing of a putative nonstructural precursor protein of hepatitis C virus. *J Virol* 1993; 67: 4665-4675
- Eckart MR, Selby M, Masiarz F, Lee C, Berger K, Crawford K, Kuo C, Kuo G, Houghton M, Choo QL. The hepatitis C virus encodes a serine protease involved in processing of the putative nonstructural proteins from the viral polyprotein precursor. *Biochem Biophys Res Commun* 1993; 192: 399-406
- Grakoui A, McCourt DW, Wychowski C, Feinstone SM, Rice CM. Characterization of the hepatitis C virus-encoded serine proteinase: determination of proteinase-dependent polyprotein cleavage sites. *J Virol* 1993; 67: 2832-2843
- Manabe S, Fuke I, Tanishita O, Kaji C, Gomi Y, Yoshida S, Mori C, Takamizawa A, Yosida I, Okayama H. Production of nonstructural proteins of hepatitis C virus requires a putative viral protease encoded by NS3. *Virology* 1994; 198: 636-644
- Tomei L, Failla C, Santolini E, De Francesco R, La Monica N. NS3 is a serine protease required for processing of hepatitis C virus polyprotein. *J Virol* 1993; 67: 4017-4026
- Grakoui A, Wychowski C, Lin C, Feinstone SM, Rice CM. Expression and identification of hepatitis C virus polyprotein cleavage products. *J Virol* 1993; 67: 1385-1395
- Matsuura Y, Suzuki T, Suzuki R, Sato M, Aizaki H, Saito I, Miyamura T. Processing of E1 and E2 glycoprotein of hepatitis C virus expressed in mammalian and insect cells. *Virology* 1994; 205: 141-150
- Hiramatsu N, Dash S, Gerber MA. HCV cDNA transfection to HepG2 cells. *J Viral Hepat* 1997; 4 Suppl 1: 61-67
- Seipp S, Mueller HM, Pfaff E, Stremmel W, Theilmann L, Goeser T. Establishment of persistent hepatitis C virus infection and replication *in vitro*. *J Gen Virol* 1997; 78: 2467-2476
- Rumin S, Berthillon P, Tanaka E, Kiyosawa K, Trabaud MA, Bizollon T, Gouillat C, Gripon P, Guguen-Guillouzo C, Inchauspe G, Trepo C. Dynamic analysis of hepatitis C virus replication and quasispecies selection in long-term cultures of adult human hepatocytes infected *in vitro*. *J Gen Virol* 1999; 80: 3007-3018
- Lohmann V, Korner F, Koch J, Herian U, Theilmann L, Bartenschlager R. Replication of subgenomic hepatitis C virus RNAs in a hepatoma cell line. *Science* 1999; 285: 110-113
- Song ZQ, Hao F, Min F, Ma QY, Liu GD. Hepatitis C virus infection of human hepatoma cell line 7721 *in vitro*. *World J Gastroenterol* 2001; 7: 685-689
- Bartenschlager R, Lohmann V. Novel cell culture systems for the hepatitis C virus. *Antiviral Res* 2001; 52: 1-17
- Lohmann V, Korner F, Dobierzewska A, Bartenschlager R. Mutations in hepatitis C virus RNAs conferring cell culture adaptation. *J Virol* 2001; 75: 1437-1449
- Pietschmann T, Lohmann V, Rutter G, Kurpanek K, Bartenschlager R. Characterization of cell lines carrying self-replicating hepatitis C virus RNAs. *J Virol* 2001; 75: 1252-1264
- Ni YH, Chang MH, Lue HC, Hsu HY, Wang MJ, Chen PJ, Chen DS. Posttransfusion hepatitis C virus infection in children. *J Pediatr* 1994; 124: 709-713
- Luengrojanakul P, Vareesangthip K, Chainuvati T, Murata K, Tsuda F, Tokita H, Okamoto H, Miyakawa Y, Mayumi M. Hepatitis C virus infection in patients with chronic liver disease or chronic renal failure and blood donors in Thailand. *J Med Virol* 1994; 44: 287-292
- Hsu HH, Donets M, Greenberg HB, Feinstone SM. Characterization of hepatitis C virus structural proteins with a recombinant baculovirus expression system. *Hepatology* 1993; 17: 763-771
- Yan BS, Liao LY, Leou K, Chang YC, Syu WJ. Truncating the putative membrane association region circumvents the difficulty of expressing hepatitis C virus protein E1 in *Escherichia coli*. *J Virol Methods* 1994; 49: 343-351
- Zhu LX, Kong YY, Wang Y, Li GD. Effect of downstream sequence on the cleavage of envelop protein 1 signal sequence in hepatitis C virus. *Acta Biochim Biophys Sin* 2001; 33: 682-686
- Moss B, Elroy-Stein O, Mizukami T, Alexander WA, Fuerst TR. New mammalian expression vectors. *Nature* 1990; 348: 91-92
- Li Y, Li G, Kong Y, Wang Y, Wang Y, Wen Y. Expression of structural proteins of hepatitis C virus (HCV) in mammalian cells. *Science in China (Series C)* 1998; 41: 47-55
- Wang Y, Okamoto H, Tsuda F, Nagayama R, Tao QM, Mishiro S. Prevalence, genotypes and isolate (HC-C2) of hepatitis C virus in Chinese patients with liver disease. *Journal of Medical Virology* 1993; 40: 254-260
- Liu J, Zhu L, Zhang X, Lu M, Kong Y, Wang Y, Li G. Expression, purification, immunological characterization and application of *E. coli*-derived hepatitis C virus E2 proteins. *Biotechnology and Applied Biotechnology* 2001; 34: 109-119
- Hijikata M, Kato N, Ootsuyama Y, Nakagawa M, Ohkoshi S, Shimotohno K. Hypervariable regions in the putative glycoprotein of hepatitis C virus. *Biochem Biophys Res Commun* 1991; 175: 220-228
- Weiner AJ, Brauer MJ, Rosenblatt J, Richman KH, Tung J, Crawford K, Bonino F, Saracco G, Choo QL, Houghton M, Han JH. Variable and hypervariable domains are found in the regions of HCV corresponding to the flavivirus envelope and NS1 proteins and the pestivirus envelope glycoproteins. *Virology* 1991; 180: 842-848
- Taylor DR, Shi ST, Romano PR, Barber GN, Lai MMC. Inhibition of the interferon-inducible protein kinase PKR by HCV E2 protein. *Science* 1999; 285: 107-110
- Tarentino AL, Gomez CM, Plummer TH. Deglycosylation of asparagine-linked glycans by peptide:N-glycosidase F. *Biochemistry* 1985; 24: 4665-4671
- Tai T, Yamashita K, Ogata-Arakawa M, Koide N, Muramatsu T. Structural studies of two ovalbumin glycopeptides in relation to the endo-beta-N-acetylglucosaminidase specificity. *J Biol Chem* 1975; 250: 8569-8575
- Kaku H, Goldstein JJ. Snowdrop lectin. *Methods Enzymol* 1989; 179: 327-331

- 43 Shibuya N, Berry JE, Goldstein JJ. One-step purification of murine IgM and human alpha 2-macroglobulin by affinity chromatography on immobilized snowdrop bulb lectin. *Arch Biochem Biophys* 1988; 267: 676-680
- 44 Inudoh M, Nyunoya H, Tanaka T, Hijikata M, Kato N, Shimotohno K. Antigenicity of hepatitis C virus envelope proteins expressed in Chinese hamster ovary cells. *Vaccine* 1996; 14: 1590-1596
- 45 Sato K, Okamoto H, Aihara S, Hoshi Y, Tanaka T, Mishiro S. Demonstration of sugar moiety on the surface of HCV recovered from the circulation of infected humans. *Virology* 1993; 196: 354-357
- 46 Cocquerel L, Duvet S, Meunier JC, Pillez A, Cacan R, Wychowski C, Dubuisson J. The transmembrane domain of hepatitis C virus glycoprotein E1 is a signal for static retention in the endoplasmic reticulum. *J Virol* 1999; 73: 2641-2649
- 47 Flint M, McKeating JA. The C-terminal region of the hepatitis C virus E1 glycoprotein confers localization within the endoplasmic reticulum. *J Gen Virol* 1999; 80: 1943-1947
- 48 Duvet S, Cocquerel L, Pillez A, Cacan R, Verbert A, Moradpour D, Wychowski C, Dubuisson J. Hepatitis C virus glycoprotein complex localization in the endoplasmic reticulum involves a determinant for retention and not retrieval. *J Biol Chem* 1998; 273: 32088-32095
- 49 Cocquerel L, Meunier JC, Pillez A, Wychowski C, Dubuisson J. A retention signal necessary and sufficient for endoplasmic reticulum localization maps to the transmembrane domain of hepatitis C virus glycoprotein E2. *J Virol* 1998; 72: 2183-2191
- 50 Mottola G, Jourdan N, Castaldo G, Malagolini N, Lahm A, Serafini-Cessi F, Migliaccio G, Bonatti A. New determinant of endoplasmic reticulum localization is contained in the juxtamembrane region of the ectodomain of hepatitis C virus glycoprotein E1. *J Biol Chem* 2000; 275: 24070-24079
- 51 Martire G, Viola A, Iodice L, Lotti LV, Gradini R, Bonatti S. Hepatitis C virus structural proteins reside in the endoplasmic reticulum as well as in the intermediate compartment/cis-Golgi complex region of stably transfected cells. *Virology* 2001; 280: 176-182
- 52 Baumert TF, Ito S, Wong DT, Liang TJ. Hepatitis C virus structural proteins assemble into viruslike particles in insect cells. *J Virol* 1998; 72: 3827-3836

Edited by Schmid R and Pang LH

• VIRAL LIVER DISEASES •

DNA immunization with fusion genes encoding different regions of hepatitis C virus E2 fused to the gene for hepatitis B surface antigen elicits immune responses to both HCV and HBV

Jing Jin, Jian-Ying Yang, Jing Liu, Yu-Ying Kong, Yuan Wang, Guang-Di Li

Jing Jin, Jian-Ying Yang, Jing Liu, Yu-Ying Kong, Yuan Wang, Guang-Di Li, Institute of Biochemistry and Cell Biology, Shanghai Institutes for Biological Sciences, Chinese Academy of Science, Shanghai 200031, China
Supported by the National High-Technology Program of China, No. 863-102-07-02-02

Correspondence to: Yuan Wang and Guang-Di Li, Institute of Biochemistry and Cell Biology, Shanghai Institutes for Biological Sciences, Chinese Academy of Sciences, 320 Yue-Yang Road, Shanghai 200031, China. wangyuan@server.shnc.ac.cn
Telephone: +86-21-64374430 Ext 5326 Fax: +86-21-64338357
Received 2001-12-05 Accepted 2002-01-23

Abstract

AIM: Both Hepatitis B virus (HBV) and Hepatitis C virus (HCV) are major causative agents of transfusion-associated and community-acquired hepatitis worldwide. Development of a HCV vaccine as well as more effective HBV vaccines is an urgent task. DNA immunization provides a promising approach to elicit protective humoral and cellular immune responses against viral infection. The aim of this study is to achieve immune responses against both HCV and HBV by DNA immunization with fusion constructs comprising various HCV E2 gene fragments fused to HBsAg gene of HBV.

METHODS: C57BL/6 mice were immunized with plasmid DNA expressing five fragments of HCV E2 fused to the gene for HBsAg respectively. After one primary and one boosting immunizations, antibodies against HCV E2 and HBsAg were tested and subtyped in ELISA. Splenic cytokine expression of IFN- γ and IL-10 was analyzed using an RT-PCR assay. Post-immune mouse antisera also were tested for their ability to capture HCV viruses in the serum of a hepatitis C patient *in vitro*.

RESULTS: After immunization, antibodies against both HBsAg and HCV E2 were detected in mouse sera, with IgG2a being the dominant immunoglobulin sub-class. High-level expression of INF- γ was detected in cultured splenic cells. Mouse antisera against three of the five fusion constructs were able to capture HCV viruses in an *in vitro* assay.

CONCLUSION: The results indicate that these fusion constructs could efficiently elicit humoral and Th1 dominant cellular immune responses against both HBV S and HCV E2 antigens in DNA-immunized mice. They thus could serve as candidates for a bivalent vaccine against HBV and HCV infection. In addition, the capacity of mouse antisera against three of the five fusion constructs to capture HCV viruses *in vitro* suggested that neutralizing epitopes may be present in other regions of E2 besides the hypervariable region 1.

Jin J, Yang JY, Liu J, Kong YY, Wang Y, Li GD. DNA immunization with fusion genes encoding different regions of hepatitis C virus E2 fused to the gene for hepatitis B surface antigen elicits immune responses to both HCV and HBV. *World J Gastroenterol* 2002;8(3):505-510

INTRODUCTION

Both Hepatitis B virus (HBV) and Hepatitis C virus (HCV) are major causative agents of transfusion-associated and community-acquired hepatitis worldwide^[1,2]. It is estimated that there are 250 million HBV carriers in the world and more than 10% of chronically infected HBV patients eventually develop cirrhosis and hepatocellular carcinoma^[3]. About 2-3% of the world population are HCV carriers. More than 70% of HCV infections become chronic, among which 5-20% progress to liver cirrhosis and hepatocellular carcinoma^[4,5]. Available HBV vaccines have proven to be safe and effective in preventing HBV infection. However, high costs, exclusion of some escape mutants and neonatal intolerance are eliminating their wide use^[6]. So far, no vaccine is available against HCV infection. IFN- γ treatment is the only useful therapy available. However, only 20-30% of treated patients develop long-term responses^[7]. Therefore, HBV and HCV infections pose a worldwide health threat and the development of uniformly effective vaccines of affordable prices is an urgent task.

DNA immunization, which allows the *de novo* synthesis of antigens in host's cells, is able to elicit protective humoral and cellular immune responses in several animal models of viral infection^[8-10]. The cellular context for *de novo* synthesized proteins to achieve proper maturation is a particularly important advantage for proteins such as those constituting viral envelopes whose maturation requires the help of additional cellular factors. Increasing data showed that DNA immunization against HBsAg elicited strong humoral and cellular immune responses that protect chimpanzees against the challenge with HBV. Moreover, DNA immunization in transgenic mice expressing HBsAg in the liver resulted in the clearance of HBsAg and long-term control of transgene expression, suggesting that DNA immunization is a potential tool in the treatment of HBV chronic carriers^[11-15]. DNA immunization with HCV E2 protein that was believed to carry the major neutralization epitopes of HCV^[16] also was studied in several animal models including primates^[17-21]. These studies demonstrated that DNA immunization with HCV E2 elicited strong humoral and cellular immune responses in various animals, though it did not elicit sterilizing immunity in chimpanzees against the challenge with a monoclonal homologous virus. The DNA immunization did appear to modify the infection and might have prevented the progression to chronicity, suggesting that DNA vaccine could be a promising approach for HCV treatment.

The objective of this research was to simultaneously stimulate immune responses against both HBV and HCV by DNA immunization with fusion constructs comprising of various HCV E2 gene fragments fused to the HBsAg gene of HBV. HBsAg carries all the information required for membrane translocation, particle assembly and secretion from mammalian cells. We have previously shown that HBsAg carrying HBV preS1 (21-47) at its truncated carboxyl terminal end could present the preS1 epitope on the surface of the chimeric particle and induce preS1 specific antibodies in mice^[22-24]. Moreover, humoral and cellular immune responses were successfully induced via

direct injection of the plasmid containing the HBsAg-preS1 fusion gene^[15]. These data indicated that gene fragments of proper size could be fused to the C-terminal of HBsAg without affecting particle assembly and secretion, and were capable of inducing immune responses against both HBsAg and the fused epitope. Although the epitopes on envelope protein E2 are not very clear yet, there have been some successful experiments to determine the immune determinants^[25-27]. Based on these previous findings, five fragments of HCV-E2 were selected in the hydrophilic region of E2 protein and fused to the truncated 3' end of HBsAg gene. The humoral and cellular immune responses of the plasmids expressing fusion proteins were evaluated. Furthermore, virus-capture ability of antibodies against those HCV-E2 fragments was also examined. The results are opening a new approach to the development of a bivalent vaccine against HBV and HCV, and lead to a better understanding of the immunological property of HCV-E2.

MATERIALS AND METHODS

Expression plasmids

Five HCV E2 gene fragments (A to E) were amplified from pUC18/E (E1-E2 gene of HCV genome type 1b inserted in pUC18)^[28] with following primers:

Fragment	Sense Primer	Antisense Primer
A(384-413)	P1 CGGCGTTGTATACACACCTACG	P2 TGGGAATTCAAAGCTGGATTTC
B(414-443)	P3 GAAATCGTATACGTGAACACCA	P4 CCGAATTCAGTAGAACAGCGCG
C(460-489)	P5 CATGGCCGTATACCGCTCCATTG	P6 GTCGAATTCAGTAGTCCAGCA
D(490-519)	P7 TTGCTGGGTATACCACTCCGA	P8 GAGAATTCAGTGTCTCCACCAC
E(529-549)	P9 GGTGGGGGTATACGATCGCTC	P10 TACGAATTCACCAAGTGCCTGCGG

AccI and *EcoRI* sites were introduced in sense and antisense primers, respectively. After digestion with *AccI* and *EcoRI*, PCR products were inserted downstream from the HBV S gene in pcDNA3S^[29] to obtain pcDNA3SE2-A, pcDNA3SE2-B, pcDNA3SE2-C, pcDNA3SE2-D and pcDNA3SE2-E (Figure 1). A fragment coding for amino acids 384 to 649 of HCV-E2 was also amplified from pUC18/E with primers P11 (5'-CCGGCGGATCCATGAACACC-3') and P12 (5'-GCGAATTCATCCTCGAGTCCAG-3'). PcDNA3E2 was constructed by inserting this PCR product digested with *Bam*HI and *EcoRI* into the MCS of pcDNA3 (Figure 1).

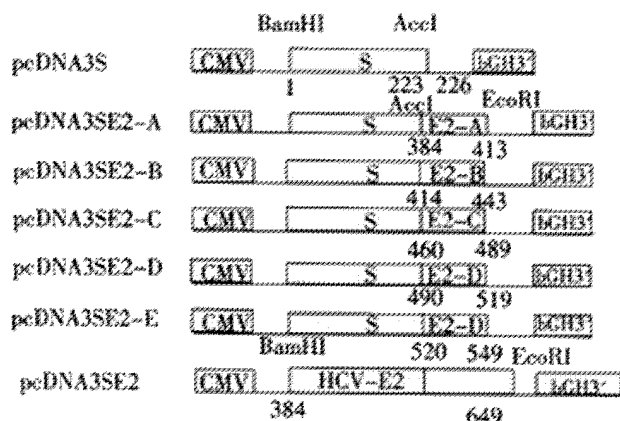


Figure 1 Schematic diagram of the expression plasmids. The coordinates below the bars refer to the corresponding amino acid residues of HBV surface antigen (HBsAg) and HCV E2 protein. The fusion genes were under the control of CMV immediate early promoter in pcDNA3. Bovine growth hormone (bGH) 3'-untranslated sequences were used as polyadenylation signals.

ELISA for transiently expressed HBV surface antigen

COS-M6 cells were maintained in Dulbecco's Modified Eagle's

medium (DMEM) supplemented with 5% fetal calf serum (Gibco, BRL, USA). 10 μ g of plasmid DNA and 5 μ g of an internal control pSK110, which expresses β -galactosidase, were transfected into 5 $\times 10^5$ COS-M6 cells by calcium phosphate co-precipitation method. Forty-eight hours after transfection, cells and media were collected. The activity of β -galactosidase in cell lysate obtained by cycles of freezing and thawing was analyzed to normalize the variation of transfection efficiency among different samples. HBsAg in cell lysates and media was determined with a commercial ELISA kit (Sino-American Co., Shanghai, China). The kit was adapted for quantitative measurements of HBsAg using purified yeast derived HBsAg (National Vaccine and Serum Institute, Beijing, China) as potency standard. Results were presented as means of three independent experiments^[23,30].

Western Blotting of transiently expressed products

HeLa cells were maintained in DMEM supplemented with 5% fetal calf serum. To enhance the expression level of fusion genes, cells were first infected with vaccinia virus vTT7 that expresses T7 RNA polymerase at a M.O.I. of 10 pfu per cell^[31]. Two hours post-infection, 1-2 $\times 10^5$ cells were transfected with 10 μ g of plasmid DNA by calcium phosphate method. Eighteen hours after transfection, cells were collected and cell lysate was electrophoresed on a 12.5% SDS-PAGE and subsequently electro-blotted onto nitrocellulose membrane. After blocking for 1h with 5% powdered lipid-free milk in PBST (PBS containing 0.1% Tween 20), the membrane was incubated with anti-HBs McAb H116 (kindly provided by Dr. E. Hildt, Munich, Germany) or anti-HCV E2 (450-565) polyclonal antiserum RE2-116^[32], followed by incubation with HRP conjugated secondary antibody (Dako Co., Denmark). Signals were detected by enhanced chemi-luminescence (ECL) blotting analysis system (Amersham-Pharmacia Co., UK).

DNA immunization of mice

C57BL/6 (H-2^b) mice were purchased from Shanghai Laboratory Animal Center. Groups of five female mice, 6-8 weeks old, were injected with 100 μ g of expression plasmids into regenerated tibialis anterior (TA) muscles 5 days after treatment of 100 μ l 10⁻⁵mol/l cardiotxin (Sigma, USA)^[15,29]. Four weeks later, the mice were boosted in the same way.

Serologic tests

Sera were collected by tail bleeding at different time points pre-and post-injection and assayed for anti-HBs and anti-HCV-E2 by ELISA. Microwell plates were coated with serum derived HBsAg particles^[29] (Kehua Co., Shanghai, China), or 0.1 μ g/well HCV-E2 (385-565) expressed in *E. Coli*^[32]. After blocking with 5% powdered lipid-free milk in PBST (PBS containing 0.1% Tween 20), serial two-fold dilutions of sera were added. The bound antibodies were detected with HRP-conjugated rabbit anti-mouse IgG (1:1000) (Dako Co., Denmark) after extensive washing with PBST. Sera from mice immunized with pcDNA3 vector at 1 in 20 dilution were used as negative controls. A positive result was defined as an absorbance value of great than twice the absorbance of negative control with a cutoff of 0.050. Seroconversion was defined as giving a positive reading at 1:20 dilution. Antibody titres of pooled seroconverted animal sera were set as the highest dilution giving a positive reading (end-point dilution method)^[22,32].

To type the subclasses of IgG, mouse sera of each group were collected 6 weeks after the first immunization, and the titers of IgG1 and IgG2a antibodies assayed individually by a similar end-point dilution method, using the HRP-conjugated rabbit anti-mouse IgG1 and IgG2a (Serotec Co., Oxford, UK) for detection.

Splenic cytokine expression test

Expression of IFN- γ and IL-10 were assayed semi-quantitatively as described^[33,34]. Mice were killed 10 weeks after the first injection and spleens were removed aseptically. The single cell suspensions of the splenocytes were prepared and maintained in DMEM supplemented with 5% fetal calf serum and 5×10^{-5} M β -ME at a density of 10^7 cells per well. Cells were stimulated with 0.5 μ g/ml rDNA yeast derived HBsAg (National Vaccine and Serum Institute, Beijing, China), followed by culture at 37°C. At 0, 24, 48 hr post-stimulation, splenic cells were sampled. Total RNA was extracted with Trizol (Gibco, BRL, USA) and reverse transcribed with random hexamer primers (New England Biolabs Inc, Beverly, USA.). Messenger RNAs for IFN- γ and IL-10 were semi-quantitated by competitive RT-PCR^[33,34]. Splenic cells from mice immunized with pcDNA3 and mitogen ConA (5 μ g/ml) served as a negative and a positive control respectively.

Analysis of the virus capture capability of immune sera

The virus capture capability of antibodies in immune sera was assessed according to the method of affinity capture RT-PCR (AC-RT-PCR) detection of HEV in patient stool specimens^[35] with a few modifications. Briefly, 0.5ml microcentrifuge tubes were coated with 50 μ l goat anti-mouse IgG F(ab')₂ (0.02 μ g/ μ l, Jackson ImmunoResearch Laboratories, Inc., West Grove, USA), capped and incubated at room temperature for 1hr. After blocking with 5% powdered lipid-free milk in PBST for 15 min at 37°C and overnight at 4°C, tubes were aspirated and washed with 150 μ l PBST. The mouse sera were adjusted to same titre of 1:80 by dilution with PBS, to avoid the variations of the results caused by different antibody titers in different samples. Tubes were subsequently loaded with 25 μ l properly diluted mouse immune sera and 25 μ l HCV-RNA-PCR-positive patient's serum (1.6×10^7 HCV genome Equivalent [Geq] per ml, provided by Dr. X. Zhang, Ruijin Hospital, Shanghai, China) diluted 1:50 in PBS. The mixtures were mixed gently and incubated for 1 hr at room temperature and overnight at 4°C. Tubes were then washed three times with 150 μ l wash buffer (25 mM Tris-HCl pH8.0, 75mM KCl, 2.5mM MgCl₂). Captured virus was detected with a commercial HCV PCR testing kit (Sino-American Co., Shanghai, China) which specifically amplifies a 225 bp fragment in the 5' UTR of HCV RNA. HCV which was captured directly by a conformation specific monoclonal antibody (McAb) against HCV-E2, 219A2, (kindly provided by Dr. S. Abrignani, IRIS, Siena, Italy) was used as positive control.

RESULTS

Transient expression of HBsAg-HCV E2 fusion proteins Five expression plasmids containing the HCV-E2 coding sequences (corresponding to amino acids 384-413, 414-443, 460-489, 490-519, 529-549) fused to the 3' end of HBV-S gene were constructed as described in "Materials and Methods". COS-M6 cells were then transfected with these plasmids respectively.

Forty-eight hours post-transfection, the presence of HBsAg fusion protein in the cell lysates and culture media was measured with HBsAg ELISA. HBsAg was detected in both the cell lysates and culture media, indicating that the fusion constructs were able to express and secrete HBsAg efficiently (Figure 2).

Expressed HBsAg and HCV-E2 fusion proteins were also evaluated by Western Blot. They were separated by SDS-PAGE gel, followed by incubation with HBsAg specific McAb H116 (Figure 3A). Compared with HBsAg expressed by pcDNA3S (Figure 1), which contained the major surface gene of HBV only and displayed 24000 and 27000 protein bands for the unglycosylated and glycosylated forms respectively (Figure 3A, lane1)^[29], all the fusion antigens showed slower migratory bands (27000 and 29000), indicating

successful expression of the fusion proteins. Two fusion constructs SE2-B (414-443) and SE2-D (490-519) displayed additional bands at 31000, which might result from multi-glycosylation. Expressed fusion proteins SE2-C (460-489), SE2-D (490-519) and SE2-E (529-549) were also incubated with polyclonal antibody RE2-116. The band pattern in the Western Blots (Figure 3B) was consistent with that in Figure 3A, suggesting that these fusion proteins possess both HBV-S and HCV-E2 antigenicity. SE2-A(384-413) and SE2-B(414-443) were not assayed for HCV-E2, since they did not locate in the reactive region (450-565) of RE2-116. By contrast, the non-fused truncated E2(384-649) (Figure 1) displayed only a single band as large as the expected unglycosylated product (Figure 3B, lane 1).

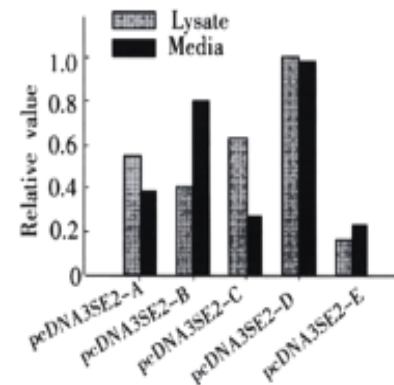


Figure 2 Comparison of the expression and secretion level of fusion proteins in COS cells.

pcDNA3SE2-A, pcDNA3SE2-B, pcDNA3SE2-C, pcDNA3SE2-D, pcDNA3SE2-E are the plasmids expressing HBsAg fused with different HCV E2 fragments. The HBsAg in the culture medium (gray) and cell lysates (black) was measured by a commercial ELISA kit (Sino-American Co., Shanghai, China). Results were presented as means of three independent experiments (see Materials and Methods). The amount of HBsAg expressed by pcDNA3SE2-D in cell lysates was arbitrarily taken as 1.0.

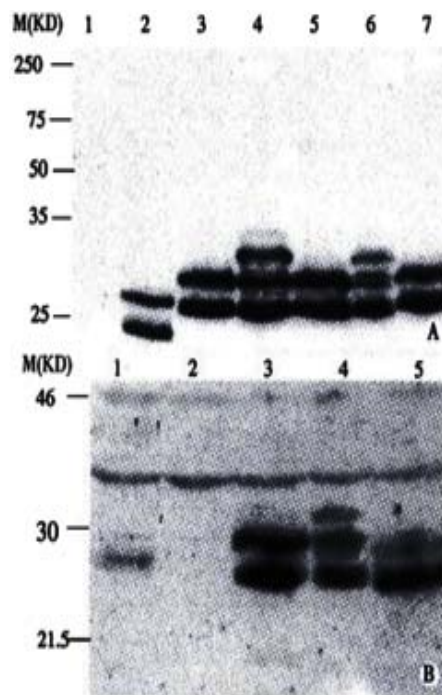


Figure 3 Characterization of the fusion antigens transiently expressed in HeLa cells by Western blotting.

After separation by a 12.5% SDS-PAGE, the proteins were blotted onto a nitrocellulose membrane and incubated with (A) anti-S McAb (H166, 1:300 diluted), (B) anti-HCV E2 (450-565) polyclonal antiserum RE2-116 (1:500 diluted) respectively. (A) lane 1-7, fusion proteins expressed by pcDNA3, pcDNA3S, pcDNA3SE2-A, pcDNA3SE2-B, pcDNA3SE2-C, pcDNA3SE2-D and pcDNA3SE2-E respectively. (B) lane 1-5, fusion proteins expressed by pcDNA3SE2-C, pcDNA3SE2-D, pcDNA3SE2-E respectively.

Humoral responses to fusion antigens in DNA-immunized mice

C57BL/6 mice were injected with HCV-E2 and HBV-S fusion constructs. As shown in Table 1, the immunized mice produced antibodies against both HBsAg and HCV-E2 after the first injection, and the seroconversion rate increased quickly after the boost, reaching 100% at week 6 or 8. Antibodies were still detectable after 24 weeks. Impressively, the anti-HCV E2 antibody titers elicited in mice immunized with fusion constructs were much higher than that induced in mice injected with pcDNA3E2 (up to 40 fold difference), which contained non-fused HCV E2(384-649). Compared with the humoral response induced by pcDNA3S, all the fusion constructs were able to induce equivalent or slightly smaller anti-HBs antibody responses.

Subsets of IgG against both HBsAg and HCV-E2 were also determined. The IgG profiles specific to HBsAg indicated the obvious predominance of IgG2a (Figure 4A), while IgG profiles specific to HCV-E2 varied among different constructs (Figure 4B). Only pcDNA3SE2-A and pcDNA3SE2-D induced predominant IgG2a against HCV-E2, suggesting that the T helper responses elicited against these two fragments were Th1 dominant.

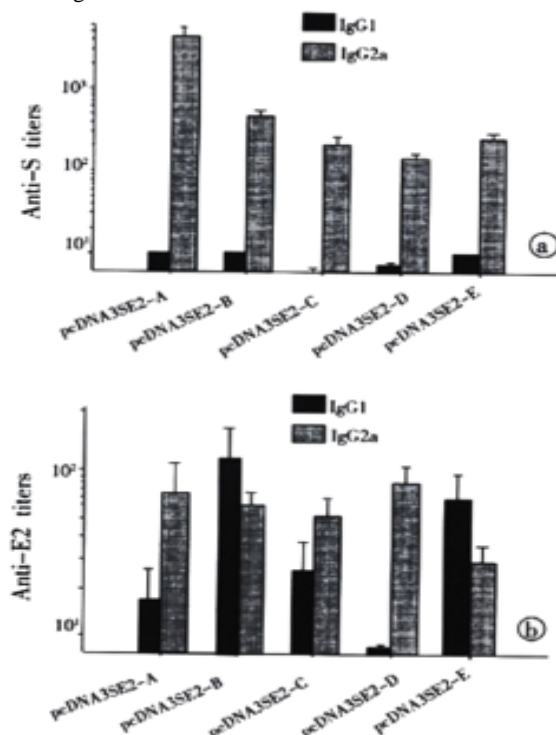


Figure 4 IgG subtypes profile of antibodies against HBsAg and HCV E2. Sera collected from mice 6 weeks after boosting were assayed for the IgG1 and IgG2a antibodies against HBsAg and HCV E2. For each group of 5 mice, titers of IgG1 and IgG2a antibodies were determined individually by serial two-fold dilution titration methods using HRP-conjugated rabbit anti-mouse IgG1 and IgG2a (Serotec Co., Oxford, UK) for detection. (as described in Materials and Methods). The arithmetic mean \pm standard deviation (SD) ($n=5$) is shown. (A) Anti-HBs, (B) Anti-HCV E2.

Expression of cytokines in the cultured splenic cells from DNA-immunized mice

After the *in vitro* stimulation of splenic cells derived from immunized mice, expressions of cytokines were analyzed by competitive RT-PCR. 24 hrs post-stimulation with rDNA yeast derived HBsAg (National Vaccine and Serum Institute, Beijing, China), high levels of IFN- γ were detected in the splenic cells from the mice immunized with pcDNA3SE2-A, pcDNA3SE2-B, pcDNA3SE2-C and pcDNA3SE2-E (Figure 5). The IL-10 expression was also detectable, but weaker than IFN- γ expression.

Table 1A Sero-conversion Ratios and Titres of Anti-HBsAg in DNA Immunized Mice

Weeks	DNAImmunogen					
	pcDNA3S	pcDNA3SE2-A	pcDNA3SE2-B	pcDNA3SE2-C	pcDNA3SE2-D	pcDNA3SE2-E
0 ^a	(0/5)	(0/5)	(0/5)	(0/5)	(0/5)	(0/5)
2	(5/5)	(1/5)	(1/5)	(1/5)	(1/5)	(2/5)
4 ^b	1280 ^c (5/5)	1280(4/5)	640(2/5)	320(2/5)	320(2/5)	320(4/5)
6	10240(5/5)	10240(5/5)	5120(4/5)	5120(4/5)	5120(5/5)	2560(5/5)
8	5120(5/5)	5120(5/5)	5120(5/5)	5120(5/5)	5120(5/5)	5120(5/5)
10	5120(5/5)	5120(5/5)	2560(4/5)	2560(5/5)	2560(5/5)	5120(5/5)
16	1280(5/5)	1280(5/5)	640(4/5)	320(5/5)	640(5/5)	80(5/5)
24	1280(5/5)	1280(5/5)	640(4/5)	320(5/5)	640(5/5)	80(5/5)

Note: Groups of mice ($n=5$) were injected i.m. with the respective plasmids, and anti-HBsAg antibody titers were measured at different time points by ELISA. Sera from mice immunized with pcDNA3 vector were used as negative controls and showed no reactivity with any coated antigens (data not shown). For sero-conversion, 1:20 starting dilution were assayed and the sera giving positive reading were taken as converted one. To determine antibody titers, serial two-fold dilutions of pooled seroconverted immune sera were incubated in antigen-coated wells. A positive result was defined as an absorbance value of greater than twice the absorbance of the negative control with a cutoff of 0.050(also see Materials and Methods). At week 2 only sero-conversion testing was performed at 1:20 dilution. ^athe first immunization; ^bthe second immunization (boost); ^c(n/n); sero-conversion ratio, numbers of sero-converted mice relative to the total number tested; ^dtiter; reciprocal of the two-fold dilution factor at end point; pools of seroconverted sera from test groups were tested.

Table 1B Sero-conversion Ratios and Titres of Anti-HCV-E2 in DNA Immunized Mice

Weeks	DNAImmunogen					
	pcDNA3S	pcDNA3SE2-A	pcDNA3SE2-B	pcDNA3SE2-C	pcDNA3SE2-D	pcDNA3SE2-E
0 ^a	(0/5)	(0/5)	(0/5)	(0/5)	(0/5)	(0/5)
2	(1/5)	(2/5)	(1/5)	(1/5)	(1/5)	(1/5)
4 ^b	40 ^c (2/5)	320(3/5)	160(1/5)	320(3/5)	320(2/5)	320(1/5)
6	160(5/5)	640(5/5)	640(5/5)	2560(5/5)	2560(5/5)	5120(4/5)
8	880(5/5)	640(5/5)	320(5/5)	5120(5/5)	5120(5/5)	5120(4/5)
10	80(5/5)	160(5/5)	320(5/5)	5120(5/5)	5120(5/5)	5120(4/5)
16	80(5/5)	80(5/5)	160(5/5)	160(5/5)	320(5/5)	80(4/5)
24	40(5/5)	40(5/5)	80(5/5)	80(5/5)	160(5/5)	40(4/5)

Note: Groups of mice ($n=5$) were injected i.m. with the respective plasmids, and seroconversion ratio and anti-HCV E2 antibody titers were measured at different time points by ELISA. With the exception of coating antigen (E2 (385-565)), all experimental procedures were the same as described in Table 1A. ^athe first immunization; ^bthe second immunization (boost); ^c(n/n); sero-conversion ratio, numbers of sero-converted mice relative to the total number tested; ^dtiter; reciprocal of the two-fold dilution factor at end point, pools of positive sera from test groups were tested.

Virus-capture ability of antisera from DNA-immunized mice

To test the virus-capture capability of antibodies elicited in response to DNA immunization, affinity-capture-RT-PCR (AC-RT-PCR) was performed as described in "Materials and Methods". The HCV virions bound to anti-HCV-E2 were detected by nested RT-PCR to amplify a specific fragment in the 5'-UTR of HCV genome. The results indicated that immune sera of mice immunized with pcDNA3SE2-A, pcDNA3SE2-B and pcDNA3SE2-D were able to capture HCV virions in the serum of a hepatitis C patient *in vitro* (Figure 6).

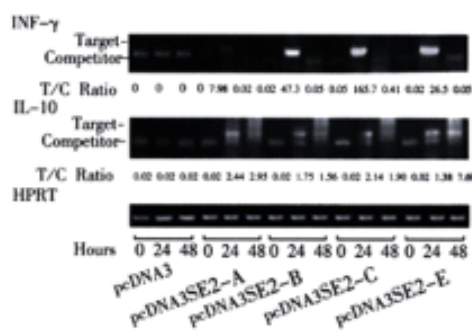


Figure 5 IFN- γ and IL-10 mRNA expression. mRNA was isolated from splenic cells of immunized mice after stimulation with HBsAg for 0, 24, 48 hours. IFN- γ and IL-10 mRNA expression was

determined by semi-quantitative RT-PCR after standardization of the cDNA concentration by amplification of HPRT. Level of expression is indicated as ratio of target to competitor, calculated from densitometric analysis of their PCR products. (High ratio indicates high expression of target mRNA).

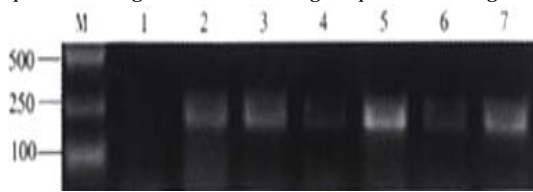


Figure 6 Detection of HCV captured by mouse antisera by nested RT-PCR. After immuno-capture of HCV from hepatitis C patient serum (1.6×10^7 HCV GEq per ml) by antisera from groups of mice immunized with pcDNA3, pcDNA3SE2-A, pcDNA3SE2-B, pcDNA3SE2-C, pcDNA3SE2-D and pcDNA3SE2-E (lane 1 to lane 6), viruses were detected by nested RT-PCR using the HCV RT-PCR testing kit (Sino-America Co., Shanghai, China). Lane 7, the positive control using McAb against HCV E2 to capture HCV. Lane M, molecular markers.

DISCUSSION

In this report, five fusion constructs comprising various fragments within the hydrophilic region of HCV-E2 fused to the 3' end of the S gene of HBV were constructed. The immune responses of mice to immunization with these fusion constructs indicated that all five constructs were able to elicit strong antibody responses against both HBsAg and HCV-E2. Importantly, antibody typing showed the HBsAg specific Th1 like responses, which were consistent with the high levels of IFN- γ expression in cultured spleen cells from the immunized mice after stimulation with HBsAg. The IgG subtype responses to HCV-E2 also showed E2 specific Th1 like responses to E2-A and E2-D. Since Th1 like response is essential for triggering a wide range of cellular responses against infectious agents, including NK cell responses, CTL responses and inflammatory reactions, the results of the DNA immunization with our fusion plasmids suggest a promising strategy to clear both HBV and HCV in the host.

The excellent vaccine potential of our constructs may be ascribed to the use of HBsAg as a carrier. HBsAg has the advantage of assembling into large secretable particles, which form a virus-like polymeric structure that enhances antigenic stability and provides a high-density presentation to antigen-presenting cells (APC). HBsAg has been used successfully as vaccine carrier to present various antigens^[15,23,29,36,37]. The successful immune responses to both HBV S and HCV E2 in these reports support our preliminary observation that antigens of a proper size fused to C-terminal of HBsAg could be successfully presented without affecting the immunogenicity of HBsAg. Moreover, our fusion constructs were able to elicit higher levels of antibody responses to HCV E2, compared to pcDNA3E2 that encodes only a truncated HCV-E2 (384-649). This of course suggests that fusion to HBsAg may help these fragments to be presented more effectively to APCs, and hence induce stronger humoral responses against HCV-E2. These fusion constructs may turn out to be promising candidates for the vaccines against HCV and HBV.

It is well established that the intact E2 glycoproteins expressed alone or together with E1 (E1-E2 heterodimer) are retained in the endoplasmic reticulum^[38] and that E2 proteins expressed in mammalian cells without the signal sequence at the C-terminus of E1 are not glycosylated^[39]. Consistently, we also observed that the truncated E2 (384-649) was expressed in unglycosylated form in mammalian cells. However, the use of HBsAg as carrier seems to give rise to expression of fusion proteins carrying HCV-E2 epitopes in glycosylated and secretable form, which emphasizes the advantage of HBsAg as a carrier. Notably, two products, SE2-B and SE2-D expressed by pcDNA2SE2-B and pcDNA3SE2-D, produced an additional 31000 glycosylated form, suggesting that in addition to the glycosylation site in HBsAg, some sites in fragment B and D also may be glycosylated. Since glycosylation is a decisive factor for biological molecules to carry out correct biological functions, the additional glycosylation of the fusion constructs may elicit immune responses similar to that of natural

infections by the HCV. This may be an additional reason that our constructs are able to elicit strong immune responses.

The results presented here also suggest that the DNA immunization with different HCV E2 fragments fused to HBsAg may be a useful approach to screen for epitopes or immune determinants on HCV-E2. Nakano *et al.*^[18] inserted different regions of HCV E2 into the preS2 region of HBV surface protein, and evaluated the humoral immune responses of these fusion constructs via DNA immunization. Their study also suggest that fusion constructs of E2 with HBsAg might be an efficient way to identify restricted immunogenic domains within E2. In our study, each of the chosen E2 fragments contained only 30 amino acids, it provides a possibility to study the antigenic domains of HCV E2 more precisely. Antibody responses and IgG subtype typing against these E2 fragments suggest that B- and T- epitopes were present in fragment D(490-519). Furthermore, the results of virus-capture assay showed that HCV virions in the serum of a hepatitis C patient could be captured by immune sera against SE2-A, SE2-B and SE2-D *in vitro*. In particular, antibodies against fragment D exhibited the strongest ability to capture HCV virions. Because the ability of antibodies to bind viruses is a prerequisite for neutralizing viruses *in vivo* and preventing bodies from being infected, our data suggest that besides HVR1-containing fragment A, fragments B and D probably also harbour neutralizing epitopes. So far, only HVR1 has been confirmed to be an important epitope^[40-48] whose corresponding antibody can neutralize the binding of HCV-E2 to susceptible cells *in vitro*, and prevent HCV infection after *in vitro* neutralization^[42,43]. Recently, correlation between circulating antibodies against HVR1 and resolution of chronic hepatitis C has been confirmed^[49]. However, the high variability of HVR1 interferes with the development of HVR1-based vaccines. Some researchers suggested that there may be B-cell epitopes located downstream from HVR1^[17,18,50]. Rosa *et al.*^[43] speculated that there may be at least one additional neutralizing epitope located somewhere other than HVR1 of HCV E2, this was based on the finding that HVR-1 peptide failed to completely block the binding of HCV to susceptible cells. Our results suggest that potential neutralizing epitopes may be present within fragments B (414-443) and D (490-519) that are downstream from HVR1. Since fragments B and D are relatively more conservative than HVR1, it would seem that vaccines containing fragments B and/or D may be more promising than that containing only HVR1. Further studies on these neutralizing epitopes are under way, which hopefully will lead to a better understanding of the immunological property of HCV E2, and facilitate the design of efficient HCV vaccines.

ACKNOWLEDGMENT

The authors are grateful to Dr. E. Hildt for providing monoclonal antibody (McAb) H166, Dr. S. Abrignani for McAb 219A2, Dr. Yuan ZH for HRP-Rabbit antibody against mouse IgG1 and IgG2a, Dr. Zhang XX for HCV patient serum and Qu D for her help in cytokine test.

REFERENCES

- 1 Choo QL, Kuo G, Weiner AJ, Overby LR, Bradley DW, Houghton M. Isolation of a cDNA clone derived from a blood-borne non-A, non-B viral hepatitis genome. *Science* 1989;244:359-362
- 2 Kuo G, Choo QL, Alter HJ, Gitnick GL, Redeker AG, Purcell RH, Miyamura T, Dienstag JL, Alter MJ, Stevens CE. An assay for circulating antibodies to a major etiologic virus of human non-A, non-B hepatitis. *Science* 1989;244:362-364
- 3 Tiollais P, Buendia MA. Hepatitis B virus. *Sci Am* 1991;264:48-54
- 4 Alter MJ, Margolis HS, Krawczynski K, Judson FN, Mares A, Alexander WJ, Hu PY, Miller JK, Gerber MA, Sampliner RE. The natural history of community-acquired hepatitis C in the United States: the Sentinel Counties chronic non-A, non-B hepatitis study team. *N Engl J Med* 1992;327:1899-1905
- 5 Saito I, Miyamura T, Ohbayashi A, Harada H, Katayama T, Kikuchi S, Watanabe Y, Koi S, Onji M, Ohta Y. Hepatitis C virus infection is associated with the development of hepatocellular carcinoma. *Proc Natl Acad Sci USA* 1990;87:6547-6549
- 6 Thanavala Y. Novel approaches to vaccine development against HBV. *J Biotechnol* 1996;44:67-73

- 7 Fried MW, Sambrook J. Therapy of hepatitis C. *Semin Liver Dis* 1995; 15:82-91
- 8 Wayne CL, Michael B. DNA Vaccine. *Crit Rev Immunol* 1998;18:449-484
- 9 Donnelly JJ, Ulmer JB, Liu MA. Immunization with DNA. *J Immunol Meth* 1994;176:145-152
- 10 McDonnell WM, Askari FK. DNA Vaccines. *N Engl J Med* 1996;334:42-45
- 11 Davis HL, Michel ML, Whalen RG. DNA-based immunization induces continuous secretion of hepatitis B surface antigen and high levels of circulating antibody. *Human Mol Genetics* 1993;2:1847-1851
- 12 Michel ML, Davis HL, Schleef M, Mancini M, Tiollais P, Whalen RG. DNA-mediated immunization to the hepatitis B surface antigen in mice: Aspects of the humoral response mimic hepatitis B viral infection in humans. *Proc Natl Acad Sci USA* 1995;92:5307-5311
- 13 Mancini M, Davis H, Tiollais P, Michel ML. DNA-based immunization against the envelope proteins of the hepatitis B virus. *J Biotechnol* 1996;44:47-57
- 14 Mancini M, Hadchouel M, Davis HL, Whalen RG, Tiollais P, Michel ML. DNA-mediated immunization in a transgenic mouse model of the hepatitis B surface antigen chronic carrier state. *Proc Natl Acad Sci USA* 1996;93:12496-12501
- 15 Hui J Y, Mancini M, Li G D, Wang Y, Tiollais P, Michel M-L. Immunization with a plasmid encoding a modified hepatitis B surface antigen carrying the receptor binding site for hepatocytes. *Vaccine* 1999;17:1771-1778
- 16 Choo QL, Kuo G, Ralston R, Weiner A, Chien D, Van Nest G, Han J, Berger K, Thudium K, Kuo C. Vaccination of chimpanzees against infection by the hepatitis C virus. *Proc Natl Acad Sci USA* 1994;91:1294-1298
- 17 Tedeschi V, Akatsuka T, Shih JWK, Battagay M, Feinstone SM. A specific antibody response to HCV E2 elicited in mice by intramuscular inoculation of plasmid DNA containing coding sequences for E2. *Hepatology* 1997;25:459-462
- 18 Nakano I, Maertens G, Major ME, Vitvitski L, Dubuisson J, Fournillier A, De Martynoff G, Trepo C, Inchauspe G. Immunization with plasmid DNA encoding hepatitis C virus envelope E2 antigenic domains induces antibodies whose immune reactivity is linked to the injection mode. *J Virol* 1997;71:7101-7109
- 19 Fornis X, Emerson SU, Tobin GJ, Mushahwar IK, Purcell RH, Bukh J. DNA immunization of mice and macaques with plasmids encoding hepatitis C virus envelope E2 protein expressed intracellularly and on the cell surface. *Vaccine* 1999;17:1992-2002
- 20 Fournillier A, Depla E, Karayiannis P, Vidalin O, Maertens G, Trepo C, Inchauspe G. Expression of noncovalent hepatitis C virus envelope E1-E2 complexes is not required for the induction of antibodies with neutralizing properties following DNA immunization. *J Virol* 1999;73:7497-7504
- 21 Fornis X, Payette PJ, Ma X, Satterfield W, Eder G, Mushahwar IK, Govindarajan S, Davis HL, Emerson SU, Purcell RH, Bukh J. Vaccination of chimpanzees with plasmid DNA encoding the hepatitis C virus (HCV) envelope E2 protein modified the infection after challenge with homologous monoclonal HCV. *Hepatology* 2000;32:618-25
- 22 Xu X, Li GD, Kong YY, Yang HL, Zhang ZC, Cao HT, Wang Y. A modified hepatitis B virus surface antigen with the receptor-binding site for hepatocytes at its C-terminus: Expression, antigenicity and immunogenicity. *J Gen Virol* 1994;75:3673-3677
- 23 Hui JY, Li GD, Kong YY, Wang Y. Expression and characterization of chimeric hepatitis B surface antigen particles carrying preS epitopes. *J Biotechnol* 1999;72:49-59
- 24 Yang JY, Jin J, Kong YY, Wei J, Zhang ZC, Li GD, Wang Y, Yuan HY, Li YY. Purification and characterization of recombinant hepatitis B virus surface antigen SS1 expressed in *Pichia pastoris*. *Acta Biochem Biophys Sin* 2000;32:503-508
- 25 Koshy R, Inchauspe G. Evaluation of hepatitis C virus protein epitopes for vaccine development. *Trends Biotechnol* 1996;149:364-369
- 26 Fournillier A, Nakano I, Vitvitski L, Depla E, Vidalin O, Maertens G, Trepo C, Inchauspe G. Modulation of immune responses to hepatitis c virus envelope E2 protein following injection of plasmid DNA using single of combined delivery routes. *Hepatology* 1998;28:237-244
- 27 Lee JW, Kim KM, Jung SH, Lee KJ, Choi EC, Sung YC, Kang CY. Identification of a domain containing B-cell epitopes in hepatitis C virus E2 glycoprotein by using mouse monoclonal antibodies. *J Virol* 1999;73:11-18
- 28 Wang Y, Okamoto H, Tsuda F, Naqayama R, Tao QM, Mishiro S. Prevalence, genotypes, and an isolate (HC-C2) of Hepatitis C Virus in Chinese patients with liver disease. *J Med Virol* 1993;40:254-260
- 29 Hui JY, Li GD, Kong YY, Yuan Wang. DNA-based immunization against hepatitis B surface antigen carrying preS epitopes. *Chinese Sci Bull* 1999;44:620-623
- 30 Feng Y, Kong YY, Wang Y, Qi GR. Intracellular inhibition of the replication of hepatitis B virus by hammerhead ribozyme. *J Gastroenterol Hepatol* 2001;16:1125-1130
- 31 Fuerst TR, Niles EG, Studier FW, Moss B. Eukaryotic transient-expression system based on recombinant vaccinia virus that synthesizes bacteriophage T7 RNA polymerase. *Proc Natl Acad Sci USA* 1986;83:8122-8126
- 32 Liu J, Zhu LX, Zhang XX, Lu M, Kong YY, Wang Y, Li GD. Expression, purification, immunological characterization and application of *Escherichia coli*-derived hepatitis C virus E2 proteins. *Biotechnol Appl Biochem* 2001;34:109-119
- 33 Sun B, Wells J, Goldmuntz E, Silver P, Remmers EF, Wilder RL, Caspi RR. A simplified, competitive RT-PCR method for measuring rat IFN- γ mRNA expression. *J Immunol Methods* 1996;195:139-148
- 34 Sun B, Rizzo LZ, Sun SH, Chan CC, Wiggert B, Wilder RL, Caspi RR. Genetic susceptibility to experimental autoimmune uveitis involves more than a predisposition to generate a T helper-1-like or a T helper-2-like response. *J Immunol* 1997;159:1004-1011
- 35 He JK, Binn LN, Caudill JD, Asher LV, Longer CF, Innis BL. Antiserum generated by DNA vaccine binds to hepatitis E virus (HEV) as determined by PCR and immune electron microscopy (IEM): application for HEV detection by affinity-capture RT-PCR. *Virus Res* 1999;62:59-65
- 36 Prange R, Werr M, Birkner M, Hilfrich R, Strecker RE. Properties of modified hepatitis B virus surface antigen particles carrying preS epitopes. *J Gen Virol* 1995;76:2131-2140
- 37 Major ME, Vitvitski L, Mink MA, Schleier M, Whalen RG, Trepo C, Inchauspe G. DNA-based immunization with chimeric vectors for the induction of immune responses against the Hepatitis C virus nucleocapsid. *J Virol* 1995;69:5798-5805
- 38 Duvet S, Cocquerel L, Pillez A, Cacan R, Verbert A, Moradpour D, Wychowski C, Dubuisson J. Hepatitis C virus glycoprotein complex localization in the endoplasmic reticulum involves a determinant for retention and not retrieval. *J Biol Chem* 1998;273:32088-32095
- 39 Saito T, Sherman GJ, Kurokohchi K, Guo ZP, Donets M, Yu MY, Berzofsky JA, Akatsuka T, Feinstone SM. Plasmid DNA-based immunization for hepatitis C virus structural proteins: immune responses in mice. *Gastroenterology* 1997;112:1321-1330
- 40 Weiner AJ, Geysen HM, Christopherson C, Hall JE, Mason TJ, Saracco G, Bonino F, Crawford K, Marion CD, Crawford KA. Evidence for immune selection of hepatitis C virus (HCV) putative envelope glycoprotein variants: potential role in chronic HCV infections. *Proc Natl Acad Sci USA* 1992;89:3468-3472
- 41 Zibert A, Schreier E, Roggendorf M. Antibodies in human sera specific to hypervariable region 1 of hepatitis C virus can block viral attachment. *Virology* 1995;208:653-661
- 42 Scarselli E, Cerino A, Esposito G. Occurrence of antibodies reactive with more than one variant of the putative envelope glycoprotein (gp70) hypervariable region 1 in viremic hepatitis C virus-infected patients. *J Virol* 1995;69:4407-4412
- 43 Rosa D, Campagnoli S, Moretto C, Guenzi E, Cousens L, Chin M, Dong C, Weiner AJ, Lau JY, Choo QL, Chien D, Pileri P, Houghton M, Abrignani S. A quantitative test to estimate neutralizing antibodies to the hepatitis C virus: cytofluorimetric assessment of envelope glycoprotein 2 binding to target cells. *Proc Natl Acad Sci USA* 1996;93:1759-1763
- 44 Farci P, Shimoda A, Wong D, Cabezon T, De Gioannis D, Strazzer A, Shimizu Y, Shapiro M, Alter HJ, Purcell RH. Prevention of hepatitis C virus infection in chimpanzees by hyperimmune serum against the hypervariable region 1 of the envelope 2 protein. *Proc Natl Acad Sci USA* 1996;93:15394-15399
- 45 Zibert A, Dudziak P, Schreier E, Roggendorf M. Characterization of antibody response to hepatitis C virus protein E2 and significance of hypervariable region 1-specific antibodies in viral neutralization. *Arch Virol* 1997;142:523-534
- 46 Esumi M, Ahmed M, Zhou YH, Takahashi H, Shikata T. Murine antibodies against E2 and hypervariable region 1 cross-reactively capture Hepatitis C virus. *Virology* 1998;251:158-164
- 47 Watanabe K, Yoshioka K, Ito H, Ishigami M, Takagi K, Utsunomiya S, Kobayashi M, Kishimoto H, Yano M, Kakumu S. The hypervariable region 1 protein of Hepatitis C virus broadly reactive with sera of patients with chronic Hepatitis C has a similar amino acid sequence with the consensus sequence. *Virology* 1999;264:153-158
- 48 Shang DZ, Zhai WW, Allain JP. Broadly cross-reactive, high-affinity antibody to hypervariable region 1 of the Hepatitis C virus in rabbits. *Virology* 1999;258:396-405
- 49 Ishii K, Rosa D, Watanabe Y, Katayama T, Harada H, Wyatt C, Kiyosawa K, Aizaki H, Matsuura Y, Houghton M, Abrignani S, Miyamura T. High titers of antibodies inhibiting the binding of envelope to human cells correlate with natural resolution of chronic hepatitis C. *Hepatology* 1998;28:1117-1120
- 50 Mink MA, Benichou S, Madaule P, Tiollais P, Prince AM, Inchauspe G. Characterization and mapping of a B-cell immunogenic domain in hepatitis C virus glycoprotein using a yeast peptide library. *Virology* 1994;200:246-255

• BASIC RESEARCH •

Effects of Yigan Decoction on proliferation and apoptosis of hepatic stellate cells

Xi-Xian Yao, You-Wei Tang, Dong-Mei Yao, He-Ming Xiu

Xi-Xian Yao, Dong-Mei Yao, Department of Gastroenterology, The Second Hospital of Hebei Medical University, Shijiazhuang 050000, Hebei Province, China

You-Wei Tang, He-Ming Xiu, Department of Geriatrics, Bethune International Peace Hospital, Shijiazhuang 050082, Hebei Province, China

Supported by Hebei Province Administration Bureau of TCM, No. 200001

Correspondence to: Dr. Xi-Xian Yao, Department of Gastroenterology, The Second Hospital of Hebei Medical University, Shijiazhuang 050000, Hebei Province, China. yaioxian@263.net

Telephone: +86-311-7814356

Received 2001-06-03 Accepted 2001-12-08

Abstract

AIM: To investigate the effects of Chinese herb Yigan Decoction on proliferation and apoptosis of the hepatic stellate cells (HSC) *in vitro*.

METHODS: The study *in vitro* was carried out in the culture of HSC lines. Various concentrations of Yigan Decoction were added and incubated. Cell proliferation was detected with MTT colorimetric assay. Cell apoptosis was detected by electron microscopy, flow cytometry and TUNEL.

RESULTS: The proliferation of HSC was inhibited by Yigan Decoction, which depending on dose and time significantly. The HSC proliferation rates of groups at the end concentrations 144 and 72(g·L⁻¹) were 21.62% and 40.54% respectively, significantly lower than that of normal control group ($P < 0.01$). The HSC proliferation rates of groups at the end concentrations 36, 18 and 9(g·L⁻¹) were 54.05%, 45.95% and 51.35% respectively, lower than that of control group ($P < 0.05$). When the end concentration was 4.5g·L⁻¹, the proliferation rate was 83.78%, which appeared no significant differences compared with control group. At the same concentrations of 18g·L⁻¹, the inhibitory effects of Yigan Decoction at 24h, 48h and 72h time point were observed, the effects were time-dependent, and reached a peak at 72h. Meanwhile, it was showed that the inducing effects of Yigan Decoction on HSC apoptosis were dose-dependent and time-dependent. The apoptosis index(AI) was detected by TUNEL. After Yigan Decoction had been incubated for 48h at the end concentration of 18g·L⁻¹, the AI (14.5±3.1)% was significantly higher than that of control group (4.3±1.3)% ($P < 0.01$). When visualized under transmission electron microscopy, some apoptotic stellate cells were found, i.e. dilated endoplasmic reticulum, irregular nuclei, chromatin condensation and heterochromatin ranked along inside of nuclear membrane. By flow cytometry detection, after HSC was treated with Yigan Decoction at different concentrations of 36, 18 and 9(g·L⁻¹) for 48 h, AI (%) were 13.3±3.2, 10.7±2.7 and 10.1±2.5 respectively, which were significantly higher than that of control group(4.1±1.9) ($P < 0.01$). At the same concentration of 18g·L⁻¹ for 24h, 48h and 72h, AI (%) were 9.3±1.8, 10.7±2.7 and 14.6±4.3 respectively, which were significantly higher than that of control group ($P < 0.01$).

CONCLUSION: Yigan Decoction could significantly inhibit HSC proliferation and increase the apoptosis index of HSC dose-dependently and time-dependently, which may be related to its mechanism of antifibrosis.

Yao XX, Tang YW, Yao DM, Xiu HM. Effects of Yigan Decoction on proliferation and apoptosis of hepatic stellate cells. *World J Gastroenterol* 2002;8(3):511-514

INTRODUCTION

As the mechanisms of hepatic fibrosis have been gradually clarified and thus, many attempts to treat hepatic fibrosis have been made recently. But up to date there is still no effective way to treat hepatic fibrosis^[1]. Recent insights^[2-11] into the molecular pathogenesis of hepatic fibrosis and the efficacy of TCM have provided hope for the foreground of successful therapy, such as compound 861^[12], Kangxianfang^[13], Fuzhenghuayu decoction^[14-16], Ganyanping^[17] etc. Yigan Decoction, which was designed in our lab, was used in clinical setting for nearly twenty years. Our clinical practice has revealed that it has a marked curative effect on treating chronic liver diseases^[18]. Hepatic sinusoidal cells such as the hepatic stellate cells (HSC), endothelial cells or Kupffer cells are deeply involved in hepatic fibrogenesis or fibrolysis. Recent studies have made their morphology and functions clear. A wealth of evidence now indicates that HSC is the key to produce fibrosis which served as the major source of fibrillar and nonfibrillar matrix proteins. Quiescent HSC synthesize low levels of matrix proteins, but as a result of injury, HSC could be proliferated and transformed to myofibroblast, a process termed activation^[4]. So to inhibit HSC activation and proliferation and induce apoptosis of the activated HSC is one of the most important strategies for preventing and curing liver fibrosis. HSC cultured in uncoated plastic plates *in vitro* spontaneously undergo activation and share the similar features of cell activation *in vivo*^[19]. This culture-induced activation has been extensively studied as a model of the activation secondary to liver fibrogenesis. In order to testify the action of Yigan Decoction on liver fibrosis and investigate its mechanism, the effects of Chinese herb Yigan Decoction on the proliferation and apoptosis of HSC *in vitro* were observed.

MATERIALS AND METHODS

Cell culture

HSC lines (CFSC) (established by Professor Greenwel) were provided by Southwest Hospital, Third Military Medical University. The phenotype was activated HSC^[20, 21]. Cells were cultured in RPMI1640 (Gibco) medium plus 100mL·L⁻¹ fetal calf serum, penicillin 1×10⁵U·L⁻¹ and streptomycin 100mg·L⁻¹, and kept in a controlled atmosphere (5% CO₂) incubator at 37°C.

Drug treatment

Yigan Decoction consists of Radix Salviae Miltiorrhizae, Radix Angelicae Sinensis, Radix Paeoniae Rubra and Hirudo, etc. The decoction was made by Hebei Institute of Gastroenterology, containing 0.72g of crude herbs in each milliliter. Exponentially growing cells were seeded in plates for 24h and treated with Yigan Decoction at

various concentrations (144, 72, 36, 18, 9 and $4.5\text{g}\cdot\text{L}^{-1}$) for 24h, 48h and 72h, respectively. The cells not treated with this drug served as control cells.

Dose-dependent effects of Yigan Decoction on cell proliferation

Colorimetric MTT assays^[23] were used to observe cell proliferation. HSC were incubated in 96 well plates. The concentration of cells was modulated to $1\times 10^8\cdot\text{L}^{-1}$. After cultured for 24h, Yigan Decoction was added in different concentrations such as 144, 72, 36, 18, 9 and $4.5\text{g}\cdot\text{L}^{-1}$ for 48h. Each group was arranged three duplicate wells. After the supernatant was extracted and 0.05% MTT solution 10 μL was added to all wells for 4h, DMSO 100 μL was added for coloration. After a few minutes at room temperature to ensure that all crystals were dissolved, the optic-metric density (OD) was read on ELISA reader at test wavelength of 570nm and referent wavelength of 630nm.

Time-dependent effects of Yigan Decoction on cell proliferation

The cultured cells were grown up to logarithmic growth phase, digested with $2.5\text{g}\cdot\text{L}^{-1}$ trypsin. The concentration of cells was modulated to $1\times 10^8\cdot\text{L}^{-1}$. HSC were incubated in 24 well plates. Each well was added with 1mL. After being cultured for 24h, Yigan Decoction (50 μL) was added into wells at the same end concentration of $18\text{g}\cdot\text{L}^{-1}$. Cell proliferation was observed at different times, i.e., 24h, 48h and 72h after the herb was treated, each was arranged three duplicate wells. The number of HSC was counted at the end of each time.

Apoptosis examined by TUNEL

In situ cell death detection kits were purchased from Boehringer Mannheim Company, Germany. The cells were adjusted to a density of 2×10^3 cells/ cm^2 , added to 24-well plates with cover glass-slides in 0.5mL each well. After being incubated with Yigan Decoction at the end concentration of $18\text{g}\cdot\text{L}^{-1}$ for 48h, the glass slides were taken out, rinsed, fixed and stained. The negative control with omission of TUNEL enzyme was designed according to the manufacturer's manual. The cells stained with dark brown nucleus were considered as positive cells. Ten optical fields, about 500-1000 cells were selected randomly and counted in each glass-slide under the high magnification ($\times 400$) microscope. Apoptosis Index (AI) = (apoptotic cells/ total cells) $\times 100\%$.

Apoptosis examined by transmission electron microscopy

HSC were treated with Yigan Decoction at the end concentration of $18\text{g}\cdot\text{L}^{-1}$ for 48h. Then the cells were centrifugated and fixed in glutaraldehyde for observation of transmission electron microscopy.

Apoptosis examined by flow cytometry

HSC were treated with Yigan Decoction at the end concentration of 36, 18 and $9\text{g}\cdot\text{L}^{-1}$ for 24h, 48h and 72h. Cells were digested by $2.5\text{g}\cdot\text{L}^{-1}$ trypsin, washed by PBS, fixed by cold ethanol at 4°C and dyed with PI (propidium iodide), and then were analyzed by flow cytometry.

Statistics

Results were expressed as mean \pm SD ($\bar{x}\pm s$). Differences between groups and differences over times were analyzed using analysis of variance and Newman-Keuls methods where appropriate. *P* values less than 0.05 were considered to be statistically significant.

RESULTS

Dose-dependent inhibitory effects of Yigan Decoction on cell proliferation

Yigan Decoction could significantly inhibit HSC proliferation dose-dependently compared with the control group (Table 1). The

inhibitory effects of groups at concentrations of 144 and $72\text{g}\cdot\text{L}^{-1}$ were stronger than those of groups at concentrations of 36, 18 and $9\text{g}\cdot\text{L}^{-1}$, and no obvious inhibitory effect was found at the herb concentration of $4.5\text{g}\cdot\text{L}^{-1}$.

Time-dependent inhibitory effects of Yigan Decoction on cell proliferation

At the end concentration of $18\text{g}\cdot\text{L}^{-1}$, HSC were significantly inhibited compared with control group. The number of cells was manually counted. The effect was time-dependent, and reached a peak at 72h ($P<0.01$) (Table 2).

Apoptosis of HSC induced by Yigan Decoction examined by TUNEL

Based on the above results that Yigan Decoction could inhibit HSC proliferation at concentrations of $9\text{--}144\text{g}\cdot\text{L}^{-1}$ from 24h to 72h, we selected the $18\text{g}\cdot\text{L}^{-1}$ of Yigan Decoction and 48h affecting period as experimental conditions so as to better compare with the results of the herb on HSC lines. After Yigan Decoction had been incubated for 48h, the AI $22.5\pm 7.1\%$ was significantly higher than that of control group $4.3\pm 1.3\%$ ($P<0.01$). Apoptotic cell is characterized by compaction of nuclear chromatin and condensation of cytoplasm. By TUNEL stain the most condensed cells demonstrated evidence of DNA fragmentation and were strongly stained (Figure 1, arrowed).

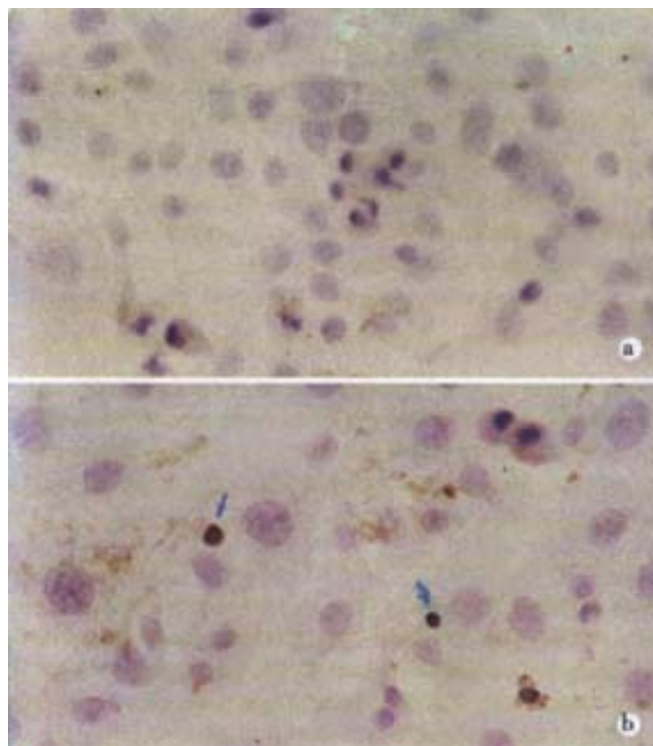


Figure 1 (A) Control HSC (TUNEL $\times 400$). (B) Apoptotic cell characterized by compaction of nuclear chromatin and condensation of cytoplasm (TUNEL $\times 400$). By TUNEL stain the most condensed cells demonstrated evidence of DNA fragmentation and were strongly staining (iu).

Apoptosis of HSC induced by Yigan Decoction examined by transmission electron microscopy

After 24~48h treatment of Yigan Decoction, we visualized under inverted microscopy. Small rounded cells were observed on the surface of the monolayer. These cells could be displaced by agitation of the tissue culture plate, demonstrating that they were very loosely adherent to the monolayer and that some were detached and floating in the culture supernatant (Figure 2). These features are compatible with HSC that have undergone programmed cell death or apoptosis^[24].

When visualized under transmission electron microscopy, the apoptotic HSC were found, i.e. dilated endoplasmic reticulum, irregular nuclei, chromatin condensation and heterochromatin ranked along inside of nuclear membrane. All of these features are characteristic of apoptosis and distinguish programmed cell death from necrosis (Figure 3).

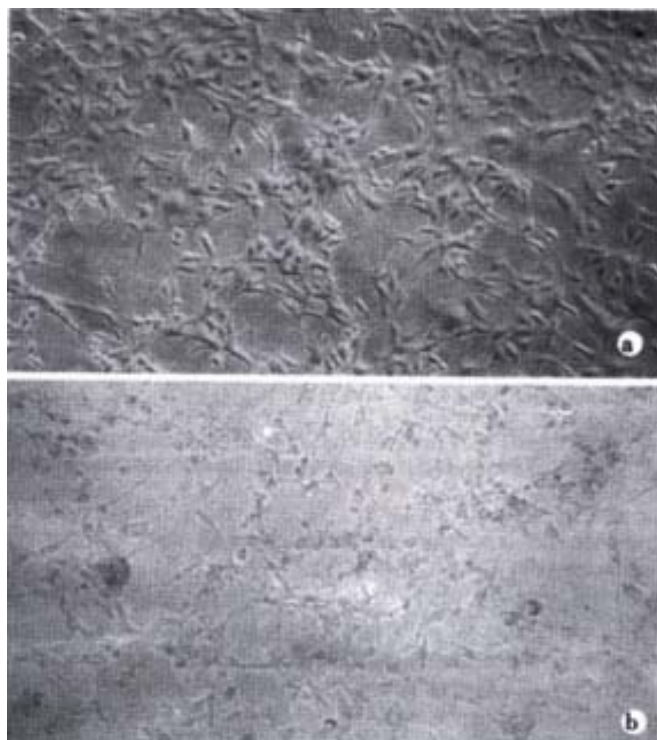


Figure 2 Morphological changes of HSC observed by light microscopy treated by Yigan Decoction. (A) Untreated cells ($\times 200$); (B) some HSC got round, detached and floating in the culture supernatant after exposure to $18\text{g}\cdot\text{L}^{-1}$ Yigan Decoction for 48h ($\times 100$).

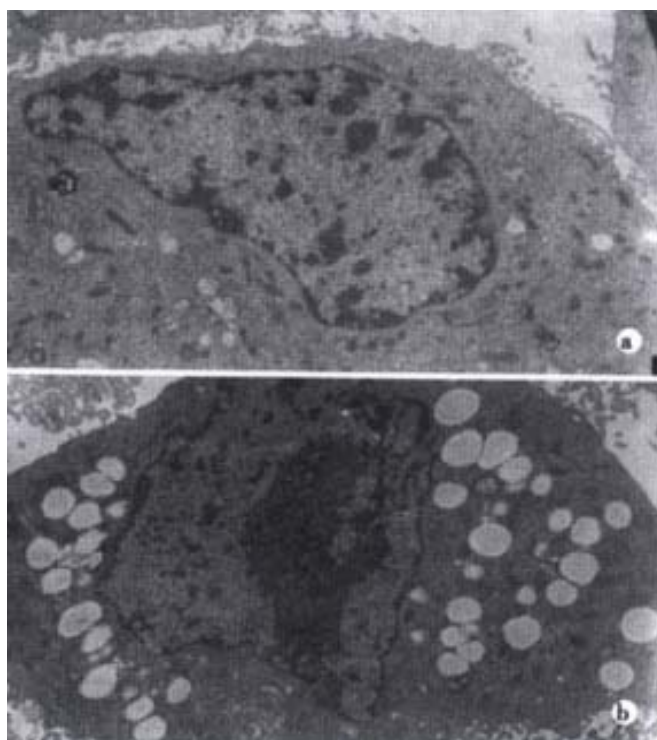


Figure 3 Ultrastructures of HSC with or without treatment with Yigan Decoction. Following 48h treatment of Yigan Decoction, dilated endoplasmic reticulum, irregular nuclei, chromatin condensation and heterochromatin ranked along inside of nuclear membrane could be found (A $5000\times$). Untreated cells (B $5000\times$).

Apoptosis examined by flow cytometry

After HSC were treated with Yigan Decoction at different concentrations of 36, 18 and $9(\text{g}\cdot\text{L}^{-1})$ for 48h, the apoptosis rate was significantly higher than that of control group ($P<0.01$) (Table 3). Our experiments showed that Yigan Decoction could increase the apoptosis rate dose-dependently and time-dependently compared with the control group. (Table 3 and 4, Figure 4).

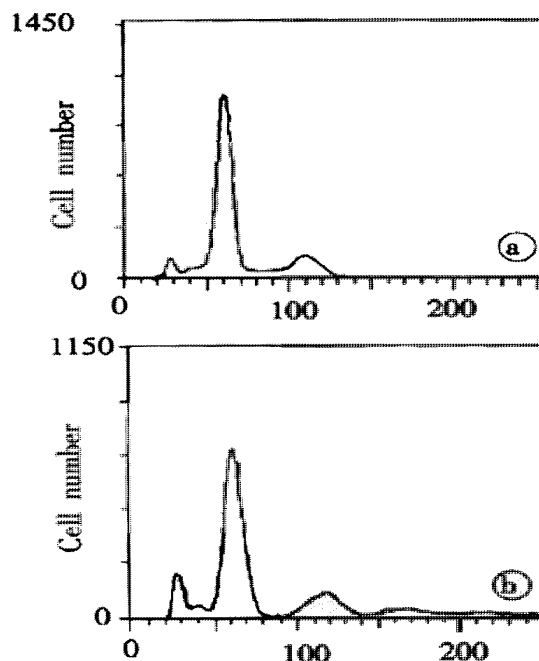


Figure 4 Flow cytometry changes. (A) Control group. (B) Yigan Decoction group.

Table 1 Effects of Yigan Decoction on HSC proliferation ($\bar{x}\pm s$)

Groups	Herb concentrations ($\text{g}\cdot\text{L}^{-1}$)	ODs	proliferation rates (%)
Yigan Decoction	144	0.08 ± 0.02^b	21.62
	72	0.15 ± 0.04^b	40.54
	36	0.20 ± 0.03^a	54.05
	18	0.17 ± 0.02^a	45.95
	9	0.19 ± 0.05^a	51.35
	4.5	0.31 ± 0.04	83.78
Control		0.37 ± 0.03	100

^a $P<0.05$, ^b $P<0.01$ vs control group.

Table 2 Effects of Yigan Decoction on HSC proliferation ($\times 10^3\cdot\text{L}^{-1}$) ($\bar{x}\pm s$)

Groups	24h	48h	72h
Control	1.440 ± 0.124	2.288 ± 0.178	2.335 ± 0.146
Yigan Decoction	1.203 ± 0.112	1.258 ± 0.098^b	1.359 ± 0.079^b

^b $P<0.01$ vs control group.

Table 3 Apoptosis indexes of Yigan Decoction on HSC ($\bar{x}\pm s$)

Groups	Herb concentrations ($\text{g}\cdot\text{L}^{-1}$)	apoptosis indexes (%)
Yigan Decoction	36	13.3 ± 3.2^b
	18	10.7 ± 2.7^b
	9	10.1 ± 2.5^b
Control		4.1 ± 1.9

^b $P<0.01$ vs control group.

Table 4 Time-dependent effects of Yigan Decoction on HSC apoptosis ($\bar{x}\pm s$)

Groups	24h	48h	72h
Control	4.5 ± 1.3	7.1 ± 1.9	8.0 ± 1.8
Yigan Decoction	9.3 ± 1.8^b	10.7 ± 2.7^b	14.6 ± 4.3^b

^b $P<0.01$ vs control group.

DISCUSSION

Recent studies have found clearly the key role of HSC in developing liver fibrosis. HSC could activate, proliferate and largely synthesize various components of extracellular matrix in chronic liver disease, that would lead to liver fibrosis^[22]. Studies suggest that HSC numbers are controlled by apoptosis in addition to proliferation during progressive fibrosis and particularly during recovery from fibrosis. The key event in the process of injury-fibrosis-recovery sequence is the loss of activated HSC mediated by apoptosis^[23]. Therefore to induce apoptosis of activated HSC is one of the most important therapeutic strategies for liver fibrosis. Recent evidence has demonstrated that a mechanism to eliminate activated HSC in culture and in animal models is inducing apoptosis. Interestingly, activated HSC are more sensitive to some mechanisms of apoptosis than quiescent HSC. Such a mechanism may serve in the future to eliminate the undesirable activated HSC without affecting their normal quiescent counterpart.

The CFSC used in present study is activated HSC. So it shared some features with activated HSC *in vivo* and could be used as a desirable cell model for the test of antifibrotic drugs. Although the desirable antifibrotic drugs have not been found up to now, some herbal decoctions have been reported to prevent fibrogenesis effectively, showing a good prospect of using Chinese herbs in treating chronic liver diseases^[24]. It was reported that Radix Salviae Miltiorrhizae (RSM) can inhibit fibroblast cells^[25]. RSM can prevent liver fibrosis if it is used for a long time^[26]. Large doses of RSM can activate collagenase and help reduce extracellular matrix. The level of P III P and laminin were decreased in patients with liver disease after treatment of RSM. Studies demonstrated that long-term treatment of RSM for 10-12wk can reduce portal vein, spleen diameters and blood flow, but the velocity of blood flow did not change^[27]. These results demonstrated the advantage of Chinese herbs in treating chronic hepatic diseases. Yigan Decoction, one of formally produced herbs, could prevent extracellular matrix production and deposit in CCl₄ induced rat liver fibrosis^[28], and improve fibrotic liver structure and liver function in patients with chronic hepatitis or cirrhosis^[18]. It is mainly composed of RSM, Radix Angelicae Sinensis (RAS), Radix Paeoniae Rubra and Hirudo, which have the actions of promoting blood circulation, removing blood stasis, shrinking the liver and spleen.

The present results suggest that Yigan Decoction could significantly inhibit HSC proliferation and increase the apoptosis rate of HSC dose-dependently and time-dependently compared with the control group ($P < 0.01$). After Yigan Decoction had been incubation for 48h, the apoptosis rate of HSC was 27.5% compared with 7.1% in the control group ($P < 0.01$). Our findings strongly suggest that inhibition of HSC proliferation and induction of HSC apoptosis may play an important role in the antifibrotic actions of Yigan Decoction. Our data may provide a new idea for the future development of therapeutic antifibrotic strategies by means of traditional Chinese medicine.

The antifibrotic effect of Yigan Decoction has been well proved by the results of experimental and clinical studies. However, Chinese herbs have very complicated components and their metabolisms are not well clarified yet. There's still a long way to go. With the ever-increasing in-depth studies about the pharmacodynamics, pharmacokinetics, reasonable combinations of drugs, the best preparation form and dosages of each herb and courses, Yigan Decoction is expected to be an effective antihepatofibrotic drug.

REFERENCES

- Brenner DA. Therapeutic strategy for liver fibrosis. *J Gastroenterol Hepatol* 1999; 14(Suppl.): A279-A280

- Wu CH. Fibrodynamics-elucidation of the mechanisms and sites of liver fibrogenesis. *World J Gastroenterol* 1999; 5: 388-390
- Liu CH, Hu YY, Wang XL, Liu P, Xu LM. Effect of salvianolic acid-A on NIH/3T3 fibroblast proliferation, collagen synthesis and gene expression. *World J Gastroenterol* 2000; 6: 361-364
- Friedman SL. The cellular basis of hepatic fibrosis. Mechanisms and treatment strategies. *N Engl J Med* 1993; 328: 1828-1835
- Liu SR, Gu HD, Li DG, Lu HM. A comparative study of fat storing cells and hepatocytes in collagen synthesis and collagen gene expression. *Xin Xiaohuabingxue Zazhi* 1997; 5: 761-762
- Gu SW, Luo KX, Zhang L, Wu AH, He HT, Weng JY. Relationship between ductile proliferation and liver fibrosis of chronic liver disease. *Shijie Huaren Xiaohua Zazhi* 1999; 7: 845-847
- Yan JC, Ma Y, Chen WB, Shun XH. Dynamic observation on liver fibrosis and cirrhosis of hepatitis B. *Huaren Xiaohua Zazhi* 1998; 6: 699-702
- Wang Y, Gao Y, Huang YQ, Yu JL, Fang SG. Gelatinase A proenzyme expression in the process of experimental liver fibrosis. *Shijie Huaren Xiaohua Zazhi* 2000; 8: 165-167
- Lu LG, Zeng MD, Li JQ, Qiu DK, Hua J, Fan ZP. Expression of intercellular adhesion molecular-1 by activated hepatic stellate cells. *Huaren Xiaohua Zazhi* 1998; 6: 567-569
- Wang X, Chen YX, Xu CF, Zhao GN, Huang YX, Wang QL. Relationship between tumor necrosis factor- α and liver fibrosis. *World J Gastroenterol* 1998; 4: 18
- Cheng ML, Wu YY, Huang KF, Luo TY, Ding YS, Lu YY, Liu RC, Wu J. Clinical study on the treatment of liver fibrosis due to hepatitis B by IFN- α 1 and traditional medicine preparation. *World J Gastroenterol* 1999; 5: 267-269
- You H, Wang BE, Wang TL, Ma XM, Zhang J. Proliferation and apoptosis of hepatic stellate cells and effects of compound 861 on liver fibrosis. *Zhonghua Ganzangbing Zazhi* 2000; 8: 78-80
- Wu JG, Li XY. Clinical studies of Kangxianfang in treating liver cirrhosis. *Xin Xiaohuabingxue Zazhi* 1997; 5: 303-304
- Hu YY, Liu C, Liu P, Gu HT, Ji G, Wang XL. Anti-fibrosis and anti-peroxidation of lipid effects of Fuzhenghuayu decoction on rat liver induced by CCl₄. *Xin Xiaohuabingxue Zazhi* 1997; 5: 485-486
- Gu HT, Hu YY, Xu LM, Liu P, Liu C. Pathological observation on effects of Fuzhenghuayu decoction on rat liver induced by CCl₄. *Zhongxiyi Jiehe Ganbing Zazhi* 1997; 7: 224-226
- Liu P, Liu C, Xu LM, Xue HM, Liu CH, Zhang ZQ. Effects of Fuzhenghuayu 319 recipe on liver fibrosis in chronic hepatitis B. *World J Gastroenterol* 1998; 4: 348-353
- Du LJ, Tang WX, Dan ZL, Zhang WY, Li SB. Protective effect of Ganyanping on CCl₄ induced liver fibrosis in rats. *Huaren Xiaohua Zazhi* 1998; 6: 21-22
- Yao XX, Fu YL, Li XL, Jia YP, An ZC, Zhang XZ. Therapeutic effect of Yigan Decoction on chronic hepatitis: a multi-center observation of 324 cases. *Hebei Yixueyuan Xuebao* 1989; 10: 231-233
- Friedman SL. Cellular sources of collagen and regulation of collagen production in liver. *Sem in Liver Dis* 1990; 10: 20-29
- Zhu YH, Hu DR. Establishment and application of hepatic stellate cells. *Shijie Huaren Xiaohua Zazhi* 1999; 7: 348-349
- Denizot F, Lang R. Rapid colorimetric assay for cell growth and survival. Modifications to the tetrazolium dye procedure giving improved sensitivity and reliability. *J Immunol Methods* 1986; 89: 271-277
- Bissell DM, Friedman SL, Maher JJ, Roll FJ. Connective tissue biology and hepatic fibrosis: Report of a conference. *Hepatology* 1990; 11: 488-498
- Iredale JP, Benyon RC, Pickering J, McCullen M, Northrop M, Pawley S, Hovell C, Arthur MJ. Mechanisms of spontaneous resolution of rat liver fibrosis. *J Clin Invest* 1998; 102: 538-549
- Jia KM. Pay more attention to the study of the treatment of hepatitis B. *Zhonghua Neike Zazhi* 2000; 39: 797-798
- Yao XX, Li XT, Li YW, Zhang XY. Clinical and experimental study of Radix Salviae Miltiorrhizae and other Chinese herbs of blood-activating and stasis-eliminating effects on hemodynamics of portal hypertension. *Zhonghua Xiaohua Zazhi* 1998; 18: 24-27
- Yao XX, Cui DL, Sun YF, Li XT. Clinical and experimental study of effect of Radix Salviae Miltiorrhizae and other blood-activating and stasis-eliminating Chinese herbs on hemodynamics of portal hypertension. *World J Gastroenterol* 1998; 4: 439-442
- Li XT, Bai WY, Wang HM, Yao XX. Study of effects of Radix salviae miltiorrhizae on portal hypertension in experimental cirrhotic dogs. *Xin Xiaohuabingxue Zazhi* 1997; 5: 421-422
- Yao XX, Tang YW, Yao DM, Xiu HM. Effect of Yigan Decoction on the expression of type I, III collagen proteins in experimental hepatic fibrosis in rats. *Shijie Huaren Xiaohua Zazhi* 2001; 9: 263-267

• BASIC RESEARCH •

Salvia miltiorrhiza monomer IH764-3 induces hepatic stellate cell apoptosis via caspase-3 activation

Xiao-Lan Zhang, Li Liu, Hui-Qing Jiang

Xiao-Lan Zhang, Li Liu, Hui-Qing Jiang, Department of Gastroenterology, The Second Hospital of Hebei Medical University, Shijiazhuang 050000 Hebei Province, China

Supported by Fund of the Scientific and Technical Department of Hebei Province, No. 01276134

Correspondence to: Professor Hui-Qing Jiang, Department of Gastroenterology, The Second Hospital of Hebei Medical University, Shijiazhuang 050000, Hebei Province, China. huiqingj@heinfo.net
Telephone: +86-311-7046901 Ext. 6513

Received 2001-12-20 Accepted 2002-01-23

Abstract

AIM: To investigate the effects of IH764-3 on HSC apoptosis, and the expression of caspase-3 protein in HSC apoptotic process.

METHODS: HSCs were cultured in medium with different IH764-3 doses ($10\mu\text{g}\cdot\text{mL}^{-1}$, $20\mu\text{g}\cdot\text{mL}^{-1}$, $30\mu\text{g}\cdot\text{mL}^{-1}$, $40\mu\text{g}\cdot\text{mL}^{-1}$) and without IH764-3, and HSC proliferation was quantitatively measured by ^3H -thymidine incorporation. The morphological changes of HSCs were observed with transmission electron microscope after exposure to the dose of $40\mu\text{g}\cdot\text{mL}^{-1}$ of IH764-3 for 48 hr. The apoptosis rates were detected by annexin V/PI and TdT-mediated dUTP nick end labeling (TUNEL). The expression of caspase-3 protein was determined by flow cytometry.

RESULTS: (1) HSC proliferation rates induced with different IH764-3 doses ($10\mu\text{g}\cdot\text{mL}^{-1}$, $20\mu\text{g}\cdot\text{mL}^{-1}$, $30\mu\text{g}\cdot\text{mL}^{-1}$, $40\mu\text{g}\cdot\text{mL}^{-1}$) were significantly reduced compared with that of the control group ($P<0.01$). (2) With the doses above, IH764-3 dose-dependently produced HSC apoptosis rates of 6.7% (9.4%), 9.3% (21.6%), 15.1% (27.2%) and 19.0% (28.4%) respectively, by annexin V and PI-labeled flow cytometry assay (or TUNEL), while it was only 2.3% (6.7%) in the control. (3) The expression of caspase-3 protein in IH764-3 groups was significantly higher than that of the control ($P<0.05$).

CONCLUSION: Within the dose range used in present study, IH764-3 can inhibit HSC proliferation, as well as enhance HSC apoptosis. Furthermore, IH764-3 can significantly increase the caspase-3 protein expression.

Zhang XL, Liu L, Jiang HQ. Salvia miltiorrhiza monomer IH764-3 induces hepatic stellate cell apoptosis via caspase-3 activation. *World J Gastroenterol* 2002;8(3):515-519

INTRODUCTION

Hepatic fibrosis occurs as a result of the accumulation of excess extracellular matrix (ECM) around the hepatic sinus and portal vein^[1-19]. Activated hepatic stellate cells (HSCs) are the main source of ECM in the process of hepatic fibrosis. Therefore, HSCs play a central role in the hepatic fibrogenesis^[20-34]. Either proliferation or apoptosis of HSCs or both may affect the population of HSCs^[35-39]. Recent studies have shown that apoptosis is the main process to eliminate the activated HSCs during the resolution of hepatic fibrosis^[40-42]. To induce the apoptosis of HSCs, therefore, might be an

important strategy for the hepatic fibrosis therapy^[43-45].

Chinese herbal medicine Salviae Miltiorrhiza, which can improve circulatory status and eliminate stasis, exhibits a series of important pharmacological effects on anti-inflammation, antioxidation, and inhibiting the platelet aggregation^[46-49]. IH764-3, extracted from Salviae Miltiorrhiza, preserves all of these beneficial effects. Furthermore, in recent studies, it has been documented that IH764-3 could play an important role in anti-fibrosis, inhibiting the proliferation of HSCs and the synthesis of collagens^[47,50]. However, there are few reports so far concerns about the effects of IH764-3 on HSC apoptosis and its mechanisms. In present study, we therefore used annexin-V/PI double labeling flow cytometry, TUNEL and transmission electron microscope to examine the effects of IH764-3 on HSC apoptosis. Meanwhile, the effects of IH764-3 on the expression of caspase-3 protein during HSC apoptosis were also observed.

MATERIALS AND METHODS

Materials

HSC line CFSC was established and kindly provided by Prof. Greenwel in America, which phenotype was activated HSCs, and derived from the CCl₄-induced cirrhotic rat^[51]. RPMI-1640 medium was purchased from GIBCO Co. Fetal calf serum was from Four Season Green Biological Co, Hangzhou, China. IH764-3 was kindly provided by Prof. Chun-Zheng Yang from Hematopathy Institute, Chinese Academy of Medical Science. ^3H -TdR was from Isotope Institute, Chinese Academy of Atomic Energy. Annexin-V cell apoptosis assay kit was purchased from Baosai Biological Technology Co, Beijing. TUNEL assay kit was from Boster Biological Engineering Co, Wuhan, China. Caspase-3 assay kit was from CLONTECH Co, USA. Goat anti-mouse FITC-IgG was the product of Microorganism Institute, Academy of Military Medical Sciences, China. Other reagents were analytically pure.

Methods

Cell culture The HSCs were thawed and plated in RPMI-1640 medium containing $100\text{mL}\cdot\text{L}^{-1}$ fetal calf serum, $100\text{KU}\cdot\text{L}^{-1}$ penicillin, $100\text{mg}\cdot\text{L}^{-1}$ streptomycin, $4\text{mmol}\cdot\text{L}^{-1}$ L-glutamine and $0.1\text{mmol}\cdot\text{L}^{-1}$ HEPES. Cells were kept in culture at 37°C in a $50\text{mL}\cdot\text{L}^{-1}$ CO₂ atmosphere and 100% humidity. The HSCs were digested with 0.25% trypsin and subcultured from one to three when the cells proliferated into a full monolayer. The first change of the culture medium was made about 24 hr after subculturing, and then the cells were subcultured again about 72 hr. Experiments were carried out while the cells were in exponential growth phase. Cells were plated in 25cm^2 plastic flasks at a density of $2\times 10^5\cdot\text{L}^{-1}$ or onto 96-well plates at a density of $5\times 10^6\cdot\text{L}^{-1}$. When the cells were nearly 100% confluent, they were continued to incubate for another 12 hr in serum-free RPMI-1640 culture medium. At that time most of the cells were in G₀ phase, they were divided into different groups. The dose-response studies were performed using different doses of IH764-3 ($10\mu\text{g}\cdot\text{mL}^{-1}$, $20\mu\text{g}\cdot\text{mL}^{-1}$, $30\mu\text{g}\cdot\text{mL}^{-1}$ and $40\mu\text{g}\cdot\text{mL}^{-1}$) and lasted for 12-48 hr, while the time-response studies were carried out at the timepoints of 12, 24, 48 and 72 hr with the dose of $30\mu\text{g}\cdot\text{mL}^{-1}$ of IH764-3.

Inhibition of cell proliferation assays HSCs were plated to triplicate wells in a 96-well plate with the concentration of $5 \times 10^3 \cdot \text{mL}^{-1}$. When the cells were nearly 100% confluent, they were cultured in serum-free medium for 12 hr. Then the medium was replaced with fresh medium containing 2% fetal calf serum and different IH764-3 doses, $1.11 \times 10^4 \text{ Bq } ^3\text{H-Thymidine}$ was added to each well. After 24 hr of incubation, HSCs were collected onto filter membrane and baked 1 hr at 100°C . The radioactivity (cpm) was determined with the beta-scintillation counter (Beckman). The inhibition of HSC proliferation was expressed by inhibitory rate, which was calculated as: inhibition rate = [(cpm of control group - cpm of IH764-3 group) / cpm of control group] $\times 100\%$.

Apoptosis detection The following methods were used to detect apoptosis: (1) Transmission electron microscope: After exposure to the dose of $40 \mu\text{g} \cdot \text{mL}^{-1}$ of IH764-3 for 48 hr, cells were trypsinized, collected, washed with PBS and centrifuged at 1200g for 10 min. The cell pellet was fixed in 4% glutaral for 2 hr, 1% osmium acid for 1 hr and dehydrated gradually, then stained by uranium acetic acid and lead citromalic acid. The cells were observed with transmission electron microscope and the ultrastructural changes were recorded. (2) Annexin-V/PI labeling to detect apoptotic rate^[52]: Briefly, the trypsinized HSCs were washed twice with PBS, stained with annexin-V (10L) and PI (5 μL) for 10 min, and the apoptotic rate was quantified by FACSCalibur flow cytometry (Becton Dickinson Inc.) at 488 nm wavelength. More than 1×10^4 cells were detected, and the results were analyzed with Modfit LT software. The stained cells were divided into three subgroups: The cells in V⁻/PI⁻ subgroup were survived cells which membrane was intact, The cells in V⁺/PI⁻ subgroup were apoptotic cells which membrane intact but with phosphatidylserine translocation; The cells in V⁺/PI⁺ subgroup were necrotic cells which membrane was impairment and with phosphatidylserine translocation. (3) Determination of apoptosis by TUNEL method: After trypsinization and collection, cells were fixed with 4% paraformaldehyde for 30 min. Apoptosis was assayed by TUNEL method. Briefly, the cells were incubated with proteinase K (5 $\mu\text{L} \cdot \text{mL}^{-1}$) at 37°C for 5 min, labeled by TdT and digoxin-d-UTP at 4°C in a humidified chamber to stay overnight, anti-digoxin antibody was added. After being incubated at 37°C for 30 min, the cells were stained with diaminobenzidine (DAB). Apoptotic cells presented as brownish stain in the nucleus, but we should pay special attention to distinguish the stained DNA fragments in cytoplasm due to some nuclear leakage. At least 500 cells were examined and the rate of apoptotic cells was calculated as the percentage of stained-cell per 100 cells.

Determination of Caspase-3 expression Trypsinized cells were washed in PBS, and fixed at 4°C in 70% ethanol overnight. Fixed cells were precipitated and washed in PBS. Cells (6×10^5) were suspended in 0.5 mL permeable buffer diluted by PBS, and subsequently incubated with anti-Caspase-3 antibody, FITC-labeled goat anti-rat IgG antibody (1:20)^[53], then cells were washed with PBS, assayed by flow cytometer. The relative quantity of the protein was expressed by Fluorescence index (FI).

Statistical analysis

Data were expressed as $\bar{x} \pm s$. One-way analysis of variance was used for multiple comparisons, and Newman-Keuls test and χ^2 test were used for intra-groups comparisons. *P* values less than 0.05 were considered to be statistically significant.

RESULTS

Effect of IH764-3 on proliferation of HSCs

Compared with the control group, IH764-3 had a significant inhibitory effect on $^3\text{H-TdR}$ incorporation; the inhibition was dose-dependent (Table 1).

Table 1 The effect of IH764-3 on $^3\text{H-TdR}$ incorporation ($\bar{x} \pm s$)

Dosage ($\mu\text{g} \cdot \text{mL}^{-1}$)	Cpm	Inhibitory rate (%)
0	19749 \pm 7222	
1	018339 \pm 5344	7.1
2	014147 \pm 1850 ^b	28.4
3	09125 \pm 916 ^b	53.8
4	05313 \pm 426 ^b	73.1

^b*P* < 0.01 vs control

Morphological changes

The shape of cells incubated with $30 \mu\text{g} \cdot \text{mL}^{-1}$ or $40 \mu\text{g} \cdot \text{mL}^{-1}$ of IH764-3 for 6 hr changed from stellate or shuttle to spherical, and the intercellular space was increased. 12 hr later, the cells began to detach from the plate and it is more remarkable at 24 hr. With the transmission electron microscope, the decreased volume, condensed chromatin and decreased nucleocytoplasmic ratio of apoptotic cell were noted. Some cells showed typical apoptotic changes: the pyknosis and margination of the nuclear chromatin. Moreover, the nuclei fragment, annular or crescent body, cytoplasm vacuoles and swollen Mitochondria were also observed. Some cells were karyolysis and turn into the specific apoptotic bodies (Figure 1).

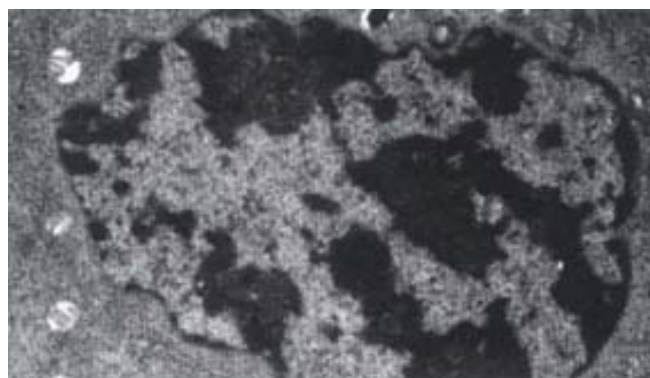


Figure 1 The apoptotic cells in $40 \mu\text{g} \cdot \text{mL}^{-1}$ IH764-3 for 48 hr (TEM 10000 \times) Apoptotic cells became small, the chromatin condensed

Annexin-V/PI combined labeling flow cytometry

The rate of apoptosis was both dose-dependent and time-dependent (Table 2A, 2B). For the $40 \mu\text{g} \cdot \text{mL}^{-1}$ group at 24 hr and $30 \mu\text{g} \cdot \text{mL}^{-1}$ group at 48-72 hr, the apoptotic cells presented worse progressive changes, most of the cells were V⁺/PI⁺ subclass, namely necrosis. The necrotic rate was 21.0-31.3%. Figure 2A, 2B.

Table 2A Apoptotic rates of HSCs exposed IH764-3 with different doses by Annexin-V/PI (%)

Time	doses	0 $\mu\text{g} \cdot \text{mL}^{-1}$	10 $\mu\text{g} \cdot \text{mL}^{-1}$	20 $\mu\text{g} \cdot \text{mL}^{-1}$	30 $\mu\text{g} \cdot \text{mL}^{-1}$	40 $\mu\text{g} \cdot \text{mL}^{-1}$
12hr		0.3	2.2	3.7	6.7	15.1
48hr		2.3	6.7	9.3	15.1	19.7

Table 2B Percentage of apoptotic HSCs exposed to IH764-3 ($30 \mu\text{g} \cdot \text{mL}^{-1}$) at different timepoints by Annexin-V/PI (%)

Time	0hr	12hr	24hr	48hr	72hr
Apoptosis rate	0.3	6.7	10.3	15.1	19.6

Detection of HSC apoptosis by TUNEL

After exposure of HSCs to different dose of IH764-3, the apoptotic indexes in experimental group by TUNEL assay at 48 hr were 9.4%

$\pm 2.6\%$ ($10\mu\text{g}\cdot\text{mL}^{-1}$), $21.6\pm 5.5\%$ ($20\mu\text{g}\cdot\text{mL}^{-1}$), $27.2\pm 6.2\%$ ($30\mu\text{g}\cdot\text{mL}^{-1}$) and $28.4\pm 6.5\%$ ($40\mu\text{g}\cdot\text{mL}^{-1}$), respectively, which were significantly higher than that in control group ($6.7\pm 0.6\%$, $P<0.01$) (Figure 3).

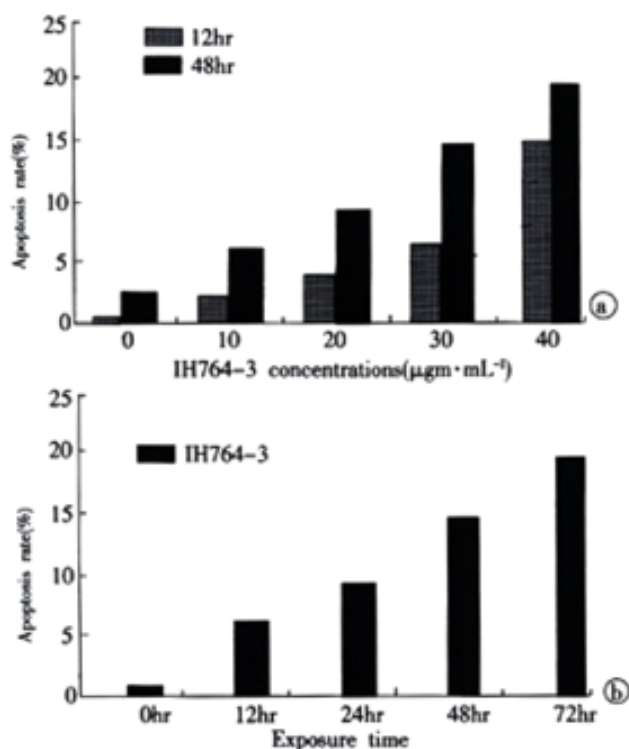


Figure 2 apoptosis rates of HSCs exposed to IH764-3. (A) dose-dependent; (B) time-dependent with the concentration of $30\mu\text{g}\cdot\text{mL}^{-1}$ of IH764-3.

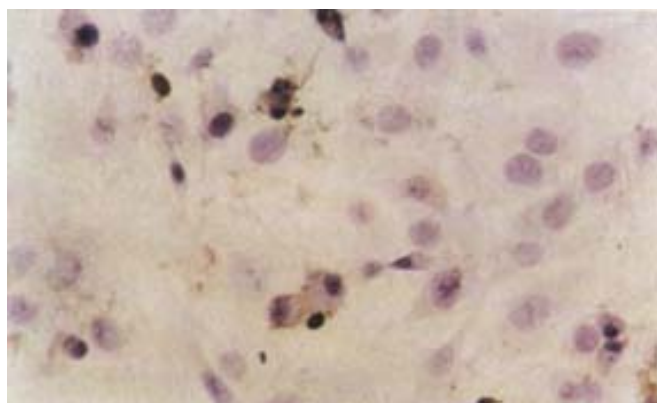


Figure 3 The apoptotic cells in $30\mu\text{g}\cdot\text{mL}^{-1}$ IH764-3 for 48hr(TUNEL10×40)

IH764-3 induced caspase-3 protein Expression in HSCs

With the given doses, IH764-3 could increase Caspase-3 protein expression dose-dependently. There was also a positive relationship between Caspase-3 protein expression and apoptosis rate (Table 3).

Table 3 Fluorescence index of caspase-3 protein in HSCs ($\bar{x}\pm s$)

Dosage ($\mu\text{g}\cdot\text{mL}^{-1}$)	Caspase-3	P value
0	175.6 ± 22.5	
10	215.1 ± 26.9	<0.01
20	231.6 ± 28.6	<0.01
30	304.7 ± 30.7	<0.01
40	338.9 ± 32.1	<0.01

DISCUSSION

The dynamic balance between the cell proliferation and apoptosis plays a key role in growth, development and maintenance of physiological functions of individuals. Once the balance is broken, varieties of pathological and pathophysiological changes will take place. HSCs are the major cells that produce ECM components and proliferated significantly in hepatic fibrosis^[36]. It has been considered that apoptosis may play at least a partial role in reducing HSC population and decreasing the production of ECM components in hepatic fibrosis, thus triggering the process of HSC apoptosis is perhaps an important strategy to resolve the hepatic fibrosis^[45,54]. IH764-3, an extract of *Salviae Miltiorrhiza*, has been proved to be an effective agent for anti-hepatic fibrosis in animal model. However, up to the present, whether its anti-fibrotic mechanism was related to the induction of HSC apoptosis or not has not been elucidated yet.

Cell apoptosis, which is different from necrosis, is an initiative cell death process that activates endogenous DNA endonuclease, with the morphological characteristics of pyknosis and the chromatin margination to become lump or crescent bodies. Then cytoplasm condenses and cell shrinks, which finally forms apoptotic bodies. However, the cell membrane is integrated and the organelles keep intact. In present study, a great deal of typical apoptotic cells was found on plates treated with IH764-3, which demonstrated that IH764-3 did trigger the HSC apoptosis.

Apoptosis is a dynamic developing process that can be divided into early phase, metaphase and late phase. It has been reported that flow cytometry is the most sensitive method to examine apoptosis^[52,53]. In early apoptotic phase, the translocation of phosphatidylserine, which has high affinity to Annexin-V, from the inner leaflet to the outer layer of the plasma membrane, could be easily recognized by Annexin-V labeling method. Moreover, when combining with PI stain, it could also distinguish from necrotic cells. In this study, we found that IH764-3 could dose-dependently induce apoptosis at 12 and 48 hr timepoints, the apoptotic rate was 2.2% in $10\mu\text{g}\cdot\text{mL}^{-1}$ group and 15.1% in $40\mu\text{g}\cdot\text{mL}^{-1}$ group. In $30\mu\text{g}\cdot\text{mL}^{-1}$ group, the apoptotic rate was time-dependent. In $40\mu\text{g}\cdot\text{mL}^{-1}$ group at 24hr and $30\mu\text{g}\cdot\text{mL}^{-1}$ group at 48-72hr, the apoptotic cells presented progressive worse advanced changes, most of the cells became necrotic, the necrotic rate reached 21.0-31.3%. Similar changes were also observed with transmission electron microscope. Thus it could be concluded that low doses of IH764-3 mainly induced apoptosis, while in high doses, it could not only induce apoptosis, but also necrosis.

The remarkable biochemical characteristic of apoptosis is the genome DNA fragmentation. This is because the activated endogenous endonuclease can degrade the connected DNA between nucleosomes into 180-200bp oligonucleotide fragments. With terminal deoxynucleotidyl transferase, utilizing exogenous biotin-labeled-free nucleotides, the free nucleotides in 3' terminal can be catalyzed to get together in a non template-dependent manner, making the break nicks of DNA is labeled. Therefore, we used TUNEL method as another way to prove the apoptosis further. The results showed that apoptosis indexes in IH764-3 groups were higher than that of the control. Furthermore, the indexes were dose-dependent in IH764-3 groups. All of the above demonstrated that IH764-3 could induce HSC apoptosis in time and dose-dependent manner, but the signal transduction process remains unclear.

Caspase-3, a key proteinase in apoptosis pathway, is one of the proteases in cysteine aspartic acid specific proteases family, and is also called as cysteine proteases P32. It splits the peptide bond at asparagic residue of specific motif sequence in substrate protein. The activated caspase-3 may cause apoptosis^[55] and results in what we saw the apoptotic signs under microscope. Caspase-3 can split inhibitory caspase activated deoxyribonuclease (ICAD) into CAD^[56,57], which

degrades DNA in nucleus.

To examine the possible mechanism of HSC apoptosis induced by IH764-3, we observed the expression of caspase-3 protein. The results showed that IH764-3 from $10\mu\text{g}\cdot\text{mL}^{-1}$ to $40\mu\text{g}\cdot\text{mL}^{-1}$ could increase the expression of caspase-3 protein. The more the apoptosis developed, the more the caspase-3 protein expressed. So we deduced that HSC apoptosis induced by IH764-3 was mediated by caspase-3 activation. Increased expression of caspase-3 protein was possibly one of the mechanisms in HSC apoptosis induced by IH764-3. Any reagents that increase caspase-3 protein expression might have a potential possibility to become new drugs to treat patients with hepatic fibrosis^[58].

ACKNOWLEDGEMENTS

The authors wish to thank Professor Greenwel for his kindly providing the cell line and Professor Chun-zheng Yang for presenting IH764-3. We also thank Dr Hong-Qun Liu and Dr Shuang Chen for their critical reading of the manuscript.

REFERENCES

- Jiang HQ, Zhang XL. Progress in the study of pathogenesis in hepatic fibrosis. *Shijie Huaren Xiaohua Zazhi* 2000;8:687-689
- Wu CH. Fibrodynamics-elucidation of the mechanisms and sites of liver fibrogenesis. *World J Gastroenterol* 1999;5:388-390
- Wang JY, Zhang QS, Guo JS, Hu MY. Effects of glycyrrhetic acid on collagen metabolism of hepatic stellate cells at different stages of liver fibrosis in rats. *World J Gastroenterol* 2001;7:115-119
- Du WD, Zhang YE, Zhai WR, Zhou XM. Dynamic changes of type α_1 , III and IV collagen synthesis and distribution of collagen-producing cells in carbon tetrachloride-induced rat liver fibrosis. *World J Gastroenterol* 1999;5:397-403
- Friedman SL. Molecular mechanisms of hepatic fibrosis and principles of therapy. *J Gastroenterol* 1997;32:424-430
- Shapiro SD, Senior RM. Matrix metalloproteinase: matrix degradation and more. *Am J Respir Cell Mol Biol* 1999;20:1100-1102
- Massova I, Kotra LP, Fridman R, Mobashery S. Matrix metalloproteinases: structure, evolution, and diversification. *FASEB J* 1998;12:1075-1095
- Benyon RC, Hovell CJ, Gaca MD, Jones EH, Iredale JP, Arthur MJ. Progelatinase A is produced and activated by rat hepatic stellate cells and promotes their proliferation. *Hepatology* 1999;30:977-986
- Knittel T, Mehde M, Kobold D, Saile B, Dinter C, Ramadori G. Expression patterns of matrix metalloproteinases and their inhibitors in parenchymal and non-parenchymal cells of rat liver: regulation by TNF- α and TGF- β 1. *J Hepatol* 1999;30:48-60
- Bai WY, Yao XX, Feng LY. The study status of liver fibrosis. *Shijie Huaren Xiaohua Zazhi* 2000;8:1267-1268
- Bahr MJ, Vincent KJ, Arthur MJ, Fowler AV, Smart DE, Wright MC, Clark IM, Benyon RC, Iredale JP, Mann DA. Control of the tissue inhibitor of metalloproteinases-1 promoter in culture-activated rat hepatic stellate cells: regulation by activator protein-1 DNA binding proteins. *Hepatology* 1999;29:839-848
- Liu HL, Li XH, Wang DY, Yang SP. Matrix metalloproteinase-2 and tissue inhibitor of metalloproteinase-1 expression in fibrotic rat liver. *World J Gastroenterol* 2000;6:881-884
- Greenwel P, Dominguez-Rosales JA, Mavi G, Rivas-Estilla AM, Rojkind M. Hydrogen peroxide: a link between acetaldehyde-elicited α_1 (I) collagen gene up-regulation and oxidative stress in mouse hepatic stellate cells. *Hepatology* 2000;31:109-116
- Friedman SL. Cytokines and fibrogenesis. *Semin Liver Dis* 1999;19:129-140
- Weng HL, Cai WM, Liu RH. Animal experiment and clinical study of effect of gamma-interferon on hepatic fibrosis. *World J Gastroenterol* 2001;7:42-48
- Yao XX. Diagnosis and treatment of hepatic fibrosis. *Shijie Huaren Xiaohua Zazhi* 2000;8:681-689
- Xiang DD, Li QF, Wang YM, Wang YF. The effect of vitamin E emulsion on procollagen III and matrix metalloproteinases-1 mRNA in hepatic stellate cells. *Shijie Huaren Xiaohua Zazhi* 1999;7:1085
- Svegliati-Baroni G, Ridolfi F, Di Sario A, Saccomanno S, Bendia E, Benedetti A, Greenwel P. Intracellular signaling pathways involved in acetaldehyde-induced collagen and fibronectin gene expression in human hepatic stellate cells. *Hepatology* 2001;33:1130-1140
- Chen PS, Zhan WR, Zhang YE, Zhang JS. The effect of hypoxia on collagen and matrix metalloproteinase hepatic stellate cells. *Shijie Huaren Xiaohua Zazhi* 2000;8:586-587
- Pinzani M, Marra F, Carloni V. Signal transduction in hepatic stellate cells. *Liver* 1998;18:2-13
- Huang GC, Zhang JS. Signal transduction in activated hepatic stellate cells. *Shijie Huaren Xiaohua Zazhi* 2001;9:1056-1060
- Carloni V, Pinzani M, Giusti S, Romanelli RG, Parola M, Bellomo G, Failli P, Hamilton AD, Sebt SM, Laffi G, Gentilini P. Tyrosine phosphorylation of focal adhesion kinase by PDGF is dependent on ras in human hepatic stellate cells. *Hepatology* 2000;31:131-140
- Zhu YH, Hu DR. The establishment and application of hepatic stellate cell lines. *Shijie Huaren Xiaohua Zazhi* 1999;7:348-349
- Zhu YH, Hu DR, Nie QH, Liu GD, Tan ZX. Study on activation and c-fos, c-jun expression of *in vitro* cultured human hepatic stellate cells. *Shijie Huaren Xiaohua Zazhi* 2000;8:299-302
- Huang GC, Zhang JS, Zhang YE. Effects of retinoic acid on proliferation, phenotype and expression of cyclin-dependent kinase inhibitors in TGF- β 1-stimulated rat hepatic stellate cells. *World J Gastroenterol* 2000;6:819-823
- Potter JJ, Rennie-Tankersley L, Anania FA, Mezey E. A transient increase in c-myc precedes the transdifferentiation of hepatic stellate cells to myofibroblast-like cells. *Liver* 1999;19:135-144
- Xiang DD, Wei YL, Li QF. Molecular mechanism of transforming growth factor β 1 on Ito cell. *Shijie Huaren Xiaohua Zazhi* 1999;7:980-981
- Lu LG, Zeng MD, Li JQ, Qiu DK, Hua J, Fan ZP. Expression of intercellular adhesion molecule-1 and hepatic stellate cell activation. *Shijie Huaren Xiaohua Zazhi* 1998;6:567-569
- Tang YW, Yao XX. The regulated role of Hepatocarcinoma cell in hepatic stellate cell activation. *Shijie Huaren Xiaohua Zazhi* 2001;9:202-204
- Huang X, Li DG, Wang ZR, Wei HS, Cheng JL, Zhan YT, Zhou X, Xu QF, Li X, Lu HM. Expression changes of activin A in the development of hepatic fibrosis. *World J Gastroenterol* 2001;7:37-41
- Liu C, Liu P, Liu CH, Zhu XQ, Ji G. Effects of Fuzhenghuayu decoction on collagen synthesis of cultured hepatic stellate cells, hepatocytes and fibroblasts in rats. *World J Gastroenterol* 1998;4:548-549
- Wei HS, Li HM, Li DG, Zhan YT, Wang ZR, Huang X, Cheng JL, Xu QF. The regulatory role of AT 1 receptor on activated HSCs in hepatic fibrogenesis: effects of RAS inhibitors on hepatic fibrosis induced by CCl $_4$. *World J Gastroenterol* 2000;6:824-828
- Vasilidou V, Lee J, Pappa A, Petersen DR. Involvement of p65 in the regulation of NF-kappa B in rat hepatic stellate cells during cirrhosis. *Biochem Biophys Res Commun* 2000;273:546-550
- Kato R, Kamiya S, Ueki M, Yajima H, Ishii T, Nakamura H, Katayama T, Fukui F. The fibronectin-derived antitumor peptides suppress the myofibroblastic conversion of rat hepatic stellate cells. *Exp Cell Res* 2001;265:54-63
- Lu P, Luo HS, Yu BP. Apoptosis and liver diseases. *Shijie Huaren Xiaohua Zazhi* 2000;8:1157-1159
- Gressner AM. The cell biology of liver fibrogenesis-an imbalance of proliferation, growth arrest and apoptosis of myofibroblasts. *Cell Tissue Res* 1998;292:447-452
- Liu WB, Wang JY. NF- κ B and apoptosis of hepatic stellate cells. *Shijie Huaren Xiaohua Zazhi* 2001;9:1054-1055
- Lang A, Schoonhoven R, Tuvia S, Brenner DA, Rippe RA. Nuclear factor kappa B in proliferation, activation, and apoptosis in rat hepatic stellate cells. *J Hepatol* 2000;33:49-58
- Saile B, Matthes N, Knittel T, Ramadori G. Transforming growth factor β and tumor necrosis factor β inhibit both apoptosis and proliferation of activated rat hepatic stellate cells. *Hepatology* 1999;30:196-202
- Gong W, Pecci A, Roth S, Lahme B, Beato M, Gressner AM. Transformation-dependent susceptibility of rat hepatic stellate cells to apoptosis induced by soluble Fas ligand. *Hepatology* 1998;28:492-502
- Iwamoto H, Sakai H, Tada S, Nakamura M, Nawata H. Induction of apoptosis in rat hepatic stellate cells by disruption of integrin-mediated cell adhesion. *J Lab Clin Med* 1999;134:83-89
- Iredale JP, Benyon RC, Pickering J, McCullen M, Northrop M, Pawley S, Hovell C, Arthur MJ. Mechanisms of spontaneous resolution of rat liver fibrosis. Hepatic stellate cell apoptosis and reduced hepatic expression of metalloproteinase inhibitors. *J Clin Invest* 1998;102:538-549
- Fischer R, Schmitt M, Bode JG, Haussinger D. Expression of the peripheral-type benzodiazepine receptor and apoptosis induction in hepatic stellate cells. *Gastroenterology* 2001;120:1212-1226
- Issa R, Williams E, Trim N, Kendall T, Arthur MJ, Reichen J, Benyon RC, Iredale JP. Apoptosis of hepatic stellate cells: involvement in resolution of biliary fibrosis and regulation by soluble growth factors. *Gut* 2001;48:548-557
- Cales P. Apoptosis and liver fibrosis: antifibrotic strategies. *Biomed Pharmacother* 1998;52:259-263
- Yang CZ, Liu RL, Liu J. The role of IH764-3 in prolyl hydroxyl of

- collagen biosynthesis. *Zhongguo Yixue Kexueyuan Xuebao* 1993;15:364-368
- 47 Wasser S, Ho JM, Ang HK, Tan CE. Salvia Miltiorrhiza reduces experimentally induced hepatic fibrosis in rats. *J Hepatol* 1998;29:760-771
- 48 Liu CH, Hu YY, Wang XL, Liu P, Xu LM. Effects of salvianolic acid-A on NIH/3T3 fibroblast proliferation, collagen synthesis and gene expression. *World J Gastroenterol* 2000;6:361-364
- 49 Cheng ML, Liu SD. The basic study and clinical research on hepatic fibrosis. 1st ed. Beijing: People's Medical Publishing House 1996:228-283
- 50 Chen YX, Li S, Fan LY, Kong XT, Yang CZ, Yu BL. The experiment study of effect on hepatic fibrosis by Salvia Miltiorrhiza monomer IH764-3. *Zhonghua Yixue Zazhi* 1998;78:636-637
- 51 Greenwel P, Schwartz M, Rossas M, Peyrol S, Grimaud JA, Rojkind M. Characterization of fat-storing cell lines derived from normal and CCl₄-cirrhotic livers. *Lab Invest* 1991;65:644-653
- 52 Boersma AW, Nooter K, Oostrum RG, Stoter G. Quantification of apoptotic cells with fluorescein isothiocyanate-labeled annexin V in chinese hamster ovary cell cultures treated with cisplatin. *Cytometry* 1996;24:123-130
- 53 Zuo LF. Flow cytometry and biomedicine. *Shenyang: Liaoning Sci Technol Publ House* 1996;213-267
- 54 Iredale JR. Hepatic Stellate Cell Behavior during Resolution of Liver Injury. *Semin Liver Dis* 2001;21:427-436
- 55 Nagata S. Apoptosis by death factor. *Cell* 1997;88:355-365
- 56 Enari M, Talianian RV, Wong WW, Nagata S. Sequential activation of ICE-like and CPP32-like proteases during Fas-mediated apoptosis. *Nature* 1996;380:723-726
- 57 Sakahira H, Enari M, Nagata S. Cleavage of CAD inhibitor in CAD activation and DNA degradation during apoptosis. *Nature* 1998;391:96-99
- 58 Wright MC, Issa R, Smart DE, Trim N, Murray GI, Primrose JN, Arthur MJP, Iredale JP, Mann DA. Gliotoxin Stimulates the Apoptosis of Human and Rat Hepatic Stellate Cells and Enhances the Resolution of Liver Fibrosis in Rats. *Gastroenterology* 2001;121:685-698

Edited by Zhu L

• BASIC RESEARCH •

Effect of Maotai liquor in inducing metallothioneins and on hepatic stellate cells

Ming-Liang Cheng, Jun Wu, Hai-Qin Wang, Lie-Ming Xue, Ying-Zhi Tan, Liu Ping, Cheng-Xiu Li, Neng-Hui Huang, Yu-Mei Yao, Lan-Zheng Ren, Lan Ye, Ling Li, Mei-Lin Jia

Ming-Liang Cheng, Jun Wu, Hai-Qin Wang, Yu-Mei Yao, Department of Infectious Diseases, Affiliated Hospital, Guiyang Medical College, Guiyang 550004, Guizhou Province, China
Lie-Ming Xue, Ying-Zhi Tan, Liu Ping, Shanghai University of Traditional Chinese Medicine, Shanghai 200020, China
Cheng-Xiu Li, Neng-Hui Huang, Lan-Zheng Ren, Lan Ye, Ling Li, Mei-Lin Jia, Department of pharmacology, Guiyang Medical College, Guiyang 550004, Guizhou Province, China
Supported by The primary sciences and technology project of Guizhou province, No. 19992015
Correspondence to: Ming-Liang Cheng, Professor Department of Infectious Diseases, Affiliated Hospital, Guiyang Medical College, Guiyang 550004, Guizhou Province, China. chengml@21cn.com
Telephone: +86-851-6782199(H), +86-851-6855119 Ext. 3263 (O)
Received 2002-05-02 Accepted 2002-05-25

Abstract

AIM: To explore the possible mechanism why drinking Maotai liquor dose not cause hepatic fibrosis.

METHODS: After being fed with Maotai for 56 days consecutively, the male SD rats were decolated for detecting the biological indexes, and the livers were harvested to examine the liver indexes and the level of hepatic metallothioneins (MT). Hepatic stellate cells (HSC) proliferation and collagen generation were also observed.

RESULTS: Hepatic MT contents were $216.0\text{ng}\cdot\text{g}^{-1}\pm 10.8\text{ng}\cdot\text{g}^{-1}$ in the rats of Maotai group and $10.0\text{ng}\cdot\text{g}^{-1}\pm 2.8\text{ng}\cdot\text{g}^{-1}$ in the normal control group, which was increased obviously in Maotai group ($P<0.05$). In the rats with grade CCL₂ poisoning induced by Maotai, hepatic MT content was $304.8\text{ng}\cdot\text{g}^{-1}\pm 12.1\text{ng}\cdot\text{g}^{-1}$ whereas in the controls with grade CCL₄ poisoning, it was $126.4\text{ng}\cdot\text{g}^{-1}\pm 4.8\text{ng}\cdot\text{g}^{-1}$ ($P<0.05$). MDA was $102.0\text{nmol}\cdot\text{g}^{-1}\pm 3.4\text{nmol}\cdot\text{g}^{-1}$ in Maotai group and $150.8\text{nmol}\cdot\text{g}^{-1}\pm 6.7\text{nmol}\cdot\text{g}^{-1}$ in the control group ($P<0.05$). When both of the groups were suffering from grade CCL₄ poisoning, hepatic MT contents was negatively correlated with MDA ($r=-0.8023$, $n=20$, $P<0.01$). The 570nmA values of each tube with HSC regeneration at concentrations of 0, 10, 50, 100, and 200g·L⁻¹ of Maotai were 0.818, 0.742, 0.736, 0.72, 0.682, and 0.604, respectively. From the concentration of 10g·L⁻¹, Maotai began to show obvious inhibitory effects against HSC, and the inhibition was concentration-dependent ($P<0.05$, $P<0.01$). Type I collagen contents in HSC were 61.4, 59.9, 50.1, 49.2, 48.7, 34.4μg·g⁻¹ at concentrations of 0, 10, 50, 100, and 200g·L⁻¹ of Maotai. At the concentration of 100-200g·L⁻¹, Maotai had obvious inhibitory effect against the secretion of type I collagen ($P<0.05$). Gene expression analysis was conducted on cells with Maotai concentrations of 0, 50, 100g·L⁻¹ respectively and the ash values of β-actin gene expression were 0.88, 0.74, and 0.59, respectively, suggesting that at the concentration of 100g·L⁻¹, Maotai could obviously inhibit gene expression of type I procollagen ($P<0.05$), but the effect was not obvious at the concentration of 50g·L⁻¹ ($P>0.05$). At the concentration of

10g·L⁻¹, HSC growth *in vitro* inhibition rates were 16.4 ± 2.3 in Maotai group and -8.4 ± 2.3 in the control group ($P<0.05$).

CONCLUSION: Maotai liquor can increase metallothioneins in the liver and inhibit the activation of HSC and the synthesis of collagen in many aspects, which might be the mechanism that Maotai liquor interferes in the hepatic fibrosis.

Cheng ML, Wu J, Wang HQ, Xue LM, Tan YZ, Ping L, Li CX, Huang NH, Yao YM, Ren LZ, Ye L, Li L, Jia ML. Effect of Maotai liquor in inducing metallothioneins and on hepatic stellate cells. *World J Gastroenterol* 2002; 8(3):520-523

INTRODUCTION

Long term alcohol abusing may result in alcoholic liver diseases, and the volume and duration of drinking has a close relationship with alcoholic liver diseases^[1-5]. According to recent studies, the main cause of alcoholic hepatic injury^[6-12] is due to acetaldehyde and hydroxy free radicals oxidized from alcohol which can injure the hepatocytes and activate the lipid peroxidation. The necrosis, inflammation, alcohol, its metabolites and lipid peroxidation are all able to activate Kupffer cells to secrete many cytokines which in turn activate hepatic stellate cells to produce various components of extracellular matrix (ECM). When a large amount of ECM is deposited in the liver, it will lead to hepatic fibrosis^[13-18]. Now many studies have demonstrated that metallothionein (MT) has the cytoprotective effect of clearing away the oxygen-derived free radicals^[19-24]. It is found^[25,26] that alcohol can induce the increase of metallothionein in rats liver, but the mechanism has not been elucidated. MT is endogenous anti-injury substance and plays a role in the defence of stress reaction^[27]. Maotai liquor has its unique brewing technique, at the same time, there are multiple microorganisms in the special geographical situations which are able to absorb abundant amino acids, vitamins and many essential microelements^[28]. It was reported by Li Xinyan *et al* that drinking Maotai liquor 150g for ten years daily did not result in significant damage to the liver, moreover, it could help protect one's health. Epidemiological study showed that no one died of liver disease in those workers who had drunk Maotai liquor for about 30 years. No obvious hepatic fibrosis or cirrhosis of liver was found in the epidemiological study of 99 workers who had a long history of drinking, or in the pathological examination of their liver needle biopsies nor were they seen in rats fed with Maotai liquor for a successive 56 days^[28]. In order to explore the effect of Maotai liquor on the liver, we observed its effect on hepatic stellate cell proliferation *in vitro*, collagen generation, gene expression and growth of human hepatic stellate cells, and the effect of Maotai liquor in inducing metallothioneins in the rats liver and the relationship between it and CCL₄ hepatic injury were also studied in order to demonstrate the possible mechanism in the inhibition on the hepatic fibrosis.

MATERIALS AND METHODS

Materials

Male SD rats, weighing (300±20)g, were purchased from the

Experimental Animal Center of the Third Military Medical University, Chongqing, China. Maotai liquor (530 ± 2) g·L⁻¹, was produced by Guizhou Maotai Distillery with bar code 6902952880026 provided by Section 4 of Guizhou Oil & Foodstuff Export and Import Company. MT standard was provided by Dr. Jie Liu in National Institute of Environmental Health Sciences, U. S. A. 3-[4,5-dimethylthiazol]-2,5-diphenyltetrazolium bromide. MTT were bought from Sigma Co., U. S. A.; trypsin was purchased from Difco. U. S. A and; 199 culture medium and MEM culture medium without calcium are the products of Gibco Co., U. S. A; newborn bovine serum (NBS) was produced by Shanghai Huamei Co.; type I rat tail collagen standard (diluted slowly with Na²-2CO₃/NaHCO₃ to 10 -200ng·L⁻¹) and rabbit anti-rat type I collagen antibody (diluted 1:500 with 0.01mol·L⁻¹ PBS) were products of Cambiolem Co.; horseradish peroxidase marker labeled goat anti-rabbit antibody (IgG-HRP, diluted 1:1000 with PBS containing 100ml·L⁻¹ NBS) was purchased from Hua Mei Company; Total protein determination agent (dcproteinassag) was the product of Biorad Co., U. S. A.; RT-PCR reaction agent and PCR marker were purchased from Promega Co.; diethylpyrocarbonate, guanidine sulfocyanate, saturated mixture of phenol and chloroform, and agarose were bought from Shanghai Sangon Co. Freezing High-speed Centrifuge (1.0R, 22R), CO₂ incubator and ultra low temperature freezer were purchased from German Heraeus Co.; inverted microscope was produced by Japanese Olympus Co.; thermostat water bath, thermostat water bath vibrator were produced by Shanghai Medical Equipment Factory; Labsystems Multiskan MS Enzyme Marker Device, was produced in Finland; Danbury CT ultrasonic membrane breaker was the product of Sonicsmaterials Co.; 90mm culture plate, 60mm culture plate, 6-well, 24-well, and 96-well culture plate were the products of Danish Nunc Co.; Beck Wallac 1410 Liquid Scintillation Counter was the product of Beckman Co. U. S. A; Watson-Marlow 101U Constant current pump was produced in U. S. A.

Effect of maotai liquor on liver MT of rats

Forty SD male rats were divided into two groups averagely. 20 rats were fed with Maotai liquor at 2mL·kg⁻¹ diluted 1:1 by distilled water once everyday for 56 days. The other 20 rats in the control group were fed with saline at the same volume. After all rats had been fed for the last time, 10 rats of each group were given mixture of CCl₄ and olive oil in a volume ratio of 1:1 at 2.5mL·kg⁻¹. All rats were sacrificed after the last feed to get blood for testing biological indexes, to calculate liver indexes by liver quantity, and to determine the content of MT in the liver by saturation method of Cd- hemoglobin, and the lipid peroxidation product of aldehyde measured by the method of thiobarbiturate.

Isolation and culture of hepatic stellate cells (HSC)

HSC were isolated by in situ perfusion. The test of cell proliferation was done by MTT. When monolayer HSC appeared in the 96-well culture plate, they were cultured in the medium containing Maotai liquor with different concentration of 1-400mg·L⁻¹ and 50g·L⁻¹ NBS for 18 hours, then 20μL MTT (5g·L⁻¹) was added in each well and continued the culture for 4 hours. After that, suspension was removed and the plate was aired, then 100μL acid isopropanol with 0.05mol·L⁻¹ HCl was added to each well, little black crystals were dissolved by agitating which formed the steady purple solution. The absorbance (A) in each well was determined by ELSIA at the wave-length of 570nm. There were 4 well in each sample. When the subculturing HSC grew into full monolayer in the 24-well culture plate, then they were cultured in the medium containing Maotai liquor with different concentration from 1mg·L⁻¹ to 400mg·L⁻¹ and 50g·L⁻¹ NBS for 24 hours.

Determination of type I collagen and total protein

After the culture was ended, it was centrifugated at 450×g at 4°C for 20 minutes. Both the suspension and cell layer were collected separately. The collected cells were dissolved by 0.2mol·L⁻¹ NaOH 0.5ml in each well and washed with 0.5ml double distilled water. Ultrasonic membrane-breaking was done for 10s at 40°C. Type I collagen in the suspension was determined by ELISA (the enzyme labelling plate was coated with type I collagen standard and samples at different concentration were kept overnight at 4°C; then IgG-HRP was used for incubation after they bound to type I collagen antibody; pyrocatechol oxidation was used for staining, and value A was obtained at 492nm wavelength by Labsystem ELISA equipment, which automatically calculated the standard curve and contents of each specimen.). Total protein in the cell layer was determined by DC protein assay kit.

Semiquantitative RT-PCR

Total RNA was isolated from HSC by phenol-chloroform extraction and isopropanol precipitation. The primer of procollagenβ1(I) was synthesized, purified and evaluated by Shanghai Sangon Company (See Table 1). One μg of total RNA was reversely transcribed according to the instructions of the RT-PCR Kit at 48°C for 45min. The PCR mixture contained 50pmol·L⁻¹ primer of procollagen β1[I] or GAPDH, 1μL 10mmol·L⁻¹ dNTPs, 2μL 25mmol·L⁻¹ MgSO₄, 5 units AMV reverse transcriptase, 5 units Tfl DNA polymerase and 10mL AMV/Tfl buffer. The PCR conditions included an initial denaturation-2min at 94°C, 30 cycles consisting of (a) 30s denaturation at 94°C;(b)1 min primer annealing at 60°C; (c) 2min elongation at 38°C; and one final step of 7min at 68°C. The PCR product or DNA marker mixed with 5μL loading buffer were electrophoresed on a 1.5% agarose gel, visualized by UV and quantified densitometrically. Procollagenβ1[I], pre-albumin, or hydroxyproline expression was calculated by determining the ratio of Procollagen α1[I], relative to β-actin mRNA.

Table 1 Primer sequence and expected PCR product length

Primer designation	Sequence	Product length
α1(I)upstream	CACCCTCAAGAGCCTGAGTC	253bp
α1(I)downstream	GTT CGGGCTGATGTACCAGT	
β-actin upstream	ACATCTGCTGGAAGGTGGAC	163bp
β-actin downstream	GGTACCACCATGTACCCAGG	

The effect of Maotai liquor on human HSC

80000 human HSC cells were inoculated in each well in the 96-well plate, and they were cultured in the DMEM medium with 100mL·L⁻¹ FBS at 37°C in a humidified atmosphere containing 5% CO₂ for 24 hours. Then they were continuously cultured in the DMEM medium with 20mL·L⁻¹ FBS for 24hours. At last they were cultured in the medium containing different concentration of Maotai liquor (Maotai liquor was diluted to 0.5g·L⁻¹, 1g·L⁻¹, 5g·L⁻¹, 10g·L⁻¹, 50g·L⁻¹ by DMEM medium with 20mL·L⁻¹ FBS or alcohol). Cells cultured in the DMEM medium with 20mL·L⁻¹ FBS was used as the control. After they were cultured for 20 hours, 20μL MTT (5g·L⁻¹) was added in each well and the culture continued for 4 hours more. Then the medium was removed, 100μL acid isopropanol with 0.05mol·L⁻¹ HCl was added in each well, after little black crystals were dissolved, value A was obtained at 570nm wavelength by Labsystem ELISA equipment and the inhibiting rate of cell proliferation was calculated.

Statistics analysis

Data were analyzed by *t* test and *q* test.

RESULTS

Effect of Maotai liquor on rats liver MT content

Maotai liquor could induce the MT in rats liver to increase to 22 times of its original level (See Table 2). It is thought that lipid peroxidation of cell membrane and the intracellular accumulation of Ca^{2+} are the important links of hepatocellular damage. In the control group, MDA in the liver was obviously increased after they were intoxicated by CCl_4 , merely Maotai liquor did not influence MDA in rats' liver. MT in rats fed with Maotai liquor when intoxicated by CCl_4 was increased obviously more than those rats they were not fed with Maotai liquor, but MDA was decreased. There was a negative relationship between MT and MDA in rats liver intoxicated by CCl_4 in the control and trial group ($r=-0.8023$, $n=20$, $P<0.01$).

Table 2 The effect of Maotai liquor on MT and MDA in rats liver ($n=10, \bar{x} \pm s$)

Group	MT($\text{ng} \cdot \text{g}^{-1}$)	MDA($\text{ng} \cdot \text{g}^{-1}$)
Control group	10.0 \pm 2.8	60.2 \pm 3.1
Maotai liquor group	216.0 \pm 10.8 ^b	60.1 \pm 2.4
CCl_4 Group	126.4 \pm 4.8 ^b	150.8 \pm 6.7 ^b
CCl_4 + Maotai liquor group	304.8 \pm 12.1 ^{bd}	102.0 \pm 3.44 ^{bd}

^b $P<0.01$, vs control group; ^d $P<0.01$, vs CCl_4 group (analysis of variance and q test)

Effect of Maotai liquor on rats' HSC

We normally obtained $(3-5) \times 10^7$ HSC from one rat. Lipid droplets in the primary HSC were obvious, but during the course of culture, lipid droplets decreased. And as they were passaged, HSC became extended, and looked like myofibroblasts. Each concentration of Maotai liquor had no effect on the shape of HSC. The absorbance (A) at 570nm of HSC in the medium with 0mg·L⁻¹, 10mg·L⁻¹, 50mg·L⁻¹, 100mg·L⁻¹ and 200mg·L⁻¹ Maotia liquor were 0.818, 0.742, 0.736, 0.72, 0.682 and 0.604, respectively. From the concentration of 10g·L⁻¹, Maotai liquor had obvious inhibiting effect on the proliferation of HSC, and the effect was enhanced with the increase of the concentration of Maotai liquor ($P<0.05$, $P<0.01$). The content of type I collagen of HSC in the medium with 0mg·L⁻¹, 10mg·L⁻¹, 50mg·L⁻¹, 100mg·L⁻¹ and 200mg·L⁻¹ Maotia liquor were 61.4 $\mu\text{g} \cdot \text{g}^{-1}$, 59.9 $\mu\text{g} \cdot \text{g}^{-1}$, 49.2 $\mu\text{g} \cdot \text{g}^{-1}$, 50.1 $\mu\text{g} \cdot \text{g}^{-1}$, 48.7 $\mu\text{g} \cdot \text{g}^{-1}$ and 34.4 $\mu\text{g} \cdot \text{g}^{-1}$, respectively. The 100-200g·L⁻¹ Maotai liquor had obvious inhibiting effect on the secretion of type I collagen ($P<0.05$). The analysis of gene expression of HSC in the 0mg·L⁻¹, 50mg·L⁻¹ and 100mg·L⁻¹ Maotia liquor group showed that the relative density of β -actin ($n=3$) analyzed by computer were 0.88, 0.74 and 0.59, respectively. The result showed that 100g·L⁻¹ Maotia liquor could significantly inhibit the gene expression of type I procollagen ($P<0.05$), but 50g·L⁻¹ Maotia liquor did not have such effect ($P>0.05$).

Table 3 The effect of Maotai liquor on HSC of human ($n=3$, $\bar{x} \pm s$)

Group	Inhibiting Rate of HSC
Alcohol group (10g·L ⁻¹)	-8.4 \pm 2.3
Maotai liquor group (0.5g·L ⁻¹)	-4.52 \pm 0.3
Maotai liquor group (1g·L ⁻¹)	12.4 \pm 10.4 ^b
Maotai liquor group (5g·L ⁻¹)	17.4 \pm 1.6 ^b
Maotai liquor group (10g·L ⁻¹)	16.4 \pm 2.3 ^b

^b $P<0.01$, vs alcohol group

Effect of Maotai liquor on the growth of HSC (See Table 3)

There were three experiment groups in our study: blank control group, control group and trial group. First alcohol was diluted to 530

g·L⁻¹ (the same concentration as Maotai liquor) and then it was dispensed to different concentrations which was the same as Maotai liquor. We used 0.5g·L⁻¹, 1g·L⁻¹, 5g·L⁻¹ and 10g·L⁻¹ Maotai liquor to study the different inhibiting effect on HSC. Our result showed that there was a significant difference between the 10g·L⁻¹ alcohol group and 10g·L⁻¹ Maotai group ($P<0.01$). That was Maotai liquor had a significant inhibiting effect on the proliferation of HSC, but alcohol did not have such effect.

DISCUSSION

MT is a low molecular weight metal-binding protein with rich cysteine existing widely in the biosphere and can be induced *in vivo* by many factors^[29-32]. MT is also a non-enzyme protein which has bioactive functions of binding heavy metals, clearing free radicals, anti-oxidation and cytoprotection. It is now the most powerful bioactive substance which can remove free radicals. In recent years, a lot of research studies show that MT can protect hepatic cells from injury and be helpful in repairing hepatocytes without inducing hepatic fibrosis^[33-38]. Induced by Maotai liquor, the increased MT in rats' liver was able to decrease the lipid peroxidation product of MDA in the liver intoxicated by CCl_4 . Our result showed that there was a negative correlation between MT and MDA in the liver and it proved that Maotai liquor was able to induce MT to antagonize the effect poisoning by CCl_4 . It may be one of the possible mechanisms in explaining why long term drinking proper volume of Maotai would not cause hepatic fibrosis or cirrhosis.

Hepatic fibrosis is an important pathologic process resulted from many chronic liver diseases and may process to liver cirrhosis. It is also the key point that many chronic liver diseases are hard to cure completely. Many investigations showed that the activation of HSC is the key point in the pathological process of hepatic fibrosis. HSC was activated by many pathological factors so that alterations in the phenotype and function of HSC happened. HSC was highly proliferated and secreted a large amount of extracellular matrix deposited in the liver which would result in hepatic fibrosis. Collagen was the most important component in the extracellular matrix^[46-48]. The degree of increase of collagen was type I>type III>type IV. The cell proliferation and the enhanced generation of collagen were the main characteristics of activation of HSC. [³H]thymidine incorporation was able to reflect the cell division and proliferation. In the inhibiting experiments of different concentration of Maotai liquor in both HSC from rats and HSC from human beings showed that Maotai liquor had a concentration-dependent inhibiting effect on the proliferation of HSC. The generation of collagen was that first the collagen gene was transcribed and then translated into procollagen and the product secreted in the extracellular matrix. Our experiment showed that Maotai liquor had inhibiting effect on the expression of collagen gene and the secretion of collagen protein, but 10g·L⁻¹ alcohol had no such inhibiting effect. All those showed that Maotai liquor could inhibit the activation of HSC in many links. The inhibiting effect of Maotai liquor in the activation of HSC and the generation of collagen may be the possible reasons why Maotai liquor can interfere with the process of hepatic fibrosis.

REFERENCES

- 1 Tang TH. Recent studies of alcoholic liver diseases. *Shijie Huaren Xiaohua Zazhi* 2000;8:56
- 2 Lin H, Lu M, Zhang YX, Wang BY, Fu BY. Induction of a rat model of alcoholic liver diseases. *Shijie Huaren Xiaohua Zazhi* 2001;9:24-28
- 3 Wu J, Liu RC, Li J, Wang WL, Hu L, Yang QZ, Liang YD, Lu YY, Cheng ML, Ding YS. To study the risk factors of hepatic cirrhosis in viral hepatitis and hepatic fibrosis. *Cina Public Health* 1999;15:394
- 4 Wu J, Cheng ML, Ding YS, Liu RC, Li J, Wang WL, Hu L. Five years follow-up survey of risk factor of virus hepatic cirrhosis. *Shijie Huaren Xiaohua Zazhi* 2000;8:1365-1367
- 5 Wei L, Tao QM. Interactions between alcohol and hepatic C. *Shijie*

- Huaren Xiaohua Zazhi 1998;6: 539-541
- 6 Sun YN. Recent studies in pathogenesis of alcoholic liver diseases. *GuowaiYiyao. Xiaohuaxi Jibing Fengece* 1999;19:97-101
- 7 Bo AH, Tian CS, Xue GP, Du JH, Xu YL. Morphology of immune and alcoholic liver diseases in rats. *Shijie Huaren Xiaohua Zazhi* 2001;9:157-160
- 8 Lu XY. Mechanism of free radicals on liver injury induced by ethanol. *Xin xiaohuabingxue Zazhi* 1997;5: 200-202
- 9 Fan JG, Zeng MD, Wang GL. Pathogenesis of fatty liver. *Shijie Huaren Xiaohua Zazhi* 1999;7:5-7
- 10 Anania FA, Womack L, Jiang M, Saxena NK. Aldehydes potentiate alpha(2)(I) collagen gene activity by JNK in hepatic stellate cells. *Free Radic Biol Med* 2001;15:30:846-857
- 11 Ruoyu Ni, Maria Anna Leo, Zhao JB, Charles S. Toxicity of β -carotene and its exacerbation by acetaldehyde in HepG2 cells. *Alcohol and Alcoholism* 2001; 36: 281-285
- 12 Zima T, Fialova L, Mestek O, Janebova M, Crkovska J, Malbohan I, Stipek S, Mikulikova L, Popov P. Oxidative stress, metabolism of ethanol and alcohol-related diseases. *J Biomed Sci* 2001;8:59-70
- 13 Fan JG, Zeng MD, Hong J, Li JQ, Qiu DK. Effects of free unsaturated fatty acids on proliferation of L-02 and HLF cell lines and synthesis of extracellular matrix. *Shijie Huaren Xiaohua Zazhi* 1998;6:502-6504
- 14 Lu LG, Zeng MD, Li JQ, Fan JG, Hua J, Fan ZP, Dai N, Qiu DK. Effect of arachidonic acid and linoleic acid on proliferation of rat hepatic stellate cells. *Shijie Huaren Xiaohua Zazhi* 1999; 7:10-12
- 15 Wu J, Zern MA. Hepatic stellate cells: a target for the treatment of liver fibrosis. *J Gastroenterol* 2000;35:665-672
- 16 Zeng MD. Fatty liver New challenge in domain of liver disease. *Zhonghua Ganzhangbing Zazhi* 2000; 8: 69
- 17 Wang Q, ren GX, Qi Z, Li ML, Song X. Evaluation of serological assay for the detection of liver fibrosis in the patients with liver diseases caused by alcohol. *Huaren Xiaohua Zazhi* 1998;6: 364-365
- 18 Lü XH, Xie YH, Fu BY, Liu CR, Wang BY. Dynamic expression of tissue inhibitor of metalloproteinase 1 in alcoholic liver disease in rats. *Shijie Huaren Xiaohua Zazhi* 2001;9:29-33
- 19 Qiu BS, Wang Y, Hu ML, Xu LY. Study on Prevention of ZnMT against membrane damage induced by MeHg. *Guangdong Weiliang Yuansu Kexue* 1999; 6: 15-181006-446X
- 20 himura N, Miyabara Y, Suzuki JS, Sato M, Aoki Y, Satoh M, Yonemoto J, Tohyama C. Induction of metallothionein in the livers of female Sprague-Dawley rats treated with 2,3,7,8-tetrachlorodibenzo-p-dioxin. *Life Sci* 2001;69:1291-1303
- 21 Park JD, Liu Y, Klaassen CD. Protective effect of metallothionein against the toxicity of cadmium and other metals(I). *Toxicology* 2001; 163:93-100
- 22 Wright J, George S, Martinez-Lara E, Carpena E, Kindt M. Levels of cellular glutathione and metallothionein affect the toxicity of oxidative stress in an established carp cell line. *Mar Environ Res* 2000;50: 503-508
- 23 Zaroogian G, Jackim E. In vivo metallothionein and glutathione status in an acute response to cadmium in Mercenaria brown cells. *Comp Biochem Physiol C Toxicol Pharmacol* 2000;127:251-261
- 24 Fabisiak JP, Pearce LL, Borisenko GG, Tyhurina YY, Tyurin VA, Razzack J, Lazo JS, Pitt BR, Kagan VE. Bifunctional anti/prooxidant potential of metallothionein: redox signaling of copper binding and release. *Antioxid Redox Signal* 1999;1:349-364
- 25 Zhou J, Cheng S. Metallothionein and Medicine. *Shengli Kexue Jinzhan* 1995;26:29
- 26 Cheng YY, Wang DL, Jiang YG, Gu JF, Wang YY. Effect of stress on the levels of metallothionein and mineral elements in Rats. *Yingyang Xuebao* 1996;18: 317-321
- 27 Tang CS, Li ZP, Su JY. Metallothionein is an endogenous protection factor against cell damage. *Beijing Yikedaxue Xuebao* 1989;21:108
- 28 Xiao Y. Preliminary explanation of the mechanism which the long-term drinking of Guizhou maotai will not induce liver fibrosis. *Zhonghua Yixue Zazhi* 2001;81:6284
- 29 Yang YX, Liu JY. Studies on zinc-induced metallothionein synthesis in rabbits. *Weiliangyuansu Yu Jiankangyanjiu* 1996;13:1-2
- 30 Zhang WQ, Tie JK, Shen HM, Xu GS, Ru BG. A preliminary study on the induction of metallothionein in rats with Aluminum administration by different ways. *Zhonghua Yufangyixue Zazhi* 1998;32:153-155
- 31 Dai JG, Yang S, Chen JH. Influence of calcium and zinc in the synthesis of hepatic metallothionein in mice. *Weisheng Dulixue Zazhi, Zhongguo Gonggong weisheng* 1997;13:95-96
- 32 Yang S, Dai JG, Chen JH. Influence of calcium and cadmium in the synthesis of hepatic metallothionein in mice. *Weisheng Dulixue Zazhi* 1996;10: 4-5
- 33 Yang S, Dai JG, Chen JH. The interaction of zinc and cadmium in the synthesis of hepatic metallothionein in mouse. *Nanjing Yikedaxue Xuebao* 1996; 16: 57-59
- 34 Nong JX, He QR, Wang SP. Relationship between metallothionein and cadmium-induced liver and kidney injury. *Shiyong Yufang Yixue* 1999;6: 177-179
- 35 He QR, Wang SP. Effects of CCl₄-induced hepatic damage on cadmium nephrotoxicity in rats. *Zhonghua Laodongweisheng Zhiyebing Zazhi* 1998;16:30-33
- 36 Mitsuyoshi H, Nakashima T, Sumida Y, Yoh T, Nakajima Y, Ishikawa H, Inaba K, Sakamoto Y, Okanoue T, Kashima K. Ursodeoxycholic acid protects hepatocytes against oxidative injury via induction of antioxidants. *Biochem Biophys Res Commun* 1999;263:537-542
- 37 Sato S, Shimizu M, Hosokawa T, Saito T, Okabe M, Niioka T, Kurasaki M. Distribution of zinc-binding metallothionein in cirrhotic liver of rats administered zinc. *Pharmacol Toxicol* 2000;87:292-296
- 38 Sato M, Sasaki M, Hojo H. Antioxidative roles of metallothionein and manganese superoxide dismutase induced by tumor necrosis factor-alpha and interleukin-6. *Arch Biochem Biophys* 1995;316:738-744
- 39 Lu LG, Zeng MD, Li JQ, Qiu DK, Hua J, Fan ZP. Expression of intercellular adhesion molecule 1 by activated hepatic stellate cell. *Shijie Huaren Xiaohua Zazhi* 1998; 6: 576-569
- 40 Zhu YH, Hu DR, Nie QH, Liu GD, Tan ZX. Study on activation and c-fos, c-jun expression of in vitro cultured human hepatic stellate cells. *Shijie Huaren Xiaohua Zazhi* 2000;8:299-302
- 41 Wang YD, Jia LW, Li CM. Hepatic content of collagens and laminin in rat model of experimental liver fibrosis. *World J Gastroenterol* 2000;6:73
- 42 Xiang DD, Wei YL, Li QF. The molecular mechanism in the effects of TGF- β 1 on Ito cell. *Shijie Huaren Xiaohua Zazhi* 1999;7:980-981
- 43 Qing JP, Jiang MD. The feature and regulation of liver stellate cell in relation with liver fibrosis. *Shijie Huaren Xiaohua Zazhi* 2001;9:801-804
- 44 Zhu YH, Hu DR, Nie QH, Liu GD, Tan ZX. Study on activation and c-fos, c-jun expression of in vitro cultured human hepatic stellate cells. *Shijie Huaren Xiaohua Zazhi* 2000;8:299-302
- 45 Lu LG, Zeng MD, Li JQ, Hua J, Fan JG, Fan ZP, Qiu DK. Effect of lipid on proliferation and activation of rat hepatic stellate cells (I). *World J Gastroenterol* 1998;4:497-499
- 46 Cheng ML, Liu SD. The basic study and clinical research on hepatic fibrosis. *Renmin Weisheng Chubanshe*, 1996;1: 30-45
- 47 Lu X, Liu CH, Xu GF, Chen WH, Liu P. Successive observation of laminin and collagen IV on hepatic sinusoid during the formation of liver fibrosis in rats. *Shijie Huaren Xiaohua Zazhi* 2001;9:260-262
- 48 Wang Y, Gao Y, Yang JZ. Gene expression of collagenase in experimental liver fibrosis. *Shijie Huaren Xiaohua Zazhi* 1999;7:1004-1006

Edited by Wu XN

• BASIC RESEARCH •

Characteristics and mechanism of enzyme secretion and increase in $[Ca^{2+}]_i$ in Saikosaponin(I) stimulated rat pancreatic acinar cells

Yi Yu, Wen-Xiu Yang, Hui Wang, Wen-Zheng Zhang, Bao-Hua Liu, Zhi-Yong Dong

Yi Yu, Wen-Xiu Yang, Hui Wang, Wen-Zheng Zhang, Bao-Hua Liu, Zhi-Yong Dong, Department of Biophysics, Nankai University, Tianjin, 300071, China

Presented at the Third East Asian Biophysics Symposium, Kyongju, Korea, May 22-26, 2000

Supported by National Natural Science Foundation of China, No. 39770910

Correspondence to: Wen-xiu Yang, Department of Biophysics, School of Physics, Nankai University, Tianjin 300071, China. yangwenx@public.tpt.tj.cn

Telephone: +86-22-23501491 Fax: +86-22-23501490

Received 2001-12-05 Accepted 2002-02-19

Abstract

AIM: This investigation was to reveal the characteristics and mechanism of enzyme secretion and increase in $[Ca^{2+}]_i$ stimulated by saikosaponin(I) [SA(I)] in rat pancreatic acini.

METHODS: Pancreatic acini were prepared from male Wistar rats. Isolated acinar cells were suspended in Eagle's MEM solution. After adding drugs, the incubation was performed at 37°C for a set period of time. Amylase of supernatant was assayed using starch-iodide reaction. Isolated acinar single cell was incubated with Fura-2/AM at 37°C, then cells were washed and resuspended in fresh solution and attached to the chamber. Cytoplasm $[Ca^{2+}]_i$ of a single cell was expressed by fluorescence ratio F340/F380 recorded in a Nikon PI Ca^{2+} measurement system.

RESULTS: Rate course of amylase secretion stimulated by SA(I) in rat pancreatic acini appeared in bell-like shape. The peak amplitude increased depended on SA(I) concentration. The maximum rate responded to 1×10^{-5} mol/L SA(I) was 13.1-fold of basal and the rate decreased to basal level at 30 min. CCK-8 receptor antagonist Bt_2 -cGMP markedly inhibited amylase secretion stimulated by SA(I) and the dose-effect relationship was similar to that by CCK-8. $[Ca^{2+}]_i$ in a single acinar cell rose to the peak at 5 min after adding 5×10^{-6} mol/L SA(I) and was 5.1-fold of basal level. In addition, there was a secondary increase after the initial peak. GDP could inhibit both the rate of amylase secretion and rising of $[Ca^{2+}]_i$ stimulated by SA(I) in a single pancreatic acinar cell.

CONCLUSION: SA(I) is highly efficient in promoting the secretion of enzymes synthesized in rat pancreatic acini and raising intracellular $[Ca^{2+}]_i$. Signaling transduction pathway of SA(I) involves activating special membrane receptor and increase in cytoplasm $[Ca^{2+}]_i$ sequentially.

Yi Y, Yang WX, Wang H, Zhang WZ, Liu BH, Dong ZY. Characteristics and mechanism of enzyme secretion and increase in $[Ca^{2+}]_i$ in Saikosaponin(I) stimulated rat pancreatic acinar cells. *World J Gastroenterol* 2002;8(3):524-527

INTRODUCTION

Bupleurum, one kind of traditional Chinese Drug, have a variety of roles in clinical practice. Our pharmacological investigations have indicated Bupleurum has significant promoting effect on enzyme

secretion in rat pancreatic acini^[1], Saikosides is the compound of the active Saikosaponin component in Bupleurum. The kinetics of enzyme secretion stimulated by Saikosides in a dose-dependent manner can be divided into first phase of high-potency secretion and later phase of low-potency secretion. The accumulation of enzyme secretion stimulated by 200 mg/L Saikosides with 30 min incubation is 6.5 folds of the basal level^[2]. Based on the results of separation, purification and identification for Saikosides^[3], we have compared the activities of nine kinds of Saikosaponins. Saikosaponin(I) [SA(I)] has the best effect of promoting secretion. The promoting effect of SA(I) increase in a dose-dependent manner, and the enzyme release stimulated by 5×10^{-5} mol/L SA(I) is 9.5 folds of basal^[4,5].

Cholecystokinin (CCK) and Carbachol (CCh) are two important secretagogues for enzyme secretion from pancreatic acini. The promoting response associated with CCK-8 is in a dose-dependent manner, and high concentrations of CCK have submaximal amylase release. Furthermore, the relative potency of CCK to mobilize intracellular Ca^{2+} is dependent on the concentration of CCK-8. At low concentration of CCK-8 (10^{-12} mol/L- 10^{-11} mol/L), it induces a series of transient increase in $[Ca^{2+}]_i$ termed "Ca²⁺ oscillations", and high concentration of CCK-8 evokes the single peak of $[Ca^{2+}]_i$ ^[6-8]. Cellular signaling transduction pathway of increase in $[Ca^{2+}]_i$ evoked by CCK-8, involves activating G protein coupled receptors by CCK-8 binding its receptor, producing inositol 1,4,5-triphosphate (IP₃) and diacylglycerol (DAG) by activating the phospholipase C (PLC), and releasing Ca^{2+} from endoplasmic reticulum (ER) by activating the IP₃ receptor^[9-14]. Increase in $[Ca^{2+}]_i$ evoked by CCK-8 and CCh not only result from ER, but from influx of extracellular Ca^{2+} ^[15-17]. Recently, it was shown that both activated PKC and elevated intracellular Ca^{2+} mediate activation of NF- κ B and *mob-1* expression by supraphysiological CCK^[18,19]. Our investigations have indicated Saikosides is also a significant Ca^{2+} -mobilizing secretagogue. The kinetics of $[Ca^{2+}]_i$ induced by Saikosides varied with two peaks, and promotion of Saikosides on pancreatic exocrine could be correlative with the kinetics of $[Ca^{2+}]_i$. The effect of 200 mg/L Saikosides was reduced by 35% and the second peak of $[Ca^{2+}]_i$ dramatically declined in Ca^{2+} -free medium^[2]. These results showed that increase in $[Ca^{2+}]_i$ evoked by SA(I) include both Ca^{2+} release from the intracellular Ca^{2+} pool and subsequent influx of Ca^{2+} through plasmic membrane.

In order to elucidate the characteristics and mechanism of enzyme secretion and increase in $[Ca^{2+}]_i$ in SA(I) stimulated rat pancreatic acinar cells, here we report an analysis in rate kinetics of SA(I) stimulated amylase secretion, Characteristics of ligand-receptor binding and kinetics of $[Ca^{2+}]_i$ evoked by SA(I) in a single cell as well as the effects of guanosine-5'-diphosphate trisodium salt (GDP) on amylase secretion and $[Ca^{2+}]_i$.

MATERIALS AND METHODS

Materials

Cholecystokinin-8 (CCK-8), Carbachol (CCh), Dibutylguanosine-3',

5'-cyclic monophosphate (Bt_2 -cGMP), Guanosine-5'-diphosphate trisodium salt (GDP), Fura2-AM, Collagenase IA, soybean trypsin inhibitor were from Sigma Chemical Co (St. Louis, MO); Other chemicals were from Tianxiangren Bio. Co. Ltd. (Beijing, China). Saikosaponin I was separated and identified by the School of Pharmaceutical Science, Beijing University.

Methods

Preparation of isolated acini Isolated pancreatic acini were prepared by the method of Duan from male Wistar rat (200-250g) that had been fasted overnight^[20]. Individual Acini were prepared by 0.3g/L collagenase digestion at 37°C and purified by centrifugation through the Eagle's MEM containing 4% bovine serum albumin. The isolated acini were then allowed to resuspend at 37°C for 30min in HEPES-buffered Ringer solution supplemented with 11.1mmol/L glucose, minimal Eagle's amino acids medium and 0.1g/L soybean trypsin inhibitor and were through gas with 1000mL/L O_2 .

Measurement of amylase release Acini were suspended in Eagle's MEM solution. After adding the drug, the incubation was performed at 37°C for a set period of time. Then the supernatant was removed and assayed for amylase. Amylase release was expressed at the ratio of the content of amylase released into the medium during the incubation to the total content. The total amylase content was estimated by measuring the amylase activity present in the acini broken at the beginning of the incubation.

Detection of cytosolic free Ca^{2+} concentration According to the method of Cui *et al.*^[21] briefly, isolated acini were incubated with 5×10^{-6} mol/L Fura-2/AM at 37°C for 40min and then washed and resuspended in fresh physiological salt solution. Isolated acini were attached to Sykus-Moor perfusion chamber and continuously superfused by a buffer medium containing agonist at 1ml/min. Stimulus was introduced by changing perfusion buffer containing relevant chemicals. Inlet perfusion buffer was pre-warmed to 37°C in a water bath. Fluorescence ratios of f340/f380 were recorded in a Nikon PI Ca^{2+} measurement system, with a pin-hole size of 0.5 focused onto the apical portion of a single acinar cell within acinar formation or formations, and a Nikon neutral density filter (#8) was placed in the excitation light path.

Statistical analysis Values of each group were expressed as $\bar{x} \pm s$. Group comparison was performed using student's *t* test. $P < 0.05$ was considered significant.

RESULTS

Rate dynamics of amylase secretion in SA(I) stimulated pancreatic acini

Under the different stimulation of 1×10^{-6} mol/L, 5×10^{-6} mol/L and 1×10^{-5} mol/L SA(I) in pancreatic acini, the amylase release accumulation from acini within 37°C incubation at different time were detected. Rate course of amylase release was obtained by differential analytics of enzyme accumulation with a computer program (Figure 1). The kinetics of rate-time effect could be divided into two phases, named by increasing phase and declining phase. With the concentration of SA(I) increasing, secreting rate rose more quickly and reached the higher peak, then it fell into basal level soon. The maximum rates of amylase secretion stimulated by 1×10^{-6} mol/L, 5×10^{-6} mol/L and 1×10^{-5} mol/L SA(I) were 3.2-fold, 7.4-fold, and 13.1-fold of basal, corresponding time at 16.5min, 14.5min, 12.5min. Those data indicated that though the SA(I) stimulated enzyme release obviously, the main promoting effect of SA(I) took place in the 20min after adding the drug, and promoting action disappeared at 30min.

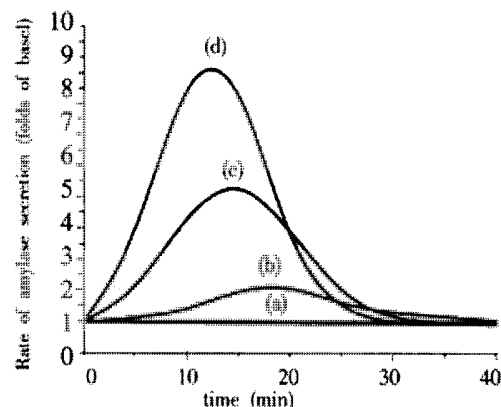


Figure 1 Rate kinetics of amylase secretion stimulated by SA(I) in the rat pancreatic acini. The results were expressed at the ratio of amylase secretion during the incubation to the basal secretion. a: basal value was standardized as 1, b: 1×10^{-6} mol/L SA(I), c: 5×10^{-6} mol/L SA(I), d: 1×10^{-5} mol/L SA(I). The values represented the $\bar{x} \pm s$ from four independent experiments.

Dose-response of inhibition of receptor antagonist on amylase secretion stimulated by SA(I)

In order to explore whether SA(I) stimulated signal was transduced through the effect of membranous receptor, the effects of CCK-8 receptor antagonist Bt_2 -cGMP and CCh receptor antagonist atropine on SA(I) stimulated amylase secretion had been studied. In Table 1, enzyme secretion induced by SA(I) was markedly depressed by Bt_2 -cGMP. The inhibitory effects of Bt_2 -cGMP on action of SA(I) and CCK-8 had similar characteristics of dose-effect relationship. Amylase secretion stimulated by secretagogues decreased within the medium containing 1×10^{-7} mol/L Bt_2 -cGMP ($^aP < 0.05$). With increasing concentration of Bt_2 -cGMP, the inhibition was enhanced ($^bP < 0.01$). 1×10^{-4} mol/L Bt_2 -cGMP decreased action of SA(I) and CCK-8 by 31.3% and 34.4% respectively.

In Table 2, atropine was observed to depress amylase secretion stimulated by CCh ($^bP < 0.01$). 1×10^{-5} mol/L atropine eliminated the promoting effect of CCh, but had no apparent inhibition on the that of SA(I) at 1×10^{-8} mol/L- 1×10^{-5} mol/L atropine range ($P > 0.05$).

Table 1 Effect of different concentrations of Bt_2 -cGMP on amylase secretion stimulated by SA(I) and CCK-8

Bt_2 -cGMP concentration (mol/L)	Amylase release (% of total)	
	1×10^{-8} mol/L CCK-8	5×10^{-6} mol/L SA(I)
Control	19.5±1.6	31.0±2.1
1×10^{-7}	17.8±1.9 ^a	27.4±2.5 ^a
1×10^{-6}	15.6±2.0 ^b	25.6±1.4 ^b
1×10^{-5}	14.0±1.2 ^b	23.1±1.8 ^b
1×10^{-4}	12.8±1.7 ^b	21.2±0.9 ^b

Rat pancreatic acini were incubated with either 1×10^{-8} mol/L CCK-8 or 5×10^{-6} mol/L SA(I) in adding different concentrations of Bt_2 -cGMP medium. After 30min, the incubation was stopped and the content of amylase in the supernatant was assayed. The values represented the $\bar{x} \pm s$ from 4 separate experiments. ^a $P < 0.05$, ^b $P < 0.01$ vs control.

Table 2 Effect of different concentrations of atropine on amylase secretion stimulated by SA(I) and CCh

Atropine concentration (mol/L)	Amylase release (% of total)	
	1×10^{-5} mol/L CCh	5×10^{-6} mol/L SA(I)
Control	15.2±1.3	30.8±3.3
1×10^{-8}	11.6±1.6 ^b	27.9±11.4
1×10^{-7}	10.5±1.2 ^b	25.1±7.4
1×10^{-6}	8.8±1.3 ^b	27.5±6.9
1×10^{-5}	8.3±1.6 ^b	25.5±6.2

Rat pancreatic acini were incubated with either 1×10^{-5} mol/L CCh or 5×10^{-6} mol/L SA(I) in adding different concentration of atropine medium. After 30min, the incubation stopped and the content of amylase in the supernatant was assayed. The values represent the $\bar{x} \pm s$ from 4 separate experiments. ^a $P < 0.05$, ^b $P < 0.01$ vs control.

Dynamics of SA(I) and CCK-8 evoked $[Ca^{2+}]_i$ in single pancreatic acinar cell

The time courses of SA(I) and CCK-8 evoked $[Ca^{2+}]_i$ in a single pancreatic acinar cell were shown in Figure 2. 1×10^{-9} mol/L CCK-8 induced a monophasic $[Ca^{2+}]_i$ spike resulting in an increase of 4.2 folds from basal and declined to basal speedily. 5×10^{-6} mol/L SA(I) evoked $[Ca^{2+}]_i$ gradually increased within 5 min after addition of SA(I), and peak of $[Ca^{2+}]_i$ was 5.0 folds of basal. Unlike CCK, $[Ca^{2+}]_i$ rose again after falling, caused a diphasic Ca^{2+} spike.

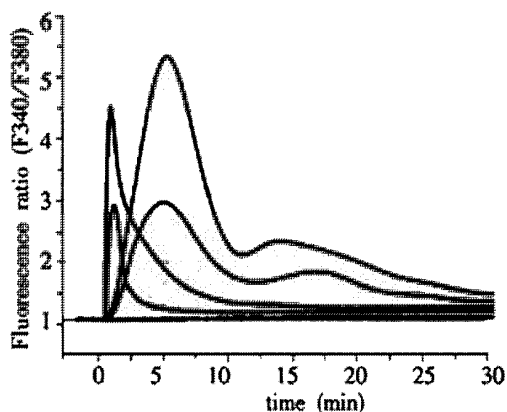


Figure 2 Kinetics of SA(I) and CCK-8 evoked $[Ca^{2+}]_i$ and effects of GDP in a single rat pancreatic acinar cell. $[Ca^{2+}]_i$ were expressed by Fluorescence ratio F340/F380. a. 1×10^{-9} mol/L CCK-8; b. 1×10^{-9} mol/L CCK-8 + 5×10^{-3} mol/L GDP; c. 5×10^{-6} mol/L SA(I); d. 5×10^{-6} mol/L SA(I) + 5×10^{-3} mol/L GDP; e. Base. Time 0 is determined by the time of adding drug.

Effects of GDP on dynamics of amylase secretion rate and $[Ca^{2+}]_i$ induced by SA(I) in pancreatic acini

Figure 3 illustrated the effects of GDP on rate change of amylase release stimulated by SA(I). GDP could inhibit the rate of amylase secretion stimulated by 5×10^{-6} mol/L SA(I), whose rate-time curve of amylase secretion was similar to that of SA(I) in configuration, but addition of 5×10^{-3} mol/L GDP decreased the maximal rate by 54%. These data suggested GDP mainly inhibited high-potency phase of amylase secretion stimulated by SA(I).

In the kinetic experiments of $[Ca^{2+}]_i$ induced by SA(I) and CCK-8 in a single pancreatic acinar cell (Figure 2), addition of 5×10^{-3} mol/L GDP inhibited 1×10^{-9} mol/L CCK-8-induced $[Ca^{2+}]_i$ peak amplitude by 39%, with similar dynamic characteristics of $[Ca^{2+}]_i$. Addition of 5×10^{-3} mol/L GDP caused diphasic spike of $[Ca^{2+}]_i$ induced by 5×10^{-6} mol/L SA(I) decrease either, this resulted in a 44% decrease of initial Ca^{2+} peak, but a secondary increase in $[Ca^{2+}]_i$ still appeared.

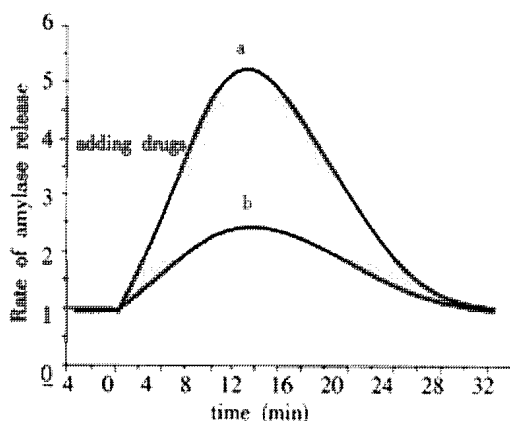


Figure 3 Inhibitory of GDP on rate course of SA(I) stimulated amylase secretion in rat pancreatic acini (base secretion rate is normalized as 1.0). a. 5×10^{-6} mol/L SA(I); b. 5×10^{-6} mol/L SA(I) + 5×10^{-3} mol/L GDP. The data points represent from four separate experiments

DISCUSSION

A series of investigation for amylase secretion stimulated by Bupleurum and its effective components show that they have the rapid and high-potency ability of promoting pancreatic acini enzyme secretion and the validity of reversing functional disorder of pancreas exocrine. From the analysis of rate kinetics of amylase secretion stimulated by SA(I) (Figure 1), within 15 min following adding SA(I), the rate of amylase secretion increased rapidly, then gradually decreased and returned to basal level at 30 min. It indicates that different from CCK to enhance the synthesis of protein^[22,23], the main effect of SA(I) is to hasten secretion of the exocrine protein synthesized and accumulated in granules.

To determine whether the stimulating signal of SA(I) on acinar cells is transduced by binding to the receptor on the cellular membrane, is the first task in the investigation of its mechanism of action. It is known that physiological functions of CCK-8 and CCh are mediated by specific types of receptors now termed the CCK_A and M₃ receptors. CCK_A and M₃ receptors belong to the receptors of G protein-coupled superfamily which transduce the stimulating signal by generation of intracellular second messengers, primarily IP₃ and DAG^[9-11,14,24]. We compared the effects of CCK-8 and CCh receptor antagonist, Bt₂-cGMP and atropine, on amylase secretion caused by SA(I) (Table 1, 2), the results showed that atropine had no detectable influence on the action of SA(I). Moreover, the dose-effect relationships of inhibition of Bt₂-cGMP on SA(I) and CCK-8 were similar. The results suggested that interaction between SA(I) and its membrane receptor initiated intracellular signaling transduction. The receptor of SA(I) has similar characteristics as that of CCK-8. To clarify the detail machinery of receptor of SA(I) will require further study.

As mentioned in our previous papers^[25], the rising dynamics of mean intracellular $[Ca^{2+}]_i$ induced by SA(I) in rat pancreatic acinar cells could produce two peaks. When pancreatic acini were incubated in Ca^{2+} -free medium, in the second step, $[Ca^{2+}]_i$ did not rise and fell to the basal level gradually, and the second peak disappeared. The finding demonstrated the Ca^{2+} release from intracellular Ca^{2+} pool resulted in the first $[Ca^{2+}]_i$ peak, and second $[Ca^{2+}]_i$ peak depending on the extracellular Ca^{2+} influx in sequence. In the present experiments of single acinar cell $[Ca^{2+}]_i$ was concordant with our previous report, 1×10^{-9} mol/L CCK-8 could cause a large transient increase in $[Ca^{2+}]_i$. But it is different from CCK-8 that the change of $[Ca^{2+}]_i$ caused by SA(I) had relatively slow rate and higher peak value. In addition, there was a secondary increase after the initial peak of $[Ca^{2+}]_i$. The data suggested SA(I) had a different mechanism from that of CCK inducing Ca^{2+} release from ER and might be through more signaling transduction pathways to initiate the intracellular calcium mobilization and subsequent extracellular calcium influx. So the intracellular increase in $[Ca^{2+}]_i$ caused by SA(I) could maintain a longer time course. These mechanisms correlated with high-potency effect of SA(I) on pancreatic exocrine. It is now known that the changes of intracellular calcium play a key role in many functions of cells. Recently, several reports showed that the spatio-temporal patterns of the intracellular calcium carried the Ca^{2+} signals to regulate gene expression and cell differentiation^[26-29]. The specificity of Ca^{2+} signal is somewhat more acute in polarized secretory cells such as pancreatic acinar cells^[30-32]. These researches suggest that such pattern of Ca^{2+} signal induced by SA(I) in our present studies may offer specific signal to modulate enzymes secretion in pancreatic acinar cells.

In addition, GDP could cause obvious decrease of amylase secretion and increase in $[Ca^{2+}]_i$ induced by SA(I). GDP mainly inhibited the early peak of $[Ca^{2+}]_i$ and high-potency phase of secretion stimulated by SA(I). The decrease of $[Ca^{2+}]_i$ anticipated the inhibition of amylase secretion in sequence (Figure 2,3). Several

investigators had reported that the increase in intracellular level of GDP could cause the inhibition of G-protein activity in pancreatic acini^[33-35]. These G-proteins, including both ras-like small GTP-binding proteins and heterotrimeric G-proteins, had important role on the release of intracellular calcium and amylase secretion stimulated by secretagogues^[14, 36-40]. More experimental data are required whether intracellular signal of stimulatory effect of SA(I) transducing to down stream through activation of G protein coupling receptor.

In summary, the results presented in this study prove that SA(I) has high-potency in stimulating the amylase secretion in rat pancreatic acini and its main effect is to promote exocytosis of enzymes synthesized by the cells. The transmembrane signal of SA(I) is transduced through interaction with its membrane receptor. Subsequently, $[Ca^{2+}]_i$ is increased by intracellular Ca^{2+} release and extracellular Ca^{2+} influx, so as to enhance the function of cellular enzyme secretion.

REFERENCES

- Chen XQ, Yang WX, Xu WS, Yang F, Kong D, Wu XZ. Stimulative action of bupleurum chinensis on amylase secretion from pancreatic acini and its dependence on Ca^{2+} . *Zhongguo Zhongxiyi Jiehe Zazhi* 1997;17:211-212
- Yang WX, Yu Y, Yao HQ, Zhao YY, Liang H. Kinetics of enzyme secretion and $[Ca^{2+}]_i$ in pancreatic acini stimulated by Saikosides. *Zhongguo Xueshu Qikan Wenzhai (Keji Kuaibao)* 1999;5:1185-1186
- Liang H, Zhao YY, Qi HY, Huang J, Zhang RY. A new saikosaponin from bupleurum DC. *Yaoxue Xuebao* 1998; 33:37-41
- Yang WX, Yu Y, Yao HQ, Wang H, Zhao YY, Liang H. Comparative research of enzyme secretion in pancreatic acini stimulated by saikosaponins. *Zhongguo Xueshu Qikan Wenzhai (Keji Kuaibao)* 1999;5: 1529-1530
- Yang WX, Yu Y, Zhao YY, Liang H, Wang H, Zhou J. The characteristics of saikosaponin-stimulated pancreatic acini protein secretion and effects of Ca^{2+} . *Nankai Daxue Xuebao* 2000;33:41-44
- Tsunoda T, Stuenkel EL, Williams JA. Oscillatory mode of calcium signaling in rat pancreatic acinar cells. *Am J Physiol* 1990; 258: C147-C155
- Williams JA, Blevins GT. Cholecystokinin and regulation of pancreatic acinar cell function. *Physiol Rev* 1993;73:709-723
- Giovanna T, Zhang BX, Xu X, Muallem S. Compartmentalization of Ca^{2+} signaling and Ca^{2+} pools in pancreatic acini. *J Bio Chem* 1994;269: 29621-29628
- Muallem S, Beeker TG. Relationship between hormonal, GTP and $Ins(1,4,5)P_3$ -stimulated Ca^{2+} uptake and release in pancreatic acinar cells. *Biochem J* 1989;263:333-339
- Yasuhiro T, Chung O. The regulatory site of functional GTP binding protein coupled to the high affinity cholecystokinin receptor and phospholipase A2 pathway is on the G- β subunit of Gq protein in pancreatic acini. *Biochem Biophys Res Com* 1995;211:648-655
- Berridge MJ. Inositol trisphosphate and calcium signaling. *Nature* 1993;361:315-325
- Takashi K, Shunsuke S, Shinji K, Toyohiko H, Chohei S, Junji K. Cholecystokinin receptor occupation and cholecystokinin-induced calcium mobilization in the early phase in rat pancreatic acini. *Biochem Biophys Acta* 1991;1094:231-237
- Xu X, Zeng WZ, Muallem S. Regulation of inositol 1,4,5-trisphosphate-activated Ca^{2+} channel by activation of G protein. *J Bio Chem* 1996; 271:11737-11744
- Verspohl EJ, Herrmann K. Involvement of G proteins in the effect of Carbachol and Cholecystokinin in rat pancreatic islets. *Am J Physiol* 1996;271:E65-E72
- Hurley TW, Ronald WB. Regulating transient and sustained changes of cytosolic Ca^{2+} in rat pancreatic acini. *Am J Physiol* 1990; 258:C54-C61
- Stephen JP, Mari SSP. Cyclic GMP mediates the agonist-stimulated increase in plasma membrane calcium entry in the pancreatic acinar cell. *J Bio Chem* 1990; 265: 12846-12853
- Anna G, Stephen P. Nitric oxide production regulates cGMP formation and calcium influx in pancreatic acinar cells. *Am J Physiol* 1994; 266:G350-G356
- Han B, Logsdon C. CCK stimulates mob-1 expression and NF- κ B activation via protein kinase C and intracellular Ca^{2+} . *Am J Physiol Cell Physiol* 2000; 278: C344-C351
- Gukovsky I, Gukovskaya AS, Blinman TA, Zaninovic V, Pandol SJ. Early NF-kappaB activation is associated with hormone-induced pancreatitis. *Am J Physiol* 1998; 275:G1402-G1414
- Duan RD, Wagner ACC, Yule DI, Williams JA. Multiple inhibitory effects of genistein on stimulus-secretion coupling in rat pancreatic acini. *Am J Physiol* 1994; 266: G303-G310
- Cui ZJ, Kanno T. Cholecystokinin analog JMV-180-induced intracellular calcium oscillations are mediated by inositol 1,4,5-trisphosphate in rat pancreatic acini. *Zhongguo Yaoli Xuebao* 2000;21: 377-380
- Bragado MJ, Groblewski GE, Williams JA. Regulation of protein synthesis by cholecystokinin in rat pancreatic acini involves PHAS-I and the p70 S6 kinase pathway. *Gastroenterology* 1998; 115:733-742
- Bragado MJ, Tashiro M, Williams JA. Regulation of the initiation of pancreatic digestive enzyme protein synthesis by Cholecystokinin in rat pancreas *in vivo*. *Gastroenterology* 2000; 119:1731-1739
- Talkad VD, Potto RJ, Metz DC, Turner RJ, Fortune KP, Bhat ST, Gardner JD. Characterization of the three different states of the cholecystokinin(CCK) receptor in pancreatic acini. *Biochem Biophys Acta* 1994;1224:103-116
- Yang WX, Yu Y, Zhang WZ, Wang H, Li XD, Zhao YY, Liang H. Inhibitory role of GDP on saikosaponin(I) stimulated enzyme secretion and rising of $[Ca^{2+}]_i$ in rat pancreatic acini. *Acta Pharmacol Sin* 2001;22: 669-672
- Bootman MD, Lipp P, Berridge MJ. The organisation and functions of local Ca^{2+} signals. *J Cell Sci* 2001; 114: 2213-2222
- Dotmentsch RE, Xu K, Lewis RS. Calcium oscillation increase the efficiency and specificity of gene expression. *Nature* 1998; 392: 933
- Kummer U, Olsen LF, Dixon CJ, Green AK, Bornberg-Bauer E, Baier G. Switching from simple to complex oscillations in calcium signaling. *J Biophys* 2000; 79:1188-1195
- West AE, Chen WG, Dalva MB, Dolmetsch RE, Kornkauer JM, Shaywitz AJ, Takasa MA, Tao X, Greenberg ME. Calcium regulation of neuronal gene expression. *Proc Natl Acad Sci USA* 2001; 98:11024
- Xu X, Zeng WZ, Diaz J, Muallem S. Spatial compartmentalization of Ca^{2+} signaling complexes in pancreatic acini. *J Biol Chem* 1996; 271: 24684-24690
- James W. Putney, Pharmacology of Capacitative Calcium Entry. *Mol Interv* 2001; 1: 84-94
- Shuttleworth TJ. Intracellular Ca^{2+} signalling in secretory cells. *J Exp Biol* 1997; 200: 303-314
- Padfield PT, Ding TG, Jamieson TD. Ca^{2+} -dependent amylase secretion from pancreatic acinar cells occurs without activation of phospholipase C linked-G-proteins. *Biochem Biophys Res commun* 1991;174:536-541
- Gasman S, Chasserot-Golaz S, Popoff MR, Aunis D, Bader MF. Involvement of Rho GTPases in calcium-regulated exocytosis from adrenal chromaffin cells. *J Cell Sci* 1999; 112: 4763-4771
- Rosales J, Ernst JD. GTP-dependent permeabilized neutrophil secretion requires a freely diffusible cytosolic protein. *J Cell Biochem* 2000; 80:37-45
- Ohnishi H, Mine T, Shibata H, Ueda N, Tsuchida T, Fujita T. Involvement of Rab4 in regulated exocytosis of rat pancreatic acini. *Gastroenterology* 1999; 116:943-952
- Dabrowski A, Vanderkuur JA, Carter-Su C, Williams JA. Cholecystokinin stimulates formation of Shc-Grb2 complex in rat pancreatic acinar cells through a protein kinase C-dependent mechanism. *J Biochem* 1996;271:27125-27129
- Ohnishi H, Samuelson LC, Yule DI, Ernst SA, Williams JA. Overexpression of Rab3D enhances regulated amylase secretion from pancreatic acini of transgenic mice. *J Clin Invest* 1997;100: 3044-3052
- Padfield PJ, Panesar N. The two phases of regulated exocytosis in permeabilized pancreatic acini are modulated differently by heterotrimeric G Proteins. *Biochem Biophys Res Com* 1998;245:332-336
- Nozu F, Tsunoda Y, Ibitayo AI, Bitar KN, Owyang C. Involvement of RhoA and its interaction with protein kinase C and Src in CCK-stimulated pancreatic acini. *Am J Physiol* 1999;276: G915-G923

Edited by Wu XN

• BASIC RESEARCH •

Effect of endotoxin on portal hemodynamic in rats

Xiang-Jun Bi, Min-Hu Chen, Jing-Hui Wang, Jie Chen

Xiang-Jun Bi, Min-Hu Chen, Jing-Hui Wang, Jie Chen, Department of Gastroenterology, First Affiliated Hospital, Sun Yat-sen University, Guangzhou 510089, Guangdong Province, China
Correspondence to: Xiang-Jun Bi, Department of Gastroenterology, First Affiliated Hospital, Sun Yat-sen University, Guangzhou 510089, Guangdong Province, China. bixj@gzsums.edu.cn
Telephone: +86-20-87334343

Received 2001-10-19 Accepted 2001-11-18

Abstract

AIM: To study the effects of endotoxin on portal hemodynamic of normal and noncirrhotic portal hypertensive rats.

METHODS: Normal rats were intraperitoneally injected with 0.1, 0.25, 0.5, 1.0, 2.0, 4.0 mg·kg⁻¹ of lipopolysaccharide(LPS) respectively, portal vein ligation(PVL) and intrahepatic portal occlusion (IPO) rats as well as sham-operated rats were treated with an intraperitoneal injection of 1.0 mg·kg⁻¹ of LPS, the portal vein pressure(PVP), portal venous flow(PVF), inferior vena cava pressure(IVCP) and portal vein resistance(PVR) were detected 4 hours after injection.

RESULTS: PVF of the 5 groups of rats accepting intraperitoneal injection of LPS were increased from 14.0 to 18.0, 22.2, 26.2, 34.8, 39.6, 38.8 mL·min⁻¹ 4 hours after injection of LPS ($P<0.01$). PVP of the 4 groups of rats accepting more than 0.1 mg/kg·b.w of LPS was increased from 1.04 to 1.25, 1.50, 1.80, 1.95, 2.05 kPa ($P<0.01$). The increments of PVF and PVP were in a dose-dependent manner of LPS. PVR of the 5 groups of rats was decreased from 51 to 42, 44, 48, 45, 44, 47 kPa·min·L⁻¹ ($P<0.05$) and no dose-dependent manner was observed. PVF of PVL, IPO and sham-operated rats increased from 22.6 to 32.8, 22.0 to 28.0, 14.0 to 34.8 mL·min⁻¹ ($P<0.01$), and PVP increased from 1.86 to 2.24, 1.74 to 1.95, 1.04 to 1.80 kPa ($P<0.01$), PVR decreased from 71 to 61, 67 to 61, 52 to 44 kPa·min·L⁻¹ after intraperitoneal injection of 1 mg·kg⁻¹ of LPS. The increments of PVF and PVP of PVL and IPO rats were significantly less than the sham-operated rats ($P<0.01$). There was no significant difference between the amounts of PVR decreased in the two groups of PHT model rats and sham-operated rats ($P>0.05$) after intraperitoneal injection 1 mg·kg⁻¹ of LPS.

CONCLUSION: Endotoxin could prompt portal hypertension of the normal and noncirrhotic portal hypertensive rats by increasing portal blood flow mainly.

Bi XJ, Chen MH, Wang JH, Chen J. Effect of endotoxin on portal hemodynamic in rats. *World J Gastroenterol* 2002;8(3):528-530

INTRODUCTION

Endotoxin is lipopolysaccharide(LPS), a component of the outer membrane of the Gram-negative bacteria, which is released from the Gram-negative bacterial cell wall. Its functional component is lipid

A. Many researchers have discovered that endotoxemia can lead to an alteration of systemic hemodynamics and some organs' blood circulation such as the lungs, liver and kidney^[1-4]. However, some researchers have displayed evidence against a role for endotoxin in the hyperdynamic circulation of rats with prehepatic portal hypertension^[5]. The activation of endotoxin occurs through a series of vaso modulators such as nitric oxide (NO), endothelin and others^[4-11]. These vaso modulators could modulate portal venous flow(PVF), portal vein resistance(PVR) and/or portal vein pressure(PVP). In patients suffering from liver cirrhosis with PHT, endotoxemia is often present and might contribute to the development of liver cirrhosis and PHT^[12-14]. Whether or not PHT models without liver cirrhosis are more sensitive to endotoxin is still unclear^[15,16]. Little has been done to study the effects of various dosages of LPS on portal hemodynamics. So, to detect what role endotoxin plays in PHT, we designed the following experiments to discover the effects of various dosages of LPS on the portal hemodynamics of both normal rats as well as non-cirrhosis PHT rats.

MATERIALS AND METHODS

Animals

Female Sprague Dawley rats weighing 200-250g were obtained from the Laboratory Animal Center of Sun Yat-sen University, and fed with standard rat chow. (1) Surgery was performed as in Yachida's method^[17]. Under penbarbital (50 mg·kg⁻¹, intraperitoneal injection) anesthesia, the portal vein was isolated and a single ligature placed around both the portal vein and a 16-gauge needle. The needle was ligated together with the portal vein and immediately removed to allow the portal vein to expand to the limit imposed by the ligature. A catheter was inserted through the mesentery vein into the portal vein and another into the inferior vena cava. Pressure transducers(Philips CM 130) recorded PVP and IVCP. PVF was recorded with an electromagnetic flow meter (Nihonkohden). The abdomen was closed and the rats were allowed to recover for 2 wks. In sham-operated rats, surgery consisted of dissection and visual inspection of the portal vein without ligature. (2) Surgery was performed as in Li's *et al*^[18] method. Under penbarbital anesthesia as above, microspheres (about 2×10^4 each time) of Sephadex LH-20(Pharmacia) were injected into the mesentery vein; injection was repeated 5 times. The portal venous and vena cava pressure were recorded as above. The abdomen was closed and the rats were allowed to recover for 2wks. Sham-operated rats above were used as a control.

Effects of LPS on portal hemodynamics

Normal rats were divided into seven groups, each group containing five rats. Rats were intraperitoneally injected with LPS(from *Escherichia coli* serotype, Sigma) at dosages of 0.1, 0.25, 0.5, 1.0, 2.0, 4.0 mg·kg⁻¹ respectively. Equivalent volumes of saline were intraperitoneally injected as a control. 4h later, anesthesia and operation were manipulated as above. A catheter was inserted through mesentery vein into portal vein and another catheter into the inferior vena cava. Pressure transducers(Philips CM 130) recorded PVP and IVCP. PVF was recorded with an electromagnetic flow meter (Nihonkohden). PVF, PVP and IVCP were checked four hours after injection and PVR was determined according to the formula: $PVR = (PVP - IVCP) / PVF$.

PHT rats were divided into PVL, IPO model, and sham-operated groups, each group containing ten rats, and then divided at random into two groups of five rats. PVL, IPO and sham-operated rats were each intraperitoneally injected with LPS at the dose of 1.0mg·kg⁻¹. The other PVL, IPO and sham-operated rats were intraperitoneally injected equivalent volumes of saline as control. PVF, PVP and IVCP were checked as above 4h after injection and PVR was determined according to the formula: $PVR=(PVP-IVCP)/PVF$.

The alteration of portal hemodynamics of the noncirrhotic and sham-operated rats after injection of LPS was analyzed. The means and increment percentages of PVF, PVP, and PVR of the PVL and IPO groups were compared with that of the sham-operated group.

Statistical analysis

Data were expressed as $\bar{x} \pm s$. Statistical analysis between groups was made by means of the student's unpaired *t* test by means of SPSS10.0 software, with *P*<0.05 being regarded as statistically significant.

RESULTS

Portal hemodynamic of model rats after operation

Just after portal vein ligation, PVF averaged 10.8mL·min⁻¹, PVP increased to 1.85kPa and PVR increased to 142kPa·min·L⁻¹. Two weeks after operation, PVF, PVP and PVR averaged 22.6mL·min⁻¹, 1.86kPa and 71kPa·min·L⁻¹. After finishing portal vein occlusion, PVF averaged 9.6mL·min⁻¹, PVP increased to 2.05kPa and PVR 180kPa·min·L⁻¹. Two weeks after operation, PVF, PVP and PVR averaged 22mL·min⁻¹, 1.74kPa and 67kPa·min·L⁻¹. PVP of the models was significantly increased the moment after operation and 2 wks after operation (*P*<0.01).

Effects of LPS on portal hemodynamic

PVF of all the groups of rats accepting intraperitoneal injection of LPS was significantly increased 4h after injection (*P*<0.01). Except for the group of rats accepting intraperitoneal injection of 0.1mg·kg⁻¹ of LPS (*P*>0.05), the other groups of rats were all significantly increased in PVP 4h after injection (*P*<0.01). PVF and PVP increased in a dose-dependent manner with increasing LPS concentration. Except for the group of rats accepting intraperitoneal injection of 0.5mg·kg⁻¹ of LPS (*P*>0.05), the other groups of rats were all decreased in PVR 4h after injection (*P*<0.05) and no dose-dependent manner of LPS was observed (Table 1).

Table 1 Effects of LPS on portal hemodynamics

Dose of LPS (mg·kg ⁻¹)	PVF (mL·min ⁻¹)	<i>P</i>	PVP (kPa)	<i>P</i>	PVR (kPa·min·L ⁻¹)	<i>P</i>
0.00	14.0±0.44		1.04±0.020		51	
0.10	18.0±0.44	0.000	1.05±0.022	0.743	42	0.001
0.25	22.2±0.66	0.000	1.25±0.026	0.000	44	0.003
0.50	26.2±0.80	0.000	1.50±0.015	0.000	48	0.086
1.00	34.8±0.80	0.000	1.80±0.023	0.000	45	0.003
2.00	39.6±0.74	0.000	1.95±0.035	0.000	44	0.001
4.00	38.8±0.33	0.000	2.05±0.022	0.000	47	0.008

Compare rats accepting intraperitoneal injection of various doses of LPS with rats not accepting LPS.

Effects of endotoxin on portal hemodynamic of PHT models

PVF and PVP of sham-operated rats increased from 14.0mL·min⁻¹ and 1.04kPa to 34.8mL·min⁻¹ and 1.80kPa. PVR decreased from 52kPa·min·L⁻¹ to 44kPa·min·L⁻¹ 4h after intraperitoneal injection of 1mg·kg⁻¹ of LPS. PVF of PVL and IPO model rats increased to 32.8mL·min⁻¹ and 28.0mL·min⁻¹ respectively; PVP increased to 2.24 kPa and 1.95 kPa respectively; and PVR decreased to 61kPa·min·L⁻¹

and 61kPa·min·L⁻¹ respectively. In the three groups of rats, intraperitoneal injection 1mg·kg⁻¹ of LPS significantly changed PVF, PVP and PVR (*P*<0.01, Table 2).

The percentages of PVF increase in the PVL, IPO and sham-operated groups of rats were 45.1%, 27.3%, and 148.6% respectively. PVP increased 20.4%, 12.1%, and 73.1% respectively. PVR increased -14.1%, -9.0%, and -15.4% respectively (Table 3). The increase of PVF and PVP in the two groups of PHT model rats were significantly different from sham-operated rats (*P*<0.01). There was no significant difference between the decrease of PVR in the two groups of PHT model rats and sham-operated rats (*P*>0.05 Table 3).

Table 2 Effects of LPS on portal hemodynamics of sham-operated and PHT rats

Group	PVF (mL·min ⁻¹)	PVP (kPa)	PVR (kPa·min·L ⁻¹)
Portal vein ligation	32.8±1.6	2.24±0.073	61
Control	22.6±1.7	1.86±0.044	71
Intrahepatic portal occlusion	28.0±2.1	1.95±0.054	61
Control	22.0±2.1	1.74±0.037	67
Sham-operated	34.8±0.7	1.80±0.046	44
Control	14.0±0.4	1.04±0.039	52

Table 3 Alteration of portal hemodynamics of the noncirrhotic and sham-operated rats after injection of LPS

Group	PVF (mL·min ⁻¹)	Increment (%)	PVP (kPa)	Increment (%)	PVR (kPa·min·L ⁻¹)	Increment (%)
PVL	10.2±0.8	45.13	0.38±0.047	20.43	-10	-14.08
IPO	6.4±1.14	27.27	0.21±0.026	12.07	-10	-8.96
Sham-operated	20.8±0.84	148.57	0.76±0.038	73.08	-8	-15.38

DISCUSSION

Portal hypertension (PHT) is mainly due to two factors, PVF and PVR. Increase of PVF could lead to portal congestion, and PVR could prevent portal output and lead to portal gore. PHT is apt to be associated with a series of cytokines and vasodilators^[19]. Endotoxin could enhance synthesis of a series of vasoconstrictors such as endothelins, as well as a series of vasodilators such as nitric oxide (NO). These modulators are able to adjust portal and systemic hemodynamics functionally. Across the cell's membrane, NO could spread to smooth muscle cells, enhance synthesis of cyclic guanosine monophosphate (cGMP), and consequently decrease intracellular Ca²⁺ concentrations, thus inducing vasorelaxation^[11]. NO could also increase cardiac output and lower the vessel's reaction to vasoconstrictors, causing systemic and splanchnic hyperdynamic circulation^[20,21]. Our research proved LPS could increase PVF of normal and noncirrhotic portal hypertensive rats and that this increase was associated with the dosage of LPS, which demonstrated increasing PVF was an important factor to form PHT. Endotoxemia could modulate the intrahepatic portal vessel and consequently alter the resistance of the intrahepatic portal vessel^[23, 24]. Endotoxin signals hepatic cells to secrete a series of cytokines such as tumor necrosis factor (TNF α) and endothelin and consequently enhances synthesis and deposition of collagens^[25-27]. Endothelin has been reported to be able to induce constriction of the smooth muscle cells of the hepatic vasculature^[28]. Endothelin can also prompt hepatic stellate cells (HSC) to proliferate and constrict^[29]. Endotoxin was thought to increase PVP by the ways above. However, endotoxin-induced increase of NO synthesized by inducible nitric oxide synthase could lead to vasorelaxation and lower the vessel's response to vasoconstrictors, which might account for the increase of PVR. Yokoyama reported the liver maintains its microcirculatory flow by vascular remodeling from the hepatic arterial vasculature following PVL^[30], which might induce the decrease of PVR in noncirrhotic

PHT rats. This research shows the PVR of normal and noncirrhotic PHT rats decreased after intraperitoneal injection of LPS, which demonstrated effectively that increasing PVF was the main factor to forming PHT.

PHT models moderate PVP through a new balance of vasoconstrictors and vasodilators^[1]. PHT model rats were reported to be sensitive to LPS^[15] by means of portal vein ligation. But Chu suggested some evidence against a role for endotoxin in the hyperdynamic circulation of rats with prehepatic portal hypertension^[5]. Our experiments show that after intraperitoneal injection of LPS, PVF and PVP of PVL and IPO model rats increased significantly less than that of sham-operated rats ($P < 0.01$). Another report found artery vessel of PVL rats more blunt to LPS and the increment of NOS was significantly less than sham-operated rats^[16], which might act as an explanation of our results. We would perform research with vasoconstrictors and vasodilators to further demonstrate our results.

REFERENCES

- Liu F, Li JX, Li CM, Leng XS. Plasm endothelin in patients with vasodilator in cirrhotic patients. *World J Gastroenterol* 2001; 7: 126-127
- Xu KD, Liu TF, Cing X. Significance of detection of plasm nitric oxide, endothelin, endotoxin in patients with liver cirrhosis. *World J Gastroenterol* 1998; 4(Suppl 2): 64
- Qin RY, Zou SQ, Wu ZD, Qiu FZ. Influence of splanchnic vascular infusion on the content of endotoxins in plasma and the translocation of intestinal bacteria in rats with acute hemorrhage necrosis pancreatitis. *World J Gastroenterol* 2000;6:577-580
- Mu Y, Shen YZ, Chu YF. Effects of tetrandrine on gastric mucosa and liver in portal hypertensive rats. *China Natl J New Gastroenterol* 1997;3:192-194
- Chu CJ, Lee FY, Wang SS, Chang FY, Lin HC, Lu RH, Wu SL, Chan CC, Tai CC, Lai IN, Lee SD. Evidence against a role for endotoxin in the hyperdynamic circulation of rats with prehepatic portal hypertension. *J Hepatol* 1999; 30: 1105-1111
- Zhang GL, Wang YH, Teng HL, Lin ZB. Effects of aminoguanidine on nitric oxide production induced by inflammatory cytokines and endotoxin in cultured rat hepatocytes. *World J Gastroenterol* 2001;7:331-334
- Feng ZJ, Feng LY, Sun ZM, Song M, Yao XX. Expression of nitric oxide synthase protein and gene in the splanchnic organs of liver cirrhosis and portal hypertensive rats. *World J Gastroenterol* 2000;6(Suppl 3):33
- Zhang GF, Zhang MA, Chen YR, Wang L. The roles of endothelin and nitric oxide in gastric mucosa injuries in rats with endotoxemia. *Shijie Huaren Xiaohua Zazhi* 2000;8(Suppl8):24
- Liu BH, Chen HS, Zhou JH, Xiao N. Effects of endotoxin on endothelin receptor in hepatic and intestinal tissues after endotoxemia in rats. *World J Gastroenterol* 2000;6:298-300
- Horie Y, Kato S, Ohki E, Tamai H, Ishii H. Role of endothelin in endotoxin-induced hepatic microvascular dysfunction in rats fed chronically with ethanol. *J Gastroenterol Hepatol* 2001;16:916-922
- Horie Y, Kimura H, Kato S, Ohki E, Tamai H, Yamagishi Y, Ishii H. Role of nitric oxide in endotoxin-induced hepatic microvascular dysfunction in rats chronically fed ethanol. *Alcohol Clin Exp Res* 2000; 24: 845-851
- Goulis J, Patch D, Burroughs AK. Bacterial infection in the pathogenesis of variceal bleeding. *Lancet* 1999; 353: 139-142
- Jia JB, Han DW, Xu RL, Gao F, Zhao LF, Zhao YC, Yan JP, Ma XH. Effect of endotoxin on fibronectin synthesis of rat primary cultured hepatocytes. *World J Gastroenterol* 1998;4:329-331
- Yang JM, Han DW, Xie CM, Liang QC, Zhao YC, Ma XH. Endotoxins enhance hepatocarcinogenesis induced by oral intake of thioacetamide in rats. *World J Gastroenterol* 1998;4:128-132
- Perez del Pulgar S, Pizcueta P, Engel P, Bosch J. Enhanced monocyte activation and hepatotoxicity in response to endotoxin in portal hypertension. *J Hepatol* 2000; 32: 25-31
- Heller J, Sogni P, Tazi KA, Chagneau C, Poirel O, Moreau R, Lebrec D. Abnormal regulation of aortic NOS2 and NOS3 activity and expression from portal vein-stenosed rat after lipopolysaccharide administration. *Hepatology* 1999; 30: 698-704
- Yachida S, Ikeda K, Kaneda K, Goda F, Maeba T, Maeta H. Preventive effect of preoperative portal vein ligation on endotoxin-induced hepatic failure in hepatectomized rats is associated with reduced tumour necrosis factor alpha production. *Br J Surg* 2000; 87: 1382-1390
- Li XN, Benjamin IS, Alexander B. A new rat model of portal hypertension induced by intraportal injection of microspheres. *World J Gastroenterol* 1998; 4: 66-69
- Perez del Pulgar S, Pizcueta P, Engel P, Bosch J, Rodes J. Neutrophil adhesion is impaired in the mesentery but not in the liver sinusoids of portal hypertensive rats. *Am J Physiol Gastrointest Liver Physiol* 2001; 280: G1351-1319
- Roberts LR, Kamath PS. Pathophysiology of variceal bleeding. *Gastrointest Endosc Clin N Am* 1999; 9: 167-174
- Wiest R, Groszmann RJ. Nitric oxide and portal hypertension: its role in the regulation of intrahepatic and splanchnic vascular resistance. *Semin Liver Dis* 1999; 19: 411-426
- Huang YQ, Xiao SD, Mo JZ, Zhang DZ. Effects of nitric oxide synthesis in hibitor in long/term treatment on hyperdynamic circulatory state in cirrhotic rats. *World J Gastroenterol* 2000;6(Suppl3):31
- Bauer M, Bauer I, Sonin NV, Kresge N, Baveja R, Yokoyama Y, Harding D, Zhang JX, Clemens MG. Functional significance of endothelin B receptors in mediating sinusoidal and extrasinusoidal effects of endothelins in the intact rat liver. *Hepatology* 2000; 31: 937-947
- Gandhi CR, Kuddus RH, Nemoto EM, Murase N. Endotoxin treatment causes an upregulation of the endothelin system in the liver: amelioration of increased portal resistance by endothelin receptor antagonism. *J Gastroenterol Hepatol* 2001; 16: 61-69
- Cho JJ, Hoher B, Herbst H, Jia JD, Raehl M, Hahn EG, Riecken EO, Schappan D. An oral endothelin-A receptor antagonist blocks collagen synthesis and deposition in advanced rat liver fibrosis. *Gastroenterology* 2000; 118: 1169-1178
- Wang X, Chen YX, Xu CF, Zhao GN, Huang YX, Wang QL. Relationship between tumor necrosis factor- α and liver fibrosis. *World J Gastroenterol* 1998;4:18
- Chu YK, Wu JS, Ma QJ, Gao DM, Wang X. Plasm TNF- α levels during the formation of liver cirrhosis and portal hypertension in rats. *Huaren Xiaohua Zazhi* 1998;6:755-756
- Garcia PJ, Zhang JX, Sonin N, Nakanishi K, Clemens MG. Ischemia/reperfusion induces an increase in the hepatic portal vasoconstrictive response to endothelin-1. *Shock* 1999; 11: 325-329
- Petrowsky H, Schmandra T, Lorey T. Endothelin-induced contraction of the portal vein in cirrhosis. *Eur Surg Res* 1999; 31: 289-296
- Yokoyama Y, Baveja R, Sonin N. Hepatic neovascularization after partial portal vein ligation: novel mechanism of chronic regulation of blood flow. *Am J Physiol Gastrointest Liver Physiol* 2001;280:G21-31

Edited by Pagliarini R

• BASIC RESEARCH •

The role of endotoxin, TNF- α , and IL-6 in inducing the state of growth hormone insensitivity

Ping Wang, Ning Li, Jie-Shou Li, Wei-Qin Li

Ping Wang, Ning Li, Jie-Shou Li, Wei-Qin Li, Medical College of Nanjing University, Research Institute of General Surgery, Jinling Hospital, Nanjing 210002, Jiangsu Province, China

Supported by the key project of the tenth-five foundation of PLA, No. 01Z011.

Correspondence to: Ping Wang, Research Institute of General Surgery, Jinling Hospital, 305 Zhong Shan East Road, Nanjing 210002, Jiangsu Province, China. wpmd@yahoo.com

Telephone: +86-25-4826808 Ext 58067

Received 2001-12-05 Accepted 2002-01-28

Abstract

AIM: Critical illnesses such as sepsis, trauma, and burns cause a growth hormone insensitivity, which leads to an increased negative nitrogen balance. Endotoxin is generously released into blood under these conditions and stimulates the production of proinflammatory cytokines such as TNF- α , IL-6, and IL-1, which may play a very important role in inducing the growth hormone insensitivity. The objective of this current study was to investigate the role of endotoxin, TNF- α and IL-6 in inducing the growth hormone insensitivity at the receptor and post-receptor levels.

METHODS: Spague-Dawley rats were injected with endotoxin, TNF- α , and IL-6, respectively and part of rats injected with endotoxin was treated with exogenous somatotropin simultaneously. All rats were killed at different time points. The expression of IGF-I, GHR, SOCS-3 and β -actin mRNA in the liver was detected by RT-PCR and the GH levels were measured by radioimmunoassay, the levels of TNF- α and IL-6 were detected by ELISA.

RESULTS: There was no significant difference in serum GH levels between experimental group and control rats after endotoxin injection, however, liver IGF-I mRNA expression had been obviously down-regulated in endotoxemic rats. Liver GHR mRNA expression also had a predominant down-regulation after endotoxin injection. The lowest regulation of liver IGF-I mRNA expression occurred at 12h after LPS injection, being decreased by 53% compared with control rats. For GHR mRNA expression, the lowest expression occurred at 8h and had a 81% decrease. Although SOCS-3 mRNA was weakly expressed in control rats, it was strongly up-regulated after LPS injection and had a 7.84 times increase compared with control rats. Exogenous GH could enhance IGF-I mRNA expression in control rats, but it did fail to prevent the decline in IGF-I mRNA expression in endotoxemic rats. Endotoxin stimulated the production of TNF- α and IL-6, and the elevated IL-6 levels was shown a positive correlation with increased SOCS-3 mRNA expression. The liver GHR mRNA expression was obviously down-regulated after TNF- α iv injection and had a 40% decrease at 8h, but the liver SOCS-3 mRNA expression was the 4.94 times up-regulation occurred at 40min after IL-6 injection.

CONCLUSION: The growth hormone insensitivity could be induced by LPS injection, which was associated with down-

regulated GHR mRNA expression at receptor level and with up-regulated SOCS-3 mRNA expression at post-receptor level. The in vivo biological activities of LPS were mediated by TNF- α and IL-6 indirectly, and TNF- α and IL-6 may exert their effects on the receptor and post-receptor levels respectively.

Wang P, Li N, Li JS, Li WQ. The role of endotoxin, TNF- α , and IL-6 in inducing the state of growth hormone insensitivity. *World J Gastroenterol* 2002;8(3):531-536

INTRODUCTION

Infection especially severe intra-abdominal infection is characterized by catabolic status associated with severe protein loss and negative nitrogen balance^[1-7]. Meantime, the levels of many important hormones such as glucocorticoid, insulin and growth hormone (GH) do not decline, but their biological activities have reduced obviously. Critical illnesses such as sepsis, trauma and burns can usually cause a elevated level of growth hormone at early stage, however the insulin-like growth factor I (IGF-I), which is a growth hormone-dependent growth factor that inhibits protein breakdown, has been showing decreased predominantly, this phenomenon indicating a status of growth hormone insensitivity^[8-12]. In this condition, the administration of high doses of recombinant human growth hormone could not improve negative nitrogen balance, in contrary, it may lead to other metabolic disorders and result in increased morbidity and mortality^[13].

Endotoxin is generously released into blood under the infected condition and stimulates the production of proinflammatory cytokines such as TNF- α , IL-6, and IL-1^[14-18], which play very important roles in inducing the GH insensitivity. The GH insensitivity can occur at receptor and post-receptor levels, the receptor level associates with down-regulated GHR mRNA expression^[19, 20]; the post-receptor insensitivity mainly occurs on the intracellular signal transduction pathway of growth hormone. Recent studies have suggested that the SOCS protein family, especially SOCS-3 play a very important role on this level^[21, 22]. In this study, we investigated whether the GH insensitivity could be induced by LPS, TNF- α and IL-6 iv injection, and what kind of roles they played.

MATERIALS AND METHODS

Animals

All experimental procedures were carried out in compliance with the appropriate institutional and national ethical guidelines for work with laboratory animals. 156 adolescent male Spague-Dawley rats (240-260g) were obtained from animal center of Jinling Hospital (Nanjing, China). They were given free access to food and water for three days before experiments.

Endotoxin and cytokines preparation

Escherichia coli lipopolysaccharide (LPS; serotype O111:B4 phenol extract), obtained from Sigma Chemical (St. Louis, MO), was resuspended in sterile endotoxin-free saline to obtain 4mg/ml

solutions. The recombinant rat TNF- α and IL-6 provided by Pepto Tech EC Ltd (London, England), were resuspended in sterile endotoxin-free saline to obtain 100000U/ml solutions. Human growth hormone, kindly provided by Serono, was resuspended in sterile endotoxin-free saline to obtain a 1mg/ml solution.

Experimental protocols

Male Spague-Dawley rats (provided by Animal Center of Jingling Hospital), weighing 250 ± 10 g, were given free access to food and water for three days before experiments. Rats were anesthetized with ether and received LPS, GH, TNF- α , IL-6, and saline injection. LPS, TNF- α , and IL-6 were administered through superficial dorsal veins of penis and GH was injected subcutaneously. All rats were killed at different time points; blood of rats with LPS injected was collected and centrifuged at 500g for 10min at 4°C to collect serum. Livers were removed, flash-frozen in liquid nitrogen, and stored at -80°C until homogenate preparation and RNA extraction.

Effect of endotoxin on liver expression of IGF-I, GHR, and SOCS-3 mRNA

After the 3-day adaptation period, 42 rats were randomly divided into laboratory group ($n=36$) and control group ($n=6$), LPS ($7.5\text{mg}\cdot\text{kg}^{-1}$ iv) was administered to the laboratory group, every six rats were killed at 1h, 2h, 4h, 8h, 12h, and 24h after injection. The control rats were given intravenous saline.

Effect of GH on liver expression of IGF-I, GHR, and SOCS-3 mRNA along with endotoxin injection

After 3-day adaptation period, 24 rats were divided into 4 groups (6 rats/group). The first group received one injection of LPS ($7.5\text{mg}\cdot\text{kg}^{-1}$ iv) and one injection of saline (sc), the second group received one injection of GH ($1.5\text{mg}\cdot\text{kg}^{-1}$ sc) and one injection of saline (iv), the third group received one injection of LPS ($7.5\text{mg}\cdot\text{kg}^{-1}$ iv) and one injection of GH ($1.5\text{mg}\cdot\text{kg}^{-1}$ sc), the fourth group received two injections of saline. All rats were killed at 10h after injection.

Effects of TNF- α and IL-6 on liver expression of GHR and SOCS-3 mRNA

After the 3-day adaptation period, 102 rats were randomly divided into laboratory group ($n=96$) and control group ($n=6$). Rat recombinant TNF- α and IL-6 ($100000\text{U}/\text{kg}\cdot\text{wt}$) were injected through the same pathway and every six rats were killed after 20min, 40min, 1h, 2h, 4h, 8h, 12h and 24h. The control rats were given intravenous saline.

Analysis of mRNA by RT-PCR

Fresh-frozen liver samples were homogenized and total RNA was performed using TRIZOL Reagent (Biobasic Inc, Scarborough, Ontario, Canada). With Access RT-PCR system kit (Promega Corporation, Madison, WI), the cDNA synthesis and amplification was done in one tube following the manufacture's instructions. In brief, $1\mu\text{g}$ RNA, $1\mu\text{M}$ primers for SOCS-3, GHR, IGF-I and β -actin were added to each reaction mixture respectively, which included 0.2mM dNTP, 1mM MgSO_4 , AMV reverse transcriptase 5U , Tfl DNA polymerase 5U , and AMV/Tfl $5\times$ buffer $10\mu\text{L}$. The reaction final volume was $50\mu\text{L}$ and was covered with $30\mu\text{L}$ mineral oil. RT-PCR reaction was run in the following procedures: (1)Reverse transcription: 48°C for 45min, 1 cycle. (2)AMV RT inactivation and RNA/cDNA/primers denaturation: 94°C for 2min, 1 cycle. (3) Second strand cDNA synthesis and PCR amplification: denaturation 94°C for 30s, annealing 60°C for 1min, extension 68°C for 2min, 28 cycles for SOCS-3 and 21 cycles for GHR and IGF-I, β -actin as intra-control to be amplified along with SOCS-3, GHR and IGF-I. (4)

Final extension: 68°C for 7min, 1 cycle. $5\mu\text{L}$ each RT-PCR reaction was electrophoresed in a 1.7% Metaphor agarose (FMC Bioproducts, Rockland, ME) gel and stained with ethidium bromide. Products of RT-PCR reactions were photographed and analyzed by densitometry. The expression of IGF-I, GHR, and SOCS-3 mRNA in laboratory group is represented as a percentage or times compared with their expression in control group.

Polymerase chain reaction primers were as follows: IGF-I sense, (5') CAC ATC TCT TCT ACC TGG CAC TC (3'); IGF-I antisense, (5') GGA TGG AAC GAG CTG ACT TTG TA (3'), to give a 270 base pair product; GHR sense, (5') CTG GGT TGA GTT CAT TGA GCT GGA T (3'); GHR antisense, (5') TGT AGA GGG GAG TTG GTG GGT TGA C (3'), to give a 394 base pair product; SOCS-3 sense, (5') ACC AGC GCC ACT TCT TCA CG (3'); and SOCS-3 antisense, (5') GTG GAG CAT CAT ACT GAT CC (3'), to give a 450 base pair product; β -actin sense, (5') CAT TTC CGG TGC ACG ATG GAG (3'); β -actin antisense, (5') GCC ATC CTG CGT CTG GAC CTG (3'), to give a 599 base pair production. All primers spanned at least one intron of genomic DNA.

Serum levels of GH, TNF- α and IL-6

Blood was obtained from the inferior vena cava at the time of sacrifice. Serum growth hormone levels was measured by radioimmunoassay according to manufacture's instructions (Northern Isotope Co, Beijing, China). Serum samples were analyzed for TNF- α and IL-6 content by enzyme-linked immunosorbent assay according to manufacture's instructions (BioSource International, Camarillo, CA).

Statistics analysis

All data are expressed as means \pm SEM. Correlation between data was analyzed with linear regression. Comparisons between two groups were performed using an unpaired Student's t test. Differences were considered statistically significant when $P < 0.05$.

RESULTS

Levels of serum growth hormone after endotoxin injection

The levels of serum growth hormone at each time points after LPS injection had no significant difference compared with control rats, it maintained a relatively stable status (Table 1).

Table 1 Serum GH levels in LPS injected rats at different time points and control rats

	<i>n</i>	GH levels(ng/ml)
Control	6	2.19 ± 0.48
1h	6	1.85 ± 0.37^a
2h	6	1.95 ± 0.45^a
4h	6	1.76 ± 0.27^a
8h	6	1.79 ± 0.27^a
12h	6	1.77 ± 0.20^a
24h	6	1.79 ± 0.55^a

^aStatistically no difference compared with control rats.

Liver IGF-I mRNA expression

Liver IGF-I mRNA expression had already declined by 25% vs. control rats at 8 hours. On the time of 12 hours, we observed the lowest level of expression, which was a 53% decrease compared with control rats. It did not recover to the normal level and had a 15% reduction at 24 hours (Figure 1A, 1B). Although exogenous GH administration in control rats significantly enhanced the liver IGF-I mRNA expression, it did fail to prevent its decline in endotoxemic rats (Figure 1C).

Liver GHR mRNA expression

Liver GHR mRNA expression had already down-regulated by 45% at 2 hours after LPS injection, the lowest regulation occurred at 8 hours, which was a 89% decrease compared with control rats. After 24 hours, it did not recover to the normal level and had a 44% decrease (Figure 2A, 2B). the exogenous GH administration had no effect on the liver GHR mRNA expression in control and endotoxemic rats (Figure 2C).

Liver SOCS-3 mRNA expression

The liver SOCS-3 mRNA was weakly expressed in control rats, however, it was strongly up-regulated by 7.84 times *vs.* control rats at 1 hour after LPS injection. This level was maintained at 2 hours and it still had a 1.8 times increase at 24 hours (Figure 3A, 3B). the exogenous GH infusion had no effect on the liver SOCS-3 mRNA expression in control and endotoxemic rats (Figure 3C).

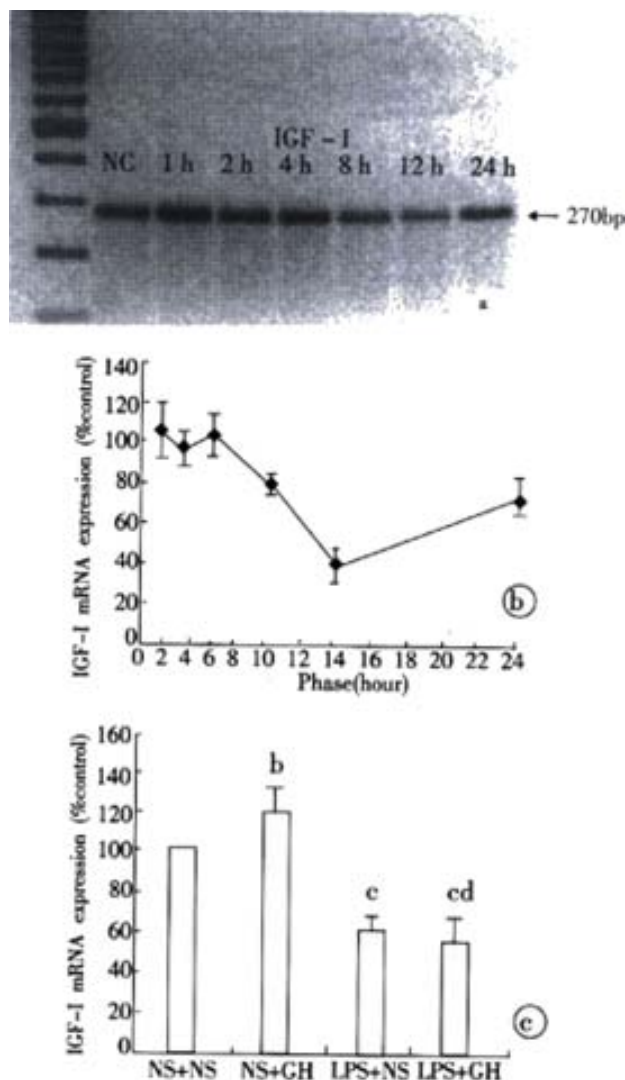


Figure 1 (A, B) Liver IGF-I mRNA expression response to endotoxin injection at different time points. (C) Liver IGF-I mRNA expression after single GH injection and endotoxin injection along with or without GH injection. ^b*P*<0.05 compared with NS+NS group, ^c*P*<0.01 *vs* NS+NS group, ^d*P*>0.05 compared with LPS+NS group. NS as saline injection.

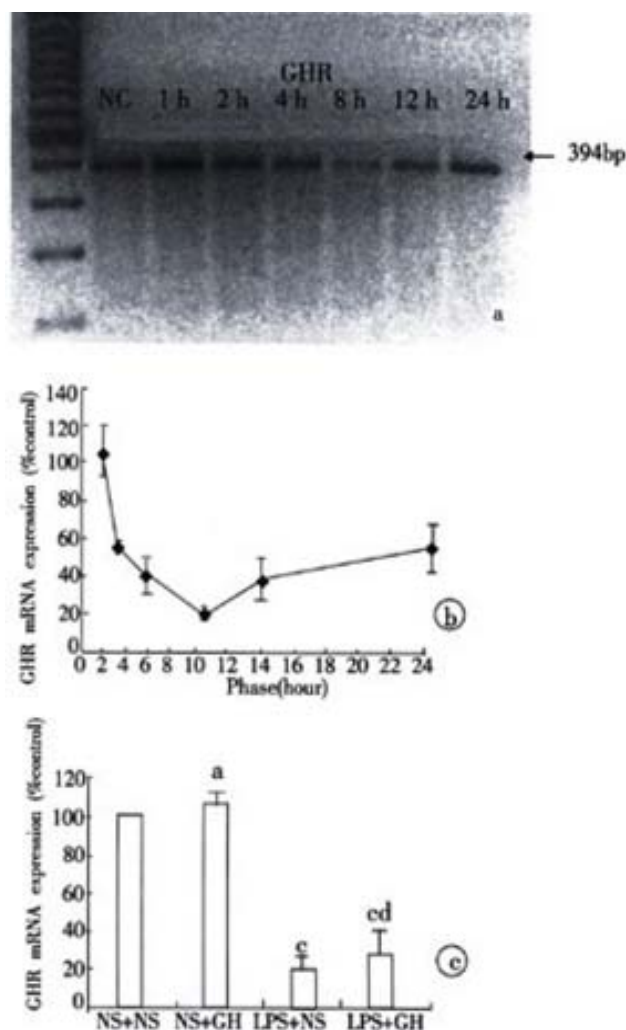


Figure 2 (A, B) Liver GHR mRNA expression responded to endotoxin injection at different time points. (C) Liver GHR mRNA expression after single GH injection and endotoxin injection along with or without GH injection. ^a*P*>0.05 compared with NS+NS group, ^c*P*<0.01 *vs* NS+NS group, ^d*P*>0.05 compared with LPS+NS group. NS as saline injection.

Levels of serum TNF- α and IL-6 after LPS injection and the correlation between liver SOCS-3 mRNA expression and IL-6 concentration

The TNF- α level was increased rapidly after LPS injection, but it decreased obviously from the second hour and returned to the normal level at 4h. The IL-6 level was also elevated rapidly after LPS injection; it got to the highest level at 2h and then decreased gradually (Table 2). Linear regression analysis was shown a positive correlation of IL-6 with liver SOCS-3 mRNA expression ($r=0.935$, $P<0.01$).

Table 2 Serum TNF- α and IL-6 levels in LPS injected rats at different time points and control rats

	<i>n</i>	TNF- α levels(pg/ml)	IL-6 levels(pg/ml)
Control	6	<20	<8
1h	6	342.80 \pm 50.01	1438.74 \pm 323.07
2h	6	75.81 \pm 11.50	1678.03 \pm 126.57
4h	6	<20	1332.67 \pm 120.95
8h	6	<20	142.59 \pm 48.07
12h	6	<20	48.75 \pm 10.57
24h	6	<20	46.82 \pm 11.64

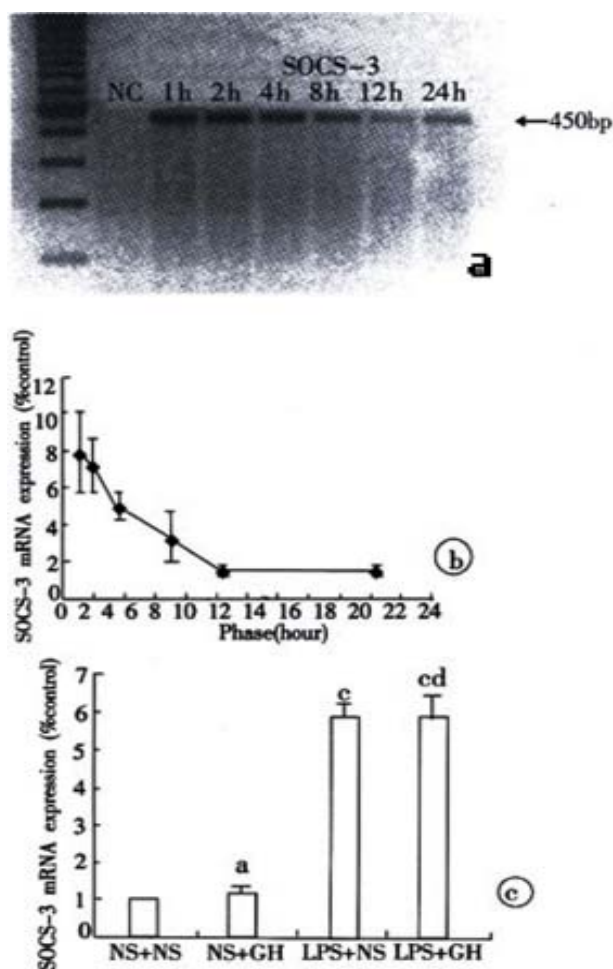


Figure 3 (A, B) Liver SOCS-3 mRNA expression response to endotoxin injection at different time points. (C) Liver SOCS-3 mRNA expression after endotoxin injection along with or without GH injection. ^a*P*>0.05 compared with NS+NS group, ^c*P*<0.01 vs NS+NS group, ^d*P*>0.05 compared with LPS+NS(7.5) group. NS as saline injection.

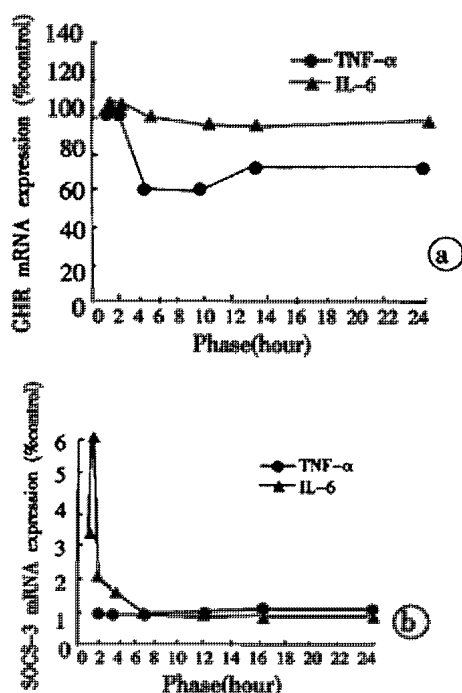


Figure 4 Liver GHR(A) and SOCS-3(B) mRNA expression response to TNF-α and IL-6 iv injection at different time points.

Effects of TNF-α and IL-6 on liver expression of GHR and SOCS-3 mRNA

The liver GHR mRNA expression after TNF-α injection had already down-regulated at 4 hours and it reached the lowest level at 8 hours, which was a 40% decrease compared with control rats. At 24 hours, a 27% reduction still existed. The IL-6 injection had no effect on the liver GHR mRNA expression at different time points (Figure 4A). The liver SOCS-3 mRNA had weak expressions at all time points after TNF-α injection, no difference could be found compared with control rats. The IL-6 injection was able to up-regulate rapidly the liver SOCS-3 mRNA expression, the latter showing a 2.73 times increase at 20 minutes and the highest level occurred at 40 minutes with a 4.94 times increase compared with control rats (Figure 4B).

DISCUSSION

In this report, using an experimental method of *E. coli* endotoxin infusion in laboratory rats, we have found endotoxin-induced growth hormone insensitivity. At 12 hours after LPS injection, there was no difference in serum growth hormone concentration between the experimental and control rats, however, the liver IGF-I mRNA expression had already declined obviously. In control rats, the liver IGF-I mRNA expression was up-regulated by 25% after exogenous GH administration, but in endotoxemic rats, GH did fail to prevent the decline in liver IGF-I mRNA expression. Several groups have observed that decreased IGF-I may result from a state of GH insensitivity. Ross *et al*^[8] reported low circulating IGF-I levels in critically ill patients despite elevated GH secretion. More recently, the study^[19] showed that after a single injection of LPS in rats, plasma IGF-I level remained low despite the fact that GH level had returned to normal value. In agreement with these authors, our study support the possibility that the GH insensitivity maybe one of the important factors for the reduced liver IGF-I mRNA expression after LPS injection.

Growth hormone insensitivity can occur at receptor and post receptor levels, on the receptor level GH insensitivity is associated with the reduced GHR numbers on target cell surface^[19,20]. Because of the shorter half-life of liver GHR (30-40min)^[23] and the decreased liver GHR mRNA expression by endotoxin, these led to the reduced GHR synthesis. Our results shown that liver GHR mRNA expression was obviously down-regulated after LPS injection, manifested that LPS had effect on the receptor level GH insensitivity indeed.

The factor of post-receptor level GH insensitivity has caused more and more attention recently, and it is associated with a novel family of suppressor of cytokine signalling (SOCS) which includes eight members (SOCS-1 to SOCS-7 and CIS) that act in a classical negative feedback loop to regulate cytokine signal transduction^[24-29]. SOCS-3 is a strong inhibitor on growth hormone intracellular signal transduction^[30-32].

Once growth hormone binds to its receptor, the intracellular signal transduction is activated through JAK-STAT pathway^[33,34]. The first activated tyrosine kinase is JAK2, which promotes the tyrosyl phosphorylation of both JAK2 itself and signal transducer and activator of transcription 5b (STAT 5b). Phosphorylated STAT 5b causes its dimerization and then the dimerized STAT 5b translocates into the nucleus, where it binds with high affinity to the promoters of various target genes and then activates the gene transcription such as IGF-I. SOCS-3 can block the GH intracellular JAK/STAT-dependent signaling pathway at different levels^[35-44], including competitively inhibits the phosphorylation of STAT 5b. Binds to GHR and leads to the degradation of GHR-JAK2 compound directly or indirectly through Elongin B and Elongin C, in the end the JAK2 kinase loses its activity. Through binding to GHR, SOCS-3 can inhibit the JAK2 kinase activity directly. Our experiment observed that after LPS injection, liver SOCS-3 mRNA expression was rapidly up-regulated with a 7.84 times increase at 1 hour compared with the weak expression in control rats, this

indicating that LPS induced the production of post-receptor GH insensitivity.

The *in vivo* biological activities of LPS are largely mediated by the production of proinflammatory cytokines such as tumor necrosis factor- α (TNF- α), interleukin-1 β (IL-1 β), and IL-6^[45-50], which is illustrated in our experiment by the marked stimulation of the secretion of TNF- α and IL-6 in blood. TNF- α and IL-6 had different roles in inducing the GH insensitivity, TNF- α injection leading to a reduced expression of liver GHR mRNA, and IL-6 being associated with the up-regulated SOCS-3 mRNA expression after injection. The elevated IL-6 levels stimulated by LPS had significant positive correlation with the increased liver SOCS-3 mRNA expression induced by LPS.

The mechanisms of TNF- α -induced GHR mRNA suppression was mostly mediated by inhibition of Sp transactivator binding to the L2 promoter of GHR gene^[51], the other way might be associated with some other cytokines stimulated by TNF- α , such as IL-1^[52]. Both IL-6 and GH, belonging to the cytokine receptor superfamily, can transduce their signal from cell surface to nucleus through the same JAK-STAT pathway^[53-55]. Hence, the elevated IL-6 levels stimulated by LPS promoted the increased expression of SOCS-3 mRNA, which not only had a negative feedback to IL-6 biological activities, but also inhibited the GH intracellular signal transduction^[56-60].

In summary, our study observed that the growth hormone insensitivity could be induced by endotoxin, which suggested that the endotoxin played a very important role in inducing the GH insensitivity. The endotoxin not only had predominant effect on the GHR gene expression, but also induced the phenomenon of negative feedback loop at post-receptor level. The toxic effect of endotoxin was mostly mediated by TNF- α and IL-6 indirectly, and TNF- α mainly had effect on the receptor gene expression, but for IL-6, it mainly caused the negative feedback loop at post-receptor level.

REFERENCES

- Wu XN. Current concept of pathogenesis of severe acute pancreatitis. *World J Gastroenterol* 2000;6:32-36
- Wu XN. Treatment revisited and factors affecting prognosis of severe acute pancreatitis. *World J Gastroenterol* 2000;6:663-665
- Zhang JJ, Dong WF, Zhu ZY. The clinical significance and rational evaluation of early nutritional support in severe head-injured patients. *World J Gastroenterol* 2000;6(Suppl3):20
- Chen QP. Enteral nutrition and acute pancreatitis. *World J Gastroenterol* 2001;7:185-192
- Mitch WE, Bailey JL, Wang X, Jurkovitz C, Newby D, Price SR. Evaluation of signals activating ubiquitin-proteasome proteolysis in a model of muscle wasting. *Am J Physiol* 1999;276:C1132-C1138
- Breuille D, Voisin L, Contrepoint M, Arnal M, Rose F, Obled C. A sustained rat model for studying the long-lasting catabolic state of sepsis. *Infect Immun* 1999;67:1079-1085
- Voisin L, Breuille D, Combaret L, Pouyet C, Taillandier D, Aurousseau E, Obled C, Attia D. Muscle wasting in a rat model of long-lasting sepsis results from the activation of lysosomal, Ca²⁺-activated, and ubiquitin-proteasome proteolytic pathways. *J Clin Invest* 1996;97:1610-1617
- Ross BJM, Chew SL. Acquired growth hormone resistance. *Eur J Endocrinol* 1995; 132:655-660
- Bhutta ZA, Bang P, Karlsson E, Hagenas L, Nizami SQ, Soder O. Insulin-like growth factor I response during nutritional rehabilitation of persistent diarrhoea. *Arch Dis Child* 1999;80:438-442
- Vary TC, Dardevet D, Grizard J, Voisin L, Buffiere C, Denis P, Breuille D, Obled C. Differential regulation of skeletal muscle protein turnover by insulin and IGF-I after bacteremia. *Am J Physiol* 1998;275:E584-E593
- Bjarnason R, Wickelgren R, Hermansson M, Hammarqvist F, Carlsson B, Carlsson LMS. Growth hormone treatment prevents the decrease in insulin-like growth factor I gene expression in patients undergoing abdominal surgery. *J Clin Endocrinol Metab* 1998;83:1566-1572
- Hobler SC, Williams AB, Fischer JE, Hasselgren PO. IGF-I stimulates protein synthesis but does not inhibit protein breakdown in muscle from septic rats. *Am J Physiol* 1998;274:R571-R576
- Takala J, Roukonen E, Webster NR, Nielsen MS, Zandstra DF, Vundelinckx G, Hinds CJ. Increased mortality associated with growth hormone treatment in critically ill adults. *N Engl J Med* 1999;341:785-792
- Wang JY, Wang XL, Liu P. Detection of serum TNF- α , IFN- γ , IL-6 and IL-8 in patient with hepatitis B. *World J Gastroenterol* 1999;5:38-40
- Sanlioglu S, Williams CM, Samavati L, Butler NS, Wang G, McCray PB, Ritchie TC, Hunninghake GW, Zandi E, Engelhardt JF. Lipopolysaccharide induces rac1-dependent reactive oxygen species formation and coordinates tumor necrosis factor- α secretion through IKK regulation of NF- κ B. *J Biol Chem* 2001;276:30188-30198
- Ebong SJ, Goyyert SM, Nemzek JA, Kim J, Bolgos GL, Remick DG. Critical role of CD14 for production of proinflammatory cytokines and cytokine inhibitors during sepsis with failure to alter morbidity or mortality. *Infect Immun* 2001;69:2099-2106
- Krakauer T. Suppression of endotoxin- and staphylococcal exotoxin-induced cytokines and chemokines by a phospholipase C inhibitor in human peripheral blood mononuclear cells. *Clin Diagn Lab Immunol* 2001;8:449-453
- Massoudy P, Zahler S, Becker BF, Braun SL, Barankay A, Meisner H. Evidence for inflammatory responses of the lungs during coronary artery bypass grafting with cardiopulmonary bypass. *Chest* 2001;119:31-36
- Defalque D, Brandt N, Ketelslegers JM, Thissen JP. GH insensitivity induced by endotoxin injection is associated with decreased liver GH receptors. *Am J Physiol* 1999;276:E565-E572
- Hermansson M, Wickelgren RB, Hannarquist F, Bjarnason R, Wennstrom I, Wernerman J, Carlsson B, Carlsson LM. Measurement of human growth hormone receptor messenger ribonucleic acid by a quantitative polymerase reaction-based assay: demonstration of reduced expression after elective surgery. *J Clin Endocrinol Metab* 1997;82:421-428
- Nicholson SE, Hilton DJ. The SOCS protein: a new family of negative regulators of signal transduction. *J Leuko Biol* 1998;63:665-668
- Alexander WS, Starr R, Metcalf D, Nicholson SE, Farley A, Elefanti AG, Brysha M, Kile BT, Richardson R, Baca M, Zhang JG, Willson TA, Viney EM, Sprigg NS, Rakar S, Corbin J, Mifsud S, Dirago L, Cary D, Nicola NA, Hilton DJ. Suppressors of cytokine signaling (SOCS): negative regulators of signal transduction. *J Leukoc Biol* 1999;66:588-592
- Frick GP, Tai LR, Baumbach WR, Goodman HM. Tissue distribution, turnover, and glycosylation of the long and short growth hormone receptor isoforms in rat tissues. *Endocrinology* 1998;139:2824-2830
- Kreba DL, Hilton DJ. SOCS proteins: negative regulators of cytokine signaling. *Stem Cells* 2001;19:378-387
- Stoiber D, Kovarik P, Cohnsey S, Johnston JA, Steinlein P, Decker T. Lipopolysaccharide induces in macrophages the synthesis of the suppressor of cytokine signaling 3 and suppresses signal transduction in response to the activating factor IFN- γ . *J Immunol* 1999;163:2640-2647
- Pezet A, Favre H, Kelly PA, Edery M. Inhibition and restoration of prolactin signal transduction by suppressor of cytokine signaling. *J Biol Chem* 1999;274:24497-24502
- Bjerkbak C, Haschimi KE, Frantz JD, Flier JS. The role of SOCS-3 in leptin signaling and leptin resistance. *J Biol Chem* 1999;274:30059-30065
- Hilton DJ, Richardson RT, Alexander WS, Viney EM, Willson TA, Sprigg NS, Starr R, Nicholson SE, Metcalf D, Nicola NA. Twenty proteins containing a C-terminal SOCS box form five structural classes. *Proc Natl Acad Sci USA* 1998;95:114-119
- Gisselbrecht S. The CIS/socs proteins: a family of cytokine-inducible regulators of signaling. *Euro Cytokine Network* 1999;10:463-470
- Mao Y, Ling PR, Fitzgibbons TP, McCowen KC, Frick GP, Bistrrian BR, Smith RJ. Endotoxin-induced inhibition of growth hormone receptor signaling in rat liver *in vivo*. *Endocrinology* 1999;140:5505-5515
- Petra TE, Amilcar FM, Anneli SE, Lena S, Gunnar N. Growth hormone regulation of SOCS-2, SOCS-3, and CIS messenger ribonucleic acid expression in the rat. *Endocrinology* 1999;140:3693-3704
- Adams TE, Hansen JA, Starr R, Nicola NA, Hilton DJ, Billestrup N. Growth hormone preferentially induces the rapid, transient expression of SOCS-3, a novel inhibitor of cytokine receptor signaling. *J Biol Chem* 1998;273:1285-1287
- Argetsinger LS, Christin CS. Mechanism of signaling by growth hormone receptor. *Physiol Rev* 1996;74:1089-1107
- Han Y, Leaman DW, Watling D, Rogers NC, Groner B, Kerr IM, Wood WI, Stark GR. Participation of JAK and STAT proteins in growth hormone-induced signaling. *J Biol Chem* 1996;271:5947-5952
- Hansen JA, Lindberg K, Hilton DJ, Nielsen JH, Billestrup N. Mechanism of inhibition of growth hormone receptor signaling by suppressor of cytokine signaling proteins. *Mol Endocrinol* 1999;13:1832-1843
- Ram PA, Waxman DJ. SOCS/CIS protein inhibition of growth hormone-stimulated STAT5 signaling by multiple mechanisms. *J Biol Chem* 1999;274:35553-35561
- Zhang JG, Farley A, NicholSEN SE, Willson TA, Zugarot LM, Simpsont RJ, Moritz RL, Cary D, Richardson R, Hausmann G, Kile BJ, Kent SBH, Alexander WS, Metcalf D, Hilton DJ, Nicola NA, Baca M. The conserved SOCS box motif in suppressors of cytokine signaling binds to elongin B and C and may couple bound proteins to proteasomal degradation. *Proc Natl Acad Sci USA* 1999;96:2071-2076
- Biosclair YR, Wanf JR, Shi JR, Hurst KR, Ooi GT. Role of the suppressor of cytokine signaling-3 in mediating the inhibitory effects of

- interleukin-1 β on the growth hormone-dependent transcription of the acid-labile subunit gene in liver cells. *J Biol Chem* 2000;275:3841-3847
- 39 Schaefer F, Chen Y, Tsao T, Nouri P, Rabkin R. Impaired JAK-STAT signal transduction contributes to growth hormone resistance in chronic uremia. *J Clin Invest* 2001;108:467-475
- 40 Kamizono S, Hanada T, Yasukawa H, Minoguchi S, Kato R, Minoguchi M, Hattori K, Hatakeyama S, Yada M, Morita S, Kitamura T, Kato H, Nakayama K, Yoshimura A. The SOCS box of SOCS-1 accelerates ubiquitin-dependent proteolysis of TEL-JAK2. *J Biol Chem* 2001;276:12530-12538
- 41 Ram PA, Waxman DJ. Role of the cytokine-inducible SH2 protein CIS in desensitization of STAT5b signaling by continuous growth hormone. *J Biol Chem* 2000;275:39487-39496
- 42 Sasaki F, Yasukawa I, Shouda T, Kitamura T, Dikic I, Yoshimura A. CIS3/SOCS-3 suppresses erythropoietin(EPO) signaling by binding the EPO receptor and JAK2. *J Biol Chem* 2000;275:29338-29347
- 43 Cohnsey SJ, Sanden D, Cacalano NA, Yoshimura A, Mui A, Migone TS, Johnston JA. SOCS-3 is tyrosine phosphorylated in response to interleukin-2 and suppresses STAT5 phosphorylation and lymphocyte proliferation. *Mol Cell Biol* 1999;19:4980-4988
- 44 Song MM, Shuai K. The suppressor of cytokine signaling (SOCS)1 and SOCS3 but not SOCS2 proteins inhibit interferon-mediated antiviral and antiproliferative activities. *J Biol Chem* 1998;273:35056-35062
- 45 Dinarello CA. proinflammatory cytokines. *Chest* 2000;118:503-508
- 46 Iwagaki A, Porro M, Pollack M. Influence of synthetic antiendotoxin peptides on lipopolysaccharide(LPS) recognition and LPS-induced proinflammatory cytokine responses by cell expressing membrane-bound CD14. *Infect Immun* 2000;68:1655-1663
- 47 Zhao B, Brauner A, Li YH, Normark S. Expression of and cytokine activation by Escherichia coli curli fibers in human sepsis. *J Infect Diseases* 2000;181:602-612
- 48 Bruggen TVD, Jenhuis SN, Raaij EV, Verhouf J, Asbeck BSV. Lipopolysaccharide-induced tumor necrosis factor alpha production by human monocytes involves the Raf-1/MEK1-MEK2/ERK1-ERK2 pathway. *Infect Immun* 1999;67:3824-3829
- 49 Soltys J, Quinn MT. Modulation of endotoxin- and enterotoxin-induced cytokine release by in vivo treatment with β -(1,6) branched β -(1,3)-glucan. *Infect Immun* 1999;67:244-252
- 50 Thissen JP, Verniers J. Inhibition by interleukin-1 β and tumor necrosis factor- β of the insulin-like growth factor I messenger ribonucleic acid response to growth hormone in rat hepatocyte. *Endocrinology* 1997;138:1078-1084
- 51 Denson LA, menon RK, Shaufl A, Bajwa HS, Williams CR, Karpen SJ. TNF- α downregulates murine hepatic growth hormone receptor expression by inhibiting Sp1 and Sp3 binding. *J Clin Invest* 2001; 107:1451-1458
- 52 Wolf M, Bohm S, Brand M, Kreymann G. Proinflammatory cytokines interleukin-1 β and tumor necrosis factor- α inhibit growth hormone stimulation of insulin-like growth factor I synthesis and growth hormone receptor mRNA levels in cultured rat liver cells. *Eur J Endocrinol* 1996;135:729-737
- 53 Heinrich PC, Behrmann I, Newen GM, Schaper F, Graeve L. Interleukin-6-type cytokines signaling through the gp130/Jak/STAT pathway. *Biochem J* 1998;334:297-314
- 54 Kishimoto T, Akira S, Narazaki M, Taga T. Interleukin-6 family of cytokines and gp130. *Blood* 1995;86:1243-1254
- 55 Chen TS, wang LH, Farrar WL. Interleukin 1 activates androgen receptor-mediated gene expression through a signal transducer and activator of transcription 3-dependent pathway in LNCap prostate cancer cells. *Cancer Res* 2000;60:2132-2135
- 56 Paul C, Seilliez I, Thissen JP, Cam AL. Regulation of expression of the rat SOCS-3 gene in hepatocytes by growth hormone, interleukin-6 and glucocorticoids. *Eur J Biochem* 2000;267:5849-5857
- 57 Narazaki M, Fujimoto M, Matsumoto T, Morita Y, Saito H, Kajita T, Yashizaki K, Naka T, Kishimoto T. Three distinct domains of SSI-1/SOCS-1/JAB protein are required for its suppression of interleukin-6 signaling. *Proc Natl Acad Sci USA* 1998;95:13130-13134
- 58 Nicholson SE, Willson TA, Farley A, Starr R, Zhang JG, Baca M, Alexander WS, Metcalf D, Hilton DJ, Nicola NA. Mutational analyses of the SOCS proteins suggest a dual domain requirement but distinct mechanisms for inhibition of LIF and IL-6 signal transduction. *EMBO J* 1999;18:375-385
- 59 Terstegen L, Gatsios P, Bode JG, Schaper F, Heinrich PC, Graeve L. The inhibition of interleukin-6-dependent STAT activated protein kinases depends on tyrosine 795 in the cytoplasmic tail of glycoprotein 130. *J Biol Chem* 2000;275:18810-18817
- 60 Schmitz J, Weissenbach M, Haan S, Heinrich PC, Schaper F. SOCS-3 exerts its inhibitory function on interleukin-6 signal transduction through the SHP2 recruitment site of gp130. *J Biol Chem* 2000;275:12848-12856

Edited by Zhao P

• BASIC RESEARCH •

Distribution of constitutive nitric oxide synthase in the jejunum of adult rat

Yan-Min Chen, Zhong-Ming Qian, Jian Zhang, Yan-Zhong Chang, Xiang-Lin Duan

Yan-Min Chen, Jian Zhang, Yan-Zhong Chang, Xiang-Lin Duan, Life Science College, Hebei Normal University, Shijiazhuang 050016, Hebei Province, China

Zhong-Ming Qian, Department of Applied Biology and Chemical Technology, The Hong Kong Polytechnic University, Hung Hom, Kowloon, Hong Kong

Supported by Natural Science Foundation of Hebei Province; Education Department Foundation of Hebei Province. No. 2002136.

Correspondence to: Xiang-Lin Duan, Life Science College, Hebei Normal University, Shijiazhuang 050016, Hebei Province, China. dxlzh@sj-user.he.cninfo.net

Telephone: +86-311-6049941 Ext.86480 Fax: +86-311-5828784

Received 2002-01-11 Accepted 2002-01-28

Abstract

AIM: To study the distribution of the constitutive nitric oxide synthase (NOS) in the jejunum of adult rat.

METHODS: The distribution of endothelial NOS (eNOS) was detected by immunohistochemistry. Immunofluorescence histochemical dual staining technique were used for studying the distribution of neuronal NOS (nNOS) and eNOS. The dual stained slides were observed under a confocal laser scanning microscope.

RESULTS: Positive neuronal NOS (nNOS) and endothelial NOS (eNOS) cells were found to be distributed in lamina propria of villi, and the epithelial cell was not stained. eNOS was mainly located in submucosal vascular endothelia, while nNOS was mainly situated in myenteric plexus. Some cells in the villi had both nNOS and eNOS. More than 80% of the cells were positive for both nNOS and eNOS, the rest cells were positive either for nNOS or for eNOS.

CONCLUSION: The two constitutive nitric oxide synthases are distributed differently in the jejunum of rat. nNOS distributed in myenteric plexus is a neurotransmitter in the non-adrenergic non-cholinergic (NANC) inhibitory nerves. eNOS distributed in endothelial and smooth muscle cells of blood vessels plays vasodilator role. eNOS and nNOS are coexpressed in some cells of lamina propria of villi. NO generated by those NOS is very important in the physiological and pathological process of small intestine.

Chen YM, Qian ZM, Zhang J, Chang YZ, Duan XL. Distribution of constitutive nitric oxide synthase in the jejunum of adult rat. *World J Gastroenterol* 2002;8(3):537-539

INTRODUCTION

Nitric oxide (NO) is an intercellular and endocellular signal molecule, and has an important role in the physiological process of intestine. For example, NO can regulate muscular contraction and blood circulation of the intestine^[1,2]. Nitric oxide synthase (NOS) is widely distributed in the intestine, and has several isoforms, such as constitutive nitric oxide synthase (nNOS and eNOS) and inducible NOS (iNOS)^[3]. In previous studies, NOS was mostly located in small intestine and could be shown by enzyme cytochemistry, but different isoforms of NOS^[4-8] could not be distinguished. In order to study the characteristics and distribution of NOS,

immunohistochemistry and immunofluorescence histochemical dual staining technique were used to investigate the distribution of the constitutive nitric oxide synthase (NOS) in the jejunum of adult rat, to provide morphological basis of digestive physiology.

MATERIALS AND METHODS

Specimens

Segments (1-2cm) of the jejunum were removed from decapitated male Sprague-Dawley rats (250-300g) and placed immediately in a fixative consisting of 4% paraformaldehyde and 0.1 M phosphate buffer (PB, pH7.4). The fixed jejunum segments were rinsed for at least 12h at 4°C in 0.1 M PB (pH7.2) containing 30% sucrose, and then cryostat sections were made at 6µm thickness and mounted onto glass slides.

Reagents

Rabbit anti-rat eNOS antibody and SP kit were purchased from Beijing Zhongshan Biotechnical Company. Mouse anti-rat nNOS antibody, FITC-conjugated anti-mouse IgG and PE-conjugated anti-rabbit IgG were purchased from Wuhan Boster Biological Technology Company.

Immunohistochemistry

Immunohistochemical staining for eNOS was performed using SP technique with the following procedure.

(1)The slides were washed in 0.01 M phosphate-buffered saline (PBS). Endogenous peroxidase was blocked by 0.3% H₂O₂ in methanol for 25 minutes, followed by incubation in normal goat serum for 30 minutes at room temperature. (2)The slides were incubated with a 1 : 75 dilution of the primary rabbit anti-rat eNOS antibody for 12 hour at 4°C. A biotin-streptavidin detection system was employed with diaminobenzidine as the chromogen. (3)Then the slides were washed with PBS and incubated with a reagent (biotinylated anti-immunoglobulin) for 60 minutes at 37°C. After rinsing in PBS, the slides were incubated with the peroxidase-conjugated streptavidin label for 60 minutes at 37°C, and incubated with diaminobenzidine and H₂O₂ for 5 minutes. Finally the sections were counterstained with hematoxylin.

Immunofluorescence histochemical dual-staining technique

The slides were incubated with normal goat serum for 30 minutes, followed by incubation with rabbit anti-rat eNOS antibody and mouse anti-rat nNOS antibody for 48 hour at 4°C. Then, These were washed with PBS and incubated with FITC-conjugated anti-mouse IgG and PE-conjugated anti-rabbit IgG for 24 hour at 4°C. After rinsing in PBS, the slides were observed under a confocal laser scanning microscope (MR/A₂, Nikon). Excitation of FITC and PE were 488 and 495 nm respectively, emission of FITC and PE were 525 and 578 nm. 0.01 M PBS was used as a substitute for primary antibody for negative control groups.

RESULTS

Immunohistochemistry showed that eNOS was localized in the cytoplasm solely. eNOS was distributed mainly in the endothelia of submucosa vessels. Part of the smooth muscle of submucosa vessels was also positive

for eNOS (Figure 1). There were strongly positive substances in the cells of lamina propria of the villi, and in the cells near the striated border of villous epithelia. The epithelial cells were unstained (Figure 2).

Under the confocal laser scanning microscope, the positive substances of nNOS labeled by FITC were green, and those of eNOS

labeled by PE were red. The positive substances of nNOS were distributed mainly in myenteric plexus, rarely in the submucosal plexus (Figure 3). In the lamina propria of the villi, more than 80% of the cells were positive for both nNOS and eNOS, the rest of them were positive either for nNOS or for eNOS (Figure 4 and 5).

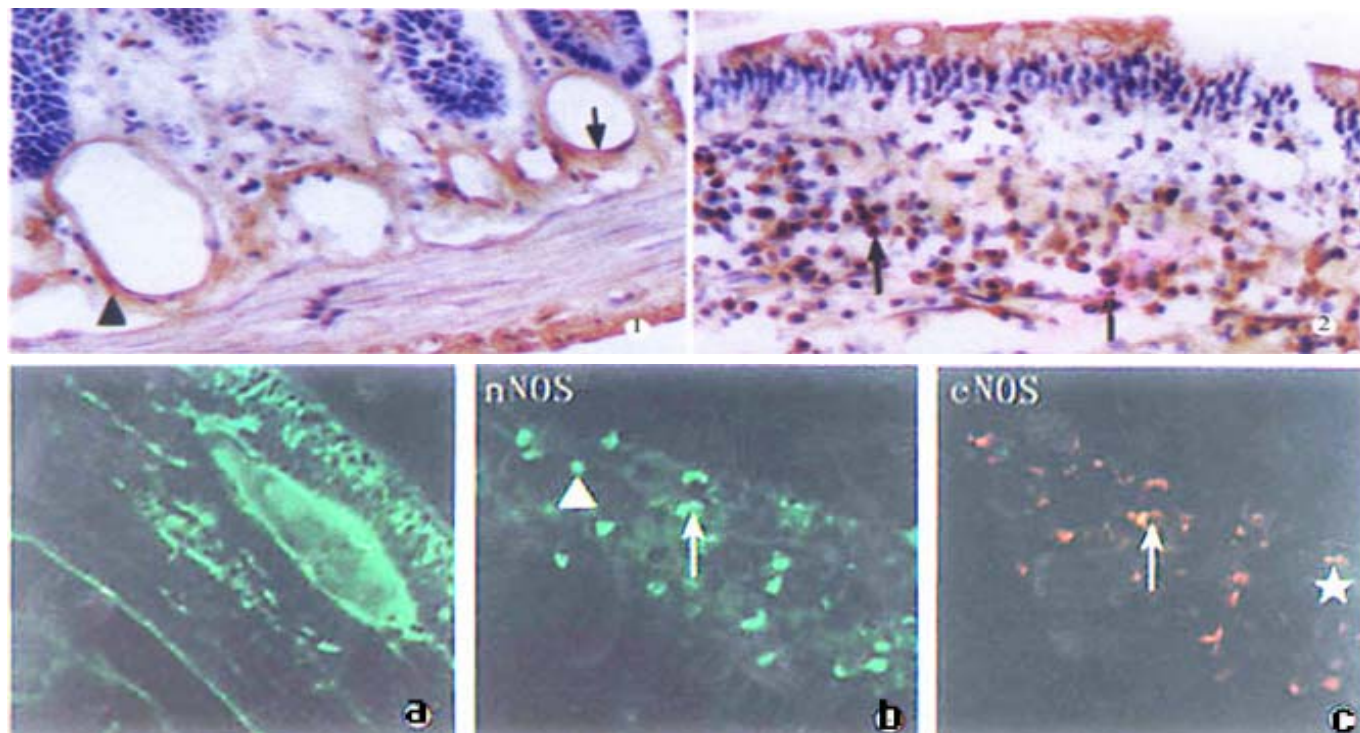


Figure 1 Immunohistochemical stain of eNOS in jejunal submucosa, showing the positive endothelium(↑) and microvascular smooth muscle(▲). ×170

Figure 2 Immunohistochemical stain of eNOS in jejunal villi, showing the positive cell in the proper layer(↑). ×170

Figure 3-4-5 Immunofluorescence histochemical double-stain in jejunum observed under a confocal laser scanning microscope, fig3 showing the positive substances of nNOS were distributed mainly in myenteric plexus. ×350 fig4 and fig5 showing the nNOS-positive cell(▲), the eNOS-positive cell(★) and double-stained cell(↑) in the proper layer of villi. ×250

DISCUSSION

The two constitutively expressed, Ca^{2+} -dependent NOS isoforms previously identified in neurons (nNOS) and endothelial cells (eNOS) are now known to be distributed more widely^[9-11]. eNOS is found in cardiac myocytes^[12,13], epithelial cells^[14-16], human platelets^[17] and various neurons, particularly the pyramidal neurons of the hippocampus, where it is coexpressed with nNOS^[18]. nNOS is found in the cytoskeleton of fast-contracting skeletal muscle fibers^[19]. In our study, we found nNOS and eNOS were coexpressed in some cells of lamina propria of the villi. NO generated by those cells plays an important role in absorption and protection of microvasculature. Inhibition of endogenous NOS by N_G -nitro-L-arginine methyl ester (L-NAME) caused secretion of water and ions, and this secretion was reversed by administration of the NOS substrate L-arginine^[20]. Previous studies indicated that norepinephrine^[21, 22], somatostatin^[23], and neuropeptide Y^[24] increased ileal water and ion absorption at a similar magnitude to that observed with L-arginine. It is consistent with the hypothesis that endogenous NO has a proabsorptive influence in the intestine in the basal state. Furthermore, endogenous NO can reduce the vascular albumin leakage provoked by lipopolysaccharide (LPS)^[25] and maintain microvascular integrity^[26-29].

Our study showed that nNOS was distributed mainly in the myenteric plexus, rarely in submucosal plexus. Recent pharmacological and physiological studies demonstrated that NO is a neurotransmitter in the non-adrenergic non-cholinergic (NANC)

inhibitory nerves of the gut^[30-34]. During nerve stimulation, NO generated by nNOS in nerve terminals regulates the release of vasoactive intestinal polypeptide (VIP) when diffuses to muscle cells to participate in muscle relaxation^[35-38]. Teng *et al*^[39] found eNOS was selectively expressed in rabbit gastric and human intestinal smooth muscle cells. In turn, VIP acts on smooth muscle cells to generate NO. The NO formed in the muscle cells constitutes the predominant component (60-80%) of NO formed during nerve stimulation.

Using NOS histochemistry and endothelial cell immunohistochemistry, Nichols *et al*^[40] provided the first anatomic evidence of NOS in both endothelial and smooth muscle cells of submucosal blood vessels in the intestines of rat and human, but he could not distinguish the isoform. We found eNOS was distributed in the endothelial and smooth muscle cells of submucosal blood vessels. This particular localization of eNOS was unexpected since only the inducible isoform of NOS had been reported in the vascular smooth muscle cells^[41-44]. These anatomical data strongly supported the proposed vasodilator role of NO in the mammalian gastrointestinal tract. There is both basal and stimulated release of NO from the endothelium. Stimulated NO release is affected by certain antagonists (acetylcholine, ATP, or bradykinin) or by physical stimuli such as fluid shear stress^[45-49] or low arterial PO_2 ^[50]. Vascular smooth muscle-derived NO behaves as an autocrine factor that plays a role in modulation of vasodilator tone and represents a reserve pool of NOS, which may be required when the tissue is under a local stress. The

source of NO within the vascular wall, either intimal or medial, should be a consideration in future studies in terms of the relative contribution of these sources to vasodilator tone in the gut wall.

REFERENCES

- Eskandari MK, Kalff JC, Billiar TR, Lee KK, Bauer AJ. LPS-induced muscularis macrophage nitric oxide suppresses rat jejunal circular muscle activity. *Am J Physiol* 1999;277:G478-486
- Konomi H, Meedeniya AC, Simula ME, Toouli J, Saccone GT. Characterization of circular muscle motor neurons of the duodenum and distal colon in the Australian brush-tailed possum. *J Comp Neurol* 2002;443:15-26
- Peng X, Wang SL. Nitric oxide and gastrointestinal movement. *Shijie Huaren Xiaohua Zazhi* 1998; 6:445-446
- Peng X, Feng JB, Wang SL. Distribution of nitric oxide synthase in stomach wall in rats. *World J Gastroenterol* 1999;5:92
- Nichols K, Staineds W, Krantis A. Nitric oxide synthase distribution in the rat intestine: a histochemical analysis. *Gastroenterology* 1993; 105:1651-1661
- Bagyanszki M, Roman V, Fekete E. Quantitative distribution of NADPH-diaphorase-positive myenteric neurons in different segments of the developing chicken small intestine and colon. *Histochem J* 2000;32:679-684
- Peng X, Feng JB, Wang SL. Nitric oxide synthase distribution in myenteric plexus of rat digestive tract. *Shijie Huaren Xiaohua Zazhi* 1998;6:250-252
- Wilhelm M, Batori Z, Pasztor I, Gabriel R. NADPH-diaphorase positive myenteric neurons in the ileum of guinea-pig, rat, rabbit and cat: a comparative study. *Eur J Morphol* 1998;36:143-152
- Bredt DS, Hwang PM, Glatt CE, Lowenstein C, Reed RR, Snyder SH. Cloned and expressed nitric oxide synthase structurally resembles cytochrome P-450 reductase. *Nature* 1991;351:714-718
- Busconi L, Michel T. Endothelial nitric oxide synthase: N-terminal myristoylation determines subcellular localization. *J Biol Chem* 1993; 268:8410-8413
- Marsden PA, Schappert KT, Chen HS, Flowers M, Sundell CL, Wilcox JN, Lamas S, Michel T. Molecular cloning and characterization of human endothelial nitric oxide synthase. *FEBS Lett* 1992;307:287-293
- Feron O, Belhassen L, Kobzik L, Smith TW, Kelly RA, Michel T. Endothelial nitric oxide synthase targeting to caveolae: specific interactions with caveolin isoforms in cardiac myocytes and endothelial cells. *J Biol Chem* 1996;271:22810-22814
- Balligand JL, Kobzik L, Xan XQ, Kaye DM, Belhassen L, O'hera DS, Kelly RA, Smith TW, Michel T. Nitric oxide-dependent parasympathetic signaling is due to activation of constitutive endothelial nitric oxide synthase in cardiac myocytes. *J Biol Chem* 1995;270:14582-14586
- Kobzik L, Bredt DS, Lowenstein CJ, Drazen J, Gaston B, Sugarbaker D, Stamler JS. Nitric oxide synthase in human and rat lung: immunocytochemical and histochemical localization. *Am J Respir Cell Mol Biol* 1993;9:371-377
- Lamas S, Marsden PA, Li GK, Tempst P, Michel T. Endothelial nitric oxide synthase: molecular cloning and characterization of a distinct constitutive enzyme isoform. *Proc Natl Acad Sci* 1992;89:6348-6352
- Shaul PW, North AJ, Wu LC, Wells LB, Brannon TS, Lau KS, Michel T, Margraf LR, Star RA. Endothelial nitric oxide synthase is expressed in cultured human bronchial epithelium. *J Clin Invest* 1994;94:2231-2236
- Sase K, Michel T. Expression of constitutive endothelial nitric oxide synthase in human blood platelets. *Life Sci* 1995;57:2049-2055
- Dinerman JL, Dawson TM, Schell J, Snowman A, Snyder SH. Endothelial nitric oxide synthase localized to hippocampal pyramidal cells: implications for synaptic plasticity. *Proc Natl Acad Sci USA* 1994;91:4214-4218
- Nakane M, Schmidt HW, Pollock JS, Forseman U, Murad F. Cloned human brain nitric oxide synthase is highly expressed in skeletal muscle. *FEBS Lett* 1993;316:175-180
- Barry MK, Aloisi JD, Pickering SP, Yeo CJ. Nitric oxide modulates water and electrolyte transport in the ileum. *Ann Surg* 1994;219:382-388
- Yano CJ, Couse NF, Antiohos C, Zinner MJ. The effect of norepinephrine on intestinal transport and perfusion pressure in the isolated perfused rabbit ileum. *J Surg Res* 1988;44:617-624
- Yao CJ, Couse NF, Zinner MJ. Discrimination between alpha1 and alpha2 adrenergic receptors in the isolated perfused ileum. *Surgery* 1988;104:130-136
- Anthone GJ, Bastidas JA, Orandle MS, Yao CJ. Direct proabsorptive effect of octreotide on ionic transport in the small intestine. *Surgery* 1990;108:1136-1142
- Anthone GJ, Orandle MS, Wang BH, Yao CJ. Neuropeptide Y induced intestinal absorption: mediation by α_2 -adrenergic receptors. *Surgery* 1991;110:1132-1138
- Crouser ED, Julian MW, Weinstein DM, Fahy RJ, Bauer JA. Endotoxin-induced ileal mucosal injury and nitric oxide dysregulation are temporally dissociated. *Am J Respir Crit Care Med* 2000;161:1705-1712
- László F, Morschl E, Pávó I, Whittle BJR. Nitric oxide modulates the gastrointestinal plasma extravasation following intraabdominal surgical manipulation in rats. *Eur J Pharmacol* 1999;375:211-215
- Iwashita E, Miyahara T, Hino K, Tokunaga T, Wakisaka H, Sawazaki Y. High nitric oxide synthase activity in endothelial cells in ulcerative colitis. *J Gastroenterol* 1995;30:551-554
- Tan B, He SY, Deng HW, Li YJ. Effect of quercetin on adhesion of platelets to microvascular endothelial cells *in vitro*. *Acta Pharmacol Sin* 2001;22:851-856
- Laszlo F, Whittle BJ, Moncada S. Time-dependent enhancement or inhibition of endotoxin-induced vascular injury in rat intestine by nitric oxide synthase inhibitors. *Br J Pharmacol* 1994;111:1309-1315
- Takeuchi T, Nioka S, Yamaji M, Okishio Y, Ishii T, Nishio H, Takatsuji K, Hata F. Decrease in participation of nitric oxide in nonadrenergic, noncholinergic relaxation of rat intestine with age. *Jpn J Pharmacol* 1998;78:293-302
- Nakao K, Takahashi T, Utsunomiya J, Owyang C. Extrinsic neural control of nitric oxide synthase expression in the myenteric plexus of rat jejunum. *J Physiol* 1998;507:549-560
- Shah S, Nathan L, Singh R, Fu YS, Chaudhuri G. E2 and not P4 increases NO release from NANC nerves of the gastrointestinal tract: implications in pregnancy. *Am J Physiol Regul Integr Comp Physiol* 2001;280:R1546-1554
- Shah S, Hobbs A, Singh R, Cuevas J, Ignarro LJ, Chaudhuri G. Gastrointestinal motility during pregnancy: role of nitrergic component of NANC nerves. *Am J Physiol Regul Integr Comp Physiol* 2000; 279:R1478-1485
- Correia NA, Oliveira RB, Ballejo G. Pharmacological profile of nitrergic nerve-, nitric oxide-, nitrosoglutathione- and hydroxylamine-induced relaxations of the rat duodenum. *Life Sci* 2000;68:709-717
- Vittoria A, Costagliola A, Carrese E, Mayer B, Cecio A. Nitric oxide-containing neurons in the bovine gut, with special reference to their relationship with VIP and galanin. *Arch Histol Cytol* 2000;63:357-368
- Simula ME, Brookes SJ, Meedeniya AC, Toouli J, Saccone GT. Distribution of nitric oxide synthase and vasoactive intestinal polypeptide immunoreactivity in the sphincter of Oddi and duodenum of the possum. *Cell Tissue Res* 2001;304:31-41
- Ekelund M, Ekblad E. Intestinal adaptation in atrophic rat ileum is accompanied by supersensitivity to vasoactive intestinal peptide, pituitary adenylate cyclase-activating peptide and nitric oxide. *Scand J Gastroenterol* 2001;36:251-257
- Konturek SK, Konturek PC. Role of nitric oxide in the digestive system. *Digestion* 1995;56:1-13
- Teng B, Murthy KS, Kuemmerle JF, Grider JR, Sase K, Michel T, Makhoul GM. Expression of endothelial nitric oxide synthase in human and rabbit gastrointestinal smooth muscle cells. *Am J Physiol* 1998; 275:G342-351
- Nichols K, Staines W, Rubin S, Krantis A. Distribution of nitric oxide synthase activity in arterioles and venules of rat and human intestine. *Am J Physiol* 1994; 267:G270-275
- Charpie JR, Webb RC. Vascular myocyte-derived nitric oxide is an autocrine that limits vasoconstriction. *Biochem Biophys Res Commun* 1993;194:763-768
- Hirafuji M, Tsunoda M, Machida T, Hamaue N, Endo T, Miyamoto A, Minami M. Reduced expressions of inducible nitric oxide synthase and cyclooxygenase-2 in vascular smooth muscle cells of stroke-prone spontaneously hypertensive rats. *Life Sci* 2002;70:917-926
- Teng X, Li D, Catravas JD, Johns RA. C/EBP-beta mediates iNOS induction by hypoxia in rat pulmonary microvascular smooth muscle cells. *Circ Res* 2002;90:125-127
- Teng X, Zhang H, Snead C, Catravas JD. Molecular mechanisms of iNOS induction by IL-1 beta and IFN-gamma in rat aortic smooth muscle cells. *Am J Physiol Cell Physiol* 2002;282:C144-152
- Busse R, Mulsch A. Endothelium-derived relaxing factor: nitric oxide. *Mol Aspects Inflam* 1991;42:189-205
- Busse R, Mulsch A, Fleming I, Hecker M. Mechanisms of nitric oxide release from the vascular endothelium. *Circulation* 1993;87(Suppl.V):18-26
- Ignarro LJ, Wood KS, Fukuto JM. Continuous basal formation of endothelium-derived relaxing factor and muscle-derived relaxing factor, both of which are nitric oxide. *J Cardiovasc Pharmacol* 1991;17(suppl.3):S229-S233
- Lamontagne D, Pohl U, Busse R. Mechanical deformation of vessel wall and shear stress determine the basal EDRF release in the intact coronary vascular bed. *Circ Res* 1992;70:123-130
- Pohl U, Holtz J, Busse R, Bassenge E. Crucial role of endothelium in the vasodilator response to increased flow *in vivo*. *Hypertension* 1986;8:37-44
- Pohl U, Busse R. Hypoxia stimulates the release of endothelium-derived relaxant factor. *Am J Physiol* 1989;256(Heart Circ Physiol 25):H1595-H1600

• BASIC RESEARCH •

Evidences for vagus nerve in maintenance of immune balance and transmission of immune information from gut to brain in STM-infected rats

Xi Wang, Bai-Ren Wang, Xi-Jing Zhang, Zhen Xu, Yu-Qiang Ding, Gong Ju

Xi Wang, Bai-Ren Wang, Zhen Xu, Yu-Qiang Ding, Gong Ju, Institute of Neuroscience, Fourth Military Medical University, Xi'an 710032, Shaanxi Province, China

Xi-Jing Zhang, Department of Anesthesiology, Xi Jing Hospital, Fourth Military Medical University, Xi'an 710032, Shaanxi Province, China
Supported by National Natural Science Foundation, No. 39830130

Correspondence to: Gong Ju, Institute of Neurosciences, The Fourth Military Medical University, Xi'an, P.R. China. jugong@fmmu.edu.cn
Telephone: +86-29-3374557 Fax: +86-29-3246270

Received 2001-11-02 Accepted 2001-11-27

Abstract

AIM: To determine whether *Salmonella Typhimurium* (STM) in gastrointestinal tract can induce the functional activation of brain, whether the vagus nerve involves in signaling immune information from gastrointestinal tract to brain and how it influences the immune function under natural infection condition.

METHODS: Animal model of gastrointestinal tract infection in the rat was established by an intubation of *Salmonella Typhimurium* (STM) into stomach to mimic the condition of natural bacteria infection. Subdiaphragmatic vagotomy was performed in some of the animals 28 days before infection. The changes of Fos expression visualized with immunohistochemistry technique in hypothalamic paraventricular nucleus (PVN) and supraoptic nucleus (SON) were counted. Meanwhile, the percentage and the Mean Intensities of Fluorescent (MIFs) of CD4+ and CD8+ T cells in peripheral blood were measured by using flow cytometry (FCM), and the pathological changes in ileum and mesenteric lymph node were observed in HE stained sections.

RESULTS: In bacteria-stimulated groups, inflammatory pathological changes were seen in ileum and mesenteric lymph node. The percentages of CD4+ T cells in peripheral blood were decreased from $42\% \pm 4.5\%$ to $34\% \pm 4.9\%$ ($P < 0.05$) and MIFs of CD8+ T cells were also decreased from 2.9 ± 0.39 to 2.1 ± 0.36 ($P < 0.05$) with STM stimulation. All of them proved that our STM-infection model was reliable. Fos immunoreactive (Fos-ir) cells in PVN and SON increased significantly with STM stimulation, from 189 ± 41 to 467 ± 62 ($P < 0.05$) and from 64 ± 21 to 282 ± 47 ($P < 0.05$) individually, which suggested that STM in gastrointestinal tract induced the functional activation of brain. Subdiaphragmatic vagotomy attenuated Fos expression in PVN and SON induced by STM, from 467 ± 62 to 226 ± 45 ($P < 0.05$) and from 282 ± 47 to 71 ± 19 ($P < 0.05$) individually, and restored the decreased percentages of CD4+ T cells induced by STM from $34\% \pm 4.9\%$ to original level $44\% \pm 6.0\%$ ($P < 0.05$). In addition, subdiaphragmatic vagotomy itself also decreased the percentages of CD8+ T cells (from $28\% \pm 3.0\%$ to $21\% \pm 5.9\%$, $P < 0.05$) and MIFs of CD4+ (from 6.6 ± 0.6 to 4.9 ± 1.0 , $P < 0.05$) and CD8+ T cells (from 2.9 ± 0.39 to 1.4 ± 0.34 , $P < 0.05$). Both of them

manifested the important role of vagus nerve in transmitting immune information from gut to brain and maintaining the immune balance of the organism.

CONCLUSION: Vagus nerve does involve in transmitting abdominal immune information into the brain in STM infection condition and play an important role in maintenance of the immune balance of the organism.

Wang X, Wang BR, Zhang XJ, Xu Z, Ding YQ, Ju G. Evidences for vagus nerve in maintenance of immune balance and transmission of immune information from gut to brain in STM-infected rats. *World J Gastroenterol* 2002;8(3):540-545

INTRODUCTION

It has been suggested in recent studies that the vagus nerve, the tenth cranial nerve, might play an important role in transmitting immune information into the brain^[1-5]. However, this conclusion is based on the experiments in which cytokines, endotoxins or exotoxins were usually used as immune stimulators through intraperitoneal or intravenous injection. All these immune stimulations, however, are non-natural and the role of vagus in natural infection condition has not been established yet. *Salmonella Typhimurium* (STM) belongs to the group B of *Salmonella*. It can infect both human beings and animals through gastrointestinal tract and leads to a local or general infection by inhibiting the host immune system^[6]. Thus, in the current experiments we introduced *Salmonella Typhimurium* (STM) into stomach to mimic the natural bacteria infection in gastrointestinal tract and to reassess the role of vagus in transmission of immune signal by subdiaphragmatic vagotomy. The production of c-fos, an immediately early gene, has been used as a morphological marker of functionally activated brain neurons^[7-15]. In the present study we observed the STM-induced Fos expression in hypothalamic paraventricular nucleus (PVN) and supraoptic nucleus (SON) and the effect of vagotomy. We also studied the importance of integrity of vagus nerve in the balance of T cell subpopulations.

MATERIALS AND METHODS

Animals

Adult male Sprague Dawley albino rats (180-210g, offered by Animal Center, Fourth Medical University) were used. Rats were housed individually in a temperature-controlled room in a natural light/dark cycle, with food and water available freely. The animals were trained for adaptation to handling and gastric intubation before the following procedures started.

Procedures

Subdiaphragmatic vagotomy Rats were anesthetized with pentobarbital sodium (40mg/kg, i.p.) and subjected to a complete subdiaphragmatic vagotomy ($n=10$) or sham operation ($n=10$). Briefly, after laparotomy, the two trunks of vagus were identified under an operating microscope. Both trunks were cut off close to the

diaphragm. For sham vagotomy, the vagus was similarly exposed but was not cut. After surgery, a recovery period of 28 days was allowed.

Preparation of STM Wild strain of STM (offered by Laboratory of Bacteria, Xijing Hospital, Fourth Medical University) was preserved in freeze-dried powder before use. In order to enhance the pathogenicity of the bacteria, STM were sub-cultured in mice abdomen (Kunming mice offered by Animal Center, Fourth Medical University) for 3 times and then the number of the bacteria was adjusted to 10^{10} /ml for use.

Intubation of STM Rats ($n=20$) were divided into 4 groups randomly, 5 for each. Group 1, saline(NS) + sham operation; 2, NS + vagotomy; 3, STM + sham operation; 4, STM + vagotomy. Food was taken away from the rats 24h prior to intubating STM or saline. After anesthetized with ether, all rats were intubated with 30g/L NaHCO_3 300 μl to neutralize gastric acid. Then the animals of groups 3 and 4 were gastrically intubated with STM (10^{10} in saline, 1ml) and in the others (Groups 1 and 2) 1 ml of saline were given.

Perfusion and Sectioning After intubation for 22h, all rats were deeply anesthetized with pentobarbital (80mg/kg) and 1ml of blood was taken via heart as quickly as possible. The rats were then perfused transcardially with saline 100ml followed by 4% paraformaldehyde in 0.1M phosphate buffer (PB) 500ml, pH 7.4, at 4°C. Blood was anti-coagulated with heparin. Brains, part of ileum and mesenteric lymph node were taken out and cryoprotected in 20% sucrose in 0.1 M PB overnight at 4°C. Frontal sections in 50 μm -thickness were cut through whole brains with a microtome and collected in cold cryoprotectant and stored at -20°C until immunohistochemistry processing. Serial ileum and mesenteric lymph node sections in 5 μm -thickness were cut with a cyostat and mounted onto slides coated with gelatin and stored at -20°C until histochemistry processing.

HE staining of ileum and mesenteric lymph node sections Slides of ileum and mesenteric lymph node were immersed successively in dimethylbenzene (10min \times 2), graded ethanol (100% 5min \times 2, 95% 2min, 80% 2min, 70% 2min and distilled water 2min), Harris hematoxylin (5-10min) and 10% acid ethanol for several seconds. After rinsed with tap water for 30min, slides were immersed again successively in distilled water (10-30min), graded ethanol (70%, 80%, and 95% 2min for each), 0.5% eosin (5-10min), 95% ethanol from several seconds to minutes, 100% ethanol (5min \times 2) and dimethylbenzene (10min \times 2). At last, the slides were sealed with gum and observed under a light microscope (Olympus B \times 60).

Flow cytometry (FCM) of blood T Cell Blood CD4+ and CD8+ T lymphocytes were labeled by using indirect immunofluorescent labeling method. First, 80 μl of anti-coagulated blood was incubated with mice anti rat CD4 mAb (1:100, Serotec company) or 15 μl of mice anti rat CD8 mAb (1:100, Serotec company) for 30min at 4°C, then with 40 μl of goat anti mice IgG-FITC (1:100, Serotec company) after washing twice with 0.01Mol/L Phosphate-buffered saline (PBS). FCM was used to detect the percentages and the Mean Intensities of Fluorescence (MIFs) of CD4+ and CD8+ T cells.

Immunohistochemistry of Brain Sections ABC immunohistochemical technique was used to detect Fos-immunoreactive (Fos-ir) cells in brain. One-in-five of brain sections were incubated with primary antibody raised from rabbit against Fos protein (Sigma Inc.) at a dilution of 1:3000. After incubation at room temperature for 36h, sections were rinsed with 0.01Mol/L Phosphate-buffered saline (PBS) (10min \times 3) and then incubated with biotinylated secondary antibody against rabbit IgG (Sigma Inc, diluted at 1:500) at room temperature for 4h. After rinsing with 0.01Mol/L PBS (10min \times 3), sections were incubated with avidin-biotin-horseradish peroxidase

(1:500, Sigma Inc.) at room temperature for 2h. The reaction product was visualized with amine nickel sulfate-enhanced 3,3'-diaminobenzidine (DAB) method. The sections were dehydrated in graded ethanol, cleared with dimethylbenzene, and coverslipped with gum.

Counting of Fos-ir cells Sections of hypothalamus were observed with a light microscope (Olympus BX60). The number of Fos-ir cells was quantified by counting immunostained nuclei in PVN or SON at two consecutive typical sections with an image analysis system (Leica Quantimet 570 C). The number of Fos-positive nuclei in PVN or SON was the group mean \pm SE.

Statistical analyses All data were expressed as mean \pm SE and were analyzed by one-way ANOVA. Post hoc analysis was done by using the Student-Newman-Keuls (SNK) multiple comparison test. A value of $P<0.05$ was considered significant.

RESULTS

HE staining

Inflammation change was seen in ileum and mesenteric lymph node in the rats stimulated with STM. There are numerous bacilli in ileum cavity in the infected rats. The structure of the villus of the infected ileum was destroyed (Figure E2), part of epithelial cells were scaled, and many neutrophil, red blood cell and fibroblast infiltrated into the villus. At the same time, secondary lymphoid folliculi appeared in mesenteric lymph node (Figure E4). Figures.E1 and E3 show the normal tissue image of the villus and mesenteric lymph node in saline-treated rat.

FCM

Table 1 shows the percentages and MIFs of CD4+and CD8+ T cells in every group.

Figure1 A shows that subdiaphragmatic vagotomy itself in normal animals had no evident effect on the percentages of CD4+ T cells, but the stimulation of STM itself in sham-operated animals decreased the percentages of CD4+ T cells from $42\% \pm 4.5\%$ to $34\% \pm 4.9\%$ ($P<0.05$) and after subdiaphragmatic vagotomy the decreased percentages of CD4+ T cells in STM stimulated rats restored from $34\% \pm 4.9\%$ to $44\% \pm 6.0\%$, the level of non- STM stimulated rats ($P<0.05$).

Figure1 B shows that subdiaphragmatic vagotomy itself in NS+operation animals decreased MIFs of CD4+ T cells from 6.6 ± 0.6 to 4.9 ± 1.0 ($P<0.05$), indicating the inhibition of subdiaphragmatic vagotomy to CD4+ T cells.

Figure1 C and Figure1 D show that subdiaphragmatic vagotomy itself in normal rats decreased the percentages of CD8+ T cells (from $28\% \pm 3.0\%$ to $21\% \pm 5.9\%$, $P<0.05$) as well as MIFs of CD8+ T cells (from 2.9 ± 0.39 to 1.4 ± 0.34 , $P<0.05$). STM stimulation itself in sham-operated rats also depressed the percentages of CD8+ T cells (from $28\% \pm 3.0\%$ to $21\% \pm 5.9\%$, $P>0.05$) and MIFs of CD8+ T cells (from 2.9 ± 0.39 to 2.1 ± 0.36 , $P<0.05$). Subdiaphragmatic vagotomy in STM-challenged rats aggravated the inhibition of STM to the percentages of CD8+ T cells (from $23\% \pm 2.0\%$ to $17\% \pm 5.8\%$, $P<0.05$) and MIFs of CD8+ T cells (from 2.1 ± 0.36 to 1.1 ± 0.06 , $P<0.05$).

Table 1 Percentages (%) and MIF of CD8+ and CD4+ T cells ($\bar{x} \pm s$)

	NS+sham	NS+vagotomy	STM+sham	STM+vagotomy
CD4	42 \pm 4.5	46 \pm 4.6	34 \pm 4.9 ^b	44 \pm 6.0 ^a
CD4 MIF	6.6 \pm 0.6	4.9 \pm 1.0 _b	6.8 \pm 1.1	6.1 \pm 1.0
CD8	28 \pm 3.0	21 \pm 5.9 ^b	23 \pm 2.0	17 \pm 5.8 ^a
CD8 MIF	2.9 \pm 0.39	1.4 \pm 0.34 ^b	2.1 \pm 0.36 ^b	1.1 \pm 0.06 ^a

^a $P<0.05$ vs STM+sham; ^b $P<0.05$ vs NS+sham

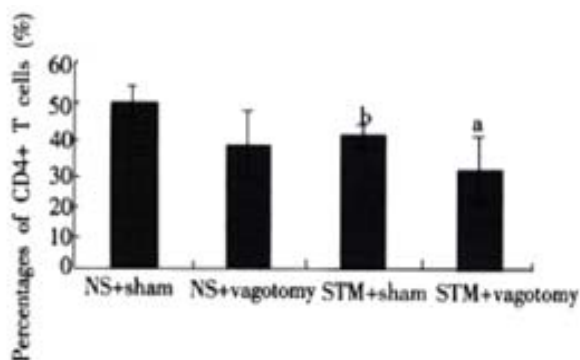


Figure 1A Percentages of blood CD4+ T cells. ^a $P < 0.05$ vs. STM+sham, ^b $P < 0.05$ vs NS+sham

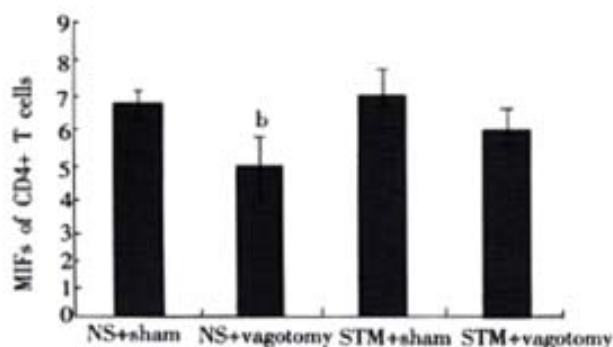


Figure 1B The Mean Intensities of Fluorescence (MIFs) of blood CD4+ T cells. ^b $P < 0.05$ vs NS+sham

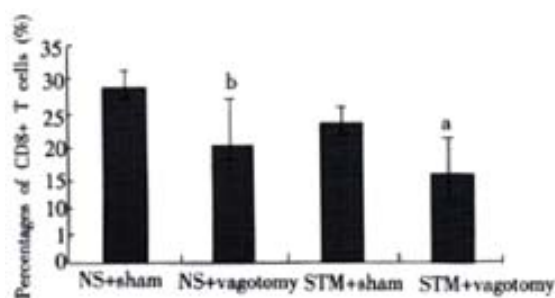


Figure 1C Percentages of blood CD8+ T cells. ^a $P < 0.05$ vs STM+sham, ^b $P < 0.05$ vs NS+sham

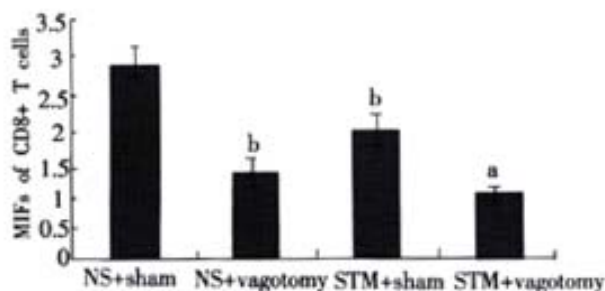


Figure 1D The Mean Intensities of Fluorescence (MIFs) of blood CD8+ T cells. ^a $P < 0.05$ vs STM+sham; ^b $P < 0.05$ vs NS+sham

Immunohistochemistry

Table 2 shows the number of Fos-ir cells in PVN and SON in each group. The numbers of Fos-ir cells in PVN and SON of STM+sham-operated rats increased significantly compared with that of NS+sham from 189 ± 41 to 467 ± 62 ($P < 0.05$) and from 64 ± 21 to 282 ± 47 ($P < 0.05$) individually (Figures.E5, E6, E9, E10). The positive neuron distributed in both magnocellular and parvocellular portions of

PVN as well as dorsal and ventral parts of SON. Fos expressions were attenuated in PVN and SON in the rats of STM+vagotomy group compared with that of STM+sham group from 467 ± 62 to 226 ± 45 ($P < 0.05$) and from 282 ± 47 to 71 ± 19 ($P < 0.05$) individually (Figures. E6, E7, E10, E11), but it was still higher than that of saline-treated animal (189 ± 41 and 64 ± 21 individually). There was no significant changes of Fos expression in NS + vagotomy rats compared with NS + sham rats (Figures.E5, E8, E9, E12).

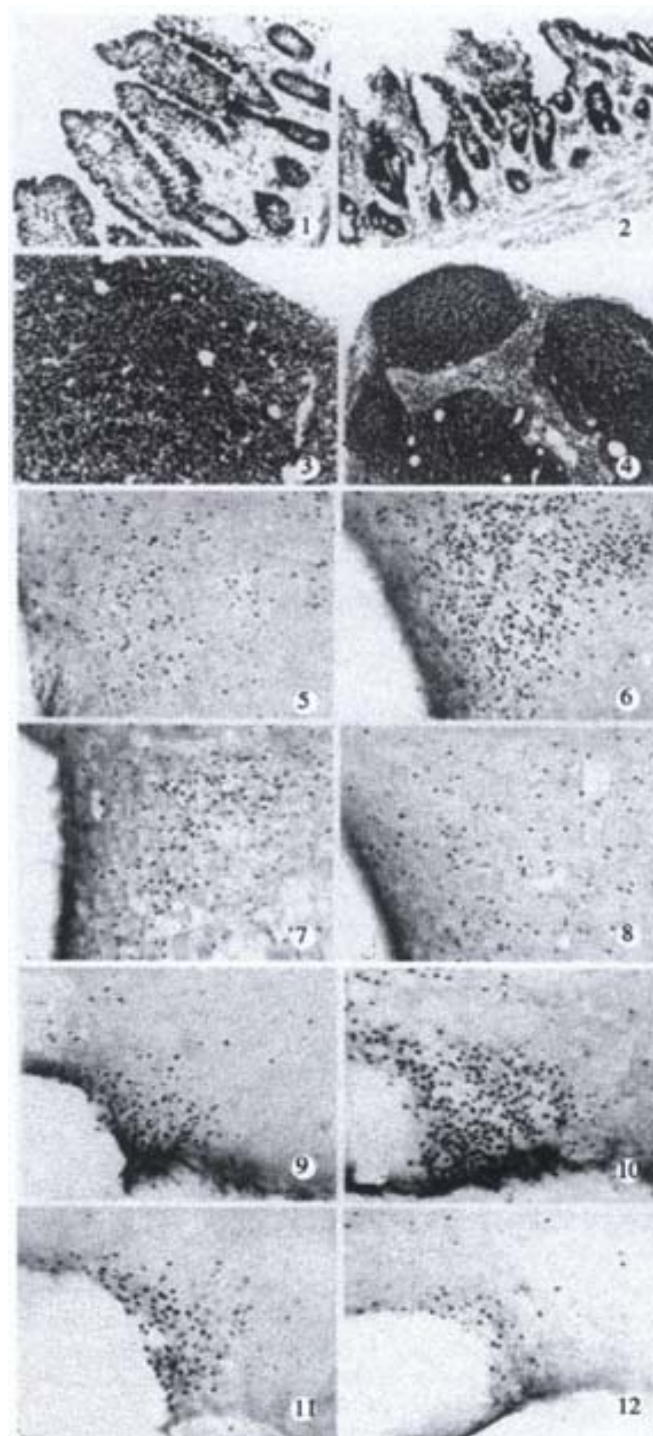


Figure 2 In Figures E 1 and 3 show the normal structures of the villus and mesenteric lymph node in saline-injected rats; 2 and 4 show the villus and mesenteric lymph node in STM-challenged rats. 5 and 9 show Fos expression in PVN and SON respectively in NS + sham rats; 6 and 10 show Fos expressions in PVN and SON respectively in STM + sham rat; 7 and 11 show Fos expressions in PVN and SON respectively in STM + vagotomy rat; 8 and 12 show Fos expressions in PVN and SON respectively in NS + vagotomy rat. $\times 50$

Table 2 Numbers of Fos-ir Cells in PVN and SON ($\bar{x} \pm s$)

	NS + sham	NS + vagotomy	STM + sham	STM + vagotomy
PVN	189±41	131±38	467±62 ^a	226±45 ^b
SON	64±21	49±22	282±47 ^a	71±19 ^b

^a*P*<0.05 vs NS + Sham; ^b*P*<0.05 vs STM + sham

DISCUSSION

More and more evidences have shown that there is a complicated bidirectional inter-relationship between nervous system and immune system^[4,16-23]. Immune signals produced during antigen challenge can be transmitted into central nervous system (CNS) and influence the function of the latter. In turn, CNS can modulate the activity of immune system. However, it is still an unsolved problem up to now how the immune signals are transmitted into CNS. Two of hypotheses have been proposed^[1-4]: one is through humoral route and the other, via neural pathway. Among the neural pathways the vagus nerve in transferring peripheral immune signals into CNS has been paid more attention to^[1-5,24,25]. A large amount of evidences indicate that vagus plays an important role in surveying the peripheral immune information into CNS. For example, subdiaphragmatic vagotomy inhibits a series of brain-mediated responses to peripheral administration of lipopolysaccharide (LPS), IL-1 β or TNF- β , such as induction of IL-1 β mRNA within mice brain^[26,27], activation of hypothalamic corticotropin-releasing hormone neurons and ACTH secretion^[28,29], LPS-induced fever in guinea pigs^[30], Fos immunoreactivity in primary afferent neurons of the vagus^[31], the inhibition of social exploration^[32], a monophasic fever^[33], the hyperalgesia^[34,35] etc. Administration of IL-1 β in hepatic portal vein induced afferent discharges of hepatic branch of vagus, but the discharges disappeared in vagotomy rats^[36]. Nucleus tractus solitarius lesions attenuated the first fever peak induced by intraperitoneal injection of IL-1 β ^[37]. All of the above mentioned experiments indicate that intact vagus is necessary for transmitting the immune information from periphery, especially from peritoneal cavity, to the brain. According to the anatomical structure of vagus, the abdominal organs such as liver, stomach, intestines, lymph node, etc. are innervated mostly by subdiaphragmatic vagus and the vagus contains important visceral sensory afferent fibers from abdominal organs^[38,39]. Thus, we conjecture that subdiaphragmatic vagus may play an important role in transmitting the abdominal immune information into the brain and is important in maintaining immune balance.

All the immune challenges used in previous studies were bacterial toxins such as LPS or immune cytokines injected intraperitoneally or intravenously. In this experiment we established a rat model of gastrointestinal tract infection by STM intubation to mimic the natural infection and a subdiaphragmatic vagotomy was performed to further observe the role of vagus in immune signal transmission. According to aetiology, STM can invade intestinal mucosa and largely reproduce, and then further spread into the drained mesenteric lymph nodes and disseminate via the bloodstream^[40]. STM is an intracellular Gram-negative bacterial pathogen that infects both phagocytic and non-phagocytic cells^[6,40-43]. It can inhibit the host immune system and cause a range of diseases including enteric fever and gastroenteritis^[6]. It has been reported that the depletion of either CD4⁺ or CD8⁺ T cells by STM impairs their ability to transfer protective immunity to virulent *S. typhimurium*^[6]. These studies indicate that CD4⁺ and CD8⁺ T cells act synergistically to control infection with virulent *S. typhimurium*^[6,44,45]. In our experiment the villus of the infected ileum was destroyed, part of epithelial cells scaled, and the number of neutrophils, red blood cells as well as fibroblasts increased in the villus. At the same time, secondary lymphoid folliculus stimulated with STM emerged in mesenteric lymph nodes. The percentages of

CD4⁺ and CD8⁺ T cells and MIFs of CD8⁺ T cells of peripheral blood were all inhibited, which was consistent with the previous reports. These changes induced by STM suggest that our STM infection model was reliable.

The result showed that in NS+sham rats Fos proteins expressed in a few of PVN and SON neurons, which suggests that in normal condition some PVN and SON neurons are active, and may be related to the modulation of routine metabolic activities. After being stimulated with STM the number of Fos-ir cells significantly increased in PVN and SON. It indicated that these cells were activated by STM-challenge. It is well known that CNS, especially hypothalamus, involves in modulation of acute immune reaction^[46]. PVN and SON, which are two most important nuclei in hypothalamus related to autonomic function, are mainly composed of three kinds of neurons neurochemically: oxytocinergic, vasopressinergic and CRH neurons^[46]. All of these three kinds of neurons can involve in neuroimmunomodulation^[46]. Yang *et al.*^[46] reported that, as the neuroimmunomodulation integrating center, hypothalamic PVN modulates the immune function through three pathways: The first is CRH -ACTH-adrenal cortex axis, the second is oxytocin neuroendocrine pathway, and the third is PVN-spinal cord sympathetic preganglionic projection. Although we can't determine which kind of neurons were activated in this experiment since we did not apply double-labeling technique to identify them, we proposed from the observation of distribution of Fos positive neurons in the subnuclei of PVN and SON that, maybe, all these three kind neurons were activated.

But, how the immune signals are transmitted into the brain is an important and unsolved question. Is it through vagus or humoral pathway, or both of them? What we focused on in the present study was the role of vagus in the sensation and transmission of immune signals to brain. So, we severed subdiaphragmatic vagus to observe whether the Fos expressions in PVN and SON induced by STM infection and the T cell subpopulation were influenced. After subdiaphragmatic vagotomy, Fos expressions in PVN and SON were attenuated. At the same time we found that the decreased percentage of CD4⁺ T cells in STM-infected rats restored after subdiaphragmatic vagotomy. These results indicate the importance of intact subdiaphragmatic vagus in signaling immune information from abdominal organs to CNS. We tend to conclude from our results that subdiaphragmatic vagus does play a role in transferring immune information into brain during the abdominal inflammatory phase.

However, the detailed mechanism about how vagus nerve senses the immune stimulation and transfers it into electric signal is still not fully understood. It is known that macrophages, dendritic cells, and other immune cells detect and present antigens and respond by releasing proinflammatory mediators, such as IL-1 β , IL-6 and TNF- α ^[23,47,48]. Goehler *et al.*^[47] found that between the fibers of abdominal vagus there exist immune cells which can produce IL-1 β . IL-1 β acts to both coordinating the peripheral immune response and signaling the CNS^[49]. The globe cells of vagus paraganglia near liver hilus could be stained by biotinylated IL-1 receptor antagonist^[50] and by anti rat IL-1 receptor type I antibody^[51], which suggested the possibility for vagus to sense the local IL-1. We^[51] and others^[52] also have reported that the primary sensory neurons in nodose ganglia of vagus contain IL-1 receptor protein and mRNA, which indicates that vagus nerve probably can sense IL-1 directly.

It is necessary to point out that vagus is definitely not the only route for immune signal getting into the brain, since it is found in the present study that although the number of STM stimulation-induced Fos expressed neurons in hypothalamus is attenuated after vagotomy, the number is still higher than that in control. So the humoral pathways or other nerves may also involve in the immune signals transmission in some degree, which still needs further study.

Our results also showed that subdiaphragmatic vagotomy itself decreased the percentages of CD8⁺ T cells and MIFs of CD4⁺ and CD8⁺ T cells, which indicated the importance of intact vagus in maintaining the host immune balance. This is also accordant with our previous study^[53]. As we know that CD4⁺ and CD8⁺ T cells are necessary in clearing STM^[6,54,55]. Vagotomy inhibits the subpopulation of T cells, which is a disadvantage to STM clearance and only aggravate the inhibition to CD4⁺ and CD8⁺ T cells induced by STM. How does the vagus influence the phenotype of lymphatic cells? Vagus contains both afferent and efferent fibers innervating abdomen. The former can transmit abdominal information into CNS and the latter innervates some immune organs or immune cells, such as abdominal lymph node. When we cut off subdiaphragmatic vagotomy, on the one hand, the abdominal immune information can't be transmitted into the brain; on the other hand, the brain can't influence the abdominal immune organizations via vagus. We suppose that this is probably the answer.

In summary, subdiaphragmatic vagus is able to signal immune information from abdomen into the brain and intact vagus is necessary in maintaining the host immune balance.

REFERENCES

- 1 Maier SF, Goehler LE, Fleshner M, Watkins LR. The role of the vagus in cytokine-to-brain communication. *Ann N Y Acad Sci* 1998; 840: 289-300
- 2 Goehler LE, Gaykema RPA, Hansen MK, Anderson K, Maier SF, Watkins LR. Vagal immune-to-brain communication: a visceral chemosensory pathway. *Auton Neurosci: Basic & Clinical* 2000; 85: 49-59
- 3 Dantzer R, Konsman PJ, Bluthé RM, Kelley KW. Neural and humoral pathways of communication from the immune system to the brain: parallel or convergent? *Auton Neurosci: Basic & Clinical* 2000; 85: 60-65
- 4 Watkins LR, Maier SF, Goehler LE. Cytokine-to-brain communication: a review & analysis of alternative mechanisms. *Life Sci* 1995; 57: pp1011-1026
- 5 Wang X, Wang BR, Ju G. The role of the vagus nerve in transmitting immune information into the brain. *Shanghai Mianyixue Zazhi* 2000; 20:192-194
- 6 Lo WF, Ong H, Metcalf ES, Soloski MJ. T cell responses to Gram-negative intracellular bacterial pathogens: A role for CD8⁺ T cells in immunity to Salmonella infection and the involvement of MHC class Ib molecules. *J Immunol* 1999; 162: 5398-5406
- 7 Stephen MS, Frank RS. Early response genes as markers of neuronal activity and growth factor action. *Adv in Neurol* 1993; 59: 273-284
- 8 Xu ZC, Jiang XH. Advance and development of Early response genes in neuroscience research. *Shengli Kexue Jinzhan* 1997; 28: 49-51
- 9 Wang X, Wang BR, Duan XL, Ju G. The basal expression of Fos in the rat under the normal life situation. *Zhongguo Shenjing Jiepouxue Zazhi* 2000; 16: 353-358
- 10 Matsunaga W, Takamata A, Bun H, Nakashima T. LPS-induced Fos expression in oxytocin and vasopressin neurons of the rat hypothalamus. *Brain Res* 2000; 858: 9-18
- 11 Zhang X, Ju G. The induction and display of c-fos oncogene. *Shengli Kexue Jinzhan* 1991; 22: 299-303
- 12 Arnold FJL, Bueno MDL, Shiers H, Hancock DC, Evan GI, Herbert J. Expression of c-fos in regions of the basal limbic forebrain following intracerebroventricular corticotropin-releasing factor in unstressed or stressed male rats. *Neurosci* 1992; 51: pp377-390
- 13 Imaki T, Shhibasaki T, Hotta M, Demura H. Intracerebroventricular administration of corticotropin-releasing factor induces c-fos mRNA expression in brain regions related to stress responses: comparison with pattern of c-fos mRNA induction after stress. *Brain Res* 1993; 616: 114-125
- 14 Morgan JJ, Cohen DR, Hempstead JL, Curran T. Mapping patterns of c-fos expression in the central nervous system after seizure. *Science* 1987; 237: 192-197
- 15 Hare AS, Clarke G, Tolchard S. Bacterial lipopolysaccharide-induced changes in FOS protein expression in the rat brain: correlation with thermoregulatory changes and plasma corticosterone. *J Neuroendocrinol* 1995; 7: 791-799
- 16 Borovikova LV, Lvanona S, Zhang M, Yang H, Botchkina GI, Watkins LR, Wang H, Abumrad N, Eaton JW, Tracey JK. Vagus nerve stimulation attenuates the systemic inflammatory response to endotoxin. *Nature* 2000; 405: 458-462
- 17 Erricsson A, Arias C, Sawchenko PE. Evidence for an intramedullary prostaglandin-dependent mechanism in the activation of stress-related neuroendocrine circuitry by intravenous interleukin-1. *J Neurosci* 1997; 17: 7166-7179
- 18 Ivanov AI, Kulchitsky VA, Sugimoto N, Simons CT, Romanovsky AA. Does the formation of lipopolysaccharide tolerance require intact vagal innervation of the liver? *Auton Neurosci: Basic and Clinical* 2000; 85: 111-118
- 19 Downing JEG, Miyan JA. Neural immunoregulation: emerging roles for nerves in immune homeostasis and disease. *Immunol Today* 2000; 21: 281-289
- 20 Roth J, Souza GEP. Fever induction pathways: evidence from responses to systemic or local cytokine formation. *Braz J Med Biol Res* 2001; 34: 301-314
- 21 Watkins LR, Maier SF. Implications of immune-to-brain communication for sickness and pain. *Proc Natl Acad Sci* 1999; 96: pp7710-7713
- 22 Shanks N, Windle RJ, Perks PA, Harbuz MS, Jessop DS, Ingram CD, Lighman SL. Early-life exposure to endotoxin alters hypothalamic-pituitary-adrenal function and predisposition to inflammation. *Proc Natl Acad Sci* 2000; 97: 5645-5650
- 23 Ling YL, Meng AH, Zhao XY, Shan BE, Zhang JL, Zhang XP. Effect of cholecystokinin on cytokines during endotoxic shock in rats. *World J Gastroenterol* 2001; 7: 667-671
- 24 Romanovsky AA. Thermoregulatory manifestations of systemic inflammation: lessons from vagotomy. *Auton Neurosci: Basic and Clinical* 2000; 85: 39-48
- 25 Blatteis CM, Li SX. Pyrogenic signaling via vagal afferents: what stimulates their receptors? *Auton Neurosci: Basic and Clinical* 2000; 85: 66-71
- 26 Laye S, Bluthé RM, Kent S, Combe C, Medina C, Parnet P, Kelley K, Dantzer R. Subdiaphragmatic vagotomy blocks induction of IL-1 β mRNA in mice brain in response to peripheral LPS. *Am J Physiol* 1995; 268:R1327-R1331
- 27 Hansen MK, Taishi P, Chen Z, Krueger JM. Vagotomy blocks the induction of interleukin-1 (IL-1) mRNA in the brain of rats in response to systemic IL-1. *J Neurosci* 1998; 18: 2247-2253
- 28 Gaykema RPA, Dijkstra I, Tilders RJH. Subdiaphragmatic vagotomy suppresses endotoxin-induced activation of hypothalamic corticotropin-releasing hormone neurons and ACTH secretion. *Endocrinol* 1995; 136: 4717-4720
- 29 Kapcala LP, He RJ, Gao Y, Pieper JO, Detolla LJ. Subdiaphragmatic vagotomy inhibits intra-abdominal interleukin-1 β stimulation of adrenocorticotropin secretion. *Brain Res* 1996; 728: 247-254
- 30 Sehic E, Blatteis CM. Blockade of lipopolysaccharide-induced fever by subdiaphragmatic vagotomy in guinea pigs. *Brain Res* 1996; 726: 160-166
- 31 Gaykema RPA, Goehler LE, Tilders FJ, Bol J GJM, McGorry M, Fleshner M, Maier SF, Watkins LR. Bacterial endotoxin induces Fos immunoreactivity in primary afferent neurons of the vagus. *Neuroimmunomodulation* 1998; 5: 234-240
- 32 Luheshi GN, Bluthé RM, Rushorforth D, Mulcahy N, Konsman JP, Goldbach M, Dantzer R. Vagotomy attenuates the behavioural but not the pyrogenic effects of interleukin-1 in rats. *Auton Neurosci: Basic and Clinical* 2000; 85: 127-132
- 33 Romanovsky AA, Simons CT, Szekely M, Kulchitsky VA. The vagus nerve in the thermoregulatory response to systemic inflammation. *Am J Physiol* 1997; 273: R407-R413
- 34 Watkins LR, Wiertelak EP, Goehler LE, Smith KP, Martin D, Maier SF. Characterization of cytokine-induced hyperalgesia. *Brain Res* 1994; 654: 15-26
- 35 Watkins LR, Goehler LE, Reiton J, Brewer MT, Maier SF. Mechanisms of tumor necrosis factor- α (TNF- α) hyperalgesia. *Brain Res* 1995; 692: 244-250
- 36 Nijima A. The afferent discharges from sensors for interleukin 1 β in the hepatoportal system in the anesthetized rat. *J Auton Nerv Sys* 1996; 61: 287-291
- 37 Gordon FJ. Effect of nucleus tractus solitarius lesions on fever produced by interleukin-1 β . *Auton Neurosci: Basic and Clinical* 2000; 85: 102-112
- 38 Berthoud HR, Neuhuber WL. Functional and chemical anatomy of the afferent vagal system. *Auton Neurosci: Basic & Clinical* 2000; 85: 1-17
- 39 Dou DB, Cai G. Regulation of the stomach motility function. *Shijie Huaren Xiaohua Zazhi* 1999; 7: 353-354
- 40 Niedergang F, Sirard JC, Blanc CT, Kraehenbuhl JP. Entry and survival of Salmonella Typhimurium in dendritic cells and presentation of recombinant antigens do not require macrophage-specific virulence factors. *Proc Natl Acad Sci* 2000; 97: 14650-14655
- 41 Portillo FGD, Finlay B. Salmonella invasion of nonphagocytic cells induces formation of macropinosomes in the host cell. *Infect and Immun* 1994; 62: p4641-4645

- 42 Cookson BT, Bevan MJ. Identification of a natural T cell epitope presented by Salmonella-infected macrophages and recognized by T cells from orally immunized mice. *J Immunol* 1997; 158: 4310-4319
- 43 Weinstein DL, Carsiotis M, Lissner CR, O'Brien AD. Flagella help Salmonella typhimurium survive within murine macrophages. *Infect and Immun* 1984; 46: p819-825
- 44 Tite JP, Dougan G, Chatfield SN. The involvement of tumor necrosis factor in immunity to Salmonella infection. *Infect and Immun* 1991; 147: 3161-3164
- 45 Nauciel C. Role of CD4⁺ T cells and T-independent mechanisms in acquired resistance to Salmonella typhimurium infection. *Infect and Immun* 1990; 145: 1265-1269
- 46 Yang H, Wang L, Ju G. Evidence for hypothalamic paraventricular nucleus as an integrative center of neuroimmunomodulation. *Neuroimmunomodulation* 1997; 4: 120-127
- 47 Goehler LE, Gaykema RPA, Nguyen KT, Lee JE, Tilders FJH. Interleukin-1 β in immune cells of the abdominal vagus: a link between the immune and nervous system? *J Neurosci* 1999; 19: 2799-2806
- 48 Xia B. Pathogeny and mechanism of inflammatory bowel disease. *Shijie Huaren Xiaohua Zazhi* 2001; 9: 245-250
- 49 Maier SF, Wiertelak EP, Martin D, Wakins LR. Interleukin-1 mediates the behavioral hyperalgesia produced by lithium chloride and endotoxin. *Brain Res* 1993; 623: 321-324
- 50 Goehler LE, Relton JK, Dripps D, Kiechle R, Tartaglia N, Maier SF, Watkins LR. Vagal paranganglia bind biotinylated interleukin-1 receptor antagonist: a possible mechanism for immune-to-brain communication. *Brain Res Bul* 1997; 43: 357-364
- 51 Wang X, Wang BR, Duan XL, Liu HL, Ju G. The expression of IL-1 receptor type I in nodose ganglion and vagal paranganglion in the rat. *Zhongguo Shenjing Kexue Zazhi* 2000; 16: 90-93
- 52 Ek M, Kurosawa M, Lundeborg T, Ericsson A. Activation of vagal afferents after intravenous injection of interleukin-1 β : role of endogenous prostaglandins. *J Neurosci* 1998; 18: 9471-9479
- 53 Wang X, Cao YX, Wang BR, Xu Z, Jin L, Duan XL, Ju G. The influence of subdiaphragmatic vagotomy on CD4⁺/CD8⁺ T cells in peripheral blood. *Xibao Fenzi Yu Mianyixue Zazhi* 2000; 16: 230-231
- 54 Mesorley SJ, Cookson BT, Jenkins MK. Characterization of CD4⁺ T cells responses during natural infection with Salmonella typhimurium. *J Immunol* 2000; 164: 986-993
- 55 Sandrine P, Paolo TB, Marika P, Charles N. Th1 response in Salmonella typhimurium-infected mice with a high or low rate of bacterial clearance. *Infect and Immun* 1997; 65: 4509-4514

Edited by Hu DK

• BASIC RESEARCH •

Relationship between lymphocyte apoptosis and endotoxin translocation after thermal injury in rats

Pei-Yuan Xia, Jiang Zheng, Hong Zhou, Wen-Dong Pan, Xiao-Jian Qin, Guan-Xia Xiao

Pei-Yuan Xia, Department of Pharmacy and Clinical Pharmacology, Southwestern Hospital, Third Military Medical University, Chongqing 400038, China
Jiang Zheng, Hong Zhou, Wen-Dong Pan, Xiao-Jian Qin, Guan-Xia Xiao, Institute of Burn Research, Southwestern Hospital, Third Military Medical University, Chongqing 400038, China

Supported by the National Basic Research Priorities Programme of China, No. G199905403

Correspondence to: Pei-Yuan Xia, M. D., ph. D., Department of Pharmacy and Clinical Pharmacology, Southwestern Hospital, Third Military Medical University, Chongqing 400038, China. xiapy61@mail.tmmu.com.cn

Received 2001-11-02 Accepted 2001-12-04

Abstract

AIM: To investigate the relationship between lymphocyte apoptosis in peripheral blood, spleen and mesenteric lymph nodes (MLN) and endotoxin translocation after thermal injury in rats.

METHODS: In a Wistar rat model inflicted with 30% TBSA III degree scalding, serum LPS levels in portal vein and vena cava were quantified by tachypleus amebocyte lysate (TAL) technique. The analysis of peripheral blood lymphocyte was employed in situ Cell Death Detection Kit and evaluated by flow cytometry. Apoptotic lymphocytes in paraffin-embedded spleen and MLN sections were examined by histologic analysis, in situ deoxynucleotidyl transferase dUTP nick-end labeling (TUNEL) and peroxidase (POD) staining. The images were taken by Coolcd camera system, and the count and optical density value (transmission light) of apoptotic lymphocytes were analyzed with software Spot and Imagine proplus 4.10a (IPP4.10a).

RESULTS: In the period of 3 to 48 postburn hours (PBHs) serum LPS level ($\times 10^3$ EU·L⁻¹) in portal vein (2.11 ± 0.02 , 5.66 ± 0.20 , 3.70 ± 0.22 , 2.56 ± 0.28 , 0.90 ± 0.11) was higher than that in vena cava (0.63 ± 0.01 , 1.53 ± 0.18 , 0.83 ± 0.32 , 0.52 ± 0.12 , 0.23 ± 0.02 , $P < 0.01$), but both increased sharply in postburn rats ($P < 0.01$) and reached a peak at 6 PBH. Analysis of apoptotic lymphocytes showed that the proportion (%) of postburn apoptotic cells was much higher than that in healthy rats (8.34 ± 1.53 , 8.13 ± 1.81 , 20.77 ± 3.94 , 23.90 ± 3.92 , 11.23 ± 1.35 and 13.26 ± 2.09 at 3, 6, 12, 24, 48 and 72 PBH, respectively, $vs 3.99 \pm 1.72$, $P < 0.01$), especially after 6 PBH. The concentrations of lymphocytic apoptosis at 12 and 24 PBH were markedly higher than that at other time points. Meantime, few apoptotic lymphocytes were found in normal MLN, but increased postburn obviously (3 ± 1 $vs 546 \pm 83$, 285 ± 39 , 149 ± 30 , 58 ± 10 , 36 ± 11 and 33 ± 9 in turn, $P < 0.01$), especially at 3 PBH, whereas apoptotic lymphocytes were concentrated in splenic cortex before the burn and decreased obviously during 72 PBHs (499 ± 186 $vs 12 \pm 8$, 19 ± 15 , 12 ± 7 , 100 ± 15 , 123 ± 25 and 226 ± 26 in turn, $P < 0.01$) though a slight rise was found in the medulla after 24 PBH. Optical density of apoptotic lymphocytes was significantly reduced in spleen in the 24 PBHs and raised in MLN during 48 PBHs than that prior to the burn, respectively.

CONCLUSION: Gut-origin LPS is a major cause of endotoxemia taken place early in rats following severe thermal injury and could induce extensive lymphocyte apoptosis in blood and MLN, which suggests an immunosuppression state could follow the initial injury and favors a septic state based on apoptotic mechanism.

Xia PY, Zheng J, Zhou H, Pan WD, Qin XJ, Xiao GX. Relationship between lymphocyte apoptosis and endotoxin translocation after thermal injury in rats. *World J Gastroenterol* 2002;8(3):546-550

INTRODUCTION

Endotoxin or lipopolysaccharide (LPS) is a major cause of the local inflammation and septic shock and has been shown to impair host immune defense^[1-10]. With the experimental endotoxemia or sepsis in C3H/HeN (endotoxin-sensitive) mice, it was demonstrated in recent studies that LPS could cause thymic atrophy and bring about the increased apoptotic lymphocytes in thymus, spleen and gut-associated lymphatic tissue^[11-13]. Since the lymphocytes appear essential to both competent immune function and to the control of inflammatory response^[14,15], the lymphocyte apoptosis induced by LPS may play important roles in the development and regulation of the immune system, especially in the gut-dysfunction situations induced by sepsis or severe injuries. Endotoxemia in the patients with severe injury has been suggested to be an important factor in the systemic inflammatory response syndrome (SIRS)^[16,17]. It was found in the previous *in-vivo* study that gut-origin endotoxemia following the intestinal mucosal barrier dysfunction could occur in early postburn period and lead to the injury of systemic organs such as lungs, liver etc^[18,19]. Although the exact routes by which translocating LPS reach the blood and systemic organs are not known with certainty, most researchers believed that LPS was capable of translocating from the gut via both the mesenteric lymphatics and the portal blood^[20]. Because the mesenteric lymph nodes (MLN) receives its lymphatic drainage from the small intestine, cecum and proximal colon, we believed that MLN should be a major site and pathway of translocated gut-origin LPS. However, little has been known about lymphocyte apoptosis in circulating blood and MLN induced by endotoxin translocation after thermal injury and the relationship between them.

The present experiments were performed in severe scalded rats to determine the effects of gut-origin LPS translocation on the apoptosis of lymphocytes in circulating blood, spleen and MLN, and to investigate the relationship between them.

MATERIALS AND METHODS

Animals and reagents

Forty-two adult Wistar rats weighing 235-345g were randomly distributed in the normal control and 6 thermal injury groups, i.e. 3, 6, 12, 24, 48 and 72h after scalding. Each group contained 6 animals (half males and half females). Rats in the thermal injury groups were inflicted with 30% total burn surface area (TBSA) III degree scalding on their back after anesthetized with 30mg/kg of

intraperitoneal pentobarbital. Then under general anesthesia at the different time points after the thermal injury, the blood of rats' portal vein and vena cava were collected for LPS test and the isolation of peripheral blood lymphocyte, respectively. MLN and spleen were harvested by aseptic manipulation and fixed in 10mL·L⁻¹ paraformaldehyde solution (pH 7.4) for 24h. All chemicals used in this study were purchased from Sigma Chemical Co. (USA) unless specified otherwise. Endotoxin-free glassware and plasticware were prepared by baking at 250°C for 1.5h and radiating with ⁶⁰Co, respectively.

Determination of serum LPS levels in portal vein and vena cava

Sera were obtained from the blood samples of portal vein and vena cava by clotting for 60min on ice and then centrifuged at 2500g at 4°C for 5min respectively, filtered, aliquoted, and frozen at -70°C. After all serum samples were collected, the serum LPS levels were determined with a commercially available kit for tachypleus amebocyte lysate (TAL) technique (Zhanjiang A & C Biological Ltd, Zhanjiang, China) according to the manufacture's guidelines.

Isolation and preparation of lymphocyte

Lymphocyte in the heparinized blood from vena cava were isolated by density gradient centrifugation using ficoll-hypaque (d=1.077) followed by two washing steps in phosphate buffered saline (PBS) and lysis of residual erythrocytes using nine volumes of an ice-cold isotonic ammonium chloride solution (NH₄Cl 155mmol·L⁻¹, KHCO₃ 10mmol·L⁻¹, EDTA 0.1mmol·L⁻¹) to one volume of cell pellet at 4°C for 7min^[21]. Lymphocytes were greater than 98% as analyzed by microscopy using Hemacolor staining (Merk, Germany). Cell viability was greater than 97% as assessed by the trypan blue exclusion test. Isolated lymphocytes were maintained in a glass bottle in RPMI 1640-medium without fetal calf serum (endotoxin-free; Gibco BRL, Life Technologies, USA) at a concentration of 1×10⁹ cells·L⁻¹ in 5mL·L⁻¹ CO₂ at 37°C for 2h to exclude macrophage before the analysis of apoptosis. Then the cells were collected by centrifugation and washed twice in PBS.

Flow cytometric analysis of apoptotic lymphocyte

The analysis of apoptotic lymphocytes was performed by an in situ Cell Death Detection Kit, Fluorescein (Roche, Germany). The procedures in brief was according to the manufacture's guidelines as follows: lymphocyte were suspended and fixed with 40mL·L⁻¹ paraformaldehyde solution (pH 7.4), rinsed in PBS twice, and incubated in permeabilization solution (1 g·L⁻¹ Triton X-100 in 1 g·L⁻¹ sodium citrate) for 2min on ice. The cells were again rinsed in PBS, centrifuged and incubated in terminal deoxynucleotidyl transferase (TdT)-mediated dUTP nick end labeling (TUNEL) reaction mixture for 1h at 37°C in a humidified atmosphere at dark. Then cells were rinsed in PBS again. TUNEL fluorescence of individual nuclei in a final volume of 500μL cells solution was analyzed by an FACS Calibur (Becton Dickinson, USA), while gating on physical parameters was enacted to exclude cell debris. A minimum of 10000 events were counted per sample. The results were reported as the percentage of hypodiploid (fragmented) nuclei reflecting the relative proportion of apoptotic cells.

Analysis of apoptotic lymphocytes in spleen and MLN

Paraffin-embedded spleen and MLN tissue were cut into sections of 5μm and mounted on Vectabond Reagent slides, deparaffinized and rehydrated through xylene, graded ethanol to distilled water. Then the tissue sections were pre-treated with 20mg·L⁻¹ proteinase K for 30min, and analyzed with an in situ Cell Death Detection Kit, POD (Roche, USA) according to the manufacture's guidelines. Each

experiment set up by TUNEL reaction mixture without terminal transferase served as negative control. The images were taken by Cooled camera system, and the count and optical density (OD) value of apoptotic lymphocytes were analyzed with software Spot and Imagine proplus 4.10a (IPP 4.10). The counts and optical density values (transmission light) of TUNEL-POD positive lymphocytes in spleen and MLN were determined in three high-resolution fields selected randomly in the area concentrated positive apoptotic lymphocytes and two thousand cells per field were counted per slides.

Statistical analysis

All the data was analyzed by Student's *t* test and expressed as $\bar{x} \pm s$. The statistical difference $P < 0.05$ was considered as significantly and $P < 0.01$ as very significant.

RESULTS

Serum LPS in portal vein and vena cava increased after thermal injury

Serum LPS levels in portal vein and vena cava increased sharply postburn ($P < 0.01$) and reached to a peak level at 6 PBH and decreased thereafter. LPS level in portal vein was higher than that in the vena cava ($P < 0.01$) in the period of 3 to 48 PBHs, but both decreased to near control level at 72 PBH (Figure 1).

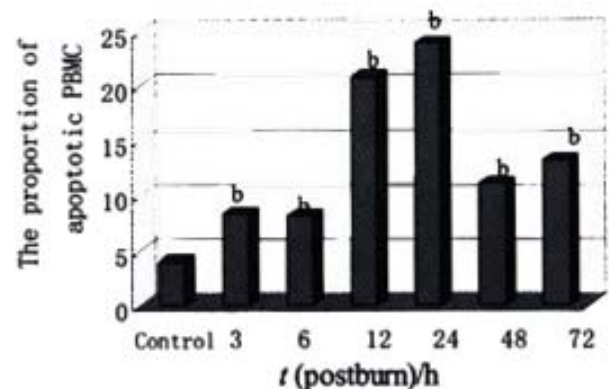


Figure 1 Comparison of the LPS levels postburn in portal vein and in vena cava. ^b $P < 0.01$, vs control; ^c $P < 0.01$, portal vein vs vena cava

Apoptosis of lymphocytes

Lymphocytes isolated from the circulation of healthy rats exhibited a low proportion of apoptotic cells at (3.99±1.72)%, but increased obviously during the whole postburn period of the experiment ($P < 0.01$), especially after 6 PBH. The concentrations of lymphocytic apoptosis at 12 and 24 PBH were markedly higher than that at other time points (Figure 2,3).

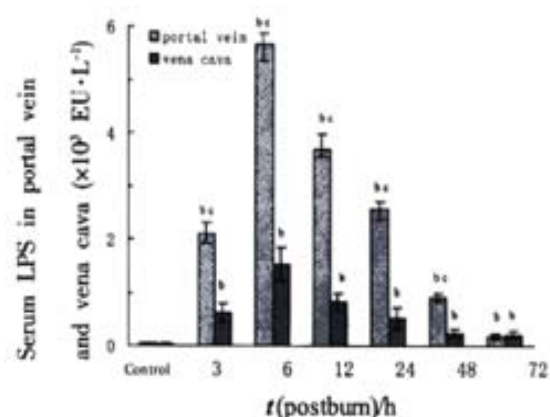


Figure 2 The relative proportions of apoptotic lymphocytes postburn. ^b $P < 0.01$, vs control

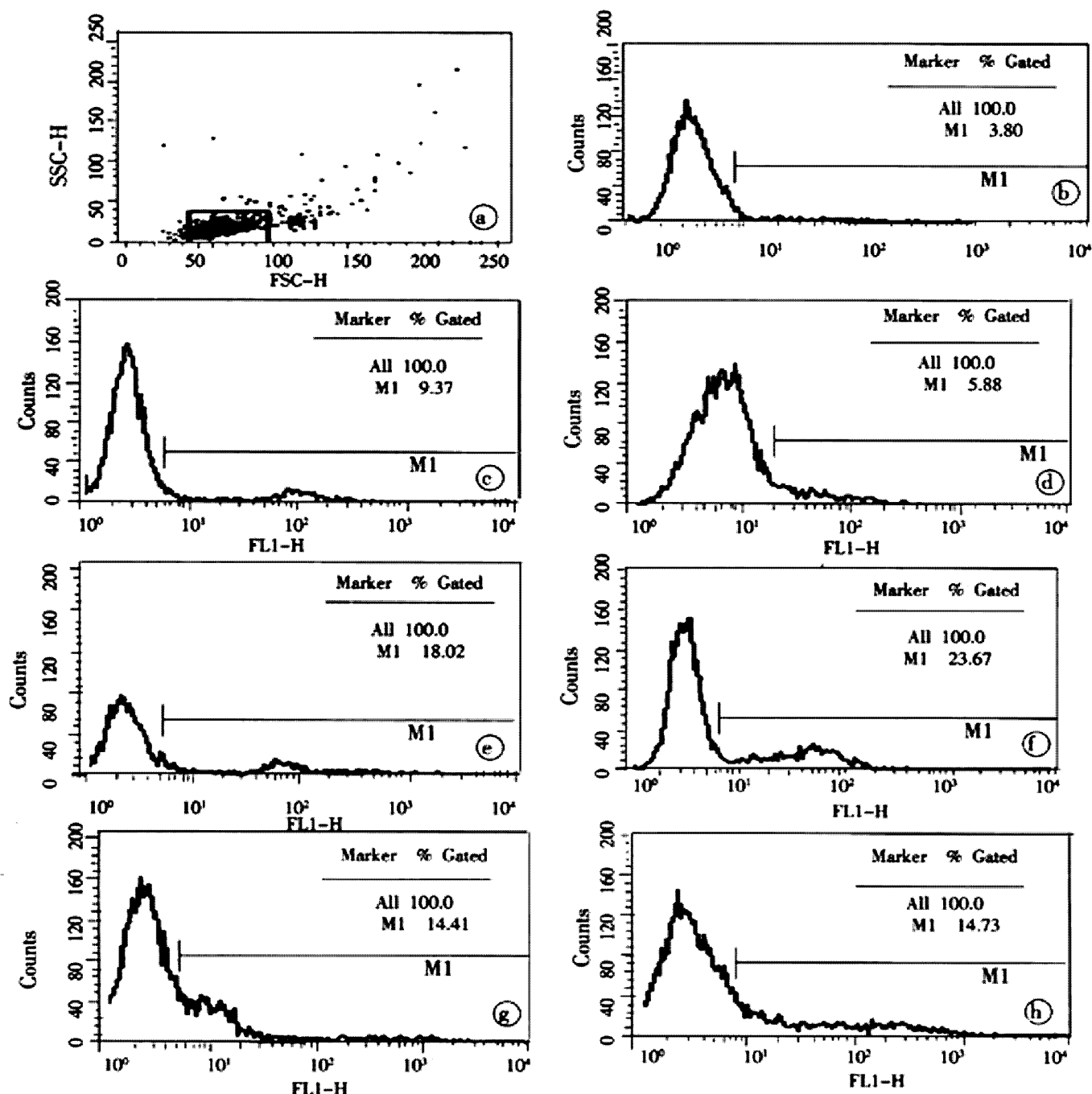


Figure 3 The results of typical flow cytometric analysis of postburn apoptotic lymphocytes. a, b, c, d, e, f, g and h were the relative proportion of apoptotic lymphocytes isolated from one rat in the control and group 3, 6, 12, 24, 48 and 72 PBH, respectively.

Apoptotic lymphocytes in spleen and MLN

It was shown by the results of TUNEL-POD staining and the counts of apoptotic lymphocytes that the apoptotic cells were few in normal MLN (Figure 4a), but increased postburn obviously ($P < 0.01$), especially at 3 PBH (Figure 4b, Table 1). Opposite to MLN, apoptotic lymphocytes were concentrated in spleen cortex before burn (Figure 4c), but decreased obviously during 3 to 72 PBHs ($P < 0.01$) though a slight rise was found in the medulla after 24 PBH (Figure 4d, Table 1). Since the principle of TUNEL-POD is to label the fragmented genomic DNA, the biochemical hallmark of apoptotic cell, the color density of nuclei staining could indirectly reflect the extent of DNA fragmentation. Optical density of TUNEL-POD staining in apoptotic lymphocytes was significantly reduced in spleen in the 24 PBHs, but raised in MLN during 48 PBHs than that before burn, respectively (Table 2).

Table 1 Apoptotic lymphocyte counts in 2000 total cells of spleen and MLN

Tissue	Healthy control	t(postburn)/h					
		3	6	12	24	48	72
Spleen	499±186	12±8 ^b	19±15 ^b	12±7 ^b	100±15 ^b	123±25 ^b	226±26 ^b
MLN	3±1	546±83 ^b	285±39 ^b	149±30 ^b	58±10 ^b	36±11 ^b	33±9 ^b

^b $P < 0.01$, vs control

Table 2 The optical density values(transmission light) of TUNEL-POD positive lymphocytes in spleen and MLN

Tissue	Healthy control	t(postburn)/h					
		3	6	12	24	48	72
Spleen	0.54±0.03	0.30±0.02 ^b	0.35±0.12 ^b	0.36±0.03 ^b	0.36±0.02 ^b	0.44±0.19	0.52±0.12
MLN	0.24±0.06	0.83±0.16 ^b	0.96±0.25 ^b	0.62±0.16 ^b	0.45±0.04 ^b	0.35±0.07 ^b	0.29±0.04

^b $P < 0.01$, vs control

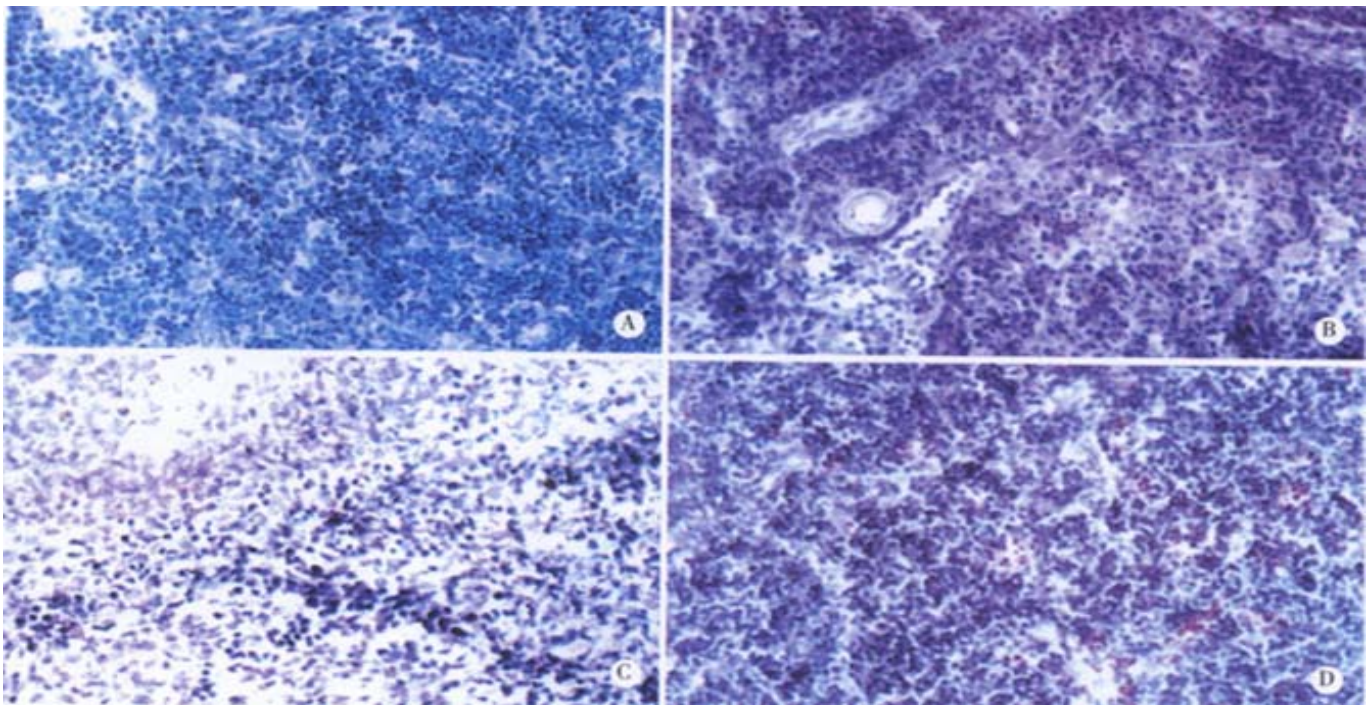


Figure 4 Apoptotic lymphocytes in spleen and MLN. (TUNEL-POD staining $\times 400$, the nuclei stained brown are positive apoptotic cells). a: MLN from the healthy rat; b: MLN from the rat at 3 PBH; c: Spleen from the healthy rat; d: Spleen from the rat 24 PBH.

DISCUSSION

Translocation of gut bacteria and endotoxin is a common situation after severe trauma, probably as a consequence of loss of physical integrity of the mucosal barrier, increments in permeability, or impaired local immune function resulted from ischemia-reperfusion injury of intestine. The gut-origin LPS translocated to the portal circulation or gut lymphatics has been thought to subsequently initiate a septic process leading to the development of SIRS^[22]. In this study, the LPS levels in portal vein and vena cava increased sharply after the severe thermal injury (Figure 1) indicating that endotoxin could enter the blood circulation in the early period of trauma and might be a main cause of endotoxemia.

The gastrointestinal tract contains numerous immune effector and regulatory cells of lymphoid and myeloid origin that are thought to play a critical role in host defense against enteric infections^[23]. And at a systemic level, the lymphocytes, through the production of regulatory cytokines, are important in mediating and controlling the host immune response. This was well illustrated by the spontaneous appearance of gastrointestinal inflammatory disease in a number of animals deficient in different cytokines, including IL-2 and IL-10, etc^[24-26]. Thus, the increased lymphocyte apoptosis in circulatory blood and gut-associated lymphoid tissues must impair the balance between the functions of host defense and immune tolerance in the gut immune system^[27,28]. The observation presented here provided some evidence that local and systemic pathologic lymphocyte apoptosis following an initial event of injury could impair the immune system. In the scalded rats, the counts of apoptotic lymphocytes in peripheral blood and MLN increased dramatically during the whole 72 PBHs, and reached a peak level at 12-24 PBHs and 3 PBH, respectively (Figure 2,3, 4, Table 1, 2). The results of lymphocyte apoptosis in MLN were consistent with that reported by Mongini *et al*^[22]. Moreover, It was surprised to observe the apoptotic lymphocytes in the spleen decreased obviously after thermal injury in this study (Figure 4, Table 1, 2) though splenic lymphocyte seemed to be less sensitive to apoptosis triggered by LPS

and oxidative stress^[11,12,29]. Specifically, we also found that splenic apoptotic lymphocytes were located mainly in the cortex in healthy rats, but being present in the medulla after thermal injury. The implications of these results are unclear. During normal lymphocyte development, immature lymphocytes are located in the cortex and migrate to the medulla in the course of maturation. The depletion of cortical lymphocytes by apoptosis may be one mechanism of eliminating potentially autoreactive immune cells^[22]. As for the decreased splenic apoptotic lymphocytes in the scalded rats, whether it is a reaction induced by the lymphocyte apoptosis in peripheral blood remains to be clarified.

Taking that both change tendency of lymphocyte apoptosis and serum LPS level after thermal injury into consideration, it was found that the peak level of lymphocyte apoptosis appeared earlier in MLN and much later in circulatory blood than that of LPS in the blood. The results indicated that MLN was an advanced station in the routing of the LPS translocation and suggested that the translocation of gut-origin LPS was a major factor of lymphocyte apoptosis in rats with severe burn injury. Furthermore, LPS translocated into the blood could lead to a further breakdown of gut immune barrier and thus accelerate the entrance of enteric bacteria and their toxins into the circulation^[30] and result in an immunosuppressive state due to the induction of lymphocyte apoptosis^[14,22,31]. This might explain why the peak level of apoptotic lymphocytes came forth much later in circulatory blood than that in MLN.

In addition to our observations in the present study, thymocyte and mucosal lymphocyte apoptosis after thermal injury had been recently reported^[32,33]. Although in these two studies the increased lymphocyte apoptosis in thymus and gut-associated lymphoid tissue seemed mainly due to the increased corticosterone concentration in plasma and in the lymphoid tissue, the presence of lymphocyte apoptosis in the peripheral blood, thymus and gut-associated lymphoid tissue following injury could explain the immunosuppressive state following such injury. In fact, decreased lymphocyte apoptosis in

sepsis can improve survival by overexpression of Bcl-2 in transgenic mice^[34]. In summary, we can reach the conclusion that an immunosuppression state could follow the initial injury and favor a septic state based on apoptotic mechanism, and that the immunosuppressive state after the thermal injury can be the event induced by translocation of gut-origin LPS and bacteria spreading to other tissues, and which in turn causes a recurrence of sepsis.

REFERENCES

- Bouchon A, Facchetti F, Weigand MA, Colonna M. TREM-1 amplifies inflammation and is a crucial mediator of septic shock. *Nature* 2001; 410: 1103-1107
- Yi JH, Ni RY, Luo DD, Li SL. Intestinal flora translocation and overgrowth in upper gastrointestinal tract induced by hepatic failure. *World J Gastroenterol* 1999;5:327-329
- Wray GM, Foster SJ, Hinds CJ, Thiemermann C. A cell wall component from pathogenic and non-pathogenic gram-positive bacteria (peptidoglycan) synergises with endotoxin to cause the release of tumour necrosis factor- α , nitric oxide production, shock, and multiple organ injury/dysfunction in the rat. *Shock* 2001; 15: 135-142
- Zhu L, Yang ZC, Li A, Cheng DC. Protective effect of early enteral feeding on postburn impairment of liver function and its mechanism in rats. *World J Gastroenterol* 2000;6:79-83
- Schultz MJ, Olszyna DP, de-Jonge E, Verbon A, van-Deventer SJ, van-der-Poll T. Reduced ex vivo chemokine production by polymorphonuclear cells after in vivo exposure of normal humans to endotoxin. *J Infect Dis* 2000; 182: 1264-1267
- Fu WL, Xiao GX, Yue XL, Hua C, Lei MP. Tracing method study of bacterial translocation in vivo. *World J Gastroenterol* 2000;6:153-155
- Liu BH, Chen HS, Zhou JH, Xiao N. Effects of endotoxin on endothelin receptor in hepatic and intestinal tissues after endotoxemia in rats. *World J Gastroenterol* 2000; 6:298-300
- Zuo GQ, Gong JP, Liu CA, Li SW, Wu XC, Yang K, Li Y. Expression of lipopolysaccharide binding protein and its receptor CD14 in experimental alcoholic liver disease. *World J Gastroenterol* 2001;7:836-840
- Heagy W, Hansen C, Nieman K, Cohen M, Richardson C, Rodriguez JL, West MA. Impaired ex vivo lipopolysaccharide-stimulated whole blood tumor necrosis factor production may identify "septic" intensive care unit patients. *Shock* 2000; 14: 271-277
- Zhang GL, Wang YH, Teng HL, Lin ZB. Effects of aminoguanidine on nitric oxide production induced by inflammatory cytokines and endotoxin in cultured rat hepatocytes. *World J Gastroenterol* 2001; 7: 331-334
- Zhang YH, Takahashi K, Jiang GZ, Kawai M, Fukada M, Yokochi T. In vivo induction of apoptosis (programmed cell death) in mouse thymus by administration of lipopolysaccharide. *Infect Immun* 1993; 61: 5044-5048
- Manhart N, Vierlinger K, Habel O, Bergmeister LH, Gotzinger P, Sautner T, Spittler A, Boltz-Nitulescu G, Marian B, Roth E. Lipopolysaccharide causes atrophy of Peyer's patches and an increased expression of CD28 and B7 costimulatory ligands. *Shock* 2000; 14: 478-483
- Wang SD, Huang KJ, Lin YS, Lei HY. Sepsis-induced apoptosis of the thymocytes in mice. *J Immunol* 1994;152:5014-5021
- Hotchkiss RS, Swanson PE, Freeman BD, Tinsley KW, Cobb JP, Matuschak GM, Buchman TG, Karl IE. Apoptotic cell death in patients with sepsis, shock, and multiple organ dysfunction. *Crit Care Med* 1999; 27: 1230-1251
- Hotchkiss RS, Chang KC, Swanson PE, Tinsley KW, Hui JJ, Klender P, Xanthoudakis S, Roy S, Black C, Grimm E, Aspiotis R, Han Y, Nicholson DW, Karl IE. Caspase inhibitors improve survival in sepsis: a critical role of the lymphocyte. *Nat Immunol* 2000; 1: 496-501
- Pape HC, Remmers D, Grotz M, Schedel I, von-Glinski S, Oberbeck R, Dahlweit M, Tscherne H. Levels of antibodies to endotoxin and cytokine release in patients with severe trauma: does posttraumatic dysergy contribute to organ failure? *J Trauma* 1999; 46: 907-913
- Crespo E, Macias M, Pozo D, Escames G, Martin M, Vives F, Guerrero JM, Acuna-Castroviejo D. Melatonin inhibits expression of the inducible NO synthase II in liver and lung and prevents endotoxemia in lipopolysaccharide-induced multiple organ dysfunction syndrome in rats. *FASEB J* 1999; 13: 1537-1546
- Hotchkiss RS, Schmiege RE, Swanson PE, Freeman BD, Tinsley KW, Cobb JP, Karl IE, Buchman TG. Rapid onset of intestinal epithelial and lymphocyte apoptotic cell death in patients with trauma and shock. *Crit Care Med* 2000; 28: 3207-3217
- Goris RJA, Bebbler IPT, Mollen RMH, Koopman JP. Dose selective decontamination of the gastrointestinal tract prevent multiple organ failure. *Arch Surg* 1991; 126: 561-562
- Alexander JW, Gianotti L, Pyles T, Carey MA, Babcock GF. Distribution and survival of *Escherichia coli* translocating from the intestine after thermal injury. *Ann Surg* 1991; 213: 558-567
- Ertel W, Keel M, Infanger M, Ungethüm U, Steckholzer U, Trentz O. Circulating mediators in serum of injured patients with septic complications inhibit neutrophil apoptosis through up-regulation of protein-tyrosine phosphorylation. *J Trauma* 1998; 44: 767-775
- Mongini C, Ruybal PH, Garcia RH, Mocetti E, Escalada A, Christiansen S, Argibay P. Apoptosis in gut-associated lymphoid tissue: a response to injury or a physiologic mechanism? *Transplant Proc* 1998; 30: 2673-2676
- Malstrom C, James S. Inhibition of murine splenic and mucosal lymphocyte function by enteric bacterial products. *Infect Immun* 1998; 66: 3120-3127
- Sadlack B, Merz H, Schorle H, Schimpl A, Feller AC, Horak I. Ulcerative colitis-like disease in mice with a disrupted interleukin-2 gene. *Cell* 1993; 75: 253-261
- Kulkarni AB, Huh CG, Becker D, Geiser A, Lyght M, Flanders KC, Roberts AB, Sporn MB, Ward JM. Transforming growth factor (1 null mutation in mice causes excessive inflammatory response and early death. *Proc Natl Acad Sci USA* 1993; 90: 770-774
- Kuhn R, Lohler J, Rennick D, Rajewsky K, Muller W. Interleukin-10-deficient mice develop chronic enterocolitis. *Cell* 1993; 75: 263-274
- Ayala A, Xu YX, Ayala CA, Sonefeld DE, Karr SM, Evans TA, Chaudry IH. Increased mucosal B-lymphocyte apoptosis during polymicrobial sepsis is a Fas ligand but not an endotoxin-mediated process. *Blood* 1998; 91: 1362-1372
- Andjelic S, Khanna A, Suthanthiran M, Nikolic ZJ. Intracellular Ca²⁺ elevation and cyclosporin A synergistically induce TGF- β 1-mediated apoptosis in lymphocytes. *J Immunol* 1997; 158: 2527-2534
- Freeman BD, Reaume AG, Swanson PE, Epstein CJ, Carlson EJ, Buchman TG, Karl IE, Hotchkiss RS. Role of CuZn superoxide dismutase in regulating lymphocyte apoptosis during sepsis. *Crit Care Med* 2000; 28: 1701-1708
- Navaratnam RLN, Morris SE, Traber DL, Flynn J, Woodson L, Linares H, Herndon DN. Endotoxin (LPS) increased mesenteric vascular Resistance (MVR) and bacterial translocation. *J Trauma* 1990; 30: 1104-1115
- Kurita-Ochiai T, Fukushima K, Ochiai K. Butyric acid-induced Apoptosis of murine thymocytes, splenic T cells, and human jurkat T cells. *Infect Immun* 1997; 65: 35-41
- Fukuzuka K, Edwards CK 3rd, Clare-Salzer M, Copeland EM 3rd, Moldawer LL, Mozingo DW. Glucocorticoid and Fas ligand induced mucosal lymphocyte apoptosis after burn injury. *J Trauma* 2000; 49: 710-716
- Nakanishi T, Nishi Y, Sato EF, Ishii M, Hamada T, Inoue M. Thermal injury induces thymocyte apoptosis in the rat. *J Trauma* 1998; 44: 143-148
- Hotchkiss RS, Swanson PE, Knudson CM, Chang KC, Cobb JP, Osborne DF, Zollner KM, Buchman TG, Korsmeyer SJ, Karl IE. Overexpression of Bcl-2 in transgenic mice decreases apoptosis and improves survival in sepsis. *J Immunol* 1999; 162: 4148-4150

Edited by Wu XN

• BASIC RESEARCH •

Expression of CD14 protein and its gene in liver sinusoidal endothelial cells during endotoxemia

Jian-Ping Gong, Li-Li Dai, Chang-An Liu, Chuan-Xin Wu, Yu-Jun Shi, Sheng-Wei Li, Xu-Hong Li

Jian-Ping Gong, Chang-An Liu, Chuan-Xin Wu, Yu-Jun Shi, Sheng-Wei Li, Xu-Hong Li, Department of General Surgery, the Second College of Clinical Medicine & the Second Affiliated Hospital of Chongqing University of Medical Science, Chongqing, 400010, China

Li-Li Dai, Department of Digestive Disease, the Second College of Clinical Medicine & the Second Affiliated Hospital of Chongqing University of Medical Science, Chongqing, 400010, China

Supported by the National Natural Science Foundation of China, No. 39970719, 30170919

Correspondence to: Dr Jian-Ping Gong, Department of General Surgery, the Second College of Clinical Medicine & the Second Affiliated Hospital of Chongqing University of Medical Science, 74 Linjiang Road, Chongqing 400010, China. gongjianping11@hotmail.com

Telephone: +86-23-85541610 Fax: +86-23-63822815

Received 2001-11-15 Accepted 2001-12-10

Abstract

AIM: To observe expression of CD14 protein and CD14 gene in rat liver sinusoidal endothelial cells (LSECs) during endotoxemia, and the role of CD14 protein in the activation of lipopolysaccharide (LPS)-induced LSECs.

METHODS: Wistar rat endotoxemia model was established first by injection of a dose of LPS (5mg/kg, Escherichia coli O111:B4) via the tail vein, then sacrificed after 0h, 3h, 6h, 12h, and 24h, respectively. LSECs were isolated from normal and LPS-injected rats by an in situ collagenase perfusion technique. The isolated LSECs were incubated with rabbit anti-rat CD14 polyclonal antibody, then stained with goat anti rabbit IgG conjugated fluorescein isothiocyanate (FITC) and flow cytometric analysis (FCM) was performed. The percentage and mean fluorescence intensity (MFI) of CD14-positive cells were taken as the indexes. LSECs were collected to measure the expression of CD14 mRNA by in situ hybridization analysis. The isolated LSECs from normal rats were incubated firstly with anti-CD14 antibody, then stimulated with different concentrations of LPS, and the supernatants of these cells were then collected for measuring the levels of tumor necrosis factor (TNF)- α and Interleukin (IL)-6 with ELISA.

RESULTS: In rats with endotoxemia, LSECs displayed a strong MFI distinct from that of control rats. CD14 positive cells in rats with endotoxemia were 54.32%, 65.83%, 85.64%, and 45.65% at 3h, 6h, 12h, and 24h respectively, there was significant difference when compared to normal group of animals (4.45%) ($P < 0.01$). The expression of CD14 mRNA in isolated LSECs was stronger than that in control rats. In LPS group, the levels of TNF- α and IL-6 were $54 \pm 6 \text{ ng} \cdot \text{L}^{-1}$, $85 \pm 9 \text{ ng} \cdot \text{L}^{-1}$, $206 \pm 22 \text{ ng} \cdot \text{L}^{-1}$, $350 \pm 41 \text{ ng} \cdot \text{L}^{-1}$, $366 \pm 42 \text{ ng} \cdot \text{L}^{-1}$ and $103 \pm 11 \text{ ng} \cdot \text{L}^{-1}$, $187 \pm 20 \text{ ng} \cdot \text{L}^{-1}$, $244 \pm 26 \text{ ng} \cdot \text{L}^{-1}$, $290 \pm 31 \text{ ng} \cdot \text{L}^{-1}$, and $299 \pm 34 \text{ ng} \cdot \text{L}^{-1}$, respectively at different concentration points. In anti-CD14 group, the levels of TNF- α and IL-6 were $56 \pm 5 \text{ ng} \cdot \text{L}^{-1}$, $67 \pm 8 \text{ ng} \cdot \text{L}^{-1}$, $85 \pm 10 \text{ ng} \cdot \text{L}^{-1}$, $113 \pm 12 \text{ ng} \cdot \text{L}^{-1}$, $199 \pm 22 \text{ ng} \cdot \text{L}^{-1}$ and $104 \pm 12 \text{ ng} \cdot \text{L}^{-1}$, $125 \pm 12 \text{ ng} \cdot \text{L}^{-1}$, $165 \pm 19 \text{ ng} \cdot \text{L}^{-1}$, $185 \pm 21 \text{ ng} \cdot \text{L}^{-1}$, and $222 \pm 23 \text{ ng} \cdot \text{L}^{-1}$, respectively at

different concentration points. There was significant difference between the two groups ($P < 0.01$).

CONCLUSION: LSECs can synthesize CD14 protein and express CD14 gene during endotoxemia. CD14 protein plays an important role in the activation of LPS-induced LSECs. This finding has important implications for the understanding of the mechanisms by which LPS may injure liver sinusoidal endothelial cells during sepsis.

Gong JP, Dai LL, Liu CA, Wu CX, Shi YJ, Li SW, Li XH. Expression of CD14 protein and its gene in liver sinusoidal endothelial cells during endotoxemia. *World J Gastroenterol* 2002;8(3):551-554

INTRODUCTION

Lipopolysaccharide (LPS) has been shown to play a key role in the pathogenesis of severe sepsis and septic shock caused by gram-negative bacteria. LPS stimulates monocytes and macrophages to release proinflammatory mediators, such as tumor necrosis factor (TNF)- α and interleukins^[1-10]. Recent studies have reported that LPS-binding protein (LBP) and LPS receptor CD14 mediate responses of activated monocytes, macrophages and other cells to LPS^[11-13]. CD14 is a 55-kDa glycoprotein with multiple leucine-rich repeats and was first described as a myeloid differentiation antigen^[14]. CD14 has been identified as receptor for complexes of LPS and LBP. It is known that CD14 is linked to the cell membrane by a glycosylphosphatidylinositol anchor in myeloid lineage cells, and it plays a pivotal role in the activation of LPS-induced monocytes and macrophages^[15, 16]. But it is not yet clear whether CD14 is expressed by vascular endothelial cells. Indeed, it has been generally accepted that endothelial cells do not express CD14^[17]. Soluble CD14 (sCD14) is thought to facilitate LPS-induced activation of endothelial cells^[18]. However, recent studies have shown that endothelial cells are sensitive to low concentration of LPS and anti-CD14 antibodies can block endothelial cell activation even in the absence of serum, which is an observation inconsistent with the concept that endothelial cells do not express CD14^[19]. Our aim was to demonstrate that liver sinusoidal endothelial cells (LSECs) synthesize CD14 protein and express CD14 gene in rats with endotoxemia, and the role of CD14 protein in the activation of LPS-induced LSECs.

MATERIALS AND METHODS

Reagents

LPS (Escherichia coli O111: B4) and collagenase (type IV) were purchased from Sigma Chemical Company (St. Louis, Mo.). A rabbit anti-rat CD14 polyclonal antibody was purchased from Santa Cruz Biotechnology (Santa Cruz, Calif). Fluorescein isothiocyanate (FITC)-IgG were purchased from Zhongshan Biotechnology Company (Beijing, China). In situ hybridization analysis kit of CD14 mRNA was purchased from Boshide Biotechnology Company (Wuhan, China).

Animals

Male Wistar rats, which were pathogen-free and weighed

approximately 225g each, were purchased from the Animal Center of Chongqing University of Medical Science. The rats were exposed each day to 12h of light and darkness respectively. Rodent chow and water were provided ad libitum. Experimental protocols were approved by the Institutional Care and Use Committee of Chongqing University of Medical Science.

The endotoxemia model of animals

The Wistar rat endotoxemia model was established as described previously^[20]. In brief, animals were injected with a dose of LPS (5mg/kg, Escherichia coli O111: B4) via the tail vein, then the sacrificed after 3h, 6h, 12h, and 24h, respectively. There were six rats at each time point. Other six rats were used as control group (0h).

LSECs isolation

LSECs were isolated from normal and LPS-injected rats by an in situ collagenase perfusion technique, modified as described previously^[21]. In brief, livers were removed after a portal vein perfusion with Hanks' balanced salt solution (HBSS) and the homogenate was digested in a solution of 0.5% collagenase. LSECs were separated from other nonparenchymal cells by two cycles of differential centrifugation (50×g for 2min) and further purified over a 30% Percoll gradient. LSECs purity exceeded 90% as assessed by light microscopy, and viability was typically greater than 95% as determined by trypan blue exclusion assay.

Determination of CD14 mRNA by in situ hybridization

In situ hybridization was performed as described previously^[22]. Positive result: positive location was blue.

Flow cytometric analysis

Expression of CD14 protein in LSECs was examined by flow cytometric analysis as described previously^[23]. In brief, LSECs were incubated with rabbit anti-rat CD14 polyclonal antibody (1ug/ml) after washing, and then cells were incubated with goat anti-rabbit immunoglobulin G labeled with FITC. After being washed three times, 10000 cells were analyzed by flow cytometry (Coulter, USA), and the percentage and mean fluorescence intensity (MFI) of CD14-positive cells were taken as the indexes.

Blocking test of anti-CD14 antibody

To determinate the role of CD14 in the activation of LPS-induced LSECs, LSECs were isolated from normal rats. These cells were harvested and adjusted to a concentration of 1×10^6 /ml/well and were divided into two groups. Group of LPS: LSECs were incubated at different concentrations of LPS (0, 0.01ug/ml, 1ug/ml, 10ug/ml, and 100ug/ml). Group of anti-CD14 antibody blockade: LSECs were pre-incubated for 30min with 0.2ml CD14 antibody (1:100 dilution) before different concentrations of LPS were added. Supernatants were then collected for measuring the levels of TNF- α and IL-6 with ELISA.

Statistical analysis

All results were expressed as mean \pm SEM. Statistical differences between means were determined by using Student's *t* test. The value of $P < 0.01$ was considered significant.

RESULTS

Binding of FITC to LSECs

To confirm expression of CD14 on LSECs, we examined the binding of FITC to the cells. CD14 positive cells were 4.45% in rats of normal group. But in rats with endotoxemia, CD14 positive cells were 54.32%, 65.83%, 85.64%, and 45.65% at 3 h, 6 h, 12 h, and 24 h

respectively after stimulation of LPS, which were significant different when compared with normal group of animals ($P < 0.01$) (Figure 1).

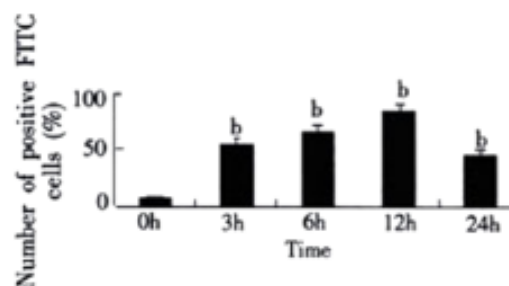


Figure 1 The percentage of positive FITC cells. ^b $P < 0.01$ vs 0h

Expression of CD14 gene in LSECs

We postulated that LSECs could express CD14 mRNA during endotoxemia. In order to examine the cell-specific expression of CD14 mRNA, freshly isolated and purified LSECs were analyzed by in situ hybridization with a riboprobe specific for rat CD14. Our analysis showed that LSECs from controls had no detectable level of CD14 mRNA. LPS treatment increased the level of CD14 mRNA in LSECs, inducing expression as early as 3h after LPS treatment. The expression of CD14 gene increased with time, reaching a maximum induction by 12h after treatment of LPS, and subsequently declined to low level by 24h.

Results of blocking test

In LPS group, with increasing of LPS concentrations, the levels of TNF- α and IL-6 in supernatant of LSECs also increased. In group of anti-CD14 antibody blockade, productions of TNF- α and IL-6 in supernatants of LSECs were obviously inhibited by Ab against CD14 when compared with LPS group ($P < 0.01$). (Figure 2 and 3)

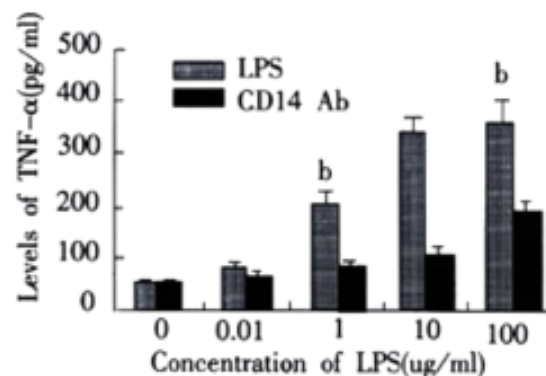


Figure 2 Effect of CD14 Ab on production of TNF- α in supernatants of LSECs. ^b $P < 0.01$ vs CD14 Ab

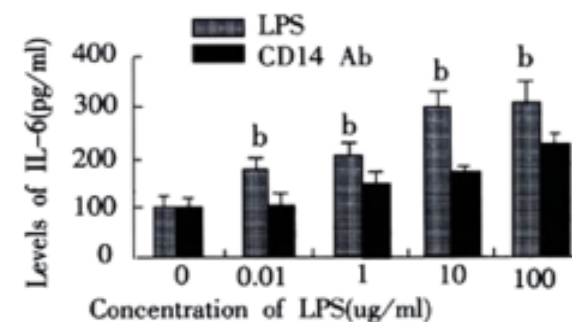


Figure 3 Effect of CD14 Ab on production IL-6 in supernatants of LSECs. ^b $P < 0.01$ vs CD14 Ab

DISCUSSION

CD14 as a key LPS signaling molecule was first reported to be expressed in monocyte-macrophage system^[4,12,23]. Recent works have showed that the CD14 antigen is expressed in many types of cells and tissues^[20, 24-32]. But it is not yet clear whether vascular endothelial cells could synthesize CD14 protein and express CD14 gene. Beekhuizen *et al* reported endothelial cells did not express CD14. With method of in situ hybridization, Fearn *et al*^[24] found that endothelial cells did not express CD14 protein. Wang *et al*^[18] considered that sCD14 was thought to facilitate LPS-induced activation of endothelial cells. But, Lee *et al*^[33] found CD14-negative murine pre-B cells (70Z/3), which were unresponsive to low concentrations of LPS (0.1ng/ml) even in the presence of serum, showed responses to LPS when transfected with CD14. Surprisingly, anti-CD14 antibody blocked endothelial cell activation by LPS even in the absence of serum, which is an observation inconsistent with the concept that endothelial cells do not express CD14 protein.

In this experiment, we selected LSECs to represent vascular endothelial cells as targets of our experiment, and determined whether LSECs could synthesize CD14 protein and express CD14 gene. We found: (1)LSECs from normal rats did not synthesize CD14 protein and express CD14 gene, but the synthesis and expression of CD14 were markedly upregulated by LPS during endotoxemia, accompanied with the expression of CD14 mRNA, which showed that CD14 protein in LSECs was not passively acquired from serum. (2)Anti-CD14 antibody could block LSECs activation by LPS in the absence of serum, which further indicated that LSECs could synthesize and express CD14 molecules.

Why were our findings different from previously published data that endothelial cells were CD14 negative? We think there were a few possibilities: (1)many authors used routine passaging of multiple culture of human vascular endothelial cells (HUVEC) or HUVEC purchased from tissue culture laboratories to observe whether these cells expressed CD14, but these cells might lose CD14 gene when they were cultured at multiple passages. Jersmann *et al*^[34] reported when HUVEs were cultured at passages 3 to 5, these cells were indistinguishable from passage 1 HUVEC in a number of properties and displayed normal morphology and viability and response to TNF to the same extent as passage 1 cells. However, unlike passage 1 cells, HUVEC that had undergone multiple passing expressed extremely low amounts of CD14 protein. We used freshly isolated primary rat LSECs to study the expression of CD14 and found they could obviously synthesize and express CD14 during endotoxemia. (2) LSECs were different from other endothelial cells in location, construction, and function. LSECs are located in hepatic sinus and stimulated by LPS from gut via portal vein blood, so these cells have their property which are different from other endothelial cells^[35]. (3) The choice of Ab against CD14 for the flow cytometric analysis may have been an additional explanation for the previously reported lack of CD14 on the endothelial cells' surface. Jersmann *et al*^[34] stained HUVEC with five different primary mAbs (MY4, 2D-15C, TUK4, LeuM3, and Rmo52) against CD14, and found only MY4 and TUK4 produced a positive stain and MY4 was the most effective mAb for detection of CD14 expression in endothelial cells. We stained LSECs with rabbit anti-rats primary antibody against CD14 from Santa Cruz Biotechnology and found this Ab against CD14 was effective for detecting the expression of CD14 protein. As expression of CD14 in animals is probably different from that in humans, further investigation of the expression of CD14 among animals is going on actively in our laboratory.

REFERENCES

- Gong JP, Liu CA, Wu CX, Li SW, Shi YJ, Li XH. Nuclear factor k β activity in patients with acute severe cholangitis. *World J Gastroenterol* 2002; 8:346-349
- Gong JP, Wu CX, Liu CA, Li SW, Shi YJ, Yang K, Li Y, Li XH. Intestinal damage mediated by Kupffer cells in rats with endotoxemia. *World J Gastroenterol* 2002; 8: press
- Gong JP, Liu CA, Wu CX, Li SW, Shi YJ, Yang K, Li Y, Li XH. Liver sinusoidal endothelial cell injury by neutrophils in rats with acute obstructive cholangitis. *World J Gastroenterol* 2002; 8:342-345
- Heumann D, Adachi Y, Roy DL, Ohno N, Yadomae T, Glauser MP, Calandra T. Role of plasma, lipopolysaccharide-binding protein, and CD14 in response of mouse peritoneal exudate macrophages to endotoxin. *Infect Immun* 2001; 69: 378-385
- Merkel SM, Alexander S, Zufall E, Oliver JD, Huet-Hudson YM. Essential role for estrogen in protection against *Vibrio vulnificus*-induced endotoxic shock. *Infect Immun* 2001; 69: 6119-6122
- Rabeih L, Irinopoulou T, Cholley B, Haeflner-Cavillon N, Carreno MP. Gram-positive and Gram-negative bacteria do not trigger monocyte cytokine production through similar intracellular pathways. *Infect Immun* 2001; 69: 4590-4599
- Fry DE. Sepsis syndrome. *Am Surg* 2000; 66:126-132
- Hotchkiss RS, Karl IE. Cytokine blockade in sepsis are two better than one? *Crit Care Med* 2001; 29: 671-672
- Mathurin P, Deng QG, Keshavarzian A, Choudhary S, Holmes EW, Tsukamoto H. Exacerbation of alcoholic liver injury by enteral endotoxin in rats. *Hepatology* 2000; 32:1008-1017
- Parker SJ, Watkins PE. Experimental models of gram-negative sepsis. *Br J Surg* 2001; 88:22-30
- Nanbo A, Nishimura H, Muta T, Nagasawa S. Lipopolysaccharide stimulates HepG2 human hepatoma cells in the presence of lipopolysaccharide-binding protein via CD14. *Eur J Biochem* 1999; 260: 183-191
- Gutsmann T, Muller M, Carroll SF, Mackenzie RC, Wiese A, Seydel U. Dual role of lipopolysaccharide (LPS)-binding protein in neutralization of LPS and enhancement of LPS-induced activation of mononuclear cells. *Infect Immun* 2001; 69: 6942-6950
- Hiki N, Berger D, Mimura Y, Frick J, Dentener MA, Buurman WA, Seidelmann M, Kaminishi M, Beger HG. Release of endotoxin-binding proteins during major elective surgery: role of soluble CD14 in phagocytic activation. *World J Surg* 2000; 24: 499-506
- Ulevitch RJ, Tobias PS. Receptor-dependent mechanisms of cell stimulation by bacterial endotoxin. *Annu Rev Immunol* 1995; 13: 437-457
- Enomoto N, Yamashina S, Kono H, Schemmer P, Rivera CA, Enomoto A, Nishiura T, Nishimura T, Brenner DA, Thurman RG. Development of a new, simple rat model of early alcohol-induced liver injury based on sensitization of Kupffer cells. *Hepatology* 1999; 29: 1680-1689
- Li SW, Gong JP, Wu CX, Shi YJ, Liu CA. Lipopolysaccharide induced synthesis of CD14 proteins and its gene expression in hepatocytes during endotoxemia. *World J Gastroenterol* 2002; 8: 124-127
- Kono H, Wheeler MD, Rusyn I, Lin M, Seabra V, Rivera CA, Bradford BU, Forman DT, Thurman RG. Gender differences in early alcohol-induced liver injury: role of CD14, NF- κ B, and TNF- α . *Am J Physiol* 2000; G652-661
- Wong PM, Chung SW, Sultzner BM. Genes, receptors, signals and responses to lipopolysaccharide endotoxin. *Scand J Immunol* 2000; 51: 123-127
- Von Asmuth EJU, Dentener MA, Baxil V, Bouma MG, Leeuwenberg JFM, Buurman WA. Anti-CD14 antibodies reduce responses of cultured human endothelial cells to endotoxin. *Immunology* 1993; 80: 78-83
- Gong JP, Xu MQ, Li K, Zhu J, Han BL. Expression of CD14 in Kupffer cells induced by lipopolysaccharide. *Di-San Junyi Daxue Xuebao* 2001; 23: 425-428
- Gong JP, Han BL. Technique of isolation, culture and identification of liver cells. *Shijie Huaren Xiaohua Zazhi* 1999; 7:417-419
- Fearn C, Loskutoff DJ. Role of tumor necrosis factor alpha in induction of murine CD14 gene expression by lipopolysaccharide. *Infect Immun* 1997; 65: 4822-4831
- Gong JP, Han BL. Effects of CD14 in LPS mediating activation of Kupffer cells. *Shijie Huaren Xiaohua Zazhi* 1999; 7:875-877
- Fearn C, Kravchenko VV, Ulevitch RJ, Loskutoff DJ. Murine CD14 gene expression *in vivo*: extramylloid synthesis and regulation by lipopolysaccharide. *J Exp Med* 1995; 181: 857-866
- Li SW, Wu CX, Shi YJ, Liu CA. Lipopolysaccharide upregulates expression of CD14 gene and CD14 proteins of hepatocytes in rats. *Chin J Hepatol* 2001; 9:103-105
- Zuo GQ, Gong JP, Liu CA, Li SW, Wu XC, Yang K, Li Y. Expression of lipopolysaccharide binding protein and its receptor CD14 in experimental alcoholic liver disease. *World J Gastroenterol* 2001; 6: 836-840
- Jiang Q, Akashi S, Miyake K, Petty HR. Cutting edge: lipopolysaccharide induces physical proximity between CD14 and toll-like

- receptor 4 (TLR4) prior to nuclear translocation of NF-kB. *J Immunol* 2000; 165:3541-3544
- 28 Ikejima K, Enomoto N, Seabra V, Ikejima A, Brenner DA, Thurman RG. Pronase destroys the lipopolysaccharide receptor CD14 on Kupffer cells. *Am J Physiol* 1999; 276: G591-G598
- 29 Scott MG, Vreugdenhil ACE, Buurman WA, Hancock REW, Gold MR. Cutting edge: cationic antimicrobial peptides block the binding of lipopolysaccharide (LPS) to LPS binding protein. *J Immunol* 2000; 164:549-553
- 30 Asea A, Kraeft SK, Kurt-Jones EA, Stevenson MA, Chen LB, Fixberg RW, Koo GC, Calderwood SK. HSP70 stimulates cytokine production through a CD14-dependant pathway, demonstrating its dual role as a chaperone and cytokine. *Nature Med* 2000; 6:435-442
- 31 Haziot A, Hijiya N, Gangloff SC, Silver J, Goyert SM. Induction of a novel mechanism of accelerated bacterial clearance by lipopolysaccharide in CD14-deficient and Toll-like receptor 4-deficient mice. *J Immunol* 2001; 166:1075-1078
- 32 Perea PY, Mayadas TN, Takeuchi O, Akira S, Zaks-Zilberman, Goyert SM, Vogel SN. CD11b/CD18 acts in concert with CD14 and toll-like receptor (TLR) 4 to elicit full lipopolysaccharide and taxol-inducible gene expression. *J Immunol* 2001; 166: 574-581
- 33 Lee JD, Kato K, Tobias PS, Kirkland TN, Ulevitch RJ. Transfection of CD14 into 70Z/3 cells dramatically enhances the sensitivity to complexes of lipopolysaccharide (LPS) and LPS binding protein. *J Exp Med* 1992; 175: 1697-1703
- 34 Jersmann HPA, Hii CST, Hodge GL, Ferrante AF. Synthesis and surface expression of CD14 by human endothelial cells. *Infect Immun* 2001; 69: 479-485
- 35 Bone-Larson CL, Simpson KJ, Colletti LM, Lukacs NW, Chen SC, Lira S, Kunkel S, Hogaboam CM. The role of chemokines in the immunopathology of the liver. *Immunol Rev* 2000; 177: 8-20

Edited by Hu DK

• BASIC RESEARCH •

The effects of anisodamine and dobutamine on gut mucosal blood flow during gut ischemia/reperfusion

Sen Hu, Zhi-Yong Sheng

Sen Hu, Zhi-Yong Sheng, Burns Institute, 304th Hospital of PLA, Beijing 100037, China

Supported by the Tenth Five-Year Key Project of PLA, No.01L081
Correspondence to: Dr Sen Hu, Burns Institute, 304th Hospital of PLA, 51 Fu Cheng Road, Beijing 100037, China

Telephone: +86-10-66867397 Fax: +86-10-68429998

Received 2002-01-26 Accepted 2002-02-20

Abstract

AIM: To determine if anisodamine is able to augment mucosal perfusion during gut I/R ischemia-reperfusion.

METHODS: A jejunal sac was formed in Sprague Dawley rat. A Laser Doppler probe and a tonometer were inserted into the sac which was filled with saline. The superior mesenteric artery was occluded (SMAO) for 60 minutes followed by 90 minutes of reperfusion. At the end of 60 minutes of SMAO, either 0.2mg/kg of anisodamine or dobutamine was injected into the jejunal sac. Laser Doppler mucosal blood flow and regional PCO_2 (PrCO_2) measurements were made.

RESULTS: Mucosal blood flow was significantly increased at 30, 60 and 90 minutes of reperfusion (R_{30} , R_{60} , R_{90}) when intraluminal anisodamine or dobutamine was present compared to intraluminal saline only ($44 \pm 3.3\%$ or $48 \pm 4.1\%$ vs $37 \pm 2.6\%$ at R_{30} , $57 \pm 5.0\%$ or $56 \pm 4.7\%$ vs $45 \pm 2.7\%$ at R_{60} , $64 \pm 3.3\%$ or $56 \pm 4.2\%$ vs $48 \pm 3.4\%$ at R_{90} , respectively $P < 0.05$). Blood flow changes were also reflected by lowering of jejunal PrCO_2 measurements after intraluminal anisodamine or dobutamine compared with that of the saline controls ($41 \pm 3.1\text{mmHg}$ or $44 \pm 3.0\text{mmHg}$ vs $49 \pm 3.7\text{mmHg}$ at R_{30} , $38 \pm 3.7\text{mmHg}$ or $40 \pm 2.1\text{mmHg}$ vs $47 \pm 3.8\text{mmHg}$ at R_{60} , $34 \pm 2.1\text{mmHg}$ or $39 \pm 3.0\text{mmHg}$ vs $46 \pm 3.4\text{mmHg}$ at R_{90} , respectively, $P < 0.05$). Most interesting finding was that there were significantly higher mucosal blood flow and lower jejunal PrCO_2 in anisodamine group than those in dobutamine group at 90 minutes of reperfusion ($64 \pm 3.3\%$ vs $56 \pm 4.2\%$ for blood flow or $34 \pm 2.1\text{mmHg}$ vs $39 \pm 3.0\text{mmHg}$ for PrCO_2 , respectively, $P < 0.05$), suggesting that anisodamine had a more lasting effect on mucosal perfusion than dobutamine.

CONCLUSION: Intraluminal anisodamine and dobutamine can augment mucosal blood flow during gut I/R and alleviate mucosal acidosis. The results provided beneficial effects on the treatment of splanchnic hypoperfusion following traumatic or burn shock.

Hu S, Sheng ZY. The effects of anisodamine and dobutamine on mucosal blood flow during gut ischemia/reperfusion. *World J Gastroenterol* 2002;8(3):555-557

INTRODUCTION

With remarkable advancement in our understanding of shock and greater ability to resuscitate patients from shock, few people today died of hypovolemic shock. However there still exists an inadequate

splanchnic perfusion, especially gut ischemia, despite apparent normalization of global hemodynamic parameters. Clinical and experimental studies have implicated gut hypoperfusion as an important inciting event which contributes to gut origin sepsis and multiple organ dysfunction^[1-10]. To improve gut perfusion, thus averting compensated shock, is still an important goal of resuscitation of shock^[11,12]. Anisodamine and dobutamine are commonly used as antishock drugs, as they can improve the microcirculation flow and splanchnic perfusion^[13-16]. Anisodamine, an anticholinergic drug extract from a Chinese herb *Anisodus tanguticus*, also processes many other beneficial effects such as inhibition of thromboxane synthesis and protection of cell from reperfusion injury^[17-20]. Some researches indicated that anisodamine and dobutamine augmented gut perfusion during the shock^[21,22], but there was no report concerning their intraluminal effects on mucosal blood flow and metabolism in the gut. The purpose of this study is to investigate the effects of local administration of anisodamine and dobutamine on mucosal blood flow and PrCO_2 in a gut ischemia-reperfusion (I/R) rat model.

MATERIALS AND METHODS

Animal model

Male Sprague-Dawley rats weighing 350-450 grams were employed after acclimatization to the experimental environment. Rats were fasted overnight but allowed free access to water. Anesthesia was induced and maintained with 2% isoflurane and body temperature maintained at 37°C by the use of a warming blanket. Through an upper midline laparotomy, a segment of jejunum measuring 16cm in length was isolated 5cm distal to the ligament of Treitz with preservation of its mesentery. The isolated loop was closed at both ends with 3-0 silk ligatures^[23,24]. The superior mesenteric artery (SMA) was isolated at its origin and clamped for 60 minutes, followed by release of the clamp and restoration of blood to the intestine for 90 minutes to produce gut ischemia and reperfusion injury (I/R injury). At the time of release of the clamp, either 0.2mg/kg of anisodamine or dobutamine was injected into the jejunal sac. At the conclusion of the experiment, cardiac puncture and exsanguination were used to achieve euthanasia.

Animals were divided into three groups: Group one ($n=15$): I/R + anisodamine + saline; group two ($n=15$): I/R + dobutamine + saline and group three ($n=10$): I/R + saline as control.

Measurement of mucosal blood flow

A Teflon-coated laser optic flow probe (Peri flux PF409, flexible probe with 0.25mm fiber separation) was inserted through a small enterotomy at the proximal end of the jejunal sac and it was positioned along the antimesenteric border of the jejunum to the center of the sac. Mucosal blood flow was continuously recorded with a laser Doppler flow monitor (Peri Flux 4001 Master; Perimed, Jaarnfalla, Sweden). Blood flow measurements using Laser Doppler flow meters are not absolute but rather indicate flow in arbitrary perfusion units. Measurements were taken as the average flow over a five-minute period following an initial 30 minute period of stabilization. The quality of the signal was monitored by visualization on the computer screen so that motion artifact and noise were excluded from measurement^[25,26].

Measurement of PCO₂ (PrCO₂)

In the same animal, a 5F saline tonometer was inserted through a small enterotomy at the distal end of the sac and positioned to the center of the sac. The system was allowed to equilibrate for 30 minutes at which time a baseline PrCO₂ measurement was obtained by discarding the first 0.3ml saline from the tonometer balloon and using the remaining 0.7ml for analysis (model 1610 pH/blood gas analyzer, Milano, Italy). Regional PCO₂ (PrCO₂) was calculated using the following formula: PrCO₂=measure PCO₂×EF. EF=equilibration factor, and based on the equilibration period for saline which gained from the handbook^[27-29].

Doppler measurements and PrCO₂ determinations were made every 30 minutes throughout the experimental period.

Statistics

Data were reported as mean ±SEM and were analyzed by one-way analysis of variance (ANOVA) or student *t* test, significance was set at *P*<0.05.

RESULTS

Laser doppler flow

Table 1 showed the effects of anisodamine and dobutamine on gut mucosal blood flow. Laser Doppler baseline flow (arbitrary units) was not different among groups. Flow dropped significantly during ischemia, with a reduction to 12% of baseline level, but notably not down to zero. With reperfusion, flow increased over time in all groups (*P*<0.05) but did not reach baseline by 90 minutes. When compared to saline group, mucosal blood flow were higher in the anisodamine and dobutamine groups (*P*<0.05) throughout the reperfusion period. Blood flow was also significantly higher at 90 minutes after reperfusion in anisodamine group compared with dobutamine animals (*P*<0.05).

Table 1 Effects of anisodamine and dobutamine on gut mucosal blood flow (%)

Goups	B	I ₆₀	R ₃₀	R ₆₀	R ₉₀
Anisodamine	98±3.8	14±3.9	44±3.3 ^{ab}	57±5.0 ^{ab}	64±3.3 ^{abc}
Dobutamine	100±5.2	18±2.1	48±4.1 ^{ab}	56±4.7 ^{ab}	56±4.2 ^{ab}
Saline	103±6.9	16±3.4	37±2.6 ^a	45±2.7 ^a	48±3.4 ^a

Mean ± SEM; **P*<0.05, vs I₆₀; ^b*P*<0.05, vs saline; ^c*P*<0.05, vs Dobutamine; B, baseline; I₆₀, ischemia 60 minutes; R₃₀, reperfusion 30 minutes; R₆₀, reperfusion 60 minutes; R₉₀, reperfusion 90 minutes.

Tonometry PrCO₂

Table 2 depicts jejunal PrCO₂ during I/R. Jejunal PrCO₂ did not differ in baseline among the groups, but it was significantly increased at 60 minutes of ischemia in all groups, amounting to 204% of baseline level. With reperfusion, PrCO₂ dropped over time in all groups (*P*<0.05), but did not reach the baseline. When compared with saline group, PrCO₂ values were lower in the anisodamine and dobutamine groups (*P*<0.05) throughout reperfusion period. There were no significant differences between anisodamine group and dobutamine animals at 30 and 60 minutes of reperfusion, but by 90 minutes of reperfusion anisodamine administration resulted in a significantly lower PrCO₂ than dobutamine (*P*<0.05).

Table 2 Effects of anisodamine and dobutamine on PrCO₂ (mm Hg)

Goups	B	I ₆₀	R ₃₀	R ₆₀	R ₉₀
Anisodamine	28±2.2	55±3.9	41±3.1 ^{ab}	38±3.7 ^{ab}	34±2.1 ^{abc}
Dobutamine	31±3.8	61±7.8	44±3.0 ^a	40±2.1 ^{ab}	39±3.0 ^{ab}
Saline	26±2.5	57±5.4	49±3.7	47±3.8 ^a	46±3.4 ^a

Mean ± SEM; **P*<0.05, vs I₆₀; ^b*P*<0.05, vs saline; ^c*P*<0.05, vs Dobutamine; B, baseline; I₆₀, ischemia 60 minutes; R₃₀, reperfusion 30 minutes; R₆₀, reperfusion 60 minutes; R₉₀, reperfusion 90 minutes

DISCUSSION

Both laboratory and clinical studies have demonstrated that splanchnic perfusion remains significantly impaired following resuscitation in traumatic, hemorrhagic and septic shock^[30-33]. Intravital video microscopic studies by Flynn *et al*^[34,35] have shown that although inflow and premucosal arterioles return to normal after resuscitation from hemorrhagic shock, there is a progressive arteriolar constriction resulting in a decrease in blood flow. There have been few reports about effects of intraluminal vasoactive agents on gut mucosal blood flow during both ischemia and reperfusion. It has been demonstrated that dobutamine could augment gut microcirculatory blood flow in septic shock^[36,37]. Observation in extensively burned patients by Sheng, *et al*^[22] have shown that intravenous administration of anisodamine 12 hours postburn resulted in a significant elevation in gastric pH and decrease in plasma level of TNF. In a porcine model of 30% TBSA full-thickness burn, anisodamine (0.4mg/kg) infused intravenously for one hour could increase portal blood flow, and it showed a positive correlation with intestinal pH^[38]. The use of Laser Doppler-measured tissue perfusion is a reliable technique that has been validated in the assessment of gastrointestinal mucosal blood flow, and the results were shown to correlate with other techniques of measurement of local blood flow^[33,38]. Recently, its use as a clinical tool for assessing jejunal mucosal perfusion had also been demonstrated^[39]. In this study with advanced Laser Doppler technique, we further demonstrated the beneficial effect of anisodamine on gut mucosal perfusion during I/R injury in comparison with dobutamine. The results showed that intraluminal anisodamine or dobutamine did increase mucosal blood flow throughout reperfusion as compared to intraluminal saline only. Blood flow augmentation was reflected by lower jejunal PrCO₂ measurements with intraluminal anisodamine or dobutamine. The most interesting finding was that there were significantly lower jejunal PrCO₂ and higher mucosal blood flow in anisodamine group than those in dobutamine at 90 minutes of reperfusion, suggesting that anisodamine had a more lasting effect on mucosal perfusion than dobutamine.

Tissue CO₂ gas tonometry provides an indirect measurement of perfusion and/or mucosal metabolic stress. Gastric tonometry, in particular, has been suggested as a tool to monitor splanchnic perfusion in experimental animals and critically ill patients^[40-43]. Though studies have demonstrated low gastric intramucosal pH (pHi) is a good predictor of poor outcome in critically ill patients, no improvement in outcome has been ascertained when patients are resuscitated based on the results of gastric tonometry^[44-46]. In this study we used 5F gut tonometry, in which the air pocket can be matched with rat small bowel sac, and the results are more accurate than gastric tonometry in detecting gut perfusion and metabolism^[47-50]. In our study significant increases in gut PrCO₂ following gut I/R were found, which could be markedly reduced by intraluminal anisodamine or dobutamine. These results might suggest that anisodamine or dobutamine is capable of augmenting mucosal blood flow, thus improving gut mucosal metabolism.

In conclusion, we have demonstrated in this laboratory model of gut ischemia and reperfusion that intraluminal anisodamine or dobutamine could augment mucosal blood flow, alleviate mucosal acidosis, improve metabolism in mucosal cell. These results provided reliable evidence to clinicians to adopt anisodamine or dobutamine in the treatment of splanchnic hypoperfusion, especially gut mucosal blood flow reduction following traumatic or burn shock.

REFERENCES

- Heithan TH, Kone BC, Mercer DW, Moody FG, Weisbrodt NW, Moore FA. Postinjury multiple organ failure: The role of the gut. *Shock* 2001; 15:1-10
- Moore FA. The role of the gastrointestinal tract in postinjury multiple organ

- failure. *Am J Surg* 1999;178:449-453
- 3 Zhang LY, Wang ZG, Zhu PF, Qin HJ. Gut barrier function disturbance posterior to hemorrhagic shock resuscitation in rats. *Shijie Huaren Xiaohua Zazhi* 2001;9:767-770
- 4 Hu S, Sheng ZY, Zhou BT, Guo ZR, Lu JY, Xue LB, Jin H, Sun XQ, Sun SR, Li JY, Lu Y. Study on delay two-phase multiple organ dysfunction syndrome. *Chin Med J* 1998;111:101-108
- 5 Hu S, Sheng ZY, Zhou BT, Xue LB, Jin H, Lu Y, Lin HY. Experimental study on hemodynamic changes in the development of multiple organ dysfunction syndrome. *Zhongguo Weizhongbing Jijiu Yixue* 1996;8:707-709
- 6 Reed LL, Mangano R, Martin M, Hochman M, Kocka F, Barrett J. The effect of hypertonic saline resuscitation on bacterial translocation after hemorrhagic shock in rats. *Surgery* 1991;110:685-690
- 7 Tamion F, Richard V, Lyoumi S, Daveau M, Bonmarchand G, Leroy T, Thuillez C, Lebreton JP. Gut ischemia and mesenteric synthesis of inflammatory cytokines after hemorrhagic or endotoxic shock. *Am J physiol* 1997;273:G314-G321
- 8 Moore EE, Moore FA, Franciose RJ, Kim FJ, Biffl, Banerjee A. Postischemia gut serves as a priming bed for circulating neutrophils that provoke multiple organ failure. *J Trauma* 1994;37:881-887
- 9 Magnotti LJ, Upperman JS, Xu DZ, Lu Q, Deitch EA. Gut derived mesenteric lymph but not portal blood increases endothelial cell permeability and promotes lung injury after hemorrhagic shock. *Ann Surg* 1998;228:518-527
- 10 Schmidt H, Secchi A, Wellmann R, Bach A, Bohrer H, Gebhard MM, Martin E. Effect of endotoxemia on intestinal villus microcirculation in rats. *J Surg Res* 1996;61:521-526
- 11 Fiddian-Green RG, Haglund U, Gutierrez, Shoemaker WC. Goals for the resuscitation on shock. *Crit Care Med* 1993;21:S25-S31
- 12 Friedman G, Silva E, Vincent JL. Has the mortality of septic shock changed with time? *Crit Care Med* 1998;26:2078-2086
- 13 Martin C, Viviani X, Arnaud S, Viale R, Rougon T. Effects of norepinephrine plus dobutamine or norepinephrine alone on left ventricular performance of septic shock patients. *Crit care Med* 1999;27:1708-1713
- 14 Hoogenberg K, Smit AJ, Girbes AJ. Effects of low-dose dopamine on renal and systemic hemodynamics during incremental norepinephrine infusion in healthy volunteers. *Crit Care Med* 1998;26:260-265
- 15 Backer DD, Zhang HB, Cherkhaoui S, Borgers M, Vincent JL. Effects of dobutamine on hepato-splanchnic hemodynamics in an experimental model of hyperdynamic endotoxic shock. *Shock* 2001;15:208-214
- 16 Yang XH. Mechanism of the protective effect of anisodamine in gut ischemia injury. *Zhongguo Bingli Shengli Zazhi* 1988;4:134-136
- 17 Huang YS, Li A, Yang ZC. Roles of thromboxane and its inhibits anisodamine in burn shock. *Burns* 1990;16:249-253
- 18 Shi LB, Peng SY, Meng XY, Liu YB, Peng CH. The role of platelet activating factor in hepatic ischemia-reperfusion injury and the protective effect of anisodamine. *Zhongguo Weizhongbing Jijiu Yixue* 2001;13:220-222
- 19 Jang CG, Yang GT, Tang Y. Influence of Anisodamine on neuronal apoptosis after cerebral reperfusion in the rats. *Zhongguo Jijiu Zazhi* 2001;21:131-133
- 20 Meng XK, Shi LB, Peng SY, Peng CH, Wu YL, Sheng HW. Experimental study of anisodamine against hepatic ischemia-reperfusion injury. *Zhongguo Jijiu Yixue* 2001;21:4-6
- 21 Joly LM, Monchi M, Cariou A. Effects of dobutamine on gastric mucosal perfusion and hepatic metabolism in patients with septic shock. *Am J Respir Crit Care Med* 1999;160:1983-1986
- 22 Sheng ZY, Gao WY, Guo ZR, He LX. Anisodamine restores bowel circulation in burn shock. *Burns* 1997;23:142-146
- 23 Wilson TH. Methods. IN: Wilson TH, ed. *Intestinal Absorption*. Philadelphia: W. B. Saunders Co 1962:20-39
- 24 Hu S, Kozar RA, Moore FA, Sheng ZY. Enteral feeding of glucose increases intestinal mucosal blood flow during intestinal ischemia/reperfusion injury. *Zhonghua Shaoshang Zazhi* 2001;17:139-141
- 25 Wang P, Zhou M, Cioffi WG, Bland KI, Zheng F, Chaudry IH. Is prostacyclin responsible for producing the hyperdynamic response during early sepsis? *Crit Care Med* 2000;28:1534-1539
- 26 Elizalde JJ, Hernandez C, Liach J, Monton C, Bordes JM, Pique JM, Torres A. Gastric intramucosal acidosis in mechanically ventilated patients: role of mucosal blood flow. *Crit Car Med* 1998;26:827-832
- 27 Dawson AM, Trenchard D, Guz A. Small bowel tonometer: assessment of small gut mucosal oxygen tension in dog and man. *Nature* 1965; 206: 943-945
- 28 Heinonen PO, Jousela IT, Blomqvist KA. Validation of air tonometric measurement of gastric regional concentration of CO₂ in critically ill septic patients. *Intensive Care Med* 1977;23:524-529
- 29 McKinley BA, Marvin RG, Moore FA. Gastric and intestinal mucosal regional PCO₂ following shock resuscitation: changes with small intestinal enteral feeding. *Shock* 1999;11:S72-73
- 30 Fiddian-Green RG. Associations between intramucosal acidosis in the gut and organ failure. *Crit Care Med* 1993;21:S103-107
- 31 Grossie B, Weisbrodt NW. Inhibition of small intestinal transit by ischemia/reperfusion in the rat. *Dig Dis Sci* 1998;43:1585-1587
- 32 Wang P, Shou M, Rana MW. Differential alterations in microvascular perfusion in various organs during early and late sepsis. *Am J Physiol* 1992;263:G38-G43
- 33 Wang P, Hauptman JG, Chaudry IH. Hemorrhage produces depression in microvascular blood flow that persists despite fluid resuscitation. *Circ Shock* 1990;32:307-318
- 34 Flynn WJ, Cryer HG, Garrison RH. Pentoxifylline restores intestinal microvascular blood flow during resuscitated hemorrhagic shock. *Surgery* 1991;110:350-356
- 35 Flynn WJ, Gosche JR, Garrison RN. Intestinal blood flow is restored with glutamine or glucose infusion after hemorrhage. *J Surg Res* 1992;52:499-504
- 36 Gutierrez G, Clark C, Brown K SD, Price K, Ortiz L, Nelson C. Effect of dobutamine on oxygen consumption and gastric intramucosal pH in septic patients. *Am J Respir Crit Care Med* 1994;150:324-329
- 37 Nevriere R, Chagnon JL, Vallet B, Lebleu N, Marechal X, Mathieu D, Wattel F, Dupuis B. Dobutamine improves gastrointestinal mucosal blood flow in a porcine model of endotoxic shock. *Crit Care Med* 1997; 25:1371-1377
- 38 Gao WY, Sheng ZY, Gou ZR, He LX, Xiong DX, Song HF, Zhang SX, Ma NS, Chang GY. Protective effect of anisodamine on intestine in the early period of burn shock. *Jiefangjun Yixue Zazhi* 1995;20:88-91
- 39 Thoren A, Elam M, Ricksten S. Differential effects of dopamine, dopexamine, and dobutamine on jejunal mucosal perfusion early after cardiac surgery. *Crit Care Med* 2000;28:2338-2343
- 40 Temmesfeld-Wollbrück B, Szalay A, Olschewski H. Advantage of buffered solutions or automated capnometry in air-filled balloons for use in gastric tonometry. *Intensive Care Med* 1997;23:423-427
- 41 Knudson G, Bermudez KM, Doyle CA, Mackersie RC, Hopf HW, Morabito D. Use of tissue oxygen tension measurements during resuscitation from hemorrhagic shock. *J Trauma* 1997;42:608-611
- 42 Hu S, Sheng ZY, Zhou BT, Xue LB, Jin H. Changes in gastrointestinal intramucosal pH in goats resuscitated from hypovolemic shock. *Zhongguo Weizhongbing Jijiu Yixue* 1997;9:708-710
- 43 Marik P, Lorenzana A. Effect of tube feeding on the measurement of gastric intramucosal pH. *Crit Care Med* 1996;24:1498-1500
- 44 Gomersall CD, Joynt GM, Freebairn RC, Hung V, Buckley CA, Oh TE. Resuscitation of critically ill patients based on the results of gastric tonometry: A prospective, randomized, controlled trial. *Crit Care Med* 2000;28:607-614
- 45 Kirton OC, Windsor J, Wedderburn R, Hudson-Civetta J, Shatz DV, Mataragas NR, Civetta JM. Failure of splanchnic resuscitation in the acutely injured trauma patient correlates with multiple organ-system failure and length of stay in the ICU. *Chest* 1998;113:1064-1069
- 46 Ivatury RR, Simon RJ, Islam S, Fuego A, Rohman M, Stahl WM. A prospective randomized study of resuscitation after major trauma: Global oxygen transport induces versus organ-specific gastric mucosal pH. *J Amer Col Surg* 1996;183:145-154
- 47 Walley KR, Friesen BP, Humer MF, Phang PT. Small bowel tonometry is more accurate than gastric tonometry in detecting gut ischemia. *J Appl Physiol* 1998;85:1770-1777
- 48 Barry B, Mallick A, Hartley G, Bodenham, Vucevic M. Comparison of air tonometry with gastric tonometry using saline and other equilibrating fluids: an in vivo and in vitro study. *Intensive Care Med* 1998; 24:777-784
- 49 Noone RB, Bolden JE, Mythen NG, Vaslef SN. Comparison of the response of saline tonometry and an automated gas tonometry device to a change in CO₂. *Crit Care Med* 2000;28:3728-3733
- 50 Thorburn K, Hatherill M, Roberts PC, Durward A, Tibby SM, Murdoch IA. Evaluation of the 5-French saline paediatric gastric tonometer. *Intensive Care Med* 2000;26:973-980

Edited by Wu XN

• CLINICAL RESEARCH •

Presence and density of common bile duct microlithiasis in acute biliary pancreatitis

Maciej Kohut, Andrzej Nowak, Ewa Nowakowska-Dulawa, Tomasz Marek

Maciej Kohut, Andrzej Nowak, Ewa Nowakowska-Dulawa, Tomasz Marek, Department of Gastroenterology, Central Clinical Hospital, Silesian Academy of Medicine, Katowice, Poland

Supported by Silesian Medical Academy scientific grants - NN-4-173-94, NN-1-161-95, NN-4-200-96, NN-1-248-97

Correspondence to: Maciej Kohut, Department of Gastroenterology, Silesian Academy of Medicine, Medyków 14,40 - 752 Katowice, Poland. maciej.2250177@pharmanet.com.pl

Telephone: +48-32-7894401 Fax: +48-32-2523119

Received 2002-01-11 Accepted 2002-03-07

Abstract

AIM: Common bile duct microlithiasis (CBDM) is found in majority of patients with acute biliary pancreatitis (ABP) and no CBD stones in fluoroscopy during urgent ERCP. It is unclear, however, whether CBDM is a cause or the result of the disease. This prospective study was done to investigate the presence and density of CBDM in patients with ABP, when endoscopic retrograde cholangiopancreatography (ERCP) was done in different periods from the onset of the disease.

METHODS: One hundred fifty one consecutive patients with ABP and no CBDS on ERCP, performed as an urgent (<24h of admission) procedure, (101 - with gallbladder stones, 50 post-cholecystectomy patients), treated during last 4 years were prospectively included to the study. The presence and density of CBDM (cholesterol monohydrate crystals-CMCs and calcium bilirubinate granules-CBGs) in bile collected directly from common bile duct during ERCP was prospectively calculated according to Juniper and Burson criteria. High density of crystals was considered, when we found >10CMCs and/or >25 clusters of CBGs on 1 slide.

RESULTS: CBD microlithiasis was present in given number of patients: on d1-30/34 (88.2%), on d2 41/49 (83.7%), on d3-23/33 (69.6%), on d4-7-24/35 (68.6%) [*P* for trend=0.018]. In patients with CBD microlithiasis the high density of crystals was observed in given number of patients: on d1-27/30 (90%), on d2-34/41 (82.9%), on d3-18/23 (78.3%), on d4-7-16/24 (66.7%) [*P* for trend=0.039].

CONCLUSION: In patients with ABP and no CBDS on ERCP, CBD microlithiasis is observed in the majority of patients, especially during the first day of the disease. Density of CBD microlithiasis is the highest in the first day of the disease. This suggests that CBD microlithiasis can be the cause and not the result of ABP.

Kohut M, Nowak A, Nowakowska-Dulawa E, Marek T. Presence and density of common bile duct microlithiasis in acute biliary pancreatitis. *World J Gastroenterol* 2002;8(2):558-561

INTRODUCTION

Some cases of acute biliary pancreatitis (ABP) are due to the biliary microcrystals (microlithiasis). The pathogenesis of acute pancreatitis (AP) produced by biliary crystals is unknown. It is probably related to the temporary impaction or migration of very small stones or

clusters of crystals at the level of the ampoule of Vater. The mechanism of such pancreatitis is presumably the same as that when "normal size" biliary stones are impacted in the ampoule of Vater in the onset of the disease^[1,2]. Literature on this problem started with simple case reports^[3-5]. In the end of 1980's and the beginning of 1990's some larger series of patients with acute pancreatitis possibly associated with biliary sludge or microlithiasis were presented^[1,6-10]. However, most of patients presented in these papers suffered from acute pancreatitis classified as so called "idiopathic" pancreatitis, as they do not bear gallbladder sludge, gallbladder stones and they did not have the history of cholecystectomy.

The methodology of these reports was based on the microscopic bile examination (MBE), which was a widely used technique in the diagnosis of gallstone disease before the advent of modern imaging procedures such as ultrasonography^[11,12]. Almost all authors studied gallbladder bile obtained after stimulated gallbladder contractions via either blindly or endoscopically placed tube at the level of the papilla of Vater. Even in one of the best papers by Lee *et al*^[6] the common bile duct bile has been investigated only in less than half of the patients. In the rest of cases the stimulated gallbladder bile was the matter of study. The minority of authors studied the bile obtained directly from the biliary tree on ERCP or via the T-tube placed in common bile duct during cholecystectomy with choledochotomy^[13,14].

To our knowledge the study of common bile duct microlithiasis (CBDM) in patients with gallbladder stones or prior cholecystectomy and no CBD stones on ERCP is scanty^[13,14]. In our previous paper we have found CBDM in vast majority of ABP cases (76%)^[15]. One can argue, however, that the CBD microlithiasis can be the result and not the cause of the disease-CBD microlithiasis can be produced in the biliary tree due to the obstructed outflow of bile. This cholestasis can be related to the compression of distal common bile duct stone made by swollen pancreatic head during acute pancreatitis. Thus, we conducted the study of the presence and density of CBD microlithiasis in patients with ABP and no CBD stones on ERCP performed in the different periods from the onset of the disease. The aims of our work were to study the presence of CBD microlithiasis in different periods from the onset of the acute biliary pancreatitis, and the density of CBD microlithiasis in patients with microlithiasis in different periods from the onset of acute biliary pancreatitis.

MATERIALS AND METHODS

Materials

The study had been performed between September 1993 and January 1997 in the Department of Gastroenterology of the Silesian Academy of Medicine in Katowice, which is the reference centre for gastrointestinal diseases for approximately 4 million inhabitants area. Informed consent was obtained from all the subjects. Protocol of the study was approved by the local Ethics Committee in February 1993.

Methods

ERCP was done urgently - up to 24 hours of admission. Only patients with no more than 7 days from the onset of ABP were included to the study. We included patients with gallbladder stones or patients previously cholecystectomized. Patients without suspected biliary pathology [e.g. with pancreas divisum or with metabolic

(hyperlipidaemia) acute pancreatitis] were excluded. Patients with alcoholic pancreatitis were also excluded. The diagnostic criteria for ABP were (both criteria must be present): (1) Typical clinical picture (epigastric pain), elevated levels of pancreatic enzymes (exceeding at least 3 times upper normal range), typical patterns of pancreatitis in abdominal imaging methods (ultrasonography, CT-scan), and (2) History of gallstones (e.g. cholecystectomy), positive laboratory criteria of biliary etiology of acute pancreatitis according to Goodman *et al*^[16], gallstones on ultrasonography.

After the cannulation of the orifice of the ampoule of Vater was verified and the diagnostic catheter was placed in the common bile duct by injection of contrast medium (Meglumine diazotriacetate, Uropolinum, Polfa, Poland), the examiner confirmed that there were no "macroscopic" bile duct stones on fluoroscopy and X-ray films. Then the CBD bile was collected by manual suction through the standard ERCP catheters (Olympus and Boston Scientific companies) to the sterile syringe attached to the proximal end of the catheter. Approximately 5mL of bile was achieved from every patient. All the following procedures were done in the sterile conditions. Immediately after the collection the bile sample was divided into two parts of the same volume. One part was examined immediately, while the second one was incubated in the temperature of 37°C for 24h. The presence of biliary microlithiasis was recorded as the combined result from both microscopic bile examinations. We established the diagnosis of CBD microlithiasis when at least we found crystals (immediately after incubation or on both microscopic bile examinations). The patients did not receive any antibiotic treatment prior to ERCP that can influence microscopic bile examination due to the drug precipitation in the bile.

The sample of bile was centrifuged 12 000 r·min⁻¹ for 10 min. Centrifugation enables to separate bile from the contrast medium we used during ERCP. The contrast medium floated over the bile after centrifugation. The sediment found on the bottom of the bile was than examined under direct and polarising light microscope, equipped with a heating stage. The same was done on the next day with the second portion of incubated bile. Three slides with bile sediment were examined for each sample. We prospectively used criteria of Juniper and Burson for counting crystals, as shown in Table 1^[17]. Cholesterol monohydrate crystals (CMC) were identified on the basis of their rhomboid shape and their birefringence under cross - polarisation. Calcium bilirubinate granules (CBG) were identified on the basis of their reddish - brown colour and tendency to aggregate^[17]. The number of crystals were graded as 1 - 4 when present and 0 when absent. Grades 1 - 4 corresponded to the grades specified by Juniper and Burson^[17]. A positive result (at once, after incubation or both) for CMCs was taken if graded 1 - 4, and for CBGs if graded 3 - 4 (> 25 crystals per slide). The diagnosis of high density of crystals was done only if we have found > 10 CMCs and/or > 25 CBGs per one slide - as proposed by Juniper and Burson^[17]. These criteria were derived directly from the original paper of Juniper and Burson, who discovered, that some cases with small number of calcium bilirubinate granules (graded 1 and 2, < 25 crystals per slide) were healthy and did not present cholelithiasis. All the bile samples were examined by one of the investigators, who were unaware of any clinical information.

The data were prospectively collected in the purpose-made database and analysed with the statistical package STATISTICA 5.0PL. The results are expressed as $\bar{x} \pm s$. Unpaired t Student tests (Fisher's exact test - two-sided or Mann-Whitney's test when needed) and chi - 2 test when appropriate were used for statistical analyses. The level < 0,05 was considered as statistically significant.

RESULTS

Demographic clinical and biochemical data of all the patients are shown in Table 2. The comparison of the characteristics of the

patients with and without microlithiasis is given in the Table 3. There were no differences in the sex, mean age, the presence of gallbladder stones, mean BMI, mean levels of biochemical cholestasis (bilirubin, alkaline phosphatase and alanine transaminase) of patients in both subgroups. Presence and density of common bile duct microlithiasis (CBDM) in patients with acute biliary pancreatitis and no CBD stones on ERCP done in different periods from the onset of the disease are presented in Figures 1 and 2, respectively. The results showed statistically significant decrease in the presence of microlithiasis, when the patient moved away from the onset of acute biliary pancreatitis. We observed also the fall in the presence of high density of microlithiasis. The highest density was in the first day of acute biliary pancreatitis, falling down in next days of the disease. These results also achieved the statistical significance.

Table 1 System of Juniper and Burson for counting microlithiasis^[4]

Number of crystals per one slide	Grading
<10	+
10-25	++
25-40	+++
>40	++++

Table 2 Demographic, clinical and biochemical data of all patients with no common bile duct stones on ERCP

All cases		
Number of patients		
151		
Sex (M : F)		
49 : 102		
Age (years) ($\bar{x} \pm s$)		
53.9(± 15.7)		
Number of cases with gallbladder stones		
101		
Number of cases with prior cholecystectomy		
50		
Number of cases with Goodman's criteria of		
129		
ABP present (at least 1 criterion)		
Biochemical		
values (range, mean and SD)	Bilirubin ($\mu\text{mol}\cdot\text{L}^{-1}$)	17-3065 4.57(± 44.03)
	Alkaline phosphatase ($\text{IU}\cdot\text{L}^{-1}$)	57-556216.5(± 115.3)
	Alanine transaminase ($\text{IU}\cdot\text{L}^{-1}$)	16-1335351.2(± 252.8)

Normal levels of liver enzymes in our lab:

- Bilirubin <17 $\mu\text{mol}\cdot\text{L}^{-1}$)
- Alkaline phosphatase <110 $\text{IU}\cdot\text{L}^{-1}$)
- ALT <40 $\text{IU}\cdot\text{L}^{-1}$)

Table 3 Demographic, clinical and biochemical features of patients in relation to the diagnosis of common bile duct microcrystals (Fischer's s exact test or U Mann-Whitney's test when needed)

Feature	Microcrystals present (n=118)	Microcrystals absent (n=33)	P
Women	91	11	0.066
Men	27	22	0.066
Age[years] (mean)	52.4	54.2	0.623
Gallbladder stones present	81	20	0.770
BMI (mean)	27.8	28.7	0.490
Number of cases with Goodman's criteria of ABP present (at least 1 criterion)	106	23	0.670
Bilirubin [$\text{mol}\cdot\text{L}^{-1}$] (mean)	54.4	49.3	0.607
Alkaline phosphatase [$\text{IU}\cdot\text{L}^{-1}$] (mean)	213.7	178.9	0.148
Alanine transaminase [$\text{IU}\cdot\text{L}^{-1}$] (mean)	350.4	383.4	0.577

Results of microscopic bile examination (types of detected crystals) are shown in Figure 3. Calcium bilirubinate granules present alone (50% of cases with microlithiasis) were found the most frequently on MBE (Figure 3). CBGs together with CMCs were present in 43.2% cases with microlithiasis. Cholesterol monohydrate crystals were present alone only in 6.8% of patients with microlithiasis. We did not record any case of microspherulites.

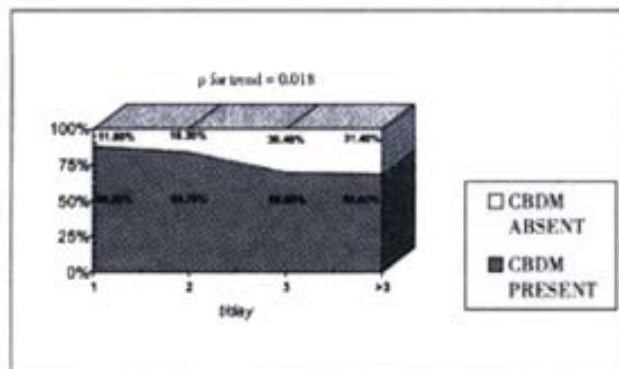


Figure 1 The presence of common bile duct microlithiasis (CBDM) in patients with acute biliary pancreatitis in different periods from the onset of the disease. (Fischer's exact test or Mann-Whitney's test when needed).

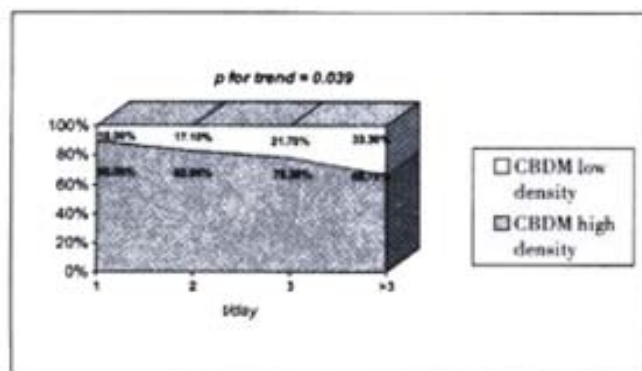


Figure 2 The density of common bile duct microlithiasis (CBDM) in patients with crystals on ERCP in different periods from the onset of the disease. (Fischer's exact test or Mann-Whitney's test when needed).

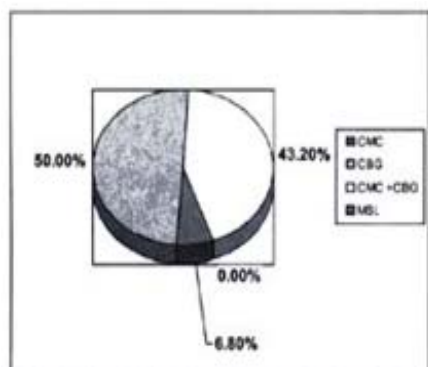


Figure 3 Types of detected microcrystals.
CMC - cholesterol monohydrate crystals
CBG - calcium bilirubinate granules
MSL - microspherulites

DISCUSSION

Duodenal bile fractions was microscopically checked since decades in search for gallstone disease^[11, 12, 17]. This method has shown the sensitivity and specificity around 70-90%. The microscopic examination of stimulated gallbladder bile collected via the tube, placed either under radiological guidance or endoscope in the duodenum at the level of the papilla has been shown to be reliable in the diagnosis of gallstone disease as well^[18, 19]. Both methods of

MBE had lost its attractivity after the advent of ultrasonographic examination of the gallbladder and bile ducts. However, the bile is still examined in some patients, especially with acute pancreatitis of uncertain origin^[1,3,4-10]. Common bile duct bile has been microscopically examined in patients with endoscopically placed naso - biliary tube or surgically placed T - tube in CBD^[13]. Sensitivity of 100% of such microscopic examination for CBD stones recognition was reported^[13].

In another study common bile duct bile was obtained directly from the duct during ERCP^[14]. We have shown the sensitivity of 85% in the diagnosis of choledocholithiasis^[14] and the same methodology was used in this study.

Our study was designed to find out the presence and density of CBD microlithiasis in patients with acute biliary pancreatitis and no CBD stones on ERCP, when ERCP was done in different periods from the onset of the ABP. ABP was diagnosed according to the typical abdominal symptoms of acute pancreatitis, ultrasound and CT changes of pancreatic gland and the presence of gallbladder stones or prior cholecystectomy. All the patients presented also a significant (more than $2 \times N$) elevation of at least one of biochemical markers of cholestasis (alkaline phosphatase, alanine transaminase, and bilirubin).

ERCP is one of the diagnostic standards in choledocholithiasis. This method can give false (positive and negative) results, but the sensitivity and specificity of the method is believed to be above 90-95%^[20]. In this respect, we can exclude almost all cases with CBD stones during fluoroscopy with high confidence that our group of patients contains really no cases with CBD stones.

No one of the tested biochemical parameters achieved statistical significance as a marker of microcrystals (Table 2). Similar values of biochemical data in patients with or without microlithiasis can be explained by the finding of signs of recent stone passage through the papilla of Vater in some patients. Swollen papilla with enlarged (usually quite easy to cannulate) reddish orifice, sometimes with a drop of blood, were found on ERCP in some ABP patients, mostly without microlithiasis. In these patients elevated biochemical markers were seen, as in patients with microlithiasis and without recent passage signs. The absence of microlithiasis in patients with signs of recent passage of stone may be explained so called "flushing out" mechanism after decompression of bilio - pancreatic duct system. This deserves further studies.

Microcrystals within the biliary tree are present intermittently^[19]. We observed very high percentage of microlithiasis in studied group of patients with ABP. This can be explained by the fact that majority of cases were admitted and ERCP performed on first three days of the disease. In previous studies, done few weeks or even months after the acute episode of acute pancreatitis, the percentage of cases with microlithiasis was lower^[3,5,7-9,11,12,18].

The main idea behind our study was to exclude the biliary microlithiasis as the result of acute pancreatitis. The presented results confirmed our presumption, that the percentage of cases with microlithiasis fell down, when the beginning of the acute pancreatitis was becoming distant. The percentage of patients with high density of microlithiasis also falls down with time. We can speculate that the high density microlithiasis was potentially more harmful in the sense, that it can easily aggregate at the level of the orifice of the ampoule of Vater, leading to the obstruction of the outflow of pancreatic juice. It suggests, that microlithiasis is the cause and not the result of the acute pancreatitis.

Results of microscopic bile examinations, found in this study (Figure 3), confirm previous observation, that calcium bilirubinate granules (CBG) are more frequently found in patients with AP^[1, 6, 7]. CBG were present alone (50%) or in association with CMC (43.2%) of all cases with microlithiasis. CMC were found alone in only 6.8% of cases. Previously CMCs were also less frequently found in endoscopically obtained duodenal bile, than in gallbladder bile in the same patient^[21].

In our opinion one important etiopathogenetic conclusion comes from the study: microlithiasis can provoke acute biliary pancreatitis. Crystals can irritate the papilla, leading to inflammation of the papilla and obstructed outflow of pancreatic juice. If very high percentage of patients with microcrystals is present in the first day of ABP and if the high percentage of high density microlithiasis is also present in the first day of the disease, it seems logical to perform next step - the investigation of the influence of endoscopic sphincterotomy in such patients.

List of abbreviations

ABP	- acute biliary pancreatitis
CBD	- common bile duct
CBDS	- common bile duct stones
CBDM	- common bile duct microlithiasis
CMCs	- cholesterol monohydrate crystals
CBGs	- calcium bilirubinate granules
ERCP	- endoscopic retrograde cholangiopancreatography

Meetings presentations

Parts of this work were presented as abstracts during:

1. 6th United Gastroenterology Week, Birmingham, UK, 18-23 October 1997 (Gut 1997; 41 (3): P241).
2. DDW, New Orleans, USA 17-20 May 1998 (Gastrointest Endosc 1998; 47: AB 124).
3. 11th World Congress of Gastroenterology, Vienna, Austria 6-11 September 1998 (Digestion 1998; 54: 494: 3441).

REFERENCES

- 1 Ros E, Navarro S, Bru C, Garcia-Puges A, Valderrama R. Occult microlithiasis in "idiopathic" acute pancreatitis-prevention of relapses by cholecystectomy or ursodeoxycholic acid therapy. *Gastroenterology* 1991; 101:1701-1709
- 2 Acosta JM, Pellegrini CA, Skinner DB. Aetiology and pathogenesis of acute biliary pancreatitis. *Surgery* 1980; 88: 118-124
- 3 Perrota G, Pugliese G, Esposito R. Acute pancreatitis and biliary microlithiasis. A study of biliary sediment. *G Chir* 1989; 10: 646-648
- 4 Block MA, Priest RJ. Acute pancreatitis related to grossly minute stones in a radiographically normal gallbladder. *Am J Dig Dis* 1967; 12: 945-948
- 5 Negro P, Flati G, Flati D. Occult gallbladder microlithiasis causing acute recurrent pancreatitis. *Acta Chir Scand* 1984; 150: 503-506
- 6 Lee SP, Nichols JF, Park HZ. Biliary sludge as a cause of acute pancreatitis. *N Eng J Med* 1992; 326: 589-593
- 7 Neoptolemos JP, Davidson BR, Winder AF, Vallance D. Role of duodenal bile crystals analysis in the investigation of "idiopathic" pancreatitis. *Br J Surg* 1988; 75: 450-453
- 8 Reyez-Lopez A, Mino-Fugerolas G, Costan-Rodero G, Perez-Rodriguez E, Montero-Alvarez JL, Cabrera D. Value of duodenal drainage in the etiologic diagnosis of acute pancreatitis. *Rev Esp Enferm Dig* 1993; 83: 363-366
- 9 Bel FJ, Aparisis L, Garcia-Tell G, Rosello J, Rodrigo J. Biliary drainage in the diagnosis of microlithiasis. Value in acute idiopathic pancreatitis and in patients with pain in the right hypochondrium. *Rev Esp Enferm Dig* 1994; 85: 343-347
- 10 Humbert P, Casals A, Boix J. Usefulness of microscopic study of the duodenal bile in the diagnosis of pancreatitis of unknown cause. *Rev Esp Enferm* 1989; 75: 471-474
- 11 Lyon BBV. Diagnosis and treatment of diseases of the gallbladder and biliary ducts. *Am J Med Assoc* 1919; 73: 980-986
- 12 Bockus HL, Shay H, Willard JM. Comparison of bile drainage and cholecystography in gallstone disease with special reference to bile microscopy. *J Am Med Assoc* 1931; 96: 311-317
- 13 Agarwal DK, Choudhuri G, Saraswat VA, Negi TS. Utility of biliary microscopic analysis in predicting composition of common bile stones. *Scand J Gastroenterol* 1994; 29: 352-354
- 14 Buscail L, Escourrou J, Delvaux M, Guimbaud R, Nicolet T, Freximos J. Microscopic examination of bile directly collected during endoscopic cannulation of the papilla. Utility in patients with suspected microlithiasis. *Dig Dis Sci* 1992; 37: 116-120
- 15 Nowak A, Kohut M, Nowakowska-Dulawa E, Marek TA, Kaczor R. Common bile duct microlithiasis in patients with acute biliary pancreatitis and no CBD stones on ERCP. *Digestion* 1998; 59: 494
- 16 Goodman AJ, Neoptolemos JP, Carr-Locke DL, Finlay DB, Fossard DP. Detection of gallstones after acute pancreatitis. *Gut* 1985; 26: 125-132
- 17 Juniper K, Burson EN. Biliary tract studies II. The significance of biliary crystals. *Gastroenterology* 1957; 32: 175-211
- 18 Abbas A, Baumann R, Schutlz JF. Cristaux de cholesterol et lithiase biliaire. Interet de l' etude de la bile recueillie par tubage duodenal. *Gastroenterol Clin Biol* 1984; 8: 454-457
- 19 Marks JW, Bonorris G. Intermittency of cholesterol crystals in duodenal bile from gallstone patients. *Gastroenterology* 1984; 87: 622-627
- 20 Prat F, Amouyal G, Amouyal G, Pelletier G, Choury AD, Buffet C, Etienne JP. Prospective controlled study of endoscopic ultrasonography and endoscopic retrograde cholangiography in patients with suspected common bile duct lithiasis. *Lancet* 1996; 346: 75-79
- 21 Janowitz P, Swobodnik W, Weschler JG, Zoller A, Kuhn K, Ditschuneit H. Comparison of gallbladder bile and endoscopically obtained duodenal bile. *Gut* 1990; 31: 1407-1410

Edited by Pan BR and Zhang JZ

• CLINICAL RESEARCH •

HCV-specific cytokine induction in monocytes of patients with different outcomes of hepatitis C

Rainer P. Woitas, Uwe Petersen, Dirk Moshage, Hans H. Brackmann, Bertfried Matz, Tilman Sauerbruch, Ulrich Spengler

Rainer P. Woitas, Uwe Petersen, Dirk Moshage, Tilman Sauerbruch, Ulrich Spengler, Department of Internal Medicine I, University of Bonn, 53105 Bonn, Germany

Hans H. Brackmann, Institute of Experimental Hematology, University of Bonn, 53105 Bonn, Germany

Bertfried Matz, Institute of Medical Microbiology and Immunology, University of Bonn, 53105 Bonn, Germany

Correspondence to: Dr. Rainer P. Woitas, Medizinische Klinik, Poliklinik I, -Allgemeine Innere Medizin-, Universität Bonn, Sigmund-Freud-Strasse 25, D-53105 Bonn, Germany. woitas@uni-bonn.de

Received 2002-03-12 Accepted 2002-04-25

Abstract

AIM: Cytokine release by macrophages critically determines the type of immune response to an antigen. Therefore, we studied hepatitis C virus (HCV)-specific induction of interleukins-1 β , -10, -12 (IL-1 β , IL-10, IL-12), and tumor necrosis factor- α (TNF- α) in monocytes.

METHODS: Intracellular cytokine expression was studied by flow cytometry in 23 patients with chronic hepatitis C, 14 anti-HCV seropositives without viremia and 11 controls after stimulation of peripheral blood mononuclear cells with recombinant core, NS3, NS4, NS5a and NS5b proteins.

RESULTS: Patients with HCV viremia revealed greater spontaneous expression of IL-1 β , TNF- α , and IL-10. Furthermore, greater than twofold higher IL-10 expression was induced by the HCV antigens in chronic hepatitis C than in the other two groups ($P < 0.05$). In contrast, neither IL-12 nor TNF- α was induced preferentially.

CONCLUSION: In chronic hepatitis C antigen-specific cytokine induction in monocytes is apparently shifted towards predominant IL-10 induction - not counterbalanced by antiviral type 1 cytokines. This may contribute to persistent viral replication.

Woitas RP, Petersen U, Moshage D, Brackmann HH, Matz B, Sauerbruch T, Spengler U. HCV-specific cytokine induction in monocytes of patients with different outcomes of hepatitis C. *World J Gastroenterol* 2002;8(3):562-566

INTRODUCTION

Resistance or susceptibility to viral infections is critically linked to cytokine release, which can be polarized towards a type 1 (IFN- γ , TNF- α , IL-2) or type 2 (IL-4, IL-10, IL-13) pattern in helper as well as cytotoxic T lymphocytes^[1]. Type 1 and type 2 T lymphocytes are not derived from different lineages but develop from the same precursors, and their differentiation is influenced by the environment during priming. The most important signals are cytokines themselves: IL-12 produced by activated macrophages is the principal cytokine

inducing type 1 responses, whereas the development of type 2 T lymphocytes is induced by IL-4 and IL-10.

Hepatitis C virus (HCV) infection frequently leads to persistent viral replication, which may be facilitated by selective alterations in the host's immune response^[2]. In this context, studies of T cell functions in patients with chronic hepatitis C have indicated an inappropriately low production of antiviral type 1 cytokines in response to HCV antigens^[3-7] possibly facilitating persistent infection. However, it is not clear, whether the imbalance in the cytokine pattern is due to direct alterations of T cell function or a consequence of altered T cell priming. Because of their critical role for the type of immune reaction triggered in response to an antigen, we used flow cytometric detection of intracytoplasmic cytokines to study at the single cell level the HCV-specific induction of IL-1 β , IL-10, IL-12 and TNF- α in peripheral blood monocytes.

MATERIALS AND METHODS

Patients

Three groups of patients were included into this study: Group 1 consisted of 23 patients with chronic hepatitis C (male, $n=20$; female, $n=3$; median age 33, range 21-61), elevated liver enzymes and detectable HCV-RNA in the serum. The mean virus load was 6.3×10^6 copies/mL (SD 1.0×10^6 copies/mL) (Quantiplex™ HCV RNA 2.0 assay, Chiron, Emeryville, CA). Group 2 consisted of 14 carefully selected patients with previous HCV infection (male, $n=12$; female, $n=2$; median age 28.5, range 18-63), who had consistently normal aminotransferases without detectable viral RNA on repeated examination over at least 2 years. Finally, 11 anti-HCV negative volunteers (male, $n=5$; female, $n=6$; median age 30, range 24-66) served as a control group (group 3).

There were no significant differences between the two anti-HCV groups with respect to total immunoglobulin levels, and all were free from cryoglobulins or autoantibodies. None of the individuals in this study had hepatitis B virus or human immunodeficiency virus co-infection. The study was approved by the local ethical committee and conformed to the ethical guidelines of the 1975 Declaration of Helsinki.

Diagnosis of HCV Infection

HCV antibodies were detected with a microparticle enzyme immunoassay (MEIA) (AxSYM, Abbott, Wiesbaden, Germany) according to the instructions of the manufacturer. Positive results were confirmed by dot immunoassay (Matrix, Abbott, Wiesbaden, Germany). HCV RNA was detected with a nucleic acid purification kit (Viral Kit, Qiagen, Hilden, Germany) followed by reverse transcription and nested polymerase chain reaction as described elsewhere^[8]. Quantitative determination of HCV RNA copies was done via branched DNA technology (Chiron, Emeryville, CA). In group 1, genotypes of the infecting HCV strains were determined by the INNO-LiPA HCV II test (Innogenetics, Zwijndrecht, Belgium) except one patient, who could not be genotyped. This group revealed

the following isolates: 1a ($n=8$), 1b ($n=9$), 2b ($n=1$), 3a ($n=1$), and mixed ($n=3$; genotypes 1b/2b; 2a/2c; 4c/4d).

Patients of group 2 were characterized by genotype-specific antibodies to NS4 (Murex, Abbott Wiesbaden, Germany). Serotypes 1 and 4 were found in 10 and 1 patients, respectively. Three patients had indeterminate serotypes.

HCV antigens

The purified recombinant proteins [r-core (truncated): aa 1-115, r-NS3: aa 1007-1534, r-NS4: aa 1616-1862, r-NS5: aa 2007-2268] derived from the HCV-1 prototype sequence^[9] were purchased from Mikrogen, Munich, Germany. The bacterial lipopolysaccharide content of the proteins was between 4.0-20 pg/ μ g recombinant protein as determined by the Limulus assay. Lipopolysaccharide from *E. coli* OH101 (Sigma, Munich, Germany) was used in the control experiments.

Antibodies

Fluorescein isothiocyanate (FITC)- and phycoerythrin (PE)-labelled antibodies were purchased from the following companies: FITC- and PE-labelled -anti-CD14 (mouse IgG2b, clone MÖP9) from Becton Dickinson (Heidelberg, Germany); FITC- and PE-labelled anti-IL-1 β (mouse IgG1, clone H9.5) was purchased by Holtzel Diagnostica (Cologne, Germany). Anti-IL-10/PE (rat IgG2a, clone JES3-19F1), anti-IL-12/PE (mouse IgG1, clone C11.5.14), anti-TNF- α /PE (mouse IgG1, clone MAb11) as well as appropriate isotype controls from Pharmingen (Hamburg, Germany). Unlabelled mAbs for blocking experiments were purchased from Pharmingen (Hamburg, Germany) except for IL-1 β that was a gift of Holtzel Diagnostica (Cologne, Germany).

Cells and cell culture

PBMC (1.1×10^6 /ml) isolated from fresh EDTA blood by Ficoll density-gradient centrifugation (Biochrom, Berlin, Germany) were resuspended in low endotoxin level culture medium (RPMI 1640, Biochrom, Berlin, Germany) containing 10% autologous human serum, 100 units/ml penicillin, 100 units/ml streptomycin and incubated at 37°C with 5% CO₂ in 96 well microtiter plates (Sarstedt, Berlin, Germany) in the presence of recombinant HCV proteins (1 μ g/ml) or LPS (10-200 ng/ml). Kinetic experiments showed that the antigen-specific cytokine induction indicated a maximum after 12 hours of stimulation. Further experiments revealed 1.0 μ M monensin (Sigma, Munich Germany) for 12 hours to be optimal to enhance the signal/noise ratio as well as to exclude relevant toxicity^[10-12].

Dual-colour flow cytometry for immunophenotyping and intracytoplasmic staining of cytokines

CD14 and intracytoplasmic cytokines were detected by direct immunofluorescence using a paraformaldehyde (PFA)-saponin procedure with 4% PFA as fixative and 0.2% saponin for permeabilisation. In brief, cultured cells were washed twice in Hank's balanced salt solution (HBSS) (Gibco, Eggenstein, Germany) and stained for the surface markers (20 minutes incubation at 4°C in the dark). After one further wash, the cells were fixed in ice cold HBSS containing 4% PFA for 5 minutes and washed again. Cells were resuspended in HBSS containing 0.2% saponin (saponin buffer). Then cytokine specific antibodies diluted in saponin buffer were added at a concentration of 0.5-3.0 μ g/ml and incubated for 30 minutes at room temperature in the dark. Cells were washed in saponin buffer and analyzed by dual-colour flow cytometry on a FACS Sort

flowcytometer (Becton Dickinson, Heidelberg, Germany). Forward and side scatter as well as gating for CD14⁺ cells were used to identify monocytes. The data were analyzed with the CellQuest (software (Becton Dickinson) after counting 5000 CD14⁺ cells. All experiments were performed in triplicate.

To ensure specificity of the cytokine staining procedures, the binding of each mAb was blocked with an excess of unlabelled mAb.

Statistics

Results are given as median and range. Differences between the groups were analyzed by the Kruskal-Wallis test, Mann-Whitney *U* test and Wilcoxon signed rank test, as appropriate. All calculations were performed on a personal computer with Statview 4.5 software (Abacus Concepts inc., Berkeley CA, USA). *P* values <0.05 were regarded as significant.

RESULTS

Using flowcytometric detection of intracytoplasmic cytokines in combination with CD14 staining, we were able to specifically measure spontaneous as well as HCV antigen-induced production of IL-1 β , IL-10, IL-12 and TNF- α in peripheral blood monocytes (Figure 1). Following stimulation with LPS, intracytoplasmic expression of the cytokines did not show statistically significant differences between the study groups for the cytokines with the exception of IL-1 β , which was higher in patients with chronic hepatitis C when compared to the controls (Table 1). Cytokine production after 12 hours of HCV-specific stimulation together with the corresponding spontaneous and LPS-induced production is summarized in Table 1.

With respect to spontaneous production of IL-1 β , TNF- α , IL-10, and IL-12, there was considerable individual variability which was most pronounced in the group with chronic hepatitis C. The numbers of monocytes with detectable spontaneous production of IL-12 were low in general (0.1-5.1%) and on average not significantly different between the three study groups. In contrast, average numbers with detectable spontaneous production of IL-1 β , TNF- α , and IL-10 were higher in patients with chronic hepatitis C than in aviremic anti-HCV seropositives. However, due to considerable inter-individual variations, these differences between the groups reached statistical significance only for IL-1 β and IL-10 ($P < 0.05$).

Antigen-specific stimulation of peripheral blood mononuclear cells resulted in increased numbers of monocytes with production of IL-1 β , TNF- α , IL-10, and IL-12 in each study group for most of the tested HCV proteins (Table 1). However, after stimulation with the HCV proteins core, NS3, NS4, NS5a, and NS5b, the numbers of IL-1 β and IL-10 producing monocytes were at least twofold higher in patients with chronic hepatitis C than in aviremic anti-HCV seropositives and the controls ($P < 0.05$ for each HCV protein). In contrast, statistically significant differences ($P < 0.05$) in the numbers of TNF- α and IL-12 producing monocytes between patients with chronic hepatitis C and the other groups were only seen after stimulation with HCV core and NS5b (Table 1). The marked difference in the balance between IL-1 β and IL-10 producing monocytes, and TNF- α and IL-12 producing ones among the patients with chronic hepatitis C is illustrated in Figure 2, which shows the stimulation experiments with recombinant NS4 as a representative example. Since stimulation of monocytes was performed in the presence of T cells, we undertook control experiments with untouched isolated monocytes. When these purified monocytes were stimulated with HCV antigens or LPS, the cells showed a similar behaviour although the number of cytokine producing macrophages was strongly reduced compared to the PBMC assays (data not shown).

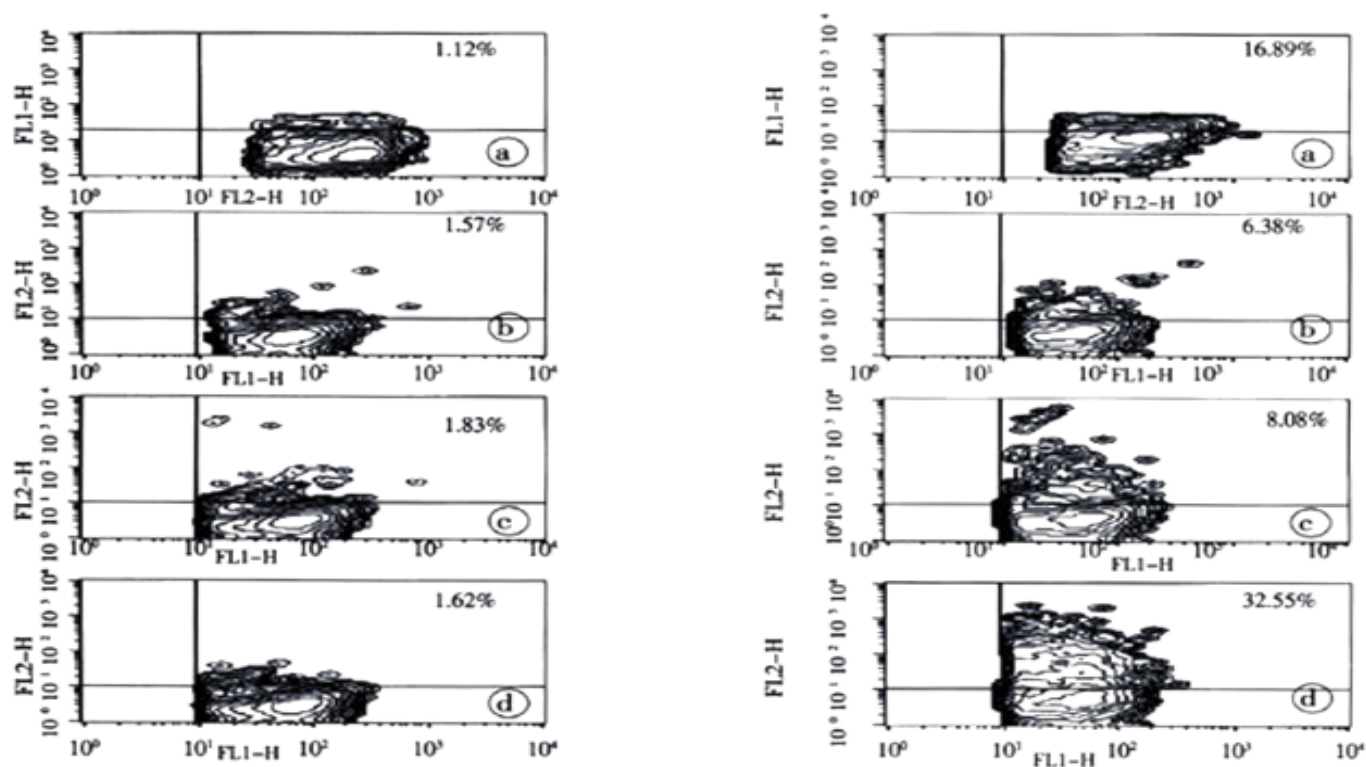


Figure 1 Contour plots of cytokine expression in CD14⁺ cells. These contour plots show representative experiments for the detection of spontaneous expression (buffer control, left column) and HCV NS5b-induced expression (1 μ g/mL, right column) of IL-1 β (a), IL-10 (b), IL-12 (c) and TNF- α (d) in peripheral blood CD14⁺ monocytes of patient # 23 with chronic hepatitis C at 12 hours of incubation.

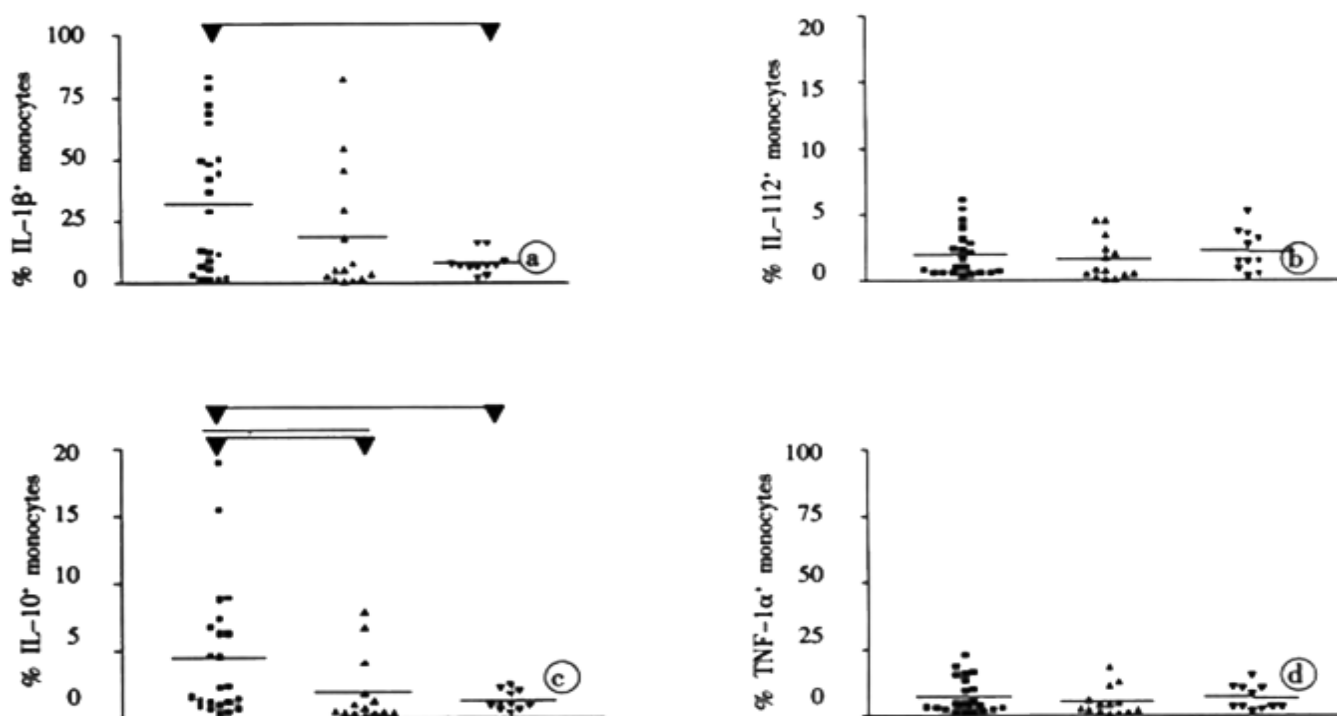


Figure 2 Induction of cytokines by the HCV NS4 protein. The graph displays the fractions of IL-1 β (a), IL-10 (b), IL-12 (c) and TNF- α (d) producing monocytes 12 hours after stimulation with recombinant NS4 protein (1 μ g/mL) for patients with chronic hepatitis C (filled squares), aviremic anti-HCV seropositives (upward triangles), and non-HCV related controls (downward triangles). Each dot represents the mean percentage of a single patient obtained from triplicate experiments. The horizontal bar gives the mean of each group.

Table 1 CD14⁺ monocytes with detectable intracellular cytokine expression

	Chronic hepatitis C (n=23)		Aviremic anti-HCV seropositives (n=14)		Controls (n=11)	
	% CD14 ⁺ monocytes	§ Significance	% CD14 ⁺ monocytes	§ Significance	% CD14 ⁺ monocytes	§ Significance
IL-1β						
Spontaneous expression	13.6 [0.3-82.1]	a, b	1.9 [0.4-65.5]		2.1 [0.6-4.7]	
Expression after stimulation with						
Core	21.5 [0.9-84.8]	a, b, c	3.1 [0.1-69.6]	c	2.8 [0.6-8.3]	
NS3	42.0 [1.1-91.1]	a, b, c	7.0 [0.6-71.8]	c	6.1 [1.6-31.6]	c
NS4	28.3 [0.4-82.4]	a, b, c	4.6 [0.2-81.8]		6.2 [1.6-15.5]	c
NS5a	34.3 [0.4-87.2]	a, b, c	3.3 [0.1-77.8]	c	8.3 [1.7-14.5]	c
NS5b	27.6 [1.7-89.9]	a, b, c	6.2 [0.8-75.3]	c	4.8 [0.8-30.3]	
LPS	55.5 [7.6-96.5]	b	36.2 [4.0-97.0]		24.1 [9.4-48.7]	
IL-10						
Spontaneous expression	1.4 [0.2-8.6]	a, b	0.4 [0.1-6.1]		0.7 [0.1-1.3]	
Expression after stimulation with						
Core	2.6 [0.3-24.4]	a, b, c	0.6 [0.1-8.3]	c	1.0 [0.2-1.8]	
NS3	2.4 [0.2-20.2]	a, b, c	0.8 [0.2-9.8]	c	0.8 [0.2-2.3]	c
NS4	2.0 [0.2-18.8]	a, b, c	0.5 [0.0-7.7]		0.9 [0.2-2.1]	c
NS5a	2.0 [0.2-16.9]	a, b, c	0.7 [0.1-7.9]	c	1.0 [0.1-3.2]	c
NS5b	3.7 [0.1-22.4]	a, b, c	0.7 [0.1-12.6]	c	0.7 [0.2-5.4]	
LPS	12.4 [0.2-39.8]		6.4 [0.3-25.0]		6.0 [0.5-19.1]	
IL-12						
Spontaneous expression	0.8 [0.2-5.1]		0.5 [0.2-3.1]		0.6 [0.1-2.3]	
Expression after stimulation with						
Core	2.0 [0.2-8.1]	a	0.7 [0.1-3.1]		1.1 [0.3-3.2]	
NS3	1.8 [0.5-16.3]	c	1.1 [0.2-5.3]	c	1.6 [0.2-12.2]	c
NS4	1.0 [0.3-6.1]	c	0.8 [0.8-4.5]		4.5 [0.3-5.2]	c
NS5a	1.5 [0.3-9.1]	c	0.8 [0.1-3.7]	c	1.5 [0.2-3.7]	c
NS5b	2.2 [0.3-40.1]	b,c	1.0 [0.3-5.2]	c	0.9 [0.2-6.1]	
LPS	18.7 [0.7-61.8]		6.2 [0-12.7]		11.8 [2.4-33.5]	
TNF-α						
Spontaneous expression	3.2 [0.1-39.5]		0.8 [0.2-12.0]		1.3 [0.4-3.4]	
Expression after stimulation with						
Core	6.9 [0.3-51.3]	b, c	1.5 [0.1-12.8]	c	1.7 [0.3-6.1]	c
NS3	5.4 [0.2-40.7]		2.9 [0.4-16.4]	c	3.7 [0.9-23.3]	c
NS4	3.1 [0.2-21.9]		2.7 [0.1-17.7]	c	2.9 [1.1-14.6]	c
NS5a	4.30 [0.1-22.7]		1.8 [0.2-11.1]	c	4.0 [1.3-8.3]	c
NS5b	10.9 [0.7-53.8]	a, b, c	2.3 [0.4-23.2]	c	2.0 [0.9-9.6]	c
LPS	35.0 [1.50-91.2]		21.3 [1.5-51.4]		31.5 [12.1-47.9]	

§ Significances:

 a= $P < 0.05$ Chronic HCV infection vs. aviremic anti-HCV seropositives (Kruskal-Wallis test and Mann-Whitney U test)

 b= $P < 0.05$ Chronic HCV infection vs. Controls (Kruskal-Wallis test and Mann-Whitney U test)

 c= $P < 0.05$ Stimulated vs. spontaneous cytokine expression (Wilcoxon signed rank test)

Data are given as median+ range.

DISCUSSION

Impaired function of macrophages has been described repeatedly in infection with HCV and also the closely related Dengue virus^[13-17]. Our study adds to these observation that in chronic hepatitis C altered macrophage function may also comprise the pattern of cytokines produced in response to HCV antigens. Of note, the various cytokines appeared to be involved differentially. Despite considerable individual variability, we found significantly greater average numbers of monocytes with spontaneous IL-1β and IL-10 production in patients with chronic hepatitis than that in aviremic anti HCV seropositives or the HCV-naïve controls. This finding appears to be compatible with in vivo pre-activation of the monocytes from patients with chronic hepatitis C. However, the numbers of monocytes with spontaneous IL-12 production did not reveal any conspicuous differences between our study groups. Thus far, studies on the cytokine production in hepatitis C have produced conflicting results for macrophages, mainly because monocytes were assessed only indirectly by measuring cytokines in the supernatants of peripheral blood mononuclear cells after stimulation with mitogen or LPS. This flowcytometric study is the first investigation, which provides HCV-specific data for monocytes at the single cell level in a more or less physiological environment that enables natural interactions to take place between the monocytes and other peripheral blood mononuclear cells, e.g. CD4⁺ T lymphocytes. Control experiments with untouched isolated monocytes showed that these interactions were crucial for an effective cytokine induction. Despite similar behaviour after stimulation the amount of cytokine

producing macrophages was strongly reduced (data not shown). With the flowcytometric approach, we could demonstrate that the numbers of IL-1β⁺ and IL-10⁺ monocytes increased significantly upon stimulation with the HCV antigens, whereas a similar induction of TNF-α and IL-12 was not observed.

After exposure to the HCV proteins a slight increase in the number of monocytes with expression of IL-1β, TNF-α, IL-10, and IL-12 was also seen in the HCV-naïve control group. This finding most likely indicates a non-specific stimulatory effect of the HCV antigens on the monocytes, probably due to small amounts of contaminating endotoxin. Compared to this non-specific effect this results indicate marked (2-7 fold) antigen-specific induction of IL-1β and IL-10 in response to all HCV antigens, but a less prominent induction of IL-12 and TNF-β in response to HCV core and NS5b in the group with chronic hepatitis C.

Similar responses were occasionally seen in few patients of our aviremic anti-HCV seropositive group. However, we cannot exclude completely that HCV replication below the detection limit of PCR technique was present in some of these patients, despite the fact that the group of aviremic anti-HCV seropositives was selected carefully to ensure that these patients had gained immune-mediated control of their HCV infection. Thus persistent low level viremia might be an explanation for the occasional altered cytokine responses in this group.

In general, our findings are in line with a previous report by Kakumu *et al.*, who reported increased IL-10 levels but unaltered IL-12 production in mononuclear cells of patients with chronic hepatitis

C^[18]. Furthermore, increased spontaneous TNF- α expression in patients with chronic hepatitis C is in line with previous work published by Kishihara and co-workers^[19]. As our flowcytometric approach enabled interactions between the monocytes and other immunoregulatory cells, which are important for the generation of antigen-specific responses, it was not unexpected that our results differed from those studies, which used purified monocytes^[20]. Thus, we could not confirm reduced numbers of IL-1 β and TNF- α monocytes in chronic hepatitis C, as has been reported for purified monocytes from patients with chronic hepatitis C by Mendoza and co-workers^[21].

The reasons for altered macrophage functions in chronic hepatitis C are unclear at present. Although HCV RNA has been detected in macrophages of a variable proportion of patients with chronic hepatitis C^[22], the reported percentages of HCV-RNA positive monocytes seem to be too low as to explain the altered cytokine induction by a direct infection of the monocytes^[23]. Persistent antigenic stimulation due to chronic hepatitis C viremia provides a better alternative explanation. For instance, continued production of HCV antigens may lead to the formation of antigen-antibody complexes, which can bind to Fc γ receptors on immunocompetent cells. Fc γ receptor ligation on monocytes will then result in reversal of macrophage pro-inflammatory responses as IL-10 up-regulation together with a reciprocal inhibition of IL-12 production can result from such Fc γ receptor triggering^[24]. Likewise, the blunted TNF- α responses observed in our *in vitro* stimulation experiments are likely to reflect altered immunoregulation, because loss of inducible TNF- α secretion has been well documented in pre-activated monocytes^[25].

Irrespective of the underlying cause, altered cytokine production by macrophages in chronic hepatitis C is likely to have important functional consequences. The high proportion of macrophages, which produce IL-1 β either spontaneously or after antigen-specific challenge may indicate that these macrophages are pre-conditioned towards pro-inflammatory reactions. However, proinflammatory cytokines required for efficient antiviral responses such as IL-12 and TNF- α show blunted responses to the HCV antigens. On the contrary, cytokine production appeared to be markedly biased towards IL-10 already at the level of the macrophages. Due to the pivotal role of monocytes and macrophages for the initiation of immune responses, the uniform up-regulation of IL-10 in response to HCV antigens, not counterbalanced by IL-12, may explain poor HCV-specific type I cytokine responses, which have been observed repeatedly in chronic hepatitis C^[3-7]. Thus, altered cytokine production by monocytes and macrophages might contribute to HCV persistence, because these cells may not support sufficiently effective antiviral immune responses.

ACKNOWLEDGMENTS

We gratefully acknowledge Eva-Maria Althausen, Department of Internal Medicine I and Bettina Kochan, Institute of Medical Microbiology and Immunology for excellent technical assistance. This work was supported by a generous grant of the Joachim Kuhlmann AIDS-Stiftung.

REFERENCES

- Abbas AK, Murphy KM, Sher A. Functional diversity of helper T lymphocytes. *Nature* 1996; 383:787-793
- Cerny A, Chisari FV. Pathogenesis of chronic hepatitis C: immunological features of hepatic injury and viral persistence. *Hepatology* 1999; 30:595-601
- Lechmann M, Woitas RP, Langhans B, Kaiser R, Ihlenfeldt HG, Jung G, Sauerbruch T, Spengler U. Decreased frequency of HCV core-specific peripheral blood mononuclear cells with type 1 cytokine secretion in chronic hepatitis C. *J Hepatol* 1999; 31:971-978
- Malaguarnera M, Di Fazio I, Laurino A, Pistone G, Restuccia S, Trovato BA. Decrease of interferon gamma serum levels in patients with chronic hepatitis C. *Biomed Pharmacother* 1997; 51:391-396
- Osna N, Silonova G, Vilgert U, Hagina E, Kuse V, Giedraitis V, Zvirbliene A, Mauricas M, Sochnev A. Chronic hepatitis C: T-helper1/T-helper2 imbalance could cause virus persistence in peripheral blood. *Scand J Clin Lab Invest* 1997; 57:703-710
- Reiser M, Marousis CG, Nelson DR, Lauer G, Gonzalez-Peralta RP, Davis GL, Lau JY. Serum interleukin 4 and interleukin 10 levels in patients with chronic hepatitis C virus infection. *J Hepatol* 1997; 26:471-478
- Woitas RP, Lechmann M, Jung G, Kaiser R, Sauerbruch T, Spengler U. CD30 induction and cytokine profiles in hepatitis C virus core-specific peripheral blood T lymphocytes. *J Immunol* 1997; 159:1012-1018
- Woitas RP, Rockstroh JK, Beier I, Jung G, Kochan B, Matz B, Brackmann HH, Sauerbruch T, Spengler U. Antigen-specific cytokine response to hepatitis C virus core epitopes in HIV/hepatitis C virus-coinfected patients. *Aids* 1999; 13:1313-1322
- Choo QL, Kuo G, Weiner AJ, Overby LR, Bradley DW, Houghton M. Isolation of a cDNA clone derived from a blood-borne non-A, non-B viral hepatitis genome. *Science* 1989; 244:359-362
- Tartakoff AM. Perturbation of the structure and function of the Golgi complex by monovalent carboxylic ionophores. *Methods Enzymol* 1983; 98:47-59
- Jung T, Schauer U, Heusser C, Neumann C, Rieger C. Detection of intracellular cytokines by flow cytometry. *J Immunol Methods* 1993; 159:197-207
- Pickler LJ, Singh MK, Zdravski Z, Treer JR, Waldrop SL, Bergstresser PR, Maino VC. Direct demonstration of cytokine synthesis heterogeneity among human memory/effector T cells by flow cytometry. *Blood* 1995; 86:1408-1419
- Bain C, Fatmi A, Zoulim F, Zarski JP, Trepo C, Inchauspe G. Impaired allostimulatory function of dendritic cells in chronic hepatitis C infection. *Gastroenterology* 2001; 120:512-524
- Kanto T, Hayashi N, Takehara T, Tatsumi T, Kuzushita N, Ito A, Sasaki Y, Kasahara A, Hori M. Impaired allostimulatory capacity of peripheral blood dendritic cells recovered from hepatitis C virus-infected individuals. *J Immunol* 1999; 162:5584-5591
- Mathew A, Kurane I, Green S, Vaughn DW, Kalayanarooj S, Suntayakorn S, Ennis FA, Rothman AL. Impaired T cell proliferation in acute dengue infection. *J Immunol* 1999; 162:5609-5615
- Hiasa Y, Horiike N, Akbar SM, Saito I, Miyamura T, Matsuura Y, Onji M. Low stimulatory capacity of lymphoid dendritic cells expressing hepatitis C virus genes. *Biochem Biophys Res Commun* 1998; 249:90-95
- Auffermann-Gretzinger S, Keffe EB, Levy S. Impaired dendritic cell maturation in patients with chronic, but not resolved, hepatitis C virus infection. *Blood* 2001; 97:3171-3176
- Kakumu S, Okumura A, Ishikawa T, Iwata K, Yano M, Yoshioka K. Production of interleukins 10 and 12 by peripheral blood mononuclear cells (PBMC) in chronic hepatitis C virus (HCV) infection. *Clin Exp Immunol* 1997; 108:138-143
- Kishihara Y, Hayashi J, Yoshimura E, Yamaji K, Nakashima K, Kashiwagi S. IL-1 beta and TNF-alpha produced by peripheral blood mononuclear cells before and during interferon therapy in patients with chronic hepatitis C. *Dig Dis Sci* 1996; 41:315-321
- Cella M, Scheidegger D, Palmer-Lehmann K, Lane P, Lanzavecchia A, Alber G. Ligation of CD40 on dendritic cells triggers production of high levels of interleukin-12 and enhances T cell stimulatory capacity: T-T help via APC activation. *J Exp Med* 1996; 184:747-752
- Mendoza EC, Paglieroni TG, Zeldis JB. Decreased phorbol myristate acetate-induced release of tumor necrosis factor-alpha and interleukin-1 beta from peripheral blood monocytes of patients chronically infected with hepatitis C virus. *J Infect Dis* 1996; 174:842-844
- Bouffard P, Hayashi PH, Acevedo R, Levy N, Zeldis JB. Hepatitis C virus is detected in a monocyte/macrophage subpopulation of peripheral blood mononuclear cells of infected patients. *J Infect Dis* 1992; 166:1276-1280
- Mellor J, Haydon G, Blair C, Livingstone W, Simmonds P. Low level or absent *in vivo* replication of hepatitis C virus and hepatitis G virus/GB virus C in peripheral blood mononuclear cells. *J Gen Virol* 1998; 79:705-714
- Sutterwala FS, Noel GJ, Salgame P, Mosser DM. Reversal of proinflammatory responses by ligating the macrophage Fc gamma receptor type I. *J Exp Med* 1998; 188:217-222
- Haas JG, Baeuerle PA, Riethmuller G, Ziegler-Heitbrock HW. Molecular mechanisms in down-regulation of tumor necrosis factor expression. *Proc Natl Acad Sci USA* 1990; 87:9563-9567

• CLINICAL RESEARCH •

Coinfection of TT virus and response to interferon therapy in patients with chronic hepatitis B or C

Yung-Chih Lai, Ruey-Tyng Hu, Sien-Sing Yang, Chi-Hwa Wu

Yung-Chih Lai, Ruey-Tyng Hu, Sien-Sing Yang, Chi-Hwa Wu, Liver Unit, Department of Internal Medicine, Cathay General Hospital, Taipei, Taiwan
Correspondence to: Sien-Sing Yang, MD, Liver Unit, Cathay General Hospital, 280 Jen-Ai Rd., Sec. 4, Taipei, Taiwan 106. yangss@seed.net.tw
Telephone: +886-2-2708-2121 Ext. 3121

Received 2002-03-30 Accepted 2001-05-25

Abstract

AIM: To investigate the serum positive percentage of TT virus (TTV) in patients with chronic hepatitis B or C and the response of the coinfecting TTV to interferon (IFN) during IFN therapy for chronic hepatitis B and C.

METHODS: We retrospectively studied the serum samples of 70 patients with chronic hepatitis who had received IFN- α therapy from January 1997 to June 2000, which included 40 cases of hepatitis B and 30 hepatitis C. All the patients had been followed up for at least 6 months after the end of IFN therapy. The serum TTV DNA was detected using the polymerase chain reaction (PCR) before and every month during the course of IFN treatment.

RESULTS: TTV infection was detected in 15% (6/40) of the chronic hepatitis B group and 30% (9/30) of the chronic hepatitis C group. Loss of serum TTV DNA during IFN therapy occurred in 3 of 6 patients (50%) and 6 of 9 (67%) of hepatitis B and C groups, respectively. Seronegativity of TTV was found all during the first month of IFN therapy in the 9 patients. There was no correlation between the seroconversion of TTV and the biochemical changes of the patients.

CONCLUSION: TTV is not infrequently coinfecting in patients with chronic hepatitis B and C in Taiwan, and more than half of the TTV infections are IFN-sensitive. However, the loss of serum TTV DNA does not affect the clinical course of the patients with chronic hepatitis B or C.

Lai YC, Hu RT, Yang SS, Wu CH. Coinfection of TT virus and response to interferon therapy in patients with chronic hepatitis B or C. *World J Gastroenterol* 2002;8(3):567-570

INTRODUCTION

In 1997, a novel DNA virus was isolated from a patient with post-transfusion hepatitis of unknown etiology in Japan, and was designated as TT virus (TTV) after the initials of the index patient^[1]. From then on TTV has been studied worldwide. Now we know that TTV genome is non-enveloped, circular, single-stranded DNA and comprises 3,852 bases with a particle size of 30-50nm. These findings suggest that TTV is closely related to the Circoviridae^[2,3].

In the original studies from Japan, the agent was found in 34/290 (12%) of healthy donors, compared to 9/19 (47%) of patients with fulminant non-A to G hepatitis and 41/90 (46%) with non-A-G chronic liver disease^[2]. In 72 patients with chronic liver disease in the United Kingdom, TTV DNA was demonstrated in 18 cases (25%), compared to 10% of 30 cases of healthy controls^[4]. Chronic liver

disease caused by hepatitis B virus (HBV) and hepatitis C virus (HCV) infection is common in Taiwan^[5,6] and interferon (IFN) has been used for the treatment of chronic infections. Therefore, we aimed to study the serum positive percentage of TTV infection in such patients who had received IFN therapy and also to see the response of TTV to IFN during the course of the treatment.

MATERIALS AND METHODS

Patients

We retrospectively studied the frozen-stored serum samples from the patients who had received IFN therapy for chronic hepatitis B and C at Cathay General Hospital from January 1997 to June 2000.

For chronic hepatitis B, we only included the cases with both positive HBsAg (Auszyme, Abbott Lab., North Chicago, IL) and positive HBeAg [HBe (rDNA) EIA, Abbott Lab.]. Hepatitis C was confirmed with positive results for the anti-HCV antibody (Murex anti-HCV, version III, Murex Diagnostics Ltd., Dartford, England). All the cases had elevated serum alanine transaminase (ALT) levels for more than 6 months and had had at least three documented occasions of levels higher than twice the upper limit of normal (<35 IU/L), at least 1 month apart, and within 6 months prior to enrollment. All the patients underwent liver biopsy within 1 month before the start of IFN treatment. The diagnosis of chronic liver disease was based on clinical and pathological results. Serum samples taken from the patients were stored at -70°C until use.

None of our patients was alcoholic, an intravenous drug abuser or homosexual. None had received hepatotoxic drugs, herbal medicine or immuno-suppressive therapy within the 6 months prior to IFN therapy. Patients with metabolic liver diseases including hemochromatosis, Wilson's disease or α -1 anti-trypsin deficiency and autoimmune hepatitis were excluded by clinical and laboratory examinations. None had decompensated liver function (prolonged prothrombin time >3 seconds, serum total bilirubin >3.0 mg/dl, or serum albumin <3.0 gm/dl), chronic renal failure, clotting abnormalities, or serious neurological disorders. Those who coinfecting with both HBV and HCV were also excluded. Informed consent for the IFN therapy and examinations, including virological assays, was obtained from all the patients.

Laboratory assays

The patients underwent blood biochemical tests every week for the initial 4 weeks and every 2 weeks thereafter during the treatment until 24 weeks. After the end of the treatment, the patients were followed up at 4-week intervals for 12 months.

Serum samples from hepatitis C patients were examined for HCV RNA using reverse transcription-nested polymerase chain reaction (PCR) with primers for the 5'-noncoding region of HCV RNA. Genotyping of HCV RNA was assayed by PCR with type-specific primers^[7]. Serum HBV DNA was quantified with the use of a signal amplified solution hybridization antibody capture assay (Hybrid capture system, Digene, Gaithersburg, MD, USA). The presence of serum HCV RNA or HBV DNA was determined before the initiation of IFN therapy, at the end of therapy, and at 24 weeks after the completion of therapy.

Detection of TTV DNA

Serum TTV DNA was determined in specimens before the initiation of IFN therapy and regularly checked every 1 month during the course of the treatment. TTV DNA was examined using the PCR method with nested primers as previously described^[8]. Briefly, DNA was extracted from 100 μ L of serum using a QIAMP blood kit (QIAGEN Ltd., Crawley, UK) and resuspended in 50 μ L of elution buffer. For the first round of PCR, 25 μ L of reaction mixture containing 2 μ L of the cDNA sample, 1 \times PCR buffer (10mM tris-HCl pH 9.0, 50mM KCl, 1.5mM MgCl₂, 0.01% gelatin, and 0.1% Triton X-100), 10mM of each dNTP, 100ng of each outer primer T-1 (sense: 5'-ACA GAC AGA GGA GAA GGC AAC ATG-3') and T-2 (anti-sense: 5'-CTA CCT CCT GGC ATT TTA CC-3'), and 1 unit of Taq DNA polymerase was amplified in a thermal cycler (Perkin-Elmer Cetus, Norwalk, CT) for 30 cycles. One microliter of the PCR products was re-amplified for another 30 cycles with 100ng of inner primers, T-3 (sense: 5'-GGC AAC ATG TTA TGG ATA GAC TGG-3') and T-4 (anti-sense: CTG GCA TTT TAC CAT TTC CAA AGT T-3'). The amplified products were separated by 3% agarose gel electrophoresis and stained with ethidium bromide.

Interferon therapy

For the patients with chronic hepatitis B, 10 million units (mu) of recombinant interferon alfa-2b (Intron A, Schering-Plough, Co. Kenilworth, NJ, USA) was subcutaneously administered three times weekly for 24 weeks. For those with hepatitis C, 4.5 million units of recombinant alfa-2a (Roferon-A, F. Hoffmann-La Roche Ltd., Basle, Switzerland) was used subcutaneously three times a week for 24 weeks. The response to IFN was classified into two patterns according to the serum ALT level. Patient who had normalized serum ALT level (<35 IU/L) during therapy and remained constant for up to 6 months after the end of therapy was considered to have a biochemical sustained response. Non-sustained response was defined as serum ALT level that could not be normalized either at the end of therapy or during the follow-up period. The virological sustained response was defined as the absence of HBV DNA and HBeAg for hepatitis B, HCV RNA for hepatitis C and TTV DNA for TTV infection at 6 months after the end of therapy.

Statistical analysis

Data were analyzed by Student's *t* test, Chi-squared test with Yates' correction or Fisher's exact test where appropriate. All statistical tests were two-sided. A *P* value of less than 0.05 was considered significant.

RESULTS

The sera of 70 patients were studied, which included 40 patients with chronic hepatitis B and 30 patients with chronic hepatitis C (Table 1). The difference of ages between the two groups was statistically significant (*P*<0.001). In those with chronic hepatitis B, the mean age was 33 years; whereas in the chronic hepatitis C group, it was 41 years. As for the gender distribution and serum ALT levels, there was no statistically significant difference between the two groups.

Serum TTV DNA could be detected in 6 cases (15%) of chronic hepatitis B and 9 cases (30%) of chronic hepatitis C. However, the difference was not statistically significant (*P*=0.130) (Table 1).

During IFN therapy loss of serum TTV DNA was found in 3 of 6 (50%) TTV-positive patients with chronic hepatitis B and 6 of 9 (67%) TTV-positive patients with chronic hepatitis C (Table 2). Because this was a retrospective study and the doses of IFN used for chronic hepatitis B and C were different, we could not compare the rate of TTV disappearance between the two groups. Of interest,

disappearance of serum TTV DNA occurred during the first 4 weeks of IFN therapy in all the 9 cases despite the regimen of treatment or the type of chronic viral hepatitis (Table 2). In addition, serum ALT levels did not change when TTV disappeared from the serum. Serum TTV DNA was still examined every 4 weeks after the cessation of IFN therapy in the 9 cases of TTV seroconversion and had continued for 24 weeks. There was no case having the re-emergence of TTV DNA during this follow-up period.

Disappearance of TTV occurred in different genotypes of chronic hepatitis C (1a: 1/1 case, 1b: 3/5 cases, 2a: 1/2 cases, 2b: 1/1 case.). However, the number of cases was small.

In the group of chronic hepatitis B, 10 patients had virological persistent response to IFN therapy, and all the 10 patients also had biochemical persistent response. Whereas, only one patient (1/3 cases) with virological persistent response of TTV DNA had biochemical persistent response (Table 3). If we further exclude the patient with concomitant loss of HBV DNA, HBeAg and TTV DNA, none of the patients (0/2 cases) with TTV virological persistent response had biochemical persistent response.

In the group of chronic hepatitis C, all the 7 patients with virological persistent response of HCV RNA to IFN therapy had biochemical persistent response, and 2 patients (2/6 cases) with virological sustained response of TTV DNA had biochemical persistent response (Table 4). Nevertheless, none of the patients (0/4 cases) of TTV virological sustained response had biochemical persistent response after exclusion of 2 patients of concomitant loss of TTV DNA and HCV RNA.

Table 1 Demographic data and serum positive percentage of TTV in the two groups

Type	Sex (M/F)	Age (yr)	ALT (IU/L)	TTV DNA	
				No.Positive	%
B ^a (n=40)	29/11	33±8 ^c	133±65	6	15
C ^b (n=30)	24/6	41±9	121±60	9	30

^aChronic hepatitis B group. ^bChronic hepatitis C group. ^c*P*<0.001.

Table 2 Loss of serum TTV DNA during IFN therapy in the two groups

	Time of IFN Therapy (weeks)						Total
	4	8	12	16	20	24	
B ^a	3	0	0	0	0	0	3
C ^b	6	0	0	0	0	0	6

Data are presented as case number. ^aChronic hepatitis B group. ^bChronic hepatitis C group.

Table 3 Relationship between viral and biochemical responses in the group of chronic hepatitis B

	Virological SR	
	HBV (n=10)	TTV (n=3)
Biochemical SR (+)	10	1
Biochemical SR (-)	0	2

SR: sustained response, *P*=0.038, by Fisher's exact test

Table 4 Relationship between viral and biochemical responses in the group of chronic hepatitis C

	Virological SR	
	HCV (n=7)	TTV (n=6)
Biochemical SR (+)	7	2
Biochemical SR (-)	0	4

SR: sustained response, *P*=0.021, by Fisher's exact test

DISCUSSION

Epidemiologic studies have confirmed that TTV is a parenterally transmitted agent as demonstrated by donor-recipient linkage in transfused patients and by a high prevalence among hemophiliacs and intravenous drug abusers^[9-11]. In general, TTV is common in populations at risk of infection with blood-borne viruses^[2,12-14]. Many hepatitis viruses share the same modes of transmission, thus multiple viral infections may occur in a given patient^[15].

Coinfection of TTV has been observed frequently in patients with chronic hepatitis B or C^[4]. Chronic infection of hepatitis B or C virus is common in Taiwan. Thus, we made use of such patients who underwent interferon treatment to study the TT virus. In our series TTV DNA was detected in 15% of chronic hepatitis B and 30% of chronic hepatitis C, which were comparable to the results of Kao *et al*^[16], (22% and 37%, respectively) and apparently higher than that (10%) of healthy adults in Taiwan^[8]. In a prior study by Naoumov *et al*, TTV infection was detected in 21% of 33 patients with chronic hepatitis C and 20% of 10 patients with chronic hepatitis B^[4]. In Thailand, Tanaka *et al*, also found that 36% of 59 patients with HBsAg (+) and 36% of 10 patients with HCV RNA (+) had TTV infection^[17]. Several other studies also reported that the serum positive rates of TTV DNA in the patients with chronic hepatitis C, and the range was 20-46%^[18-20]. The variation might be due to the different primers used for the detection of TTV DNA. These results imply that HBV, HCV, and TTV may share common modes of transmission^[16].

The interferons possess antiproliferative, antiviral and immunomodulant properties^[21]. Extensive clinical trials have confirmed the efficacy of recombinant interferon-alfa for patients with chronic hepatitis B, C and D^[22-26]. However, because the causal role of TTV in liver disease has not been established, there is only a few papers which studied the response of TTV to IFN therapy. Taking advantage of previous research of IFN therapy for chronic hepatitis B and C, we were able to retrospectively study the prevalence of TTV in these patients and to see the response of TTV to IFN treatment. In our study, loss of serum TTV DNA during IFN therapy was noted in 50% (3/6) of chronic hepatitis B and 67% (6/9) of chronic hepatitis C. Regrettably, the comparison of these results was not feasible because this was a retrospective study and the doses of IFN used in two groups were different. Kao *et al*^[16], had similar results and they found that 41% (17/41) of patients with HCV and TTV coinfection lost serum TTV DNA at 24 weeks after the end of IFN therapy for chronic hepatitis C. Virological sustained response of TTV DNA after IFN therapy was detected to be 40-55% in patients coinfecting with chronic hepatitis C according to the recently published reports^[18-20, 27]. These findings suggest that TTV was actually vulnerable and responsive to IFN therapy. In addition, all the 9 IFN-responsive cases in our series lost their TTV DNA within the first 4 weeks of IFN therapy. This kind of seroconversion occurred in the same way in both hepatitis B and C groups, but we need more cases to further observe and confirm this phenomenon. With the results above, we know that TTV could be divided into 2 types according to the response to IFN therapy: IFN-sensitive and IFN-resistant. For the IFN-sensitive virus, the 4-week course of IFN therapy was enough to cause the seronegativity of TTV DNA. Moreover, virological sustained response could be achieved in all the 9 IFN-sensitive cases.

TTV was detected in patients with different genotypes of chronic hepatitis C. Loss of serum TTV DNA during IFN therapy occurred in all the genotypes in our study. The conversion rate between each genotype could not be compared because the number of patients was not enough. Nevertheless, the loss of serum TTV DNA during IFN therapy did not seem to be associated with the genotype of HCV.

Investigations of TTV showed considerable diversity among different isolates. The genetic diversity has continued to expand as

more and more isolates have been studied^[2,4,12]. The different response patterns to IFN therapy must be related to the genetic diversity. Comparison of partial viral DNA nucleotide sequences and phylogenetic analysis done by Chayama *et al*^[27] showed that viral strains that had a high identity to the prototype virus were more resistant to IFN than those showing low nucleotide sequence identity. The variants with multiple substitutions in the genomic sequence were more apt to be eliminated by IFN. Further analysis with new genotyping assays will reveal more information in this field.

During the course of IFN treatment, we did not find any correlation between the seroconversion of TTV DNA and the change of serum ALT levels. Although TTV was sensitive to IFN therapy in many subjects, the improvement in ALT levels after IFN therapy was not attributable to the eradication of TTV but rather to that of HCV or HBV. The disappearance of TTV DNA had no effect on the biochemical response to IFN therapy^[18,20]. According to such results, TTV may lack pathogenicity or clinical association with liver disease in these patients, which is consistent with the conclusions of many other reports^[4,8,28,29].

In summary, the serum positive percentage of TTV in chronic hepatitis B or C in our series was not low. During the IFN therapy for chronic hepatitis B or C, disappearance of coinfecting TTV occurred in more than half of the patients. IFN-sensitive TTV usually lost its DNA during the first month of treatment. Genotyping of TTV might further clarify the cause of diverse responses to IFN therapy. The finding that the disappearance of TTV DNA did not affect the clinical course of chronic hepatitis favors the null hypothesis of no significant association of TTV with liver disease.

REFERENCES

- 1 Nishizawa T, Okamoto H, Konishi K, Yoshizawa H, Miyakawa Y, Mayumi M. A novel DNA virus (TTV) associated with elevated transaminase levels in posttransfusion hepatitis of unknown etiology. *Biochem Biophys Res Commun* 1997; 241:92-97
- 2 Okamoto H, Nishizawa T, Kato N, Ukita M, Ikeda H, Iizuka H. Molecular cloning and characterization of a novel DNA virus (TTV) associated with posttransfusion hepatitis of unknown etiology. *Hepatology Research* 1998; 10:1-16
- 3 Mushahwar IK, Erker JC, Muerhoff AS, Leary TP, Simon JN, Birkenmeyer LG. Molecular and biophysical characterization of TT virus; evidence for a new virus family infecting humans. *Proc Natl Acad Sci USA* 1999; 96:3177-3182
- 4 Naoumov N, Petrova EP, Thomas MG, Williams R. Presence of a newly described human DNA virus (TTV) in patients with liver disease. *Lancet* 1998; 352:195-197
- 5 Chen DS. Hepatitis B virus infection, its sequelae, and prevention in Taiwan. In: Okuda K, Ishak KG, editors. *Neoplasm of the liver*. Tokyo: Springer Verlag 1987; 71-80
- 6 Chen DS, Kao G, Sung JL, Lai MY, Sheu JC, Chen PJ. Hepatitis C virus infection in an area hyperendemic for hepatitis B and chronic liver disease: the Taiwan experience. *J Infect Dis* 1990; 162: 817-822
- 7 Kao JH, Chen PJ, Yang PM, Lai MY, Sheu JC, Wang TH. Interfamilial transmission of hepatitis C virus: the important role of infections between spouses. *J Infect Dis* 1992; 166: 900-903
- 8 Kao JH, Chen W, Hsiang SC, Chen PJ, Lai MY, Chen DS. Prevalence and implication of TT virus infection: minimal role in patients with non-A-E hepatitis in Taiwan. *J Med Virol* 1999; 59: 307-312
- 9 Yang SS, Wu CH, Chen TH, Huang YY, Huang CS. TT viral infection through blood transfusion: retrospective investigation on patients in a prospective study of post-transfusion hepatitis. *World J Gastroenterol* 2000; 6: 53-56
- 10 Desai SM, Muerhoff AS, Leary TP. Prevalence of TT virus infection in US blood donors and populations at risk for acquiring parenterally transmitted viruses. *J Infect Dis* 1999; 179:1242-1244
- 11 MacDonald DM, Scott GR, Clutterbuck D. Infrequent detection of TT virus infection in intravenous drug users, prostitutes, and homosexual men. *J Infect Dis* 1999; 179:686-689
- 12 Hohne M, Berg T, Muller AR, Schreier E. Detection of sequences of TT virus, a novel DNA virus, in German patients. *J Genl Virol* 1998; 79:2761-2764
- 13 Poovorawan Y, Theamboonlers A, Jantaradsamee P, Kaew-in N, Hirsch P, Tangkitvanich P. Hepatitis TT virus infection in high-risk groups.

- Infection* 1998; 26:355-358
- 14 Takayama S, Yamazaki S, Matsuo S, Sugii S. Multiple infection of TT virus (TTV) with different genotypes in Japanese hemophiliacs. *Biochem Biophys Res Commun* 1999; 256: 208-211
- 15 Pontisso P, Ruvoletto MG, Fattovich G, Chemello L, Galloini A, Ruol A. Clinical and virological profiles in patients with multiple hepatitis virus infections. *Gastroenterology* 1993; 105:1529-1533
- 16 Kao JH, Chen W, Chen PJ, Lai MY, Chen DS. TT virus infection in patients with chronic hepatitis B or C: influence on clinical, histological and virological features. *J Med Virol* 2000; 60: 387-392
- 17 Tanaka H, Okamoto H, Luengrojanakul P, Chainuvati T, Tsuda F, Tanaka T. Infection with an unenveloped DNA virus (TTV) associated with posttransfusion non-A to G hepatitis in hepatitis patients and healthy blood donors in Thailand. *J Med Virol* 1998; 56: 234-238
- 18 Watanabe H, Saito T, Kawamata O, Shao L, Aoki M, Terui Y. Clinical implication of TT virus superinfection in patients with chronic hepatitis C. *Am J Gastroenterol* 2000;95:1776-1780
- 19 Akahane Y, Sakamoto M, Miyazaki Y, Okada S, Inoue T, Ukita M. Effect of interferon on a nonenveloped DNA virus (TT virus) associated with acute and chronic hepatitis of unknown etiology. *J Med Virol* 1999;58:196-200
- 20 Hagiwara H, Hayashi N, Mita E, Oshita M, Kobayashi I, Iio S. Influence of transfusion-transmitted virus infection on the clinical features and response to interferon therapy in Japanese patients with chronic hepatitis C. *J Viral Hepat* 1999;6:463-469
- 21 Baron S, Tying SK, Fleischmann WR, Coppenhaver DH, Niesel DW, Klimpel GR. The interferons: mechanisms of action and clinical applications. *JAMA* 1991; 266: 1375-1383
- 22 Hoofnagle JH. Therapy of acute and chronic viral hepatitis. *Adv Intern Med* 1994; 39:241-275
- 23 Woo MH, Burnakis TG. Interferon alfa in the treatment of chronic viral hepatitis B and C. *Ann Pharmacother* 1997; 31: 330-337
- 24 Di Bisceglie AM, Fong TL, Fried MW, Swain MG, Baker B, Korenman J. A randomized controlled trial of recombinant alpha-interferon therapy for chronic hepatitis B. *Am J Gastroenterol* 1993; 88:1887-1892
- 25 Poynard T, Bedossa P, Chevallier M, Mathurin P, Lemonnier C, Trepo C. A comparison of three interferon alfa-2b regimens for the long-term treatment of chronic non-A, non-B hepatitis. *N Engl J Med* 1995; 332: 1457-1462
- 26 Iino S, Hino K, Kuroki T, Suzuki H, Yamamoto S. Treatment of chronic hepatitis C with high-dose interferon alpha-2b. A multicenter study. *Dig Dis Sci* 1993; 38: 612-618
- 27 Chayama K, Kobayashi M, Tsubota A, Kobayashi M, Arase Y, Suzuki Y. Susceptibility of TT virus to interferon therapy. *J Gen Virol* 1999;80: 631-634
- 28 Kanda T, Yokosuka O, Ikeuchi T. The role of TT virus infection in acute viral hepatitis. *Hepatology* 1999; 29: 1905-1908. Utsunomiya S, Yoshioka K, Wakita T, Seno H, Takagi K, Ishigami M. TT virus infection in hemodialysis patients. *Am J Gastroenterol* 1999; 94: 3567-3570

Edited by Zhang JZ

• CLINICAL RESEARCH •

Epidemiological and histopathological study of relevance of Guizhou Maotai liquor and liver diseases

Jun Wu, Ming-Liang Cheng, Guo-Hao Zhang, Rong-Wei Zhai, Neng-Hui Huang, Cheng-Xiu Li, Tian-Yong Luo, Shuang Lu, Zhi-Qin Yu, Yu-Mei Yao, Ying-Ying Zhang, Lan-Zhen Ren, Lan Ye, Ling Li, Hui-Na Zhang

Jun Wu, Ming-Liang Cheng, Tian-Yong Luo, Shuang Lu, Zhi-Qin Yu, Yu-Mei Yao, Ying-Ying Zhang, Department of Infectious Diseases, Affiliated Hospital, Guiyang Medical College, Guiyang 550004, Guizhou Province, China
Guo-Hao Zhang, Hospital of Doutai Distillery, Renhuai 563000, Guizhou Province, China

Rong-Wei Zhai, Shanghai university of Medical Sciences, Shanghai 200025, China
Neng-Hui Huang, Cheng-Xiu Li, Lan-Zhen Ren, Lan Ye, Ling Li, Hui-Na Zhang, Department of pharmacology, Guiyang Medical College, Guiyang 550004, Guizhou Province, China

Supported by The primary sciences and technology project of Guizhou province., No. 19992015

Correspondence to: Jun Wu, Department of Infectious Diseases, Affiliated Hospital, Guiyang Medical College, Guiyang 550004, Guizhou Province, China. wuwuj@21cn.com

Telephone: +86-851-6702233(H), +86-851-6855119 Ext.3263 (O)

Received 2002-05-02 Accepted 2002-05-25

Abstract

AIM: To explore the relevance of Maotai liquor and liver diseases.

METHODS: Epidemiological study was conducted on groups of subjects, each consisting of 3 subjects from the Maotai liquor group consisting of 99 individuals and one from the non-alcoholic control group consisting of 33 individuals. Liver biopsy was performed on 23 volunteers from Guizhou Maotai Distillery who had a constant and long history of drinking Maotai liquor. Experimental histopathological study was conducted as follows: sixty male Wistar rats were divided into 3 groups randomly and fed with Maotai liquor, ordinary white wine, and physiological saline respectively for a period of 8 and 12 weeks. The rats were sacrificed in batches, then serum ALT, AST, TBil, and AKP were measured. Rat livers were harvested to measure the liver indexes, GSH, and MDA. Histopathological examinations were also performed. Another eighty mice were randomly divided into 4 groups and fed with Maotai (at different dosages of 10 ml·kg⁻¹ and 20 ml·kg⁻¹), ethanol, and physiological saline. The animals were sacrificed after 4 weeks and serum ALT was determined. Then the livers were harvested and liver indexes and MDA were measured.

RESULTS: The incidence rate of hepatic symptoms, splenomegaly, liver function impairment, reversal of Albumin/Globulin and increased diameter of portal veins in the Maotai liquor group were 1.0%(1/99), 1.0%(1/99), 1.0%(1/99), 1.0%(1/99), 0(0/99) and 0(0/99), 0(0/99), 0(0/99), 0(0/99), 0(0/99), respectively. There was no significant difference between the Maotai group and the non-alcoholic control group ($P>0.05$). Various degree of fatty infiltration of hepatocytes was found in the 23 volunteers receiving liver biopsy, but there was no obvious hepatic fibrosis or cirrhosis. A comparison was made between the Maotai liquor group and the ordinary white wine group. It was found that hepatic MDA in rats and mice were 0.33 ± 0.10 and 0.49 ± 0.23 respectively in Maotai group and 0.61 ± 0.22 and 0.66 ± 0.32 in the ordinary white wine group; MDA had an obvious decrease in the Maotai liquor group ($P<0.05$);

hepatic GSH were $0.12\text{mg}\cdot\text{g}^{-1}\pm0.06\text{mg}\cdot\text{g}^{-1}$ in rats of the Maotai liquor group and $(0.08\pm0.02)\text{mg}\cdot\text{g}^{-1}$ in white wine group, it was obviously increased in the Maotai liquor group ($P<0.05$). After the 20 rats had been fed with ordinary white wine for 8 weeks consecutively, disarranged hepatocyte cords, fatty infiltration of hepatocytes, and fibrous septa of varying widths due to hepatic connective tissues proliferation were observed; after 12 weeks, the fibrous tissue proliferation continued and early cirrhosis appeared. Compared with the ordinary white wine group, fatty infiltration was observed in the 8-week and 12-week groups, but no necrosis or fibrosis or cirrhosis was found in the Maotai liquor group ($P<0.05$).

CONCLUSION: Maotai liquor may cause fatty liver but not hepatic fibrosis or cirrhosis, and it can strengthen lipid peroxidation in the liver.

Wu J, Cheng ML, Zhang GH, Zhai RW, Huang NH, Li CX, Luo TY, Lu S, Yu ZQ, Yao YM, Zhang YY, Ren LZ, Ye L, Li L, Zhang HN. Epidemiological and histopathological study of relevance of Guizhou Maotai liquor and liver diseases. *World J Gastroenterol* 2002;8(3):571-574

INTRODUCTION

Alcohol can cause fatty liver, hepatitis and liver cirrhosis^[1-5]. A lot of research showed that there was a close relationship between liver diseases and alcohol content of liquor. If one drinks ardent spirits 80 to 150g daily for more than ten years, he will get alcoholic hepatitis, hepatic fibrosis, liver cirrhosis and even hepatocellular carcinoma^[6-13]. Maotai liquor has a very unique brewing technique which is different from that for ordinary white wine, and there are multiple microorganisms in the special geographical situations which are able to absorb abundant amino acids, vitamins and many essential microelements^[14], so the taste of Maotai is very sweet and pure. A study on 40 individuals reported by Li et al showed that drinking Maotai liquor more than 150g daily for ten years would not cause liver injury. Our previous study showed that Maotai liquor was able to induce increase of metallothioneins(MT), inhibit the proliferation of hepatic stellate cell (HSC) and generation of collagen and enhance the effect of antioxidation^[15]. Our study has initially interpreted the anti-fibrosis mechanism of Maotai liquor. A study was conducted on groups of subjects from Guizhou Maotai Distillery, each consisting of 3 subjects from the Maotai liquor group of 99 individuals who had a constant and long history of drinking Maotai liquor and one from the non-alcoholic control group of 33 individuals. Liver biopsy was performed on some of them and liver biopsy and serological tests in rats and mice fed with Maotai liquor were performed in order to explore the effect of Maotai liquor has on the liver.

MATERIALS AND METHODS

Materials

One hundred and thirty two individuals from Guizhou Maotai Distillery, aged from 30 to 60 years old, were divided into Maotai

liquor group consisting of 99 individuals and non-alcoholic control group consisting of 33 individuals. All members of the Maotai liquor group have the capacity for liquor of more than 250g.d⁻¹ and drinking history of longer than ten years. There was no significant difference between the two groups in sex and age. The male Wistar rats weighing (300±20)g were employed in this study (Provided by Experimental Animal center, the Third Military Medical University); the mice of Kunming species weighing (22±2)g (Provided by Experimental Animal center, Guiyang Medical College) were also used. Maotai liquor of (530±2)g·L⁻¹ was produced by Guizhou Maotai Distillery, China, whose code bar was 6902952880026; the ordinary white wine of (530±2)g·L⁻¹ was provided by the Fourth Department of Guizhou Food Export and Import Company.

Methods

Questionnaires were prepared in advance including sex, age, drinking history (capacity and duration), history of liver diseases, and history of gastropathy, etc. Physical examination, abdominal B ultrasound (the size of liver and spleen, diameter of portal vein), serum ALT, A/G, LN and HA were also done at the same time. Liver biopsy was performed in twenty three volunteers from the Maotai group, the liver tissue was fixed by formalin of 40g·L⁻¹, embedded by paraffin, sectioned and stained by HE. Sixty male Wistar rats were randomly divided into Maotai liquor group, ordinary white wine group and normal control group. Rats in the wine group were fed with 2mL·kg⁻¹ Maotai liquor and 2mL·kg⁻¹ ordinary white wine both of which were diluted one fold by distilled water, and in the control group were fed with the same volume of saline. All rats were fed once everyday continuously for 8 weeks, and after the last feed, 15 rats were fasted for 20 hours and then sacrificed to get blood for testing serum ALT, AST, TBil and AKP were tested, and Rat livers were harvested to measure the liver indexes, GSH, MDA, the liver tissue was embedded, sectioned and stained with HE. The remaining 5 rats in each group were sacrificed for histopathological examination after fed for 12 weeks. Eighty mice (40male, 40female) were randomly divided into 4 groups [two Maotai groups (at different dosage of 1 mL·kg⁻¹ and 2 mL·kg⁻¹), ethanol group, and physiological saline group]. Mice were fed with dosage of 1 mL·kg⁻¹ and 2 mL·kg⁻¹ Maotai in the two Maotai groups respectively. In the ethanol group, mice were fed (with) 53 g·L⁻¹ ethanol at dosage of 1 mL·kg⁻¹, they were fed once everyday for 4 weeks. After the last feed, the mice were killed to measure serum ALT, the liver indexes and MDA. Questionnaires were done by special messenger, and were examined and verified by persons in charge of the study.

Statistic analysis

The data were analyzed by *t* test and χ^2 test.

RESULTS

Epidemiologic analysis

The 98 individuals who had a long history of wine drinking had no symptoms abnormal, signs or liver function; only one who had a history of hepatitis showing cirrhosis of liver. He had symptoms of liver disease, splenomegaly, lightly increase of ALT and reversed A/G. There was no increase in the diameter of portal vein trunk in those individuals, compared with that of the control group, ($P>0.05$). None of those who had a history of drinking Maotai for more than 30 years died of liver diseases. (See Table 1). There was a slight increase of serum LN, but a significant increase of HA, ($P<0.05$) (See Table 2). All twenty three individuals in the Maotai group who had biopsy had varying degrees of fatty infiltration of hepatocytes. One of them had slight necrosis, but none had obvious hepatic fibrosis or cirrhosis of liver, in compared with that of the white wine group ($P<0.05$).

Experimental study in rats

Neither Ordinary white wine nor Maotai liquor had obvious effect on ALT, AST, TBil, ALP and liver indexes in rats fed for 8 weeks, compared to the normal control group. There was no significant difference between them ($P>0.05$) (See Table 3); but Maotai liquor was able to increase the level of GSH and decrease the level of liver MDA (See Table 4). There were no obvious pathologic changes in rat liver of the normal control group (See figure 1). In the ordinary white wine group, all twenty rats had disarrangement of hepatocyte cords, fatty infiltration and hyperplasia of fibrous tissue which formed the fibrous septa (See Figure 2) after they had been fed for 8 weeks. The fibrous tissue had further hyperplasia in the rats of the 12-week group and there were also signs of early cirrhosis of liver (See figure 3). But after the Maotai group had been fed for 8 weeks and 12 weeks, all rats had fatty infiltration, 17 were mild degree and 3 were moderate degree; all were devoided of necrosis of hepatocytes, hepatic fibrosis and cirrhosis ($P<0.05$) (See figure 4,5) when compared with that of the white wine group.

Table 1 Epidemiologic study of the Relationship between Guizhou Maotai liquor and Liver Diseases

	Group	Number	Positive	
			Number	Rate (%)
History of	Maotai Group	99	1	1.0
liver disease	Control Group	33	0	0
Symptoms of	Maotai Group	99	1	1.0
liver disease	Control Group	33	0	0
Hepatomegaly	Maotai Group	99	15	15.2
	Control Group	33	3	9.1
Splenomegaly	Maotai Group	99	1	1.0
	Control Group	33	0	0
Abnormal ALT	Maotai Group	99	1	1.0
	Control Group	33	0	0
Reversed A/G	Maotai Group	99	1	1.0
	Control Group	33	0	0
Portal trunk	Maotai Group	99	0	0
widening	Control Group	33	0	0

Table 2 Serum ALT, LN, and HA in Maotai Group ($\bar{x}\pm s$)

Group	<i>n</i>	ALT(nkat·L ⁻¹)	LN(μg·L ⁻¹)	HA(μg·L ⁻¹)
Control Group	33	683±150	88±24	106±32
Maotai Group	99	650±100	132±71 ^a	293±194 ^a

^a $P<0.05$, vs control group

Table 3 The effect of Maotai wine to the liver function of rats ($n=20$, $\bar{x}\pm s$)

Group	Serum biochemical index				Liver index and biochemical index		
	ALT (nkat·L ⁻¹)	AST (nkat·L ⁻¹)	Tbil (nmol·L ⁻¹)	AKP (nkat·L ⁻¹)	Index (g·kg ⁻¹)	GSH (mg·g ⁻¹)	MDA (A)
Saline	517±233	300±150	12.68±6.47	350±217	27.93±8.64	0.06±0.01	0.66±0.24
Ordinary white wine	567±167	300±67	13.54±2.50	433±67	29.19±4.41	0.08±0.02	0.61±0.22
Maotai wine	533±183	283±133	11.54±6.20	450±133	27.81±2.11	0.12±0.06 ^a	0.33±0.10 ^a

^a $P<0.05$, vs control group

Table 4 The effect of Maotai wine to the liver function of mice ($n=20$, $\bar{x}\pm s$)

Group	Dosage (mL·kg ⁻¹)	ALT (nkat·L ⁻¹)	liver index (mg·g ⁻¹)	MDA (A)
Saline	10	316±83	40.34±7.54	0.69±0.21
Alcohol	10	333±83	40.96±7.21	0.66±0.32
Maotai wine	10	383±133	43.8±8.79	0.49±0.23 ^a
Maotai wine	20	250±100	39.48±3.84	0.46±0.12 ^a

^a $P<0.05$, vs control group

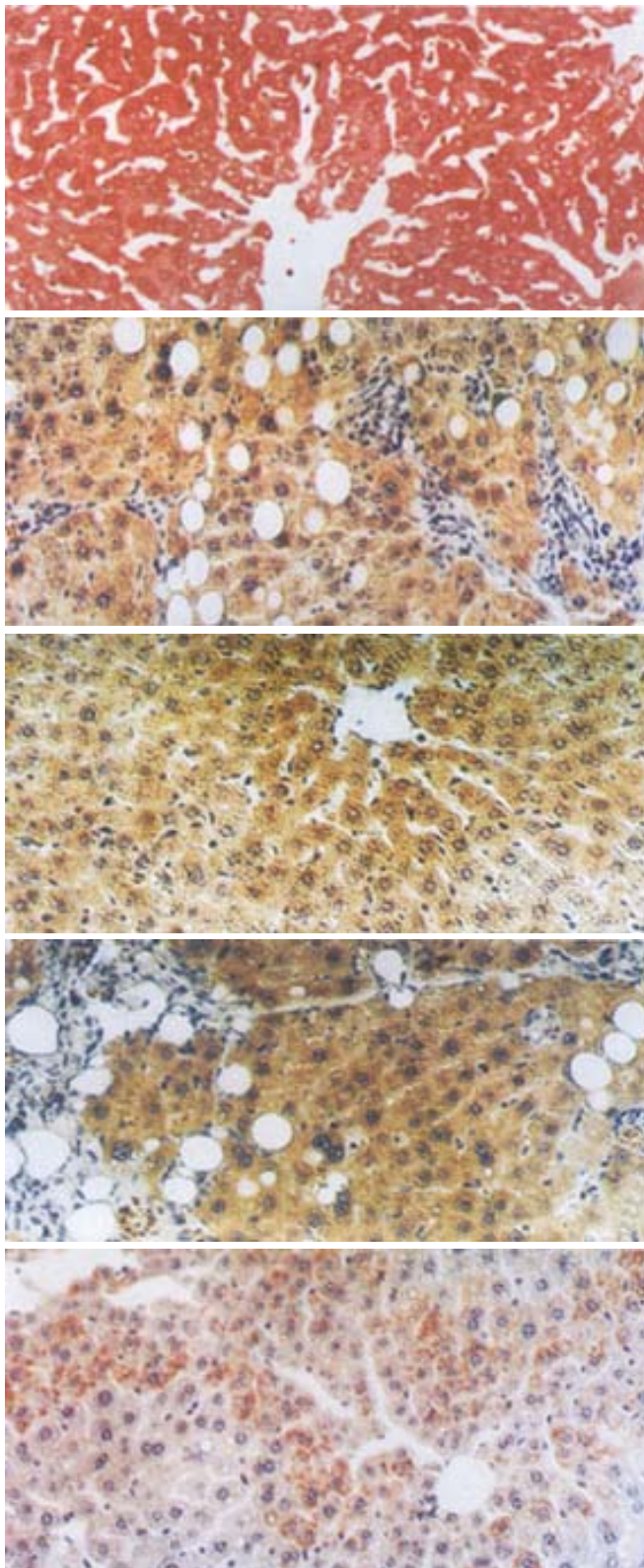


Figure 1 Normal liver tissue, hepatic cords were well arranged, the structure of hepatic lobule were intact. (HE.×200)

Figure 2 After fed with alcohol for 8 weeks, disorganized hepatic cords, fatty infiltration, mesenchymal hyperplasia, and fibrosis could be seen. (HE.×200)

Figure 3 After fed with alcohol for 12 weeks, there were fatty infiltration of hepatocytes, hyperplasia of connective tissue, and early manifestation of cirrhosis. (HE.×200)

Figure 4 After fed with Maotai liquor for 8 weeks, there were a few infiltrating inflammatory cells, normally arranged hepatic cords, liver sinusoids were dilated and lipid droplet could be seen in hepatocytes. (HE.×200)

Figure 5 After fed with alcohol for 12 weeks, brown changes and lipid droplet could be obviously seen in hepatocytes. (HE.×200)p

DISCUSSION

About 40% of those who drank 150g ardent spirits every day would have fatty liver and alcoholic hepatitis^[15]. Alcoholic fatty liver diseases can be manifested as fatty liver, alcoholic hepatitis, hepatic fibrosis and cirrhosis of liver, frequently they are overlapping. And fatty liver can proceed to hepatic fibrosis via inflammatory progress. The varying pathology of alcoholic fatty liver diseases have similar pathogenesis in hepatic fibrosis and cirrhosis^[16-22]. They are mainly caused by activation of HSC, resulting in excessive deposition and relatively insufficient degradation of ECM. Alcohol, acetaldehyde, lipid, fatty acids, etc can activate and stimulate Kupffer cells to secrete many cytokines which activate HSC to produce various components of ECM, as collagen, laminin, and hyaluronic acid, etc.

In recent years, studies have shown alcohol has direct damage effect to the hepatocytes^[23-32]. Alcohol can be oxidized to acetaldehyde with elimination hydroxy free radicals, which causes lipid peroxidation, hepatocytic damage and apoptosis. Lipid peroxidation and its metabolic products malondialdehyde (MDA) and free radicals have strong cellular toxicity^[33-37]. GSH^[38-44] being an antioxidant is able to inhibit lipid peroxidation, and is also involved in hepatic detoxication, thus it can process cytoprotective effect. MT is a low molecular weight metal-binding protein rich in thioaminopropionic acid. Studies in recent years showed that MT has the effects of eliminating hydroxy free radicals and other oxidation products, being also protective^[45-49].

Hepatic pathological changes of human being and animals show that Maotai liquor can lead to fatty infiltration in the liver, but no obvious hepatic fibrosis or cirrhosis of liver. Similar findings were shown in epidemiological study, B mode ultrasound and liver biopsy in the Maotai liquor group. One died of liver diseases in this group.

By contrast, various widths of fibrous septa and cirrhosis can be seen in the liver of rats fed ordinary white wine. Why is fatty infiltration in which Maotai liquor group dose not lead to liver fibrosis and cirrhosis of liver? The answer is that Maotai liquor was able to lower the MDA level in the rats and mice liver and increase the level of liver GSH as comparing with those in the ordinary white wine group, $P < 0.05$. It also showed that Maotai liquor had the inhibitory effect on lipid peroxidation and was cytoprotective. Moreover, study in vitro showed that Maotai liquor could increase MT which was the most powerful bioactive substance of scavenging free radicals and antagonizing liver damage. Maotai liquor may also inhibit the activation of hepatic stellate cells and generation of collagen.

Our study revealed that Maotai liquor was able to elevate the level of workers' serum LN and HA in Maotai liquor group vs. ordinary white wine group, ($P < 0.05$). It may be related with the activation of hepatic stellate cells (HSC) by ethanol, acetaldehyde, lipid and fatty acid. The elevation of LN was mild, but HA was very obvious whose reason may be that the serum level of HA was related with the ability of hepatic secretion and the renal excretion. In the acute hepatic injury caused by alcohol, inflammation and drugs, the level of serum HA may be very high, but it only points at a possible hepatic fibrosis or the early stage of hepatic fibrosis because researches show that the level of HA is not very high, even normal, in the late stage of hepatic fibrosis^[50].

As one of the three most famous distilled spirits of the world, Maotai liquor was brewed with open solid state fermentation in a special geographical environment, so it has formed its own style which is hard for others to imitate. According to the analysis of the nutritive component in Maotai liquor in recent years, in every 100 ml Maotai Liquor, there were 18mg protein, 6667 u superoxide dismutase (SOD), 0.06 mg vitamin B₁, 0.1 mg vitamin B₂ and 1.19 mg vitamin C, 0.022 mg manganese (Mn), 0.026 mg copper (Cu), 0.42 mg iron (Fe), 1.0 mg potassium (Ka), and <0.005 mg zinc (Zn); 4.7 mg methanol, 4.7 mg aldehyde compounds. And there were also 18 kinds of amino acids and 6 kinds of essential amino acids

except acimeton and tryptophan which were never found in the Jiang flavor white wine before Maotai. There were SOD and multiple human essential microelements in Maotai liquor, especially rich in Fe, Mn and Cu. The components of methanol, benzene and aldehyde were much lower than it was ruled in the international standard.

REFERENCES

- Cheng ML, Liu SD. The basic study and clinical research on hepatic fibrosis. *Renmin Weisheng Chubanshe* 1996;84-86
- Sun YN. Recency studies in Pathogenesis of alcoholic liver diseases. *Guowai Yiyao. Xiaohuaxi Jibing Fengce* 1999;19:97-101
- Fan JG, Zeng MD, Wang GL. Pathogenesis of fatty liver. *Shijie Huaren Xiaohua Zazhi* 1999;7:5-7
- Tang TH. Recent studies of alcoholic liver diseases. *Shijie Huaren Xiaohua Zazhi* 2000;8:56
- Miyano S, Maeyama S, Iwaba A, Ogata S, Koike J, Kishi M, Uchikoshi T. A clinicopathological study of acute hepatitis in heavy drinkers, unrelated to hepatitis A, B, or C viruses. *Alcohol Clin Exp Res* 2001;25:69S-74S
- Wu J, Liu RC, Li J, Wang WL, Hu L, Yang QZ, Liang YD, Lu YY, Cheng ML, Ding YS. To study the risk factors of hepatic cirrhosis in hepatitis virus and hepatic fibrosis. *Cina Public Health* 1999;15:394
- Wu J, Cheng ML, Ding YS, Liu RC, Li J, Wang WL, Hu L. Five years follow-up survey of risk factor of virus hepatic cirrhosis. *Shijie Huaren Xiaohua Zazhi* 2000;8:1365-1367
- Pan RM, Shao XD. Clinical characteristics of alcoholic liver disease. *World J Gastroenterol* 1998;4:95-96
- Huang Z, Tian DL, Yuan AH. Experimental animal models with alcoholic liver diseases. *Huaren Xiaohua Zazhi* 1998;6:712-713
- Liu WW. Etiological studies of hepatocellular carcinoma. *Shijie Huaren Xiaohua Zazhi* 1999;7:93-95
- Gu GW, Zhou HG. New concept in etiology of liver cancer. *Huaren Xiaohua Zazhi* 1998;6:185-187
- Pan RM, Shao XD. Clinical characteristics of alcoholic liver disease. *World J Gastroenterol* 1998;4:95-96
- Bellentani S, Saccoccio G, Costa G, Tiribelli C, Mancini F, Sodde M, Croce LS, Sasso F, Pozzato G, Cristiani G, Brandi G. Drinking habits as co-factors of risk for alcohol induced liver damage. *Gut* 1997;41:845-850
- Xiao Y. Preliminary explanation of the mechanism which long term drinking of Guizhou maotai will not incur liver fibrosis. *Zhonghua Yixue Zazhi* 2001;81:628
- Wang JY. Clinical Epidemiology of fatty liver. *Zhonghua Ganzangbing Zazhi* 2000;8:115
- Fan JG, Zeng MD, Hong J, Li JQ, Qiu DK. Effects of free unsaturated fatty acids on proliferation of L-02 and HLF cell lines and synthesis of extracellular matrix. *Shijie Huaren Xiaohua Zazhi* 1998;6:502-504
- Sun DL, Sun SQ, Li TZ, Lu XL. Serologic study on extracellular matrix metabolism in patients with viral liver cirrhosis. *Huaren Xiaohua Zazhi* 1999;0:55-56
- Lü XH, Xie YH, Fu BY, Liu CR, Wang BY. Dynamic expression of tissue inhibitor of metalloproteinase 1 in alcoholic liver disease in rats. *Shijie Huaren Xiaohua Zazhi* 2001;9:29-33
- Lu LG, Zeng MD, Li JQ, Fan JG, Hua J, Fan ZP, Dai N, Qiu DK. Effect of arachidonic acid and linoleic acid on proliferation of rat hepatic stellate cells. *Shijie Huaren Xiaohua Zazhi* 1999; 7:10-12
- Kishore R, McMullen MR, Nagy LE. Stabilization of tumor necrosis factor α mRNA by chronic ethanol: role of A+U rich elements and p38 mitogen activated protein kinase signaling pathway. *J Biol Chem* 2001;10
- Wu J, Zern MA. Hepatic stellate cells: a target for the treatment of liver fibrosis. *J Gastroenterol* 2000;35:665-672
- Anania FA, Womack L, Jiang M, Saxena NK. Aldehydes potentiate α (2)(I) collagen gene activity by JNK in hepatic stellate cells. *Free Radic Biol Med* 2001; 30:846-857
- Ruoyu Ni, Maria Anna Leo, Jingbo Zhao and Charles S. Toxicity of α -carotene and its exacerbation by acetaldehyde in HepG2 cells. *Alcohol and Alcoholism* 2001; 36: 281-285
- Zhang B, Zhang DF, Ren H. Resistance of Bcl-2 adenovirus vector to HepG2 cell apoptosis induced by ethanol. *Zhonghua Ganzangbing Zazhi* 2000;8:215-217
- Slukvin II, Boor PJ, Jerrells TR. Initiation of alcoholic fatty liver and hepatic inflammation with a specific recall immune response in alcohol-consuming C57Bl/6 mice. *Clin Exp Immunol* 2001;125:123-133
- Deaciuc IV, Nikolova-Karakashian M, Fortunato F, Lee EY, Hill DB, McClain CJ. Apoptosis and dysregulated ceramide metabolism in a murine model of alcohol-enhanced lipopolysaccharide hepatotoxicity. *Alcohol Clin Exp Res* 2000;24:1557-1565
- Lu LG. Hepatic sieve and fatty liver. *Zhonghua Ganzangbing Zazhi* 2000;8:115
- Lin H, Lü M, Zhang YX, Wang BY, Fu BY. Induction of a rat model of alcoholic liver diseases. *Shijie Huaren Xiaohua Zazhi* 2001;9:24-28
- Bo AH, Tian CS, Xue GP, Du JH, Xu YL. Morphology of immuno and alcoholic liver diseases in rats. *Shijie Huaren Xiaohua Zazhi* 2001;9:157-160
- Yang CF, Chen XM, Liu J, Zheng WX, Chang W. Study of the effect of alcohol on liver lipid peroxidation in the rat. *Xiandai Yufang Yixue* 1996;23:141-143
- MacDonald GA, Bridle KR, Ward PJ, Walker NI, Houghlum K, George DK, Smith JL, Powell LW, Crawford DH, Ramm GA. Lipid peroxidation in hepatic teatosis in humans is associated with hepatic fibrosis and occurs predominately in acinar zone 3. *J Gastroenterol Hepatol* 2001;16:599-606
- Zima T, Fialova L, Mestek O, Janebova M, Crkovska J, Malbohan I, Stipek F, Mikulikova L, Popov P. Oxidative stress, metabolism of ethanol and alcohol-related diseases. *J Biomed Sci* 2001;8:59-70
- Lu XY. Mechanism of free radicals on liver injury induced by ethanol. *Xin Xiaohuabingxue Zazhi* 1997;5: 200-202
- Degoul F, Sutton A, Mansouri A, Cepanec C, Degott C, Fromenty B, Beaugrand M, Valla D, Pessayre D. Homozygosity for alanine in the mitochondrial targeting sequence of superoxide dismutase and risk for severe alcoholic liver disease. *Gastroenterology* 2001;120:1468-1474
- Poli G. Pathogenesis of liver fibrosis: role of oxidative stress. *Mol Aspects Med* 2000;21:49-98
- Mutlu-Turkoglu U, Dogru-Abbasoglu S, Aykac-Toker G, Mirsal H, Beyazyurek M, Uysal M. Increased lipid and protein oxidation and DNA damage in patients with chronic alcoholism. *J Lab Clin Med* 2000;136:287-291
- French SW. Intragastric ethanol infusion model for cellular and molecular studies of alcoholic liver disease. *J Biomed Sci* 2001;8:20-27
- Tang YP, Yang GZ, Lu HL, Tu YQ, Zhang Y. Effects of external glutathione in protection against organ injury after infection. *Zunyi Yixueyuan Xuebao* 1999;22: 85-87
- Shi JS, Sheng MP, Li F. protection from DEN carcinogenesis by glutathione in rat hepatoma model. *Zunyi Yixueyuan Xuebao* 1998; 21:1-5
- Dai DW, Wu SM, Qi QE, Li M, Chen HJ, Chai W. Effects of glutamine on intracellular reduced glutathione in cultured human intestinal epithelial cells with anoxia/reoxygenation. *Zhonghua Binglischengli Zazhi* 1999;15: 128-130
- Li J, Tu BQ, Yang TS, Liu JJ, Jia FM. Alteration of glutathione in RBC in patients with liver cirrhosis and its clinical significance. *Xinxiaohua Zazhi* 1996;4:18-19
- Sun GY, Liu WW. Free radicals and Digestive system neoplasms. *Huaren Xiaohua Zazhi* 1998;6:272-273
- Soltys K, Dikdan G, Koneru B. Oxidative stress in fatty livers of obese Zucker rats: rapid amelioration and improved tolerance to warm ischemia with tocopherol. *Hepatology* 2001;34:13-18
- Yu JC, Jiang ZM, Li DM. Glutamine: a precursor of glutathione and its effect on liver. *World J Gastroenterol* 1999;5:143-146
- Nishimura N, Miyabara Y, Suzuki JS, Sato M, Aoki Y, Satoh M, Yonemoto J, Tohyama C. Induction of metallothionein in the livers of female Sprague-Dawley rats treated with 2,3,7,8-tetrachlorodibenzo-p-dioxin. *Life Sci* 2001;69:1291-1303
- Park JD, Liu Y, Klaassen CD. Protective effect of metallothionein against the toxicity of cadmium and other metals(1). *Toxicology* 2001; 163:93-100
- Wright J, George S, Martinez-Lara E, Carpena E, Kindt M. Levels of cellular glutathione and metallothionein affect the toxicity of oxidative stressors in an established carp cell line. *Mar Environ Res* 2000;50: 503-508
- Zaroogian G, Jackim E. In vivo metallothionein and glutathione status in an acute response to cadmium in *Mercenaria mercenaria* brown cells. *Comp Biochem Physiol C Toxicol Pharmacol* 2000;127:251-261
- Fabisiak JP, Pearce LL, Borisenko GG, Tyhurina YY, Tyurin VA, Razzack J, Lazo JS, Pitt BR, Kagan VE. Bifunctional anti/prooxidant potential of metallothionein: redox signaling of copper binding and release. *Antioxid Redox Signal* 1999;1:349-364
- Kong XT. Early Diagnosis of hepatic fibrosis. *Zhonghua Ganzangbing Zazhi* 2000;8:241-242

Edited by Wu XN

• CLINICAL RESEARCH •

Clinical significance of plasma D-dimer and von Willebrand factor levels in patients with ulcer colitis

Gang Xu, Ke-Li Tian, Guo-Ping Liu, Xue-Jun Zhong, Shao-Ling Tang, Yan-Ping Sun

Gang Xu, Guo-Ping Liu, Xue-Jun Zhong, Shao-Ling Tang, Yan-Ping Sun, Department of Gastroenterology, Chinese PLA 456 Hospital of PLA, Jinan 250031, Shandong Province, China

Ke-Li Tian, Department of Biochemistry, Shandong University, Jinan 250062, Shandong Province, China

Correspondence to: Gang Xu, Institute of Gastroenterology, First Military Medical University, Guangzhou 510515, Guangdong Province, China. gangxujn@263.net

Telephone: +86-20-85141544

Received 2001-09-14 Accepted 2001-10-29

Abstract

AIM: To investigate the levels of D-dimer(DD) and von Willebrand factor(vWF) and the relationship between DD and vWF in ulcerative colitis(UC) patients.

METHODS: A total of 29 plasma specimens were obtained from patients with ulcerative colitis (male 13, female 16), aged 21-47 years (33 ± 11). Disease activity was assessed by Truelove-Writeria. Patients with a score of above 5 were regarded as having active colitis. Twenty healthy people(male 12, female 8), aged 19-53 years(31 ± 14), served as normal controls. Blood samples were taken from an antecubital vein puncture. Blood(1.8 mL) was injected into the tubes containing sodium citrate (0.13 mmol/L). The plasma was obtained by centrifugation at $3000\text{ r}\cdot\text{min}^{-1}$ for 10 min, and stored at $-80\text{ }^{\circ}\text{C}$ until assayed by ELISA.

RESULTS: The mean plasma levels of DD and vWF in active UC patients were significantly higher than those of the controls (0.69 ± 0.41 vs 0.27 ± 0.11 , $P<0.01$; 143 ± 46 vs 103 ± 35 , $P<0.01$). The mean plasma levels of DD in the patients with active disease were higher than those with inactive disease(0.69 ± 0.41 vs 0.48 ± 0.29 , $P<0.05$). The levels of vWF were not different between active and inactive patients. DD levels were positively related to vWF levels($r=0.574$, $P<0.01$). There was no significant difference between levels of DD and vWF and the scope of disease and sex of the patients.

CONCLUSION: vWF is an important feature and a good marker of UC; intravascular thrombus and endothelial cell dysfunction were found in UC patients; and the combined test of DD and vWF is helpful to distinguish the activity of the UC patients.

Xu G, Tian KL, Liu GP, Zhong XJ, Tang SL, Sun YP. Clinical significance of plasma D-dimer and von Willebrand factor levels in patients with ulcer colitis. *World J Gastroenterol* 2002;8(3):575-576

INTRODUCTION

The pathogenesis of ulcerative colitis(UC) is still unknown^[1,2]. Some studies suggested that intestinal vascular injury caused by intramural vascular thrombosis or vasculitis was considered as a potential pathogenetic mechanism of inflammatory bowel disease. The D-Dimer (DD) is known to be a special fibrin degradation product, which is used as an index of fibrin turnover and intravascular

thrombogenesis^[3]. von willebrand factor(vWF) is released from endothelial cells, which is used as a marker for endothelial damage^[4]. In this study, we investigated the change of DD and vWF levels in UC patients and the relationship between these two markers.

MATERIALS AND METHODS

Patients

A group of 29 patients (male 13, female 16), aged 21-47 years(33 ± 11), were diagnosed by routine clinical, radiologic, endoscopic and histologic means(excluding heart and brain vessel diseases, diabetes and other diseases that affect blood coagulation). Disease activity was assessed by Truelove-Writeria. Patients with a score of above 5 were regarded as having active colitis. Meanwhile 20 healthy people(male 12, female 8), aged 19-53 years (31 ± 14), served as normal controls.

Measurement of plasma DD and vWF levels

Blood samples were taken from an antecubital vein puncture. Blood (1.8 mL) was injected into the tubes containing sodium citrate(0.13 mmol/L). The plasma was obtained by centrifugation at $3000\text{ r}\cdot\text{min}^{-1}$ for 10 min, and stored at $-80\text{ }^{\circ}\text{C}$ until assayed by ELISA(The Sun Biotechnology Company, Fujian, China).

Statistical analysis

Statistical analysis of mean value of DD and vWF levels were made by Student's *t* test and Student -Newman-keuls's test. $P<0.05$ was considered to be significant.

RESULTS

DD and vWF levels in patients with UC

The mean plasma levels of DD and vWF in active UC patients were significantly higher than those of the controls ($P<0.01$, Table 1). The mean plasma levels of DD in the patients with active disease were higher than that of inactive disease ($P<0.05$). The levels of vWF had no difference between active and inactive patients. DD levels was positively related to vWF levels($r=0.574$, $P<0.01$).

Table 1 Changes of DD and vWF levels in patients with UC ($\bar{x}\pm s$)

	<i>n</i>	DD(mg/l)	vWF(%)
controls	20	0.27 ± 0.11	102.75 ± 34.91
UC active	17	0.69 ± 0.41^{ab}	142.71 ± 45.96^a
Inactive	12	0.48 ± 0.29^a	135.00 ± 26.25^a

^a $P<0.01$, vs control; ^b $P<0.05$, vs inactive

Table 2 The levels of DD and vWF in different sex and scope of disease ($\bar{x}\pm s$)

	<i>n</i>	DD(mg/l)	vWF (%)
Sex			
Male	13	0.58 ± 0.11	142.84 ± 42.85
Female	16	0.55 ± 0.15	138.75 ± 36.75
Scope of disease			
Rectum-sigmoid	15	0.58 ± 0.27	137.11 ± 36.87
Left-side	9	0.59 ± 0.26	138.78 ± 42.22
Colon	5	0.63 ± 0.41	143.60 ± 51.60

DD and vWF levels in gender of disease and scope of disease

DD and vWF levels seemed to be increased with the scope of disease gradually, but differences were not significant with different scope of disease. There was no statistical difference between males and females (Table 2).

DISCUSSION

Von willebrand factor(vWF) is a high molecular weight multimeric glycoprotein, synthesized and released by vascular endothelial cells and megakaryocytes. It has two functions: firstly, this glycoprotein carries factor VIII in the circulation and is required for factor VIII stability in the plasma. Serving as the carrier for factor VIII, vWF may also coordinate formation of the fibrin rich thrombus at the site of endothelial cell injury; secondly, this glycoprotein may mediate initial platelet adhesion to the subendothelium by linking to specific platelet membrane receptors and to constituents of subendothelial connective tissues. This is pertinent to the damage of the vascular endothelium^[5]. Most of plasma vWF is derived from endothelial cells rather than from platelets under normal circumstances, suggesting that vWF is a good marker of endothelial dysfunction^[6,7]. Clinically, in vitro and animal studies support the concept that increased levels of circulating vWF reflect endothelial cell damage or injury^[8]. Elevated vWF levels have been demonstrated in the patients with inflammatory vascular disease and associated disorders, including rheumatoid arthritis, systemic sclerosis, systematic lupus erythematosus, Felty's syndrome, giant cell arteritis and polyarteritis nodosa. Intestinal vascular injury caused by intramural vascular thrombosis or vasculitis is considered as a potential pathogenetic mechanism of inflammatory bowel disease. We investigated the role of vascular injury in the pathogenesis of UC by examining the levels of plasma vWF. The results showed that vWF levels were more significantly raised in the active or inactive patients with UC, as compared with the controls. The levels of vWF were unrelated to the scope of the disease, and there was no statistical difference between males and females. Our results confirmed and extended those of other investigators^[9], showing that concentration of circulation vWF is elevated in UC patients. Our results supported the hypothesis that intestinal endothelial cell damage was an important feature of UC and proved that vWF was a good marker of UC.

It is well known that DD is a marker of ongoing intravascular thrombogenesis. In the previous researches, DD test was established as a useful aid in the diagnosis of the deep-vein thrombosis of the lower limbs and pulmonary embolism^[10]. Some reports showed higher DD levels in patients with coronary artery disease, Sickle cell disease, systemic lupus erythematosus, several sorts of neoplasms^[11,12] and acute pancreatitis^[13]. Weber's results showed that DD levels were higher in patients with UC^[14]. Our results showed significantly higher DD levels in patients with UC, both in active and inactive patients, as compared with the controls. It confirmed the presence of intravascular thrombus in UC patients. Thus anticoagulant treatment, with either warfarin or heparin, may have a positive influence on UC.

Several reports indicated that DD is used as a marker of

inflammation. Elevated level is a well-established marker of acute-phase reaction and may reflect the presence of inflammation^[12,15]. Our results showed that DD levels were significantly higher in patients with active UC than those with inactive UC, but there was no statistical difference in vWF levels between active and inactive UC patients. There was positive correlation between vWF and DD, we therefore, proposed that the combined test of DD and vWF is helpful to distinguish the activity of the UC patients.

REFERENCES

- 1 Cui HF, Jiang XL. Treatment of corticosteroids-resistant ulcerative colitis with oral low molecular weight heparin. *World J Gastroenterol* 1999;5:448-450
- 2 Das KM, Farag SA. Current medical therapy of inflammatory bowel disease. *World J Gastroenterol* 2000; 6:483-489
- 3 Danesh J, Whincup P, Walker M, Lennon L, Thomson A, Appleby P, Rumley A, Lowe GD. Fibrin D-dimer and coronary heart disease: prospective study and meta-analysis. *Circulation* 2001;103:2323-2327
- 4 Goldsmith I, Kumar P, Carter P, Blann AD, Patel RL, Lip GY. Atrial endocardial changes in mitral valve disease: a scanning electron microscopy study. *Am Heart J* 2000; 140: 777-845
- 5 Jager A, van-Hinsbergh VW, Kostense PJ, Emesis JJ, Nijpels G, Dekker JM, Heine RJ, Bouter LM, Stehouwer CD. Increased levels of soluble vascular cell adhesion molecule 1 are associated with risk of cardiovascular mortality in type 2 diabetes: the Hoorn study. *Diabetes* 2000; 49:485-491
- 6 Feng D, Bursell SE, Clermont AC, Lipinska I, Aiello LP, Laffel L, King GL, Tofler GH. von Willebrand factor and retinal circulation in early-stage retinopathy of type 1 diabetes. *Diabetes care* 2000;23:1694-1698
- 7 Alborno L, Alvarez D, Otero JC, Gadano A, Salviu J, Gerona S, Sorroche P, Villamil A, Mastai R. von Willebrand factor could be an index of endothelial dysfunction in patients with cirrhosis: relationship to degree of liver failure and nitric oxide levels. *J Hepatol* 1999;30:451-455
- 8 Makris TK, Stavroulakis GA, Dafni UG, Gialeraki AE, Krespi PG, Hatzizacharias AN, Tsoukala CG, Vythoulkas JS, Kyriakidia MK. ACE/DD genotype is associated with hemostasis balance disturbances reflecting hypercoagulability and endothelial dysfunction in patients with untreated hypertension. *Am Heart J* 2000;140:760-765
- 9 Meucci G, Pareti F, Vecchi M, Saibeni S, Bressi C, Franchis R. Serum von Willebrand factor levels in patients with inflammatory bowel disease are related to systemic inflammation. *Scand J Gastroenterol* 1999;34:287-290
- 10 Righimi M, Goehring C, Bounameaux H, Perrier A. Effects of age on the performance of common diagnostic tests for pulmonary embolism. *Am J Med* 2000;109:357-361
- 11 Blackwell K, Haroon Z, Broadwater G, Berry D, Harris L, Iglehart JD, Dewhirst M, Greenberg C. Plasma D-dimer levels in operable breast cancer patients correlate with clinical stage and axillary lymph node status. *J Clin Oncol* 2000; 18:600-608
- 12 Kohno I, Inuzuka K, Itoh Y, Nakahara K, Eguchi Y, Sugo T, Soe G, Sakata Y, Murayama H, Matsuda M. A monoclonal antibody specific to the granulocyte-derived elastase-fragment D species of human fibrinogen and fibrin: its application to the measurement of granulocyte-derived elastase digests in plasma. *Blood* 2000;95:1721-1728
- 13 Xu G, Zhong XJ, Guo WM, Sui RL, Tang SL, Sun YP. D-dimer and von Willebrand factor levels in acute pancreatitis patients. *Shijie Huaren Xiaohua Zazhi* 1999;7:1088-1089
- 14 Weber P, Husemann S, Vielhaber H, Zimmer KP, Nowak-Gottl U. Coagulation and fibrinolysis in children, adolescents, and young adults with inflammatory bowel disease. *J Pediatr Gastroenterol Nutr* 1999;28: 418-422
- 15 Kim SB, Chi HS, Park JS, Hong CD, Yang WS. Effect of increasing serum albumin on plasma D-dimer, von Willebrand factor, and platelet aggregation in CAPD patients. *Am J Kidney Dis* 1999;33:312-317

Edited by Ma JY